NOVEL APPROACHES TO TARGET THE IMMUNE SYSTEM IN GASTROINTESTINAL CANCERS

EDITED BY: Gianluigi Giannelli, Erica Villa and Maria L. Martinez Chantar
PUBLISHED IN: Frontiers in Immunology and Frontiers in Oncology

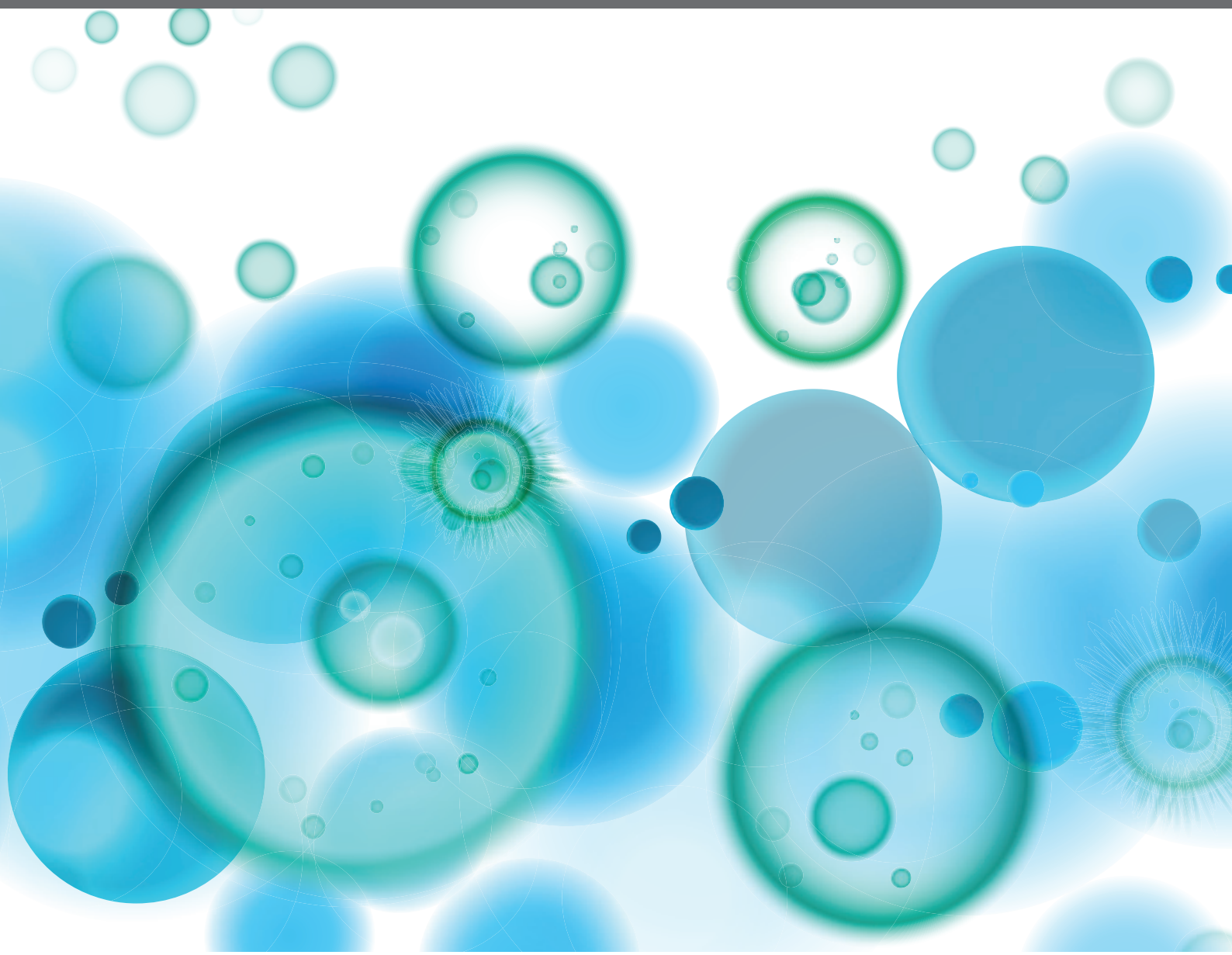

frontiers Research Topics

ISSN 1664-8714
ISBN 978-2-88974-261-5
DOI 10.3389/978-2-88974-261-5

About Frontiers

Frontiers is more than just an open-access publisher of scholarly articles: it is a pioneering approach to the world of academia, radically improving the way scholarly research is managed. The grand vision of Frontiers is a world where all people have an equal opportunity to seek, share and generate knowledge. Frontiers provides immediate and permanent online open access to all its publications, but this alone is not enough to realize our grand goals.

Frontiers Journal Series

The Frontiers Journal Series is a multi-tier and interdisciplinary set of open-access, online journals, promising a paradigm shift from the current review, selection and dissemination processes in academic publishing. All Frontiers journals are driven by researchers for researchers; therefore, they constitute a service to the scholarly community. At the same time, the Frontiers Journal Series operates on a revolutionary invention, the tiered publishing system, initially addressing specific communities of scholars, and gradually climbing up to broader public understanding, thus serving the interests of the lay society, too.

Dedication to Quality

Each Frontiers article is a landmark of the highest quality, thanks to genuinely collaborative interactions between authors and review editors, who include some of the world's best academicians. Research must be certified by peers before entering a stream of knowledge that may eventually reach the public - and shape society; therefore, Frontiers only applies the most rigorous and unbiased reviews.
Frontiers revolutionizes research publishing by freely delivering the most outstanding research, evaluated with no bias from both the academic and social point of view. By applying the most advanced information technologies, Frontiers is catapulting scholarly publishing into a new generation.

What are Frontiers Research Topics?

Frontiers Research Topics are very popular trademarks of the Frontiers Journals Series: they are collections of at least ten articles, all centered on a particular subject. With their unique mix of varied contributions from Original Research to Review Articles, Frontiers Research Topics unify the most influential researchers, the latest key findings and historical advances in a hot research area! Find out more on how to host your own Frontiers Research Topic or contribute to one as an author by contacting the Frontiers Editorial Office: frontiersin.org/about/contact

NOVEL APPROACHES TO TARGET THE IMMUNE SYSTEM IN GASTROINTESTINAL CANCERS

Topic Editors:
Gianluigi Giannelli, National Institute of Gastroenterology S. de Bellis Research Hospital (IRCCS), Italy
Erica Villa, University of Modena and Reggio Emilia, Italy
Maria L. Martinez Chantar, CIC bioGUNE, Spain

Citation: Giannelli, G., Villa, E., Chantar, M. L. M., eds. (2022). Novel Approaches to Target the Immune System in Gastrointestinal Cancers. Lausanne: Frontiers Media SA. doi: 10.3389/978-2-88974-261-5

Table of Contents

frontiers in Immunology

REVIEW
published: 06 August 2019
doi: 10.3389/fimmu.2019.01816

Is There a Place for Immunotherapy for Metastatic Microsatellite Stable Colorectal Cancer?

François Ghiringhelli[*†] *and Jean-David Fumet*[†‡]

Department of Medical Oncology, Centre Georges François Leclerc, Dijon, France

Immunotherapy using checkpoint inhibitor targeting PD-1 and PD-L1 revolutionized the treatment of microsatellite instable metastatic colon cancer. Such treatment is now a standard of care for these patients. However, when used as monotherapy checkpoint inhibitors targeting PD-1 and PD-L1 are not effective in metastatic colorectal cancer patients with microsatellite stable tumors. Recent advances in biology provide a rationale for this intrinsic resistance and support the evaluation of combination therapy to reverse resistance. This article will highlight recent findings on the mechanism of intrinsic resistance and recent advances in clinical trials for combination therapy.

Keywords: colorectal cancer, checkpoint inhibitor, mismatch repair deficiency, combination therapy, PD-1, PD-L1

OPEN ACCESS

Edited by:
Gianluigi Giannelli,
National Institute of Gastroenterology S. de Bellis Research Hospital (IRCCS), Italy

Reviewed by:
Gordon Freeman,
Dana–Farber Cancer Institute, United States
Ruggero De Maria,
Catholic University of the Sacred Heart, Italy

***Correspondence:**
François Ghiringhelli
fghiringhelli@cgfl.fr
orcid.org/0000-0002-5465-8305

†These authors have contributed equally to this work

‡Jean-David Fumet
orcid.org/0000-0002-9444-941X

Specialty section:
This article was submitted to Cancer Immunity and Immunotherapy, a section of the journal Frontiers in Immunology

Received: *04 June 2019*
Accepted: *18 July 2019*
Published: *06 August 2019*

Citation:
Ghiringhelli F and Fumet J-D (2019) Is There a Place for Immunotherapy for Metastatic Microsatellite Stable Colorectal Cancer? Front. Immunol. 10:1816. doi: 10.3389/fimmu.2019.01816

INTRODUCTION

Tumor microenvironment (TME) plays an important role in cancer progression and in the response to therapy. Increasing data in the literature underlines that CD8 T cells and tumor-infiltrating lymphocyte (TIL) accumulation in the tumor bed are biomarkers of good outcome in most types of cancers (1). In the context of colorectal cancer, the presence of CD8 T cells in the tumor bed and invasive margin is strongly associated with outcome. Jerome Galon's team's publications have shown that time to recurrence and overall survival strongly correlate with the strength of the *in-situ* adaptive immune reaction in the colon tumor core and invasive margin (2, 3). They proposed that solid tumors' intra-tumoral immune context (i.e., type, functional orientation, density, and location of immune cells) could be a dominant determinant of clinical outcome (4). These data underline that colorectal cancers are frequently widely invaded by immune cells and suggest that immunotherapy could be a suitable therapy for such patients. Based on this observation, anti PD-1 mAb was tested in advanced metastatic colorectal cancers. However, initial reports of phase I trials were very disappointing, with only 1 of 33 patients with colorectal cancer with objective clinical response to this treatment (5, 6). Importantly, the responding patient differed from others due to the mismatch-repair deficiency (dMMR). dMMR is a small fraction of whole colorectal cancer. dMMR status is due to a mutation in genes involved in DNA mismatch repair (MLH1, MSH2, MSH6, PMS2, EPCAM). Such mutations can be exclusively somatic or constitutional, in the context of Lynch syndrome. These tumors represent around 15% of localized colorectal tumors and about 3–4% of metastatic colon cancers (7). Recently, Le et al. reported a phase 2 clinical trial to evaluate the efficacy of pembrolizumab, an anti PD-1 immune checkpoint blocker, in colorectal cancer patients with either dMMR or proficient MMR (pMMR status). In this trial, only treatment-refractory metastatic colon cancer patients were included. Objective response was 40% in patients with dMMR tumors, while no patient had an objective response in the pMMR group. The median progression-free survival reached 5 months in dMMR patients but only 2 months in pMMR patients (8). Such data support that checkpoint inhibitors targeting PD-1 are

only effective in dMMR tumors. In this review, we will explain why dMMR tumors are sensitive to checkpoint inhibitors and we will study the different mechanisms of pMMR tumors' intrinsic resistance and how to circumvent them.

RATIONALE OF CHECKPOINT INHIBITORS' EFFICACY IN MICROSATELITE INSTABLE TUMORS

dMMR status relies on epigenetic silencing or mutations in DNA mismatch repair genes (9, 10). This anomaly induces genetic aberrations due to DNA replication errors in microsatellites, short tandemly repeated DNA sequences. Such an anomaly is called microsatellite instability (9) and is classically diagnosed by the variable length of DNA microsatellites, some mononucleotide and dinucleotide repeats. dMMR mutations induce accumulation of DNA replication errors in both coding and non-coding DNA regions, which can be point or frameshift mutations (9). This mechanism induces mutation accumulation at a 10- to 50-fold higher rate than in pMMR tumors. The inactivation of MMR increased the mutational burden and led to dynamic mutational profiles, which resulted in the persistent generation of neoantigens, whereas MMR-proficient cells exhibited stable mutational load and neoantigen profiles over time (11). Consequently, when present in the coding sequence such mutations induce the generation of a large number of neoantigens, which could be presented as neoantigenic peptides by HLA molecules of both tumor and antigen presenting cells and be recognized as foreign antigens by T cells (12). Such a mechanism could explain why dMMR tumors present higher CD8 cytotoxic T and Th1 helper cells infiltration, resulting in a better prognosis when tumors are non-metastatic (10). Mutant neoantigens are recognized by tumor-antigen-specific T cells, present in growing tumors, and able to limit both tumor growth and metastatic process. In experimental settings, these CD8 T cells can be reactivated following treatment with anti-PD-1/anti-CTLA-4 and mediate tumor rejection (13). So, we can hypothesize that a high level of neoantigens in localized tumor dMMR tumors might explain their better prognosis via a more robust immunoediting. In the metastatic setting, we could hypothesize that CD8 and Th1 infiltrating dMMR tumors are exhausted and could be reactivated by checkpoint inhibitors (14).

In dMMR tumors, CD8 and Th1 express high levels of multiple checkpoints inhibitors such as programmed death-1 (PD-1), cytotoxic T lymphocyte–associated antigen 4 (CTLA4), and lymphocyte activation gene 3 (LAG3) in comparison to pMMR tumors (15). These markers underline that intratumoral T cells present an exhausted status. Exhausted CD8 T cells are T cells that emerge during chronic antigen stimulation. These cells are initially effector cells, which produce a high level of cytotoxic molecules and interferon gamma (IFNγ). In the absence of complete tumor eradication, the sustained antigen stimulation restrains T cells' capacity to produce cytotoxic molecules and inflammatory cytokines such as IFNγ (16). In addition, dMMR colorectal cancer (CRC) may present an increased expression of tumor PD-L1, which has been correlated with checkpoint inhibitor efficacy in different tumor types in a retrospective study (17). Such data might explain both checkpoint inhibitors' efficacy in such tumors and absence of spontaneous tumor eradication due to T cell exhaustion [(12); **Figure 1**].

MECHANISM OF INTRINSIC RESISTANCE IN MICROSATELITE STABLE TUMORS

Immunoexclusion

Immunohistological analysis of colon cancer revealed that CD8 infiltration is mainly located in the invasive margin around tumors (18). Among dMMR tumors, T cells were more abundant at the invasive margin than in the tumor core, thus suggesting that a mechanism of immunoexclusion could be involved in the absence of T cells in the tumor core. Absence of T cells in the tumor core may blunt the efficacy of checkpoint inhibitors (19).

Some experimental data on mice preclinical models of pMMR colon cancer summarize this phenomenon. Transforming growth factor–β (TGFβ), an immunosuppressive cytokine associated with bad prognosis, was observed in the tumor bed of preclinical models of colon cancer (20, 21). TGFβ acts on the fibroblastic stroma, increases fibrosis and limits tumor core T cell invasion. Inhibition of TGFβ using a pharmacological inhibitor or a mAb promotes T cell recruitment to the tumor bed and efficacy of checkpoint inhibitors (22). Recently bifunctional checkpoint inhibitor, the fusion protein M7824, comprising the extracellular domain of human TGFβRII linked to the C-terminus of human anti-PD-L1, was developed and showed important efficacy in preclinical models. M7824 treatment promoted CD8+ T cell and NK cell activation, and both of these immune populations were required for optimal M7824-mediated tumor control. M7824 was superior to TGFβ- or αPD-L1-targeted therapies when in combination with a therapeutic cancer vaccine (23).

Immunoexclusion could also be related to tumor cells' intrinsic mechanism. pMMR tumors are characterized by the presence of the activation of WNT/β-catenin signaling. In contrast, this pathway is rarely activated in dMMR colon tumors (24). Previous data obtained in melanoma underline that WNT/β-catenin signaling activation is involved in the mechanism of immune exclusion. WNT/β-catenin signaling induces transcriptional repression of chemokine genes such as CCL4, essential for intratumoral homing of dendritic cells to the tumor bed. In particular, CCL4 expression induces recruitment of Batf3 positive dendritic cells which are essential for T cell priming, activation and recruitment to the tumor site (25, 26). Activation of tumor-intrinsic WNT/β-catenin signaling was also tested in TCGA pan cancer data (27). This analysis across 31 tumors determined that 28 (90%), including colon cancer, showed activated β-catenin signaling in the non-T cell-inflamed subset, demonstrating this observation is relevant in most cancer types. Targeting WNT/β-catenin could be a strategy to improve immunotherapy efficacy (28).

Lack of Antigens

To induce an antitumor immune response, tumor cells must contain antigens detected by cytotoxic T cells. pMMR tumors

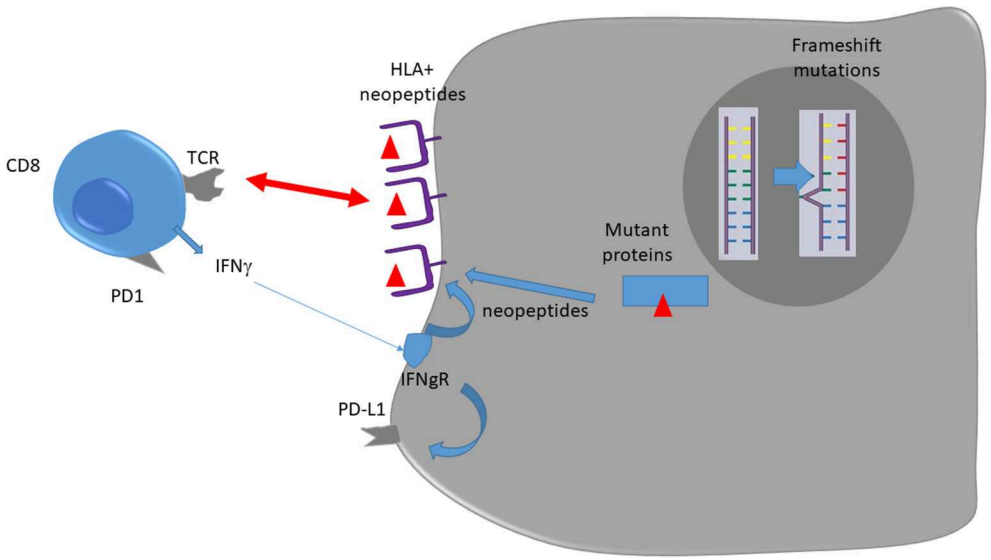

FIGURE 1 | Immune response against dMMR tumors.

have fewer mutations than dMMR tumors. Recent literature shows that there is a strong association between mutation presence and response rate to checkpoint inhibitors used as monotherapy (29). The number of non-synonymous mutations is called the tumor mutational burden (TMB). The median TMB of a pMMR tumor is 4 mutations/MB, which classifies this tumor as a low TMB tumor. In comparison, TMB mean of dMMR tumor is 30 mutations/MB (30). However, the median number of mutations in pMMR is similar to the one found in ovarian cancer or hepatocellular carcinoma, which present some response to checkpoint inhibitor used as monotherapy. Such data suggest that additional mechanisms other than TMB explain resistance to checkpoint inhibitors in pMMR tumors.

Despite the lack of antigens in pMMR tumors most colon cancer tumors are infiltrated by CD8 T cells. There is evidence that tumor-specific T cells targeting neoantigens play a role in tumor control (13, 14, 29, 31), but in most tumor types antigen specificities are unknown. A hypothesis to explain the lack of efficacy could be that CD8 tumor infiltrating cells are non-tumor specific cells and classify as bystander cells. In a recent Nature paper (29), the authors studied the antigen specificity of CD8 tumor infiltrated cells in human lung and colorectal cancer. They observed that only very few $CD8^+$ TILs are specific for tumor antigens. Most TILs recognize a wide range of infectious epitopes such as Epstein–Barr virus, cytomegalovirus or influenza virus. Similarly, specific T cell response was tested in another report concerning melanoma, colon cancer and ovarian cancer (32). While in melanoma tumors specific T cells represent 60% of tumor infiltrated CD8, in ovarian cancer and colon cancer they represent only 5 and 9%, respectively. Such data underlines that only a minority of CD8 TILs recognize tumor antigens in pMMR tumors, therefore a lack of antigen specificity may at least partly explain resistance to immunotherapy.

Activation of the mitogen activated protein kinase (MAPK) pathway is found in around 60% of pMMR colon cancers due to a constitutive activation of the small GTPase K-Ras (Kirsten rat sarcoma viral oncogene homolog) or other N-RAS (neuroblastoma rat sarcoma viral oncogene homolog). Such mutations are more frequent in pMMR than in dMMR tumors and lead to a constitutive activation of the downstream pathway effectors molecules MEK (Mitogen/Extracellular signal regulated Kinase) and ERK1 and/or ERK2 (33, 34). Activation of the MAPK pathway reduces MHC class I molecule expression on tumor cells of different cancer types such as melanoma, breast cancer and colon cancer (35–37). Pre-clinical experiments showed that MAPK inhibition, using MEK inhibitors, resulted in MHC class I molecules upregulation in tumor cells and increased CD8 T infiltration in tumor core (38). Such data provide a rationale to combine MEK inhibitors and checkpoint inhibitors in RAS mutated tumors to enhance MHC class I molecule expression and to enhance tumor recognition by infiltrated CD8 T cells (39). Based on these results a phase I with cobimetinib and atezolizumab was started and confirmed biological activity of this combination in CD8 T cells recruitment and induction of HLA expression (40). Subsequently, a phase III trial was then started in patients with pMMR advanced treatment-refractory colorectal cancer and compared the combination of cobimetinib and atezolizumab with atezolizumab alone or regorafenib (41). Neither atezolizumab monotherapy nor combination atezolizumab and cobimetinib demonstrated significantly improved OS compared to regorafenib.

IMMUNOSUPPRESSION

In addition to effector populations, like CD8 T cells and antigen presenting cells, the presence of immunosuppressive cells may

control antitumor immune response and could blunt the efficacy of checkpoint inhibitors. The two main immunosuppressive cells are FOXP3 regulatory T cells (Tregs) and the myeloid derived suppressor cells (MDSC).

Tregs have the capacity to inhibit most immune cells. These cells accumulate during tumor growth and are frequently associated with poor prognosis in various types of cancers (42–46). However, in colorectal cancers their role is complex. Indeed, some studies looking at FOXP3 positive cell accumulation in colorectal tumors suggest that a better prognosis is associated with the presence of such infiltrates (30, 45–48). This event probably relies on the fact that T cell infiltration is a strong surrogate marker of good prognosis in colorectal cancer and that Foxp3 accumulation is strongly correlated with accumulation of other immune cells (15, 49). The role of Treg infiltration in colorectal cancer became even more complex with the discovery of two types of Tregs in colon cancer. These two types of cells could be differentiated by their level of Foxp3 expression (low vs. high) (50). Only FOXP3 high cells are immunosuppressive and their accumulation in colon cancer is a surrogate marker of poor prognosis. In contrast, Foxp3 low non-suppressive Treg cells are not a factor of bad prognosis. These cells are associated with the presence of *Fusobacterium nucleatum* which is also associated with dMMR status (51). Together, such data raise the hypothesis that dMMR tumors are infiltrated with Foxp3 low non-suppressive Tregs, which are recruited due to the presence of *Fusobacterium nucleatum* and also probably due to other chemoattractant agents, while pMMR tumors are mainly invaded by Foxp3 high immunosuppressive Tregs which blunt immune response. Depletion of FOXP3 high Treg cells from tumor tissues may augment antitumor immunity and should be tested in combination with checkpoint inhibitors in pMMR tumors.

Myeloid-derived suppressor cells (MDSC) are a heterogeneous population of myeloid cells with monocytic and neutrophilic phenotypes. These cells are blocked at immature stages of differentiation and exert an immunosuppressive role in both innate and adaptive immune cells. These cells are absent in healthy humans but accumulate in blood, lymph nodes, bone marrow, and tumors during cancer growth (52, 53). The accumulation of MDSC was tested in colon cancer and a high level of MDSC was found in the blood of patients with metastatic colorectal cancers (54). This MDSC accumulation is associated with poor prognosis. Preclinical data underline that MDSC elimination could induce CD8 T cell accumulation and reactivation at the tumor site (55), thus suggesting that elimination of such immunosuppressive cells could enhance the efficacy of checkpoint inhibitors.

Secondary immunosuppression due to induction of checkpoint inhibitor expression might also be relevant. We recently reported higher expression of immune checkpoints in dMMR tumors in comparison to pMMR tumors. Immune checkpoint expression is associated with intrinsic poor prognosis in dMMR tumors while its expression does not have an impact on pMMR tumor prognosis (15). Such data suggest that immune checkpoints may be clinically more relevant in dMMR tumors, providing a rationale for a better efficacy of these therapies in this category of colorectal cancer.

ROLE OF ANGIOGENESIS

Neoangiogenesis has a major role during tumor development. Several oncogenic pathways lead to the production of Vascular Endothelial Growth Factor (VEGF), the main proangiogenic factor during cancer growth (56–58). VEGF acts as a specific proliferating agent for endothelial cells through interaction with its specific receptors, VEGFR1 and R2. Both VEGF and its receptors are expressed at high levels in human colon carcinomas and in tumor associated endothelial cells (59–61). However, few data compare angiogenesis in dMMR and pMMR colorectal cancer. A recent biological study (62) tested the presence in the blood of healthy volunteers and patients bearing metastatic dMMR or pMMR colorectal cancers of endothelial progenitor cells and VEGF. Both parameters were increased in patients with dMMR tumors, suggesting a more important dependency of these tumors to angiogenesis.

VEGF is known to have an important and deleterious effect on the immune system. Notably, VEGF could blunt dendritic maturation through STAT3 induction in myeloid cells. VEGF is also known to affect immunosuppression. VEGF could promote MDSC accumulation (63). In patients with cancer, a correlation between disease stage, VEGF-A levels and MDSC accumulation was observed (64, 65). This accumulation is related to the positive effect of VEGFR2 on STAT3 activation, which induces expansion and activation of MDSCs (66, 67). VEGF could also promote Treg cell expansion. In particular, dendritic cell and MDSC activation by VEGF induces IL-10 and TGF-β. These events promote Treg cell expansion (66, 68, 69). VEGF-A could also directly induce Treg proliferation due to their high expression level of VEGFR2 (70). Finally, VEGF is also produced by type 2 tumor-associated macrophages (TAM), which accumulate in colorectal cancer and are associated with poor prognosis (71–74).

VEGF production in the tumor bed induces pathological vascularization which could lead to insufficient vascularization and hypoxia. Such hypoxia is well-known to impede CD8 TILs-mediated lysis of tumor cells (75). VEGF-A neutralization induces tumor vasculature normalization and restores CD8 TILs' effector functions. Taken together, these results show a direct link between tumor vasculature normalization and enhanced immune cell infiltration.

The above-described data provide a rationale to use anti-VEGF therapies to limit immunosuppression and to restore an effective antitumor immune response. In mice, anti-VEGF antibody could enhance dendritic cell maturation, resulting in an increase in number and functions of tumor infiltrating dendritic cells (76). Anti VEGF-A or tyrosine kinase inhibitor like sunitinib also led to a significant reduction of MDSCs in peripheral blood in animal models (77–79). Moreover, anti-VEGF could also decrease Treg accumulation due to a direct effect on VEGFR2 and an indirect effect on dendritic cells and MDSCs (70). In patients with colorectal cancer, treatment with chemotherapy and bevacizumab was shown to decrease Treg accumulation and proliferation [(70); **Figure 2**].

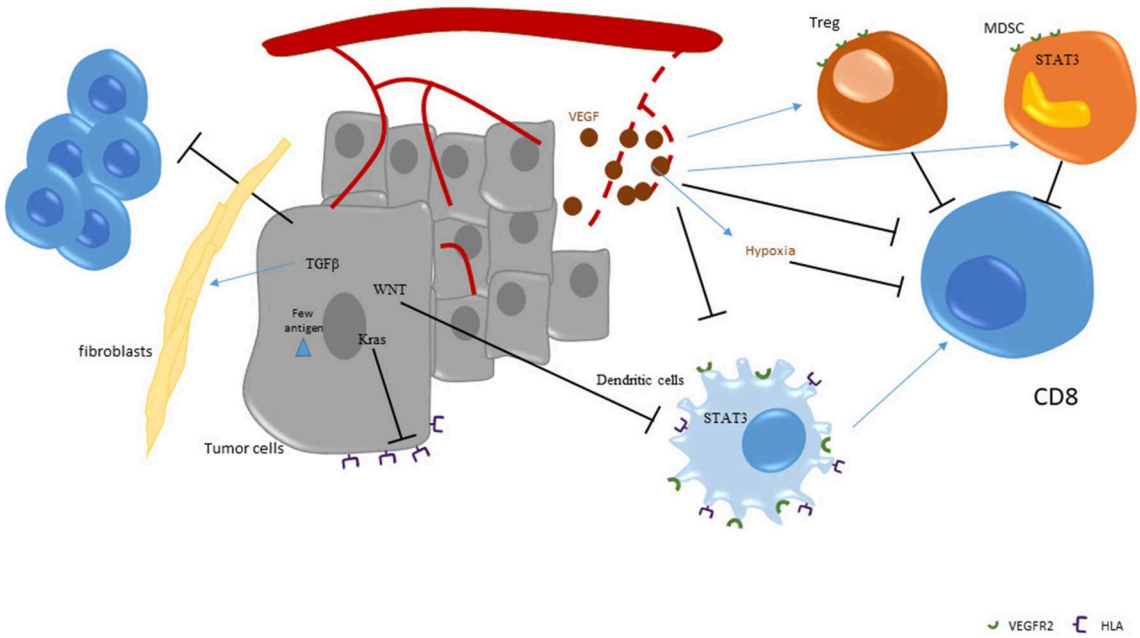

FIGURE 2 | Strategies of immunoescape in pMMR tumors.

HOPE, SUCCESS, AND FAILURE OF CURRENT CLINICAL TRIALS FOR PMMR COLORECTAL CANCER

First, clinical trials in patients with advanced disease show that monotherapy with anti PD-1 is not effective in pMMR colon cancer. The seminal report from Le et al. observed no RECIST objective response in pMMR patients. Nevertheless, two patients with stable disease were observed and a progression-free survival rate of 11% at 20 weeks was found (2 of 18 patients; 95% CI, 1–35) (8). Recently, Chen et al. (80), reported the efficacy of the combination of durvalumab and tremelimumab in heavily pretreated pMMR colorectal cancer in a randomized phase II study. One hundred and twenty patients were included. Patients in an immunotherapy group presented a median OS of 6.6 months vs. 4.1 months in the control arm (0.70; 90% CI (0.53–0.92); $p = 0.03$). In contrast, no difference was observed in terms of progression-free survival. Treatment toxicity was classical for such therapy. This trial suggests that anti-PD-L1 plus anti-CTLA4 combination therapy could have a modest effect in patients previously pretreated for colorectal cancer with a pMMR tumor.

Regorafenib, a potent inhibitor of angiogenic and oncogenic kinases, reduced TAM in tumor models. The combination of regorafenib plus a PD1 exhibited superior tumor growth suppression compared to either treatment alone in murine models. Consequently, a phase 1B study tested the combination of regorafinib and nivolumab in 25 pMMR previously-treated colorectal cancer patients. Regorafenib dose was reduced to 80 mg due to skin toxicities. Objective tumor response was observed in 7 pMMR colon cancer patients given 29% of response rate. The blood immunomonitoring showed a reduction of the FoxP3^{hi}CD45RA^{-}Tregs fraction at the tumor response (81) NCT03406871.

Chemotherapy could be used to promote immune response via a mechanism called immunogenic cell death (82). Oxaliplatin is known to induce this process. Cancer cells killed by oxaliplatin express calreticulin on the cell surface and release HMGB1, ATP, and Type I interferon. Calreticulin is recognized by dendritic cells which then phagocyte dead bodies. HMGB1 and ATP promote antigen presentation and activation of dendritic cells, resulting in optimal activation of CD8 T cells. Then Type I interferon induces an important recruitment of CD8 to the tumor bed (83). Our group showed that 5-fluorouracil could induce MDSC elimination (55, 84). Therefore, combination of oxaliplatin and 5-Fluorouracil could target both MDSC dependent immunosuppression and activation of effector T cells via immunogenic cell death. However, in preclinical models, FOLFOX regimen was also shown to induce PD-1 expression in CD8 T cells and PD-L1 expression in macrophage and myeloid cells, in a type II interferon dependent manner (85), suggesting that FOLFOX combination with an anti-PD-1 mAb (86) might be useful.

A phase II trial involving 30 patients tested the combination of FOLFOX with pembrolizumab in untreated, unresectable pMMR colorectal cancer. A total of 53% of patients had a RECIST

objective response at 24 weeks, with a disease control rate of 100% at 8 weeks (87). Survival data are awaited to determine if such combination is better than FOLFOX alone. Our group also initiated a trial, in first line pMMR patients with RAS mutated colorectal cancer, to test the combination of FOLFOX plus durvalumab and tremelimumab (88). This study is still ongoing.

As with chemotherapy, preclinical data support the capacity of radiotherapy to induce immunogenic cell death and promote activation of antitumoral immune response. However, the radiotherapy schedule may modulate its immune effect. Conventional or hypofractionated radiotherapy induces the release of DNA in the cytoplasm of cancer cells. Such cytoplasmic DNA is recognized by a DNA sensor, STING, which induces Type I IFN production. Without this Type I IFN production, no immune effect of radiotherapy or combination therapy with radiotherapy and checkpoint inhibitor could be observed (89, 90). Surprisingly, a high dose of hypofractionated radiotherapy induced exonuclease TREX1 expression. This exonuclease degrades cytoplasmic DNA and limits Type I IFN production. These data strongly support that the schedule of radiotherapy must be adapted to boost immune response.

In the setting of colorectal cancer, some small trials currently test the combination of checkpoint inhibitors and radiotherapy. A phase II, study test pembrolizumab plus radiotherapy vs. pembrolizumab and surgical ablation of metastases in patients with advanced, refractory pMMR CRC. One partial response in a total of 11 patients was observed in the radiotherapy plus immunotherapy group (91). Many clinical trials are ongoing with external radiotherapy or radioembolization of liver metastases (NCT03104439, NCT03007407, NCT03102047, NCT02837263, NCT03005002, NCT02888743).

Since VEGF has immunosuppressive functions, it can be hypothesized that the use of immunotherapy in combination with anti-VEGF therapies might be useful. Combination of atezolizumab with FOLFOX and bevacizumab was tested in first-line metastatic CRC. This treatment led to a 53% objective response and a median progression-free survival of 14.1 months (92). Survival data are awaited to determine if such combination is better than FOLFOX bevacizumab. Biological data show an induction of cytotoxic T cell signatures and PD-L1 expression as well as CD8+ T-cell accumulation. Based on these data, a maintenance trial called MODUL was initiated in patients with pMMR RAS mutated colorectal cancer. Fist line induction therapy with FOLFOX and bevacizumab was initiated, and if patients had a good response then they were randomized between capacitabine plus bevacizumab with or without atezolizumab maintenance regimen (93). No difference was observed in terms of progression-free survival and overall survival.

Mab targeting EGFR could promote antibody-dependent cytotoxicity and CD8 infiltration as well as antitumor immune response in colorectal cancer (94). Based on these results, association of cetuximab and pembrolizumab was tested in RAS wild-type pMMR colorectal cancer previously pretreated by chemotherapy. In the first treated patients, durable (>16 weeks) disease control was observed in 6/9 patients (95). Trials testing FOLFOX cetuximab plus avelumab in first line (NCT03174405) and nivolumab, ipilimumab with panitumumab in patients with metastatic, refractory, RAS wild-type, pMMR colon cancer (NCT03442569) are ongoing.

RATIONALE FOR NEW COMBINATION THERAPIES

New emerging therapies are currently in development. The first strategy targets the poor antigenicity of pMMR colorectal cancer. Vaccination represents a valuable strategy to artificially induce an antitumor immune response and enhance T cell recruitment to tumor bed. The classical strategy uses shared cancer antigens as tumor vaccines. Vaccines can use whole proteins, specific peptides or whole allogeneic cells. As an example, a vaccine called GVAX was developed for colorectal cancer. This vaccine consists of irradiated allogeneic colon cells modified to express granulocyte-macrophage colony-stimulating factor (GM-CSF). A trial currently tests this therapy with pembrolizumab for advanced pMMR tumors (NCT02981524). An alternative strategy is the usage of a personalized peptide vaccine. Next-generation sequencing on tumor tissue is performed to detect the specific neoantigen of patients' tumors. Then, specific peptides which bind to patient human leukocyte antigen (HLA) and coding for the neoantigen are synthetized. Trials are ongoing to test the combination of this strategy with checkpoint inhibitors (NCT03794128, NCT03480152).

Alternative strategies to enhance immunogenicity could rely on oncolytic vaccines. Such a virus could kill cancer cells and induce a local immune response. Multiple viral platforms are currently under evaluation. Recently, a phase II trial of FOLFOX plus bevacizumab with or without an oncolytic reovirus was performed in RAS mutated colon cancer. An increased response was observed with the virus, but with a shorter median duration of response. Decreased treatment intensity with standard agents occurred and may contributed to the lack of benefit of the virotherapy (96). To induce T cell recruitment, T cell bispecific antibodies could be another solution. An antibody which recognizes both CD3 and a surface tumor antigen induces T cell activation and forces them to detect and kill cancer cells. A drug called TCB-CEA was developed and targets the carcinoembryonic antigen (CEA), which is frequently expressed by colon cancer (97). Evidence of antitumor activity in advanced colorectal cancer was reported in a phase 1 trial which tested CEA-TCB plus atezolizumab (97). Increased intratumoral CD3 T cell infiltration was observed, but some major side effects such as cytokine storm were reported, which raised some caution on the development of this drug.

Another strategy relies on elimination of immunosuppressive cells or molecules. To target MDSC and immunosuppressive macrophages, some inhibitors of CSF1R are currently in development in combination with anti PD-1/PDL1 (i.e., NCT02777710, NCT02452424, NCT02829723, NCT02880371). Some other drugs targeting STAT3 (NCT02851004, NCT03647839) or Bruton's Kinase (NCT03332498) or CCR5 (NCT03631407, NCT03274804) are also in development with anti PD-1/PD-L1 to fight against immunosuppressive myeloid cells. Adenosine is also a major immunosuppressive

molecule produced by both MDSC and Tregs. This molecule is generated by CD73 and CD39 molecules which degrade extracellular ATP. Therefore, combination of CD39 or CD73 inhibitors with checkpoints to reduce immunosuppression might be relevant. Clinical trials with anti PD1/PDL1 and anti-CD73 or anti-adenosine receptor are ongoing (NCT02503774, NCT03207867, NCT03549000).

CONCLUSION AND FUTURE DIRECTIONS

pMMR tumors are complex for immunotherapy. Despite CD8 T cell infiltration and clear demonstration that CD8 infiltrates are associated with tumor outcome, anti-PD-1 monotherapy is ineffective. Mechanisms such as lack of antigen, RAS, WNT pathway activation and immunosuppression could explain this observation. Recent advances in the understanding of immune responses generated several hypotheses to overcome resistance to checkpoint inhibitors in this pathology. While some disappointing results were observed with MEK inhibitors and antiangiogenic agents, some promising results are observed with radiotherapy or chemotherapy in first line.

New strategies involving vaccination, bispecific mAbs, STAT3 inhibitors and drugs targeting immunosuppression are tested and will probably change the face of pMMR cancer treatments.

AUTHOR CONTRIBUTIONS

All authors listed have made a substantial, direct and intellectual contribution to the work, and approved it for publication.

REFERENCES

1. Fridman WH, Pagès F, Sautès-Fridman C, Galon J. The immune contexture in human tumours: impact on clinical outcome. *Nat Rev Cancer*. (2012) 12:298–306. doi: 10.1038/nrc3245
2. Pagès F, Berger A, Camus M, Sanchez-Cabo F, Costes A, Molidor R, et al. Effector memory T cells, early metastasis, and survival in colorectal cancer. *N Engl J Med*. (2005) 353:2654–66. doi: 10.1056/NEJMoa051424
3. Galon J, Costes A, Sanchez-Cabo F, Kirilovsky A, Mlecnik B, Lagorce-Pagès C, et al. Type, density, and location of immune cells within human colorectal tumors predict clinical outcome. *Science*. (2006) 313:1960–4. doi: 10.1126/science.1129139
4. Galon J, Angell HK, Bedognetti D, Marincola FM. The continuum of cancer immunosurveillance: prognostic, predictive, and mechanistic signatures. *Immunity*. (2013) 39:11–26. doi: 10.1016/j.immuni.2013.07.008
5. Brahmer JR, Drake CG, Wollner I, Powderly JD, Picus J, Sharfman WH, et al. Phase I study of single-agent anti-programmed death-1 (MDX-1106) in refractory solid tumors: safety, clinical activity, pharmacodynamics, and immunologic correlates. *J Clin Oncol*. (2010) 28:3167–75. doi: 10.1200/JCO.2009.26.7609
6. Topalian SL, Hodi FS, Brahmer JR, Gettinger SN, Smith DC, McDermott DF, et al. Safety, activity, and immune correlates of anti-PD-1 antibody in cancer. *N Engl J Med*. (2012) 366:2443–54. doi: 10.1056/NEJMoa1200690
7. Fabrizio DA, George TJ, Dunne RF, Frampton G, Sun J, Gowen K, et al. Beyond microsatellite testing: assessment of tumor mutational burden identifies subsets of colorectal cancer who may respond to immune checkpoint inhibition. *J Gastrointest Oncol*. (2018) 9:610–7. doi: 10.21037/jgo.2018.05.06
8. Le DT, Uram JN, Wang H, Bartlett BR, Kemberling H, Eyring AD, et al. PD-1 blockade in tumors with mismatch-repair deficiency. *N Engl J Med*. (2015) 372:2509–20. doi: 10.1056/NEJMoa1500596
9. Smyrk TC, Watson P, Kaul K, Lynch HT. Tumor-infiltrating lymphocytes are a marker for microsatellite instability in colorectal carcinoma. *Cancer*. (2001) 91:2417–22. doi: 10.1002/1097-0142(20010615)91:12<2417::AID-CNCR1276>3.0.CO;2-U
10. Ogino S, Nosho K, Kirkner GJ, Kawasaki T, Meyerhardt JA, Loda M, et al. CpG island methylator phenotype, microsatellite instability, BRAF mutation and clinical outcome in colon cancer. *Gut*. (2009) 58:90–6. doi: 10.1136/gut.2008.155473
11. Germano G, Lamba S, Rospo G, Barault L, Magrì A, Maione F, et al. Inactivation of DNA repair triggers neoantigen generation and impairs tumour growth. *Nature*. (2017) 552:116–20. doi: 10.1038/nature24673
12. Llosa NJ, Cruise M, Tam A, Wicks EC, Hechenbleikner EM, Taube JM, et al. The vigorous immune microenvironment of microsatellite instable colon cancer is balanced by multiple counter-inhibitory checkpoints. *Cancer Discov*. (2015) 5:43–51. doi: 10.1158/2159-8290.CD-14-0863
13. Fehlings M, Simoni Y, Penny HL, Becht E, Loh CY, Gubin MM, et al. Checkpoint blockade immunotherapy reshapes the high-dimensional phenotypic heterogeneity of murine intratumoural neoantigen-specific CD8+ T cells. *Nat Commun*. (2017) 8:562. doi: 10.1038/s41467-017-00627-z
14. Gubin MM, Zhang X, Schuster H, Caron E, Ward JP, Noguchi T, et al. Checkpoint blockade cancer immunotherapy targets tumour-specific mutant antigens. *Nature*. (2014) 515:577–81. doi: 10.1038/nature13988
15. Marisa L, Svrcek M, Collura A, Becht E, Cervera P, Wanherdrick K, et al. The balance between cytotoxic T-cell lymphocytes and immune checkpoint expression in the prognosis of colon tumors. *JNCI J Natl Cancer Inst*. (2018) 110:68–77. doi: 10.1093/jnci/djx136
16. Wherry EJ, Kurachi M. Molecular and cellular insights into T cell exhaustion. *Nat Rev Immunol*. (2015) 15:486–99. doi: 10.1038/nri3862
17. Kim ST, Klempner SJ, Park SH, Park JO, Park YS, Lim HY, et al. Correlating programmed death ligand 1 (PD-L1) expression, mismatch repair deficiency, and outcomes across tumor types: implications for immunotherapy. *Oncotarget*. (2017) 8:77415–23. doi: 10.18632/oncotarget.20492
18. Pagès F, Mlecnik B, Marliot F, Bindea G, Ou FS, Bifulco C, et al. International validation of the consensus immunoscore for the classification of colon cancer: a prognostic and accuracy study. *Lancet*. (2018) 391:2128–39. doi: 10.1016/S0140-6736(18)30789-X
19. Yoon HH, Shi Q, Heying EN, Muranyi A, Bredno J, Ough F, et al. Intertumoral heterogeneity of CD3+ and CD8+ T-cell densities in the microenvironment of DNA mismatch-repair-deficient colon cancers: implications for prognosis. *Clin Cancer Res*. (2019) 25:125–33. doi: 10.1158/1078-0432.CCR-18-1984
20. Owyang SY, Zhang M, Walkup GA, Chen GE, Grasberger H, El-Zaatari M, et al. The effect of CT26 tumor-derived TGF-β on the balance of tumor growth and immunity. *Immunol Lett*. (2017) 191:47–54. doi: 10.1016/j.imlet.2017.08.024
21. Calon A, Lonardo E, Berenguer-Llergo A, Espinet E, Hernando-Momblona X, Iglesias M, et al. Stromal gene expression defines poor-prognosis subtypes in colorectal cancer. *Nat Genet*. (2015) 47:320–9. doi: 10.1038/ng.3225
22. Tauriello DVF, Palomo-Ponce S, Stork D, Berenguer-Llergo A, Badia-Ramentol J, Iglesias M, et al. TGFβ drives immune evasion in genetically reconstituted colon cancer metastasis. *Nature*. (2018) 554:538–43. doi: 10.1038/nature25492
23. Knudson KM, Hicks KC, Luo X, Chen JQ, Schlom J, Gameiro SR. M7824, a novel bifunctional anti-PD-L1/TGFβ Trap fusion protein, promotes anti-tumor efficacy as monotherapy and in combination with vaccine. *Oncoimmunology*. (2018) 7:e1426519. doi: 10.1080/2162402X.2018.1426519
24. Panarelli NC, Vaughn CP, Samowitz WS, Yantiss RK. Sporadic microsatellite instability-high colon cancers rarely display immunohistochemical evidence of Wnt signaling activation. *Am J Surg Pathol*. (2015) 39:313–7. doi: 10.1097/PAS.0000000000000380
25. Spranger S, Bao R, Gajewski TF. Melanoma-intrinsic β-catenin signalling prevents anti-tumour immunity. *Nature*. (2015) 523:231–5. doi: 10.1038/nature14404

26. Spranger S, Dai D, Horton B, Gajewski TF. Tumor-residing Batf3 dendritic cells are required for effector T cell trafficking and adoptive T cell therapy. *Cancer Cell.* (2017) 31:711–723.e4. doi: 10.1016/j.ccell.2017.04.003
27. Luke JJ, Bao R, Sweis RF, Spranger S, Gajewski TF. WNT/β-catenin pathway activation correlates with immune exclusion across human cancers. *Clin Cancer Res.* (2019) 25:3074–83. doi: 10.1158/1078-0432.CCR-18-1942
28. Krishnamurthy N, Kurzrock R. Targeting the Wnt/beta-catenin pathway in cancer: update on effectors and inhibitors. *Cancer Treat Rev.* (2018) 62:50–60. doi: 10.1016/j.ctrv.2017.11.002
29. Yarchoan M, Hopkins A, Jaffee EM. Tumor mutational burden and response rate to PD-1 inhibition. *N Engl J Med.* (2017) 377:2500–1. doi: 10.1056/NEJMc1713444
30. Chalmers ZR, Connelly CF, Fabrizio D, Gay L, Ali SM, Ennis R, et al. Analysis of 100,000 human cancer genomes reveals the landscape of tumor mutational burden. *Genome Med.* (2017) 9:34. doi: 10.1186/s13073-017-0424-2
31. Liu XS, Mardis ER. Applications of immunogenomics to cancer. *Cell.* (2017) 168:600–12. doi: 10.1016/j.cell.2017.01.014
32. Scheper W, Kelderman S, Fanchi LF, Linnemann C, Bendle G, de Rooij MAJ, et al. Low and variable tumor reactivity of the intratumoral TCR repertoire in human cancers. *Nat Med.* (2019) 25:89–94. doi: 10.1038/s41591-018-0266-5
33. Grimaldi AM, Simeone E, Ascierto PA. The role of MEK inhibitors in the treatment of metastatic melanoma. *Curr Opin Oncol.* (2014) 26:196–203. doi: 10.1097/CCO.0000000000000050
34. Larkin J, Ascierto PA, Dréno B, Atkinson V, Liszkay G, Maio M, et al. Combined vemurafenib and cobimetinib in *BRAF* -mutated melanoma. *N Engl J Med.* (2014) 371:1867–76. doi: 10.1056/NEJMoa1408868
35. Hu-Lieskovan S, Mok S, Homet Moreno B, Tsoi J, Robert L, Goedert L, et al. Improved antitumor activity of immunotherapy with BRAF and MEK inhibitors in *BRAF* ^{V600E} melanoma. *Sci Transl Med.* (2015) 7:279ra41. doi: 10.1126/scitranslmed.aaa4691
36. Ledys F, Klopfenstein Q, Truntzer C, Arnould L, Vincent J, Bengrine L, et al. RAS status and neoadjuvant chemotherapy impact CD8+ cells and tumor HLA class I expression in liver metastatic colorectal cancer. *J Immunother Cancer.* (2018) 6:123. doi: 10.1186/s40425-018-0438-3
37. Loi S, Dushyanthen S, Beavis PA, Salgado R, Denkert C, Savas P, et al. RAS/MAPK activation is associated with reduced tumor-infiltrating lymphocytes in triple-negative breast cancer: therapeutic cooperation between MEK and PD-1/PD-L1 immune checkpoint inhibitors. *Clin Cancer Res.* (2016) 22:1499–509. doi: 10.1158/1078-0432.CCR-15-1125
38. Hermel DJ, Ott PA. Combining forces: the promise and peril of synergistic immune checkpoint blockade and targeted therapy in metastatic melanoma. *Cancer Metastasis Rev.* (2017) 36:43–50. doi: 10.1007/s10555-017-9656-2
39. Ebert PJR, Cheung J, Yang Y, McNamara E, Hong R, Moskalenko M, et al. MAP kinase inhibition promotes T cell and anti-tumor activity in combination with PD-L1 checkpoint blockade. *Immunity.* (2016) 44:609–21. doi: 10.1016/j.immuni.2016.01.024
40. Bendell JC, Bang Y-J, Chee CE, Ryan DP, McRee AJ, Chow LQ, et al. A phase Ib study of safety and clinical activity of atezolizumab (A) and cobimetinib (C) in patients (pts) with metastatic colorectal cancer (mCRC). *J Clin Oncol.* (2018) 36:560. doi: 10.1200/JCO.2018.36.4_suppl.560
41. Bendell J, Ciardiello F, Tabernero J, Tebbutt N, Eng C, Di Bartolomeo M, et al. LBA-004Efficacy and safety results from IMblaze370, a randomised Phase III study comparing atezolizumab+cobimetinib and atezolizumab monotherapy vs regorafenib in chemotherapy-refractory metastatic colorectal cancer. *Ann Oncol.* (2018) 29:mdy208.003. doi: 10.1093/annonc/mdy208.003
42. Nishikawa H, Sakaguchi S. Regulatory T cells in cancer immunotherapy. *Curr Opin Immunol.* (2014) 27:1–7. doi: 10.1016/j.coi.2013.12.005
43. Curiel TJ, Coukos G, Zou L, Alvarez X, Cheng P, Mottram P, et al. Specific recruitment of regulatory T cells in ovarian carcinoma fosters immune privilege and predicts reduced survival. *Nat Med.* (2004) 10:942–9. doi: 10.1038/nm1093
44. Sato E, Olson SH, Ahn J, Bundy B, Nishikawa H, Qian F, et al. Intraepithelial CD8+ tumor-infiltrating lymphocytes and a high CD8+/regulatory T cell ratio are associated with favorable prognosis in ovarian cancer. *Proc Natl Acad Sci USA.* (2005) 102:18538–43. doi: 10.1073/pnas.0509182102
45. deLeeuw RJ, Kost SE, Kakal JA, Nelson BH. The prognostic value of FoxP3+ tumor-infiltrating lymphocytes in cancer: a critical review of the literature. *Clin Cancer Res.* (2012) 18:3022–9. doi: 10.1158/1078-0432.CCR-11-3216
46. Sinicrope FA, Rego RL, Ansell SM, Knutson KL, Foster NR, Sargent DJ. Intraepithelial effector (CD3+)/regulatory (FoxP3+) T-cell ratio predicts a clinical outcome of human colon carcinoma. *Gastroenterology.* (2009) 137:1270–9. doi: 10.1053/j.gastro.2009.06.053
47. Salama P, Phillips M, Grieu F, Morris M, Zeps N, Joseph D, et al. Tumor-infiltrating FOXP3 $^{+}$ T regulatory cells show strong prognostic significance in colorectal cancer. *J Clin Oncol.* (2009) 27:186–92. doi: 10.1200/JCO.2008.18.7229
48. Frey DM, Droeser RA, Viehl CT, Zlobec I, Lugli A, Zingg U, et al. High frequency of tumor-infiltrating FOXP3 $^{+}$ regulatory T cells predicts improved survival in mismatch repair-proficient colorectal cancer patients. *Int J Cancer.* (2010) 126:2635–43. doi: 10.1002/ijc.24989
49. Becht E, de Reyniès A, Giraldo NA, Pilati C, Buttard B, Lacroix L, et al. Immune and stromal classification of colorectal cancer is associated with molecular subtypes and relevant for precision immunotherapy. *Clin Cancer Res.* (2016) 22:4057–66. doi: 10.1158/1078-0432.CCR-15-2879
50. Saito T, Nishikawa H, Wada H, Nagano Y, Sugiyama D, Atarashi K, et al. Two FOXP3+CD4+ T cell subpopulations distinctly control the prognosis of colorectal cancers. *Nat Med.* (2016) 22:679–84. doi: 10.1038/nm.4086
51. Hamada T, Zhang X, Mima K, Bullman S, Sukawa Y, Nowak JA, et al. *Fusobacterium nucleatum* in colorectal cancer relates to immune response differentially by tumor microsatellite instability status. *Cancer Immunol Res.* (2018) 6:1327–36. doi: 10.1158/2326-6066.CIR-18-0174
52. Apetoh L, Végran F, Ladoire S, Ghiringhelli F. Restoration of antitumor immunity through selective inhibition of myeloid derived suppressor cells by anticancer therapies. *Curr Mol Med.* (2011) 11:365–72. doi: 10.2174/156652411795976574
53. Marvel D, Gabrilovich DI. Myeloid-derived suppressor cells in the tumor microenvironment: expect the unexpected. *J Clin Invest.* (2015) 125:3356–64. doi: 10.1172/JCI80005
54. Limagne E, Euvrard R, Thibaudin M, Rébé C, Derangère V, Chevriaux A, et al. Accumulation of MDSC and Th17 cells in patients with metastatic colorectal cancer predicts the efficacy of a FOLFOX-bevacizumab drug treatment regimen. *Cancer Res.* (2016) 76:5241–52. doi: 10.1158/0008-5472.CAN-15-3164
55. Vincent J, Mignot G, Chalmin F, Ladoire S, Bruchard M, Chevriaux A, et al. 5-Fluorouracil selectively kills tumor-associated myeloid-derived suppressor cells resulting in enhanced T cell-dependent antitumor immunity. *Cancer Res.* (2010) 70:3052–61. doi: 10.1158/0008-5472.CAN-09-3690
56. Takahashi Y, Kitadai Y, Bucana CD, Cleary KR, Ellis LM. Expression of vascular endothelial growth factor and its receptor, KDR, correlates with vascularity, metastasis, and proliferation of human colon cancer. *Cancer Res.* (1995) 55:3964–8.
57. Warren RS, Yuan H, Matli MR, Gillett NA, Ferrara N. Regulation by vascular endothelial growth factor of human colon cancer tumorigenesis in a mouse model of experimental liver metastasis. *J Clin Invest.* (1995) 95:1789–97. doi: 10.1172/JCI117857
58. Tokunaga T, Oshika Y, Abe Y, Ozeki Y, Sadahiro S, Kijima H, et al. Vascular endothelial growth factor (VEGF) mRNA isoform expression pattern is correlated with liver metastasis and poor prognosis in colon cancer. *Br J Cancer.* (1998) 77:998–1002. doi: 10.1038/bjc.1998.164
59. Samamé Pérez-Vargas JC, Biondani P, Maggi C, Gariboldi M, Gloghini A, Inno A, et al. Role of cMET in the development and progression of colorectal cancer. *Int J Mol Sci.* (2013) 14:18056–77. doi: 10.3390/ijms140918056
60. Goon PK, Lip GY, Boos CJ, Stonelake PS, Blann AD. Circulating endothelial cells, endothelial progenitor cells, and endothelial microparticles in cancer. *Neoplasia.* (2006) 8:79–88. doi: 10.1593/neo.05592
61. De Smedt L, Lemahieu J, Palmans S, Govaere O, Tousseyn T, Van Cutsem E, et al. Microsatellite instable vs. stable colon carcinomas: analysis of tumour heterogeneity, inflammation and angiogenesis. *Br J Cancer.* (2015) 113:500–9. doi: 10.1038/bjc.2015.213
62. Otto W, Macrae F, Sierdzinski J, Smaga J, Król M, Wilinska E, et al. Microsatellite instability and manifestations of angiogenesis in stage IV of sporadic colorectal carcinoma. *Medicine.* (2019) 98:e13956. doi: 10.1097/MD.0000000000013956

63. Gabrilovich D, Ishida T, Oyama T, Ran S, Kravtsov V, Nadaf S, et al. Vascular endothelial growth factor inhibits the development of dendritic cells and dramatically affects the differentiation of multiple hematopoietic lineages *in vivo*. *Blood*. (1998) 92:4150–66.
64. Almand B, Clark JI, Nikitina E, van Beynen J, English NR, Knight SC, et al. Increased production of immature myeloid cells in cancer patients: a mechanism of immunosuppression in cancer. *J Immunol*. (2001) 166:678–89. doi: 10.4049/jimmunol.166.1.678
65. Almand B, Resser JR, Lindman B, Nadaf S, Clark JI, Kwon ED, et al. Clinical significance of defective dendritic cell differentiation in cancer. *Clin Cancer Res*. (2000) 6:1755–66.
66. Huang B, Pan PY, Li Q, Sato AI, Levy DE, Bromberg J, et al. Gr-1+CD115+ immature myeloid suppressor cells mediate the development of tumor-induced T regulatory cells and T-cell anergy in tumor-bearing host. *Cancer Res*. (2006) 66:1123–31. doi: 10.1158/0008-5472.CAN-05-1299
67. Nefedova Y, Huang M, Kusmartsev S, Bhattacharya R, Cheng P, Salup R, et al. Hyperactivation of STAT3 is involved in abnormal differentiation of dendritic cells in cancer. *J Immunol*. (2004) 172:464–74. doi: 10.4049/jimmunol.172.1.464
68. Yang R, Cai Z, Zhang Y, Yutzy WH, Roby KF, Roden RB. CD80 in immune suppression by mouse ovarian carcinoma–associated Gr-1 $^{+}$ CD11b $^{+}$ myeloid cells. *Cancer Res*. (2006) 66:6807–15. doi: 10.1158/0008-5472.CAN-05-3755
69. Ghiringhelli F, Puig PE, Roux S, Parcellier A, Schmitt E, Solary E, et al. Tumor cells convert immature myeloid dendritic cells into TGF-β-secreting cells inducing CD4 $^{+}$ CD25 $^{+}$ regulatory T cell proliferation. *J Exp Med*. (2005) 202:919–29. doi: 10.1084/jem.20050463
70. Terme M, Pernot S, Marcheteau E, Sandoval F, Benhamouda N, Colussi O, et al. VEGFA-VEGFR pathway blockade inhibits tumor-induced regulatory T-cell proliferation in colorectal cancer. *Cancer Res*. (2013) 73:539–49. doi: 10.1158/0008-5472.CAN-12-2325
71. Hanada T, Nakagawa M, Emoto A, Nomura T, Nasu N, Nomura Y. Prognostic value of tumor-associated macrophage count in human bladder cancer. *Int J Urol*. (2000) 7:263–9. doi: 10.1046/j.1442-2042.2000.00190.x
72. Lissbrant IF, Stattin P, Wikstrom P, Damber JE, Egevad L, Bergh A. Tumor associated macrophages in human prostate cancer: relation to clinicopathological variables and survival. *Int J Oncol*. (2000) 17:445–51. doi: 10.3892/ijo.17.3.445
73. Salvesen HB, Akslen LA. Significance of tumour-associated macrophages, vascular endothelial growth factor and thrombospondin-1 expression for tumour angiogenesis and prognosis in endometrial carcinomas. *Int J Cancer*. (1999) 84:538–43. doi: 10.1002/(SICI)1097-0215(19991022)84:5<538::AID-IJC17>3.3.CO;2-2
74. Leek RD, Lewis CE, Whitehouse R, Greenall M, Clarke J, Harris AL. Association of macrophage infiltration with angiogenesis and prognosis in invasive breast carcinoma. *Cancer Res*. (1996) 56:4625–9.
75. Noman MZ, Buart S, Van Pelt J, Richon C, Hasmim M, Leleu N, et al. The cooperative induction of hypoxia-inducible factor-1 and STAT3 during hypoxia induced an impairment of tumor susceptibility to CTL-mediated cell lysis. *J Immunol*. (2009) 182:3510–21. doi: 10.4049/jimmunol.0800854
76. Gabrilovich DI, Ishida T, Nadaf S, Ohm JE, Carbone DP. Antibodies to vascular endothelial growth factor enhance the efficacy of cancer immunotherapy by improving endogenous dendritic cell function. *Clin Cancer Res*. (1999) 5:2963–70.
77. Kusmartsev S, Eruslanov E, Kübler H, Tseng T, Sakai Y, Su Z, et al. Oxidative stress regulates expression of VEGFR1 in myeloid cells: link to tumor-induced immune suppression in renal cell carcinoma. *J Immunol*. (2008) 181:346–53. doi: 10.4049/jimmunol.181.1.346
78. Ozao-Choy J, Ma G, Kao J, Wang GX, Meseck M, Sung M, et al. The novel role of tyrosine kinase inhibitor in the reversal of immune suppression and modulation of tumor microenvironment for immune-based cancer therapies. *Cancer Res*. (2009) 69:2514–22. doi: 10.1158/0008-5472.CAN-08-4709
79. Xin H, Zhang C, Herrmann A, Du Y, Figlin R, Yu H. Sunitinib inhibition of Stat3 induces renal cell carcinoma tumor cell apoptosis and reduces immunosuppressive cells. *Cancer Res*. (2009) 69:2506–13. doi: 10.1158/0008-5472.CAN-08-4323
80. Chen EX, Jonker D, Kennecke HF, Berry SR, Couture F, Ahmad CE, et al. CCTG CO.26 trial: a phase II randomized study of durvalumab (D) plus tremelimumab (T) and best supportive care (BSC) versus BSC alone in patients (pts) with advanced refractory colorectal carcinoma (rCRC). *J Clin Oncol*. (2019) 37:481. doi: 10.1200/JCO.2019.37.4_suppl.481
81. Yarchoan M, Johnson BA, Lutz ER, Laheru DA, Jaffee EM. Targeting neoantigens to augment antitumour immunity. *Nat Rev Cancer*. (2017) 17:209–22. doi: 10.1038/nrc.2016.154
82. Pfirschke C, Engblom C, Rickelt S, Cortez-Retamozo V, Garris C, Pucci F, et al. Immunogenic chemotherapy sensitizes tumors to checkpoint blockade therapy. *Immunity*. (2016) 44:343–54. doi: 10.1016/j.immuni.2015.11.024
83. Galluzzi L, Buqué A, Kepp O, Zitvogel L, Kroemer G. Immunogenic cell death in cancer and infectious disease. *Nat Rev Immunol*. (2017) 17:97–111. doi: 10.1038/nri.2016.107
84. Bruchard M, Mignot G, Derangère V, Chalmin F, Chevriaux A, Végran F, et al. Chemotherapy-triggered cathepsin B release in myeloid-derived suppressor cells activates the Nlrp3 inflammasome and promotes tumor growth. *Nat Med*. (2013) 19:57–64. doi: 10.1038/nm.2999
85. Dosset M, Vargas TR, Lagrange A, Boidot R, Végran F, Roussey A, et al. PD-1/PD-L1 pathway: an adaptive immune resistance mechanism to immunogenic chemotherapy in colorectal cancer. *Oncoimmunology*. (2018) 7:e1433981. doi: 10.1080/2162402X.2018.1433981
86. Liu WM, Fowler DW, Smith P, Dalgleish AG. Pre-treatment with chemotherapy can enhance the antigenicity and immunogenicity of tumours by promoting adaptive immune responses. *Br J Cancer*. (2010) 102:115–23. doi: 10.1038/sj.bjc.6605465
87. Shahda S, Noonan AM, Bekaii-Saab TS, O'Neil BH, Sehdev A, Shaib WL, et al. A phase II study of pembrolizumab in combination with mFOLFOX6 for patients with advanced colorectal cancer. *J Clin Oncol*. (2017) 35:3541. doi: 10.1200/JCO.2017.35.15_suppl.3541
88. Fumet JD, Isambert N, Hervieu A, Zanetta S, Guion JF, Hennequin A, et al. Phase Ib/II trial evaluating the safety, tolerability and immunological activity of durvalumab (MEDI4736) (anti-PD-L1) plus tremelimumab (anti-CTLA-4) combined with FOLFOX in patients with metastatic colorectal cancer. *ESMO Open*. (2018) 3:e000375. doi: 10.1136/esmoopen-2018-000375
89. Vanpouille-Box C, Demaria S, Formenti SC, Galluzzi L. Cytosolic DNA Sensing in Organismal Tumor Control. *Cancer Cell*. (2018) 34:361–378. doi: 10.1016/j.ccell.2018.05.013
90. Vanpouille-Box C, Alard A, Aryankalayil MJ, Sarfraz Y, Diamond JM, Schneider RJ, et al. DNA exonuclease Trex1 regulates radiotherapy-induced tumour immunogenicity. *Nat Commun*. (2017) 8:15618. doi: 10.1038/ncomms15618
91. Segal NH, Kemeny NE, Cercek A, Reidy DL, Raasch PJ, Warren P, et al. Non-randomized phase II study to assess the efficacy of pembrolizumab (Pem) plus radiotherapy (RT) or ablation in mismatch repair proficient (pMMR) metastatic colorectal cancer (mCRC) patients. *J Clin Oncol*. (2016) 34:3539. doi: 10.1200/JCO.2016.34.15_suppl.3539
92. Wallin J, Pishvaian MJ, Hernandez G, Yadav M, Jhunjhunwala S, Delamarre L, et al. Abstract 2651: clinical activity and immune correlates from a phase Ib study evaluating atezolizumab (anti-PDL1) in combination with FOLFOX and bevacizumab (anti-VEGF) in metastatic colorectal carcinoma. *Cancer Res*. (2016) 76:2651. doi: 10.1158/1538-7445.AM2016-2651
93. Arnold D, Schmoll H-J, de Gramont A, Ducreux M, Grothey A, O'Dwyer P, et al. LBA-10 * MODUL - a multicentre randomised clinical trial of biomarker-driven therapy for the 1st-line maintenance treatment of metastatic colorectal cancer (mCRC): a highly adaptable signal-seeking approach. *Ann Oncol*. (2015) 26:iv121. doi: 10.1093/annonc/mdv262.10
94. MacDonald F, Zaiss DMW. The immune system's contribution to the clinical efficacy of EGFR antagonist treatment. *Front Pharmacol*. (2017) 8:575. doi: 10.3389/fphar.2017.00575
95. Boland PM, Hutson AD, Maguire O, Minderman H, Fountzilas C, Iyer RV. A phase Ib/II study of cetuximab and pembrolizumab in RAS-wt mCRC. *J Clin Oncol*. (2018) 36:834. doi: 10.1200/JCO.2018.36.4_suppl.834

96. Jonker DJ, Tang PA, Kennecke H, Welch SA, Cripps MC, Asmis T, et al. A randomized phase II study of FOLFOX6/bevacizumab with or without pelareorep in patients with metastatic colorectal cancer: IND.210, a Canadian cancer trials group trial. *Clin Colorectal Cancer.* (2018) 17:231–239.e7. doi: 10.1016/j.clcc.2018.03.001
97. Argilés G, Saro J, Segal NH, Melero I, Ros W, Marabelle A, et al. LBA-004Novel carcinoembryonic antigen T-cell bispecific (CEA-TCB) antibody: preliminary clinical data as a single agent and in combination with atezolizumab in patients with metastatic colorectal cancer (mCRC). *Ann Oncol.* (2017) 28:mdx302.003. doi: 10.1093/annonc/mdx302.003

Conflict of Interest Statement: The authors declare that the research was conducted in the absence of any commercial or financial relationships that could be construed as a potential conflict of interest.

frontiers in Oncology

ORIGINAL RESEARCH
published: 10 December 2019
doi: 10.3389/fonc.2019.01401

Interleukin-24 Regulates T Cell Activity in Patients With Colorectal Adenocarcinoma

Yang Zhang[1], *Ye Liu*[2] *and Yuechao Xu*[1]*

[1] Department of Gastrointestinal Surgery, The First Hospital of Jilin University, Changchun, China, [2] Intensive Care Unit, 964th Hospital of PLA, Changchun, China

Interleukin (IL)-24 plays a potential anti-tumor activity in colorectal cancer in a dose-dependent manner. However, the immunoregulatory role of IL-24 to peripheral and tumor-infiltrating T cell function in colorectal cancer was not fully elucidated. In this study, twenty-nine colorectal adenocarcinoma patients and fifteen healthy individuals were enrolled. IL-24 expression and IL-24 receptor (IL-20R1, IL-20R2, and IL-22R1) mRNA relative level was measured by ELISA and real-time PCR, respectively. $CD4^+$ and $CD8^+$ T cells were purified from peripheral bloods and cancer specimens, and were stimulated with low (10 ng/ml) and high (100 ng/ml) concentration of recombinant IL-24. $CD4^+$ T cells activity was assessed by measurement of Th cell percentage, transcriptional factors, and cytokine production. $CD8^+$ T cells activity was evaluated by investigation of cytotoxic molecules, target cell death, and interferon-γ (IFN-γ) secretion. IL-24 was decreasingly expressed in both peripheral bloods and cancer tissues in colorectal adenocarcinoma patients. However, IL-20R1 and IL-20R2 was comparable between healthy controls and colorectal adenocarcinoma patients. Low concentration of IL-24 suppressed $CD4^+$ T cell proliferation. In contrast, high concentration of IL-24 not only promoted $CD4^+$ T cell proliferation, but also enhanced $CD4^+$ T cell activity, which mainly presented as up-regulation of Th1/Th17 frequency, T-bet/RORγt mRNA, and IFN-γ/IL-17 production but down-regulation of Treg percentage, FoxP3 mRNA, and IL-10/IL-35 secretion. Moreover, high concentration of IL-24 also increased perforin and granzyme B expression in $CD8^+$ T cells, and elevated cytolytic and non-cytolytic activity of $CD8^+$ T cells, which presented as induction of target cell death and elevation of IFN-γ expression. However, low concentration of IL-24 did not affect bioactivity of $CD8^+$ T cells. The current data indicated that IL-24 might regulate T cell function in a dose-dependent manner. High-concentration of IL-24 might promote anti-tumor immune responses in development novel therapeutic approaches to colorectal adenocarcinoma.

Keywords: colorectal cancer, interleukin-24, T lymphocytes, immunoregulation, anti-tumor

OPEN ACCESS

Edited by:
Maria L. Martinez Chantar, CIC bioGUNE, Spain

Reviewed by:
Amedeo Amedei, University of Florence, Italy
*Kia Joo Puan, Singapore Immunology Network (A*STAR), Singapore*

***Correspondence:**
Yuechao Xu
forever981024@vip.qq.com; forever981024@tom.com

Specialty section:
This article was submitted to Cancer Immunity and Immunotherapy, a section of the journal Frontiers in Oncology

Received: *06 August 2019*
Accepted: *27 November 2019*
Published: *10 December 2019*

Citation:
Zhang Y, Liu Y and Xu Y (2019) Interleukin-24 Regulates T Cell Activity in Patients With Colorectal Adenocarcinoma. Front. Oncol. 9:1401. doi: 10.3389/fonc.2019.01401

INTRODUCTION

Colorectal cancer is the third most commonly diagnosed malignancy and the fourth leading cause of tumor-related death all over the world, accounting for ∼1.4 million newly diagnosed cases and almost 0.7 million deaths annually (1–3). Although colorectal cancer incidence and mortality rates have been stabilizing or declining in a number of high human development index countries, the rapid increases in incidence and mortality of colorectal cancer are observed in medium or low income countries (4) and in patients <40 years old (5, 6). Moreover, most cases of colorectal cancer develop slowly over several years through adenocarcinoma sequence despite strong hereditary components (7). The therapeutic approaches for colorectal cancer are surgery, neoadjuvant radiotherapy (for rectal cancer), and adjuvant chemotherapy (for stage III/IV and high-risk stage II colon cancer) (7). However, the 5-year survival rate for colorectal cancer patients ranges from more than 90% in stage I patients to slightly higher than 10% in stage IV patients (8). Thus, it is pivotal to better understand the biological and immunological mechanism for colorectal cancer progression and clinical relevant insights for management of the disease.

Interleukin (IL)-24, which is also called melanoma differentiation associated gene-7, is a IL-20 cytokine family member and is expressed primarily in T cells and marcophages (9, 10). IL-24 receptor belongs to type II cytokine receptor family, and consists of two heterodimeric receptor complexes, IL-20R1/IL-20R2 and IL-22R1/IL-20R2 (11). IL-24 is a potential anti-tumor agent and affects a broad array of cancers, which selectively inhibits tumor cell growth, invasion, metastasis, and angiogensis, induces cancer-selective apoptosis, stimulates anti-cancer immune response, sensitizes cancer call to therapies (12, 13). Importantly, IL-24 is a dose-dependent cytokine, and different concentrations of IL-24 may present completely contrary bioactivity. Low concentration of IL-24 promotes inflammatory cytokine expression, leading to the proinflammatory response. In contrast, high concentration of IL-24 strongly induces apoptosis of cancer cells (12, 14). IL-24 expression was remarkably correlated with histological differentiation, but inversely correlated with the degree of lymph node involvement in rectal cancer (15), which played an important anti-tumor role for colon cancer therapy (16, 17) and even reversed multidrug resistance to chemotherapy in human colorectal cancer cells (18). However, few studies focused on the regulatory activity of IL-24 to immune cell function in colorectal cancers. Thus, we hypothesized that IL-24 also modulates $CD4^+$ and $CD8^+$ T cell activity in colorectal adenocarcinoma patients in a dose-dependent manner. To test this possibility, the effects of different concentrations of recombinant IL-24 stimulation on $CD4^+$ and $CD8^+$ T cells from colorectal adenocarcinoma patients were investigated in cell culture system *in vitro*.

MATERIALS AND METHODS

Enrolled Subjects

The current study protocol was approved by the Ethics Committee of The First Hospital of Jilin University, and written consent form was obtained from each enrolled subjects. A total of 24 colorectal adenocarcinoma patients, who were hospitalized and underwent surgery between July 2107 and December 2018 in Department of Gastrointestinal Surgery of The First Hospital of Jilin University, were enrolled in this study. Blood samples, fresh colorectal adenocarcinoma specimens and patient-matched normal tissues were obtained. No patients received chemotherapy, radiotherapy, or immunomodulatory therapy prior to surgery. The tumor-node-metastasis (TNM) stages were evaluated according to the American Joint Committee on Cancer/Union for International Cancer Control TNM classification (7th ed.). For healthy controls, 15 healthy individuals with matched age and sex ratio, who received routine medical health test in our hospital, were also enrolled for blood sampling. The clinical characteristics of enrolled subjects were shown in **Table 1**.

Peripheral Blood Mononuclear Cells (PBMC) and Tumor-Infiltrating Lymphocytes (TIL) Isolation

PBMCs were isolated using Ficoll-Hypaque (Sigma, St. Louis, MO, USA) density gradient centrifugation from anticoagulant peripheral bloods of all enrolled subjects. TILs were isolated from tissue specimens, which were passed through 70 μm-pore strainers. Cells were treated with Collagenase D (0.5 mg/ml) at 37°C for 30 min, and then were resuspended in 44% Percoll in RPMI 1640 (*vol*/*vol*). The resuspended cells were layered over 56% Percoll in PBS (*vol*/*vol*), and were centrifuged at 850 × *g* for 30 min. The interphase, which contained TILs, was collected and washed twice. TILs were cultured in RPMI 1640 supplemented with 10% fetal bovine serum at a concentration of 10^6/ml.

$CD4^+$ and $CD8^+$ T Cells Purification

$CD4^+$ and $CD8^+$ T cells were purified from PBMCs and TILs using human $CD4^+$ T Cell Isolation Kit (Miltenyi, Bergisch Galdbach, Germany) and human $CD8^+$ T Cell Isolation Kit (Miltenyi), respectively, according to the instructions from manufacturer. The purity of enriched cells was more than 95% as determined by flow cytometry analysis.

TABLE 1 | Clinical characteristics of enrolled subjects.

	Colorectal adenocarcinoma	Healthy control
Cases (*n*)	29	15
Sex (male/female)	19/10	10/5
Age (years)	55.7 ± 10.1	56.2 ± 7.4
Tumor site (right-sided/left-sided/transverse)	14/9/6	Not available
Differentiation (well/moderate/poor)	7/18/4	Not available
TNM stage (I/II/III/IV)	12/14/3/0	Not available

Cell Culture

Purified $CD4^+$ T cells or $CD8^+$ T cells were stimulation with recombinant human IL-24 (R&D System, Minneapolis, MN, USA; final concentration: 10 ng/ml or 100 ng/ml) for 24 h in the presence of anti-CD3/CD28 (eBioscience, San Diego, CA, USA; final concentration: 1 μg/ml). In certain experiments, 5×10^4 of IL-24 stimulated $CD8^+$ T cells from HLA-A2 restricted patients were co-cultured in direct contact and in parallel in indirect contact system with 2.5×10^5 of colorectal adenocarcinoma cell line CACO-2, which was also HLA-A2 restricted (19), for 48 h in the presence of anti-CD3/CD28 (Invitrogen eBioscience; final concentration: 1 μg/ml). Briefly, in direct contact co-culture system, $CD8^+$ T cells and CACO-2 cells were mixed directly in a cell culture plate. In indirect contact co-culture system, $CD8^+$ T cells and CACO-2 cells were separated by a 0.4 μm-pore membrane in a Transwell culture plate (Corning, Corning, NY, USA), which allowed the passage of soluble factors only (20). Cells and supernatants were harvested for further experiments.

Enzyme Linked Immunosorbent Assay (ELISA)

The cytokine expression in the plasma or cultured supernatants was measured using commercial ELISA kits (R&D System) according to the instructions from manufacturer.

Real-Time Polymerase Chain Reaction (PCR)

Total RNA was isolated from cells or tissues using RNeasy Minikit (Qiagen, Hilden, Germany) according to the instructions from manufacturer. RNA was reversely transcribed using PrimeScript RT Master Mix (TaKaRa, Beijing, China) with random hexamers. Real-time PCR was performed using TB Green Premix *Taq* (TaKaRa). The relative gene expression was quantified by $2^{-\Delta\Delta CT}$ method using ABI7500 System Sequence Detection Software (Applied Biosystems, Foster, CA, USA). To normalize the absolute quantification according to a single reference gene, kinetic PCR reactions has to be performed for β-actin on all experimental samples and the relative abundance values are calculated for internal control as well as for the target gene. For each target gene sample, the relative abundance value obtained is divided by the value derived from the control sequence (β-actin) in the corresponding target gene. The normalized values for different samples can then directly be compared. The primer sequences were shown in **Table 2**.

Cellular Proliferation Assay

Cellular proliferation was measured using Cell Counting Kit-8 (CCK-8; Beyotime, Wuhan, Hubei Province, China) according to the instructions from manufacturer.

Flow Cytometry

$CD4^+$ T cells were stained with anti-CD3-APC Cy7 (clone SK7; BD Pharmingen, San Jose, CA, USA), anti-CD4-PerCP (clone S3.5; Invitrogen eBioscience) along with anti-interferon-γ (IFN-γ)-FITC (clone 4S.B3; Invitrogen eBioscience; for intracellular staining), anti-FoxP3-PE (clone 150D/E4; Invitrogen eBioscience; for intracellular staining) and anti-IL-17A-APC (clone eBio64DEC17; Invitrogen eBioscience; for intracellular staining). $CD8^+$ T cells were stained with anti-CD3-APC Cy7 (clone SK7; BD Pharmingen), anti-CD8-APC (clone 17D8; Invitrogen eBioscience) along with anti-perforin-PE (clone delta G9; Invitrogen eBioscience; for intracellular staining), anti-granzyme B-PE (clone GB11; Invitrogen eBioscience; for intracellular staining), or anti-Fas ligand (FasL, CD178)-PE (clone NOK-1; Invitrogen eBioscience; for surface staining), respectively. Acquisitions were performed using Cell Quest Pro Software (BD Biosciences Immunocytometry Systems, San Jose, CA, USA) in a FACS Aira II analyzer (BD Biosciences Immunocytometry Systems). Data were analyzed using FlowJo Software Version 8.4.2 for Windows (Tree Star, Ashland, OR, USA).

Cytotoxicity of Target CACO-2 Cells

The cytotoxicity of target CACO-2 cells was assessed by measurement of lactate dehydrogenase (LDH) expression in cultured supernatants at the end of incubation period using LDH Cytotoxicity Assay Kit (Beyotime) according to the instructions from manufacturer. A low-level LDH control was represented as LDH expression in CACO-2 cells, while a high-level LDH control was represented as LDH expression in Triton X-100-treated CACO-2 cells. The percentage of target cell death was calculated using the following equation: (experimental value – low-level LDH control)/(high-level LDH control – low-level LDH control) × 100%.

Statistical Analysis

Data were analyzed using SPSS 21.0 Version for Windows (SPSS, Chicago, IL, USA). Shapiro-Wilk test was used for normal distribution assay. The parameters following normal and skewed distribution were shown in **Table S1**. Variables following normal distribution were presented as mean ± standard

TABLE 2 | Primer sequences for real-time PCR.

Primer	Sequence
IL-24 forward	5′-GGR TTG TTC CCT GTG TCA TT-3′
IL-24 reverse	5′-GCG CTG CTT AAA GAA TGA CT-3′
IL-20R1 forward	5′-TCA AAC AGA ACG TGG TCC CAG TG-3′
IL-20R1 reverse	5′-TCC GAG ATA TTG AGG GTG ATA AAG-3′
IL-20R2 forward	5′-GCT GGT GTC CAC TCA CTG AAG GT-3′
IL-20R2 reverse	5′-TCT GTC TGG CTG AAG GCG CTG TA-3′
IL-22R1 forward	5′-CCC CAG ACA ACG GTC TAC AGC AT-3′
IL-22R1 reverse	5′-GGG TCA GGC CGA AGA ACT CAT AT-3′
T-bet forward	5′-CGG CTG CAT ATC GTT GAG GT-3′
T-bet reverse	5′-GTC CCC ATT GGC ATT CCT C-3′
ROR-γt forward	5′-AGT CGG AAG GCA AGA TCA GA-3′
ROR-γt reverse	5′-CAA GAG AGG TTC TGG GCA AG-3′
FoxP3 forward	5′-CCT CCC CCA TCA TAT CCT TT-3′
FoxP3 reverse	5′-TTG GGG TTT GTG TTG AGT GA-3′
β-actin forward	5′-AGC GGG AAA TCG TGC GTG-3′
β-actin reverse	5′-CAG GGT ACA TGG TGG TGC C-3′

deviation. Student's *t*-test was used for comparison between two groups. One-way ANOVA followed by Tukey test for multiple comparison was used for comparison among groups. Variables following skewed distribution were presented as median [Q1, Q3]. Mann-Whitney test was used for comparison between two groups. Kruskal-Wallis test followed by Dunn's multiple comparison test was used for comparison among groups. A $P < 0.05$ was considered as statistical difference.

RESULTS

IL-24 Was Decreasingly Expressed in Colorectal Adenocarcinoma

We firstly screened the protein and mRNA expression profile of IL-24 in colorectal adenocarcinoma patients. IL-24 concentration in the plasma was measured by ELISA. Plasma IL-24 expression was robustly reduced in colorectal adenocarcinoma patients when compared with healthy controls (20.21 ± 8.15 ng/ml vs. 98.51 ± 18.94 ng/ml; Student's *t*-test, $P < 0.0001$, **Figure 1A**). However, there were no significant differences of IL-24 concentration among colorectal adenocarcinoma patients with different tumor site (One-way ANOVA, $P > 0.05$), different differentiation (One-way ANOVA, $P > 0.05$), or in different TNM stages (One-way ANOVA, $P > 0.05$). IL-24 mRNA relative level was also semi-quantified in peripheral T cells by real-time PCR. IL-24 mRNA expression was also notably down-regulated in both peripheral $CD4^+$ and $CD8^+$ T cells from colorectal adenocarcinoma patients when compared with those from healthy individuals (Student's *t*-tests, all $P < 0.0001$, **Figures 1B,C**). Furthermore, IL-24 mRNA was also investigated in tumor tissue and tumor-infiltrating T cells from colorectal adenocarcinoma patients. IL-24 mRNA relative level in tumor tissue was decreased when compared with non-tumor tissue (Mann-Whitney test, $P < 0.0001$, **Figure 1D**). Similarly, IL-24 mRNA expression in tumor-infiltrating $CD4^+$ and $CD8^+$ T cells was also remarkably reduced when compared with those from non-tumor tissue (Mann-Whitney tests, all $P < 0.0001$, **Figures 1E,F**). However, there were no significant differences of peripheral or tissue resident IL-24 mRNA relative level among colorectal adenocarcinoma patients with different tumor site (Kruskal-Wallis test, $P > 0.05$), different differentiation (Kruskal-Wallis test, $P > 0.05$), or in different TNM stages (Kruskal-Wallis test, $P > 0.05$).

IL-20R1 and IL-20R2 Did Not Significantly Changed in Colorectal Adenocarcinoma

mRNA expression corresponding to the component of IL-24 receptor, including IL-20R1, IL-20R2, and IL-22R1, was semi-quantified in peripheral and tumor-infiltrating $CD4^+$ and $CD8^+$ T cells. IL-20R1 mRNA relative level was comparable in peripheral $CD4^+$ and $CD8^+$ T cells between colorectal adenocarcinoma patients and healthy individuals (Student's *t*-tests, $P < 0.05$, **Figures 2A,B**). IL-20R2 mRNA relative level was also comparable in peripheral T cells between

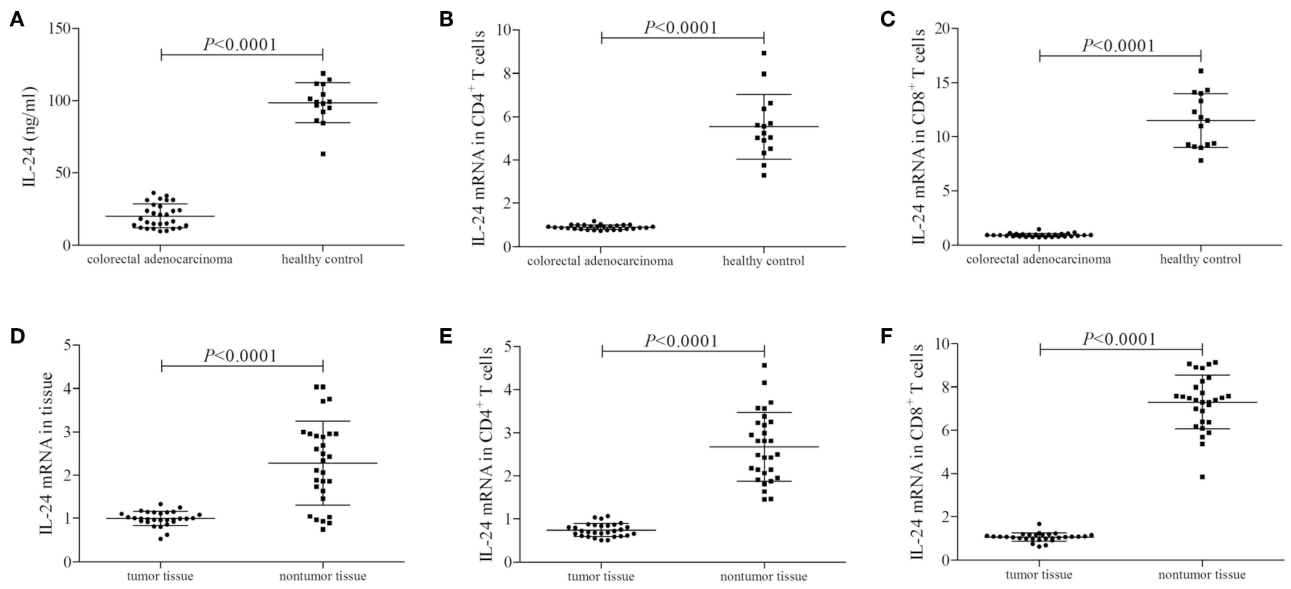

FIGURE 1 | IL-24 expression profile in colorectal adenocarcinoma patients. Plasma IL-24 concentration was measured by ELISA in all enrolled subjects (29 of colorectal adenocarcinoma patients and 15 of healthy controls). IL-24 mRNA relative level was measured by real-time PCR in tumor tissue, peripheral and tumor-infiltrating $CD4^+$ and $CD8^+$ T cells. **(A)** IL-24 expression in the plasma was reduced in colorectal adenocarcinoma patients. **(B)** IL-24 mRNA expression was down-regulated in peripheral $CD4^+$ T cells from colorectal adenocarcinoma patients. **(C)** IL-24 mRNA expression was also down-regulated in peripheral $CD8^+$ T cells from colorectal adenocarcinoma patients. **(D)** IL-24 mRNA expression was decreased in colorectal adenocarcinoma tissue. **(E)** IL-24 mRNA expression was down-regulated in tumor-infiltrating $CD4^+$ T cells from colorectal adenocarcinoma tissue. **(F)** IL-24 mRNA expression was down-regulated in tumor-infiltrating $CD8^+$ T cells from colorectal adenocarcinoma tissue. Individual level of each subject was shown. Student's *t*-test, One-way ANOVA, or Mann-Whitney test was used for comparison.

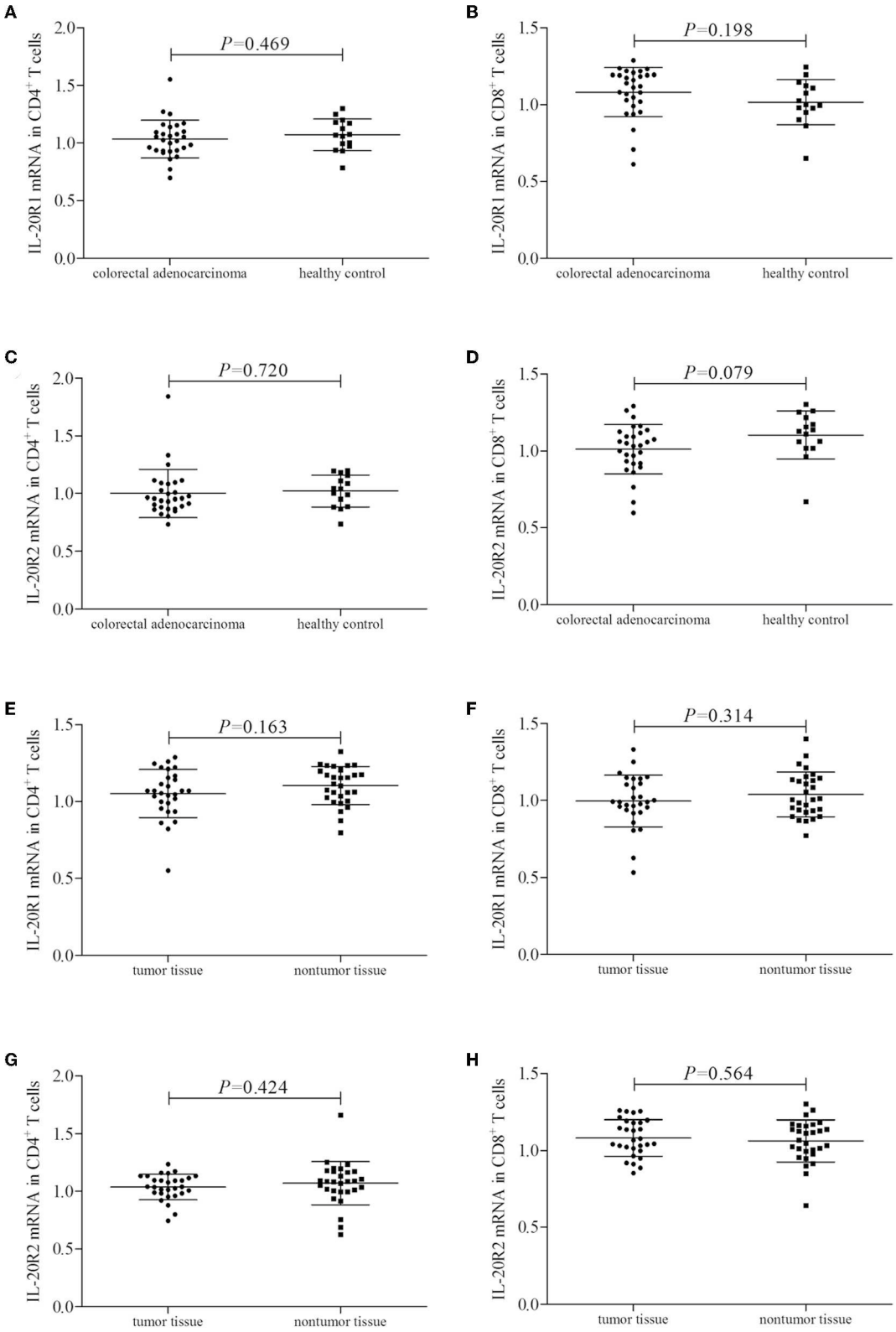

FIGURE 2 | IL-24 receptor component expression in colorectal adenocarcinoma patients. IL-20R1, IL-20R2, and IL-22R2 mRNA relative level was semi-quantified in peripheral and tumor-infiltrating $CD4^+$ and $CD8^+$ T cells from all enrolled subjects (29 of colorectal adenocarcinoma patients and 15 of healthy controls). **(A)** IL-20R1

(Continued)

FIGURE 2 | mRNA in peripheral $CD4^+$ T cells. **(B)** IL-20R1 mRNA in peripheral $CD8^+$ T cells. **(C)** IL-20R2 mRNA in peripheral $CD4^+$ T cells. **(D)** IL-20R2 mRNA in peripheral $CD8^+$ T cells. **(E)** IL-20R1 mRNA in tumor-infiltrating $CD4^+$ T cells. **(F)** IL-20R1 mRNA in tumor-infiltrating $CD8^+$ T cells. **(G)** IL-20R2 mRNA in tumor-infiltrating $CD4^+$ T cells. **(H)** IL-20R2 mRNA in tumor-infiltrating $CD8^+$ T cells. IL-20R1 and IL-20R2 mRNA was comparable in peripheral and tumor-infiltrating $CD4^+$ and $CD8^+$ T cells between colorectal adenocarcinoma patients and healthy individuals, and between tumor tissue and non-tumor tissue. Individual level of each subject was shown. Student's *t*-test was used for comparison.

two groups (Student's *t*-tests, $P < 0.05$, **Figures 2C,D**). IL-20R1/IL-20R2 expression presented similar trends in tumor-infiltrating T cells. IL-20R1 and IL-20R2 mRNA was also comparable in tumor-infiltrating $CD4^+$ and $CD8^+$ T cells between colorectal adenocarcinoma tissue and non-tumor tissue (Student's *t*-tests, $P < 0.05$, **Figures 2E–H**). However, IL-22R1 mRNA was undetectable in either $CD4^+$ or $CD8^+$ T cells.

High Concentration of IL-24 Stimulation Enhanced $CD4^+$ T Cell Activity in Colorectal Adenocarcinoma

10^5 of peripheral or tumor-infiltrating $CD4^+$ T cells from colorectal adenocarcinoma patients were stimulated with low concentration (10 ng/ml) or high concentration (100 ng/ml) of recombinant human IL-24 for 24 h. CCK-8 results showed that 10 ng/ml of IL-24 stimulation slightly inhibited both peripheral and tumor-infiltrating $CD4^+$ T cells proliferation (Tukey tests, $P = 0.024$ and $P = 0.041$, respectively, **Figure 3A**). In contrast, 100 ng/ml of IL-24 stimulation significantly promoted $CD4^+$ T cells proliferation (Tukey tests, $P < 0.0001$, **Figure 3A**). The percentage of Th1 ($CD4^+IFN\text{-}\gamma^+$), Th17 ($CD4^+IL\text{-}17^+$), and regulatory T cells (Treg, $CD4^+FoxP3^+$) was assessed by flow cytometry. The gating strategy for $CD4^+$ T cells was shown in **Figure S1**. The representative flow dots was shown in **Figures 3B–D**, respectively. Low concentration of IL-24 stimulation did not affect the peripheral Th1 percentage (Tukey test, $P = 0.642$, **Figure 3B**), however, significantly down-regulated tumor-infiltrating Th1 percentage ($1.30 \pm 0.19\%$ vs. $1.67 \pm 0.28\%$, Tukey test, $P < 0.0001$, **Figure 3B**). In contrast, high concentration of IL-24 robustly increased both peripheral and tumor-infiltrating Th1 frequency (Tukey tests, $P < 0.0001$, **Figure 3B**). However, IL-24 did not influence either peripheral or tumor-infiltrating Th17 percentage in either low or high concentration manner (One-way ANOVA, $P > 0.05$, **Figure 3C**). Furthermore, low concentration of IL-24 slightly up-regulated tumor-infiltrating Treg frequency, but this difference failed to achieve statistical significance ($10.01 \pm 2.24\%$ vs. $8.97 \pm 2.08\%$, Tukey test, $P = 0.098$, **Figure 3D**). However, low concentration of IL-24 did not affect peripheral Treg frequency (Tukey test, $P = 0.217$, **Figure 3D**). Importantly, high concentration of IL-24 remarkably reduced both peripheral and tumor-infiltrating Treg frequency (Tukey tests, all $P < 0.0001$, **Figure 3D**).

mRNA expression of transcriptional factors of $CD4^+$ T cells, including T-bet (Th1 transcriptional factor), retinoic acid receptor-related orphan receptor-γt (ROR-γt, Th17 transcriptional factor), and FoxP3 (Treg transcriptional factor), was semi-quantified by real-time PCR. Low concentration of IL-24 did not affect T-bet mRNA relative level in either peripheral or tumor-infiltrating $CD4^+$ T cells (Tukey tests, $P > 0.05$, **Figure 4A**). In contrast, high concentration of IL-24 robustly elevated T-bet mRNA relative level in $CD4^+$ T cells (Tukey tests, $P < 0.0001$, **Figure 4A**). IL-24 stimulation did not influence ROR-γt mRNA expression in $CD4^+$ T cells (One-way ANOVA, $P > 0.05$, **Figure 4B**), which were similar to the trends of Th17 percentage. Moreover, low concentration of IL-24 promoted FoxP3 mRNA expression in tumor-infiltrating $CD4^+$ T cells (Tukey test, $P = 0.012$, **Figure 4C**). However, high concentration of IL-24 notably down-regulated FoxP3 mRNA relative level in both peripheral and tumor-infiltrating $CD4^+$ T cells (Tukey tests, $P < 0.0001$, **Figure 4C**). Cytokine production in the cultured supernatants was measured by ELISA. Th1-secreting cytokine IFN-γ was comparable between unstimulated and 10 ng/ml of IL-24 stimulated $CD4^+$ T cells (Dunn's multiple comparison tests, $P > 0.05$, **Figure 4D**). One hundred Nanograms per milliliter of IL-24 stimulation enhanced IFN-γ expression in both peripheral and tumor-infiltrating $CD4^+$ T cells (Dunn's multiple comparison tests, $P < 0.0001$, **Figure 4D**). IL-24 stimulation did not affect Th17-secreting cytokine IL-17 production by $CD4^+$ T cells (One-way ANOVA, $P > 0.05$, **Figure 4E**). Expression of Treg-secreting cytokine, IL-35 and IL-10, presented similar trends of Tregs frequency and FoxP3 mRNA. Low concentration of IL-24 did not influence IL-35 and IL-10 production by $CD4^+$ T cells (Tukey tests, $P > 0.05$, **Figures 4F,G**), while high concentration of IL-24 dampened IL-35 and IL-10 expression in cultured $CD4^+$ T cells (Tukey tests, $P < 0.0001$, **Figures 4F,G**).

High Concentration of IL-24 Promoted $CD8^+$ T Cell Function in Colorectal Adenocarcinoma

10^5 of peripheral or tumor-infiltrating $CD8^+$ T cells from colorectal adenocarcinoma patients were stimulated with low concentration (10 ng/ml) or high concentration (100 ng/ml) of recombinant human IL-24 for 24 h. CCK-8 results showed that 10 ng/ml of IL-24 stimulation did not affect $CD8^+$ T cells proliferation (Tukey tests, $P > 0.05$, **Figure 5A**). However, 100 ng/ml of IL-24 stimulation significantly increased $CD4^+$ T cells proliferation (Tukey tests, all $P < 0.05$, **Figure 5A**). Cytotoxic molecules in $CD8^+$ T cells, including perforin, granzyme B, and FasL, were assessed by flow cytometry. The gating strategy for $CD8^+$ T cells was shown in **Figure S2**.The representative histograms were shown in **Figures 5B–D**, respectively. Perforin and granzyme B was expressed in almost all $CD8^+$ T cells. Mean Fluorescence Intensity (MFI) corresponding to perforin and granzyme B was then analyzed. As shown in **Figures 5B,C**, low concentration of

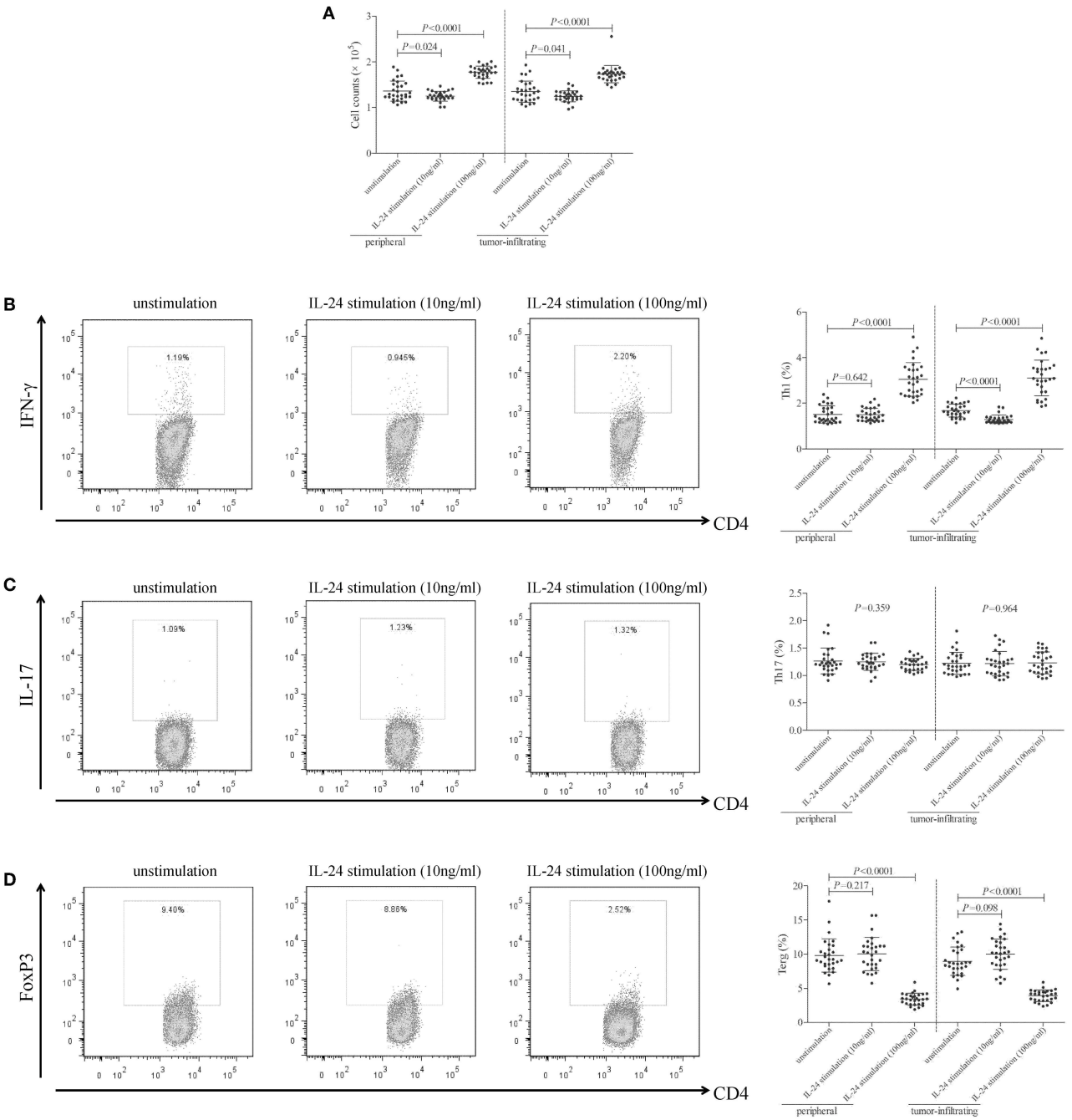

FIGURE 3 | Influence of recombinant IL-24 stimulation on peripheral and tumor-infiltrating CD4$^+$ T cell activity in colorectal adenocarcinoma. 10^5 of purified CD4$^+$ T cells from colorectal adenocarcinoma patients ($n = 29$) were stimulated with low concentration (10 ng/ml) or high concentration (100 ng/ml) of recombinant human IL-24 for 24 h. **(A)** Cellular proliferation was measured by CCK-8, and was compared among groups (One-way ANOVA, $P < 0.0001$). **(B)** Representative flow dots of CD4$^+$IFN-γ^+ Th1 cells were shown in unstimulated, 10 ng/ml of IL-24 stimulated, and 100 ng/ml of IL-24 stimulated cells. Percentage of Th1 cells was compared among groups (One-way ANOVA, $P < 0.0001$). **(C)** Representative flow dots of CD4$^+$IL-17$^+$ Th17 cells were shown in unstimulated, 10 ng/ml of IL-24 stimulated, and 100 ng/ml of IL-24 stimulated cells. Percentage of Th17 cells was compared among groups (One-way ANOVA, $P > 0.05$). **(D)** Representative flow dots of CD4$^+$FoxP3 $^+$ Treg were shown in unstimulated, 10 ng/ml of IL-24 stimulated, and 100 ng/ml of IL-24 stimulated cells (One-way ANOVA, $P < 0.0001$). Percentage of Treg was compared among groups. Individual level of each subject was shown. One-way ANOVA and Tukey test for multiple comparison was used for comparison.

IL-24 did not affect either perforin or granzyme B expression in CD8$^+$ T cells (Tukey tests, $P > 0.05$), while high concentration of IL-24 promoted perforin and granzyme B expression in both peripheral and tumor-infiltrating CD8$^+$ T cells (Tukey tests, $P < 0.05$). Furthermore, ∼60% of CD8$^+$ T cells expressed FasL. However, there were no significant differences of either FasL$^+$ cell

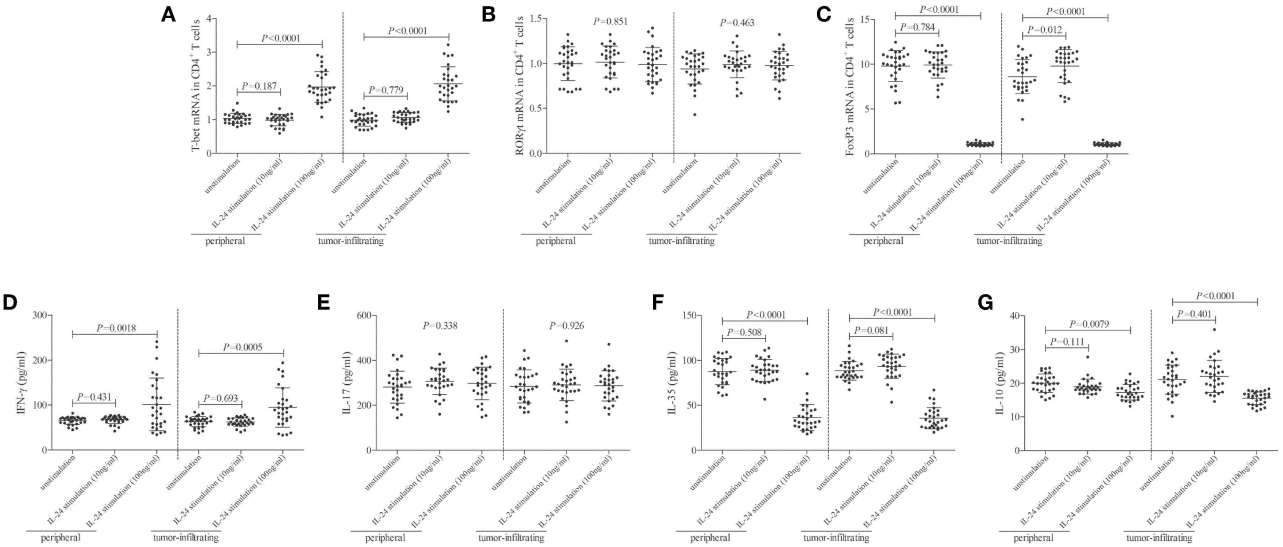

FIGURE 4 | Influence of recombinant IL-24 stimulation on transcriptional factor and cytokine production of peripheral and tumor-infiltrating CD4$^+$ T cells in colorectal adenocarcinoma. 10^5 of purified CD4$^+$ T cells from colorectal adenocarcinoma patients ($n = 29$) were stimulated with low concentration (10 ng/ml) or high concentration (100 ng/ml) of recombinant human IL-24 for 24 h. mRNA expression of transcriptional factors, including **(A)** T-bet (One-way ANOVA, $P < 0.0001$), **(B)** ROR-γt (One-way ANOVA, $P > 0.05$), and **(C)** FoxP3 (One-way ANOVA, $P < 0.0001$), were semi-quantified by real-time PCR, and were compared among groups. Expression of cytokines in cultured supernatants, including **(D)** IFN-γ (Kruskal-Wallis test, $P < 0.05$), **(E)** IL-17 (One-way ANOVA, $P > 0.05$), **(F)** IL-35 (One-way ANOVA, $P < 0.0001$), and **(G)** IL-10 (One-way ANOVA, $P < 0.001$), was measured by ELISA, and were compared among groups. Individual level of each subject was shown. One-way ANOVA, Tukey test for multiple comparison, Kruskal-Wallis test, Dunn's multiple comparison test was used for comparison.

frequency or FasL MFI among unstimulated and IL-24 stimulated CD8$^+$ T cells (Tukey tests, $P > 0.05$, **Figure 5D**).

CD8$^+$ T cells, which were purified from twelve HLA-A2 restricted colorectal adenocarcinoma patients, were stimulated with recombinant IL-24 for 24 h, and were then co-cultured with CACO-2 cells (effector: target = 1: 5) in both direct contact and indirect contact manner. Supernatants were harvested 48 h post co-culture. In direct contact co-culture system, high concentration of IL-24 (100 ng/ml), but not low concentration, stimulated CD8$^+$ T cells induced higher percentage of target CACO-2 cell death (Tukey tests, $P < 0.001$, **Figure 6A**). However, neither high nor low concentration of IL-24 promoted CD8$^+$ T cells-induced cell death in indirect contact co-culture system (Tukey tests, $P > 0.05$, **Figure 6B**). Furthermore, high concentration of IL-24, but not low concentration, treated CD8$^+$ T cells enhanced IFN-γ production in both direct and indirect contact co-culture system (Tukey tests, $P < 0.05$, **Figures 6C,D**).

DISCUSSION

In the current study, IL-24 was decreasingly expressed in both peripheral bloods and cancer tissues in colorectal adenocarcinoma, but did not correlate with either histological differentiation or TNM staging. IL-24 receptor component, IL-20R1 and IL-20R2, was comparable in CD4$^+$/CD8$^+$ T cells between normal controls and colorectal adenocarcinoma. However, IL-22R2 was undetectable in T cells. Furthermore, low concentration (10 ng/ml) of IL-24 stimulation dampened CD4$^+$ T cell proliferation, but not affected bioactivity of either CD4$^+$ or CD8$^+$ T cells. In contrast, high concentration (100 ng/ml) of IL-24 stimulation promoted both CD4$^+$ and CD8$^+$ T cell function, which presented as increase of Th1/Th17 cells and elevation of cytolytic and non-cytolytic activity of peripheral and tumor-infiltrating CD8$^+$ T cells. The current results suggested an important immunomodulatory function of IL-24 to T cells in a dose-dependent manner in colorectal adenocarcinoma.

It was well accepted that IL-24 mediated cancer cell-specific death and apoptosis *via* multiple signaling pathways (21–23). Significantly lower IL-24 expression predicted poorer prognosis in lung adenocarcinoma (24), breast cancer (25), head and neck squamous cell carcinoma (26), and lymphoma (27, 28). IL-24^{high} adenocarcinoma patients showed a notably higher incidence of apoptotic tumor cell death, and displayed favorable post-therapy prognosis as compared with IL-24^{low} patients (24). Similarly, colorectal cancer tissue revealed significantly lower IL-24 level, which was associated with 5-year survival rate (17). This was consistent with our present findings, which indicated a robust decline of IL-24 in colorectal adenocarcinoma tissues, as well as in peripheral and tumor-infiltrating T cells from colorectal adenocarcinoma patients. However, down-regulation of IL-24 level did not correlate with either histological differentiation or TNM staging, which diversely reported previously (15). This might partly due to the differences in detection and semi-quantification methods. Collectively, reduced expression of circulating and tissue-resident IL-24 might contribute to pathogenesis and progression of colorectal adenocarcinoma.

Controversy remains as to the regulatory activity of IL-24 to immune systems in infectious diseases. Parasite-specific

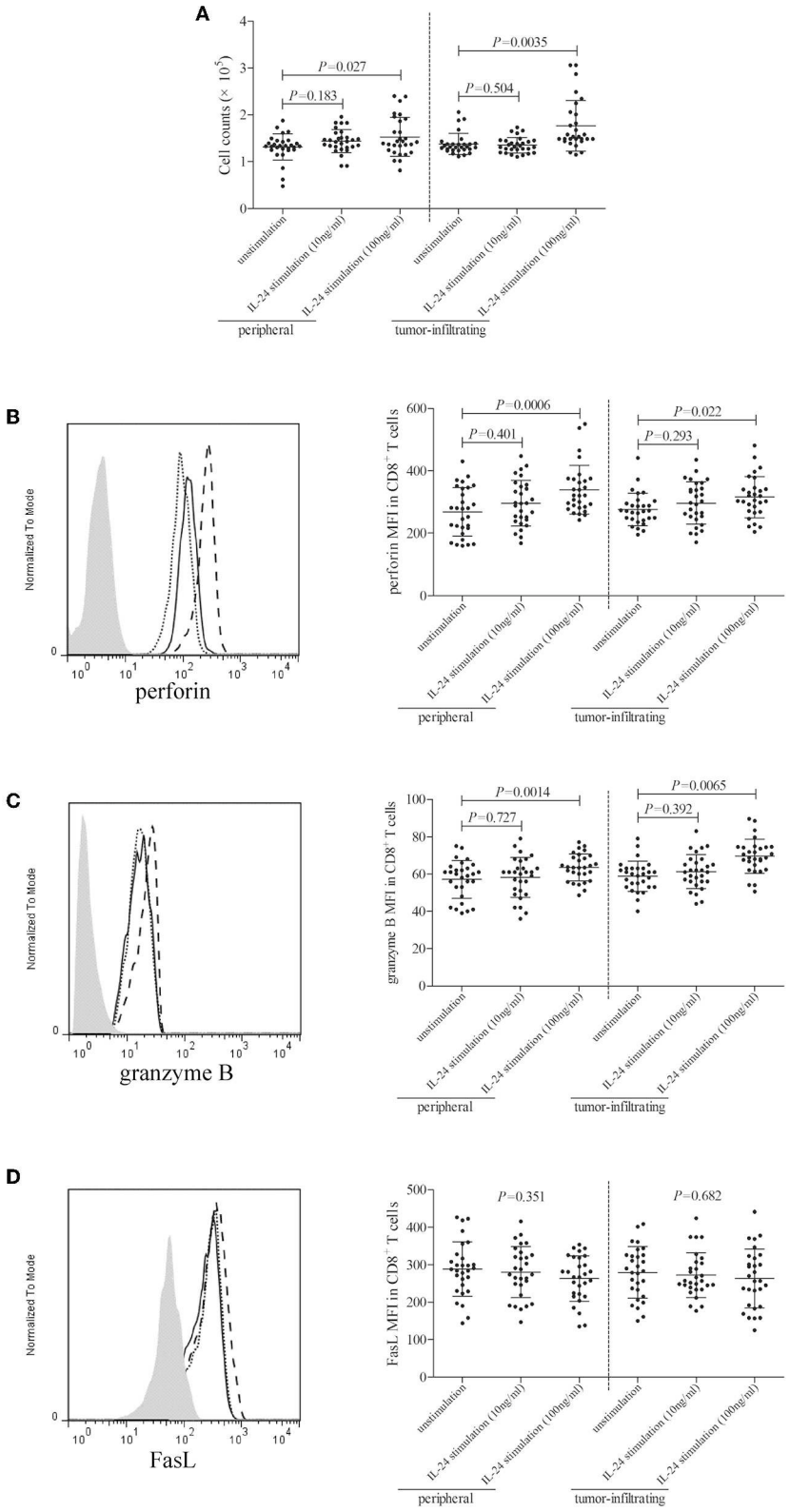

FIGURE 5 | Influence of recombinant IL-24 stimulation on peripheral and tumor-infiltrating CD8$^+$ T cell activity in colorectal adenocarcinoma. 10^5 of purified CD8$^+$ T cells from colorectal adenocarcinoma patients ($n = 29$) were stimulated with low concentration (10 ng/ml) or high concentration (100 ng/ml) of recombinant human

(Continued)

FIGURE 5 | IL-24 for 24 h. **(A)** Cellular proliferation was measured by CCK-8, and was compared among groups (One-way ANOVA, $P < 0.05$). **(B)** perforin, **(C)** granzyme B, and **(D)** FasL expression was assessed by flow cytometry, and representative histograms were shown. MFI corresponding to **(B)** perforin (One-way ANOVA, $P < 0.01$), **(C)** granzyme B (One-way ANOVA, $P < 0.05$), and **(D)** FasL (One-way ANOVA, $P > 0.05$) was compared among groups. Individual level of each subject was shown. One-way ANOVA and Tukey test for multiple comparison was used for comparison.

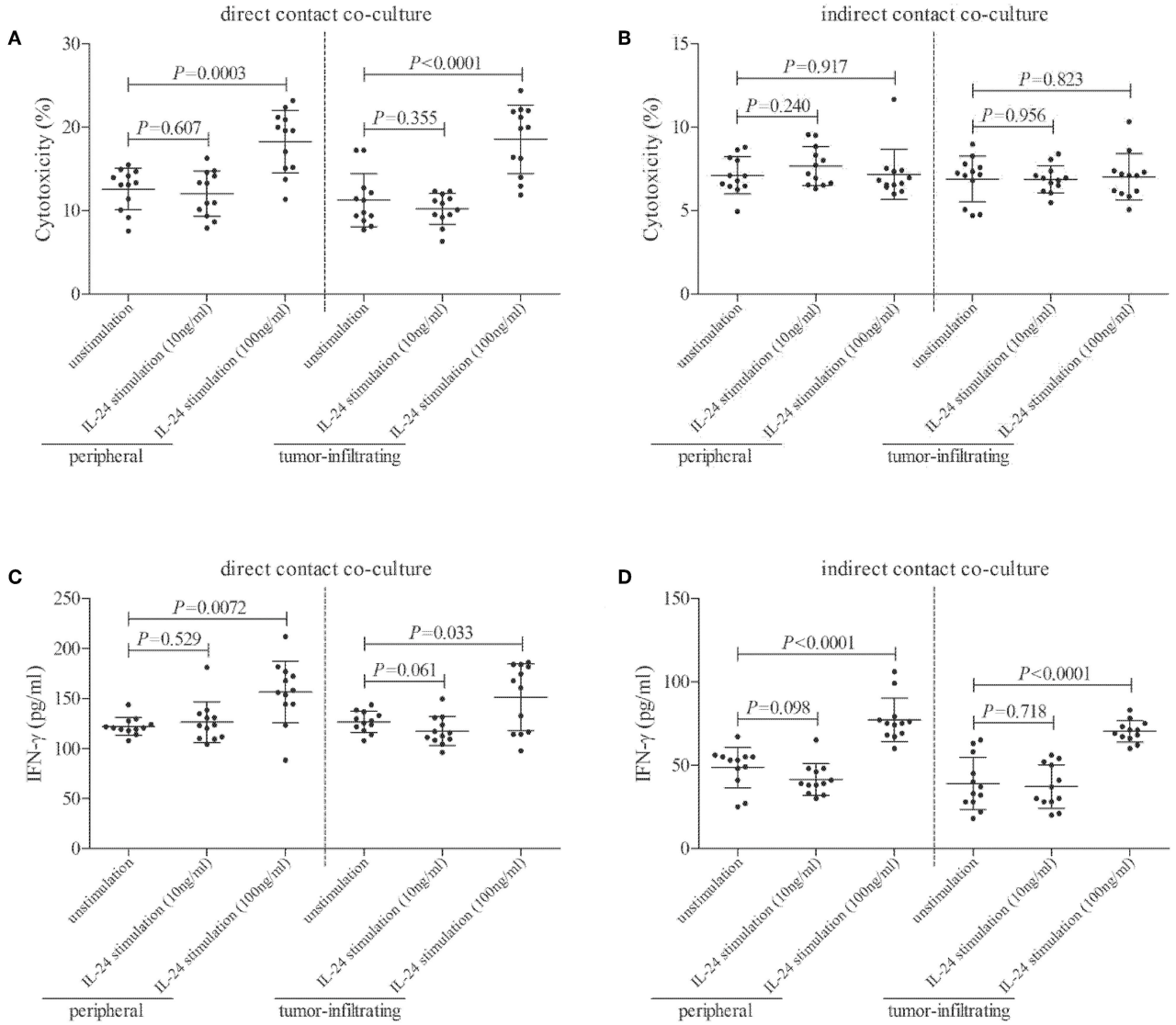

FIGURE 6 | Influence of recombinant IL-24 stimulation on cytolytic and non-cytolytic function of $CD8^+$ T cells in colorectal adenocarcinoma. $CD8^+$ T cells were purified from HLA-A2 restricted colorectal adenocarcinoma patients ($n = 12$), and were stimulated low concentration (10 ng/ml) or high concentration (100 ng/ml) of recombinant human IL-24 for 24 h. 5×10^4 of IL-24 stimulated $CD8^+$ T cells were co-cultured in direct contact and in parallel in indirect contact system with 2.5×10^5 of colorectal adenocarcinoma cell line CACO-2 for 48 h. Cytotoxicity of target CACO-2 cells was calculated by measurement of LDH expression in the cultured supernatants. IFN-γ and TNF-α expression in the cultured supernatants was measured by ELISA. **(A)** Cytotoxicity of target CACO-2 cells in direct contact co-culture system (One-way ANOVA, $P < 0.01$). **(B)** Cytotoxicity of target CACO-2 cells in indirect contact co-culture system (One-way ANOVA, $P > 0.05$). **(C)** IFN-γ expression in direct contact co-culture system (One-way ANOVA, $P < 0.001$). **(D)** IFN-γ expression in indirect contact co-culture system (One-way ANOVA, $P < 0.0001$). Individual level of each subject was shown. One-way ANOVA and Tukey test for multiple comparison was used for comparison.

$CD4^+$ and $CD8^+$ T cells expressing IL-19 and IL-24 was significantly increased in human lymphatic filariasis (29), and the elevation of IL-19 and IL-24 in turn modulated $CD4^+$ and $CD8^+$ T cell function during filarial infections, which presented as down-regulation of Th1/Tc1 and Th17/Tc17 cells (30). Similarly, the increased expression of IL-19 and IL-24 in active pulmonary tuberculosis patients also mediated decreased expression of Th1/Tc1 and Th17/Tc17 cytokine in $CD4^+$ and

$CD8^+$ T cells (31). In contrast, IL-24 stimulated neutrophils to produce IFN-γ and IL-12, subsequently activating $CD8^+$ T cells during Salmonella typhimurium infection both *in vitro* and *in vivo* (32). However, IL-24 was originally identified as a tumor suppressor cytokine. Thus, modulation of IL-24 to immune cells from cancer patients might be completely different. Adenovirus-mediated IL-24 vaccinated mice showed increased production of IFN-γ and higher proliferative activity in spleonocytes, which was mainly elevated in $CD8^+$ T cells, but not $CD4^+$ T cells (33). Importantly, IL-24 also enhanced IFN-γ secretion by T cells and promoted cytotoxicity of $CD8^+$ T cells in a colon cancer mouse model (34). But the role of direct regulatory activity of IL-24 to tumor-infiltrating T cells in colorectal adenocarcinoma patients still needed further elucidation.

We firstly investigated the expression profile of IL-24 receptor in T cells. There were no significant differences of IL-20R1 and IL-20R2 in peripheral and tissue-resident T cells between healthy individuals and colorectal adenocarcinoma patients, as well as between normal and tumor tissues. However, IL-22R1 could not be detected in either $CD4^+$ or $CD8^+$ T cells. This was consistent with the previous findings, which demonstrated that IL-22 receptor was strictly expressed on the tissue but absent on immune cells (35). Thus, signaling through IL-24 in regulation of T cells was dependent on the expression of IL-20R1/IL-20R2 heterodimeric complex, which was also the receptor for IL-20 (11). Furthermore, since anti-tumor property of IL-24 was dose-dependent, we also chose two different concentration (10 ng/ml as low concentration and 100 ng/ml as high concentration) of recombinant IL-24 for stimulation based on the plasma IL-24 level in colorectal adenocarcinoma patients and healthy individuals. Low concentration of IL-24 inhibited $CD4^+$ T cell proliferation and dampened tumor-infiltrating Th1 response. In contrast, high concentration of IL-24 robustly promoted $CD4^+$ T cell proliferation, enhanced Th1 and Th17 response, and inhibited Treg response in colorectal adenocarcinoma patients. This was similar to the *in vivo* findings that administration of 50 μg recombinant IL-24 promoted $CD4^+$ T cells response, especially increased IFN-γ production in colon cancer mouse model (34). This was partly due to the sufficient ligation of high concentration IL-24 to IL-20R1/IL-20R2, which fully activated down-stream signaling pathways in $CD4^+$ T cells. However, the current results suggested low percentages of Th1 and Th17 cells in both peripheral and tumor-infiltrating $CD4^+$ T cells from colorectal adenocarcinoma patients. This was contrast with the previous reports which showed ∼45% of Th1 (36) and 5% of Th17 (37) within colorectal cancer-infiltrating $CD4^+$ T cells. The difference might be due to different antibody clones used for staining or variations in geographic location and host genetic background, because several studies on Chinese population also revealed similar and low frequency of Th1 and Th17 cells (38, 39).

$CD8^+$ T cells induced tumor rejection *via* both cytolytic (direct target cell cytotoxicity) and non-cytolytic (cytokine production) function (20, 40, 41). There were two independent pathways, perforin/granzyme B pathway and Fas/FasL interaction, which contributed to the cytolytic activity of $CD8^+$ T cells (42). Low concentration of IL-24 did not affect the bioactivity of $CD8^+$ T cells. However, high concentration of IL-24 also notably increased $CD8^+$ T cell proliferation, and elevated perforin/granzye B, but not FasL expression in $CD8^+$ T cells from peripheral and tumor-infiltrating $CD8^+$ T cells from colorectal adenocarcinoma patients. This indicated that high concentration of IL-24 mainly influenced perforin/granzyme B pathway for cytolytic function of $CD8^+$ T cells in colorectal adenocarcinoma. The cytolytic and non-cytolytic function of $CD8^+$ T cells was also distinguished in direct contact and indirect contact co-culture system. High concentration of IL-24 promoted both peripheral and tumor-infiltrating $CD8^+$ T cells-induced cytotoxicity only in direct contact co-culture system, while IFN-γ production was elevated in both systems. The current results demonstrated that non-cytolytic activity of $CD8^+$ T cells was insufficient for colorectal ademocarcinoma rejection, although IL-24 promoted both cytolytic and non-cytolytic function of $CD8^+$ T cells.

The limitation of the current study was that the majority of enrolled patients was in stage I and stage II (26 out of 29). This was due to the fact that we need to analyze the TILs from colorectal carcinoma patients who underwent surgery. However, most patients in stage IV already lost the opportunity for operation, while biopsy samples were insufficient for TILs isolation. Thus, no patients in stage IV was enrolled.

In conclusion, down-regulation of circulating and tissue-resident IL-24 in colorectal adenocarcinoma was inadequate for developing anti-tumor activity. IL-24 regulated T cell function in a dose-dependent manner. High-concentration of IL-24 promoted peripheral and tumor-infiltrating $CD4^+$ and $CD8^+$ T cell function, which provided novel therapeutic approaches to colorectal adenocarcinoma.

DATA AVAILABILITY STATEMENT

The datasets generated for this study are available on request to the corresponding author.

ETHICS STATEMENT

The studies involving human participants were reviewed and approved by the Ethics Committee of The First Hospital of Jilin University. The patients/participants provided their written informed consent to participate in this study.

AUTHOR CONTRIBUTIONS

YZ and YL performed the study. YZ and YX enrolled patients. YZ, YL, and YX analyzed the data and prepared the manuscript. YX supervised the study.

ACKNOWLEDGMENTS

We thank all the volunteers who generously participated in this study.

SUPPLEMENTARY MATERIAL

The Supplementary Material for this article can be found online at: https://www.frontiersin.org/articles/10.3389/fonc.2019.01401/full#supplementary-material

REFERENCES

1. Chen W, Zheng R, Baade PD, Zhang S, Zeng H, Bray F, et al. Cancer statistics in China, 2015. *CA Cancer J Clin*. (2016) 66:115–32. doi: 10.3322/caac.21338
2. Arnold M, Sierra MS, Laversanne M, Soerjomataram I, Jemal A, Bray F. Global patterns and trends in colorectal cancer incidence and mortality. *Gut*. (2017) 66:683–91. doi: 10.1136/gutjnl-2015-310912
3. Siegel RL, Miller KD, Fedewa SA, Ahnen DJ, Meester RGS, Barzi A, et al. Colorectal cancer statistics, 2017. *CA Cancer J Clin*. (2017) 67:177–93. doi: 10.3322/caac.21395
4. Center MM, Jemal A, Smith RA, Ward E. Worldwide variations in colorectal cancer. *CA Cancer J Clin*. (2009) 59:366–78. doi: 10.3322/caac.20038
5. Campos FG. Colorectal cancer in young adults: A difficult challenge. *World J Gastroenterol*. (2017) 23:5041–4. doi: 10.3748/wjg.v23.i28.5041
6. Patel SG, Ahnen DJ. Colorectal cancer in the young. *Curr Gastroenterol Rep*. (2018) 20:15. doi: 10.1007/s11894-018-0618-9
7. Brenner H, Kloor M, Pox CP. Colorectal cancer. *Lancet*. (2014) 383:1490–502. doi: 10.1016/S0140-6736(13)61649-9
8. Ghoncheh M, Mohammadian M, Mohammadian-Hafshejani A, Salehiniya H. The incidence and mortality of colorectal cancer and its relationship with the human development index in Asia. *Ann Glob Health*. (2016) 82:726–37. doi: 10.1016/j.aogh.2016.10.004
9. Poindexter NJ, Walch ET, Chada S, Grimm EA. Cytokine induction of interleukin-24 in human peripheral blood mononuclear cells. *J Leukoc Biol*. (2005) 78:745–52. doi: 10.1189/jlb.0205116
10. Niess JH, Hruz P, Kaymak T. The interleukin-20 cytokines in intestinal diseases. *Front Immunol*. (2018) 9:1373. doi: 10.3389/fimmu.2018.01373
11. Chen J, Caspi RR, Chong WP. IL-20 receptor cytokines in autoimmune diseases. *J Leukoc Biol*. (2018) 104:953–9. doi: 10.1002/JLB.MR1117-471R
12. Sarkar D, Lebedeva IV, Gupta P, Emdad L, Sauane M, Dent P, et al. Melanoma differentiation associated gene-7 (mda-7)/IL-24: a 'magic bullet' for cancer therapy? *Expert Opin Biol Ther*. (2007) 7:577–86. doi: 10.1517/14712598.7.5.577
13. Menezes ME, Bhatia S, Bhoopathi P, Das SK, Emdad L, Dasgupta S, et al. MDA-7/IL-24: multifunctional cancer killing cytokine. *Adv Exp Med Biol*. (2014) 818:127–53. doi: 10.1007/978-1-4471-6458-6_6
14. Menezes ME, Bhoopathi P, Pradhan AK, Emdad L, Das SK, Guo C, et al. Role of MDA-7/IL-24 a multifunction protein in human diseases. *Adv Cancer Res*. (2018) 138:143–82. doi: 10.1016/bs.acr.2018.02.005
15. Choi Y, Roh MS, Hong YS, Lee HS, Hur WJ. Interleukin-24 is correlated with differentiation and lymph node numbers in rectal cancer. *World J Gastroenterol*. (2011) 17:1167–73. doi: 10.3748/wjg.v17.i9.1167
16. Chang S, Yang J, Chen W, Xie Y, Sheng W. Antitumor activity of an adenovirus harboring human IL-24 in colon cancer. *Mol Biol Rep*. (2011) 38:395–401. doi: 10.1007/s11033-010-0121-3
17. Xu S, Oshima T, Imada T, Masuda M, Debnath B, Grande F, et al. Stabilization of MDA-7/IL-24 for colon cancer therapy. *Cancer Lett*. (2013) 335:421–30. doi: 10.1016/j.canlet.2013.02.055
18. Emdad L, Lebedeva IV, Su ZZ, Sarkar D, Dent P, Curiel DT, et al. Melanoma differentiation associated gene-7/interleukin-24 reverses multidrug resistance in human colorectal cancer cells. *Mol Cancer Ther*. (2007) 6:2985–94. doi: 10.1158/1535-7163.MCT-07-0399
19. Boegel S, Lower M, Bukur T, Sahin U, Castle JC. A catalog of HLA type, HLA expression, and neo-epitope candidates in human cancer cell lines. *Oncoimmunology*. (2014) 3:e954893. doi: 10.4161/21624011.2014.954893
20. Phillips S, Chokshi S, Riva A, Evans A, Williams R, Naoumov NV. CD8(+) T cell control of hepatitis B virus replication: direct comparison between cytolytic and noncytolytic functions. *J Immunol*. (2010) 184:287–95. doi: 10.4049/jimmunol.0902761
21. Panneerselvam J, Srivastava A, Muralidharan R, Wang Q, Zheng W, Zhao L, et al. IL-24 modulates the high mobility group (HMG) A1/miR222 /AKT signaling in lung cancer cells. *Oncotarget*. (2016) 7:70247–63. doi: 10.18632/oncotarget.11838
22. Pradhan AK, Talukdar S, Bhoopathi P, Shen XN, Emdad L, Das SK, et al. mda-7/IL-24 mediates cancer cell-specific death via regulation of miR-221 and the beclin-1 axis. *Cancer Res*. (2017) 77:949–59. doi: 10.1158/0008-5472.CAN-16-1731
23. Persaud L, Mighty J, Zhong X, Francis A, Mendez M, Muharam H, et al. IL-24 promotes apoptosis through cAMP-dependent PKA pathways in human breast cancer cells. *Int J Mol Sci*. (2018) 19:3561. doi: 10.3390/ijms19113561
24. Ishikawa S, Nakagawa T, Miyahara R, Kawano Y, Takenaka K, Yanagihara K, et al. Expression of MDA-7/IL-24 and its clinical significance in resected non-small cell lung cancer. *Clin Cancer Res*. (2005) 11:1198–202.
25. Patani N, Douglas-Jones A, Mansel R, Jiang W, Mokbel K. Tumour suppressor function of MDA-7/IL-24 in human breast cancer. *Cancer Cell Int*. (2010) 10:29. doi: 10.1186/1475-2867-10-29
26. Wang L, Feng Z, Wu H, Zhang S, Pu Y, Bian H, et al. Melanoma differentiation-associated gene-7/interleukin-24 as a potential prognostic biomarker and second primary malignancy indicator in head and neck squamous cell carcinoma patients. *Tumour Biol*. (2014) 35:10977–85. doi: 10.1007/s13277-014-2392-0
27. Ma M, Zhao R, Yang X, Zhao L, Liu L, Zhang C, et al. Low expression of Mda-7/IL-24 and high expression of C-myb in tumour tissues are predictors of poor prognosis for Burkitt lymphoma patients. *Hematology*. (2018) 23:448–55. doi: 10.1080/10245332.2018.1435046
28. Ma M, Zhao R, Yang X, Zhao L, Liu L, Zhang C, et al. The clinical significance of Mda-7/IL-24 and C-myb expression in tumor tissues of patients with diffuse large B cell lymphoma. *Exp Ther Med*. (2018) 16:649–56. doi: 10.3892/etm.2018.6230
29. Anuradha R, George PJ, Hanna LE, Kumaran P, Chandrasekaran V, Nutman TB, et al. Expansion of parasite-specific CD4+ and CD8+ T cells expressing IL-10 superfamily cytokine members and their regulation in human lymphatic filariasis. *PLoS Negl Trop Dis*. (2014) 8:e2762. doi: 10.1371/journal.pntd.0002762
30. Anuradha R, Munisankar S, Dolla C, Kumaran P, Nutman TB, Babu S. Modulation of CD4+ and CD8+ T-cell function by interleukin 19 and interleukin 24 during filarial infections. *J Infect Dis*. (2016) 213:811–5. doi: 10.1093/infdis/jiv497
31. Kumar NP, Moideen K, Banurekha VV, Nair D, Babu S. Modulation of Th1/Tc1 and Th17/Tc17 responses in pulmonary tuberculosis by IL-20 subfamily of cytokines. *Cytokine*. (2018) 108:190–6. doi: 10.1016/j.cyto.2018.04.005
32. Ma Y, Chen H, Wang Q, Luo F, Yan J, Zhang XL. IL-24 protects against *Salmonella typhimurium* infection by stimulating early neutrophil Th1 cytokine production, which in turn activates CD8+ T cells. *Eur J Immunol*. (2009) 39:3357–68. doi: 10.1002/eji.200939678
33. Miyahara R, Banerjee S, Kawano K, Efferson C, Tsuda N, Miyahara Y, et al. Melanoma differentiation-associated gene-7 (mda-7)/interleukin (IL)-24 induces anticancer immunity in a syngeneic murine model. *Cancer Gene Ther*. (2006) 13:753–61. doi: 10.1038/sj.cgt.7700954
34. Ma YF, Ren Y, Wu CJ, Zhao XH, Xu H, Wu DZ, et al. Interleukin (IL)-24 transforms the tumor microenvironment and induces anticancer immunity in a murine model of colon cancer. *Mol Immunol*. (2016) 75:11–20. doi: 10.1016/j.molimm.2016.05.010
35. Sabat R, Ouyang W, Wolk K. Therapeutic opportunities of the IL-22-IL-22R1 system. *Nat Rev Drug Discov*. (2014) 13:21–38. doi: 10.1038/nrd4176
36. Niccolai E, Ricci F, Russo E, Nannini G, Emmi G, Taddei A, et al. The different functional distribution of "Not Effector" T cells (Treg/Tnull) in colorectal cancer. *Front Immunol*. (2017) 8:1900. doi: 10.3389/fimmu.2017.01900
37. Amicarella F, Muraro MG, Hirt C, Cremonesi E, Padovan E, Mele V, et al. Dual role of tumour-infiltrating T helper 17 cells in human colorectal cancer. *Gut*. (2017) 66:692–704. doi: 10.1136/gutjnl-2015-310016
38. Zhang Y, Cobleigh MA, Lian JQ, Huang CX, Booth CJ, Bai XF, et al. A proinflammatory role for interleukin-22 in the immune response to hepatitis B virus. *Gastroenterology*. (2011) 141:1897–906. doi: 10.1053/j.gastro.2011.06.051
39. Jin B, Liang Y, Liu Y, Zhang LX, Xi FY, Wu WJ, et al. Notch signaling pathway regulates T cell dysfunction in septic patients. *Int Immunopharmacol*. (2019) 76:105907. doi: 10.1016/j.intimp.2019.105907
40. Javed A, Leuchte N, Neumann B, Sopper S, Sauermann U. Noncytolytic CD8+ cell mediated antiviral response represents a strong element in the immune response of simian immunodeficiency virus-infected

long-term non-progressing rhesus macaques. *PLoS ONE*. (2015) 10:e0142086. doi: 10.1371/journal.pone.0142086

41. Yu W, Wang Y, Guo P. Notch signaling pathway dampens tumor-infiltrating CD8(+) T cells activity in patients with colorectal carcinoma. *Biomed Pharmacother*. (2018) 97:535–42. doi: 10.1016/j.biopha.2017.10.143
42. Li S, Wang Z, Li XJ. Notch signaling pathway suppresses CD8(+) T cells activity in patients with lung adenocarcinoma. *Int Immunopharmacol*. (2018) 63:129–36. doi: 10.1016/j.intimp.2018.07.033

Conflict of Interest: The authors declare that the research was conducted in the absence of any commercial or financial relationships that could be construed as a potential conflict of interest.

frontiers in Immunology

ORIGINAL RESEARCH
published: 22 January 2020
doi: 10.3389/fimmu.2019.03070

Deciphering the Crosstalk Between Myeloid-Derived Suppressor Cells and Regulatory T Cells in Pancreatic Ductal Adenocarcinoma

Carole Siret[1†], Aurélie Collignon[2†‡], Françoise Silvy[2‡], Stéphane Robert[3], Thierry Cheyrol[4], Perrine André[4], Véronique Rigot[2‡], Juan Iovanna[5], Serge van de Pavert[1], Dominique Lombardo[2], Eric Mas[2‡] and Anna Martirosyan[2‡]*

[1] Aix Marseille Univ, CNRS, INSERM, CIML, Centre d'Immunologie de Marseille-Luminy, Marseille, France, [2] Aix Marseille Univ, INSERM, CRO2, Centre de Recherche en Oncologie biologique et Oncopharmacologie, Marseille, France, [3] Aix Marseille Univ, INSERM, VRCM, Centre de Recherche Vasculaire de Marseille, Marseille, France, [4] Aix Marseille Univ, CEFOS, Centre d'exploration Fonctionnelle Scientifique, Marseille, France, [5] Aix Marseille Univ, CNRS, INSERM, Institut Paoli-Calmettes, CRCM, Centre de Recherche en Cancérologie de Marseille, Marseille, France

Pancreatic ductal adenocarcinoma (PDAC) is a fatal disease with rising incidence and a remarkable resistance to current therapies. The reasons for this therapeutic failure include the tumor's extensive infiltration by immunosuppressive cells such as myeloid-derived suppressor cells (MDSCs) and regulatory T cells (Tregs). By using light sheet fluorescent microscopy, we identified here direct interactions between these major immunoregulatory cells in PDAC. The *in vivo* depletion of MDSCs led to a significant reduction in Tregs in the pancreatic tumors. Through videomicroscopy and *ex vivo* functional assays we have shown that (i) MDSCs are able to induce Treg cells in a cell-cell dependent manner; (ii) Treg cells affect the survival and/or the proliferation of MDSCs. Furthermore, we have observed contacts between MDSCs and Treg cells at different stages of human cancer. Overall our findings suggest that interactions between MDSCs and Treg cells contribute to PDAC immunosuppressive environment.

Keywords: pancreatic cancer, immunosuppression, MDSC, Tregs, immune cell interactions

OPEN ACCESS

Edited by:
Gianluigi Giannelli, National Institute of Gastroenterology S. de Bellis Research Hospital (IRCCS), Italy

Reviewed by:
Pin Wu, Zhejiang University, China
Pierre Busson, Centre National de la Recherche Scientifique (CNRS), France

***Correspondence:**
Anna Martirosyan
anna.martirosyan@haliodx.com

[†] These authors have contributed equally to this work

[‡] Present address:
Aurélie Collignon and Anna Martirosyan, HalioDX, Luminy Biotech Entreprises, Marseille, France
Françoise Silvy, Véronique Rigot, and Eric Mas, Aix Marseille Univ, CNRS, INSERM, Institut Paoli-Calmettes, CRCM, Marseille, France

Specialty section:
This article was submitted to Cancer Immunity and Immunotherapy, a section of the journal Frontiers in Immunology

Received: *13 June 2019*
Accepted: *16 December 2019*
Published: *22 January 2020*

Citation:
Siret C, Collignon A, Silvy F, Robert S, Cheyrol T, André P, Rigot V, Iovanna J, van de Pavert S, Lombardo D, Mas E and Martirosyan A (2020) Deciphering the Crosstalk Between Myeloid-Derived Suppressor Cells and Regulatory T Cells in Pancreatic Ductal Adenocarcinoma. Front. Immunol. 10:3070. doi: 10.3389/fimmu.2019.03070

INTRODUCTION

Pancreatic ductal adenocarcinoma (PDAC) is a lethal malignancy projected to become the 2nd leading cause of cancer-related death in 2030 (1). With more than 337,000 new cases worldwide in 2012, it represents a major public health issue. The time-delayed diagnosis is due to the non-specific symptoms, as well as the lack of early detection markers (2). The median survival after diagnosis of PDAC is 4–6 months. The main reason of this poor prognosis is the resistance to most therapies, including current modalities of immune checkpoint blockade (1, 2). The therapeutic failure might result from the low level of immunogenicity of neoplastic cells, the tumor's robust immunosuppressive mechanisms, or both (2, 3). There is indeed a uniquely immunosuppressive tumor microenvironment (TME) dominant in most human PDAC. Increasing evidence suggests that the TME supports cancer initiation, progression and the development of metastasis (4, 5). The major drivers of the pro-tumorigenic microenvironment in PDAC include a highly fibrotic stroma and an extensive infiltration by immunosuppressive cell populations such as tumor-associated macrophages (TAMs), regulatory T cells (Tregs), and myeloid-derived suppressor cells (MDSCs).

These tumor characteristics provide a barrier to the delivery of cytotoxic agents and limit effector T cell infiltration at the tumor site (4, 5). In addition, the presence of immunosuppressive cells hamper effector T cell recruitment and activation leading to a profound immune dysfunction (6). Thus, it is essential to understand the mechanisms of pancreatic cancer's immune evasion to translate effective immunotherapy in this disease. In this study, we have been particularly interested in MDSCs and Treg cells which represent an essential class of immunoregulatory cells in PDAC.

MDSCs are key regulators of immune responses in many pathophysiological conditions, including cancer (7, 8). MDSCs are a heterogeneous population of cells characterized by their myeloid origin and immature state (9). These cells are endowed with highly suppressive machinery and hamper both innate and adaptive immune responses *via* different mechanisms. For instance, MDSCs are able to inhibit effector T cells leading to the failure of efficient anti-tumor responses (7–9). In the context of PDAC, it has been shown that primary and metastatic PDAC cells secrete factors involved in the induction, recruitment and survival of myeloid cells leading to accumulation of MDSCs (10, 11). These cells are indeed expanded significantly in cancer patients and tumor-bearing animals in PDAC (12). Furthermore, the targeted depletion of an MDSC subset in mouse models of PDAC is shown to unmask the tumor to adaptive immunity (13). Last, but not least the accumulation of MDSCs in the peripheral circulation of patients has been related to the extent of disease, correlates with stage and is associated with a poor prognosis (14–16).

Treg cells are crucial in mediating immune homeostasis and promoting the establishment and maintenance of peripheral tolerance. These cells regulate a diverse array of immune responses in the context of autoimmunity, allergies, microbial infections, and cancers (17, 18). While generally beneficial in the former conditions, their inhibitory activity often antagonizes protective immunity in the latter settings (19). In the context of PDAC an increased Treg prevalence has been demonstrated to be a prognostic factor (12, 20). The recruitment of Tregs occurs early, as demonstrated by their presence in pre-malignant lesions, and their prevalence increases with pancreatic tumor progression (12, 20). Moreover, it has been shown that the depletion of Treg cells in PDAC slows tumor growth and prolongs survival (21, 22).

Recently a degree of crosstalk between these 2 major populations of suppressor cells has been suggested, but incompletely defined in different cancer models (23–26). A variety of mechanisms for these interactions have been proposed, including the ability of MDSCs to promote the *de novo* development/expansion/recruitment of Treg cells (23–26). Although a strong influx of MDSCs and Treg cells has been described in PDAC (12, 20–22), there is no evidence yet on the presence of interactions between these major immunoregulatory cells in pancreatic tumors. Moreover, many unresolved questions remain. For instance, whether Tregs act on MDSCs and shape their functional differentiation remains unclear. All in all, the mechanisms of immunosuppression in different cancers, including PDAC, have not been yet fully studied from the perspective of the interplay between these major immunoregulatory cell populations. In the current study, we have identified and characterized a crosstalk between MDSCs and Treg cells in murine and human PDAC tumors. Our results further revealed that the *in vivo* depletion of MDSCs led to a significant reduction of Treg cells in the pancreatic tumors. We have next investigated the cellular mechanisms of these interactions in PDAC. Our results show that (i) MDSCs are able to induce Treg cells in a cell-cell dependent manner, (ii) Treg cells affect the survival and/or the proliferation of MDSCs. Overall, the modulation of MDSC and Treg cell interactions to alleviate tumor-induced immunosuppression might suggest a new therapeutic solution for the PDAC.

Abbreviations: PDAC, Pancreatic ductal adenocarcinoma; TME, Tumor microenvironment; TAMs, Tumor-associated macrophages; Tregs, Regulatory T cells; MDSCs, Myeloid-derived suppressor cells; TB mice, Tumor-bearing mice; ROS, Reactive Oxygen Species; RT, Room temperature; FCS, Fetal calf serum.

MATERIALS AND METHODS

Ethics Statement

The investigation was conducted in accordance with the French guidelines for animal care and the 2010/63/EU directive of the European Parliament, and was approved by the local ethics committee of Aix-Marseille University and by the Ministère de l'Enseignement Supérieur, de la Recherche et de l'Innovation. The protocols were registered under numbers APAFIS#4396-2016030709341791 and APAFIS#21966-2019091116114397. Mice were daily monitored for any behavioral and physical changes.

Mice and Cell Lines

Eight to 10 week-old C57BL/6J Rj (H-2b) mice were purchased from Janvier (Le Genest-St. Isle, France). The syngeneic tumorigenic murine pancreatic carcinoma cell line Panc02 was cultured in RPMI 1640 10% FCS 100 units/mL penicillin (Invitrogen), 100 μg/mL streptomycin and were tested negative for mycoplasma contamination.

Immunohistofluorescence

Frozen tissue sections were subjected to immunodetection after saturation with PBS 4% BSA. Sections were incubated with primary antibodies diluted in PBS 1% BSA. Gr-1$^+$ and Foxp3$^+$ and TCRγδ$^+$ cells were detected by incubation with the rat anti-Gr-1 (BD Pharmingen), the rabbit anti-Foxp3 (Abcam), and the armenian hamster anti-TCRγδ (Biolegend) antibodies, respectively. After three washes in PBS, samples were incubated for 1 h with either Alexa Fluor 488-, Alexa Fluor 594- (life technologies) or Cy3-conjugated goat (Jackson Immunoresearch) immunoglobulin [Ig], raised against rat, rabbit and armenian hamster Igs, respectively, then washed in PBS. Nuclei were labeled with Draq5 and sections were mounted in ProLong Gold (Invitrogen). Confocal microscopy acquisitions were performed using a Leica SP5 microscope coupled with a Leica scanning device (Leica Microsystems, Mannheim, Germany). Images were recorded with LAS AF Lite acquisition

software and were analyzed with the publicdomain ImageJ software (NIH; http://rsb.info.nih.gov/nih-image/).

Immunohistochemistry

Mouse Tissues

Mouse pancreatic tumors were harvested, frozen in liquid nitrogen and cut into 8 μm thick sections. Frozen slides were incubated 20 min at room temperature (RT), fixed with cold acetone for 10 min at 4°C, air-dried at RT and proceed to staining. Briefly, slides were rehydrated in TBS and endogenous peroxidase activity was blocked with Bloxall solution (Vector laboratories) for 20 min at RT. Primary antibodies (CD4, CD8, Gr-1, and Foxp3 purchased from Abcam) were incubated for 2 h at RT. After washes in TBS, slides were incubated with avidin/biotin/peroxidase complex (Vectastain kit from Vector Laboratories). Antigen detection was performed by incubation with substrate-chromogen 3,3-diaminobenzidine (DAB, Vector Laboratories). Sections were counterstained with Mayer' hematoxylin and mounted with Faramount Mounting Medium, Aqueous (Agilent). Images were captured using a BH-2 Olympus microscope with X20 objective.

Human Tissues

Some tumor samples ($n = 19$) were obtained after pancreatic resection (duodeno-pancreatectomy) from patients diagnosed with PDAC (Gastroenterology and Digestive Surgery departments, Timone Hospital, Marseille, France; CRO2 Agreement DC20131857) between February 2007 and February 2016. All specimens were evaluated by an expert pathologist. Additionally, a pancreas adenocarcinoma tissue array (#PA484; 24 cases) was purchased from Pantomics (Euromedex, France) to complete the collection. This TMA was composed of 3 normal pancreas tissues, 1 islet cells tumor and 20 pancreatic adenocarcinoma (5 stage 1; 11 stage 2; 2 stage 3; and 2 stage 4). All those samples were in duplicate. Overall we analyzed 43 human samples.

Sections (5 μm) of formalin-fixed paraffin embedded tissue were used. After paraffin removal and antigen retrieval, pancreatic tissue sections were incubated with an anti-CD4, anti-CD8, anti-CD15, anti-CD11b, and anti-Foxp3 for 2 h at RT. After washing, slides were proceed as described in the section Mouse tissues. For double staining, we used the Polink DS-MR-Hu C1 Kit (GBI Labs) to detect the anti-Foxp3 in GBI-Permanent Red (Red) and the anti-CD11b in Emerald (Green).

Orthotopic Tumor Induction

Subconfluent cultures of Panc02 cells were harvested using a 10% trypsin solution, washed twice in PBS and resuspended as single-cell suspension in matrigel. The pancreas of anesthetized mice was exposed after laparotomy. Panc02 cells were injected directly into the pancreas (0.8×10^6 cell/100 μl matrigel) using a tuberculin syringe. After suturing, mice received sub-cutaneous injections of analgesic (Buprenorphine 0.1 mg/kg) after the operation and again a few hours later.

Cell Suspension Preparation

Tumors were harvested 3 weeks after tumor cell inoculation and dissected into fragments with scissor followed by incubation with collagenase Type I-A from clostridium histolyticum (1 mg/ml in RPMI-2% FCS, Sigma Aldrich) for 30 min at 37°C under agitation. Cell suspensions were mixed every 10 min during agitation. The suspension was filtered through 70 μm strainer to remove macroscopic debris. Red blood cells were lysed using ACK Lysis buffer (Invitrogen) and cell suspension was filtered through a 30 μM strainer before flow cytometry staining and cell isolation.

Antibodies and Flow Cytometry

The following antibodies were used for flow cytometry analysis: CD45-A700, CD3-A488, CD25-APC/eFluor780, LY6C-A488, CD11b-PE/Cy5, Ly-6G(Gr-1)-APC, CD69-APC/eFluor780, CD62L-PE/Cy5, LAP(TGF-β1)-PE/Cy7, CD115-APC/eFluor780, CD127-APC/eFluor780, CCR5-PE, and isotype controls (Rat IgG1 K Isotype Control PE/Cy7, Rat IgG2b K Isotype Control PE, Rat IgG2a K Isotype Control eFluor450, Rat IgG2a K Isotype Control PE) were purchased from eBioscience; Ly-6G-PE, CD4-PE/CF594, CD8a-V450 from BD Biosciences, CD124-PE/Cy7, CD40-PB, B7H1-BV421, CD103-APC/Cy7, CTLA4-BV421, CD45-PB, F4/80-PE/Dazzle™ 594 from Ozyme.

For intracellular staining of cytokines, cells were incubated for 4 h at 37°C with monensin (GolgiStop, BD Pharmingen) before the staining. Isolated cells from the spleens or tumors were incubated with anti-CD16/CD32 antibody (BD Pharmingen) to prevent non-specific antibody binding. Surface antigens were stained with the antibodies diluted in PBS 5% FCS 2 mM ETDA and incubated for 20 min at 4°C. Dead cells were excluded using LIVE/DEAD Fixable Aqua Dead Cell Stain (Invitrogen). Intracellular stainings were performed using the Foxp3/Transcription Factor Staining Buffer Set (Ebioscience). Annexin V (Ozyme) and 7AAD (Beckman Coulter) stainings was performed according to the manufacturer's recommendations. Multiparameter analysis were performed on a Gallios flow cytometer (Beckman Coulter) and analyzed with FlowJo software (Tree Star). All flow cytometric analysis of immune cells was performed on live $CD45^+$ cells after excluding doublets.

Immune Cells Isolation

MDSCs were purified either from the spleen or the tumor using the Myeloid-Derived Suppressor Cell Isolation mouse Kit (Miltenyi Biotec) according to the manufacturer's protocol. $CD4^+CD25^+$ and $CD4^+CD25^-$ T cells were magnetically enriched from either the spleen or the tumor using $CD4^+CD25^+$ Regulatory T Cell Isolation Kit, mouse (Miltenyi Biotec). $CD4^+$ T cells were harvested after the first step of $CD4^+CD25^+$ cell's isolation. $CD8^+$ T cells were isolated from the spleen of naive mice with EasySep™ Mouse Naïve $CD8^+$ T Cell Isolation Kit (StemCell) according to manufacturer's instructions.

T Cell Proliferation Assay

Responder cells ($CD8^+$ or $CD4^+CD25^-$ T cells) were labeled with 2.5 μM CFSE (5×10^6 cell/ml RPMI; 10 min at 37°C

under agitation). CFSE labeled cells were then plated onto round bottom 96-well plates coated with CD3 antibodies (8 μg/ml; BD biosciences) in culture medium RPMI- PS-10% heat inactivated FCS, 50 μM β-Mercaptoethanol, 1% non-essential amino acids, and 1% sodium pyruvate. Purified suppressor cells (MDSCs or $CD4^+CD25^+$) were added in indicated ratios and plates were incubated at 37°C. The proliferation was measured by assessing dilution of CFSE by flow cytometry after 48 h ($CD8^+$) or 72 h ($CD4^+CD25^-$) with CD3/CD28 stimulation (CD28 1 μg/ml). Controls were wells with responder cells without suppressor cells. Treg suppression assay were performed in the presence of IL-2 (50 U/ml).

Detection of ROS and Arginase-1 Activity

The cell permeant reagent 2′,7′-dichlorofluorescin diacetate (DCFDA; Thermo Fisher Scientific) was used for the measurement of ROS production by MDSCs. 1×10^5 purified MDSCs or $CD8^+$ cells were incubated at 37°C in PBS without serum in the presence of DCFDA (2 μM) for 10 min, washed twice with cold PBS, before flow cytometry staining and analysis. Since the non-labeled cells cultured alone showed some auto-fluorescence, the ratio between the mean DCFDA fluorescence and the mean of cells auto-fluorescence was calculated.

For measuring arginase 1 activity, 2×10^5 purified MDSCs were lysed on ice in 50 μl lysis buffer (0.1% Triton X100, 100 μg/ml pepstatin, 100 μg/ml aprotinin, and 100 μg/ml antipain). Arginase 1 activity was assessed in supernatant of frozen cell lysates using QuantichromTM Arginase assay kit (cat# DARG-100, BioAssays Systems) according to manufacturer' instructions.

Videomicroscopy Acquisitions

A Lab-Tek chambered coverglass was coated with FCS. Purified $CD4^+CD25^+$ cells are loaded by 20 μM of green cell tracker during 30 min at 37°C. These cells are deposit with purified tumoral MDSCs with a 1/2 ratio in a same lab-tek well. Cells were then placed in a temperature- and CO_2-controlled chamber mounted on an Olympus IX83 inverted microscope and incubated for 10 h. Images were captured every 20 min using an orca-flash4 camera [Hamamatsu] with a ×40 objective. All interactions persistent more than for 40 min, as well as transient interactions for 3 wells were quantified.

Light Sheet Microscopy

Immunofluorescence Tumor Wholemount Stainings

Tumors were dissected and fixed overnight in 0.4% PFA/PBS at 4°C. Prior antibody staining, tumors were permeabilized (0.4% Triton X100, 1% milk/PBS) and subsequently blocked in block solution (0.4% Triton X100, 1% milk, 5% serum/PBS). Wholemount stainings were performed by using anti-alpha smooth muscle actin directly coupled with Alexa488, anti-Foxp3, and anti-Gr-1 as primary antibodies and Alexa-dye coupled secondary antibodies diluted in block solution. Following each staining step, samples were washed several times in PBS-Tx (0.42% Triton X100/PBS) and in PBS.

Optical Clearing and Wholemount Acquisition

Tumors were cleared before acquisition on the La Vision Ultramicroscope II (LaVision BioTec, Bielefeld, Germany). After dehydration in methanol (20, 40, 60, 80, 100%, each step 1 h and overnight in 100%, samples were optically cleared first in methanol/BABB (ratio 1:1) (benzyl alcohol:benzyl benzoate, ratio 1:2) 8 h and finally in BABB overnight. Stacks were captured with a step size of 4 μm and magnification 1X. 3D reconstruction, cell counting and analysis of cell interactions are performed by using IMARIS software (Version 9.1.0, Bitplane). The Matlab function associated with Imaris software quantified the number of cells in interaction. Since lymphocytes are 8–10 μm in diameter and myeloid cells are ∼20–30 μm in diameter, here we considered that MDSCs and Treg cells are in interaction if the distance between their centroids is ≤20 μm.

T Cell/MDSC Coculture

$CD4^+$ T Cell/MDSC Coculture

MDSCs isolated from tumor were cocultured with $CD4^+$ T cells purified from TB mice spleen at ratio (MDSCs:$CD4^+$ T cells) 3:1 for 4 days in culture medium with CD3/CD28 stimulation. Co-cultures were performed in conventional dishes (96 wells U-bottom plate) or using *Transwell* chamber (0.4 μm pore) to separate the 2 cell populations; MDSCs and $CD4^+$ T cells were added in the upper and lower chambers, respectively. The percentage of $CD4^+Foxp3^+$ cells was evaluated by flow cytometry.

$CD4^+CD25^+$ Treg Cell/MDSC Coculture

MDSCs isolated from tumor were cocultured with $CD4^+CD25^+$ cells purified from spleen or tumor onto round bottom 96-well plates in culture medium with CD3/CD28 stimulation at indicated ratios. The viability of MDSCs was analyzed by flow cytometry after 24 and 48 h of co-culture and the percentage of $CD4^+Foxp3^+$ cells was evaluated after 4 days.

MDSC Depletion

To deplete MDSCs *in vivo*, mice received 2 *i.p.* injections of RB6-8C5 antibody (anti-Gr-1, 200 μg/mice diluted in sterile PBS, BioXCell) 11 and 14 days after tumor cells inoculation. Control mice received PBS or isotype control antibody (clone LTF-2, BioXCell). Animals were euthanized 3 days after the second injection, spleens and tumors were harvested to determine the efficiency of Ab-mediated depletion. For comparisons between two groups, statistical analyses were performed using a Student's *t*-test and $p < 0.05$ was considered significant.

RESULTS

PDAC Is Characterized by a Strong Accumulation of Immunosuppressive Cell Populations

An orthotopic mouse model of pancreatic cancer (27), which mimics human PDAC with regard to histological appearance, and the pattern of the disease, was used in this study. By using immunohistochemistry and multiparametric flow cytometry methods, we have performed a detailed phenotypical analysis

of the immune cell populations following tumor induction (**Figure 1**). A strong influx of immune cells characterized by an extensive infiltration of MDSCs and Treg cells in the pancreas (**Figure 1**) and the spleen (**Supplementary Figure 1**) of tumor-bearing (TB) mice was observed.

MDSCs consist of two major subsets based on their phenotypic and morphological features: granulocytic Gr-MDSCs ($Ly6G^+Ly6C^{low}$) and monocytic Mo-MDSCs ($Ly6G^-Ly6C^{high}$). At first, we examined the expression of surface molecules either associated with MDSCs (F4/80 and CD124) or involved in MDSCs-mediated immunosuppression (B7H1 and CD40) on $CD11b^+Gr\text{-}1^+$ cells in tumors (**Figure 1C**) and spleens (**Supplementary Figure 1**). We could observe a strong expression of B7H1 and CD40 on both MDSC subsets derived from tumors. However, the upregulation of F4/80 and CD124 was more substantial on Mo-MDSCs (**Figure 1C**). In order to study the systemic immune response following tumor induction, we analyzed the phenotype of these MDSC subsets. Splenic Mo-MDSCs derived from TB mice upregulated F4/80, CD124, and CD40 compared to Gr-MDSCs (**Supplementary Figure 1B**). Both subsets showed a strong expression of B7H1 at their cell surface (**Supplementary Figure 1B**).

As shown in the **Figure 1D** and **Supplementary Figure 2**, the expression of Treg-associated molecules and functional markers was then analyzed. The transcriptional factor Foxp3 serves as a lineage specification factor of murine Treg cells. Currently the most commonly used markers for Treg identification and characterization are CD4, Foxp3, CD25 (IL-2R alpha), and CD127 (IL-7R alpha). **Figure 1D** demonstrates that most of tumoral $CD4^+Foxp3^+$ Treg cells were $CD25^{high}CD127^{low}$. Tregs manifest their immunosuppressive function through the secretion of immunosuppressive soluble factors such as TGF-β, as well as cell contact mediated regulation *via* molecules like CTLA-4 (17, 18). Our data shows that Treg cells derived from tumors have an increased expression of CTLA4 and TGF-β at their surface as compared with splenic counterparts (**Figure 1D** and **Supplementary Figure 2A**). We have then studied the amounts of CD103 (Integrin α_E) that has been reported to be a hallmark of tumor-infiltrating regulatory T cells in colon cancer (28). Recent studies have described $CD103^+$ Tregs as potent suppressors of anti-tumor immune responses in TB mice (28). In our model of murine PDAC, 70% of tumoral Treg cells expressed high levels of CD103 (**Figure 1D**). It has been shown that chemokine receptors CCR5 could mediate trafficking of Treg to PDAC tumors (21). Cells within the TME, such as pancreatic stellate cells and tumor-infiltrating MDSCs, have also been reported to express high levels of Treg cell chemotactic factors, including CCL5 (20). We examined the expression of these chemokine receptors on $CD103^+$ Tregs in the tumors and spleen of PDAC mice. As show in **Figure 1D**, 20% of tumoral Treg cells up-regulated CCR5 at their surface as compared with splenic counterparts. Moreover, we have observed that at least 60% of $CD4^+Foxp3^+CCR5^+$ cells exhibited high surface amounts of CD103, while at least 30% of those cells upregulated CTLA4 (data not shown). In contrast, the expression levels of CTLA4, CD103 and CCR5 on splenic Treg cells from TB mice (**Supplementary Figure 2A**) were reduced as compared with tumor infiltrating Treg cells (**Figure 1D**).

In parallel, the recruitment and the activation of $CD4^+$ T and $CD8^+$ T cells was analyzed (**Figure 1E**). A low infiltration of both cell populations was observed in the tumors of PDAC mice. To determine whether the intratumoral T lymphocytes show evidence of activation and thus potentially contributed to efficient antitumor immunity, we further assessed the surface marker expression (CD62L and CD69) and the production of IFN-γ (**Figure 1E**). The latter is an essential cytokine in anti-tumoral immunity. While the expression of CD62L is rapidly lost upon activation, the CD69 molecule is induced on activated T cells. More than 88% of intratumoral $CD4^+$ T and $CD8^+$ T cells from PDAC mice strongly down-regulated CD62L (**Figure 1E**). Moreover, the expression of CD69 at the surface of 24% of $CD4^+$ lymphocytes and 33% of $CD8^+$ T cells was detected. Since phenotypic markers cannot conclusively determine if infiltrating T cells are truly naive or functionally inactivated, we have then measured the intracellular levels of effector molecule IFN-γ. Our data show that 10% of $CD4^+$ T and 18% of $CD8^+$ T cells from tumor produce IFN-γ suggesting an activated phenotype (**Figure 1E**). In contrast, splenic $CD4^+$ T and $CD8^+$ T cells showed low levels of CD69 expression (**Supplementary Figure 2B**). Furthermore, the production of IFN-γ by tumoral $CD4^+$ T cells was higher as compared to their splenic counterparts (**Figure 1E** and **Supplementary Figure 2B**).

Overall, our data indicate a strong influx of immune cells ($CD45^+$) following tumor induction in the pancreas of PDAC mice. We could observe an extensive myeloid cell ($CD11b^+Gr\text{-}1^+$) infiltration, as well as a strong recruitment of functionally active Treg cells into the pancreas of tumor-bearing mice. Furthermore, we identified different phenotypes of Treg cells for the expression of functional molecules depending whether the local or systemic immune responses were studied. Small numbers of activated effector T cells were present in the PDAC mice.

Thus, consistent with previous data in the genetically engineered mouse model of pancreatic cancer (KPC mice) (12), we have found that PDAC is characterized by a strong accumulation of immunosuppressive cell populations (MDSCs, Treg cells) associated with low levels of activated $CD4^+$ and $CD8^+$ T cells.

MDSCs and Treg Cells From Pancreatic Tumors Are Able to Suppress Effector Responses

MDSCs have been shown to enhance tumor growth by inhibiting immune responses and T cell proliferation (9). To determine the suppressive potential of this population, isolated $CD11b^+Gr\text{-}1^+$ cells either from the spleen of naïve mice (MDSC SN) or the spleen (MDSC STB) and pancreas (MDSC PTB) of tumor-bearing mice were incubated with $CD8^+$ T cells in both proliferation and apoptosis assays. As shown in the **Figure 2A**, at a 2:1 myeloid-to-T cell ratio, MDSCs derived from tumors (MDSC PTB) slightly decreased T cell proliferation. Moreover, at the higher myeloid-to-T cell ratios observed *ex vivo* in mice with PDAC, tumoral MDSCs exhibited a strong ability to suppress T cell proliferation in a dose-dependent manner (**Figure 2A**). In contrast, $CD11b^+Gr\text{-}1^+$ cells isolated from the spleen of naïve

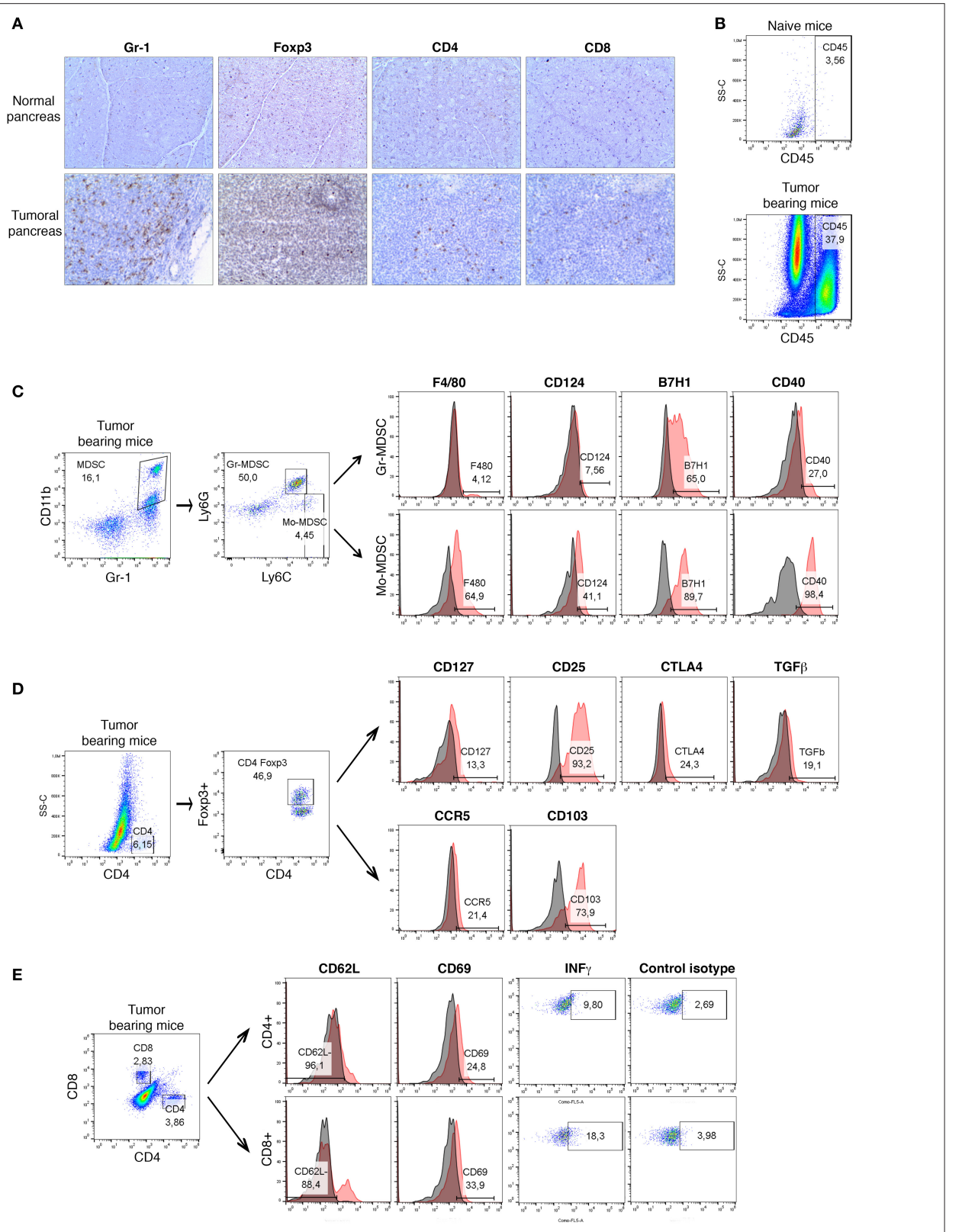

FIGURE 1 | A detailed phenotypical analysis of the immune cell populations in orthotopic mouse model of pancreatic cancer. Panc02 cells were injected in the pancreas of C57BL/6 mice ($n = 5$) and tumors were harvested 3 weeks post- inoculation. **(A)** Representative IHC analysis of Gr-1 (granulocytes), CD4, CD8, and Foxp3 (regulatory T cells) on normal pancreas ($n = 3$) and on pancreatic tumor ($n = 5$) frozen sections. Original magnification x100. Flow cytometry analysis **(B)** of

(Continued)

FIGURE 1 | $CD45^+$ immune cells in normal pancreas and pancreatic tumors, **(C)** of surface molecules F4/80, CD124, CD40, and B7H1 on Gr-MDSC ($CD11b^+Gr\text{-}1^+Ly6G^+Ly6C^{low}$) and Mo-MDSC ($CD11b^+Gr\text{-}1^+Ly6G^-Ly6C^{high}$) in pancreatic tumors, **(D)** of surface molecules CD25, CD127, CCR5, CTLA4, TGF-β, and CD103 on Treg cells ($CD45^+CD4^+Foxp3^+$) in tumors, **(E)** of activation markers CD62L and CD69, as well as the intracellular expression of IFN-γ on $CD4^+$ and $CD8^+$ T cells in tumors. Gray histograms represent isotype control and red histograms specific staining as indicated. Percentage of positive cells are shown. Three independent experiments have been performed with similar results. Representative dot plots and histograms for one of these experiments are shown. See also **Supplementary Figures 1, 2**.

or TB mice did not show any suppressive capacity (**Figure 2A**). Tumoral MDSCs also induced apoptosis of activated T cells (**Figure 2B**). Thus, MDSCs from pancreatic tumors can both suppress T cell proliferation and promote T cell death.

We next examined the presence of MDSCs functional molecules (arginase-1, ROS) which are essential for the immunosuppressive capacity of these cells (**Figure 2C**). We could observe an important up-regulation of ROS by MDSCs from PDAC tumors in contrast to $CD11b^+Gr\text{-}1^+$ cells isolated either from the spleen of naïve or TB mice (**Figure 2C**). Moreover, the tumoral MDSCs showed 3-fold more arginase-1 activity than their splenic counterparts (**Figure 2C**).

We then investigated the suppressive function of the other major immunoregulatory population in PDAC, the Treg cells (**Figure 2D**). Isolated $CD4^+CD25^-$ splenic T cells from PDAC mice were used as responders after *in vitro* CD3/CD28 stimulation. We then added isolated autologous tumoral $CD4^+CD25^+$ T cells and found that they were able to suppress CD3-induced proliferation of responder cells in a dose-dependent manner (**Figure 2D**). In these suppression assays, we identified Treg as $CD4^+CD25^+$ cells rather than $CD4^+Foxp3^+$ cells, because staining cells for Foxp3, a transcription factor, requires permeabilization. Since CD25 is also expressed by activated T cells, we evaluated CD25 expression on non-Treg populations (i.e., $CD4^+Foxp3^-$ T cells) in the pancreas of TB mice. In contrast to the majority of $CD4^+Foxp3^+$ T cells from the tumoral pancreas that expressed CD25, <30% on average of $CD4^+Foxp3^-$ T cells were $CD25^+$ in these mice (data not shown). These findings confirm the minimal activation status of effector T cells in these pancreatic neoplasms.

To summarize, our findings reveal that tumoral MDSCs display a strong suppressive capacity characterized by the inhibition of effector $CD8^+$ T cells proliferation, the induction of $CD8^+$ T cell death, as well as the production of functional molecules (arginase 1, ROS). Moreover, we have shown that Treg cells isolated from the tumors were able to suppress the proliferation of $CD4^+$ T cells.

Direct Interactions Between MDSCs and Treg Cells in PDAC

The interactions between Treg cells and MDSCs in different cancer models have been proposed to play a critical role in shaping the tumoral immunosuppressive environment. However, there is no evidence so far whether this crosstalk involves direct interactions between the two classes of immunoregulatory cells. To determine whether there are interactions between MDSCs and Treg cells in PDAC, we employed multicolor immunofluorescence imaging on tumor sections (**Figure 3**). We first determined the prevalence within the TME of cells expressing Foxp3, the lineage specification transcription factor of Treg cells, as well as of cells expressing Gr-1, defining the MDSC populations (**Figure 3A**). $Gr\text{-}1^+$ and $Foxp3^+$ cells were absent in the normal pancreas, but abundantly present within the neoplastic lesions of PDAC mice. The immune staining of tumor sections showed that some $Foxp3^+$ cells are located in close proximity to cells expressing Gr-1 (**Figure 3A**).

To further study MDSCs/Tregs interplay, we have used light sheet fluorescent microscopy (LSM), which allows long-term live 3D imaging of organism models. In our study, we have used LSM for the 3D imaging of cell interactions in whole tumors which is technically challenging and has never been reported. Since only 4% of tumor-infiltrating $CD45^+$ cells are positive for CD4 (**Figure 1E**) and only 50% of those are Treg cells (**Figure 1D**), the interactions between MDSCs and Treg cells are rare events to record and quantify. LSM technology applied to the whole pancreatic tumors allowed us to observe some of $Foxp3^+$ Treg cells to directly contact $Gr\text{-}1^+$ cells (**Figure 3B** and **Supplementary Video 1**). The quantification of these interactions has been performed on 3 different tumors (*ex vivo*) by using IMARIS software (**Figure 3C**). Consistent with the co-localization pattern observed on tumor sections (**Figure 3A**), we could observe more than 15 interactions between Treg cells and MDSCs in each analyzed PDAC tumor (**Figure 3C**). To highlight the real significance of MDSC and Treg interactions, we have to analyze their dynamic during tumor formation and progression. We have therefore quantified these interactions 1, 2, 3, and 4 weeks post-tumor induction. To do so, the tumors have been harvested at these different time points and both immunofluorescence and LSM imaging (*ex vivo* tumors) were performed. The immunofluorescence data (**Supplementary Figure 4A**) and LSM videos (**Supplementary Videos 4–7**) show an increase of MDSC and Treg cell interactions 2 weeks post-tumor induction (**Supplementary Figures 4A,B**, **Supplementary Videos 4**, **5**). The numbers of co-localizing cell populations reach a peak 3 weeks after tumor inoculation (**Supplementary Figures 4A,B**, **Supplementary Video 6**). Interestingly, at later time points (4 weeks post-tumor inoculation) we have observed an accumulation of MDSC in clusters and outside of the core tumor, while Treg cells are still found inside the tumor (**Supplementary Figures 4A**, **5**, **Supplementary Video 7**). There were fewer MDSC and Treg interactions at this stage of tumor progression. These qualitative LSM observations were quantified and confirmed as illustrated in the **Supplementary Figure 4B**. Moreover, no similar interactions were observed between MDSCs and γδT cells in the TME by using the same methodology (**Supplementary Figure 6**). Overall, our findings revealed a

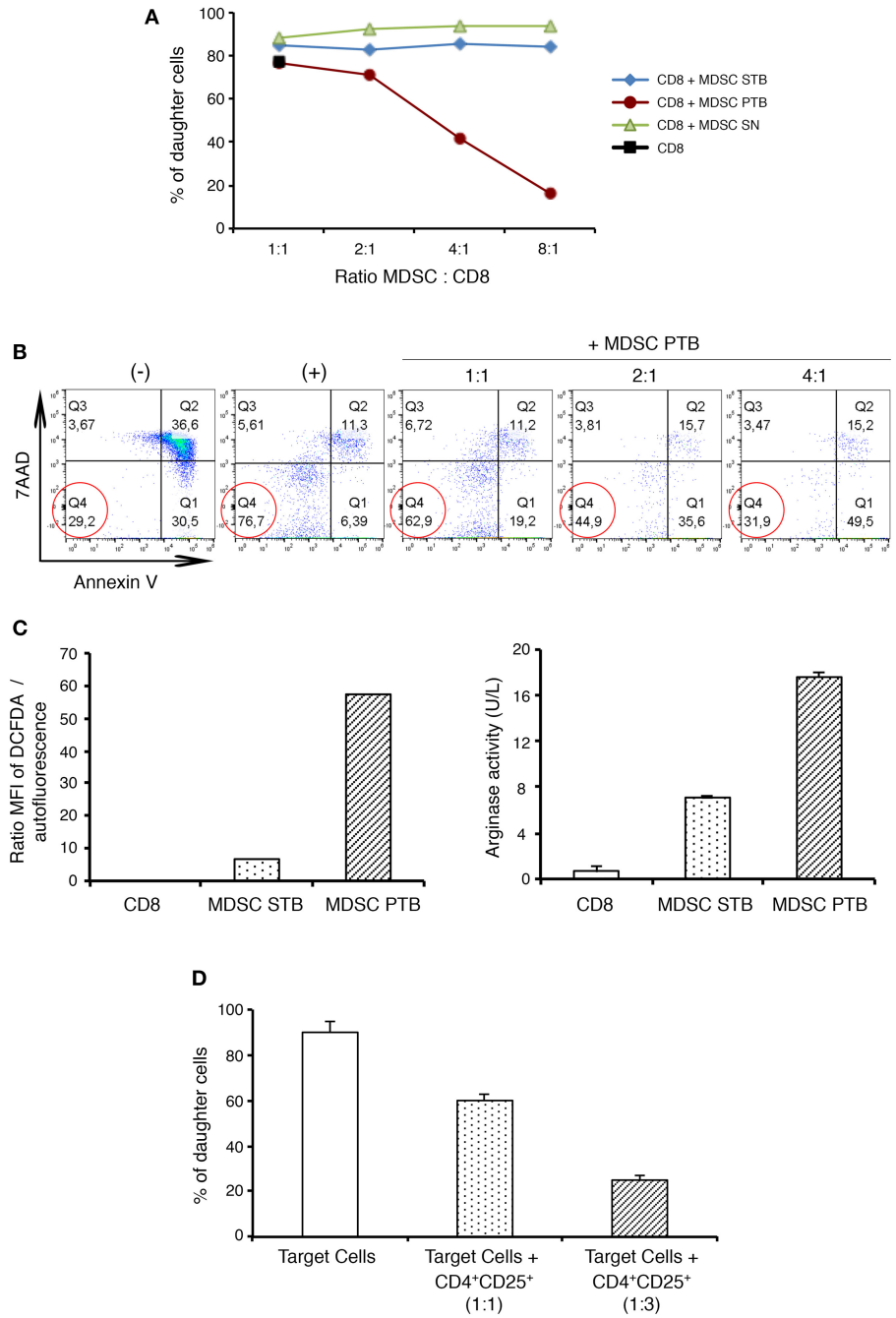

FIGURE 2 | Functional characterization of MDSCs and Treg cells in PDAC. $CD8^+$ T cells proliferation is suppressed by tumoral MDSCs. **(A)** CFSE labeled $CD8^+$ T cells were cultured with MDSCs isolated either from naive spleen (MDSC SN) or from tumor-bearing mice spleen (MDSC STB) or from tumor (MDSC PTB) at different ratios. The percentage of $CD8^+$ daughter cells was evaluated by flow cytometry after 48 h of culture with CD3/CD28 stimulation. **(B)** Tumoral MDSCs induce the death of $CD8^+$ T cells *ex vivo*. $CD8^+$ T cells were stimulated by CD3/CD28 and cultured with MDSCs isolated from tumor (MDSC PTB). Lymphocytes were then stained with cell death markers such as 7AAD and Annexin V. (–) no stimulation; (+) CD3/CD28 stimulation. **(C)** Production of ROS and arginase by MDSCs isolated either from the spleen (MDSC STB) or the tumor (MDSC PTB) of PDAC mice. $CD8^+$ T cells were used as control. Cell lysates were analyzed for arginase 1 activity by measuring the ability to convert L-arginine to urea as describe in Materials and Methods. ROS production was determined by the production of fluorescent DCFDA as described in Materials and Methods. **(D)** Naive $CD4^+CD25^-$ T cells (Target cells) proliferation is suppressed by tumoral Tregs. CFSE labeled $CD4^+CD25^-$ T cells were cultured with Treg ($CD4^+CD25^+$) cells isolated from tumor. After 72 h of culture in presence of CD3/CD28 stimulation the percentage of $CD4^+$ daughter cells was evaluated by flow cytometry.

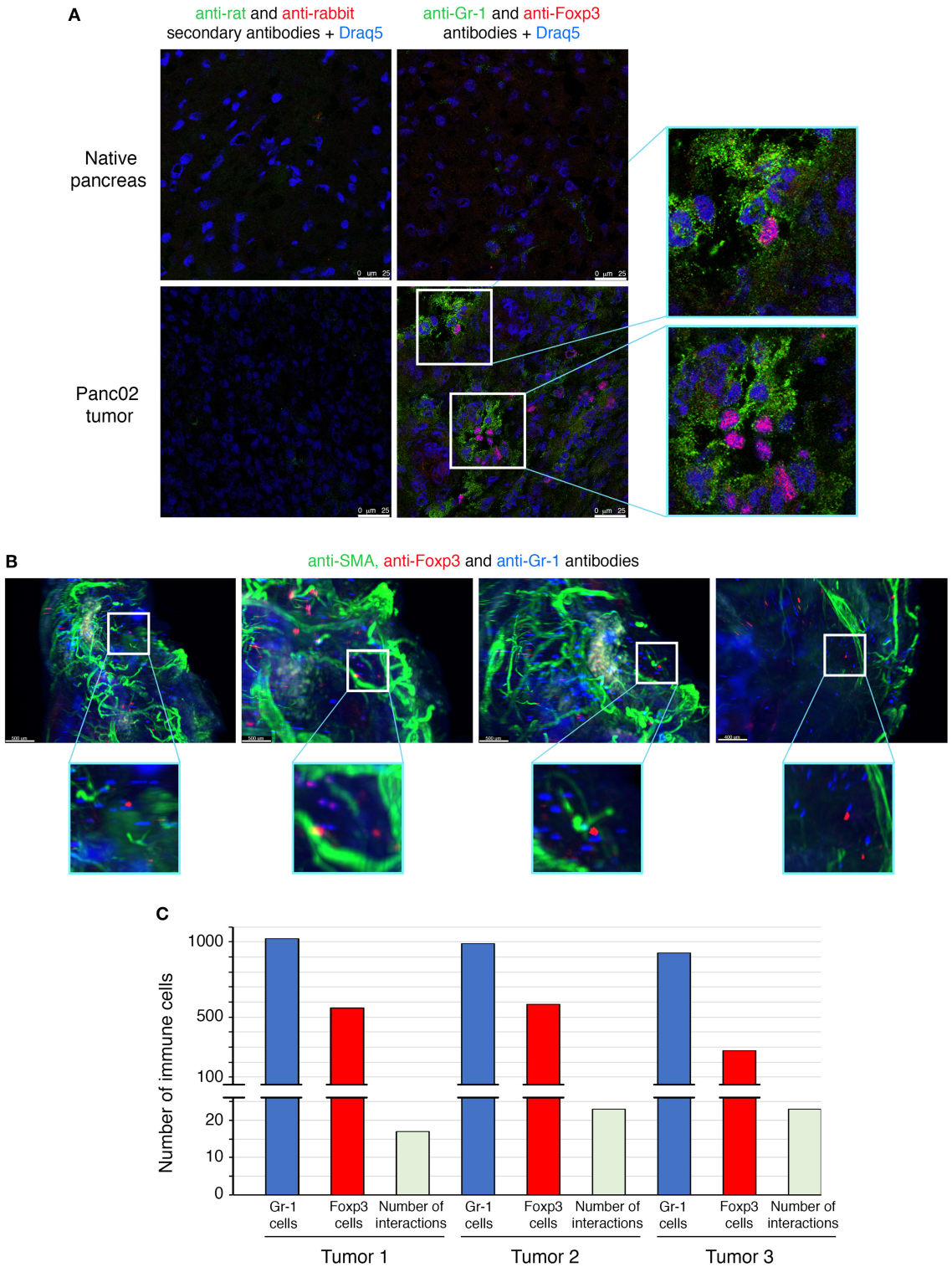

FIGURE 3 | Direct interactions between MDSCs and Treg cells in orthotopic mouse model of pancreatic cancer. Panc02 cells were injected in the pancreas of C57BL/6 mice and tumors were harvested 3 weeks post-inoculation. **(A)** Representative IHF (confocal microscopy) analysis of Gr-1 (MDSCs in green) and Foxp3 (Treg cells in red) on normal pancreas and on pancreatic tumor frozen sections. The nuclei (in blue) are stained with Draq5, a fluorescent DNA marker. Zooms show proximity between the different immune cells. Scale bar 25 μm. **(B)** Light sheet microscopy analysis of Gr-1 (MDSCs in blue) and Foxp3 (Treg cells in red) on whole cleared pancreatic tumor. Zooms show closed contacts between the two populations. Blood vessels are stained with a pericyte marker, the alpha-smooth actin (in green). Scale bar 500 μm. **(C)** Histogram represents quantification of interactions whole cleared tumors calculated with a matLab function associated with the Imaris software. See also **Supplementary Figure 3** and **Supplementary Videos 1–3**.

direct physical contact between MDSC and Treg cell in whole murine pancreatic tumors.

In order to evidence these physical interactions between Treg cells and MDSCs, we have performed videomicroscopic analysis (**Supplementary Figure 3**, **Supplementary Videos 2**, **3**). Treg ($CD4^+CD25^+$) cells purified both from spleen and pancreas of tumor-bearing mice were incubated with tumoral MDSCs and the co-cultures monitored every 20 min (**Supplementary Figure 3A**). Moreover, the persistent or transient interactions were quantified (**Supplementary Figure 3B**). Our data demonstrates physical interactions between Treg ($CD4^+CD25^+$) cells and MDSCs in PDAC.

To evaluate the influence of MDSCs on accumulation of Tregs cells *in vivo*, we depleted Gr-1^+ cells in PDAC mice (**Figure 4**). The injection of anti-Gr-1^+ antibody resulted in near complete elimination of MDSCs in spleens and pancreas of PDAC mice as assessed by flow cytometry (**Figure 4A**). Tumor masses did not generally decrease in size during this treatment window (not shown). Remarkably, *in vivo* depletion of Gr-1^+ cells in tumor-bearing mice led to a significant reduction in Treg cells ($CD4^+Foxp3^+$) in the pancreatic tumors (**Figure 4B**).

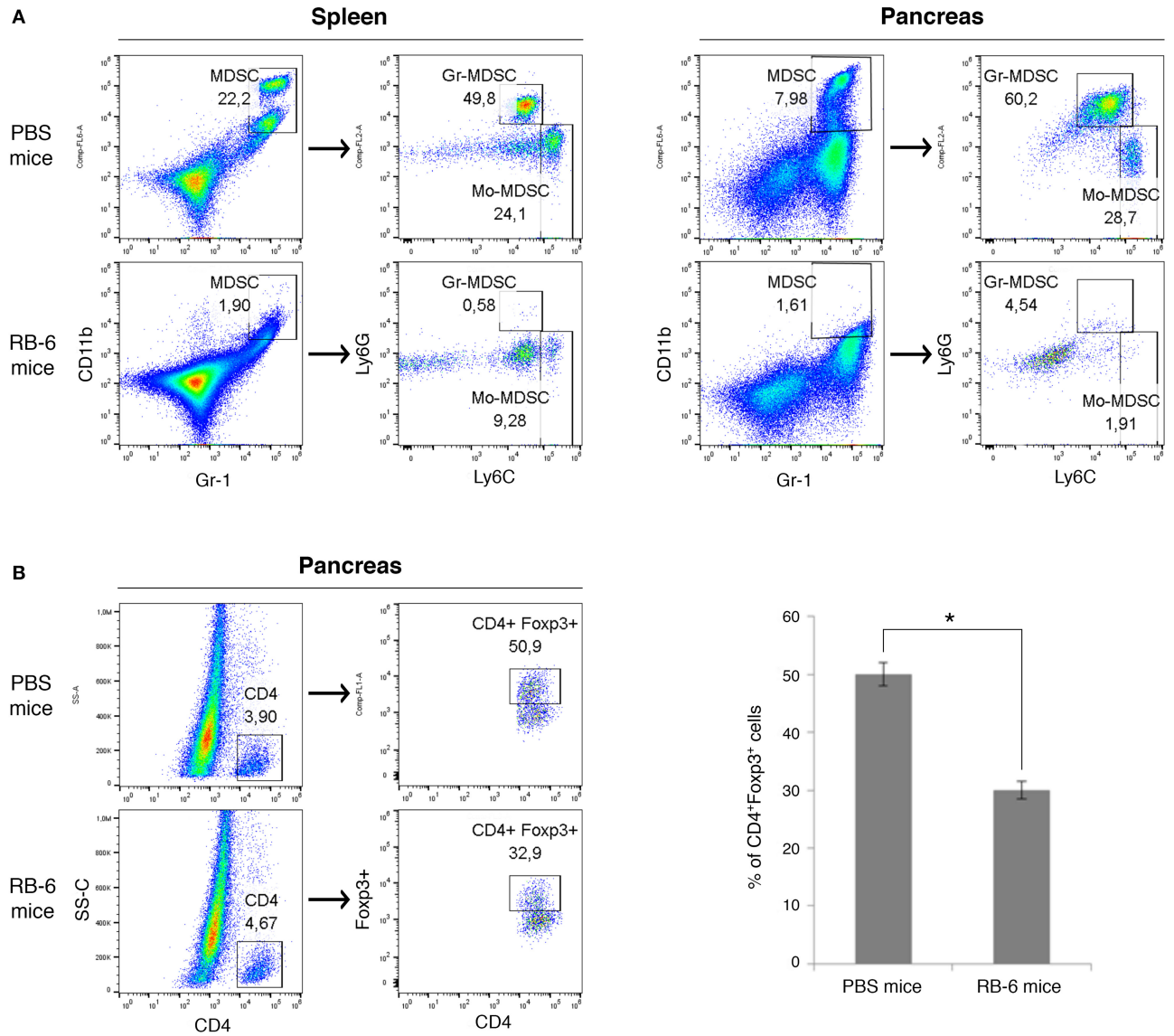

FIGURE 4 | Systemic depletion of MDSCs inhibits the recruitment of $Foxp3^+$ Tregs in pancreatic tumors. Mice were injected with Panc02 tumor cells on day 0 and Gr-1^+ cells were depleted on day 15 and 18 with intraperitoneal injection of anti-RB6 antibody (RB-6 mice). Control mice received injection of PBS (PBS mice) or isotype control antibody. Spleens and tumors were harvested 3 weeks after PDAC induction. The percentage of splenic and pancreatic MDSCs ($CD11b^+$Gr-1^+), MDSC sub-populations **(A)** and Treg cells ($CD4^+Foxp3^+$) **(B)** was evaluated by flow cytometry. Percentage of positive cells are shown. The results represent one of three independent experiments with similar data, $^*p < 0.05$.

In summary, our findings show that the systemic depletion of MDSCs inhibits the recruitment and/or induction of Foxp3$^+$ Tregs in pancreatic tumors.

A Cell-Cell Dependent Crosstalk Between Tumoral MDSCs and Treg Cells

We further investigated the cellular mechanisms of MDSC and Treg interactions in PDAC (**Figure 5**). Several studies have described the ability of MDSCs to promote the *de novo* development/expansion/recruitment of Treg cells in different tumor settings (23–26). To determine whether MDSCs in PDAC possess this ability, *ex vivo* co-culture assays were carried out (**Figures 5A,B**). We incubated either purified CD4$^+$ T cells or Treg cells with tumoral MDSCs at 1:3 ratio (**Figure 5A**). After 4 days of co-culture, we could observe in both conditions tested an increase of Treg cells in presence of tumoral MDSCs (**Figure 5A**).

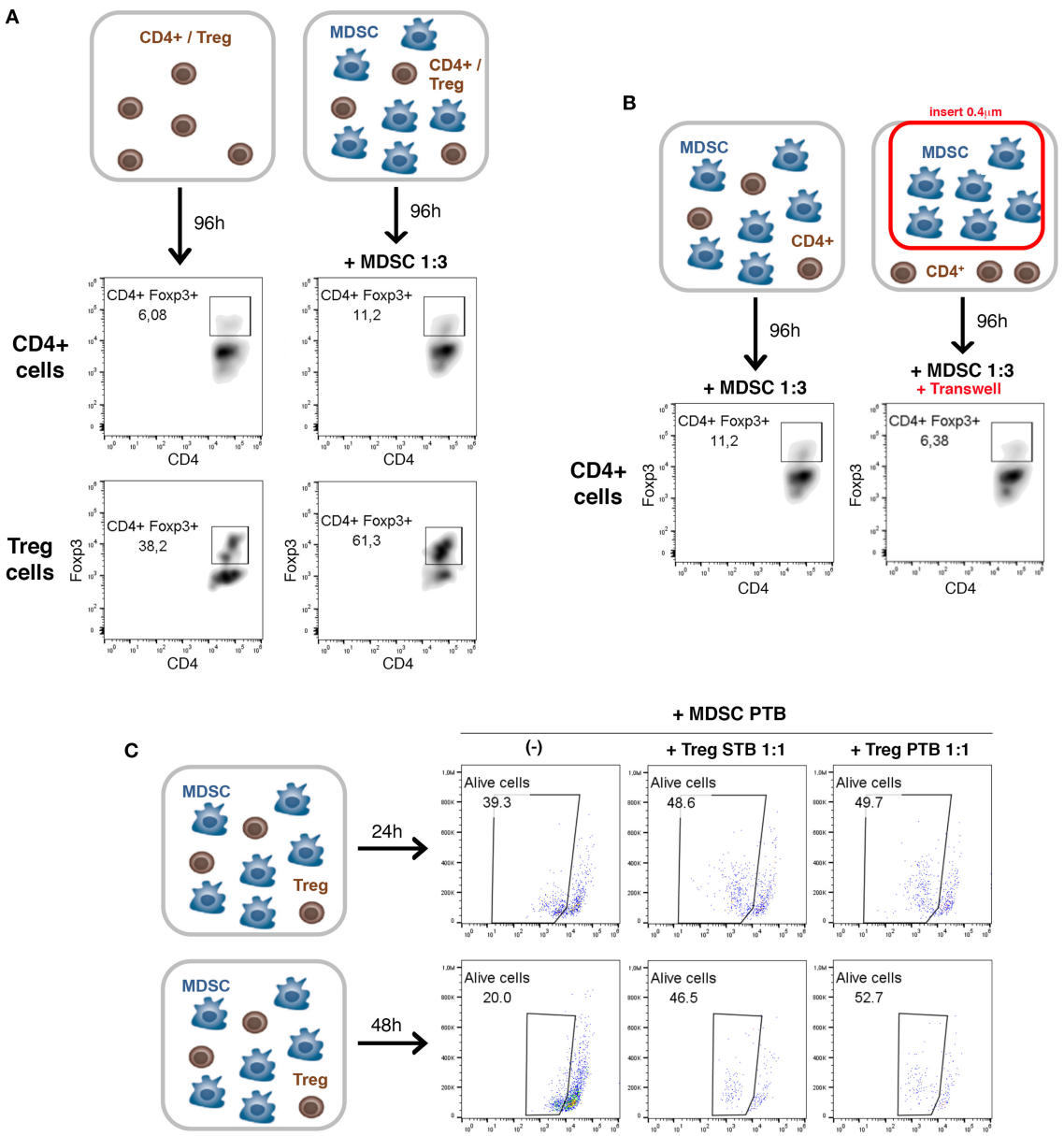

FIGURE 5 | A cell-cell dependent crosstalk between tumoral MDSCs and Treg cells. **(A)** Purified CD4$^+$ T cells or Treg cells (CD4$^+$CD25$^+$) from TB mice were cocultured with tumoral MDSCs. The percentage of CD4$^+$Foxp3$^+$ cells was evaluated by flow cytometry after 4 days of culture in the presence of CD3/CD28 stimulation. **(B)** Purified CD4$^+$ T cells from TB mice were cocultured with tumoral MDSCs at 1:3 ratio in conventional dishes or using Transwell chamber to separate the 2 cell populations. The percentage of CD4$^+$Foxp3$^+$ cells was evaluated after 4 days by flow cytometry. **(C)** Purified Treg cells (CD4$^+$CD25$^+$) from spleen of tumor-bearing mice (Treg STB) or tumor (Treg PTB) were cocultured with tumoral MDSCs for 24 or 48 h. The viability of MDSCs was then assessed by flow cytometry using *LIVE/DEAD* Fixable *Aqua* Dead stain.

These data are consistent with our *in vivo* observations of MDSCs-dependent Treg cell recruitment and/or induction in PDAC (**Figure 4**). To identify whether soluble molecules or cell-cell interaction are involved in this process, we incubated purified $CD4^+$ T cells and MDSCs in conventional dishes or using *Transwell* system (0.4 μM) to separate these 2 immune cell populations (**Figure 5B**). The induction of Treg cells by MDSCs was lost in the Transwell system suggesting that MDSC-mediated development/expansion of Treg cells was due to cell-to-cell interactions (**Figure 5B**).

Little is known on the converse impact of Treg cells on MDSCs. A novel strategy was described during the development of murine melanomas whereby Tregs shape the functional differentiation of MDSCs through the B7H1 pathway (23). Furthermore, it has been shown in B16 melanoma model that the expansion, recruitment, and activation of MDSCs occur in a Treg-dependent manner (29). In order to determine the impact of Treg cells on MDSCs in PDAC, we have performed *ex vivo* assays (**Figure 5C**). Purified Treg cells ($CD4^+CD25^+$) from spleen of tumor-bearing mice (Treg STB) or tumor (Treg PTB) were co-cultured with tumoral MDSCs. After 24 and 48 h of co-culture the percentage of alive MDSCs strongly increases in the presence of Treg cells isolated from TB mice (**Figure 5C**). Our findings reveal that Treg cells affect the survival and/or the proliferation of tumoral MDSCs.

Our results show that (i) MDSCs are able to induce Treg cell proliferation and/or development in a cell-cell dependent manner, (ii) Treg cells affect the survival and/or the proliferation of MDSCs.

Identification of MDSC and Treg Cell Crosstalk in Human PDAC

To determine whether the MDSC and Treg cell interactions are present also in the human pancreatic cancer, we have studied the expression of different immune markers (CD4, CD8,

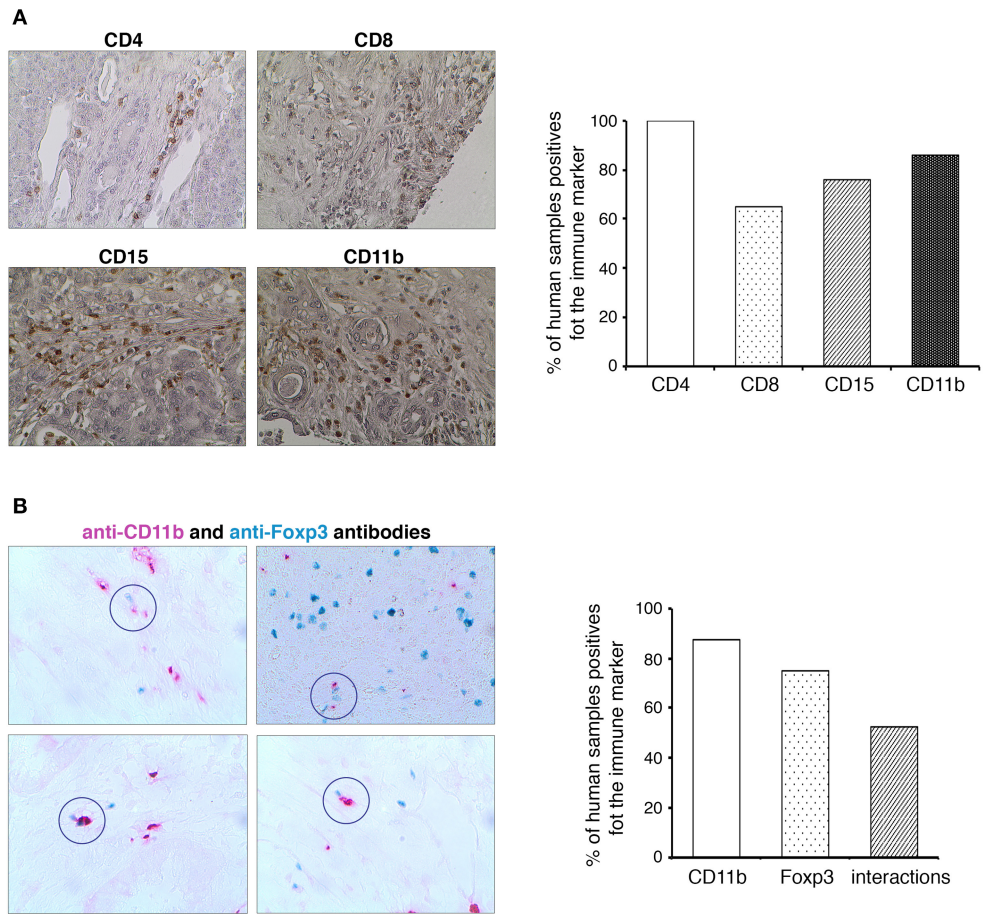

FIGURE 6 | Identification of MDSCs and Treg cells crosstalk in human PDAC. **(A)** Formalin-fixed, paraffin-embedded tissue sections of human pancreatic cancer were stained with anti-CD4, anti-CD8, anti-CD15, and anti-CD11b antibodies. All immunohistochemistry experiments were performed with the Vector Kit. Histograms show the quantification of the different immune markers expression in PDAC. Original magnification x100. **(B)** Formalin-fixed, paraffin-embedded tissue sections of human pancreatic cancer were stained with anti-Foxp3 (in Emerald) and anti-CD11b (in Permanent-red) antibodies. All immunohistochemistry experiments were performed with the GBI Labs Kit. A visual evaluation of interactions between $Foxp3^+$ and $CD11b^+$ cells was performed on human PDA tissues. Histograms show the quantification of the markers expression in PDAC and the presence of their interactions.

CD15, CD11b, Foxp3) in a cohort of PDAC patients (**Figure 6**). Similar to mouse, there are also two types of human MDSCs. Both types express CD11b; however, there is no equivalent to the mouse Gr-1 marker. Instead, human M-MDSCs are characterized by their expression of CD14 and PMN-MDSCs by their expression of CD15 (8, 9). We could not observe any immune cell infiltration in normal human pancreas (not shown). As shown in the **Figure 6A**, almost 100% of the human PDAC tissues were infiltrated by $CD4^+$ T cells, $CD8^+$ T cells, and $CD15^+$ myeloid cells. Moreover, $CD11b^+$ cells were observed in 60% of studied samples. Since the Foxp3 staining was weak, we have used GBI Labs Kit to amplify the signal. We could observe the presence of $Foxp3^+$ cells in more than 70% of tested samples (**Figure 6B**). By using the same experimental approach, we have identified and quantified the proximity between human $CD11b^+$ and $Foxp3^+$ cells. In more than 50% of analyzed PDAC patients, we have observed contacts between these cells (**Figure 6B**). Taken together these results suggest that MDSC and Treg interplay could also be present in human PDAC.

DISCUSSION

A complex relationship between the immune system and the development of pancreatic cancer has been largely described in patients and animal models. The progress in basic and translational immunology has confirmed the importance of these interactions in PDAC's prevention and prognosis (30). Neoplastic cells activate tumor-specific immune responses, but simultaneously trigger a strong immunosuppression, which is considered to be one of the main reasons for current immune-based therapy's failure (2, 5). Among the hallmarks of the immune dysfunction observed in PDAC is the recruitment and activation of immunosuppressive cells such as myeloid-derived suppressor cells and regulatory T cells. These latter shield neoplastic cells from immune detection and inhibit anti-tumoral effector responses (31).

Since the interactions between MDSCs and Treg cells are proposed to be a powerful barrier against anti-tumoral immunity in different cancer models (23–26), we have been particularly interested to study this interplay in the context of PDAC. Consistent with previous data in the genetically engineered mouse model of pancreatic cancer (KPC mice) (12), we have found that PDAC is characterized by a strong accumulation of immunosuppressive cell populations (MDSCs, Treg cells) associated with low levels of activated effector T cells. By using the innovative approach of light sheet fluorescent microscopy in whole pancreatic tumors, we have identified for the first time in a tumoral context the interactions between MDSCs and Treg cells which occurs *via* a direct physical contact. Our results further revealed that this interplay had a biological relevance since the *in vivo* depletion of MDSCs led to a significant reduction of Treg cells in the pancreatic tumors. Our findings on the biological relevance of these interactions are in concert with a previous study showing that the combination of *Listeria* vaccination and Treg depletion in a mouse model of PDAC shapes the functional differentiation of MDSCs.

Another new aspect of our study was MDSC/Treg interplay's contribution to the establishment and/or development of the immunosuppressive environment in PDAC. To better understand the mechanisms of PDAC-infiltrating MDSC and Treg crosstalk, we have used a Transwell system which allows to separate the two major immunoregulatory cell populations. Our results show that tumoral MDSCs are able to induce Treg cell proliferation and/or development in a cell-cell dependent manner. Moreover, we could observe that Treg cells affect the survival and/or the proliferation of MDSCs in PDAC. At present the molecular partners involved in the MDSC/Treg interplay are not fully understood and further studies will be needed to investigate these pathways. One candidate to consider could be the B7H1 pathway (23). It has been proposed during the development of murine melanomas whereby Tregs shape the functional differentiation of MDSCs through the B7 family molecules (23). Moreover, investigating the role of CD40 and CD80 molecules in the MDSCs/Treg crosstalk in PDAC could be promising. Indeed, the presence of these co-stimulatory molecules on MDSCs in the mouse colon and ovarian carcinomas models, respectively, is associated with Treg cells accumulation and/or functions (32, 33). Although inquiring the role of these candidates in the interactions between MDSCs and Treg cells in PDAC should be elucidated, it is important to highlight that they have an ectopic expression on different immune cell populations. This is a major obstacle for a future targeting of the crosstalk *via* their blocking by inhibitory antibodies for example. A broad transcriptomic approach might be a better tool to identify new and specific molecules involved in MDSC/Treg cell interplay in PDAC. In addition, the latter has also been reported in lung, colorectal and breast cancers, as well as in melanoma and B-cell lymphoma, suggesting that a contact-based crosstalk between these cell populations may be a general feature of tumor immune evasion (23–26). Moreover, based on our data and several other indications of a concerted immunosuppressive activity of Tregs and MDSCs in different cancer models, we expect the interactions between these major immunoregulatory cells to play a key role in PDAC development and progression.

The ability to effectively engage cancer immunity in therapies is highly promising and very challenging. The limitations encountered thus far in applying immunomodulatory strategies such as αCTLA4 and αPD1/PDL1 in PDAC to stimulate an endogenous T cell response may be the result of the profoundly suppressive effects of MDSCs and Treg cells (30, 31). Moreover, it is becoming increasingly clear that to improve the effects of conventional immune strategies in PDAC it may be necessary to target multiple forms of immune suppression simultaneously. On the other hand, safety becomes a counterbalancing concern, lest autoimmunity and organ dysfunction ensue. In summary, our study provides insights into MDSC/Treg cell crosstalk in PDAC which may help to explain the highly immunosuppressive nature of the pancreatic tumors. Should the interactions between MDSCs and Treg cells impact the tumoral

progression, it will be highly promising to target/modulate this interplay to reverse tumor-induced immunosuppression and provide an efficient therapeutic strategy for the treatment of PDAC.

DATA AVAILABILITY STATEMENT

All datasets generated for this study are included in the article/**Supplementary Material**.

ETHICS STATEMENT

The animal study was reviewed and approved by the local ethics committee of Aix-Marseille University and the Ministère de l'Enseignement Supérieur, de la Recherche et de l'Innovation. approved protocol numbers: APAFIS#4396 and APAFIS#21966.

AUTHOR CONTRIBUTIONS

AC, CS, SR, FS, VR, SP, DL, EM, and AM performed the *in vitro* and *in vivo* experiments. TC and PA helped with the *in vivo* experiments. AM conceived and supervised the study. AC, CS, SR, VR, EM, and AM analyzed data. CS, DL, VR, JI, EM, and AM contributed to discussion and wrote, illustrated, reviewed, and edited the manuscript. DL, JI, EM, and AM have acquired fundings. All authors approved the submitted version of the manuscript.

FUNDING

This work was supported by institutional funding from INSERM (Paris, France) (DL, EM, and JI), the Aix-Marseille Université (Marseille, France) (DL, EM, and JI), and by a grant INCa-DGSO-INSERM 6038 from Sites de Recherche Intégrée sur le Cancer (SIRIC) (DL, EM, and AM). This study was partly supported by research funding from the Canceropôle Provence-Alpes-Côte d'Azur (Marseille, France) (AM). This work was supported by the French National Research Agency through the Investissements d'Avenir program (France-BioImaging, ANR-10-INBS-04), FRM Amorçage jeunes équipes (AJE20150633331), ANR ACHN (ANR-16-ACHN-0011), and A*midex Chaire d'excellence.

ACKNOWLEDGMENTS

Dr. E. Lopez (Centre d'Exploration Fonctionnelle Scientifique, Campus Santé-Timone, Marseille, France) and Dr. J. Del Grande (Service d'anatomo-pathologie, Hôpital de la Timone, Marseille, France) are greatly acknowledged for their help in organization of animal experiments and diagnosis, respectively. We thank Dr. V. Schmitz and Dr. E. Raskopf (University of Bonn, Germany) for kindly providing us with the Panc02 cells. We also are deeply indebted to Dr. Pierre Golstein (Centre d'Immunologie de Marseille-Luminy, Marseille, France) for helpful discussion throughout the work.

SUPPLEMENTARY MATERIAL

The Supplementary Material for this article can be found online at: https://www.frontiersin.org/articles/10.3389/fimmu.2019.03070/full#supplementary-material

Supplementary Figure 1 | Characterization of MDSCs, Treg cells and effector T cells in the spleen of PDAC mice. C57BL/6 mice were injected with Panc02 cells in the pancreas and spleens were harvested 3 weeks post-inoculation. Spleens from naive mice were used as controls. Flow cytometry analysis of **(A)** MDSC recruitment and **(B)** of the expression of surface molecules F4/80, CD124, CD40, and B7H1 on Gr-MDSCs ($CD11b^+Gr\text{-}1^+Ly6G^+Ly6C^{low}$) and Mo-MDSCs ($CD11b^+Gr\text{-}1^+Ly6G^-Ly6C^{high}$) was performed. Gray histograms represent isotype control and red histograms specific staining as indicated. Percentage of positive cells are shown. Three independent experiments have been performed with similar results. Representative dot plots and histograms for one of these experiments are shown.

Supplementary Figure 2 | Characterization of Treg cells and effector T cells in the spleen of PDAC mice. C57BL/6 mice were injected with Panc02 cells in the pancreas and spleens were harvested 3 weeks post-inoculation. Spleens from naive mice were used as controls. Flow cytometry analysis of **(A)** the surface molecules CD127, CCR5, CTLA4, TGF-β, and CD103 on Treg ($CD45^+CD4^+Foxp3^+$), **(B)** the activation markers CD62L and CD69, as well as the intracellular expression of IFN-γ on $CD4^+$ and $CD8^+$ T cells. Gray histograms represent isotype control and red histograms specific staining as indicated. Percentage of positive cells are shown. Three independent experiments have been performed. Representative dot plots and histograms for one are shown.

Supplementary Figure 3 | Assessment of MDSC and Treg interactions in pancreatic tumors by videomicoscopy. Treg ($CD4^+CD25^+$) cells purified both from spleen or pancreas of tumor-bearing mice were loaded with FITC cell tracker and incubated with tumoral MDSCs for 10 h. Microscopic acquisition was performed every 20 min **(A)** and the percentage of total $CD4^+CD25^+$ cells bound to MDSCs was quantified 5 and 10 h post-co-culture. The ratio of persistent interactions (more than 40 min) and transient interactions was also reported **(B)**. ***Mann and Whitney analysis with p value $< 0.001\%$.

Supplementary Figure 4 | Dynamic interactions between MDSCs and Treg cells in orthotopic mouse model of pancreatic cancer. Panc02 cells were injected in the pancreas of C57BL/6 mice and tumors were harvested 1, 2, 3, and 4 weeks post-inoculation (three tumors per week). **(A)** Representative IHF (confocal microscopy) analysis of Gr-1 (MDSCs in green) and Foxp3 (Treg cells in red) on pancreatic tumor frozen sections for each week. The nuclei (in blue) are stained with Draq5, a fluorescent DNA marker. Zooms show proximity between the different immune cells. Scale bar 25 μm. **(B)** Light sheet microscopy analysis of Gr-1 (MDSCs) and Foxp3 (Treg cells) on whole cleared pancreatic tumor. Histogram represents quantification of interactions from three whole cleared tumors calculated with a matLab function associated with the Imaris software. See also **Supplementary Video 4** (1 week post-tumor inoculation), **Supplementary Video 5** (2 weeks post-tumor inoculation), **Supplementary Video 6** (3 weeks post-tumor inoculation), and **Supplementary Video 7** (4 weeks post-tumor inoculation).

Supplementary Figure 5 | Direct interactions between MDSCs and Treg cells in the center and boundary of tumors harvested at 3 and 4 weeks post-inoculation (three tumors per week). Representative IHF (confocal microscopy) analysis of Gr-1 (MDSCs in green) and Foxp3 (Treg cells in red) on pancreatic tumor frozen sections for each week. The nuclei (in blue) are stained with Draq5. Zooms show proximity between the different immune cells. Scale bar 50 μm. See also **Supplementary Video 6** (3 weeks post-tumor inoculation) and **Supplementary Video 7** (4 weeks post-tumor inoculation).

Supplementary Figure 6 | Assessment of interactions between MDSCs and γδT cells in orthotopic mouse model of pancreatic cancer. Panc02 cells were injected in the pancreas of C57BL/6 mice and tumors were harvested 1, 2, 3, and 4 weeks post-inoculation (three tumors per week). Representative IHF (confocal microscopy) analysis of Gr-1 (MDSCs in green) and TCRγδ (γδT cells in red) on pancreatic tumor frozen sections for each week. The nuclei (in blue) are stained with Draq5. Scale bar 25 μm.

Supplementary Video 1 | A direct physical contact between MDSC and Treg interactions in pancreatic tumors. Tumor 1's 3D video from LSM analysis. This video was done with the Imaris software. In green are the blood vessels stained with an anti-alpha SMA (smooth muscle actin), a pericyte marker. The blue and red spots represent, respectively, the Gr-1 and the Foxp3 positive cells. The pink and yellow spots are the Gr-1 and Foxp3 positive cells in interaction (determined with a MatLab plugin associated with Imaris software).

Supplementary Video 2 | Assessment of MDSC and Treg interactions in pancreatic tumors by videomicoscopy. Example of film showing persistent interactions.

Supplementary Video 3 | Assessment of MDSC and Treg interactions in pancreatic tumors by videomicoscopy. Example of film showing transient interactions.

Supplementary Video 4 | One week post-tumor inoculation. 3D video from LSM analysis to determine dynamic interactions between MDSC and Treg cells in pancreatic tumors at 1 week post-tumor inoculation. In green are the blood vessels stained with an anti-alpha SMA. The blue and red spots represent, respectively, the Gr-1 and the Foxp3 positive cells. The yellow spots are the Gr-1 and Foxp3 positive cells in interaction. Three tumors have been analyzed with similar results. Representative 3D video for one of these tumors are shown.

Supplementary Video 5 | Two weeks post-tumor inoculation. 3D video from LSM analysis showing dynamic interaction between MDSC and Treg cells in pancreatic tumors at 2 weeks post-tumor inoculation. Three tumors have been analyzed with similar results. Representative 3D video for one of these tumors are shown.

Supplementary Video 6 | Three weeks post-tumor inoculation. 3D video from LSM analysis showing dynamic interaction between MDSC and Treg cells in pancreatic tumors at 3 weeks post-tumor inoculation. Three tumors have been analyzed with similar results. Representative 3D video for one of these tumors are shown.

Supplementary Video 7 | Four weeks post-tumor inoculation. 3D video from LSM analysis showing dynamic interaction between MDSC and Treg cells in pancreatic tumors at 4 weeks post-tumor inoculation. Three tumors have been analyzed with similar results. Representative 3D video for one of these tumors are shown.

REFERENCES

1. Rahib L, Smith BD, Aizenberg R, Rosenzweig AB, Fleshman JM, Matrisian LM. Projecting cancer incidence and deaths to 2030: the unexpected burden of thyroid, liver, and pancreas cancers in the United States. *Cancer Res.* (2014) doi: 10.1158/0008-5472.CAN-14-0155
2. Costello E, Greenhalf W, Neoptolemos JP. New biomarkers and targets in pancreatic cancer and their application to treatment. *Nat Rev Gastroenterol Hepatol.* (2012) doi: 10.1038/nrgastro.2012.119
3. Neesse A, Michl P, Frese KK, Feig C, Cook N, Jacobetz MA, et al. Stromal biology and therapy in pancreatic cancer. *Gut*. (2011) doi: 10.1136/gut.2010.226092
4. Provenzano PP, Cuevas C, Chang AE, Goel VK, Von Hoff DD, Hingorani SR. Enzymatic targeting of the stroma ablates physical barriers to treatment of pancreatic ductal adenocarcinoma. *Cancer Cell.* (2012) doi: 10.1016/j.ccr.2012.01.007
5. Schnurr M, Duewell P, Bauer C, Rothenfusser S, Lauber K, Endres S, et al. Strategies to relieve immunosuppression in pancreatic cancer. *Immunotherapy*. (2015) doi: 10.2217/imt.15.9
6. Stromnes IM, Schmitt TM, Hulbert A, Brockenbrough JS, Nguyen H, Cuevas C, et al. T cells engineered against a native antigen can surmount immunologic and physical barriers to treat pancreatic ductal adenocarcinoma. *Cancer Cell.* (2015) doi: 10.1016/j.ccell.2015.09.022
7. Gabrilovich DI, Ostrand-Rosenberg S, Bronte V. Coordinated regulation of myeloid cells by tumours. *Nat Rev Immunol.* (2012) 12:253–68. doi: 10.1038/nri3175
8. Bronte V, Brandau S, Chen SH, Colombo MP, Frey AB, Greten TF, et al. Recommendations for myeloid-derived suppressor cell nomenclature and characterization standards. *Nat Commun.* (2016) 7:12150. doi: 10.1038/ncomms12150
9. Ostrand-Rosenberg S, Fenselau C. Myeloid-derived suppressor cells: immune-suppressive cells that impair antitumor immunity and are sculpted by their environment. *J Immunol.* (2018) 200:422–31. doi: 10.4049/jimmunol.1701019
10. Bayne LJ, Beatty GL, Jhala N, Clark CE, Rhim AD, Stanger BZ, et al. Tumor-derived granulocyte-macrophage colony-stimulating factor regulates myeloid inflammation and T cell immunity in pancreatic cancer. C*ancer Cell.* (2012) doi: 10.1016/j.ccr.2012.04.025
11. Pylayeva-Gupta Y, Lee KE, Hajdu CH, Miller G, Bar-Sagi D. Oncogenic Kras-induced GM-CSF production promotes the development of pancreatic neoplasia. *Cancer Cell.* (2012) doi: 10.1016/j.ccr.2012.04.024
12. Clark CE, Hingorani SR, Mick R, Combs C, Tuveson DA, Vonderheide RH. Dynamics of the immune reaction to pancreatic cancer from inception to invasion. *Cancer Res.* (2007) doi: 10.1158/0008-5472.CAN-07-0175
13. Stromnes IM, Brockenbrough JS, Izeradjene K, Carlson MA, Cuevas C, Simmons RM, et al. Targeted depletion of an MDSC subset unmasks pancreatic ductal adenocarcinoma to adaptive immunity. *Gut.* (2014) 63:1769–81. doi: 10.1136/gutjnl-2013-306271
14. Mundy-Bosse BL, Young GS, Bauer T, Binkley E, Bloomston M, Bill MA, et al. Distinct myeloid suppressor cell subsets correlate with plasma IL-6 and IL-10 and reduced interferon-alpha signaling in CD4+ T cells from patients with GI malignancy. *Cancer Immunol Immunother.* (2011) doi: 10.1007/s00262-011-1029-z
15. Gabitass RF, Annels NE, Stocken DD, Pandha HA, Middleton GW. Elevated myeloid-derived suppressor cells in pancreatic, esophageal and gastric cancer are an independent prognostic factor and are associated with significant elevation of the Th2 cytokine interleukin-13. *Cancer Immunol Immunother.* (2011) doi: 10.1007/s00262-011-1028-0
16. Porembka MR, Mitchem JB, Belt BA, Hsieh CS, Lee HM, Herndon J, et al. Pancreatic adenocarcinoma induces bone marrow mobilization of myeloid-derived suppressor cells which promote primary tumor growth. *Cancer Immunol Immunother.* (2012) doi: 10.1007/s00262-011-1178-0
17. Oleinika K, Nibbs RJ, Graham GJ, Fraser AR. Suppression, subversion and escape: the role of regulatory T cells in cancer progression. *Clin Exp Immunol.* (2013) doi: 10.1111/j.1365-2249.2012.04657.x
18. Nishikawa H, Sakaguchi S. Regulatory T cells in cancer immunotherapy. *Curr Opin Immunol.* (2014) 27:1–7. doi: 10.1016/j.coi.2013.12.005
19. Finotello F, Trajanoski Z. New strategies for cancer immunotherapy: targeting regulatory T cells. *Genome Med.* (2017) doi: 10.1186/s13073-017-0402-8
20. Wang X, Lang M, Zhao T, Feng X, Zheng C, Huang C, et al. Cancer-FOXP3 directly activated CCL5 to recruit FOXP3(+)Treg cells in pancreatic ductal adenocarcinoma. *Oncogene.* (2017) 36:3048–58. doi: 10.1038/onc.2016.458
21. Tan MC, Goedegebuure PS, Belt BA, Flaherty B, Sankpal N, Gillanders WE, et al. Disruption of CCR5-dependent homing of regulatory T cells inhibits tumor growth in a murine model of pancreatic cancer. *J Immunol.* (2009) doi: 10.4049/jimmunol.182.3.1746
22. Wachsmann MB, Pop LM, Vitetta ES. Pancreatic ductal adenocarcinoma: a review of immunologic aspects. *J Investig Med.* (2012) doi: 10.2310/JIM.0b013e31824a4d79
23. Fujimura T, Ring S, Umansky V, Mahnke K, Enk AH. Regulatory T cells stimulate B7-H1 expression in myeloid-derived suppressor cells in ret melanomas. *J Invest Dermatol.* (2012) 132:1239–46. doi: 10.1038/jid.2011.416
24. Serafini P, Mgebroff S, Noonan K, Borrello I. Myeloid-derived suppressor cells promote cross-tolerance in B-cell lymphoma by expanding regulatory T cells. *Cancer Res.* (2008) 68:5439–49. doi: 10.1158/0008-5472.CAN-07-6621
25. Schlecker E, Stojanovic A, Eisen C, Quack C, Falk CS, Umansky V, et al. Tumor-infiltrating monocytic myeloid-derived suppressor cells mediate CCR5-dependent recruitment of regulatory T cells favoring tumor growth. *J Immunol.* (2012) doi: 10.4049/jimmunol.1201018

26. Centuori SM, Trad M, LaCasse CJ, Alizadeh D, Larmonier CB, Hanke NT, et al. Myeloid-derived suppressor cells from tumor-bearing mice impair TGF-β-induced differentiation of $CD4^+CD25^+FoxP3^+$ Tregs from $CD4^+CD25$-FoxP3- T cells. *J Leukoc Biol.* (2012) 92:987–97. doi: 10.1189/jlb.0911465
27. Chai MG, Kim-Fuchs C, Angst E, Sloan EK. Bioluminescent orthotopic model of pancreatic cancer progression. *J Vis Exp.* 50395. doi: 10.3791/50395
28. Anz D, Mueller W, Golic M, Kunz WG, Rapp M, Koelzer VH, et al. CD103 is a hallmark of tumor-infiltrating regulatory T cells. *Int J Cancer.* (2011) doi: 10.1002/ijc.25902
29. Holmgaard RB, Zamarin D, Li Y, Gasmi B, Munn DH, Allison JP, et al. Tumor-expressed IDO recruits and activates MDSCs in a Treg-dependent manner. *Cell Rep.* (2015) doi: 10.1016/j.celrep.2015.08.077
30. Amedei A, Niccolai E, Prisco D. Pancreatic cancer: role of the immune system in cancer progression and vaccine-based immunotherapy. *Hum Vaccin Immunother.* (2014) doi: 10.4161/hv.34392
31. Kunk PR, Bauer TW, Slingluff CL, Rahma OE. From bench to bedside a comprehensive review of pancreatic cancer immunotherapy. *J Immunother Cancer.* (2016) doi: 10.1186/s40425-016-0119-z
32. Pan PY, Ma G, Weber KJ, Ozao-Choy J, Wang G, Yin B, et al. Immune stimulatory receptor CD40 is required for T-cell suppression and T regulatory cell activation mediated by myeloid-derived suppressor cells in cancer. *Cancer Res.* (2010) doi: 10.1158/0008-5472.CAN-09-1882
33. Yang R, Cai Z, Zhang Y, Yutzy WH IV, Roby KF, Roden RB. CD80 in immune suppression by mouse ovarian carcinoma-associated $Gr\text{-}1^+CD11b^+$ myeloid cells. *Cancer Res.* (2006) 66:6807–15. doi: 10.1158/0008-5472.CAN-05-3755

Conflict of Interest: The authors declare that the research was conducted in the absence of any commercial or financial relationships that could be construed as a potential conflict of interest.

frontiers in Immunology

ORIGINAL RESEARCH
published: 19 March 2020
doi: 10.3389/fimmu.2020.00224

NGS Evaluation of Colorectal Cancer Reveals Interferon Gamma Dependent Expression of Immune Checkpoint Genes and Identification of Novel IFNγ Induced Genes

Lai Xu[1†], Lorraine Pelosof[1†], Rong Wang[2†], Hugh I. McFarland[2†], Wells W. Wu[3], Je-Nie Phue[3], Chun-Ting Lee[3], Rong-Fong Shen[3], Hartmut Juhl[4], Lei-Hong Wu[5], Wei-Lun Alterovitz[6], Emanuel Petricon[7] and Amy S. Rosenberg[2*]*

[1] Office of Oncologic Diseases, Center for Drug Evaluation and Research (CDER), FDA, Silver Spring, MD, United States, [2] Office of Biotechnology Products, Division of Biotechnology Review and Research III (DBRRIII), Office of Pharmaceutical Quality (OPQ), Center for Drug Evaluation and Research (CDER), FDA, Silver Spring, MD, United States, [3] Facility for Biotechnology Resources, Center for Biologics Evaluation and Research (CBER), FDA, Silver Spring, MD, United States, [4] Indivumed GmbH, Hamburg, Germany, [5] Division of Bioinformatics and Biostatistics (DBB), National Center for Toxicological Research (NCTR), FDA, Jefferson, AR, United States, [6] HIVE, Center for Biologics Evaluation and Research (CBER), FDA, Silver Spring, MD, United States, [7] Center for Applied Proteomics and Molecular Medicine (CAPMM), George Mason University, Fairfax, VA, United States

To evaluate the expression of immune checkpoint genes, their concordance with expression of IFNγ, and to identify potential novel ICP related genes (ICPRG) in colorectal cancer (CRC), the biological connectivity of six well documented ("classical") ICPs (CTLA4, PD1, PDL1, Tim3, IDO1, and LAG3) with IFNγ and its co-expressed genes was examined by NGS in 79 CRC/healthy colon tissue pairs. Identification of novel IFNγ- induced molecules with potential ICP activity was also sought. In our study, the six classical ICPs were statistically upregulated and correlated with IFNγ, CD8A, CD8B, CD4, and 180 additional immunologically related genes in IFNγ positive (FPKM > 1) tumors. By ICP co-expression analysis, we also identified three IFNγ-induced genes [(IFNγ-inducible lysosomal thiol reductase (IFI30), guanylate binding protein1 (GBP1), and guanylate binding protein 4 (GBP4)] as potential novel ICPRGs. These three genes were upregulated in tumor compared to normal tissues in IFNγ positive tumors, co-expressed with CD8A and had relatively high abundance (average FPKM = 362, 51, and 25, respectively), compared to the abundance of the 5 well-defined ICPs (Tim3, LAG3, PDL1, CTLA4, PD1; average FPKM = 10, 9, 6, 6, and 2, respectively), although IDO1 is expressed at comparably high levels (FPKM = 39). We extended our evaluation by querying the TCGA database which revealed the commonality of IFNγ dependent expression of the three potential ICPRGs in 638 CRCs, 103 skin cutaneous melanomas (SKCM), 1105 breast cancers (BC), 184 esophageal cancers (ESC), 416 stomach cancers (STC), and 501 lung squamous carcinomas (LUSC). In terms of prognosis, based on Pathology Atlas data, correlation of GBP1 and GBP4, but not IFI30, with 5-year survival rate was favorable in CRC, BC, SKCM, and STC. Thus, further studies defining the role of IFI30, GBP1, and GBP4 in CRC are warranted.

Keywords: colorectal cancer, IFNγ gradient, immune checkpoint genes, co-expression network, novel immune checkpoint related genes

OPEN ACCESS

Edited by:
Gianluigi Giannelli, National Institute of Gastroenterology S. de Bellis Research Hospital (IRCCS), Italy

Reviewed by:
Grazia Serino, National Institute of Gastroenterology S. de Bellis Research Hospital (IRCCS), Italy
Ying Ma, University of Texas MD Anderson Cancer Center, United States

***Correspondence:**
Lai Xu
lai.xu@FDA.hhs.gov
Amy S. Rosenberg
amy.rosenberg@fda.hhs.gov

†These authors have contributed equally to this work and analyses presented herein

Specialty section:
This article was submitted to Cancer Immunity and Immunotherapy, a section of the journal Frontiers in Immunology

Received: *25 October 2019*
Accepted: *28 January 2020*
Published: *19 March 2020*

Citation:
Xu L, Pelosof L, Wang R, McFarland HI, Wu WW, Phue J-N, Lee C-T, Shen R-F, Juhl H, Wu L-H, Alterovitz W-L, Petricon E and Rosenberg AS (2020) NGS Evaluation of Colorectal Cancer Reveals Interferon Gamma Dependent Expression of Immune Checkpoint Genes and Identification of Novel IFNγ Induced Genes. Front. Immunol. 11:224. doi: 10.3389/fimmu.2020.00224

INTRODUCTION

CRC is the second leading cause of cancer-related mortality in the United States[1] (1) and, disturbingly, an increased incidence of CRC in patients <40 years of age has been reported (2). In recent years, immunotherapeutic approaches have opened important treatment options in a small subset of CRC patients with microsatellite instability high (MSI-H) tumors (3). Most CRC, however, are microsatellite stable (MSS) (4). In MSI-H CRC patients, the high response rate to the ICP blockade appears due to a higher tumor mutational burden, the presence of neoantigens and consequent infiltration by $CD8^+$ (T_C, cytotoxic T lymphocyte) CTL and higher expression levels of ICPs (5). In this regard, IFNγ has been identified as the lynchpin factor in the induction and sustained expression of ICPs on tumor and infiltrating T cells in several tumor types and thus, qPCR detection of IFNγ has been considered a potential marker of response to ICP blockade in several cancer studies including in non-small cell lung cancer (NSCLC) and cutaneous melanoma (SKCM) (6–8). However, the role of IFNγ in establishing the immunological profile of CRC has not been thoroughly investigated. This prompted us to use NGS to evaluate expression of IFN-γ in CRC tumors, its link to known IFNγ-dependent ICPs, and to identify novel ICPRGs. In this study, we evaluated expression levels of six well-known immune checkpoint genes [six ICPs (CTLA4, PD1, PDL1, Tim3, IDO1, and LAG3)] as well as potential immune checkpoint related genes (ICPRGs) also induced by IFNγ by next generation sequencing (NGS) in 79 stringently collected and preserved primary human CRCs and their patient matched normal colonic tissues. Expression levels of six ICPs were evaluated as were their relationships to expression levels of IFNγ and other immunologically pertinent genes. Based on the ICP co-expression network, we searched for potential ICP related genes (ICPRGs) in IFNγ positive tumors that may function as novel ICPs and consequently identified IFI30, GBP1 and GBP4. Based on the identified literature (9–22), IFI30, GBP1, and GBP4 suppress mouse primary T cell activation *in vitro* and mouse innate immune response *in vivo* while IFI30 and GBP1 appear to increase cell proliferation in a glioma cell line and two breast cancer cell lines but diminish cell proliferation in a colon cancer cell line. Intriguingly, however, IFI30 RNA expression is associated with better patient survival in breast cancer (12) and diffuse large B cell lymphomas (DLBCL) (14) while GPB1 RNA is associated with better patient survival in melanoma (20) but poorer prognosis in human glioblastoma (21).

MATERIALS AND METHODS

Cohort

Seventy-nine paired-tissues (79 tumor and 79 normal controls, **Table S1**) of pretreatment CRCs were collected from 38 male and 41 female patients by Indivumed GmbH (Germany) for mRNA sequencing. The purchase of these de-intified samples was exempted by FDA IRB/RIHSC. To evaluate tumor content, hematoxylin and eosin stained microscopic slices were examined by pathologists to determine the tumor cell and normal cell areas, respectively. Histologically, tumor samples had 50–70% content of cancer cells while normal samples had 0% content of cancer cells. Normal tissues were collected from a site at a minimum of 5 cm from the tumor margin. Ischemia time was 6–11 min. This short cold ischemia reduces post-surgical tissue processing artifacts (23). According to the medical pathology reports, tumors were classified as well, moderately, and poorly differentiated tumors following international guideline UICC TNM-classification (24). For the convenience of analysis, 26 stage I and II tumors were considered as low stage tumors (LSTs), while 53 stage III and IV tumors were considered as HSTs (25). In this study, a normal control adjacent to a low stage tumor is referred to as LSN. The ratio of high stage tumors vs. low stage tumors is 2–1. Among 26 low stage tumors, there were two either lymph node (LN) or lymphatic vessel (LV) positive tumors while among 53 high stage tumors, there were 28 either LN/LV positive tumors. For tumor grades, there were 17 well (low grade) differentiated, 36 moderately (medium grade) differentiated, and 26 poorly (high grade) differentiated tumors. Clinical and histopathological characteristics of the patients as well as tumor location are summarized in **Table S1**. Among these 80 tumor pairs, 79 pairs were sequenced (all except the T7/N7 pair). The information for the cohort of 50 CRC tumor pairs, 588 CRCs, 103 SKCMs, 1105 BCs, 184 ESCs, 416 STCs, and 501 LUSC for validation of six ICPs and three ICPRGs was extracted from TCGA_B38 through OncoLand (**Tables S2–S4**). As for tumor stage information of validating cohort, there were 57 LST and 82 HSTs (**Tables S1, S2**).

For protein and survival data, The Clinical Proteomic Tumor Analysis Consortium (CPTAC) (https://cptac-data-portal.georgetown.edu/) which contains Mass spectroscopy (MS) analyses of 95 CRCs (**Table S5**) and The Pathology Atlas (https://www.proteinatlas.org/humanproteome/pathology) were used.

mRNA Sequencing

RNA quality was assessed using the Agilent 2100 Bioanalyzer, with cellular RNA analyzed using the RNA 6000 Nano Kit (Agilent). Samples with an RNA Integrity Number (RIN) of 7 or higher were processed to generate libraries for mRNA sequencing following the Illumina® TruSeq Stranded mRNA Sample Preparation Guide. In this method, poly-A mRNAs were purified from 0.5 μg total RNA, fragmented and reverse-transcribed into cDNAs. Double strand cDNAs were adenylated at the 3′ ends and ligated to indexed sequencing adaptors, followed with amplification for 15 cycles. One femtomole of the sequencing libraries (median size ∼260 nt) were denatured and loaded onto a flow cell for cluster generation using the Illumina cBot. Every six samples were loaded onto each lane of a rapid run flow cell. Paired-end sequencing was carried out on a HiSeq 2500 sequencer (Illumina, San Diego, CA, USA) for 100 × 2 cycles (26). For each sample, we obtained ∼50 million 100-bp reads that passed preset filtering parameters (27).

Sequencing Data Analysis

For mRNA sequencing, Tophat V.2.0.11 was used to align reads in fastq files to the UCSC human hg19 reference genome. Cufflinks V.2.2.1 was used to assemble the transcriptome based

[1]https://www.cancer.org/cancer/colon-rectal-cancer/about/key-statistics.html

on the hg19 reference annotation, and Cuffquan/Cuffnorm (part of Cufflinks) were used in calculating relative abundance of each transcript reported as FPKM. Gene co-expression analyses were carried by Partek NGS & microarray data analysis software (25, 28, 29). Integrated Discovery (DAVID) v6.7 (https://david.ncifcrf.gov/) was used for biological pathway determination and Cytoscape (2.8.2) was used for gene co-expression networks construction.

Initial Expression Landscape of CRC

A total of 25,761 genes were detected. Because genes with higher FPKM values may have greater biological impact, we focused on genes with FPKM > 1 (25, 28). Ten thousand two hundred fifty-five genes (40% of total genes) had an average FPKM > 1 and differential expression between tumors and normal controls (False Discovery Rate (FDR) < 0.05 in ANOVA). A total of 3,893 genes (15% of total genes) with average FPKM > 1 showed no differential expression between tumor and normal controls with FDR (ANOVA) > 0.05 (25, 29).

NGS Evaluation of Immune Gene Expression

NGS is a technology that accurately quantifies gene expression and does not necessarily require further validation, as supported by the literature (25). To more fully establish NGS as a "stand alone" technology for gene quantification, we reasoned that NGS quantification of a critical hub gene should be reflected in the consequent up/downregulation of highly interconnected genes and thus examined the co-expression of IFNγ genes with T and NK cell specific genes based on the fact that IFNγ and granzymes are produced by T cells and NK cells (30). IFNγ was highly correlated (cc > 0.80) with 9 classical T and NK cell gene markers and two granzymes in IFNγ positive tumors, as assessed by NGS: CD8A [0.97], CD69 [0.93], CD52 [0.86], CD160 [0.85], CD3E [0.84], CD96 [0.83], CD8B [0.82], CD2 [0.82], CD7 [0.80], GZMA [0.80], and GZMM [0.80]) (**Table S6**). These data indicate that NGS expression profiles of immune related genes do not necessarily require validation by other gene quantification technologies, especially for hypothesis-generating studies.

RESULTS

Upregulation of Six Established ICPs Associated With Higher Expression of IFNγ in CRC

Because IFNγ has been strongly implicated in the induction of PDL1 expression in tumors, and PD1 expression in tumor infiltrating T cells (6–8), we divided 79 CRCs into those with potentially significant IFNγ expression (abundance level of FPKM > 1; 32 CRCs), designated IFNγ$^+$ (positive), and those expressing lower levels of IFNγ expression (FPKM < 1; 47 CRCs), designated IFNγ$^-$ (negative) (**Figure 1A**). The $\log_2$ FPKM plot of tumor and normal showed that IFNγ and all six well-documented ICPs were significantly upregulated ($p < 0.01$) in IFNγ positive CRCs compared to their patient matched normal tissue controls [**Figure 1B**: IFNγ (24.1-fold), IDO1 (7.8-fold), CTLA4 (2.9-fold), Tim3 (2.3-fold), PDL1 (3.0-fold), PD1 (2.1-fold) and LAG3 (1.6-fold)] while only 4 ICPs were significantly upregulated (P < 0.05) in IFNγ negative CRCs compared to their matched controls (**Figure 1C**): IFNγ (4.4-fold), IDO1 (1.4-fold), CTLA4 (1.7-fold), Tim3 (1.4-fold), PDL1 (1.3-fold), and PD1 (1.0-fold). Intriguingly, LAG3 (0.54-fold) was significantly downregulated ($p = 1.7E\text{-}0.5$) in IFNγ negative CRCs (**Figure 1C**). These data suggest that differential expression of ICPs, especially LAG3, may pertain to levels of IFNγ expression in CRCs. Regarding the quantitative relationship between IFNγ and the six ICPs, the expression levels of these six were 1.9 to 6.4 -fold higher in IFNγ positive vs. IFNγ negative tumors (**Table S7**), though even in the IFNγ positive tumors, these ICPs were expressed at relatively low abundance (average FPKM = 3–12) compared to oncogenes such as MYC, CDK4, and CCND1 (average FPKM = 105) (25), with the exception of IDO1 which is robustly upregulated (average FPKM = 89). These data suggest a positive effect of IFNγ with respect to consequent upregulation of ICPs but potentially at levels still insufficient to promote significant expression of ICP proteins on tumor and infiltrating T cells in CRC, supporting the lack of response of most of these tumors to ICP inhibitor therapeutics.

ICP Co-expression Profile in IFNγ Positive and Negative Tumors

We then performed a Pearson correlation analysis to evaluate the co-expression profile of IFNγ and the six ICPs in IFNγ positive and negative CRC, as well as in normal controls using a stringent correlation coefficient (cc) > 0.8. In IFNγ positive CRC, the following was observed: (i) IFNγ, CD8A, CD8B, and CD4 co-expression with all six ICPs genes within one network (190 genes); (ii) IFNγ and three ICPs (LAG3, Tim3, and IDO1) were defined as potential hub genes due to their substantial number of co-expressed genes ($n > 45$); and (iii) co-expression of IFNγ and six ICPs with 129 immune cell related genes (pale blue dots in **Figure 2A**) and 54 signaling genes (red dots in **Figure 2A**; **Table S8**).

In contrast, in IFNγ negative CRC, co-expression of Tim3, PDL1, and CD4 was found within one network comprised of 83 genes, but without linkage to IFNγ or other immune checkpoint genes including PD1, CTLA4, IDO1 and LAG3. Genes co-expressed with Tim3 and PDL1 consisted of 77 immune related genes (pale blue dots in **Figure 2B**) as well as six signaling genes (red dots in **Figure 2B**; **Table S8**).

In control normal colonic tissues, co-expression of two ICPs (CTLA4 and PD1) was observed but also was not linked to IFNγ and CD4, CD8A, and CD8B, or co-expression with PDL1, Tim3, LAG3, and IDO1. However, expression of CTLA4 and PD1 was noted within an 88-gene network including 63 immune related genes (pale blue dots in **Figure 2C**) as well as 25 signaling genes (red dots in **Figure 2C**; **Table S8**).

Identification of Three Novel ICPRG Genes in CRC

We next explored whether there were potential novel ICPRGs from the IFNγ co-expression network that potentially factored

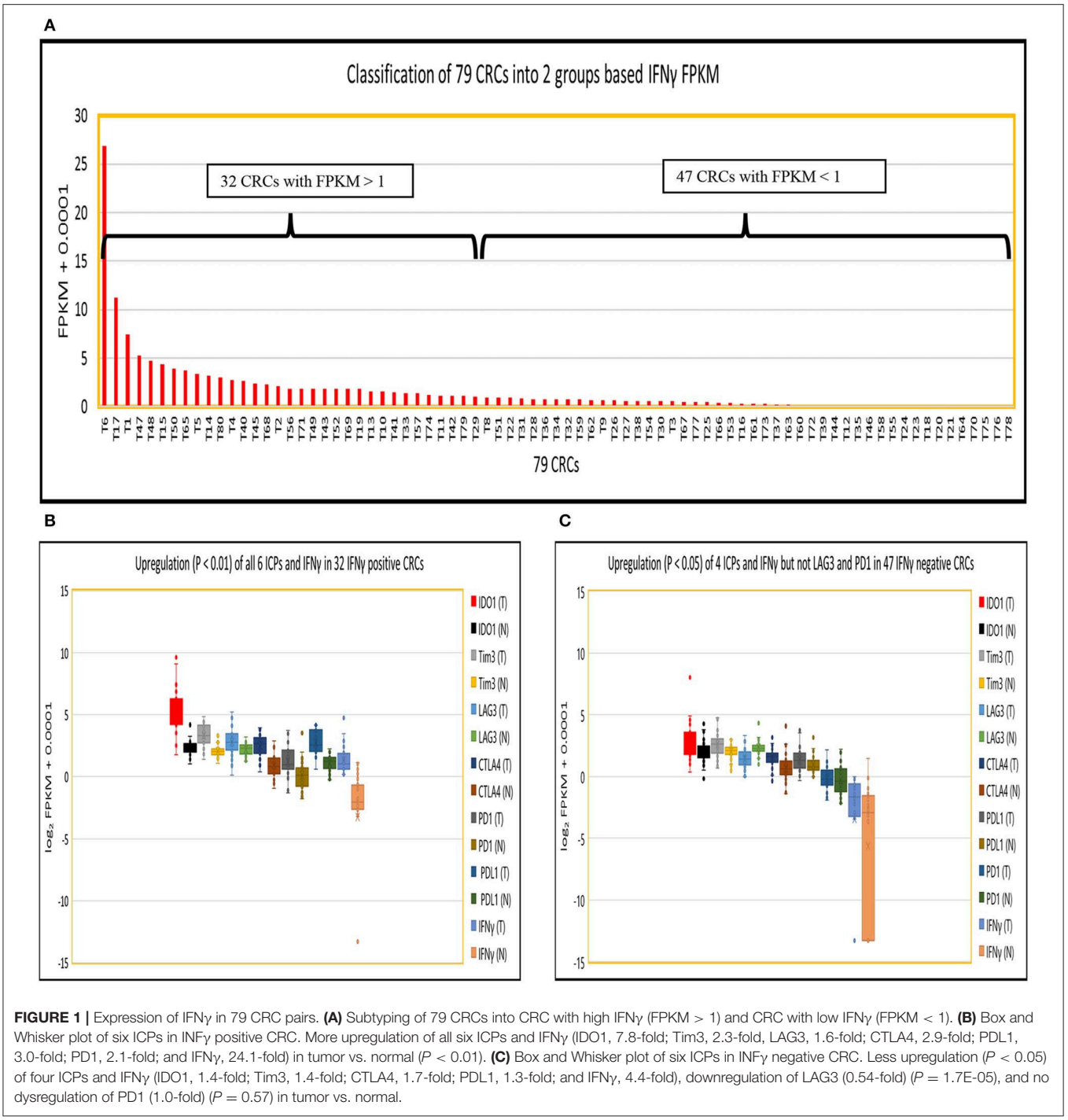

FIGURE 1 | Expression of IFNγ in 79 CRC pairs. **(A)** Subtyping of 79 CRCs into CRC with high IFNγ (FPKM > 1) and CRC with low IFNγ (FPKM < 1). **(B)** Box and Whisker plot of six ICPs in INFγ positive CRC. More upregulation of all six ICPs and IFNγ (IDO1, 7.8-fold; Tim3, 2.3-fold, LAG3, 1.6-fold; CTLA4, 2.9-fold; PDL1, 3.0-fold; PD1, 2.1-fold; and IFNγ, 24.1-fold) in tumor vs. normal ($P < 0.01$). **(C)** Box and Whisker plot of six ICPs in INFγ negative CRC. Less upregulation ($P < 0.05$) of four ICPs and IFNγ (IDO1, 1.4-fold; Tim3, 1.4-fold; CTLA4, 1.7-fold; PDL1, 1.3-fold; and IFNγ, 4.4-fold), downregulation of LAG3 (0.54-fold) ($P = 1.7E-05$), and no dysregulation of PD1 (1.0-fold) ($P = 0.57$) in tumor vs. normal.

into the refractoriness of CRC to immunotherapy. Three genes, IFI30, GBP1, and GBP4, were identified by two criteria: co-expressed (cc > 0.8) with known ICPs and upregulated by a minimum 2-fold average over normal (T/N). In IFNγ positive tumors, IFI30, GBP1, and GBP4 were significantly upregulated ($p < 0.0001$) at 2.7-, 4.2-, and 6.2-fold, respectively (**Figure 3A**) while only IFI30 and GBP1 were upregulated ($p < 0.05$) at 1.4- and 1.2-fold, respectively in IFNγ negative tumors compared to their matched normal controls (**Figure 3B**). Notably, the abundance of IFI30, GBP1 and GBP4 was substantially higher in IFNγ positive tumors (362, 51, 25 FPKM, respectively) than in IFNγ negative tumors (207, 18, 7 FPKM, respectively) (**Table S9**). These three genes have documented immune suppressive function and pro or anti-tumor roles in different types of cancers (9–23).

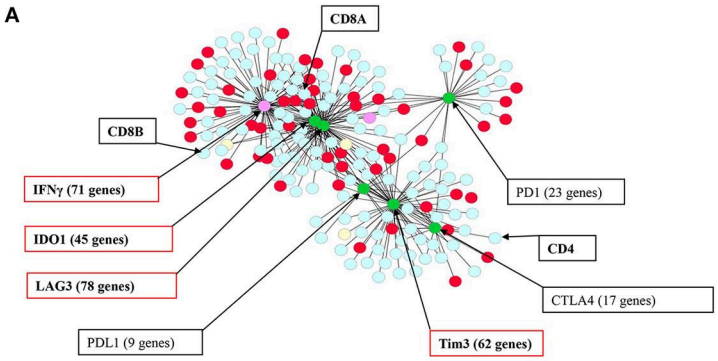

Green dot: ICP gene
Red dot: signal transduction gene
Blue dot: immune gene
Pink dot: IFNγ
Yellow dot: ICPRG

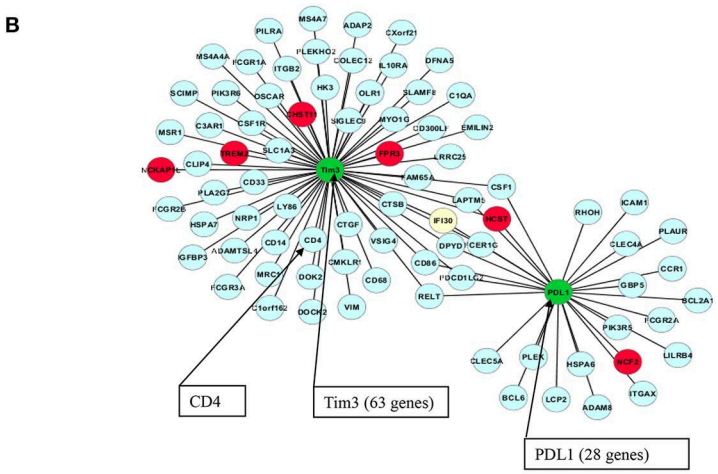

Green dot: ICP gene
Red dot: signal transduction gene
Blue dot: immune gene
Yellow dot: ICPRG

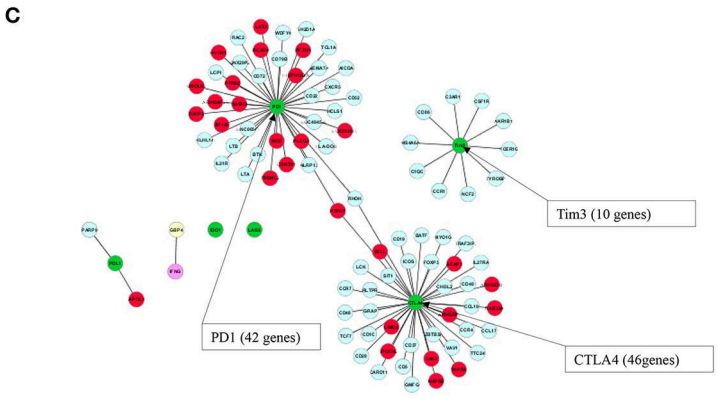

Green dot: ICP gene
Red dot: signal transduction gene
Blue dot: immune gene
Yellow dot: ICPRG

FIGURE 2 | Co-expression (cc > 0.8) of IFNγ with six ICPs in CRC. **(A)** IFNγ and all six ICPs co-expressed with CD8A/CD8B/CD4 within one 190 gene network in 32 IFNγ positive CRCs. **(B)** Tim3 and PDL1 co-expressed with CD4 within one 83 gene network in 47 IFNγ negative CRCs. **(C)** CTLA4 co-expressed with PD1 within one 88 gene expression network, but not Tim3, in normal colon without CD8/CD4.

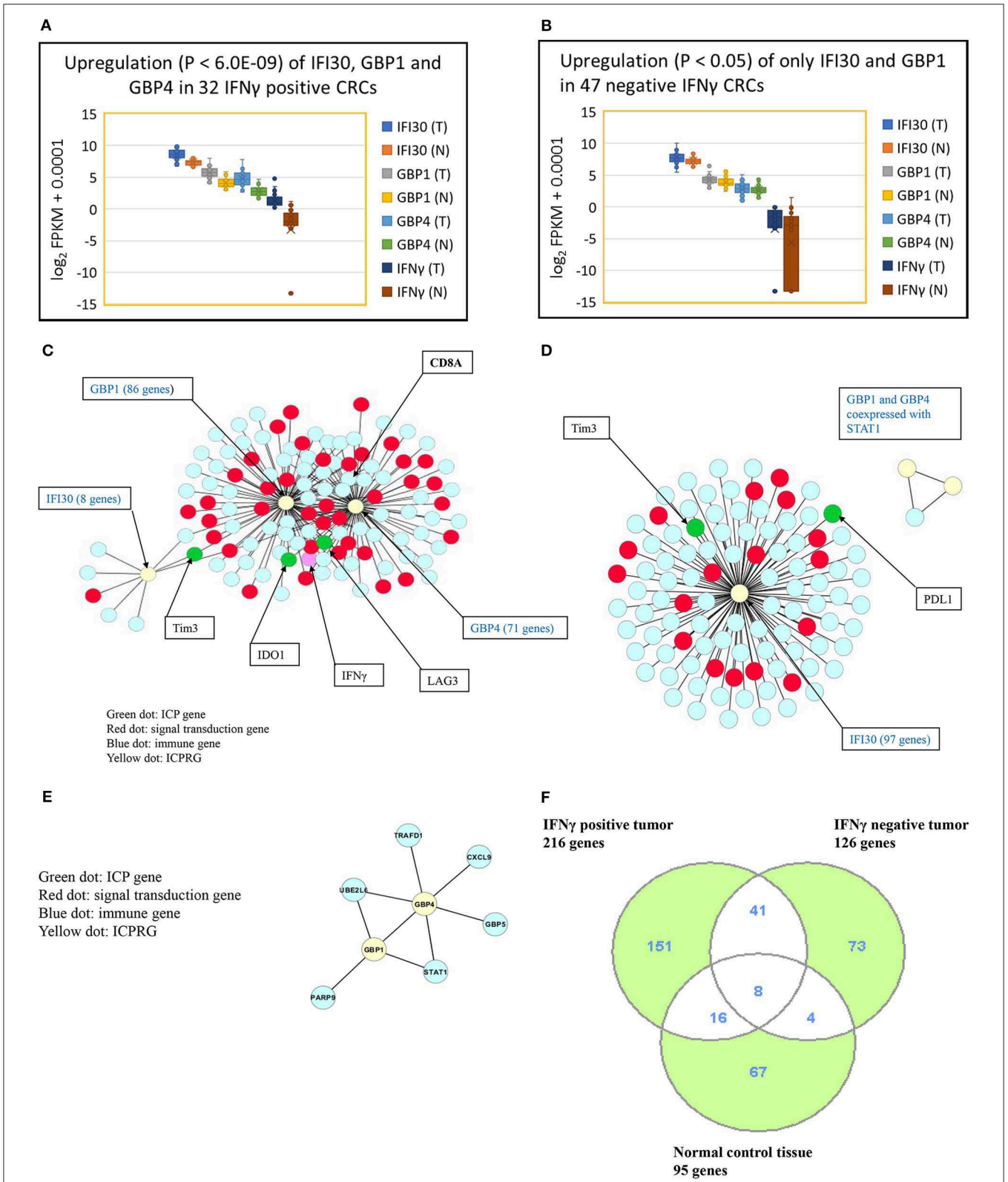

FIGURE 3 | Characterization of three ICPRGs in CRC. **(A)** Box and Whisker plot of three ICPRGs in IFNγ positive CRC. More upregulation (P < 6.0E-09) of all three ICPRGs (IFI30: 2.3-fold; GBP1: 3.1-fold, GBP4; 12.9-fold in tumor vs. normal). **(B)** Box and Whisker plot of three ICPRGs in IFNγ negative CRC. Less upregulation

(Continued)

FIGURE 3 | ($P < 0.05$) of two ICPRGs (IFI30: 1.4-fold and GBP1: 1.2-fold) and GBP4 (1.1-fold) ($P = 0.23$) in tumor vs. normal. **(C)** Co-expression of IFI30, GBP1, and GBP4 with IFNγ, IDO1, Tim3, LAG3 and CD8A within a 119 gene network in IFNγ positive CRCs. **(D)** Co-expression of IFI30 with PDL1 and Tim3 within a 101 network without CD8/CD4 in IFNγ negative CRCs. **(E)** GBP1 co-expressed with GBP4 within an eight-gene network in normal colon. **(F)** Identification of unique genes co-expressed with 10 genes (INFγ, six ICPs, and three ICPRGs) between INFγ positive and negative tumors. There are 151 unique genes in IFNγ positive tumors, 73 unique genes in IFNγ negative tumors, and 67 unique genes in normal tissue.

We then employed a Pearson correlation analysis to study the co-expression of IFNγ with the three newly identified potential ICPRGs in IFNγ positive and negative tumors as well as in normal controls. In IFNγ positive tumors, all three novel ICPRGs were co-expressed with IFNγ/CD8A and three known ICPs (IDO1, Tim3, and LAG3) within one network (total 119 genes: GBP1 and GBP4 correlated with IDO1, LAG3, and CD8A; IFI30 correlated Tim3) (**Figure 3C**). Moreover, GBP1 and GBP4 were identified as potential hub genes due to their substantial number of co-expressed genes ($n > 70$). In IFNγ negative tumors, IFI30 was co-expressed with 97 genes including Tim3 and PDL1 (but not with CD8/CD4) while GBP1 and GBP4 were only co-expressed with STAT1 (signal transducer and activator of transcription 1) but not with IFI30 or with IFNγ (**Figure 3D**). In normal colonic tissue, GBP1 and GBP4, were co-expressed within an 8 gene network, including STAT1 and GBP5 but not in association with IFNγ or IFI30 (**Figure 3E**), though IFI30 is strongly expressed in normal tissue (**Table S9**).

To address whether protein expression correlates with quantification of identified genes, we took advantage of two critical databases: Clinical Proteomic Tumor Analysis Consortium and The Pathology Atlas. The Clinical Proteomic Tumor Analysis Consortium CPTAC) (https://cptac-data-portal.georgetown.edu/) contains mass spectroscopy (MS) analyses of a cohort of 95 CRCs. By analysis of these data, we found that IFI30, GBP1, and GBP4 proteins are more abundantly expressed than are IDO1 and PD1 in this 95 CRC cohort (**Figure S1A**) (data pertaining to PDL1, Tim3, LAG3, CTLA4, and IFNγ are not available from this database) which is consistent with our findings that IFI30, GBP1, and GBP4 mRNAs (**Table S9**) were more abundant than six classical ICPs in our Indivumed and TCGA cohorts (**Table S7**).

Regarding the Pathology Atlas (https://www.proteinatlas.org/humanproteome/pathology), comprised of 5 million immunohistochemistry (IHC) images of different types of cancer, we compared the IHC data of the three novel ICP related genes and 5 classical checkpoint genes (ICPs) (CTLA4 is not available in this database) in CRC, breast cancer (BC), stomach cancer (STC) and skin cutaneous melanoma (SKCM). While 5 classical ICP proteins had low percentage staining (5–11%), the three ICP related proteins had high percentage staining (60–78%) in CRC and three other types of cancer (**Figure S1B**). This conclusion supports our findings that the proteins pertaining to the novel ICP related genes (**Table S9**), are not only markedly upregulated but are much more abundantly expressed than are the classical ICPs (**Table S7**) within tumor tissue, thus strongly supporting our gene expression data.

To gain insight into potential function of such genes in CRC, we sequenced six colon cancer cell lines (HCT15, SW480, SW620, SW116, HT29, HCT116, Colo205) and two normal colon cell lines (CCD841, HCoEpiC) and found that all 8 cell lines (both tumor and normal) had low expression of these three ICP related genes, IFNγ and six classical ICPs compared to primary tumors and normal tissues in HCA and PCA analyses (**Figures S2A,B**). The data again emphasize key differences between cell lines and primary tumors and that future functional studies, such as RNA silencing or over-expression of IFI30, GPB1, and GBP4 should be performed in primary tumors to evaluate the function of such factors in the tumor microenvironment context.

Identification of Uniquely Co-expressed Genes in IFNγ Positive vs Negative Tumors as Well as Normal Control Tissues

Because IFNγ, the six ICPs and the three ICPRGs were co-expressed with different numbers of genes in IFNγ positive and negative tumors, as well as in normal controls, we identified non-overlapping as well as overlapping genes among these groups (**Figures 2A–C**, **3C–F**) and consequently determined their related pathways with David Bioinformatics (25, 29). The results demonstrate that (i) in IFNγ positive tumors, 10 ICP and ICPRG genes (IFNγ, six ICPs and three ICPRGs) were uniquely co-expressed with 151 genes mainly related to CD8 T cell activation, inactivation, cytotoxicity, co-stimulation, response to vitamin A (T_H differentiation) and Wnt/β-catenin signaling (T cell development); (ii) in IFNγ negative tumors, three ICP and ICPRG genes (PDL1, Tim3, and IFI30) were uniquely co-expressed with 73 genes mainly related to B cell and macrophage activation, B cell antigen presentation, B cell response to lipopolysaccharide, wound healing/B cell maturation and EGFR signaling/B cell differentiation; (iii) in normal controls, 5 ICP and ICPRG genes (PD1, CTLA4, Tim3, GBP1, and GBP4) were uniquely co-expressed with 67 genes mainly related to T cell inhibition/MDSC2, lymph node development, induction of apoptosis, B cell proliferation and endoplasmic reticulum signaling/cell cycle (**Tables 1A–C**, **Table S8**). These data suggest the possible presence of distinct ICP/ICPRG involved in pathological and physiological pathways among IFNγ positive and negative tumors (two CRC subtypes) as well as in normal colonic tissues.

Close Association of IFNγ With T Cell Gene Expression in IFNγ Positive CRC

As indicated in our evaluation of NGS for gene quantification (see Methods above), in IFNγ positive tumors, higher expression levels of IFNγ correlated specifically with higher expression levels of T cell related genes including CD8α (3.5-fold), CD3ε (2.0-fold), CD4 (1.3-fold), and FOXP3 (1.5-fold) compared to IFNγ negative tumors ($p < 0.05$) but not with expression levels of genes pertaining to other immune cells ($p > 0.05$),

TABLE 1 | IFNγ dosage dependent immune checkpoint gene related pathways.

3 different groups	Total genes	Immune genes	Signaling genes
(A) NUMBER OF UNIQUELY CO-EXPRESSED GENES WITH SIX ICPs AND THREE ICPRGs IN IFNγ POSITIVE TUMOR, NEGATIVE TUMOR, AND NORMAL CONTROL			
32 IFNγ positive CRCs	151	87	64
47 IFNγ negative CRCs	73	62	11
79 normal controls	67	52	15
4 main pathways identified from 87 unique immune genes co-expressed with six **ICPs and three ICPRGs in IFNγ positive CRC**			**Pathway related genes**
(B) IMMUNE PATHWAYS AMONG IFNγ POSITIVE TUMOR, NEGATIVE TUMOR, AND NORMAL CONTROL			
CD8 T cell activation and inactivation (17 genes)			IFNγ, IDO1, LAG3, ITGAL, MICB, CD3G, CD3D, CD8A, CD8B, CD3E, SLA2, IL15, ADA, NLRC3, CD2, SPN, CD7
cytolysis (7 genes)/T cell			DNASE2, GZMM, IL2RA, GZMA, GPR65, BIRC3, SRGN
T cell co-stimulation (2 genes)			TNFSF13B, SPN
response to vitamin A (3 genes)/TH differentiation			CD38, MICB, MAP1B
4 main pathways identified from 62 unique immune genes co-expressed with six ICPs and three **ICPRGs in IFNγ negative CRC**			**Pathway related genes**
B cell and macrophage activation (7 genes)			ICAM1, PLEK, OLR1, CTGF, ITGA5, CD209, ADAM8
B cell antigen presentation (5 genes)			HCK, FCGR1A, FCER1G, COLEC12, CD14
B cell response to lipopolysaccharide (2 genes)			SLC11A1, PTAFR
wound healing (6 genes)/B cell maturation			SLC11A1, PLEK, ITGA5, ANXA5, PLAU, PLAUR
4 main pathways identified from 52 unique immune genes co-expressed with six ICPs and three **ICPRGs in normal control**			**Pathway related genes**
T cell inhibition/MDSC2 (8 genes)			CD48, ZBTB32, CARD11, LCK, FOXP3, VAV1, LCP1, CD28, CCR7
lymph node development (3 genes)/B cell			CXCR5, LTB, LTA
induction of apoptosis (2 genes)/B cell			VAV1, CD5
B cell proliferation (2 genes)			CARD11, CD40, CD19, CD79B
4 main pathways identified from 64 unique signaling genes co-expressed with six ICPs and three ICPRGs in IFNγ positive CRC			**Pathway related genes**
(C) SIGNALING TRANSDUCTION PATHWAYS AMONG IFNγ POSITIVE TUMOR, NEGATIVE TUMOR, AND NORMAL CONTROL			
Wnt/β^{-}catenin signaling (3 genes)/T cell development			NMI, RNF213, RNF31
GTPase signaling (6 genes)/T cell activation			GNGT2, GPR171, GPR174, GPR18, NCF1, SMAP2
nuclear receptor signaling (13 genes)/T cell response			ATXN7, BTN3A2, CEP170, CSTF2, CTRL, FAM78A, GTF2H4, NPL, RFX5, SFMBT2, SMCHD1, SNTB2, SNX20
phosphorylation (8 genes)/T cell activation			EVL, GSG2, HSPA1A, PPP1R16B, PTPN22, TBC1D10C, USF1, ZAP70
4 main pathways identified from 11 unique signaling genes co-expressed with six ICPs and three ICPRGs in IFNγ negative CRC			**Pathway related genes**
EGFR signaling (1 genes)/B cell differentiation			EMP3
cell-cell recognition (1 genes)/B cell receptor			ST3GAL6
phosphorylation (3 genes)/B cell receptor			ETV5, FGR, KIFC3
Ca2+ signaling (1 genes)			ITPRIP
4 main pathways identified from 15 unique signaling genes co-expressed with six ICPs and three ICPRGs in normal control			**Pathway related genes**
ER signaling (1 genes)/cell cycle			UBQLN3
phospholipase (1 genes)/B cell receptor			PLCG2
relaxin-3/RXFP3 signaling (1 genes)			RXFP3
TREM2/DAP12 signaling (1 genes) myeloid cell			TREM2

including B cells (CD19), neutrophils (CD11b), M1 macrophages (ARG1 and ARG2), and M2 macrophages (ARG2 and CCR7) (**Figure 4A**). In contrast, there were no differences ($p > 0.05$) in expression of the above 9 immune cell specific genes in normal tissues from patients with IFNγ positive vs. negative CRC (**Figure 4B**). As for T cell related cytotoxins, essential in tumor killing, stacked FPKM of 8 genes (PRF1, GZMM, GZMK, GZMH, GZMB, GZMA, FASLG, and FAS) demonstrated that these genes were more highly expressed 1.7-fold ($P = 0.037$) in IFNγ positive tumors compared to IFNγ negative tumors (**Figure S3A**). Eleven co-stimulatory genes (C10orf54 [B7-H5], BTLA4, CD86, CD80, ICOS, CD28, CD27, CD40, TNFRSF9 [4-1BB], TNFRSF18 [GITR], TNFRSF4 [OX40]) (30, 31) were expressed at higher (1.5-fold) levels in IFNγ positive vs. IFNγ negative CRC, but this did not reach statistical significance ($p = 0.30$) (**Figure S3B**). Moreover, stacked FPKM of 9 caspases (CASP2 to CASP10) (**Figure S3C**) and 9 cell cycle related genes (PRKDC, H2AFX, FANCD2, BRCA2, BRCA1, CHEK1, ATR, ATM) (**Figure S3D**) demonstrated that these genes were not significantly upregulated in IFNγ positive vs. negative tumors. These findings suggest that although IFNγ may upregulate CTL-associated proteins, it does not directly affect expression of co-stimulatory molecules (required for full T cell activation), caspases and cell cycle related genes, critical factors contributing to T cell activation and function.

In exploring further correlates of immune activation in tumors, we examined the relationship between IFNγ expression and thirteen DNA mismatch repair enzymes (MMR) (PMS2P5, PMS2P4, PMS2P3. PMS2P1, PMS2CL, PMS2, PMS1, MSH6, MSH4, MSH3, MSH2, MLH3, and MLH1), because the loss of DNA MMR function is associated with increased expression of neoantigens, immune cell recruitment and induction of ICPs (32). We did not find a difference between IFNγ expression and expression of 13 DNA MMRs (1.0-fold) ($p = 0.86$) in IFNγ positive vs. negative tumors (**Figure S3E**). Although the MSS/MSI status was available for only 7 CRCs in our cohort, 5 MSS CRCs, and two MSI CRC (**Table S1**), we found that all 10 genes (IFNγ, six ICPs, and three ICPRGs) were upregulated in MSI CRC compared to MSS CRC but this did not reach statistical significance ($P = 0.31$) in this small sample size (**Figure S3F**). Thus, the relationship between IFNγ upregulation and the presence or loss of the MMRs and MSI/MSS status needs to be studied further.

Validation of IFNγ Dependent Expression of Six Classical ICPs and Three ICPRGs in a Larger CRC Cohort

To further define the dosage impact of IFNγ on the expression of six ICPs and three ICPRGs, we generated six IFNγ expression level gradients[1] IFNγ: FPKM > 5 (4 CRCs); (1) IFNγ: FPKM = 4.9–2 (20 CRCs); (2) IFNγ: FPKM = 1.99–1(44 CRCs); (3) IFNγ: FPKM = 0.99–0.5 (73 CRCs); (4) IFNγ: FPKM = 0.49–0.01 (467 CRC); and (5) IFNγ: FPKM < 0.009 (107 CRCs) in 716 CRCs (Indivumed [79 CRCs] and TCGA [637 CRCs]) (**Figure 5A**) and examined the impact of the levels on expression of the ICPs and ICPRGs examined in our more limited cohort. We found that the expression level of IFNγ was highly co-related

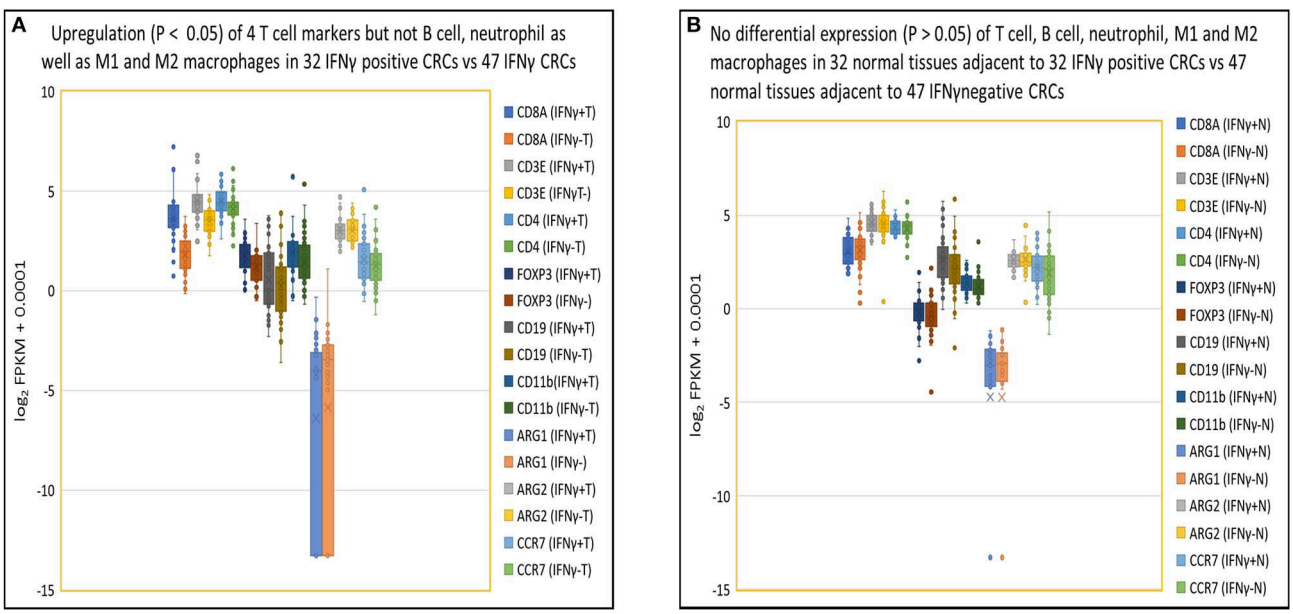

FIGURE 4 | Close association of IFNγ with T cells in tumor but not in normal tissues. **(A)** Box and Whisker plot of immune cell genes in IFNγ positive CRCs. Upregulation ($P < 0.05$) of T cells (CD8A, 3.5-fold; CD3E, 2.0-fold; CD4, 1.3-fold; FOXP3, 1.5-fold) but not B cell (CD19) (1.2-fold, $P = 0.38$), neutrophil (CD11b) (1.4-fold, $P = 0.079$), M1 (ARG1) (0.68-fold, $P = 0.62$), (ARG2) (1.0-fold, $P = 0.87$), or M2 (ARG2, CCR7) (1.2-fold, $P = 0.30$) leukocyte-related genes in IFNγ positive CRC vs. negative CRC. **(B)** Box and Whisker plot of immune cell genes in normal colon tissue. No upregulation ($P > 0.05$) of T cells (CD8A, 0.93-fold; CD3E, 1.0-fold; CD4, 1.0-fold; FOXP3, 1.1-fold), B cell (CD19) (1.4-fold), neutrophil (CD11b) (1.1-fold), MDSC1 (ARG1) (1.0-fold), (ARG2) (0.97-fold), or MDSC2 (ARG2, CCR7) (1.2-fold) leukocytes related genes in tissues adjacent to IFNγ positive and negative CRCs.

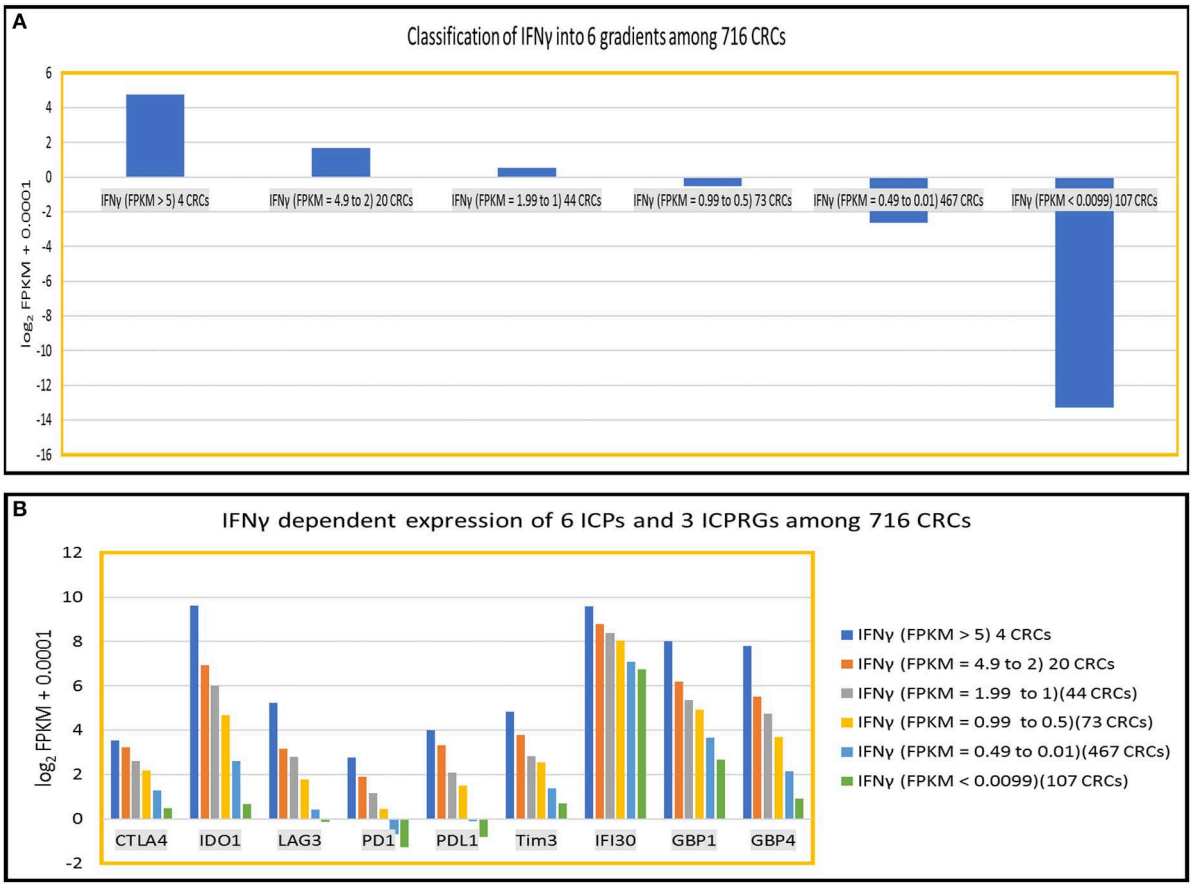

FIGURE 5 | IFNγ dependent expression of six ICPs (PDl, PDLl, CTLA4, IDOl, LAG3, Tim3) and three ICPRGs (IFI30, GBPl, GBP4) in 716 CRCs. **(A)** Classification of INFγ into six expression gradients in 716 CRCs. **(B)** IFNγ dosage dependent expression positive correlation (cc > 0.94) with six ICPs and three ICPRGs across six IFNγ expression level gradients (six CRC subsets).

(cc > 0.94) with expression levels of the six ICPs and three ICPRGs across the six IFNγ gradients (**Figure 5B**).

Regarding expression of ICPs and ICPRGs in matched normal control tissues, we found no differential expression of IFNγ, six ICPs and three ICPRGs between normal tissues adjacent to IFNγ positive vs. negative tumors (**Tables S10, S11**).

Further Confirmation of IFNγ Dependent Expression of Six Classical ICPs and Three ICPRGs Among Five Other Solid Cancer Types

To evaluate whether our findings regarding IFNγ-associated expression of six classical ICPs and three ICPRGs in CRC also applied to distinct tumor types, we compared the overall stacked $\log_2$ expression of the six ICP genes and three ICPRGs in the following tumor types: 103 skin cutaneous melanomas (SKCMs); 1,105 breast cancers (BCs); 184 esophageal cancers (ESCs); 416 stomach cancers (STCs); and 501 lung squamous carcinomas (LUSC) all from the TCGA database. Similar to the CRC findings, the overall stacked $\log_2$ FPKM expression levels of six classical ICPs [CRC: (1.73-fold, $p = 0.58$), SKCM: (3.2-fold/$p = 0.10$), BC: (27.8-fold/$P = 0.051$), ESC: (2.1-fold/$p = 0.39$)], STC: (1.9-fold/ $p = 0.51$) and LUSC: (4.4-fold/ $p = 0.10$)] (**Figure S4A**) and three ICPRGs [CRC: (4.3-fold/ $p = 0.29$), SKCM: (5.4-fold/ $p = 0.27$), BC: (3.6-fold/ $p = 0.33$), ESC: (2.8-fold/ $p = 0.36$), STC: (3.1-fold/ $p = 0.36$) and LUSC: (2.9-fold/ $p = 0.47$)] (**Figure S4B**) were increased (1.7 to 27.8-fold) in IFNγ positive (FPKM > 1) tumors vs. IFNγ negative (FPKM < 1) tumors across these cancers but without statistical significance.

Because these three ICPRGs have the potential to be novel actionable targets in cancer therapy, we further examined these individual genes by Box and Whisker plots of $\log_2$ FPKM expression levels in IFNγ positive and negative tumors of CRC, SKCM, BC, ESC, STC, and LUSC. IFI30, GBP1 and GBP4 were upregulated 2-8-fold ($p < 0.0001$) in IFNγ positive tumors vs. IFNγ negative tumors (**Figure 6**) in each of the six tumor types. Among these six cancers, only STC had a higher abundance (average FPKM) of IFI30, GBP1, and GBP4 (469, 78, 54) than did CRC (334, 47, 25) in the IFNγ positive tumors (**Table S12**). These three ICPRGs were also 24-fold more abundant than six ICPs in 5 types of normal tissues adjacent to BC, STC, LUSC, ESC,

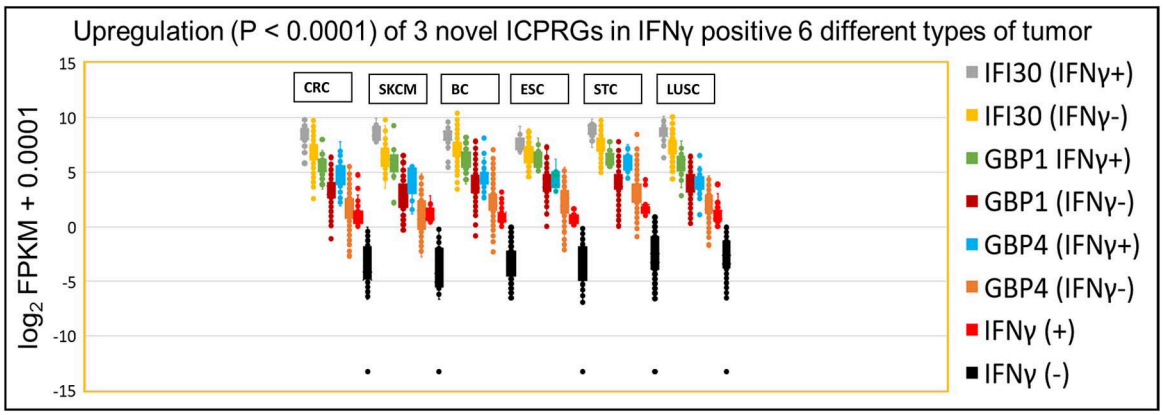

FIGURE 6 | IFNγ dependent expression of three ICPRGs among five other solid cancers in Indivmed and TCGA cohort. Box and Whisker analysis of three ICPRGs in six types of cancer. Higher three ICPRGs and IFNγ expression in IFNγ (+) 69 CRCs (IFI30, 2.9-fold; GBP1, 4.6-fold; GBP4, 7.9-fold; and IFNγ, 44-fold), 13 SKCMs (IFI30, 4.6-fold; GBP1, 8.5-fold; GBP4, 8.3-fold; and IFNγ, 55-fold), 85 BCs (IFI30, 2.3-fold; GBP1, 4.9-fold; GBP4, 4.5-fold; and IFNγ, 19-fold), 13 ESCs (IFI30, 2.0-fold; GBP1, 4.5-fold; GBP4, 4.1-fold; and IFNγ 28-fold), 71 STCs (IFI30, 2.5-fold; GBP1, 4.5-fold; GBP4, 6.2-fold; and IFNγ 23-fold), and 68 LUSCs (IFI30, 2.6-fold; GBP1, 3.4-fold; GBP4, 4.1-fold; and IFNγ 17-fold), vs. IFNγ (–) 647 CRCs, 90 SKCMs, 1,020 BCs, 171 ESCs, 345 STCs, and 433 LUSCs.

and CRC (**Table S13**) again raising the issue of whether these three genes are involved in a universal tolerance mechanism for normal tissues.

Strikingly in LUSC, all 68 IFNγ positive tumors had high expression of PD1 (FPKM $>$ 1) while all 434 IFNγ negative tumors had low expression of PD1 (FPKM $<$ 1) with a statistically significant 4.8-fold difference (**Figure S5**). These data suggest a dosage effect of IFNγ with respect to consequent expression of the six ICPs as well as for the three ICPRGs in six solid tumor types.

Correlation of Immune Genes With Clinical Parameters in CRC

To address this issue, we separated by stage the 129 CRC pairs (79 CRC pairs as well as 50 CRC pairs/TCGA_38 cohort) into 57 low stage tumors (TNM stage I/II) and 82 high stage tumors (TNM stage III/IV) and found that there was no significant difference ($p = 0.81$) in the expression of IFI30, GBP1, GBP4, PD1, PDL1, CTLA4, Tim3, LAG3, IFNγ, and IDO1 between low and high stage CRCs (**Figure S6**). Because the tumor genetic profile may impact survival, we analyzed the Pathology Atlas data and found that (i) higher expression of IFI30, GBP1 and GBP4 was associated with better 5-year survival rate in breast cancer as well as in skin cutaneous melanoma, (ii) higher expression of GBP1 and GBP4 was associated with better 5-year survival rate in colorectal and stomach cancer, and (iii) higher expression of IFI30 was associated with worse 5-year survival rate in colorectal and stomach cancer (**Table S14**). These data suggest that any impact of IFI30, GBP1, and GBP4 on tumor response to diverse therapeutics is likely tumor type and context- dependent, clearly warranting further study.

DISCUSSION

Although IFNγ secreted by immune cells promotes growth arrest of tumors by augmenting MHC class I expression, contributing to the recruitment of effector cells, mediating Treg fragility and coordinating innate and adaptive antitumor responses (33, 34), IFNγ signaling can also compromise antitumor immunity by blocking these activities through the induction of immune checkpoint inhibitory molecules on T and tumor cells (35). The overall balance and timing of IFNγ expression over the course of tumor development and the downstream consequences likely critically determine an effective vs. suppressive immune response and an immunologic profile of consideration for immunotherapeutic approaches to treatment (36). In this study, we first demonstrated the specific upregulation and co-expression of six ICPs associated with higher expression of IFNγ in CRC. These data provide the molecular basis of using more than one ICP blocker in CRC with higher IFNγ expression but not lower IFNγ expression. Then, by analysis of genes co-expressed with IFNγ, we discovered three IFNγ associated ICPRGs. These three ICPRGs are expressed at higher abundance in CRC compared to the classical ICPs (except IDO1). Furthermore, there was differential co-expression of IFNγ with other immunologically pertinent genes between IFNγ positive and negative CRCs. IFNγ, the six ICPs, and the three ICPRGs were mainly co-expressed with T cell genes related to T cell activation, cytolysis and co-stimulation in IFNγ positive tumors while 2 ICPs and one ICPRG, but not IFNγ, were mainly co-expressed with B cell genes related to B cell activation, antigen presentation and response to lipopolysaccharide in IFNγ negative tumors. These data indicate dosage dependence of IFNγ on immune regulatory mechanisms in CRC. Finally, the co-upregulation of IFNγ with six ICPs as well as three ICPRGs was strongly supported by findings in the TCGA cohorts of melanoma, colon, breast, esophageal, stomach, and lung cancer. Thus, in addition to factors such as microsatellite stability status, tumor mutational burden, and expression of checkpoint inhibitory molecules, high IFNγ expression levels could potentially be investigated as a predictive biomarker for the potential for immune responsiveness of a tumor.

In our evaluation of the six classical ICPs, LAG3 appears to be a critical hub gene with the greatest number of co-expressed genes and though upregulated in IFNγ positive tumors, was downregulated and lacking co-expressed genes in IFNγ negative tumors. Thus, LAG3 may be a marker of biologically meaningful expression levels of IFNγ and an important drug target for CRC therapy in IFNγ positive CRC. The molecular mechanisms of LAG3 immune suppression have not been extensively defined. An additional ICP expressed at higher abundance compared to the other well-known ICP was IDO1, a rate-limiting metabolic enzyme that converts tryptophan into immune suppressive kynurenines (37). IDO1 is highly expressed in multiple types of human cancer (38) and studies indicate that while single-agent treatment with IDO1 enzyme inhibitor may not substantially decrease the established cancer burden, approaches combining select therapies with IDO1 blockade may have additive or synergistic effects, as shown in animal studies (39).

Based on their co-expression with six classical ICPs and with T cell markers, it is likely that the newly identified IFNγ related proteins, IFI30, GBP1, and GBP4 are immunomodulatory and may serve, in some tumors, as ICPs. That GBP1 and GBP4 are directly co-expressed with CD8A suggests the correlation of the three ICPRGs with a higher basal level of CD8A related infiltration in IFNγ positive CRC. It is well known that $CD8^+$ T-cell infiltrates predict favorable prognosis in the majority of cancer types (40). In fact, GBP1 and GBP4 were associated with a favorable prognosis in 4 types of cancer (CRC, SKCM, BC, and STC) according to the Pathology Atlas analysis. These data are consistent with the evidence [KEYNOTE-001 trial/pembrolizumab (anti-PDL1) treatment] (41, 42) that high expression of PDL1, a classical immune suppressive check point molecule was associated with better survival among pembrolizumab-treated NSCLC and melanoma patients.

The immune and tumor related nature of these three genes are supported by the following published data: (i) IFI30 suppresses mouse primary T cell reactivity *in vitro* and mouse autoimmunity through cellular redox chemistry and ERK1/2 phosphorylation *in vivo*, promotes cell proliferation of a glioma cell line, but IFI30 RNA has been associated, with better patient survival rate in breast cancer and diffuse large B cell lymphoma (DLBCL) (9–14), (ii) GBP1 suppresses TCR signaling through lymphocyte cell-specific protein-tyrosine kinase and IL2 production in a human T cell line promotes cell proliferation/anti-apoptosis of a glioblastoma and two breast cancer cell lines, but inhibits cell proliferation of a colon cancer line. Furthermore, GBP1 reduces radioresistance of two human oral and liver cancer cell lines and correlates with better prognosis in melanoma but with poorer prognosis in human glioblastoma (15–21), (iii) GBP4 inhibits innate responses to viral infection (22) but lacks known tumor related functions to date. Thus, both knock-down and overexpression of these three genes should be tested in the future experiments to define the exact roles of these proteins within specific contexts. Additionally, there is the potential that inhibiting or stimulating them could change responses to infection and autoimmunity given their abundant expression in normal colonic tissues.

The co-expression of CTLA4 and PD1 with predominantly B cell markers and the co-expression of GBP1/GBP4 with six genes mainly related to anti-viral and microbial infection in normal intestinal epithelium [CXCL9, GBP5, STAT1, PARP9 (Poly ADP-Ribose Polymerase 9), TRAFD1 (Type Zinc Finger Domain Containing 1), and UBE2L6 (ubiquitin conjugating enzyme E2 L6)] suggest that maintenance of homeostasis, challenged by commensal bacteria, food antigens and potential autoantigens, may be maintained by B regulatory cell induction of ICPs (43–45). The relationship of these factors to mechanisms of intestinal tolerance and immunity clearly requires further study.

In summary, by applying NGS to study the expression of six classical ICPs and their co-expression networks, we found not only the well-established connection between IFNγ and the expression of ICPs in CRC, a relatively immunotherapy-refractory tumor type, but also, a novel set of ICPRGs as well as potential new hub genes which may be potential therapeutic targets. This study also provides comprehensive ICP co-expression information and fortifies the importance of NGS profiling in CRC and other tumors. The expression of higher abundance and novel ICPRG genes, including IFI30, GBP1, and GBP4, requires further evaluation of protein expression levels and immune inhibitory function in tumors.

DATA AVAILABILITY STATEMENT

The datasets generated for this study are available on request to the corresponding author.

AUTHOR CONTRIBUTIONS

RW, WW, J-NP, C-TL, and R-FS carried out experiments. RW, HM, L-HW, EP, W-LA, and LX performed data analysis. AR, LX, RW, LP, HM, EP, and HJ designed experiments and interpreted results. AR, RW, HM, LP, and LX wrote the manuscript, and all authors edited it. AR was the principal investigator of this study. All authors reviewed and approved the final manuscript.

FUNDING

This work was supported by FDA intramural program funds awarded to Amy Rosenberg (FDA/OPQ/OBP/PDUFA/2017 to 2019).

ACKNOWLEDGMENTS

The authors would like to thank Drs. Ashutosh Rao (FDA) and Gideon Blumenthal (FDA) for their critical review and comments on this manuscript.

SUPPLEMENTARY MATERIAL

The Supplementary Material for this article can be found online at: https://www.frontiersin.org/articles/10.3389/fimmu.2020.00224/full#supplementary-material

REFERENCES

1. Siegel RL, Miller KD, Jemal A. Cancer statistics, 2019. *CA Cancer J Clin.* (2019) 69:7–34. doi: 10.3322/caac.21551
2. Campos FG. Colorectal cancer in young adults: a difficult challenge. *World J Gastroenterol.* (2017) 23:5041–4. doi: 10.3748/wjg.v23.i28.5041
3. Le DT, Uram JN, Wang H, Bartlett BR, Kemberling H, Eyring AD, et al. PD-1 Blockade in tumors with mismatch-repair deficiency. *N Engl J Med.* (2015) 372:2509–20. doi: 10.1056/NEJMoa1500596
4. Cancer Genome Atlas Network. Comprehensive molecular characterization of human colon and rectal cancer. *Nature.* (2012) 487:330–7. doi: 10.1038/nature11252
5. Llosa NJ, Cruise M, Tam A, Wicks EC, Hechenbleikner EM, Taube JM, et al. The vigorous immune microenvironment of microsatellite instable colon cancer is balanced by multiple counter-inhibitory checkpoints. *Cancer Discov.* (2015) 5:43–51. doi: 10.1158/2159-8290.CD-14-0863
6. Mimura K, Teh JL, Okayama H, Shiraishi K, Kua LF, Koh V, et al. PD-L1 expression is mainly regulated by interferon gamma associated with JAK-STAT pathway in gastric cancer. *Cancer Sci.* (2018) 109:43–53. doi: 10.1111/cas.13424
7. Karachaliou N, Gonzalez-Cao M, Crespo G, Drozdowskyj A, Aldeguer E, Gimenez-Capitan A, et al. Interferon gamma, an important marker of response to immune checkpoint blockade in non-small cell lung cancer and melanoma patients. *Ther Adv Med Oncol.* (2018) 10:1758834017749748. doi: 10.1177/1758834017749748
8. Qian J, Wang C, Wang B, Yang J, Wang Y, Luo F, et al. The IFN-γ/PD-L1 axis between T cells and tumor microenvironment: hints for glioma anti-PD-1/PD-L1 therapy. *Neuroinflammation.* (2018) 15:290. doi: 10.1186/s12974-018-1330-2
9. Barjaktarević I, Rahman A, Radoja S, Bogunović B, Vollmer A, Vukmanović S, et al. Inhibitory role of IFN-gamma-inducible lysosomal thiol reductase in T cell activation. *J Immunol.* (2006) 177:4369–75. doi: 10.4049/jimmunol.177.7.4369
10. Maric M, Barjaktarevic I, Bogunovic B, Stojakovic M, Maric C, Vukmanovic S. Cutting edge: developmental up-regulation of IFN-gamma-inducible lysosomal thiol reductase expression leads to reduced T cell sensitivity and less severe autoimmunity. *J Immunol.* (2009) 182:746–50. doi: 10.4049/jimmunol.182.2.746
11. Teramoto T, Chiang HS, Takhampunya R, Manzano M, Padmanabhan R, Maric M. Gamma interferon-inducible lysosomal thioreductase (GILT) ablation renders mouse fibroblasts sensitive to dengue virus replication. *Virology.* (2013) 441:146–51. doi: 10.1016/j.virol.2013.03.017
12. Xiang YJ, Guo MM, Zhou CJ, Liu L, Han B, Kong LY, et al. Absence of gamma-interferon-inducible lysosomal thiol reductase (GILT) is associated with poor disease-free survival in breast cancer patients. *PLoS ONE.* (2014) 9:e109449. doi: 10.1371/journal.pone.0109449
13. Chen S, Wang Q, Shao X, Di G, Dai Y, Jiang X, et al. Lentivirus mediated γ-interferon-inducible lysosomal thiol reductase (GILT) knockdown suppresses human glioma U373MG cell proliferation. *Biochem Biophys Res Commun.* (2019) 509:182–7. doi: 10.1016/j.bbrc.2018.12.099
14. Rausch MP, Hastings KT. Diverse cellular and organismal functions of the lysosomal thiol reductase GILT. *Mol Immunol.* (2015) 68(2 Pt A):124–8. doi: 10.1016/j.molimm.2015.06.008
15. Forster F, Paster W, Supper V, Schatzlmaier P, Sunzenauer S, Ostler N, et al. Guanylate binding protein 1-mediated interaction of T cell antigen receptor signaling with the cytoskeleton. *J Immunol.* (2014) 192:771–81. doi: 10.4049/jimmunol.1300377
16. Quintero M, Adamoski D, Reis LMD, Ascenção CFR, Oliveira KRS, Gonçalves KA, et al. Guanylate-binding protein-1 is a potential new therapeutic target for triple-negative breast cancer. *BMC Cancer.* (2017) 17:727. doi: 10.1186/s12885-017-3726-2
17. Fukumoto M, Amanuma T, Kuwahara Y, Shimura T, Suzuki M, Mori S, et al. Guanine nucleotide-binding protein 1 is one of the key molecules contributing to cancer cell radioresistance. *Cancer Sci.* (2014) 105:1351–9. doi: 10.1111/cas.12489
18. Britzen-Laurent N, Lipnik K, Ocker M, Naschberger E, Schellerer VS, Croner RS, et al. GBP-1 acts as a tumor suppressor in colorectal cancer cells. *Carcinogenesis.* (2013) 34:153–62. doi: 10.1093/carcin/bgs310
19. Fisch D, Bando H, Clough B, Hornung V, Yamamoto M, Shenoy AR, et al. Human GBP1 is a microbe-specific gatekeeper of macrophage apoptosis and pyroptosis. *EMBO J.* (2019) 38:e100926. doi: 10.15252/embj.2018100926
20. Wang Q, Wang X, Liang Q, Wang S, Xiwen L, Pan F, et al. Distinct prognostic value of mRNA expression of guanylate-binding protein genes in skin cutaneous melanoma. *Oncol Lett.* (2018) 15:7914–22. doi: 10.3892/ol.2018.8306
21. Ji X, Zhu H, Dai X, Xi Y, Sheng Y, Gao C, et al. Overexpression of GBP1 predicts poor prognosis and promotes tumor growth in human glioblastoma multiforme. *Cancer Biomark.* (2019) 25:275–90. doi: 10.3233/CBM-171177
22. Hu Y, Wang J, Yang B, Zheng N, Qin M, Ji Y, et al. Guanylate binding protein 4 negatively regulates virus-induced type I IFN and antiviral response by targeting IFN regulatory factor 7. *J Immunol.* (2011) 187:6456–62. doi: 10.4049/jimmunol.1003691
23. Unger F, Lange N, Krüger J, Compton C, Moore H, Agrawal L, et al. Nanoproteomic analysis of ischemia-dependent changes in signaling protein phosphorylation in colorectal normal and cancer tissue. *J Transl Med.* (2016) 14:6. doi: 10.1186/s12967-015-0752-1
24. Puppa G, Sonzogni A, Colombari R, Pelosi G. TNM staging system of colorectal carcinoma: a critical appraisal of challenging issues. *Arch Pathol Lab Med.* (2010) 134:837–52. doi: 10.1043/1543-2165-134.6.837
25. Xu L, Luo H, Wang R, Wu WW, Phue JN, Shen RF, et al. Novel reference genes in colorectal cancer identify a distinct subset of high stage tumors and their associated histologically normal colonic tissues. *BMC Med Genet.* (2019) 20:138. doi: 10.1186/s12881-019-0867-y
26. Toung JM, Morley M, Li M, Cheung VG. RNA-sequence analysis of human B-cells. *Genome Res.* (2011) :991–8. doi: 10.1101/gr.116335.110
27. Xu L, Ziegelbauer J, Wang R, Wu WW, Shen RF, Juhl H, et al. Distinct Profiles for Mitochondrial t-RNAs and Small Nucleolar RNAs in Locally Invasive and Metastatic Colorectal Cancer. *Clin Cancer Res.* (2016) 22:773–84. doi: 10.1158/1078-0432.CCR-15-0737
28. Xu L, Wang R, Ziegelbauer J, Wu WW, Shen RF, Juhl H, et al. Transcriptome analysis of human colorectal cancer biopsies reveals extensive expression correlations among genes related to cell proliferation, lipid metabolism, immune response and collagen catabolism. *Oncotarget.* (2017) 8:74703–19. doi: 10.18632/oncotarget.20345
29. Wu WW, Phue JN, Lee CT, Lin C, Xu L, Wang R, et al. Robust Sub-nanomolar Library Preparation for High Throughput Next Generation Sequencing. *BMC Genomics.* (2018) 19:326. doi: 10.1186/s12864-018-4677-y
30. Kelso A, Costelloe EO, Johnson BJ, Groves P, Buttigieg K, Fitzpatrick DR. The genes for perforin, granzymes A-C and IFN-gamma are differentially expressed in single CD8(+) T cells during primary activation. *Int Immunol.* (2002) 14:605–13. doi: 10.1093/intimm/dxf028
31. Bhat P, Leggatt G, Waterhouse N, Frazer IH. Interferon-γ derived from cytotoxic lymphocytes directly enhances their motility and cytotoxicity. *Cell Death Dis.* (2017) 8:e2836. doi: 10.1038/cddis.2017.67
32. Yarchoan M, Johnson BA 3rd, Lutz ER, Laheru DA, Jaffee EM. Targeting neoantigens to augment antitumour immunity. *Nat Rev Cancer.* (2017) 17:209–22. doi: 10.1038/nrc.2016.154
33. Castro F, Cardoso AP, Gonçalves RM, Serre K, Oliveira MJ. Interferon-gamma at the crossroads of tumor immune surveillance or evasion. *Front Immunol.* (2018) 9:847. doi: 10.3389/fimmu.2018.00847
34. Wang L, Wang Y, Song Z, Chu J, Qu X. Deficiency of interferon-gamma or its receptor promotes colorectal cancer development. *J Int Cytokine Res.* (2015) 35:273–80. doi: 10.1089/jir.2014.0132
35. Ni L, Lu J. Interferon gamma in cancer immunotherapy. *Cancer Med.* (2018) 7:4509–16. doi: 10.1002/cam4.1700
36. Lin CF, Lin CM, Lee KY, Wu SY, Feng PH, Chen KY, et al. Escape from IFN-γ-dependent immunosurveillance in tumorigenesis. *J Biomed Sci.* (2017) 24:10. doi: 10.1186/s12929-017-0317-0
37. Mbongue JC, Nicholas DA, Torrez TW, Kim NS, Firek AF, Langridge WH. The role of indoleamine 2, 3-dioxygenase in immune suppression and autoimmunity. *Vaccines.* (2015) 3:703–29. doi: 10.3390/vaccines3030703
38. Liu M, Wang X, Wang L, Ma X, Gong Z, Zhang S, et al. Targeting the IDO1 pathway in cancer: from bench to bedside. *J Hematol Oncol.* (2018) 11:100. doi: 10.1186/s13045-018-0644-y

39. Muller AJ, Manfredi MG, Zakharia Y, Prendergast GC. Inhibiting IDO pathways to treat cancer: lessons from the ECHO-301 trial and beyond. *Semin Immunopathol.* (2019) 41:41–8. doi: 10.1007/s00281-018-0702-0
40. Shimizu S, Hiratsuka H, Koike K, Tsuchihashi K, Sonoda T, Ogi K, et al. Tumor-infiltrating $CD8_+$ T-cell density is an independent prognostic marker for oral squamous cell carcinoma. *Cancer Med.* (2019) 8:80–93. doi: 10.1002/cam4.1889
41. *Pembrolizumab Increases Historic Survival Rate for Certain People with Advanced Non-Small Cell Lung Cancer*. Available online at: https://www.asco.org/about-asco/press-center/news-releases/pembrolizumab-increases-historic-survival-rate-certain-people
42. *Association of PD-L1 Expression and Response to Pembrolizumab in Advanced Melanoma.* Available online at: https://www.ascopost.com/News/44059
43. Schwartz M, Zhang Y, Rosenblatt JD. B cell regulation of the anti-tumor response and role in carcinogenesis. *Int Immunol.* (2016) 28:423–33. doi: 10.1186/s40425-016-0145-x
44. Bowick GC, Airo AM, Bente DA. Expression of interferon-induced antiviral genes is delayed in a STAT1 knockout mouse model of Crimean-Congo hemorrhagic fever. *Virol J.* (2012) 9:122. doi: 10.1186/1743-422X-9-122
45. Zhang Y, Mao D, Roswit WT, Jin X, Patel AC, Patel DA, et al. PARP9-DTX3L ubiquitin ligase targets host histone H2BJ and viral 3C protease to enhance interferon signaling and control viral infection. *Nat Immunol.* (2015) 16:1215–27. doi: 10.1038/ni.3279

Conflict of Interest: HJ was employed by the company Indivumed GMBH.

The remaining authors declare that the research was conducted in the absence of any commercial or financial relationships that could be construed as a potential conflict of interest.

frontiers in Immunology

REVIEW
published: 15 April 2020
doi: 10.3389/fimmu.2020.00508

CD73's Potential as an Immunotherapy Target in Gastrointestinal Cancers

Jerry B. Harvey[1†], *Luan H. Phan*[1†], *Oscar E. Villarreal*[2†] *and Jessica L. Bowser*[1*]

[1] Department of Anesthesiology, The University of Texas Health Science Center at Houston, Houston, TX, United States, [2] Department of Gastrointestinal Medical Oncology, The University of Texas MD Anderson Cancer Center, Houston, TX, United States

CD73, a cell surface 5′nucleotidase that generates adenosine, has emerged as an attractive therapeutic target for reprogramming cancer cells and the tumor microenvironment to dampen antitumor immune cell evasion. Decades of studies have paved the way for these findings, starting with the discovery of adenosine signaling, particularly adenosine A2A receptor (A2AR) signaling, as a potent suppressor of tissue-devastating immune cell responses, and evolving with studies focusing on CD73 in breast cancer, melanoma, and non-small cell lung cancer. Gastrointestinal (GI) cancers are a major cause of cancer-related deaths. Evidence is mounting that shows promise for improving patient outcomes through incorporation of immunomodulatory strategies as single agents or in combination with current treatment options. Recently, several immune checkpoint inhibitors received FDA approval for use in GI cancers; however, clinical benefit is limited. Investigating molecular mechanisms promoting immunosuppression, such as CD73, in GI cancers can aid in current efforts to extend the efficacy of immunotherapy to more patients. In this review, we discuss current clinical and basic research studies on CD73 in GI cancers, including gastric, liver, pancreatic, and colorectal cancer, with special focus on the potential of CD73 as an immunotherapy target in these cancers. We also present a summary of current clinical studies targeting CD73 and/or A2AR and combination of these therapies with immune checkpoint inhibitors.

Keywords: CD73, adenosine, gastrointestinal cancers, immunosuppression, immunotherapy

OPEN ACCESS

Edited by:
Gianluigi Giannelli,
National Institute of Gastroenterology S. de Bellis Research Hospital (IRCCS), Italy

Reviewed by:
Arabella Young,
University of California, San Francisco, United States
Paul Andrew Beavis,
Peter MacCallum Cancer Centre, Australia

***Correspondence:**
Jessica L. Bowser
jessica.l.bowser@uth.tmc.edu

[†] *These authors have contributed equally to this work*

Specialty section:
This article was submitted to Cancer Immunity and Immunotherapy, a section of the journal Frontiers in Immunology

Received: *30 November 2019*
Accepted: *05 March 2020*
Published: *15 April 2020*

Citation:
Harvey JB, Phan LH, Villarreal OE and Bowser JL (2020) CD73's Potential as an Immunotherapy Target in Gastrointestinal Cancers. Front. Immunol. 11:508. doi: 10.3389/fimmu.2020.00508

INTRODUCTION

Gastrointestinal (GI) cancers are some of the most common cancers worldwide and a major cause of cancer-related deaths (1–5). Immune checkpoint inhibitors (ICIs), including pembrolizumab (Keytruda) and nivolumab (Opdivo), antibodies against programmed death-1 (PD-1), recently gained Food and Drug Administration (FDA) approval for use in GI cancers (**Table 1**) (6–11). While their approval has been a significant step forward in advancing clinical care, currently, few patients benefit (12). Patients benefiting the most tend to have tumors harboring deficient DNA mismatch repair (dMMR) and high microsatellite instability (MSI-H) (8, 13). dMMR and MSI-H occur together at a consistency of 90–95% (referred to as dMMR/MSI-H) (14, 15). MMR deficiency leads to high mutational rates and subsequently high presence of neoantigens, making tumor cells more likely to be recognized and destroyed by antitumor immune cells (8, 13, 16–18). Tumor-infiltrating lymphocytes are abundant in dMMR/MSI-H tumors and associate with

TABLE 1 | Summary of Food and Drug Administration approved immune checkpoint inhibitors in GI cancers.

Drug(s)	Target(s)	Therapy modality	Tumor type	Details	Objective response rate (%)	FDA approved Year	Clinical trial	ClinicalTrials.gov identifier	References (PMID)
Pembrolizumab (Keytruda)	PD-1	Humanized monocolonal antibody	Gastric Cancer	Patients with recurrent locally advanced or metastatic gastric or gastroesophageal junction adenocarcinoma whose tumors express PD-L1	60.0% (combination with cisplatin) 25.8% (single agent)	2017	KEYNOTE-059	NCT02335411	30911859
			Liver Cancer	Patients with hepatocellular carcinoma who previously received sorafenib	17%	2018	KEYNOTE-224	NCT02702414	29875066
			Colorectal Cancer	Patients with microsatellite instability-high (MSI-H) or deficient mismatch repair (dMMR) unresectable or metastatic colorectal cancer that has progressed following treatment with fluoropyrimidine, oxaliplatin, and irinotecan Also approved for any solid tumor that has tested positive for MSI-H or dMMR in patients who have had prior treatment and have no satisfactory alternative treatment options	Colorectal Cancer: 40% (dMMR) 0% (proficient MMR) Non-colorectal Cancers: 70% (dMMR)	2017	KEYNOTE	NCT01876511	26028255
Nivolumab (Opdivo)	PD-1	Humanized monocolonal antibody	Liver Cancer	Patients with advanced hepatocellular carcinoma. The approval covers the use of nivolumab in patients who have previously received sorafenib	15, 20%	2017	CheckMate 040	NCT01658878	28434648
			Colorectal Cancer	Patients with MSI-H or dMMR metastatic colorectal cancer that has progressed following treatment with fluoropyrimidine, oxaliplatin, and irinotecan	68.9%	2017	CheckMate 142	NCT02060188	28734759
Nivolumab (Opdivo) Ipilimumab (Yervoy)	PD-1 CTLA-4	Humanized monocolonal antibodies	Colorectal Cancer	Patients with MSI-H or dMMR metastatic colorectal cancer that has progressed following treatment with fluoropyrimidine, oxaliplatin, and irinotecan.	55%	2018	CheckMate 142	NCT02060188	29355075

favorable prognosis (19, 20). For comparison, the somatic mutation frequency of dMMR/MSI-H tumors is 10–100-fold to that of proficient MMR tumors (21). In contrast, ICIs as single agents have not shown meaningful benefit for proficient MMR tumors (8), which are the vast majority of GI cancer cases. MSI-H tumors account for 6–22% of gastric, 1% of pancreatic, 3% of liver, and 14–16% of colorectal cancers (22–27). Antibodies against PD-1/programmed death-ligand 1 (PD-L1) or cytotoxic T-lymphocyte-associated protein-4 (CTLA-4) are the most clinically advanced immunotherapy in cancer (12). The PD-1/PD-L1 axis promotes adaptive immune resistance by suppressing effector T cells and promoting the differentiation of regulatory T cells (Tregs). CTLA-4 also is a negative regulator of T cells; its engagement of B7-1 or B7-2 on antigen-presenting cells inhibits T cell activation (12). Preclinical and clinical efforts are pushing forward with combination ICI therapy as well as ushering in different approaches to harness the immune system to extend immunotherapy efficacy to more patients, including vaccines and viral therapy, adoptive cell transfer, and cytokine treatment (12, 28). Challenges with improving efficacy include overcoming immunosuppression activity by the tumor microenvironment, unmasking pre-existing immune cell activity, and the ability to stimulate *de novo* immunogenicity (29). In recent years, antibodies and small molecular inhibitors against CD73 have made their way into clinical trials as an attractive target for restoring antitumor immunity (30–44). This review provides a summary of current literature for CD73 in GI cancers and its potential as an immunotherapy target. We also discuss current clinical trials targeting CD73 and adenosine receptors in combination with ICI and conventional therapy and the clinical implications to GI tumors.

CD73 AND ADENOSINE RECEPTOR ACTIVITY PROMOTES IMMUNOSUPPRESSION

Ecto-5′nucleotidase (*NT5E*; CD73) serves as a pacemaker for generating extracellular adenosine. With tissue damage, inflammation, and hypoxic stress, ATP is released from stressed, necrotic, and/or apoptotic cells and is hydrolyzed stepwise by ectonucleoside triphosphate diphosphohydrolase-1 (CD39), converting ATP to AMP, and CD73, converting AMP to extracellular adenosine (**Figure 1**). ATP's activation of ATP receptors promotes inflammation, whereas subsequent breakdown of ATP to extracellular adenosine and activation of adenosine receptors dampens inflammation (**Figure 1**) (45–47). Extracellular adenosine signals though four adenosine receptors: A1R, A2AR, A2BR, and A3R (48). The earliest link of extracellular adenosine to immunosuppression include studies on the anti-inflammatory activity of methotrexate (49) and seminal studies revealing A2AR signaling as essential in suppressing tissue-devastating inflammation (50). Extracellular adenosine protects tissues by dampening inflammation with myocardial injury (51–53), acute lung injury (54–58), intestinal ischemia-reperfusion injury (59–61), and inflammatory bowel disease (62–65). Tumors exploit extracellular adenosine' to protect the cancer cells. Extracellular adenosine accumulates in tumors and suppresses cytotoxic T cells and natural killer cells (66–68). Multiple studies using syngeneic and/or spontaneous tumor models show tumor growth and metastasis is significantly reduced by genetic deletion or pharmacological blockade of CD73 or A2AR; this effect is largely due to restoring antitumor immunity (30–44, 67–70). These mice also benefit from increased chemotherapy sensitivity (36, 71) and reduced angiogenesis (71, 72). In line with these studies, many human tumors overexpress CD73 and associates with poor prognosis (36, 73–78). CD73 is also linked to drug resistance, epithelial-to-mesenchymal transition (EMT), and cancer cell proliferation and stemness (76, 79–84). Tumors also grow slower in A2BR-deficient mice and mice treated with A2BR antagonists (85–87). For the most part, activation of A2AR and to a lesser extent A2BR on several types of immune cells, summarized below, promotes immunosuppression (**Figure 1**).

Effector T Cells and T Regulatory Cells

A2AR is upregulated during inflammation on effector T cells. Its activation inhibits effector T cell proliferation, cytotoxic activity, and cytokine production [e.g., tumor necrosis factor-α (TNF-α), interferon-gamma (IFN-γ), interleukin-2 (IL-2)] (88–90). Whereas, A2AR activation on T regulatory (Treg) cells promotes Treg expansion and immunosuppressive activity [e.g., increasing forkhead box P3 (FoxP3) expression] (91). Mechanistically, these actions are linked together in a self-reinforcing loop. CD73 on Tregs generates extracellular adenosine and activates A2AR on effector T cells, suppressing effector T cell activity. Extracellular adenosine additionally activates A2AR on Tregs, promoting their expansion and activity (92). Human Tregs rarely express cell surface CD73 (93, 94), unlike mouse Tregs (92, 95). Instead, CD73 expression by surrounding cells or exosomes is considered to produce the extracellular adenosine. CD73 is expressed by populations of immune cells, stromal cells, epithelial and endothelial cells, cancer cells, and exosomes (96–98). Recently, CD39 co-expression with CD103 (integrin αE) was identified as a marker of antigen specific, tumor-reactive CD8+ T cells, having resident memory and a high capacity of recognizing and killing autologous tumor cells (99). These cells may be a strategy to improve adoptive cell therapy, which is limited by the ability to identify and expand tumor-reactive CD8+ T cells. Here, using CD39+ CD103+ to enrich the cells prior to *in vitro* expansion may increase therapy success (99). Many ongoing studies are directed at capturing and/or reinvigorating T cell-mediated antitumor responses. These studies will provide greatly to new approaches for extending and improving immunotherapy efficacy in cancer. A2AR activity also promotes peripheral T cell tolerance, skewing T cell differentiation from adaptive effector cells to adaptive FoxP3+ lymphocyte activation gene-3 (LAG-3)+ Tregs (100).

Natural Killer Cells

A2AR activation on natural killer (NK) cells inhibits NK cell maturation, proliferation, activation, production of cytotoxic cytokines (e.g., IFN-γ and TNF-α), and target cell killing (38, 101–107). Whereas, genetic deletion or pharmacological

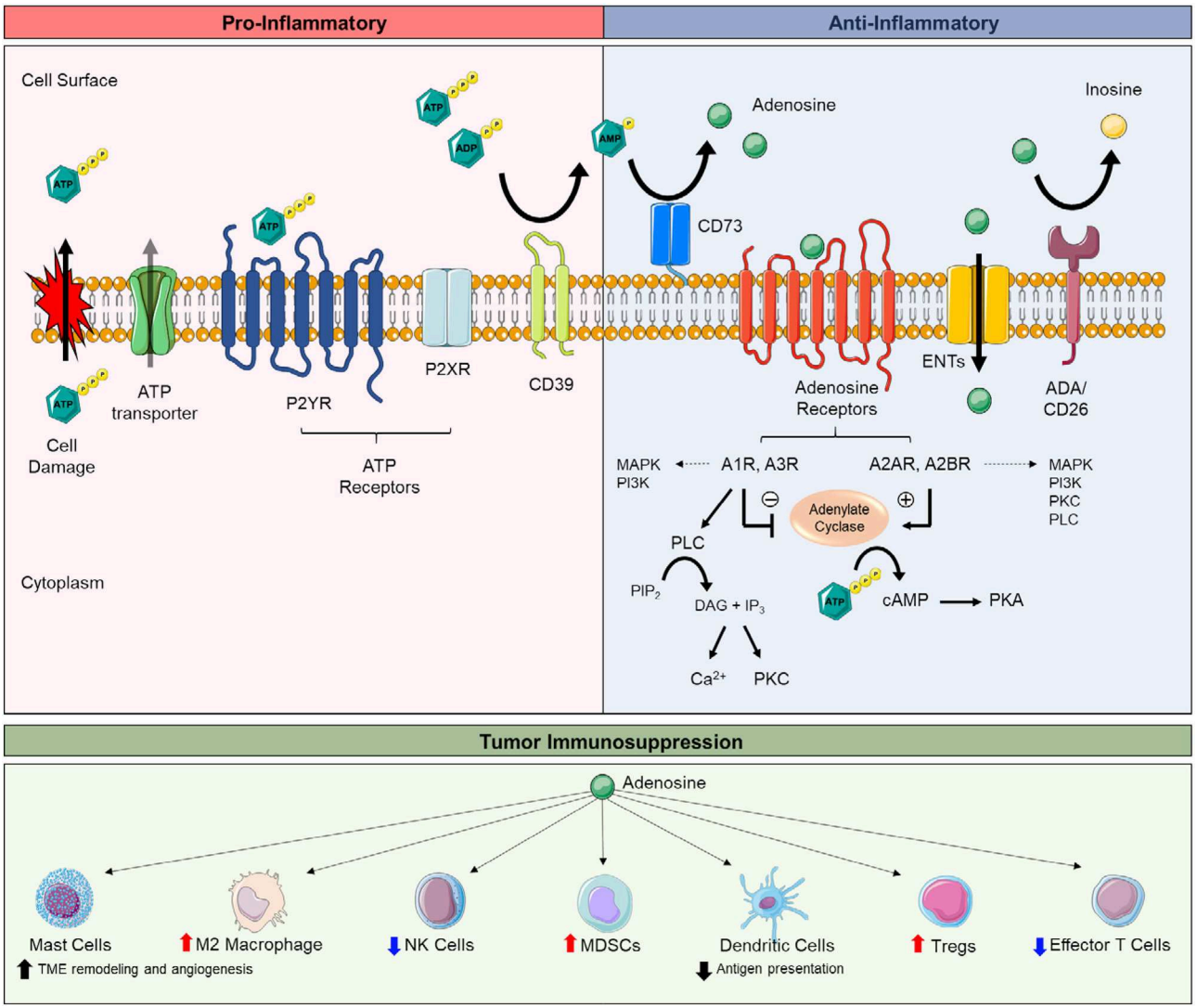

FIGURE 1 | Extracellular adenosine synthesis, adenosine receptor signaling, and adenosine-mediated immunosuppression. Extracellular adenosine and receptor signaling is part of a large cascade of ecto-enzymes (e.g., CD39, CD73), membrane transporters (e.g., ENTs), and G-protein-coupled (e.g., P2YR, adenosine receptors) and ionotrophic receptors (e.g., P2XR) known as the purinergic pathway. The purinergic pathway mediates both pro-inflammatory and anti-inflammatory responses. The breakdown of extracellular adenosine triphosphate (ATP) to extracellular adenosine is key to balancing tissue inflammation. Intracellular ATP is released by lytic (e.g., stressed and/or apoptotic/necrotic cells) and non-lytic (e.g., pannexin-1 and connexins) routes secondary to tissue damage, inflammation, and/or hypoxia. Once released, ATP activates ATP receptors (e.g., P2XR and P2YR) to promote pro-inflammatory responses, including the release of inflammatory cytokines promote lymphocyte proliferation, cell mobility, and phagocyte recruitment. ATP is dephosphorylated to extracellular adenosine by CD39, converting ATP and adenosine diphosphate (ADP) to adenosine monophosphate (AMP), and CD73, converting AMP to adenosine. Extracellular adenosine signaling through adenosine receptors (e.g., A1R, A2AR, A2BR, A3R) promotes anti-inflammatory responses, including the release of pro-tolerance cytokines, regulatory lymphocytes, and skewing toward M2 macrophages. Extracellular adenosine also can be taken up intracellularly by equilibrative nucleoside transporters (e.g., ENTs) or be further metabolized to inosine (e.g., ADA/CD26). A2AR and A2BR signaling stimulate adenylate cyclase to produce cyclic AMP (cAMP) which activates protein kinase A (PKA). A1R and A3R signaling inhibit adenylate cyclase. Adenosine receptors can activate multiple signaling pathways (e.g., MAPK, PI3K, PLC, PKC, ion channels), depending on cell and tissue types. Tumors exploit the anti-inflammatory actions of extracellular adenosine to evade antitumor immune cells. A3R activation on mast cells promotes tumor microenvironment (TME) remodeling and angiogenesis, increases the population of M2 macrophages, and promotes the accumulation of myeloid-derived suppressor cells (MDSCs) in tumors. A2AR activation on T regulatory cells (Tregs) enhances their immunosuppressive activity (e.g., suppressing effector T cells). A2AR and/or A2BR activation on natural killer (NK) cells, dendritic cells, and effector T cells dampens the antitumor activity of these cells. Abbreviations: ectonucleoside triphosphate diphosphohydrolase-1 (CD39), ecto-5′ nucleotidase (CD73), adenosine deaminase (ADA), phospholipase C (PLC), protein kinase C (PKC), diacylglycerol (DAG), phosphatidylinositol 4,5-bisphosphate (PIP_2), inositol trisphosphate (IP_3), mitogen-activated protein kinase (MAPK), phosphoinositide 3-kinase (PI3K).

blockade of A2AR or respiratory hyperoxia restores NK cell maturation, proliferative capacity, and cytotoxic function, which improves control over tumor growth, delays tumor initiation and suppresses tumor metastasis (38, 101, 102). CD73 and/or A2AR blockade or supplemental oxygen in combination with therapies promoting NK cell activity may be relevant strategies to enhance antitumor immunity. Whole-body exposure to 60% oxygen reduces tumor growth by reversing hypoxia-extracellular adenosine-mediated immunosuppression. In these preclinical studies, extracellular adenosine levels and CD39, CD73, A2AR, and A2BR gene expression decreases and coincides with increased antitumor immunity (102, 108). Hypoxia-inducible factors (HIFs) are strongly linked to increasing CD73 (109), A2AR (110), and A2BR (111) gene expression and collaborates to increase extracellular adenosine/adenosine receptor signaling for dampening inflammation (46, 47). Interestingly, recent studies show tumor cells can reprogram NK cells to gain immunosuppressive functions [e.g., increase IL-10 and transforming growth factor-β (TGF-β) production via signal transducer and activator of transcription 3 (STAT3) transcriptional activity, suppressing IFN-γ production] (112). The effects are not mediated through adenosine receptors, suggesting other mechanisms are involved and may not involve the production of extracellular adenosine (112).

Myeloid-Derived Suppressor Cells and Tumor-Associated Macrophages

CD39 and CD73 are upregulated on CD11b+ CD33+ peripheral blood and tumor-associated myeloid-derived suppressor cells (MDSCs) via TGF-β, which their ectonucleotidase activity inhibits T cell and NK cell activity (113). Granulocytic MDSCs expressing high CD39 and CD73 are described in colorectal cancer patients. These cells were found to exert robust immunosuppressive features (e.g., high PD-L1 expression) and activity that could be dampened by blocking CD39/CD73 (114). A2BR activation preferentially promotes the expansion and intratumoral accumulation of CD11b+ Gr1+ MDSCs (115). CD11b+ Gr1+ MDSCs express high CD73, which limits T cell proliferation. CD73 is also considered to facilitate MDSC expansion by generating extracellular adenosine to activate A2BR on myeloid progenitors (115). Accordingly, blocking A2BR reduces CD11b+ Gr1+ MDSCs immunosuppression and accumulation in tumors (87). Extracellular adenosine generated by cancer cells can recruit tumor-associated macrophages (TAMs), which their endonucleotiase activity, in collaboration with CD73 expression on other cells of the tumor microenvironment, further contributes (e.g., suppressing antitumor CD4+ T cell proliferation) to extracellular adenosine-mediated immunosuppression in tumors (116).

Dendritic Cells

Dendritic cells (DCs) transport tumor antigens to cytotoxic T lymphocytes for mounting antitumor immunity. A2BR activation on DCs inhibits their mobility, due to chemokine receptor downregulation, and they become tolerigenic to the tumor microenvironment (117–119). For instance, A2BR activation on DCs results in impaired allostimulatory activity and the expression of high levels of angiogenic, immunosuppressive, and tolerigenic factors [e.g., vascular endothelial growth factor (VEGF), IL-8, IL-6, IL-10, TGF-β, and idoleamine 2,3-dioxygenase (IDO)] (118). These cells cannot prime CD8+ T cells and T helper type 1 (Th1) immune responses (118–121). A2BR binding also inhibits monocyte differentiation to DCs (118, 119). A2BR blockade promotes DC activation (e.g., increased CD86 expression on CD11b- DCs), increases CD4+ and CD8+ T cell IFN-γ production, and tumor cell IFN-γ and CXCL10 expression (86), which supports the therapeutic potential of A2BR antagonists in enhancing antitumor immunity. Pharmacological agents for blocking A2BR are in clinical trials (e.g., NCT03274479; see Clinical implications section).

PRECLINICAL STUDIES TARGETING CD73 AND ADENOSINE RECEPTORS

CD73's potential as an immunotherapy target has advanced rapidly within the last decade (30–44, 67–70). Current studies focus on combination strategies, including ICIs, adoptive transfer, chemotherapy, and targeted therapy. Preclinical studies show compelling evidence for both CD73 and A2AR blockade in enhancing anti-PD-1 and anti-CTLA-4 therapy. As single agents, both CD73 and A2AR blockade are effective in controlling tumor growth and metastasis. However, the combination of these therapies is far greater at reducing tumor growth, metastatic burden, and prolonging the life of mice. These effects depend on increased IFN-γ production and CD8+ T and NK cell activity (37, 38, 40, 43, 122, 123). Notably, anti-PD-1 therapy is particularly synergized by inhibiting CD73, (37) and studies report A2AR combined with anti-PD-1 therapy is most effective with cancer cells expressing high CD73. The latter suggests CD73 expression may stratify patients likely to benefit from anti-PD-1 therapy-A2AR blockade combination (122, 123). In melanoma, CD73 is a poor pretreatment biomarker for immunotherapy, however, its expression level in relapse tumors has predictive value (41). Therefore, CD73 as a biomarker may be tumor and sample (e.g., primary, metastasis, relapse) specific. Ciforadenant (formerly, CPI-444), an oral A2AR antagonist, recently completed a first-in-human study in patients with renal cell cancer (124). Preclinical studies have shown ciforadenant combined with anti-PD-L1 or anti-CTLA-4 therapy eliminates tumors in up to 90% of mice, restores antitumor immunity, and is effective in mice that failed prior anti-PD-L1 or anti-CTLA-4 therapy (68). Moreover, ciforadenant produced an antitumor memory response in which tumor growth was completely inhibited in mice with cleared tumors when later rechallenged (68). In clinical trials, cirforadenant combined with atezolizumab (anti-PD-L1 therapy) provide great disease control and survival benefit in patients, yet without high objective response rates (124). While reasons are unclear, the Fong and colleagues predict the response is due to persistent antitumor immunity that maintains durable control over tumor growth (124). Monotherapy ciforadenant also provided disease control in some individuals (124). Mechanistically, ciforadenant suppresses the expression of multiple checkpoint pathways on

CD8+ effector T cells and CD4+ FoxP3+ Tregs and appears to have profound effects in restoring antitumor immunity at the draining lymph nodes by decreasing PD-1 and LAG-3 expression (69). Thus, a significant benefit of A2AR antagonism is its expansion of responsive cytotoxic T lymphocytes (69). A2AR and/or CD73 blockade also improves anti-CTLA-4 therapy efficacy in melanoma (43). Recently, anti-CD73 therapy combined with an agonist antibody to 4-1BB (4-1BB therapy) showed to restore antitumor immunity (125). 4-1BB is an activation-induced T cell costimulatory molecule that enhances cytotoxic T cell and NK cell activity (126, 127). 4-1BB therapy has entered into clinical trials involving GI cancer patients (NCT03330561). Poor efficacy and toxicity have been a concern in the past with 4-1BB therapy (128). Further preclinical studies are warranted.

Cancer vaccines educate the immune system to recognize cancer cells. Targeting A2AR in this setting also represents a promising strategy. Responses to melanoma and lymphoma tumor vaccines are increased in A2AR-deficient mice; these mice showed increased expansion of tumor-specific CD8+ T cells and increased survival compared to wild-type mice (129). The effectiveness of adoptive T cell transfer is also increased with genetic deletion or blockade of CD73 or A2AR. Tumor-bearing mice benefit from improved tumor control and survival due to increased infiltration and activation of adoptive T cells (30, 69, 70).

Additionally, preclinical studies show chimeric antigen receptor T (CAR T) cell efficacy is greatly increased by A2AR antagonism (130). CAR activation increases A2AR expression and suppression of mouse and human CAR T cells, which can be reversed by A2AR antagonism or genetic targeting, increasing the therapy benefit of CAR T cells. Efficacy is increased further by combination therapy (A2AR blockade and anti-PD-1 therapy) (130). Increased CD73 expression is seen in patients progressing under adoptive T cell transfer therapy (41). Accordingly, future approaches targeting CD73 in combination with A2AR blockade, anti-PD-1 therapy, and/or adoptive T cell transfer may prove beneficial. Head-to-head comparison studies blocking CD39 and CD73 (44) or CD73 and A2AR (39) also show promise for significantly increasing antitumor immunity. Co-targeting CD73 with A2AR inhibits the compensatory response of A2AR blockade to increase CD73 (39). Whereas, co-targeting CD39 with CD73 is beneficial by targeting two different mechanisms (44). Blocking CD39 elevates ATP levels. High ATP levels promote DC and macrophage antitumor activity, which adds to the antitumor immunity benefits of blocking CD73 (44). Combining CD73 anti-antibodies or small molecule inhibitors with chemotherapy or targeted therapies [e.g., antibodies against epidermal growth factor receptor (EGFR)] also shows merit in preclinical studies (36, 81). BRAF and MEK inhibitors combined with A2AR blockade show significant benefit in controlling melanoma tumor growth and metastasis in mice (42). A benefit of BRAF and MEK inhibitor combination is that it downregulates CD73 expression (42). Accordingly, this combination strategy provides the advantage of dampening CD73 expression without added drug/antibody therapy. Preclinical studies that focus on GI cancers will be essential in understanding the therapeutic potential of CD73 and/or adenosine receptor blockade in these tumors.

GASTRIC CANCER

Gastric cancer (GC) is the fifth and third most common cancer and cause of cancer deaths worldwide, respectively (1). Although incidence and death rates are declining (131), advancements in prevention and treatment remain a priority. Five year survival rates drop to 20–30% or less once the cancer moves beyond the lining of the stomach (132). The majority of GC cases are advanced stage (133). Treatment includes gastric resection, radiation, chemotherapy, and targeted therapy, including antibodies against (VEGF)/VEGF receptor 2 (VEGFR2), and HER2 (131). Recently, ICI therapy was approved for GC (**Table 1**) (6). However, most patients do not benefit. Other immunotherapies being studied in GC include combination ICI therapy, adoptive cell transfer, vaccines [e.g., melanoma-associated antigen (MAGE) A3 peptides; Bacillus Calmette-Guerin (BCG)], and agonist antibodies for costimulatory receptors [e.g., OX40 (also known as tumor necrosis factor receptor superfamily, member 4), 4-1BB] (134).

Few studies have assessed CD73 expression in GC (**Table 2**). CD73 expression is higher in GC vs. normal tissue and associates with poor tumor differentiation, increased depth of invasion, positive nodal status, presence of metastasis, advanced-stage disease, and poor overall survival (**Table 2**) (75, 135). Increased CD73 in GC may be due in part to hypoxia. Hypoxia-inducible factor-1α (HIF-1α) staining closely correlates with high CD73 expression in gastric tumors (75). In contrast, gene expression studies have shown high CD73 expression associates with favorable overall survival in GC (136). Notably, CD73 expression does not always correlate to protein expression, which may explain the differences between these studies (136). Additionally, significant heterogeneity for CD73 is seen in GC (75, 135). For example, 30–50% of advanced stage, deeply invasive, and lymph node-positive tumors express low or no CD73 (75). Significant heterogeneity for CD73 expression is also described for melanoma (41, 42). In melanoma, CD73 expression is influenced by sample type (e.g., primary, metastatic, or relapse tissue); therapy treatment; and presence of activating MAPK (e.g., *BRAF*) mutations, mitogenic and inflammatory signals [e.g., hepatocyte growth factor (HGF) and TNF-α], and necrosis (41, 42). Increased *CD73* expression with *BRAF* mutation is also seen in serous ovarian cancer; these patients have better clinical outcomes (137). *BRAF* mutations are found in 10–20% of colorectal cancer and frequently are MSI-H (138–140). CD73 expression is also impacted by *NT5E* promoter methylation, described for both melanoma and breast cancer (141, 142). Suffice to say, multiple molecular and genetic factors can affect CD73 expression in human tumors.

Looking ahead, assessing CD73 expression to common molecular and/or genetic alterations of GC and The Cancer Genome Atlas (TCGA) may help to better understand CD73 in GC (23). Studies assessing the association of CD73 expression to immune checkpoints, such as PD-L1, may also

TABLE 2 | Summary of studies assessing CD73 expression in human GI cancers.

Tumor type	Study	Findings	# of patients	Test method(s)	CD73 high advance stage tumors	Clinical significance	Reference (PMID)
Gastric Cancer	Lu et al.	CD73 expression is higher in gastric cancer vs. normal tissue; High CD73 expression is positively correlated with tumor differentiation, histology, depth of invasion, nodal status, metastasis, American Join Committee on Cancer (AJCC) stage, and poor survival	68	IHC	50%	Poor prognosis	23569336
	Jiang et al.	High CD73 expression associates with favorable overall survival in gastric cancer; Meta-analysis study reports large heterogeneity for high CD73 expression for tumors (tumors: ovarian, breast, colorectal, gastric, gallbladder, prostate, rectal, renal, bladder, head and neck cancer, and NSCLC)	Oncomine database	mRNA, IHC (meta-analysis)	–	Better overall survival	29514610
	Hu et al.	CD73 expression is higher in gastric cancer vs. normal; High CD73 associates with advanced clinical stage, deep tumor invasion, lymph node metastasis, distant metastasis, and poor survival	408 (gastric cancer; TCGA) 131 (gastric cancer; FFPE)	mRNA (TCGA), IHC, Western Blot	69%	Poor prognosis	30992388
Liver Cancer	Shrestha et al.	CD73 associates with poor overall survival and recurrence-free survival; Patients with tumors expressing high PD-L1 and high CD73 have poor prognosis	1,170 (combined datasets; GSE10143; GSE10186; GSE17856; TGCA Liver Cancer)	mRNA	–	Poor prognosis; Poor recurrence free survival in patients with high PD-L1	30057891
	Shali et al.	CD73 expression is higher in tumor vs. normal tissue; CD73 expression is positively correlated with epidermal growth factor receptor (EGFR) expression	30	IHC	–	–	30417547
	Ma et al.	CD73 expression is higher in hepatocellular carcinoma (HCC) vs. normal tissue; High CD73 expression correlates with microvascular invasion, poor differentiation increased time to recurrence, shorter overall survival, increased circulating tumor cells, and to epithelial-to-mesenchymal transition in HCC	232 (mixed: primary tumors, recurrence lesions, and metastases)	mRNA, IHC, Western Blot	57%	Poor prognosis	30971294
	Sciarra et al.	Immunohistochemistry study of CD73 expression in normal and hepatobiliopancreatic tissues; CD73 expression is present in all HCC, staining for CD73 ranges from intensity of 1+ to 3+ with a median intensity of 2+; Aberrant membranous and/or high/strong cytoplasmic expression for CD73 is seen in invasive HCC	24	IHC	CD73+ Staining Intensity = 3: 63%	–	30607549
	Snider et al.	*NT5E* is regulated by alternative splicing, producing a second transcript, *NT5E-2* in liver cirrhosis and HCC; *NT5E-2* is specific to humans and produces a protein product known as CD73 short (CD73s) that lacks enzyme activity (lacks exon 7) and is localized to the cytoplasm; *NT5E-2* is expressed at baseline in many normal human tissues; CD73s expression is 6–8-fold higher in HCC compared to normal liver tissues, whereas CD73 *(NT5E)* mRNA is dramatically deceased (>90%) in HCC	6 (HCC) 4 (Cirrhosis) 2 (Normal Liver)	mRNA, Immunofluorescence, Western Blot, Enzyme Activity	mRNA Expression HCC: *NT5E-2* = 6–8-fold increase; *NT5E* = 90% decrease	Human specific isoform for CD73, *NT5E-2* (CD73s) that lacks enzyme activity CD73s increases in HCC, whereas CD73 decreases in HCC. CD73s is restricted to the cytoplasm	25298403

(Continued)

TABLE 2 | Continued

Tumor type	Study	Findings	# of patients	Test method(s)	CD73 high advance stage tumors	Clinical significance	Reference (PMID)
	Alcedo et al.	CD73 exhibits aberrant N-linked glycosylation in HCC cells and is independent of HCC etiology, tumor stage, or fibrosis presence. Aberrant glycosylation of CD73 results in a 3-fold decrease in enzyme activity; CD73 does not correlate with tumor immune subtype in HCC	HCC samples from PanCancer Atlas Consortium (mRNA) and 33 HCC (all other assays)	mRNA, Immunofluorescence, Western Blot, Enzyme Activity, Mass Spectrometry	CD73 Enzyme Activity: aberrant glycosylation of CD73 = 3-fold decrease in enzyme activity	CD73 is aberrantly glycosylated which significantly decreases its enzyme activity	31592495
Pancreatic Cancer	Zhou et al.	CD73 expression is higher in pancreatic ductal adenocarcinoma (PDAC) vs. normal tissues; High CD73 expression associates with increased tumor size, tumor stage, TMN stage, and poor prognosis	114	mRNA, IHC	40% (TMN stage)	Poor prognosis	30927045
	Sciarra et al.	Immunohistochemistry study of CD73 expression in normal and hepatobiliopancreatic tissues; CD73 is negative in acinar and islet epithelial cells, variable in pancreatic ducts, and mildly localized to stromal cells of normal and inflamed tissues; CD73 is expressed in 100% of PDAC; CD73 is expressed in a subset of pancreatic neuroendocrine neoplasms (PanNET/PanNEC) and almost absent in acinar cell carcinoma; Different staining patterns for CD73 are observed in PDAC, well- and moderately-differentiated tumors (grade 1 and grade 2) express apical CD73 staining similar to pancreatic ducts or express mixed membrane and cytoplasm staining; Poorly-differentiated PDACs express aberrant CD73 staining; PDAC, pancreatic ductal adenocarcinoma; MCA, mucinous cystadenoma; IPMN, intraductal papillary mucinous neoplasm; PanNET/PanNEC, pancreatic neuroendocrine tumor/pancreatic neuroendocrine carcinoma; ACC, acinar cell carcinoma	42 (PDAC) 5 (MCA) 13 (IPMN) 23 (PanNET/PanNEC) 19 (ACC)	IHC	CD73+ Staining Intensity = 3: 62% (PDAC) 0% (MCA) 0% (IPMN) 4% (PanNET/PanNEC) 5% (ACC)	PDAC: poor tumor differentiation and poor overall survival	30607549
	Katsuta et al.	PanNET/PanNEC express mild to moderate CD73 and associates with invasion into adjacent organs	44	IHC	54%	Invasion into adjacent organ	26691441
Colorectal Cancer	Wu et al.	CD73 expression is higher in colorectal cancer (CRC) vs. normal tissue; High CD73 expression associates with poor tumor differentiation, advanced tumor stage, metastasis, and poor overall survival	223 (cohort 1) 135 (cohort 2)	IHC, Western Blot	–	Poor prognosis	22287455
	Zhang et al.	CD73 expression in rectal cancer only samples; CD73 expression is increased in both tumor and stromal cells; High CD73 expression in cancer cells associates with poor patient prognosis; High CD73 expression in stromal cells associates with favorable characteristics (early T and tumor-node-metastasis (TMN) stages) and overall survival; Patients with high CD73 expression in both the cancer cells and stromal cells have similar good outcomes. No CD73 expression in both cell compartments is also favorable	90	IHC	–	High CD73 expression cancer cells = poor prognosis; High CD73 expression stromal cells = favorable outcomes	25677906

(Continued)

TABLE 2 | Continued

Tumor type	Study	Findings	# of patients	Test method(s)	CD73 high advance stage tumors	Clinical significance	Reference (PMID)
	Eroglu et al.	CD73 enzyme activity is higher in CRC vs. normal tissue; CD73 enzyme activity is higher in well-differentiated tumors compared moderately/poorly differentiated; No differences in CD73 enzyme activity seen with tumor stage, extent of invasion, metastasis, or tumor morphology	38	Enzyme Histochemistry	CD73 Enzyme Activity: CD73 enzyme activity is high in well-differentiated CRC compared to moderately and poorly differentiated CRC	CD73 enzyme activity high in tumors, associates with well-differentiated tumors	11114712
	Camici et al.	CD73 enzyme activity: no difference in CRC vs. normal tissue	16	Enzyme Histochemistry	–	No association	2125239
	Jiang et al.	Several types of tumors (cervical, liver, colorectal, prostate invasive ductal breast, small cell lung cancer and lung squamous cell carcinoma) showed similar CD73 expression vs. matched normal tissue	Oncomine database	mRNA, IHC (meta-analysis)	–	No association	29514610
	Cushman et al.	High CD73 expression associates with longer progression free survival from cetuximab (anti-EGFR therapy) in patients with KRAS-wild-type and mutant tumors. Epidermal growth factor receptor (EGFR)	103	mRNA	–	Biomarker for cetuximab (anti-EGFR therapy)	25520391

be helpful. Forty percent of GC cases are PD-L1 positive (143), and preclinical studies suggest high CD73 expression in PD-1/PD-L1 expressing tumors may identify patients that would benefit from combination anti-PD-1/PD-L1 therapy and CD73 and/or A2AR blockade (122, 123). Few studies globally assess CD73 expression with other ecto-enzymes involved in ATP and adenosine synthesis and metabolism and its intracellular uptake (144), such as other E-NTPDases, ecto-nucleotide pyrophosphatases/phosphodiesterases (e.g., CD203a), nitcotinamide dinucleotide enzyme (e.g., CD38), prostatic acid phosphatase, alkaline phosphatase (45, 145, 146), adenosine deaminase, and equilibrative and concentrative nucleoside transporters (ENTs and CNTs, respectively). Reviewed recently by Boison and Yegutkin (144), this may present a major gap in developing effective adenosine-based therapies (144). Accordingly, a more global view of extracellular adenosine metabolism and signaling in GC may also prove significant.

Considering CD73/extracellular adenosine's role in immune cell escape, studies of CD73's association to *H. pylori*-mediated tumorigenesis may provide additional insight. *H. pylori* infection is responsible for up to 60% of GC cases and arises in the background of inflammation (147, 148). Immune cell evasion is important for *H. pylori* infection and supported by evidence of higher PD-L1 expression in *H. pylori* positive compared to negative gastric biopsies (149) and that *H. pylori*-induced PD-L1 expression on gastric epithelial cells converts naïve T cells to CD4+ FoxP3+ Tregs that inhibit T cell proliferation (150). CD73 expression by CD4+ CD25+ Tregs enhances *H. pylori* infection by increasing local extracellular adenosine, which suppresses IFN-γ production (151). Consistent with this, infected CD73-deficient mice experience worse gastritis and more severe inflammation (e.g., increased IL-2, TNF-α, and IFN-γ and impaired Treg function) (151). Taken together, these studies support that CD73/extracellular adenosine in collaboration with other immune checkpoints may downregulate immune cell responses necessary for recognizing and clearing transformed cells arising in chronically infected gastric tissues, thus supporting GC development. With *H. pylori* infection, CagA and VacA containing exosomes are released from gastric epithelial cells, stimulating pro-inflammatory responses and affecting the expression of tumor suppressor and oncogenic genes (152). Considering CD73 expression on exosomes promotes tumor immunosuppression (97, 98), it would be interesting to see if CD73 is also expressed on *H. pylori*-mediated exosomes and if its presence or increased presence is a biomarker for the onset of GC.

Additional studies show CD73 promotes tumor cell proliferation, migration, invasion, and stemness in GC cells (135, 153). Antitumor roles for extracellular adenosine are also reported, including AMP-kinase (AMPK)-mediated, caspase-independent apoptosis, via intracellular uptake of extracellular adenosine through ENTs, and caspase-dependent apoptosis, mediated by A1R and A3R (154, 155). ENTs passively transport nucleosides based on a concentration gradient (**Figure 1**) (156, 157). A1R and A3R signaling both inhibit adenylyl cyclase activity and can activate multiple downstream signaling pathways, including phospholipase C, producing inositol 1,

4, 5-triphosphate (IP_3) and diacylglycerol (DAG), mitogen-activated protein kinase (MAPK), and phosphoinositide 3-kinase (PI3K) (**Figure 1**) (158–160). A3R agonist, CF102, is in clinical trials for antitumor benefit in liver cancer (NCT02128958). A3R is also reported to increase HIF-1α through a non-transcription-dependent, non-HIF-1α oxygen-dependent degradation mechanism in several cancer cell lines (161). Though the role of A3R-mediated upregulation of HIF-1α is unclear, these data suggest A3R may both suppress and promote tumor progression. A2AR expression is increased in human GC tissue and correlates with poor tumor differentiation, advanced stage, lymph node positivity, and worse patient outcomes (162). Studies show A2AR, via PI3K-AKT-mTOR signaling, promotes GC cell stemness, EMT, and tumor cell migration and invasion (162). Altogether, more work is necessary to understand the role of CD73/extracellular adenosine in GC. Targeting specific adenosine receptors (e.g., A2AR) may be promising, but represents an area in need of more research.

LIVER CANCER

Liver cancer is the fourth most common cause of cancer death and sixth in terms of incidence worldwide (2). Ninety percentage of liver cancers are hepatocellular carcinoma (HCC) (163). Chronic liver disease (e.g., cirrhosis and fibrosis) is a major risk factor and most commonly caused by hepatitis B or C infection or long-term alcohol abuse (2, 164, 165). The 5-year survival rate for HCC is 18% (2). Treatment includes tumor resection, liver transplant, and targeted therapy (e.g., multi-kinase inhibitor, sorafenib) (166). However, 70% of patients do not qualify for surgery, due to advance disease, and sorafenib therapy is limited in its benefit; patient survival is prolonged only by a few months (166). ICI therapy was recently approved as second-line therapy for HCC (**Table 1**) (7, 9). Other promising immunotherapies are in development and are aimed at boosting existing or *de novo* immune responses, including vaccines and oncolytic viruses, and combination ICI therapy (167). Anticipation awaits the results of NCT03298451, a phase 3 clinical trial assessing anti-PD-L1 and anti-CTLA-4 combination therapy vs. monotherapy as better first-line options than sorafenib [HIMALAYA trial, (NCT03298451)].

In recent years, HCC has been a platform for the discovery of novel biology for CD73 in human tumors (**Table 2**) (168, 169). Studies by Snider and colleagues (168) identified an alternative splicing variant of *NT5E*, *NT5E-2* expressed in liver cirrhosis and HCC. *NT5E-2* produces a protein product, CD73-short (CD73s), and is a human-specific isoform that lacks enzyme activity and is unable to dimerize due to the loss of exon 7 with splicing (168). CD73s expression is limited to the cytoplasm and complexes with CD73 to promote proteasome-dependent degradation of CD73 (168). In HCC human tissues, CD73s expression is 6–8-fold higher compared to normal liver, whereas CD73 expression is downregulated by more than 90% (168). Accordingly, these studies indicate CD73s may be the major source of "CD73" overexpression in HCC. In contrast, other studies (170, 171) report CD73 is overexpressed in HCC and associates with poor tumor differentiation, microvascular invasion, and poor overall and recurrence-free survival (**Figure 1**) (170, 171). *NT5E-2* expression was not assessed in these studies, which is a limitation. In line with CD73s expression, Sciarra et al. (172) especially noted significant cytoplasmic CD73 expression in tumors, particularly with invasive tumors (172) (**Table 2**).

Many immunohistochemistry data for high CD73 expressing tumors, including gastric and pancreatic cancer, show significant cytoplasmic staining of CD73 (75, 77). Current commercial antibodies are not marketed to distinguish between CD73 and CD73s. Thus, other human tumors with CD73 overexpression may overexpress CD73s. Notably, *NT5E-2* is expressed at low levels in most normal human tissues and its expression increases with the onset of disease (123, 159). Currently, *NT5E-2* remains unstudied in other human tumors despite possible clinical implications. Similarly, recent studies by Alcedo et al. (169) report CD73 enzyme activity in HCC is significantly limited by aberrant glycosylation (169). The authors discovered that in HCC cells, unlike normal hepatocytes, CD73 carries abnormal N-linked glycosylation in its C-terminal catalytic domain, which greatly impairs the enzyme activity of CD73 (169). Aberrantly-glycosylated CD73 also showed to remain partially localized to the cytoplasm with golgi structural protein, GM130 (169). Importantly, these studies show that CD73 protein expression levels may not necessarily reflect its ability to generate extracellular adenosine. Studies by Snider et al. (168) and Alcedo et al. (169) are significant in that they demonstrate CD73 overexpression in human tumors can be misleading. Thus, CD73 immunohistochemistry may fall short in identifying patients likely to benefit the most from CD73 blockade therapy. As mentioned, commercial antibodies are unknown to be specific for recognizing CD73 vs. CD73s. Additionally, they are not primed for recognizing aberrant glycosylation. Instead, CD73 enzyme histochemistry is necessary, which is more challenging for clinical workups. These studies also raise questions as to how close preclinical studies of CD73/extracellular adenosine model human tumors. For instance, syngeneic and spontaneous mouse tumor models do not account for the biology of CD73s, which negatively regulates CD73 (168). A species-specific role of CD73 is also seen for arterial calcifications in humans and is not recapitulated in CD73-deficient mice (173, 174). CD73 downregulation in human tumors has been described in endometrial cancer. Its loss associates with more aggressive disease and poor overall survival (175). In normal endometrium, CD73-generated adenosine protects epithelial integrity, which CD73 loss and subsequently the loss of cell-cell adhesions promotes tumor progression (175). In contrast, in normal breast tissue, CD73 is expressed in myoepithelial cells as opposed to differentiated cells (e.g., acinar and ductal epithelial cells) (176). Myoepithelial cells are stem cell-like and exhibit highly invasive behavior similar to tumor cells (177). Consistent with this, CD73 is upregulated in cancer cells of triple-negative breast cancer (TNBC), which are tumors characterized by a gene expression signature similar to basal/myoepithelial cells (36, 177, 178). Accordingly, studies that reconcile tissue- and cell-specific roles for CD73 in normal GI tissues may help better understand CD73 in GI cancers (179, 180). Similar to

endometrial cancer (175), CD73 is downregulated in cancer cells of bladder and prostate tumors and associates with poor prognosis (181, 182). The role of CD73 in bladder and prostate epithelium is unknown. Notably, CD39 deficiency promotes both induced and spontaneous autochthonous tumors in the liver (183).

For adenosine receptors, studies show A2AR signaling via PI3K-AKT promotes HCC tumor growth and metastasis and is reversed by A2AR antagonist treatment (170). A2BR expression is increased in human HCC tissue and correlates with tumor progression and is likely due to hypoxia (184). HIF-1α increases A2BR expression in HCC cells and cancer cell proliferation (184). Recent studies by Lan and colleagues (185) show HIF-1α's induced expression of A2BR is essential in enriching breast cancer stem cells for the onset of recurrent disease (185). Studies linking A2BR to tumor progression include work in bladder (86), breast (186), colon (187), and prostate (188) cancer and involves A2BR activity on both immune and tumor cells. A2BR antagonist, ATL801, reduces metastases by more than 80% in mice, which is due to increased IFN-γ, IFN-inducible chemokine CXCL10, a ligand for CXCR3, and tumor-infiltrating CXCR3+ T cells (86). Needless to say, interests in antagonizing A2BR in human tumors are rising. Studies by Vecchio et al. (188), in prostate cancer, describe a ligand-independent, constitutively active A2BR, which drives cancer cell proliferation (188). Importantly, these studies highlight an unappreciated view that adenosine receptors in tumors may not rely on CD73/extracellular adenosine. Aberrant ligand-independent G protein-coupled receptor constitutive activity is implicated in several cancers (188). In contrast, A3R expression is increased in human HCC and A3R promotes cancer cell apoptosis (189). A3R agonist, CF102, is being evaluated as second-line therapy for HCC (NCT02128958). Increased overall survival is reported with NCT02128958 and phase 3 studies are being planned (190). Taken together, adenosine receptors as opposed to CD73 may be better predictive targets for therapeutic benefit in HCC.

PANCREATIC CANCER

Pancreatic cancer is predicted to become the second leading cause of cancer-related deaths in the United States by 2030 (3, 4). Ninety percentage of pancreatic tumors are pancreatic ductal adenocarcinoma (PDAC) while 3–5% are neuroendocrine tumors (PNETs) (191). Smoking, heavy alcohol consumption, obesity, *H. pylori* infection, and chronic pancreatitis are risk factors (192). Prognosis is incredibly poor, approximately 70% of patients will succumb to the disease in the first year (193). The 5-year survival rate is 9% (193). Standard of care for pancreatic cancer includes radiation therapy, chemotherapy, and targeted therapy (e.g., EGFR inhibitors) (192). The prevalence of therapy resistance to these treatments is a persistent problem. PDAC patients have not benefited from single agent or combination ICI therapy (194–196) despite increased expression of PD-L1 in tumors (197–199). Significant efforts are underway to improve immunotherapy efficacy, including studies investigating regulatory B cell inhibition (e.g., Bruton's Tyrosine Kinase (BTK) inhibitors), IDO inhibition, and vaccine therapy (200). Though a predominant target in B cell malignancies, BTK in PDAC is shown to induce B cell- and macrophage-mediated T cell suppression, which BTK inhibitors (i.e., ibrutinib) restore T cell-dependent antitumor immunity and improve responsiveness to chemotherapy in preclinical studies (201). BTK inhibitors also produce an unexpected anti-fibrotic effect (202). PDAC cancers are rich in stromal cells and fibro-inflammatory reactions, which support chemotherapy resistance (203). A phase 3 clinical trial of ibrutinib in combination with chemotherapy in PDAC was recently completed (April 2019; NCT02436668) (204). Results are not yet publicly available.

Studies of CD73 in human PDAC tissue have only recently emerged (**Table 2**). CD73 is upregulated in PDAC compared to normal pancreatic tissue and correlates with increased tumor size, advanced stage, lymph node involvement, metastasis, and poor prognosis (77, 80, 172). While PDAC tumors are 100% positive for CD73 expression (172), interesting staining patterns for CD73 are seen. Well- and moderately-differentiated PDAC cells express mixed membrane and cytoplasmic CD73 staining. CD73 staining intensity is low to moderate in these tumors (172). In contrast, poorly-differentiated PDAC cells have aberrant CD73 staining, including very strong cytoplasmic CD73 expression (172). The increase of cytoplasmic CD73 expression in PDAC is unclear. We previously mentioned the discovery of CD73s in HCC (168). Studies assessing *NT5E-2* (CD73s) expression may help to better understand CD73 in PDAC. CD73 expression in acinar cell carcinomas (ACC) is rare (172). ACC comprises 1–2% of pancreatic tumors and does not carry typical genomic alterations seen in PDAC, including *KRAS* and *TP53* mutations (205), which is suggestive that CD73 expression in PDAC may be linked to *KRAS* and/or *TP53* mutations. *KRAS* mutation occurs in nearly 100% of PDAC cases (206). In human colorectal cancer (CRC) and non-small cell lung cancer (NSCLC) tissue, CD73 staining is increased in *KRAS* mutant compared to wild-type tumor (207). *KRAS* alterations associate with increased CD73, CD39, A2AR, and A2BR gene expression in CRC and NSCLC cell lines, which correlates with anti-PD-1 resistance in *KRAS* mutant tumor models (207). Moreover, high CD73 expression and *KRAS* alterations associate with worse overall survival compared to patients with *KRAS* alterations and low CD73 expression tumors (207). EGFR alterations and high CD73 expression also associate with poor overall survival (TCGA pan-cancer) (207). EGFR alterations and *KRAS* mutations occur together in 67% of PDAC cases (208). Accordingly, EGFR alterations may also increase CD73 expression in PDAC. A positive association between CD73 expression and EGFR alterations is described in breast cancer (209).

CD73 expression (3+ staining) increases with aggressive disease in PDAC (172), which may be an indicator of an evolving or advancing immunosuppression phenotype. For instance, in PDAC, a decrease in CD8+ T cell infiltration into tumors is seen with the rise of infiltrating Tregs with disease progression (210). As mentioned, human Tregs rarely express cell surface CD73 (93, 94), and it is considered that

CD73-generated extracellular adenosine from other sources [e.g., cells (96) or exosomes (97, 98)] activate adenosine receptors on immune cells for immunosuppression. Accordingly, the coinciding increase of CD73 in PDAC cells may be significant in promoting extracellular adenosine-mediated immunosuppression. Other cells and cell-derived products possibly contributing are CD4+ CD73+ T cells, B cells, and CD39+ CD73+ exosomes (211). CD73+ PDAC and NSCLC cell-derived exosomes activate A3R on intratumor and peripheral mast cells, which promotes remodeling of the tumor microenvironment through increasing the expression of angiogenic factors (212, 213). Additionally, in PDAC models, tumor-infiltrating CD11b+ CD103– DCs promote tumor growth by inducing expansion of FoxP3^{neg} CD39+ CD73+ tumor-promoting Tregs (214).

Pancreatic neuroendocrine tumors and carcinomas (PanNET/PanNEC) account for 1–10% of pancreatic tumors (215, 216). Thirty to fifty percent of PanNET/PanNEC express mild to moderate CD73 expression and associates with increased malignant potential, which is similar to gastrointestinal (GI)-NET/NECs (80, 172, 217). In GI-NET/NECs, CD73 expression positively correlates with PD-L1 expression (217), which possibly anti-PD-1/PD-L1 therapy with CD73 and/or A2AR blockade may benefit these patients. Increased expression of CD73 with PanNET also associates with cancer cell stemness (e.g., aldehyde dehydroxygenase expression) and aggressive behavior (80). Filippini et al. (218) recently reported a transplantable model of mouse pancreatic tumor organoids into immunocompetent mice that recapitulate human PDAC progression and that the system serves as a suitable model for immunophenotypic studies (218). The organoid-derived isographs induce the expression of many immunosuppressive/aggressive biomarkers with tumor development and evolution, including CD73 (218). Studies using such models may provide a significant understanding of CD73/extracellular adenosine signaling in immunosuppression and the immunoevolution of PDAC.

CD73 also shows to promote drug resistance and tumor growth in PDAC cells. For instance, high CD73 expression and low miR-30a-5p expression in PDAC cells result in chemotherapy (e.g., gemcitabine) resistance (77), and CD73 knockdown inactivates AKT and extracellular signal-regulated kinase (ERK) signaling and slows cancer cell growth (77). In contrast, studies show extracellular adenosine treatment in combination with AKT inhibitor, GSK690693, reduces PDAC growth and induces tumor cell apoptosis and senescence in patient-derived xenografts (PDX). Mechanistically, the intracellular uptake of extracellular adenosine via ENTs (**Figure 1**) appears important for this response, as dipyridamole (pan-ENT inhibitor) treatment remarkably recovers cell viability (219). The difference between these studies likely relates to the subcutaneous transplanting of tumors (77) vs. tumors transplanted to the tail of the pancreas (219). Indeed, for example, CD39 deficiency can promote the development of both induced and *de novo* tumors in the liver, which is in contrast to its role in antitumor immunity of subcutaneous transplanted tumors (183, 220). It is considered that the surrounding microenvironment and interaction with these cells by the tumor likely produce different responses and outcomes. In the next several years, adopting in-depth and detailed characterization of CD73/extracellular adenosine in immunocompetent, autochthonous pancreatic cancer models, humanized models, and human organoids will be essential for better understanding the possible therapeutic benefit of targeting CD73 and adenosine receptors in pancreatic tumors.

COLORECTAL CANCER

Colorectal cancer (CRC) is the third most common cancer and the second cause of cancer-related deaths worldwide (5). CRC incidence rates are declining in the United States and are stable in most other Western countries, whereas rates are rising in Eastern Asia and Eastern Europe and likely reflect the adoption of a Western lifestyle (221, 222). CRC risk factors include obesity, Western diet, lack of physical activity, excessive alcohol use, hereditary syndromes (e.g., Lynch syndrome), and smoking (223). Treatment includes surgery, combination chemotherapy, radiation therapy, and targeted therapy, including antibodies against VEGF/VEGFR or EGFR (224). Although advances in better screening and treatment have been made in the last decade, long-term survival remains poor for metastatic CRC patients. The 5-year survival rate is <15% (225). ICI therapy was recently approved for refractory dMMR/MSI-H metastatic CRC (**Table 1**) (8, 10, 11). Of CRC cases that are dMMR/MSI-H, only 4% are metastatic. Accordingly, several approaches, including IDO inhibitors, vaccine therapy, and combination ICI therapy are being studied to extend immunotherapy efficacy to more patients (226). A better understanding of CD73/adenosine receptor signaling in CRC may help in these efforts.

Early studies assessing CD73 in CRC were part of larger efforts examining enzymatic patterns of key enzymes involved with purine metabolism and salvage, including ADA, alkaline phosphatase, hypoxanthine-guanine phosphoribosyltransferase (**Table 2**) (227, 228). Studies by Camici et al. (227) reported no difference with CD73 enzyme activity between CRC and normal tissue (227). In contrast, Eroglu et al. (228) showed higher CD73 enzyme activity in tumors compared to normal tissue (228). No associations were found with high CD73 enzyme activity and poor clinical features. Instead, high CD73 enzyme activity was associated with well-differentiated tumors and low CD73 enzyme activity associated with poorly-differentiated tumors (228). More recent studies show high CD73 expression correlates with poor tumor differentiation, lymph node involvement, advanced stage, and poor survival (78). In rectal cancer, CD73 expression in the different cell types carries different clinical prognosis (229). High CD73 expression in cancer cells and low CD73 expression in stromal cells associates with poor overall survival, whereas low CD73 expression in cancer cells and high CD73 expression in stromal cells is more favorable (229). Bladder cancer is similar. CD73 positive expression by epithelial cells predicts better progression-free survival and overall survival, whereas stromal cell CD73 positivity predicts poor outcome (230). Accordingly,

these studies support that CD73 in tumors may suppress and promote tumor progression. Although unknown, targeting tumors with dual roles for CD73 may prove challenging for CD73 inhibitor therapy.

Tumor heterogeneity is likely one explanation for the reported differences of CD73 expression in CRC. CRC tumors carry significant inter- and intra-heterogeneity (231, 232), so much so that in recent years an international consortium was formed to establish a robust molecular and genetic classification scheme for CRC. These global efforts led to the development of the consensus molecular subtypes (CMS) (233). Accordingly, future efforts assessing CD73 expression to the CMS groups (e.g., CMS1, CMS2, CMS3, CMS4) may provide a better understanding of CD73 in CRC and the possible molecular and genetic alterations that drive its downregulation and/or overexpression. Indeed, high CD73 expression in CRC may be associated with CMS2 tumors. In CRC, CD73 is a predictive biomarker of patient response to anti-EGFR therapy (234). In line with this, the CMS2 group predicts tumors that are more responsive to anti-EGFR and anti-HER2 therapy (235). Also consistent is that CD73 promotes CRC cell proliferation and tumor growth through β-catenin (WNT)/cyclin D1 signaling (236) and CMS2 tumors are characterized by WNT and MYC signaling (233). *KRAS* mutations/alterations are likely also linked to CD73 expression in CRC; discussed previously in the section on PDAC (207). Thus, investigating CD73 expression in *KRAS* mutant tumors may provide additional insight. A focus on metastatic samples may also be important. Liver metastasis occurs in 50% CRC patients (237). Recently, studies have shown high CD73 expression associates with significantly shorter time to recurrence and poor survival (238). In renal cancer patients, an adenosine high (AdenoSig^{hi}) expression signature was identified in pretreatment biopsies and associated with clinical response to A2AR antagonism (124). Similar efforts in identifying biomarker signatures may provide greatly to improving immunotherapy efficacy in CRC.

In preclinical studies, CD73 deletion increases CD8+ T cells and IFN-γ production to suppress the growth of MC-38 mouse colon cancer (32). The depletion of CD73 on CD4+ Foxp3+ Tregs also is significant in restoring antitumor immunity in this model (32). Similarly, CD39-deficient mice are resistant to MC-38 metastasis (239, 240). Whereas, overexpression of CD39 increases MC-26 mouse colon cancer cell metastasis to the liver (220). CD39 deletion does not increase the development of primary MC-26 orthotopic transplant tumors in heterozygous CD39 mice or mice transgenic for human CD39 compared to wild-type mice (220). Recent studies show support for co-targeting CD39 and CD73 in combination with ICI therapy and/or chemotherapy (44). Tumor-bearing mice benefit from increased antitumor immunity in these studies, which is due to the recovery of DC, macrophage, and effector T cell antitumor activity (44). In line with these studies, inhibiting CD39 or CD73 on MDSCs from CRC patients is effective in dampening the immunosuppressive activity of these cells (114).

Adenosine receptors may also be possible therapeutic targets. High A2AR expression associates with larger tumor size, increased tumor invasion, and higher TNM (TNM Classification of Malignant Tumors) stage in CRC (241). High A2AR expression also predicts poor patient survival and is positively correlated with PD-L1 expression (241). Consistent with the possible benefit of combined A2AR antagonist and ICI therapy (43, 68, 122, 123), studies with MC-38 cells, show A2AR antagonist, ciforadenant, combined with anti-PD-L1 or anti-CTLA-4 therapy eliminates 90% of tumors in mice by restoring antitumor immunity (68). Notably, MC-38 cells are normally highly sensitive to ICI therapy (37, 123). Additionally, in many studies, MC-38 cells are grown subcutaneously. Accordingly, it is not known how close these preclinical studies model immunosuppression and immunotherapy efficacy for CRC. A2BR is also upregulated in CRC and likely is linked to tumor hypoxia and progression (187). *In vitro* studies show A2BR expression is upregulated in CRC cells by hypoxia and promotes cancer cell proliferation, which is dampened by A2BR antagonism (187). A2BR antagonism also dampens A2BR-mediated CD73 expression by cancer-associated fibroblasts (CAFs) and CAF-associated immunosuppression activity (242). A3R is overexpressed in human CRC tissue and stimulates tumor growth via extracellular signal-regulated protein kinases 1 and 2 (ERK1/2) (243, 244). In contrast, studies also report A3R activity inhibits tumor growth by modulating glycogen synthesis kinase-3β (GSK-3β) and NF-Kappaβ (NF-κβ). A3R agonist treatment inhibits CRC cell proliferation, limits liver metastasis, and increases the cytotoxicity of chemotherapy (e.g., 5-fluorouracil) (245–247). Interestingly, treatment of CRC cells with caffeine, a non-selective adenosine receptor antagonist, inhibits A3R-mediated stabilization of HIF-1α (248). It is unclear if HIF-1α mediated by A3R promotes tumor progression or antitumor activity. HIFs are described to have pro- and antitumor activity in CRC (249). Moreover, overexpression of HIF-1α does not increase CRC tumorigenesis and does not result in spontaneous tumor formation in mice (250). Taken together, while many adenosine pathway members show evidence for possible therapeutic targeting in CRC, detailed studies in human tumors and relevant preclinical models are greatly needed.

CLINICAL IMPLICATIONS

Inhibiting CD73 (and/or A2AR) restores antitumor immunity in many preclinical studies with combination approaches showing superior efficacy. Accordingly, several clinical trials inhibiting CD73 (e.g., antibodies against CD73 or small molecule inhibitors) in combination with ICI therapy, A2AR antagonism, targeted therapy, and/or chemotherapy are underway (**Table 3**). Preliminary safety profiles report BMS-986179, an anti-CD73 humanized monoclonal antibody, and its combination with nivolumab (anti-PD-1 therapy) to be well-tolerated in patients (NCT02754141) (251). Recent studies in renal cell cancer (RCC) reported the feasibility and safety of A2AR antagonist, ciforadenant (124). Similar to preclinical studies, durable clinical benefit was associated with increased recruitment of CD8+ T cells (124). Additionally, combination therapy (ciforadenant and anti-PD-L1 therapy) showed benefit in patients who had progressed on anti-PD-1/PD-L1 therapy. Notably, patients in

TABLE 3 | Summary of clinical trials for CD73, A2AR, and A2BR in cancer.

Adenosine pathway target	Drug(s)	Target(s)	Therapy modality (adenosine pathway)	Phase	Details	Disease	Status	ClinicalTrials.gov Identifier
CD73	LY3475070 Pembrolizumab	CD73 PD-1	LY3475070: CD73 Small Molecule Inhibitor	Phase 1	Cohort A: LY3475070 administered orally Cohort B: LY3475070 + Pembrolizumab administered IV Cohort C1: LY3475070 + Pembrolizumab administered IV Cohort C2 LY3475070 administered orally Cohort D1 LY3475070 + Pembrolizumab administered IV Cohort D2: LY3475070 administered orally Cohort E: LY3475070 + Pembrolizumab administered IV	Advanced Solid Malignancies	Recruiting	NCT04148937
	Oleclumab (MEDI9447) Durvalumab (MEDI4736)	CD73 PD-L1	Oleclumab: CD73 Humanized Monoclonal Antibody	Phase 1 Phase 2	Phase I and Phase II Arm A: Paclitaxel, Carboplatin, Durvalumab, + Oleclumab Phase II Arm B: Paclitaxel, Carboplatin, + Durvalumab	Triple Negative Breast Cancer	Recruiting	NCT03616886
	Oleclumab (MEDI9447) Durvalumab	CD73 PD-L1	Oleclumab: CD73 Humanized Monoclonal Antibody	Phase 2	Experimental: Chemotherapy and radiation Experimental: Chemotherapy and pre-operative radiotherapy + Durvalumab Experimental: Chemotherapy and pre-operative radiotherapy + Durvalumab and Oleclumab	Luminal B (Breast Cancer)	Recruiting	NCT03875573
	Oleclumab (MEDI9447) Durvalumab	CD73 PD-L1	Oleclumab: CD73 Humanized Monoclonal Antibody	Phase 1	Experimental: Monotherapy, Oleclumab Experimental: Combination, Oleclumab and Durvalumab	Solid Tumors	Active, not Recruiting	NCT02503774
	TJ004309 Atezolizumab	CD73 PD-L1	TJ004309: CD73 Humanized Monoclonal Antibody	Phase 1	Dose escalated TJ004309 + Atezolizumab	Solid Tumors Metastatic Cancer	Recruiting	NCT03835949
	Oleclumab (MEDI9447) Durvalumab AZD9150 AZD6738 Vistusertib Olaparib Trasutzumab Cediranib	CD73 PD-L1 STAT3 ATR mTOR PARP HER2 VEGFR	Oleclumab: CD73 Humanized Monoclonal Antibody	Phase 2	Experimental: Durvalumab + Olaparib Experimental: Durvalumab + AZD9150 Experimental: Durvalumab + AZD6738 Experimental: Durvalumab + Vistusertib Experimental: Durvalumab + Oleclumab Experimental: Durvalumab + Trastuzumab Experimental: Durvalumab + Cediranib	Non-Small Cell Lung Cancer	Recruiting	NCT03334617
	Oleclumab (MEDI9447) Durvalumab Capivasertib Danvatirsen Paclitaxel	CD73 PD-L1 AKT STAT3 Chemotherapy	Oleclumab: CD73 Humanized Monoclonal Antibody	Phase 1 Phase 2	Experimental: Durvalumab + Paclitaxel Experimental: Durvalumab + Paclitaxel + Capivasertib Experimental: Durvalumab + Paclitaxel + Danvatirsen Experimental: Durvalumab + Paclitaxel + Oleclumab	Triple Negative Breast Cancer	Recruiting	NCT03742102
	Oleclumab (MEDI9447) Durvalumab Gemcitabine Nab-paclitaxel Oxaliplatin Leucovorin 5-FU	CD73 PD-L1 Chemotherapy	Oleclumab: CD73 Humanized Monoclonal Antibody	Phase 1 Phase 2	Arm A1: Gemcitabine + Nab-paclitaxel Arm A2: Oleclumab + Gemcitabine + Nab-paclitaxel Arm A3: Oleclumab + Durvalumab + Gemcitabine/Nab-paclitaxel Arm B1: Oxaliplatin + Leucovorin + 5-FU (mFOLFOX) Arm B2: Oleclumab + mFOLFOX	Carcinoma Metastatic Pancreatic Adenocarcinoma	Active, not Recruiting	NCT03611556
	Oleclumab (MEDI9447) Durvalumab	CD73 PD-L1	Oleclumab: CD73 Humanized Monoclonal Antibody	Phase 1	Experimental: Monotherapy, Durvalumab Experimental: Combination, Durvalumab + Oleclumab	Muscle Invasive Bladder Cancer	Recruiting	NCT03773666
	BMS-986179 Nivolumab rHUPH20	CD73 PD-1 Hyaluronidase	Oleclumab: CD73 Humanized Monoclonal Antibody	Phase 1 Phase 2	Arm A: Monotherapy, BMS-986179 Arm B: Combination Therapy, BMS-986179 + Nivolumab Arm C: Combination Therapy, BMS-986179 + rHUPH20	Malignant Solid Tumor	Recruiting	NCT02754141
	Oleclumab (MEDI9447) MEDI0562 Durvalumab Tremelilumab	CD73 OX40 PD-L1 CTLA-4	Oleclumab: CD73 Humanized Monoclonal Antibody	Phase 2	Cohort A: Oleclumab + Durvalumab Cohort B: MEDI0562 + Durvalumab Cohort C: MEDI0562 + Tremelimumab	Ovarian Cancer	Recruiting	NCT03267589

(Continued)

TABLE 3 | Continued

Adenosine pathway target	Drug(s)	Target(s)	Therapy modality (adenosine pathway)	Phase	Details	Disease	Status	ClinicalTrials.gov Identifier
CD73 A2AR	CPI-006 Ciforadenant (CPI-444) Pembrolizumab	CD73 A2AR PD-1	CPI-006: CD73 Humanized Monoclonal Antibody Ciforadenant: A2AR Antagonist	Phase 1	Cohort 1a: (escalating doses) CPI-006 Cohort 1b: (escalating doses) CPI-006 + Ciforadenant Cohort 1c: (escalating doses) CPI-006 + Pembrolizumab Cohort 2a: (selective dose) CPI-006 Cohort 2b: (selective dose) CPI-006 + Ciforadenant Cohort 2c: (selective doses) CPI-006 + Pembrolizumab	Non-Small Cell Lung Cancer Renal Cell Cancer Colorectal Cancer Triple Negative Breast Cancer Cervical Cancer Ovarian Cancer Pancreatic Cancer Endometrial Cancer Sarcoma Squamous Cell Carcinoma of the Head and Neck Bladder Cancer Metastatic Castration Resistant Prostate Cancer Non-hodgkin Lymphoma	Recruiting	NCT03454451
	Oleclumab (MEDI9447) AZD4635 Durvalumab	CD73 A2AR PD-L1	Oleclumab: CD73 Humanized Monoclonal Antibody AZD4635: A2AR Antagonist	Phase 2	Module 1: Drug: AZD4635; Drug: Durvalumab Module 2: Drug: AZD4635; Drug: Oleclumab	Prostate Cancer Metastatic Castration-Resistant Prostate Cancer	Recruiting	NCT04089553
	Oleclumab (MEDI9447) AZD4635 Osimertinib	CD73 A2AR EGFR	Oleclumab: CD73 Humanized Monoclonal Antibody AZD4635: A2AR Antagonist	Phase 1 Phase 2	Arm A: MEDI9447 + Osimertinib Arm B: MEDI9447 + AZD4635	Non-Small Cell Lung Cancer	Recruiting	NCT03381274
	NZV930 NIR178 PDR001	CD73 A2AR PD-1	NZV930: CD73 Humanized Monoclonal Antibody NIR178: A2AR Antagonist	Phase 1	Experimental: NZV930 Experimental: NZV930 + PDR001 Experimental: NZV930 + NIR178 Experimental: NZV930, NIR178, PDR001	Non-small Cell Lung Cancer (NSCLC) Triple Negative Breast Cancer Pancreatic Ductal Adenocarcinoma Colorectal Cancer Microsatellite Stable Ovarian Cancer Renal Cell Carcinoma	Recruiting	NCT03549000
	Oleclumab (MEDI9447) AZD4635 Durvalumab Abiraterone Acetate Enzalutamide Docetaxel	CD73 A2AR PD-L1 Hormone Therapy Chemotherapy	Oleclumab: CD73 Humanized Monoclonal Antibody AZD4635: A2AR Antagonist	Phase 1	Experimental: Arm A: AZD4635 monotherapy as nanoparticle suspension 125 mg BID Experimental: Arm B: AZD4635 monotherapy as nanoparticle suspension 75 mg QD Experimental: Arm C: AZD4635 monotherapy as nanoparticle suspension 100 mg QD Experimental: Arm D: AZD4635 as nanoparticle suspension 75 mg QD plus Durvalumab Experimental: Arm E: AZD4635 as nanoparticle suspension 100 mg QD plus Durvalumab Experimental: Arm EA: AZD4635 as nanoparticle suspension plus Enzalutamide Experimental: Arm AA: AZD4635 as nanoparticle suspension plus Abiraterone Acetate Experimental: Arm F: AZD4635 as nanoparticle suspension plus Durvaluamb in patients post immunotherapy with non-small cell lung cancer Experimental: Arm G: AZD4635 monotherapy as nanoparticle suspension in patients post immunotherapy with non-small cell lung cancer Experimental: Arm H: AZD4635 monotherapy as nanoparticle suspension in patients post immunotherapy with other solid tumors Experimental: Arm I: AZD4635 as nanoparticle suspension plus Durvalumab in immunotherapy naïve patients with metastatic castration resistant prostate cancer Experimental: Arm J: AZD4635 as nanoparticle suspension plus Durvalumab in immunotherapy naïve patients with metastatic castration resistant prostate cancer	Advanced Solid Malignancies Non-Small Cell Lung Cancer Metastatic Castrate-Resistant Prostate Carcinoma Colorectal Carcinoma	Recruiting	NCT02740985

(Continued)

TABLE 3 | Continued

Adenosine pathway target	Drug(s)	Target(s)	Therapy modality (adenosine pathway)	Phase	Details	Disease	Status	ClinicalTrials.gov Identifier
					Experimental: Arm K: AZD4635 monotherapy as nanoparticle suspension in immunotherapy naïve patients with colorectal carcinoma Experimental: Arm KD: AZD4635 as nanoparticle suspension plus Durvalumab in immunotherapy-naïve patients with colorectal carcinoma Experimental: Arm L: AZD4635 monotherapy as nanoparticle suspension in immunotherapy naïve patients with other solid tumours Experimental: Arm CA: AZD4635 capsule formulation monotherapy 75 mg QD Experimental: Arm CB: AZD4635 capsule formulation 50 mg QD plus Durvalumab and Oleclumab Experimental: Arm CC: AZD4635 capsule formulation 50 mg QD plus Docetaxel			
A2AR	NIR178 PDR001	A2AR PD-1	NIR178: A2AR Antagonist	Phase 2	Experimental (1): NIR178 + PDR001 Experimental (2): NIR178 BID Intermittent + PDR001 Experimental (3): Part 3, initiation of part 3 will depend on results from parts 1 and 2 Experimental (4): Japanese safety run-in part, two different dosing schedules of NIR178 will be explored	Non-small Cell Lung Cancer Renal Cell Cancer Pancreatic Cancer Urothelial Cancer Head and Neck Cancer Diffused Large B Cell Lymphoma Microsatellite Stable Colon Cancer Triple Negative Breast Cancer Melanoma	Recruiting	NCT03207867
	PBF-509 PDR001	A2AR PD-1	PBF-509: A2AR Antagonist	Phase 1 Phase 2	Drug: PBF-509_80 mg Drug: PBF-509_160 mg Drug: PBF-509_320 mg Drug: PBF-509_640 mg Drug: Combo PBF-509 (160 mg) + PDR001 Drug: Combo PBF-509 (320 mg) + PDR001 Drug: Combo PBF-509 (640 mg) + PDR001 Drug: RP2D (PBF-509+PDR001)_immuno naïve Drug: Experimental: RP2D (PBF-509+PDR001)_immuno treated	Non-small Cell Lung Cancer	Recruiting	NCT02403193
	NIR178 Spartalizumab LAG525 Capmatinib MCS110 Canakinumab	A2AR PD-1 LAG-3 c-Met M-CSF IL-1β	NIR178: A2AR Antagonist	Phase 1	Experimental: Spartalizumab + LAG525 + NIR178 Experimental: Spartalizumab + LAG525 + Capmatinib Experimental: spartalizumab + LAG525 + MCS110 Experimental: spartalizumab + LAG525 + Canakinumab	Triple Negative Breast Cancer	Recruiting	NCT03742349
	Ciforadenant (CPI-444) Atezolizumab	A2AR PD-L1	Ciforadenant: A2AR Antagonist	Phase 1	Experimental: Ciforadenant, 100 mg orally twice daily for the first 14 days of each 28-day cycle Experimental: Ciforadenant, 100 mg orally twice daily for 28 days of each 28-day cycle Experimental: Ciforadenant, 200 mg orally once daily for the first 14 days of each 28-day cycle Experimental: Ciforadenant + Atezolizumab Experimental: Ciforadenant, start with 150 mg orally twice daily for 28-day cycles; then, increase increments by 100 mg/day for 6 dose levels	Non-Small Cell Lung Cancer Malignant Melanoma Renal Cell Cancer Triple Negative Breast Cancer Colorectal Cancer Bladder Cancer Metastatic Castration Resistant Prostate Cancer	Recruiting	NCT02655822
	Ciforadenant (CPI-444) Atezolizumab Cobimetinib RO6958688 Docetaxel Pemetrexed Carboplatin Gemcitabine Linagliptin Tocilizumab Ipatasertib Idasanutlin	A2AR PD-L1 MEK CEA Chemotherapy IL-6R AKT MDM2	Ciforadenant: A2AR Antagonist	Phase 1 Phase 2	Active Comparator: Stage 1: Cohort 1: Atezolizumab Experimental: Stage 1: Cohort 1: Atezolizumab + Cobimetinib Experimental: Stage 1: Cohort 1: Atezolizumab + RO6958688 Active Comparator: Stage 1: Cohort 2: Docetaxel Experimental: Stage 1: Cohort 2: Atezolizumab + Cobimetinib Experimental: Stage 1: Cohort 2: Atezolizumab + Ciforadenant Experimental: Stage 1: Cohort 2: Atezolizumab + RO6958688 Experimental: Stage 1: Cohort 2: Atezolizumab + Ipatasertib Experimental: Stage 1: Cohort 2: Idasanutlin + Docetaxel Experimental: Stage 2: Cohort 1: Atezolizumab + Pemetrexed + Carboplatin	Carcinoma, Non-Small-Cell Lung	Recruiting	NCT03337698

(Continued)

TABLE 3 | Continued

Adenosine pathway target	Drug(s)	Target(s)	Therapy modality (adenosine pathway)	Phase	Details	Disease	Status	ClinicalTrials.gov Identifier
A2AR A2BR	AB928 IPI-549 Doxorubicin Paclitaxel	A2AR/A2BR PI3Kγ Chemotherapy	AB928: Dual A2AR and A2BR Antagonist	Phase 1	Experimental: Dose Escalation-Arm A, AB928 + Pegylated Liposomal Doxorubicin Experimental: Dose Escalation-Arm B, AB928 + Nanoparticle Albumin-bound Paclitaxel Experimental: Dose Escalation-Arm C, AB928 + Pegylated Liposomal Doxorubicin + Nanoparticle Albumin-bound Paclitaxel Experimental: Dose Expansion-TNBC-Arm 1, dose from Arm A for AB928 + Pegylated Liposomal Doxorubicin Experimental: Dose Expansion-Ovarian-Arm 2, dose from Arm A for AB928 + Pegylated Liposomal Doxorubicin Experimental: Dose Expansion-TNBC-Arm 3, dose from Arm B for AB928 + Nanoparticle Albumin-bound Paclitaxel Experimental: Dose Expansion-TNBC-Arm 4, dose from Arm C for AB928 + IPI-549 + Pegylated Liposomal Doxorubicin	Triple Negative Breast Cancer (TNBC) Ovarian Cancer	Recruiting	NCT03719326
	AB928 mFOLFOX	A2AR/A2BR Chemotherapy	AB928: Dual A2AR and A2BR Antagonist	Phase 1	Experimental: Dose Escalation, AB928 + mFOLFOX Experimental: Dose Expansion-GE, dose from escalation for AB928 + mFOLFOX Experimental: Dose Expansion-CRC, dose from escalation for AB928 + mFOLFOX	GastroEsophageal Cancer (GE) Colorectal Cancer (CRC)	Recruiting	NCT03720678
	AB928 Zimberelimab (AB122)	A2AR/A2BR PD-1	AB928: Dual A2AR and A2BR Antagonist	Phase 1	Experimental: Dose Escalation, AB928 + fixed dose of Zimberelimab (AB122) Experimental: Dose Expansion-Renal Cell Carcinoma, recommended dose for expansion AB928 + Zimberelimab (AB122) Experimental: Dose Expansion, recommended dose for expansion AB928 + Zimberelimab (AB122)	Non-small Cell Lung Cancer Squamous Cell Carcinoma of the Head and Neck Breast Cancer Colorectal Cancer Melanoma Bladder Cancer Ovarian Cancer Endometrial Cancer Merkel Cell Carcinoma GastroEsophageal Cancer Renal Cell Carcinoma Castration-resistant Prostate Cancer	Recruiting	NCT03629756
	AB928 AB154 Zimberelimab (AB122)	A2AR/A2BR TIGIT PD-1	AB928: Dual A2AR and A2BR Antagonist	Phase 2	Experimental: Arm 1, Zimberelimab Experimental: Arm 2, AB154 + Zimberelimab Experimental: Arm 3, AB928 + AB154 + Zimberelimab	Non-Small Cell Lung Cancer Non-squamous Non-Small Cell Lung Cancer Squamous Non-Small Cell Lung Cancer Lung Cancer	Recruiting	NCT04262856
	AB928 Zimberelimab (AB122) Carboplatin Pemetrexed Pembrolizumab	A2AR/A2BR PD-1 Chemotherapy	AB928: Dual A2AR and A2BR Antagonist	Phase 1	Experimental: Dose Escalation Arm A, AB928 + Carboplatin + Pemetrexed Experimental: Dose Escalation Arm B, AB928 + Carboplatin + Pemetrexed + Pembrolizumab Experimental: Dose Expansion Arm 1, recommended dose for expansion AB928 + Carboplatin + Pemetrexed in patients harboring sensitizing EGFR mutation Experimental: Dose Expansion Arm 2, recommended dose for expansion AB928 + Carboplatin + Pemetrexed + AB122 in patients harboring sensitizing EGFR mutation	Non-Small Cell Lung Cancer Metastatic Non-Small Cell Lung Cancer Non-squamous Non-small Cell Neoplasm of Lung Sensitizing EGFR Gene Mutation	Recruiting	NCT03846310
A2BR	PBF-1129	A2BR	PBF-1129: A2BR Antagonist	Phase 1	Experimental: PBF-1129_40 mg Experimental: PBF-1129_80 mg Experimental: PBF-1129_160 mg Experimental: PBF-1129_320 mg	Non-Small Cell Lung Cancer	Recruiting	NCT03274479

these trials were heavily pretreated (≥3 prior treatments) (124). It will be interesting in the future to see if CD73 and/or A2AR therapy efficacy is increased further when used in earlier lines of therapy (124). Moreover, the authors discovered responding patients carry an AdenoSig^{hi} signature (124). Assessing whether this signature can also be detected in pretreatment biopsies of other cancers and possibly primary tumors may be beneficial (124). Biomarkers or gene signatures will likely be key in identifying patients benefiting the most from CD73/adenosine receptor therapy. Clinical trials are underway for AB928, a dual A2AR/A2BR antagonist, and include a focus on GI cancers [e.g., esophageal cancer and CRC; NCT03720678 (**Table 3**)]. A favorable safety profile of AB928 combined with chemotherapy has been reported in patients (252). Future studies in GI cancers that focus on determining if adenosine-mediated resistance to immunotherapy therapy exists at diagnosis or evolves with therapy will also be of significant benefit. Encouraging early results for BMS-986179 combined with nivolumab report clinical benefit (partial response) in one or more patients with pancreatic and prostate cancer (NCT02754141) (251). Both are poorly immunogenic tumors. Preclinical studies show CD73/adenosine therapy (e.g., A2AR deletion) liberates CD8+ T cells for antitumor activity even against weakly immunogenic sarcomas (70). Therapy benefit in these studies is independent of the anatomical location of the tumor (70). Thus, therapeutic benefit across many tumors (immunogenic and non-immunogenic) is expected. Understanding factors preventing immune cells from recognizing and eliminating cancer cells will continue to be important in the advancement of immunotherapy strategies. Poor tumor immunogenicity can be a result of many features, including HLA class I molecule downregulation or loss (253); genetic, epigenetic, and chromosome alterations regulating presentation and processing of surface epitopes (254–256); expression and secretion of immunosuppressive factors (e.g., PD-1, TGF-β, adenosine) (257); and the inability of cancer cells to produce new surface epitopes that are different from what immune receptors have regularly experienced (258). Whether CD73 expression associates with dMMR/MSI-H in GI tumors and its blockade would further increase immunotherapy efficacy in these tumors is unknown. In NSCLC studies, tumor mutational burden and neoantigen burden does not associate with CD73 high or low expression (74).

Taking advantage of strong associations of CD73 with molecular and genetic alterations (e.g., *KRAS* mutation and EGFR alterations) may benefit GI cancers. Combination studies of CD73 inhibitors with anti-EGFR therapy and/or tyrosine kinase inhibitors are in clinical trials for managing resistance (**Table 3**). In CRC, high CD73 predicts patients benefiting from cetuximab (anti-EGFR therapy) (234). Benefits are the same for both wild-type and mutant *KRAS* tumors (234). It would be interesting to see the performance of combination cetuximab with CD73 inhibitors in preclinical CRC studies considering that inflammation is a mechanism of resistance to cetuximab (259). In melanoma, combination BRAF and MEK inhibitors with an A2AR antagonist induces significant tumor control in preclinical studies (41). MEK is a promising target for *KRAS*, *NRAS*, and *BRAF* mutant tumors and is being targeted in CRC (260). Recently, MEK inhibitor, cobimetinib, combined with anti-PD-L1 therapy (atezolizumab) failed to improve survival in microsatellite-stable metastatic CRC patients in a phase 3 clinical trial (261). Could the inclusion of A2AR antagonists be key to the success of these studies? AMG510, a selective inhibitor for *KRAS* (G12C) recently showed promising antitumor effects, including increasing ICI therapy sensitivity in preclinical models (262). Its combination with CD73/adenosine receptor blockade may be a promising future approach. AMG510 is in clinical trials (NCT03600883). Mentioned previously, hyperoxia induces antitumor immunity in preclinical studies, which involves the downregulation of many adenosine pathway genes (102, 108). With drug toxicity being a concern with studies pushing past two targets, approaches like this that can simultaneously dampen multiple immune checkpoints may be better tolerated and provide greater benefit (263). Although a drawback of hyperoxia therapy is that it may/does cause tissue damage (263, 264), it is interesting to consider whether this response also benefits in helping to recover antitumor immunity. Hyperoxia is in clinical trials for many conditions/diseases (ClinicalTrials.gov; hyperoxia, 87 studies).

CONCLUSIONS

Immunotherapy in GI cancers currently benefits only a few patients. Blocking adenosine signaling by inhibiting CD73 and/or A2AR/A2BR antagonism has the potential to improve antitumor immunity in these tumors. However, identifying which patients may benefit stands in the way. To aid in these efforts, a better understanding of CD73 in human GI cancers is greatly needed. This includes initiating studies that assess CD73 in addition to other ecto-enzymes involved in extracellular adenosine synthesis and metabolism as well as their association with key molecular and genetic features. A focus of CD73 expression in primary, pretreatment, and relapsed samples will also be of great value in addition to identifying predictive biomarkers or gene signatures relating to efficacy of CD73/adenosine receptor blockade. Mechanistically, studies assessing CD73/extracellular adenosine receptor activity in humanized and autochthonous tumor mouse models and patient-derived organoids will provide needed insight into the role of CD73/extracellular adenosine in these tumors. Moreover, studies in HCC have revealed CD73 overexpression in human tumors can be misleading. Future studies also incorporating this insight have the best chance of helping to better define CD73 in GI cancers.

AUTHOR'S NOTE

AUTHOR CONTRIBUTIONS

JH, LP, OV, and JB drafted, edited, and revised the manuscript. OV developed the manuscript figure.

FUNDING

JB is supported by an International Research Society Mentored Research Award. LP was funded by a McGovern Medical School at UTHealth Dean's Office Stipend Award.

REFERENCES

1. Magalhaes H, Fontes-Sousa M, Machado M. Immunotherapy in advanced gastric cancer: an overview of the emerging strategies. *Can J Gastroenterol Hepatol.* (2018) 2018:2732408. doi: 10.1155/2018/2732408
2. Villanueva A. Hepatocellular carcinoma. *N Engl J Med.* (2019) 380:1450–62. doi: 10.1056/NEJMra1713263
3. Siegel RL, Miller KD, Jemal A. Cancer statistics, 2017. *CA Cancer J Clin.* (2017) 67:7–30. doi: 10.3322/caac.21387
4. Rahib L, Smith BD, Aizenberg R, Rosenzweig AB, Fleshman JM, Matrisian LM. Projecting cancer incidence and deaths to 2030: the unexpected burden of thyroid, liver, and pancreas cancers in the United States. *Cancer Res.* (2014) 74:2913–21. doi: 10.1158/0008-5472.CAN-14-0155
5. Bray F, Ferlay J, Soerjomataram I, Siegel RL, Torre LA, Jemal A. Global cancer statistics 2018: GLOBOCAN estimates of incidence and mortality worldwide for 36 cancers in 185 countries. *CA Cancer J Clin.* (2018) 68:394–424. doi: 10.3322/caac.21492
6. Bang YJ, Kang YK, Catenacci DV, Muro K, Fuchs CS, Geva R, et al. Pembrolizumab alone or in combination with chemotherapy as first-line therapy for patients with advanced gastric or gastroesophageal junction adenocarcinoma: results from the phase II nonrandomized KEYNOTE-059 study. *Gastric Cancer.* (2019) 22:828–37. doi: 10.1007/s10120-018-00909-5
7. Zhu AX, Finn RS, Edeline J, Cattan S, Ogasawara S, Palmer D, et al. Pembrolizumab in patients with advanced hepatocellular carcinoma previously treated with sorafenib (KEYNOTE-224): a non-randomised, open-label phase 2 trial. *Lancet Oncol.* (2018) 19:940–52. doi: 10.1200/JCO.2018.36.4_suppl.209
8. Le DT, Uram JN, Wang H, Bartlett BR, Kemberling H, Eyring AD, et al. PD-1 blockade in tumors with mismatch-repair deficiency. *N Engl J Med.* (2015) 372:2509–20. doi: 10.1056/NEJMoa1500596
9. El-Khoueiry AB, Sangro B, Yau T, Crocenzi TS, Kudo M, Hsu C, et al. Nivolumab in patients with advanced hepatocellular carcinoma (CheckMate 040): an open-label, non-comparative, phase 1/2 dose escalation and expansion trial. *Lancet.* (2017) 389:2492–502. doi: 10.1016/S0140-6736(17)31046-2
10. Overman MJ, McDermott R, Leach JL, Lonardi S, Lenz HJ, Morse MA, et al. Nivolumab in patients with metastatic DNA mismatch repair-deficient or microsatellite instability-high colorectal cancer (CheckMate 142): an open-label, multicentre, phase 2 study. *Lancet Oncol.* (2017) 18:1182–91. doi: 10.1016/S1470-2045(17)30422-9
11. Overman MJ, Lonardi S, Wong KYM, Lenz HJ, Gelsomino F, Aglietta M, et al. Durable clinical benefit with nivolumab plus ipilimumab in DNA mismatch repair-deficient/microsatellite instability-high metastatic colorectal cancer. *J Clin Oncol.* (2018) 36:773–9. doi: 10.1200/JCO.2017.76.9901
12. Hazama S, Tamada K, Yamaguchi Y, Kawakami Y, Nagano H. Current status of immunotherapy against gastrointestinal cancers and its biomarkers: perspective for precision immunotherapy. *Ann Gastroenterol Surg.* (2018) 2:289–303. doi: 10.1002/ags3.12180
13. Le DT, Durham JN, Smith KN, Wang H, Bartlett BR, Aulakh LK, et al. Mismatch repair deficiency predicts response of solid tumors to PD-1 blockade. *Science.* (2017) 357:409–13. doi: 10.1126/science.aan6733
14. Cicek MS, Lindor NM, Gallinger S, Bapat B, Hopper JL, Jenkins MA, et al. Quality assessment and correlation of microsatellite instability and immunohistochemical markers among population- and clinic-based colorectal tumors results from the Colon Cancer Family Registry. *J Mol Diagn.* (2011) 13:271–81. doi: 10.1016/j.jmoldx.2010.12.004
15. Zhao P, Li L, Jiang X, Li Q. Mismatch repair deficiency/microsatellite instability-high as a predictor for anti-PD-1/PD-L1 immunotherapy efficacy. *J Hematol Oncol.* (2019) 12:54. doi: 10.1186/s13045-019-0738-1
16. McGranahan N, Furness AJ, Rosenthal R, Ramskov S, Lyngaa R, Saini SK, et al. Clonal neoantigens elicit T cell immunoreactivity and sensitivity to immune checkpoint blockade. *Science.* (2016) 351:1463–9. doi: 10.1126/science.aaf1490
17. Rizvi NA, Hellmann MD, Snyder A, Kvistborg P, Makarov V, Havel JJ, et al. Cancer immunology. Mutational landscape determines sensitivity to PD-1 blockade in non-small cell lung cancer. *Science.* (2015) 348:124–8. doi: 10.1126/science.aaa1348
18. Castle JC, Kreiter S, Diekmann J, Lower M, van de Roemer N, de Graaf J, et al. Exploiting the mutanome for tumor vaccination. *Cancer Res.* (2012) 72:1081–91. doi: 10.1158/0008-5472.CAN-11-3722
19. Dolcetti R, Viel A, Doglioni C, Russo A, Guidoboni M, Capozzi E, et al. High prevalence of activated intraepithelial cytotoxic T lymphocytes and increased neoplastic cell apoptosis in colorectal carcinomas with microsatellite instability. *Am J Pathol.* (1999) 154:1805–13. doi: 10.1016/S0002-9440(10)65436-3
20. Guidoboni M, Gafa R, Viel A, Doglioni C, Russo A, Santini A, et al. Microsatellite instability and high content of activated cytotoxic lymphocytes identify colon cancer patients with a favorable prognosis. *Am J Pathol.* (2001) 159:297–304. doi: 10.1016/S0002-9440(10)61695-1
21. Hause RJ, Pritchard CC, Shendure J, Salipante SJ. Classification and characterization of microsatellite instability across 18 cancer types. *Nat Med.* (2016) 22:1342–50. doi: 10.1038/nm.4191
22. Kim JY, Shin NR, Kim A, Lee HJ, Park WY, Kim JY, et al. Microsatellite instability status in gastric cancer: a reappraisal of its clinical significance and relationship with mucin phenotypes. *Korean J Pathol.* (2013) 47:28–35. doi: 10.4132/KoreanJPathol.2013.47.1.28
23. Cancer Genome Atlas Research Network. Comprehensive molecular characterization of gastric adenocarcinoma. *Nature.* (2014) 513:202–9. doi: 10.1038/nature13480
24. Cancer Genome Atlas Research Network. Integrated genomic characterization of pancreatic ductal adenocarcinoma. *Cancer Cell.* (2017) 32:185–203 e13.
25. Cortes-Ciriano I, Lee S, Park WY, Kim TM, Park PJ. A molecular portrait of microsatellite instability across multiple cancers. *Nat Commun.* (2017) 8:15180. doi: 10.1038/ncomms15180
26. Goumard C, Desbois-Mouthon C, Wendum D, Calmel C, Merabtene F, Scatton O, et al. Low levels of microsatellite instability at simple repeated sequences commonly occur in human hepatocellular carcinoma. *Cancer Genomics Proteomics.* (2017) 14:329–39. doi: 10.21873/cgp.20043
27. Meinel S, Blohberger J, Berg D, Berg U, Dissen GA, Ojeda SR, et al. Pro-nerve growth factor in the ovary and human granulosa cells. *Horm Mol Biol Clin Investig.* (2015) 24:91–9. doi: 10.1515/hmbci-2015-0028
28. Procaccio L, Schirripa M, Fassan M, Vecchione L, Bergamo F, Prete AA, et al. Immunotherapy in gastrointestinal cancers. *Biomed Res Int.* (2017) 2017:4346576. doi: 10.1155/2017/4346576
29. Sambi M, Bagheri L, Szewczuk MR. Current challenges in cancer immunotherapy: multimodal approaches to improve efficacy, and patient response rates. *J Oncol.* (2019) 2019:4508794. doi: 10.1155/2019/4508794
30. Jin D, Fan J, Wang L, Thompson LF, Liu A, Daniel BJ, et al. CD73 on tumor cells impairs antitumor T-cell responses: a novel mechanism of tumor-induced immune suppression. *Cancer Res.* (2010) 70:2245–55. doi: 10.1158/0008-5472.CAN-09-3109

31. Stagg J, Divisekera U, McLaughlin N, Sharkey J, Pommey S, Denoyer D, et al. Anti-CD73 antibody therapy inhibits breast tumor growth and metastasis. *Proc Natl Acad Sci USA*. (2010) 107:1547–52. doi: 10.1073/pnas.0908801107
32. Stagg J, Divisekera U, Duret H, Sparwasser T, Teng MW, Darcy PK, et al. CD73-deficient mice have increased antitumor immunity and are resistant to experimental metastasis. *Cancer Res.* (2011) 71:2892–900. doi: 10.1158/0008-5472.CAN-10-4246
33. Wang L, Fan J, Thompson LF, Zhang Y, Shin T, Curiel TJ, et al. CD73 has distinct roles in nonhematopoietic and hematopoietic cells to promote tumor growth in mice. *J Clin Invest.* (2011) 121:2371–82. doi: 10.1172/JCI45559
34. Yegutkin GG, Marttila-Ichihara F, Karikoski M, Niemela J, Laurila JP, Elima K, et al. Altered purinergic signaling in CD73-deficient mice inhibits tumor progression. *Eur J Immunol.* (2011) 41:1231–41. doi: 10.1002/eji.201041292
35. Stagg J, Beavis PA, Divisekera U, Liu MC, Moller A, Darcy PK, et al. CD73-deficient mice are resistant to carcinogenesis. *Cancer Res.* (2012) 72:2190–6. doi: 10.1158/0008-5472.CAN-12-0420
36. Loi S, Pommey S, Haibe-Kains B, Beavis PA, Darcy PK, Smyth MJ, et al. CD73 promotes anthracycline resistance and poor prognosis in triple negative breast cancer. *Proc Natl Acad Sci USA*. (2013) 110:11091–6. doi: 10.1073/pnas.1222251110
37. Allard B, Pommey S, Smyth MJ, Stagg J. Targeting CD73 enhances the antitumor activity of anti-PD-1 and anti-CTLA-4 mAbs. *Clin Cancer Res.* (2013) 19:5626–35. doi: 10.1158/1078-0432.CCR-13-0545
38. Beavis PA, Divisekera U, Paget C, Chow MT, John LB, Devaud C, et al. Blockade of A2A receptors potently suppresses the metastasis of CD73+ tumors. *Proc Natl Acad Sci USA*. (2013) 110:14711–6. doi: 10.1073/pnas.1308209110
39. Young A, Ngiow SF, Barkauskas DS, Sult E, Hay C, Blake SJ, et al. Co-inhibition of CD73, and A2AR adenosine signaling improves anti-tumor immune responses. *Cancer Cell.* (2016) 30:391–403. doi: 10.1016/j.ccell.2016.06.025
40. Hay CM, Sult E, Huang Q, Mulgrew K, Fuhrmann SR, McGlinchey KA, et al. Targeting CD73 in the tumor microenvironment with MEDI9447. *Oncoimmunology.* (2016) 5:e1208875. doi: 10.1080/2162402X.2016.1208875
41. Reinhardt J, Landsberg J, Schmid-Burgk JL, Ramis BB, Bald T, Glodde N, et al. MAPK signaling, and inflammation link melanoma phenotype switching to induction of CD73 during immunotherapy. *Cancer Res.* (2017) 77:4697–709. doi: 10.1158/0008-5472.CAN-17-0395
42. Young A, Ngiow SF, Madore J, Reinhardt J, Landsberg J, Chitsazan A, et al. Targeting adenosine in BRAF-mutant melanoma reduces tumor growth, and metastasis. *Cancer Res.* (2017) 77:4684–96. doi: 10.1158/0008-5472.CAN-17-0393
43. Iannone R, Miele L, Maiolino P, Pinto A, Morello S. Adenosine limits the therapeutic effectiveness of anti-CTLA4 mAb in a mouse melanoma model. *Am J Cancer Res.* (2014) 4:172–81. eCollection 2014.
44. Perrot I, Michaud HA, Giraudon-Paoli M, Augier S, Docquier A, Gros L, et al. Blocking antibodies targeting the CD39/CD73 immunosuppressive pathway unleash immune responses in combination cancer therapies. *Cell Rep.* (2019) 27:2411–25 e9. doi: 10.1016/j.celrep.2019.04.091
45. Linden J, Koch-Nolte F, Dahl G. Purine release, metabolism„ and signaling in the inflammatory response. *Annu Rev Immunol.* (2019) 37:325–47. doi: 10.1146/annurev-immunol-051116-052406
46. Bowser JL, Lee JW, Yuan X, Eltzschig HK. The hypoxia-adenosine link during inflammation. *J Appl Physiol.* (2017) 123:1303–20. doi: 10.1152/japplphysiol.00101.2017
47. Bowser JL, Phan LH, Eltzschig HK. The hypoxia-adenosine link during intestinal inflammation. *J Immunol.* (2018) 200:897–907. doi: 10.4049/jimmunol.1701414
48. Robeva AS, Woodard RL, Jin X, Gao Z, Bhattacharya S, Taylor HE, et al. Molecular characterization of recombinant human adenosine receptors. *Drug Dev Res.* (1996) 39:243–52. doi: 10.1002/(SICI)1098-2299(199611/12)39:3/4<243::AID-DDR3>3.0.CO;2-R
49. Cronstein BN, Naime D, Ostad E. The antiinflammatory mechanism of methotrexate. Increased adenosine release at inflamed sites diminishes leukocyte accumulation in an *in vivo* model of inflammation. *J Clin Invest.* (1993) 92:2675–82. doi: 10.1172/JCI116884
50. Ohta A, Sitkovsky M. Role of G-protein-coupled adenosine receptors in downregulation of inflammation and protection from tissue damage. *Nature.* (2001) 414:916–20. doi: 10.1038/414916a
51. Kohler D, Eckle T, Faigle M, Grenz A, Mittelbronn M, Laucher S, et al. CD39/ectonucleoside triphosphate diphosphohydrolase 1 provides myocardial protection during cardiac ischemia/reperfusion injury. *Circulation.* (2007) 116:1784–94. doi: 10.1161/CIRCULATIONAHA.107.690180
52. Yang Z, Day YJ, Toufektsian MC, Ramos SI, Marshall M, Wang XQ, et al. Infarct-sparing effect of A2A-adenosine receptor activation is due primarily to its action on lymphocytes. *Circulation.* (2005) 111:2190–7. doi: 10.1161/01.CIR.0000163586.62253.A5
53. Rose JB, Naydenova Z, Bang A, Eguchi M, Sweeney G, Choi DS, et al. Equilibrative nucleoside transporter 1 plays an essential role in cardioprotection. *Am J Physiol Heart Circ Physiol.* (2010) 298:H771–7. doi: 10.1152/ajpheart.00711.2009
54. Eckle T, Fullbier L, Wehrmann M, Khoury J, Mittelbronn M, Ibla J, et al. Identification of ectonucleotidases CD39, and CD73 in innate protection during acute lung injury. *J Immunol.* (2007) 178:8127–37. doi: 10.4049/jimmunol.178.12.8127
55. Eckle T, Grenz A, Laucher S, Eltzschig HK. A2B adenosine receptor signaling attenuates acute lung injury by enhancing alveolar fluid clearance in mice. *J Clin Invest.* (2008) 118:3301–15. doi: 10.1172/JCI34203
56. Eckle T, Hughes K, Ehrentraut H, Brodsky KS, Rosenberger P, Choi DS, et al. Crosstalk between the equilibrative nucleoside transporter ENT2 and alveolar Adora2b adenosine receptors dampens acute lung injury. *FASEB J.* (2013) 27:3078–89. doi: 10.1096/fj.13-228551
57. Eckle T, Kewley EM, Brodsky KS, Tak E, Bonney S, Gobel M, et al. Identification of hypoxia-inducible factor HIF-1A as transcriptional regulator of the A2B adenosine receptor during acute lung injury. *J Immunol.* (2014) 192:1249–56. doi: 10.4049/jimmunol.1100593
58. Schingnitz U, Hartmann K, Macmanus CF, Eckle T, Zug S, Colgan SP, et al. Signaling through the A2B adenosine receptor dampens endotoxin-induced acute lung injury. *J Immunol.* (2010) 184:5271–9. doi: 10.4049/jimmunol.0903035
59. Hart ML, Jacobi B, Schittenhelm J, Henn M, Eltzschig HK. Cutting edge: A2B adenosine receptor signaling provides potent protection during intestinal ischemia/reperfusion injury. *J Immunol.* (2009) 182:3965–8. doi: 10.4049/jimmunol.0802193
60. Taha MO, Miranda-Ferreira R, Simoes RS, Abrao MS, Oliveira-Junior IS, Monteiro HP, et al. Caricati-neto: role of adenosine on intestinal ischemia-reperfusion injury in rabbits. *Transplant Proc.* (2010) 42:454–6. doi: 10.1016/j.transproceed.2010.01.019
61. Haddad MA, Miranda-Ferreira R, Taha NS, Maldonado VC, Daroz RR, Daud MO, et al. Effect of adenosine on injury caused by ischemia and reperfusion in rats: functional and morphologic study. *Transplant Proc.* (2012) 44:2317–20. doi: 10.1016/j.transproceed.2012.07.057
62. Friedman DJ, Kunzli BM, A-Rahim YI, Sevigny J, Berberat PO, Enjyoji K, et al. From the cover: CD39 deletion exacerbates experimental murine colitis and human polymorphisms increase susceptibility to inflammatory bowel disease. *Proc Natl Acad Sci USA.* (2009) 106:16788–93. doi: 10.1073/pnas.0902869106
63. Louis NA, Robinson AM, MacManus CF, Karhausen J, Scully M, Colgan SP. Control of IFN-alphaA by CD73: implications for mucosal inflammation. *J Immunol.* (2008) 180:4246–55. doi: 10.4049/jimmunol.180.6.4246
64. Aherne CM, Saeedi B, Collins CB, Masterson JC, McNamee EN, Perrenoud L, et al. Epithelial-specific A2B adenosine receptor signaling protects the colonic epithelial barrier during acute colitis. *Mucosal Immunol.* (2015) 8:1324–38. doi: 10.1038/mi.2015.22
65. Aherne CM, Collins CB, Rapp CR, Olli KE, Perrenoud L, Jedlicka P, et al. Coordination of ENT2-dependent adenosine transport and signaling dampens mucosal inflammation. *JCI Insight.* (2018) 3. doi: 10.1172/jci.insight.121521
66. Blay J, White TD, Hoskin DW. The extracellular fluid of solid carcinomas contains immunosuppressive concentrations of adenosine. *Cancer Res.* (1997) 57:2602–5.

67. Ohta A, Gorelik E, Prasad SJ, Ronchese F, Lukashev D, Wong MK, et al. A2A adenosine receptor protects tumors from antitumor T cells. *Proc Natl Acad Sci USA*. (2006) 103:13132–7. doi: 10.1073/pnas.0605251103
68. Willingham SB, Ho PY, Hotson A, Hill C, Piccione EC, Hsieh J, et al. A2AR Antagonism with CPI-444 induces antitumor responses, and augments efficacy to Anti-PD-(L)1, and Anti-CTLA-4 in preclinical models. *Cancer Immunol Res.* (2018) 6:1136–49. doi: 10.1158/2326-6066.CIR-18-0056
69. Leone RD, Sun IM, Oh MH, Sun IH, Wen J, Englert J, et al. Inhibition of the adenosine A2a receptor modulates expression of T cell coinhibitory receptors and improves effector function for enhanced checkpoint blockade, and ACT in murine cancer models. *Cancer Immunol Immunother.* (2018) 67:1271–84. doi: 10.1007/s00262-018-2186-0
70. Kjaergaard J, Hatfield S, Jones G, Ohta A, Sitkovsky M. A2A adenosine receptor gene deletion or synthetic A2A antagonist liberate tumor-reactive CD8(+) T cells from tumor-induced immunosuppression. *J Immunol.* (2018) 201:782–91. doi: 10.4049/jimmunol.1700850
71. Yan A, Joachims ML, Thompson LF, Miller AD, Canoll PD, Bynoe MS. CD73 promotes glioblastoma pathogenesis, and enhances its chemoresistance via A2B adenosine receptor signaling. *J Neurosci.* (2019) 39:4387–402. doi: 10.1523/JNEUROSCI.1118-18.2019
72. Allard B, Turcotte M, Spring K, Pommey S, Royal I, Stagg J. Anti-CD73 therapy impairs tumor angiogenesis. *Int J Cancer.* (2014) 134:1466–73. doi: 10.1002/ijc.28456
73. Buisseret L, Pommey S, Allard B, Garaud S, Bergeron M, Cousineau I, et al. Clinical significance of CD73 in triple-negative breast cancer: multiplex analysis of a phase III clinical trial. *Ann Oncol.* (2018) 29:1056–62. doi: 10.1093/annonc/mdx730
74. Park LC, Rhee K, Kim WB, Cho A, Song J, Anker JF, et al. Immunologic and clinical implications of CD73 expression in non-small cell lung cancer (NSCLC) *J Clin Oncol.* (2018) 36(15_suppl):12050. doi: 10.1200/JCO.2018.36.15_suppl.12050
75. Lu XX, Chen YT, Feng B, Mao XB, Yu B, Chu XY. Expression and clinical significance of CD73 and hypoxia-inducible factor-1alpha in gastric carcinoma. *World J Gastroenterol.* (2013) 19:1912–8. doi: 10.3748/wjg.v19.i12.1912
76. Turcotte M, Spring K, Pommey S, Chouinard G, Cousineau I, George J, et al. CD73 is associated with poor prognosis in high-grade serous ovarian cancer. *Cancer Res.* (2015) 75:4494–503. doi: 10.1158/0008-5472.CAN-14-3569
77. Zhou L, Jia S, Chen Y, Wang W, Wu Z, Yu W, et al. The distinct role of CD73 in the progression of pancreatic cancer. *J Mol Med.* (2019) 97:803–15. doi: 10.1007/s00109-018-01742-0
78. Wu XR, He XS, Chen YF, Yuan RX, Zeng Y, Lian L, et al. High expression of CD73 as a poor prognostic biomarker in human colorectal cancer. *J Surg Oncol.* (2012) 106:130–7. doi: 10.1002/jso.23056
79. Lupia M, Angiolini F, Bertalot G, Freddi S, Sachsenmeier KF, Chisci E, et al. CD73 regulates stemness, and epithelial-mesenchymal transition in ovarian cancer-initiating cells. *Stem Cell Rep.* (2018) 10:1412–25. doi: 10.1016/j.stemcr.2018.02.009
80. Katsuta E, Tanaka S, Mogushi K, Shimada S, Akiyama Y, Aihara A, et al. CD73 as a therapeutic target for pancreatic neuroendocrine tumor stem cells. *Int J Oncol.* (2016) 48:657–69. doi: 10.3892/ijo.2015.3299
81. Turcotte M, Allard D, Mittal D, Bareche Y, Buisseret L, Jose V, et al. CD73 promotes resistance to HER2/ErbB2 antibody therapy. *Cancer Res.* (2017) 77:5652–63. doi: 10.1158/0008-5472.CAN-17-0707
82. Ujhazy P, Berleth ES, Pietkiewicz JM, Kitano H, Skaar JR, Ehrke MJ, et al. Evidence for the involvement of ecto-5′-nucleotidase (CD73) in drug resistance. *Int J Cancer.* (1996) 68:493–500.
83. Bavaresco L, Bernardi A, Braganhol E, Cappellari AR, Rockenbach L, Farias PF, et al. The role of ecto-5'-nucleotidase/CD73 in glioma cell line proliferation. *Mol Cell Biochem.* (2008) 319:61–8. doi: 10.1007/s11010-008-9877-3
84. Xiong L, Wen Y, Miao X, Yang Z. NT5E, and FcGBP as key regulators of TGF-1-induced epithelial-mesenchymal transition (EMT) are associated with tumor progression and survival of patients with gallbladder cancer. *Cell Tissue Res.* (2014) 355:365–74. doi: 10.1007/s00441-013-1752-1
85. Ryzhov S, Novitskiy SV, Zaynagetdinov R, Goldstein AE, Carbone DP, Biaggioni I, et al. Host A(2B) adenosine receptors promote carcinoma growth. *Neoplasia.* (2008) 10:987–95. doi: 10.1593/neo.08478
86. Cekic C, Sag D, Li Y, Theodorescu D, Strieter RM, Linden J. Adenosine A2B receptor blockade slows growth of bladder and breast tumors. *J Immunol.* (2012) 188:198–205. doi: 10.4049/jimmunol.1101845
87. Iannone R, Miele L, Maiolino P, Pinto A, Morello S. Blockade of A2b adenosine receptor reduces tumor growth and immune suppression mediated by myeloid-derived suppressor cells in a mouse model of melanoma. *Neoplasia.* (2013) 15:1400–9. doi: 10.1593/neo.131748
88. Huang S, Apasov S, Koshiba M, Sitkovsky M. Role of A2a extracellular adenosine receptor-mediated signaling in adenosine-mediated inhibition of T-cell activation and expansion. *Blood.* (1997) 90:1600–10. doi: 10.1182/blood.V90.4.1600.1600_1600_1610
89. Ohta A, Ohta A, Madasu M, Kini R, Subramanian M, Goel N, et al. A2A adenosine receptor may allow expansion of T cells lacking effector functions in extracellular adenosine-rich microenvironments. *J Immunol.* (2009) 183:5487–93. doi: 10.4049/jimmunol.0901247
90. Lappas CM, Rieger JM, Linden J. A2A adenosine receptor induction inhibits IFN-gamma production in murine CD4+ T cells. *J Immunol.* (2005) 174:1073–80. doi: 10.4049/jimmunol.174.2.1073
91. Ohta A, Kini R, Ohta A, Subramanian M, Madasu M, Sitkovsky M. The development and immunosuppressive functions of CD4(+) CD25(+) FoxP3(+) regulatory T cells are under influence of the adenosine-A2A adenosine receptor pathway. *Front Immunol.* (2012) 3:190. doi: 10.3389/fimmu.2012.00190
92. Deaglio S, Dwyer KM, Gao W, Friedman D, Usheva A, Erat A, et al. Adenosine generation catalyzed by CD39, and CD73 expressed on regulatory T cells mediates immune suppression. *J Exp Med.* (2007) 204:1257–65. doi: 10.1084/jem.20062512
93. Mandapathil M, Hilldorfer B, Szczepanski MJ, Czystowska M, Szajnik M, Ren J, et al. Generation and accumulation of immunosuppressive adenosine by human CD4+CD25highFOXP3+ regulatory T cells. *J Biol Chem.* (2010) 285:7176–86. doi: 10.1074/jbc.M109.047423
94. Burton CT, Westrop SJ, Eccles-James I, Boasso A, Nelson MR, Bower M, et al. Altered phenotype of regulatory T cells associated with lack of human immunodeficiency virus (HIV)-1-specific suppressive function. *Clin Exp Immunol.* (2011) 166:191–200. doi: 10.1111/j.1365-2249.2011.04451.x
95. Borsellino G, Kleinewietfeld M, Di Mitri D, Sternjak A, Diamantini A, Giometto R, et al. Expression of ectonucleotidase CD39 by Foxp3+ Treg cells: hydrolysis of extracellular ATP and immune suppression. *Blood.* (2007) 110:1225–32. doi: 10.1182/blood-2006-12-064527
96. Allard B, Longhi MS, Robson SC, Stagg J. The ectonucleotidases CD39, and CD73: novel checkpoint inhibitor targets. *Immunol Rev.* (2017) 276:121–44. doi: 10.1111/imr.12528
97. Clayton A, Al-Taei S, Webber J, Mason MD, Tabi Z. Cancer exosomes express CD39, and CD73, which suppress T cells through adenosine production. *J Immunol.* (2011) 187:676–83. doi: 10.4049/jimmunol.1003884
98. Morandi F, Marimpietri D, Horenstein AL, Bolzoni M, Toscani D, Costa F, et al. Microvesicles released from multiple myeloma cells are equipped with ectoenzymes belonging to canonical and non-canonical adenosinergic pathways and produce adenosine from ATP, and NAD. *Oncoimmunology.* (2018) 7:e1458809. doi: 10.1080/2162402X.2018.1458809
99. Duhen T, Duhen R, Montler R, Moses J, Moudgil T, de Miranda NF, et al. Co-expression of CD39, and CD103 identifies tumor-reactive CD8 T cells in human solid tumors. *Nat Commun.* (2018) 9:2724. doi: 10.1038/s41467-018-05072-0
100. Zarek PE, Huang CT, Lutz ER, Kowalski J, Horton MR, Linden J, et al. A2A receptor signaling promotes peripheral tolerance by inducing T-cell anergy and the generation of adaptive regulatory T cells. *Blood.* (2008) 111:251–9. doi: 10.1182/blood-2007-03-081646
101. Young A, Ngiow SF, Gao Y, Patch AM, Barkauskas DS, Messaoudene M, et al. A2AR adenosine signaling suppresses natural killer cell maturation in the tumor microenvironment. *Cancer Res.* (2018) 78:1003–16. doi: 10.1158/0008-5472.CAN-17-2826
102. Hatfield SM, Kjaergaard J, Lukashev D, Schreiber TH, Belikoff B, Abbott R, et al. Immunological mechanisms of the antitumor effects of supplemental oxygenation. *Sci Transl Med.* (2015) 7:277ra30. doi: 10.1126/scitranslmed.aaa1260

103. Miller JS, Cervenka T, Lund J, Okazaki IJ, Moss J. Purine metabolites suppress proliferation of human NK cells through a lineage-specific purine receptor. *J Immunol.* (1999) 162:7376–82.
104. Lokshin A, Raskovalova T, Huang X, Zacharia LC, Jackson EK, Gorelik E. Adenosine-mediated inhibition of the cytotoxic activity and cytokine production by activated natural killer cells. *Cancer Res.* (2006) 66:7758–65. doi: 10.1158/0008-5472.CAN-06-0478
105. Priebe T, Platsoucas CD, Nelson JA. Adenosine receptors and modulation of natural killer cell activity by purine nucleosides. *Cancer Res.* (1990) 50:4328–31.
106. Williams BA, Manzer A, Blay J, Hoskin DW. Adenosine acts through a novel extracellular receptor to inhibit granule exocytosis by natural killer cells. *Biochem Biophys Res Commun.* (1997) 231:264–9. doi: 10.1006/bbrc.1997.6077
107. Raskovalova T, Huang X, Sitkovsky M, Zacharia LC, Jackson EK, Gorelik E. Gs protein-coupled adenosine receptor signaling and lytic function of activated NK cells. *J Immunol.* (2005) 175:4383–91. doi: 10.4049/jimmunol.175.7.4383
108. Hatfield SM, Kjaergaard J, Lukashev D, Belikoff B, Schreiber TH, Sethumadhavan S, et al. Systemic oxygenation weakens the hypoxia and hypoxia inducible factor 1alpha-dependent and extracellular adenosine-mediated tumor protection. *J Mol Med.* (2014) 92:1283–92. doi: 10.1007/s00109-014-1189-3
109. Synnestvedt K, Furuta GT, Comerford KM, Louis N, Karhausen J, Eltzschig HK, et al. Ecto-5'-nucleotidase (CD73) regulation by hypoxia-inducible factor-1 mediates permeability changes in intestinal epithelia. *J Clin Invest.* (2002) 110:993–1002. doi: 10.1172/JCI0215337
110. Ahmad A, Ahmad S, Glover L, Miller SM, Shannon JM, Guo X, et al. Adenosine A2A receptor is a unique angiogenic target of HIF-2alpha in pulmonary endothelial cells. *Proc Natl Acad Sci USA.* (2009) 106:10684–9. doi: 10.1073/pnas.0901326106
111. Kong T, Westerman KA, Faigle M, Eltzschig HK, Colgan SP. HIF-dependent induction of adenosine A2B receptor in hypoxia. *FASEB J.* (2006) 20:2242–50. doi: 10.1096/fj.06-6419com
112. Neo SY, Yang Y, Julien R, Ma R, Chen X, Chen Z, et al. CD73 immune checkpoint defines regulatory NK-cells within the tumor microenvironment. *J Clin Invest.* (2020) 130:1185–98. doi: 10.1172/JCI128895
113. Li J, Wang L, Chen X, Li L, Li Y, Ping Y, et al. CD39/CD73 upregulation on myeloid-derived suppressor cells via TGF-beta-mTOR-HIF-1 signaling in patients with non-small cell lung cancer. *Oncoimmunology.* (2017) 6:e1320011. doi: 10.1080/2162402X.2017.1320011
114. Limagne E, Euvrard R, Thibaudin M, Rebe C, Derangere V, Chevriaux A, et al. Accumulation of MDSC, and Th17 cells in patients with metastatic colorectal cancer predicts the efficacy of a FOLFOX-bevacizumab drug treatment regimen. *Cancer Res.* (2016) 76:5241–52. doi: 10.1158/0008-5472.CAN-15-3164
115. Ryzhov S, Novitskiy SV, Goldstein AE, Biktasova A, Blackburn MR, Biaggioni I, et al. Adenosinergic regulation of the expansion and immunosuppressive activity of CD11b+Gr1+ cells. *J Immunol.* (2011) 187:6120–9. doi: 10.4049/jimmunol.1101225
116. Montalban Del Barrio Penski C, Schlahsa L, Stein RG, Diessner J, Wockel A, Dietl J, et al. Adenosine-generating ovarian cancer cells attract myeloid cells which differentiate into adenosine-generating tumor associated macrophages - a self-amplifying, CD39-, and CD73-dependent mechanism for tumor immune escape. *J Immunother Cancer.* (2016) 4:49. doi: 10.1186/s40425-016-0154-9
117. Hofer S, Ivarsson L, Stoitzner P, Auffinger M, Rainer C, Romani N, et al. Adenosine slows migration of dendritic cells but does not affect other aspects of dendritic cell maturation. *J Invest Dermatol.* (2003) 121:300–7. doi: 10.1046/j.1523-1747.2003.12369.x
118. Novitskiy SV, Ryzhov S, Zaynagetdinov R, Goldstein AE, Huang Y, Tikhomirov OY, et al. Adenosine receptors in regulation of dendritic cell differentiation and function. *Blood.* (2008) 112:1822–31. doi: 10.1182/blood-2008-02-136325
119. Challier J, Bruniquel D, Sewell AK, Laugel B. Adenosine and cAMP signalling skew human dendritic cell differentiation towards a tolerogenic phenotype with defective CD8(+) T-cell priming capacity. *Immunology.* (2013) 138:402–10. doi: 10.1111/imm.12053
120. Panther E, Corinti S, Idzko M, Herouy Y, Napp M, la Sala A, et al. Adenosine affects expression of membrane molecules, cytokine and chemokine release, and the T-cell stimulatory capacity of human dendritic cells. *Blood.* (2003) 101:3985–90. doi: 10.1182/blood-2002-07-2113
121. Wilson JM, Kurtz CC, Black SG, Ross WG, Alam MS, Linden J, et al. The A2B adenosine receptor promotes Th17 differentiation via stimulation of dendritic cell IL-6. *J Immunol.* (2011) 186:6746–52. doi: 10.4049/jimmunol.1100117
122. Mittal D, Young A, Stannard K, Yong M, Teng MW, Allard B, et al. Antimetastatic effects of blocking PD-1 and the adenosine A2A receptor. *Cancer Res.* (2014) 74:3652–8. doi: 10.1158/0008-5472.CAN-14-0957
123. Beavis PA, Milenkovski N, Henderson MA, John LB, Allard B, Loi S, et al. Adenosine receptor 2A blockade increases the efficacy of Anti-PD-1 through enhanced antitumor T-cell responses. *Cancer Immunol Res.* (2015) 3:506–17. doi: 10.1158/2326-6066.CIR-14-0211
124. Fong L, Hotson A, Powderly JD, Sznol M, Heist RS, Choueiri TK, et al. Adenosine 2A receptor blockade as an immunotherapy for treatment-refractory renal cell cancer. *Cancer Discov.* (2020) 10:40–53. doi: 10.1158/2159-8290.CD-19-0980
125. Chen S, Fan J, Zhang M, Qin L, Dominguez D, Long A, et al. CD73 expression on effector T cells sustained by TGF-beta facilitates tumor resistance to anti-4–1BB/CD137 therapy. *Nat Commun.* (2019) 10:150. doi: 10.1038/s41467-018-08123-8
126. Melero I, Johnston JV, Shufford WW, Mittler RS, Chen L. NK1.1 cells express 4–1BB (CDw137) costimulatory molecule and are required for tumor immunity elicited by anti-4–1BB monoclonal antibodies. *Cell Immunol.* (1998) 190:167–72. doi: 10.1006/cimm.1998.1396
127. Shuford WW, Klussman K, Tritchler DD, Loo DT, Chalupny J, Siadak AW, et al. 4–1BB costimulatory signals preferentially induce CD8+ T cell proliferation and lead to the amplification *in vivo* of cytotoxic T cell responses. *J Exp Med.* (1997) 186:47–55. doi: 10.1084/jem.186.1.47
128. Chu DT, Bac ND, Nguyen KH, Tien NLB, Thanh VV, Nga VT, et al. An update on Anti-CD137 antibodies in immunotherapies for cancer. *Int J Mol Sci.* (2019) 20:1822. doi: 10.3390/ijms20081822
129. Waickman AT, Alme A, Senaldi L, Zarek PE, Horton M, Powell JD. Enhancement of tumor immunotherapy by deletion of the A2A adenosine receptor. *Cancer Immunol Immunother.* (2012) 61:917–26. doi: 10.1007/s00262-011-1155-7
130. Beavis PA, Henderson MA, Giuffrida L, Mills JK, Sek K, Cross RS, et al. Targeting the adenosine 2A receptor enhances chimeric antigen receptor T cell efficacy. *J Clin Invest.* (2017) 127:929–41. doi: 10.1172/JCI89455
131. Sitarz R, Skierucha M, Mielko J, Offerhaus GJA, Maciejewski R, Polkowski WP. Gastric cancer: epidemiology, prevention, classification, and treatment. *Cancer Manag Res.* (2018) 10:239–48. doi: 10.2147/CMAR.S149619
132. Woo Y, Goldner B, Son T, Song K, Noh SH, Fong Y, et al. Western validation of a novel gastric cancer prognosis prediction model in US gastric cancer patients. *J Am Coll Surg.* (2018) 226:252–8. doi: 10.1016/j.jamcollsurg.2017.12.016
133. Jim MA, Pinheiro PS, Carreira H, Espey DK, Wiggins CL, Weir HK. Stomach cancer survival in the United States by race and stage (2001–2009): findings from the CONCORD-2 study. *Cancer.* (2017) 123(Suppl 24):4994–5013. doi: 10.1002/cncr.30881
134. Dolcetti R, De Re V, Canzonieri V. Immunotherapy for gastric cancer: time for a personalized approach? *Int J Mol Sci.* (2018) 19. doi: 10.3390/ijms19061602
135. Hu S, Meng F, Yin X, Cao C, Zhang G. NT5E is associated with unfavorable prognosis and regulates cell proliferation and motility in gastric cancer. *Biosci Rep.* (2019) 39. doi: 10.1042/BSR20190101
136. Jiang T, Xu X, Qiao M, Li X, Zhao C, Zhou F, et al. Comprehensive evaluation of NT5E/CD73 expression and its prognostic significance in distinct types of cancers. *BMC Cancer.* (2018) 18:267. doi: 10.1186/s12885-018-4073-7
137. Wong KK, Tsang YT, Deavers MT, Mok SC, Zu Z, Sun C, et al. BRAF mutation is rare in advanced-stage low-grade ovarian serous carcinomas. *Am J Pathol.* (2010) 177:1611–7. doi: 10.2353/ajpath.2010.100212
138. Rajagopalan H, Bardelli A, Lengauer C, Kinzler KW, Vogelstein B, Velculescu VE. Tumorigenesis: RAF/RAS oncogenes and mismatch-repair status. *Nature.* (2002) 418:934. doi: 10.1038/418934a

139. Davies H, Bignell GR, Cox C, Stephens P, Edkins S, Clegg S, et al. Mutations of the BRAF gene in human cancer. *Nature.* (2002) 417:949–54. doi: 10.1038/nature00766
140. Tran B, Kopetz S, Tie J, Gibbs P, Jiang ZQ, Lieu CH, et al. Impact of BRAF mutation and microsatellite instability on the pattern of metastatic spread and prognosis in metastatic colorectal cancer. *Cancer.* (2011) 117:4623–32. doi: 10.1002/cncr.26086
141. Wang H, Lee S, Nigro CL, Lattanzio L, Merlano M, Monteverde M, et al. NT5E (CD73) is epigenetically regulated in malignant melanoma and associated with metastatic site specificity. *Br J Cancer.* (2012) 106:1446–52. doi: 10.1038/bjc.2012.95
142. Lo Nigro C, Monteverde M, Lee S, Lattanzio L, Vivenza D, Comino A, et al. NT5E CpG island methylation is a favourable breast cancer biomarker. *Br J Cancer.* (2012) 107:75–83. doi: 10.1038/bjc.2012.212
143. Wu C, Zhu Y, Jiang J, Zhao J, Zhang XG, Xu N. Immunohistochemical localization of programmed death-1 ligand-1 (PD-L1) in gastric carcinoma and its clinical significance. *Acta Histochem.* (2006) 108:19–24. doi: 10.1016/j.acthis.2006.01.003
144. Boison D, Yegutkin GG. Adenosine metabolism: emerging concepts for cancer therapy. *Cancer Cell.* (2019) 36:582–96. doi: 10.1016/j.ccell.2019.10.007
145. Hogan KA, Chini CCS, Chini EN. The multi-faceted ecto-enzyme CD38: roles in immunomodulation, cancer, aging„ and metabolic diseases. *Front Immunol.* (2019) 10:1187. doi: 10.3389/fimmu.2019.01187
146. Vigano S, Alatzoglou D, Irving M, Menetrier-Caux C, Caux C, Romero P, et al. Targeting adenosine in cancer immunotherapy to enhance T-cell function. *Front Immunol.* (2019) 10:925. doi: 10.3389/fimmu.2019.00925
147. Parkin DM. The global health burden of infection-associated cancers in the year 2002. *Int J Cancer.* (2006) 118:3030–44. doi: 10.1002/ijc.21731
148. Sepulveda AR. Helicobacter, inflammation, and gastric cancer. *Curr Pathobiol Rep.* (2013) 1:9–18. doi: 10.1007/s40139-013-0009-8
149. Wu YY, Lin CW, Cheng KS, Lin C, Wang YM, Lin IT, et al. Increased programmed death-ligand-1 expression in human gastric epithelial cells in *Helicobacter pylori* infection. *Clin Exp Immunol.* (2010) 161:551–9. doi: 10.1111/j.1365-2249.2010.04217.x
150. Beswick EJ, Pinchuk IV, Das S, Powell DW, Reyes VE. Expression of the programmed death ligand 1, B7-H1, on gastric epithelial cells after *Helicobacter pylori* exposure promotes development of CD4+ CD25+ FoxP3+ regulatory T cells. *Infect Immun.* (2007) 75:4334–41. doi: 10.1128/IAI.00553-07
151. Alam MS, Kurtz CC, Rowlett RM, Reuter BK, Wiznerowicz E, Das S, et al. CD73 is expressed by human regulatory T helper cells and suppresses proinflammatory cytokine production, and *Helicobacter felis*-induced gastritis in mice. *J Infect Dis.* (2009) 199:494–504. doi: 10.1086/596205
152. Wang J, Yao Y, Chen X, Wu J, Gu T, Tang X. Host derived exosomes-pathogens interactions: potential functions of exosomes in pathogen infection. *Biomed Pharmacother.* (2018) 108:1451–9. doi: 10.1016/j.biopha.2018.09.174
153. Nguyen PH, Giraud J, Chambonnier L, Dubus P, Wittkop L, Belleannee G, et al. Characterization of biomarkers of tumorigenic, and chemoresistant cancer stem cells in human gastric carcinoma. *Clin Cancer Res.* (2017) 23:1586–97. doi: 10.1158/1078-0432.CCR-15-2157
154. Saitoh M, Nagai K, Nakagawa K, Yamamura T, Yamamoto S, Nishizaki T. Adenosine induces apoptosis in the human gastric cancer cells via an intrinsic pathway relevant to activation of AMP-activated protein kinase. *Biochem Pharmacol.* (2004) 67:2005–11. doi: 10.1016/j.bcp.2004.01.020
155. Tsuchiya A, Nishizaki T. Anticancer effect of adenosine on gastric cancer via diverse signaling pathways. *World J Gastroenterol.* (2015) 21:10931–5. doi: 10.3748/wjg.v21.i39.10931
156. Griffiths M, Beaumont N, Yao SY, Sundaram M, Boumah CE, Davies A, et al. Cloning of a human nucleoside transporter implicated in the cellular uptake of adenosine and chemotherapeutic drugs. *Nat Med.* (1997) 3:89–93. doi: 10.1038/nm0197-89
157. Griffiths M, Yao SY, Abidi F, Phillips SE, Cass CE, Young JD, et al. Molecular cloning and characterization of a nitrobenzylthioinosine-insensitive (ei) equilibrative nucleoside transporter from human placenta. *Biochem J.* (1997) 328 (Pt 3):739–43. doi: 10.1042/bj3280739
158. Ali H, Cunha-Melo JR, Saul WF, Beaven MA. Activation of phospholipase C via adenosine receptors provides synergistic signals for secretion in antigen-stimulated RBL-2H3 cells. Evidence for a novel adenosine receptor. *J Biol Chem.* (1990) 265:745–53.
159. Zhou QY, Li C, Olah ME, Johnson RA, Stiles GL, Civelli O. Molecular cloning and characterization of an adenosine receptor: the A3 adenosine receptor. *Proc Natl Acad Sci USA.* (1992) 89:7432–6. doi: 10.1073/pnas.89.16.7432
160. Varani K, Merighi S, Gessi S, Klotz KN, Leung E, Baraldi PG, et al. [(3)H]MRE 3008F20: a novel antagonist radioligand for the pharmacological and biochemical characterization of human A(3) adenosine receptors. *Mol Pharmacol.* (2000) 57:968–75.
161. Merighi S, Benini A, Mirandola P, Gessi S, Varani K, Leung E, et al. A3 adenosine receptors modulate hypoxia-inducible factor-1alpha expression in human A375 melanoma cells. *Neoplasia.* (2005) 7:894–903. doi: 10.1593/neo.05334
162. Shi L, Wu Z, Miao J, Du S, Ai S, Xu E, et al. Adenosine interaction with adenosine receptor A2a promotes gastric cancer metastasis by enhancing PI3K-AKT-mTOR signaling. *Mol Biol Cell.* (2019) 30:2527–34. doi: 10.1091/mbc.E19-03-0136
163. Llovet JM, Zucman-Rossi J, Pikarsky E, Sangro B, Schwartz M, Sherman M, et al. Hepatocellular carcinoma. *Nat Rev Dis Primers.* (2016) 2:16018. doi: 10.1038/nrdp.2016.18
164. Nzeako UC, Goodman ZD, Ishak KG. Hepatocellular carcinoma in cirrhotic and noncirrhotic livers. A clinico-histopathologic study of 804 North American patients. *Am J Clin Pathol.* (1996) 105:65–75. doi: 10.1093/ajcp/105.1.65
165. Mullin AS, Guo H, McCoy AB. Viewpoint: new physical insights from kinetics studies. *J Phys Chem A.* (2019) 123:3057. doi: 10.1021/acs.jpca.9b02535
166. Llovet JM, Ricci S, Mazzaferro V, Hilgard P, Gane E, Blanc JF, et al. Sorafenib in advanced hepatocellular carcinoma. *N Engl J Med.* (2008) 359:378–90. doi: 10.1056/NEJMoa0708857
167. Johnston MP, Khakoo SI. Immunotherapy for hepatocellular carcinoma: current and future. *World J Gastroenterol.* (2019) 25:2977–89. doi: 10.3748/wjg.v25.i24.2977
168. Snider NT, Altshuler PJ, Wan S, Welling TH, Cavalcoli J, Omary MB. Alternative splicing of human NT5E in cirrhosis and hepatocellular carcinoma produces a negative regulator of ecto-5'-nucleotidase (CD73). *Mol Biol Cell.* (2014) 25:4024–33. doi: 10.1091/mbc.e14-06-1167
169. Alcedo KP, Guerrero A, Basrur V, Fu D, Richardson ML, McLane JS, et al. Tumor-selective altered glycosylation, and functional attenuation of CD73 in human hepatocellular carcinoma. *Hepatol Commun.* (2019) 3:1400–14. doi: 10.1002/hep4.1410
170. Ma XL, Shen MN, Hu B, Wang BL, Yang WJ, Lv LH, et al. CD73 promotes hepatocellular carcinoma progression and metastasis via activating PI3K/AKT signaling by inducing Rap1-mediated membrane localization of P110beta and predicts poor prognosis. *J Hematol Oncol.* (2019) 12:37. doi: 10.1186/s13045-019-0724-7
171. Shrestha R, Prithviraj P, Anaka M, Bridle KR, Crawford DHG, Dhungel B, et al. Monitoring immune checkpoint regulators as predictive biomarkers in hepatocellular carcinoma. *Front Oncol.* (2018) 8:269. doi: 10.3389/fonc.2018.00269
172. Sciarra A, Monteiro I, Menetrier-Caux C, Caux C, Gilbert B, Halkic N, et al. de Leval: CD73 expression in normal and pathological human hepatobiliopancreatic tissues. *Cancer Immunol Immunother.* (2019) 68:467–78. doi: 10.1007/s00262-018-2290-1
173. St Hilaire C, Ziegler SG, Markello TC, Brusco A, Groden C, Gill F, et al. NT5E mutations and arterial calcifications. *N Engl J Med.* (2011) 364:432–42. doi: 10.1056/NEJMoa0912923
174. Joolharzadeh P, St Hilaire C. CD73 (cluster of differentiation 73) and the differences between mice, and humans. *Arterioscler Thromb Vasc Biol.* (2019) 39:339–48. doi: 10.1161/ATVBAHA.118.311579
175. Bowser JL, Blackburn MR, Shipley GL, Molina JG, Dunner K Jr, Broaddus RR. Loss of CD73-mediated actin polymerization promotes endometrial tumor progression. *J Clin Invest.* (2016) 126:220–38. doi: 10.1172/JCI79380

176. Kruger KH, Thompson LF, Kaufmann M, Moller P. Expression of ecto-5'-nucleotidase (CD73) in normal mammary gland and in breast carcinoma. *Br J Cancer*. (1991) 63:114–8. doi: 10.1038/bjc.1991.23
177. Gordon LA, Mulligan KT, Maxwell-Jones H, Adams M, Walker RA, Jones JL. Breast cell invasive potential relates to the myoepithelial phenotype. *Int J Cancer*. (2003) 106:8–16. doi: 10.1002/ijc.11172
178. Sorlie T, Perou CM, Tibshirani R, Aas T, Geisler S, Johnsen H, et al. Borresen-Dale: Gene expression patterns of breast carcinomas distinguish tumor subclasses with clinical implications. *Proc Natl Acad Sci USA*. (2001) 98:10869–74. doi: 10.1073/pnas.191367098
179. Minor M, Alcedo KP, Battaglia RA, Snider NT. Cell type- and tissue-specific functions of ecto-5'-nucleotidase (CD73). *Am J Physiol Cell Physiol.* (2019) 317:C1079–92. doi: 10.1152/ajpcell.00285.2019
180. Bowser JL, Broaddus RR. CD73s protection of epithelial integrity: thinking beyond the barrier. *Tissue Barriers.* (2016) 4:e1224963. doi: 10.1080/21688370.2016.1224963
181. Rackley RR, Lewis TJ, Preston EM, Delmoro CM, Bradley EL Jr, Resnick MI, et al. 5'-nucleotidase activity in prostatic carcinoma and benign prostatic hyperplasia. *Cancer Res*. (1989) 49:3702–7.
182. Wettstein MS, Buser L, Hermanns T, Roudnicky F, Eberli D, Baumeister P, et al. CD73 predicts favorable prognosis in patients with nonmuscle-invasive urothelial bladder cancer. *Dis Markers.* (2015) 2015:785461. doi: 10.1155/2015/785461
183. Sun X, Han L, Seth P, Bian S, Li L, Csizmadia E, et al. Disordered purinergic signaling and abnormal cellular metabolism are associated with development of liver cancer in Cd39/ENTPD1 null mice. *Hepatology.* (2013) 57:205–16. doi: 10.1002/hep.25989
184. Xiang HJ, Liu ZC, Wang DS, Chen Y, Yang YL, Dou KF. Adenosine A(2b) receptor is highly expressed in human hepatocellular carcinoma. *Hepatol Res*. (2006) 36:56–60. doi: 10.1016/j.hepres.2006.06.008
185. Lan J, Lu H, Samanta D, Salman S, Lu Y, Semenza GL. Hypoxia-inducible factor 1-dependent expression of adenosine receptor 2B promotes breast cancer stem cell enrichment. *Proc Natl Acad Sci USA*. (2018) 115:E9640–8. doi: 10.1073/pnas.1809695115
186. Panjehpour M, Castro M, Klotz KN. Human breast cancer cell line MDA-MB-231 expresses endogenous A2B adenosine receptors mediating a Ca2+ signal. *Br J Pharmacol.* (2005) 145:211–8. doi: 10.1038/sj.bjp.0706180
187. Ma DF, Kondo T, Nakazawa T, Niu DF, Mochizuki K, Kawasaki T, et al. Hypoxia-inducible adenosine A2B receptor modulates proliferation of colon carcinoma cells. *Hum Pathol.* (2010) 41:1550–7. doi: 10.1016/j.humpath.2010.04.008
188. Vecchio EA, Tan CY, Gregory KJ, Christopoulos A, White PJ, May LT. Ligand-independent adenosine A2B receptor constitutive activity as a promoter of prostate cancer cell proliferation. *J Pharmacol Exp Ther*. (2016) 357:36–44. doi: 10.1124/jpet.115.230003
189. Bar-Yehuda S, Stemmer SM, Madi L, Castel D, Ochaion A, Cohen S, et al. The A3 adenosine receptor agonist CF102 induces apoptosis of hepatocellular carcinoma via de-regulation of the Wnt, and NF-kappaB signal transduction pathways. *Int J Oncol.* (2008) 33:287–95.
190. Stemmer SM, Manojlovic NS, Marinca MV, Petrov P, Cherciu N, Ganea D, et al. A phase II, randomized, double-blind, placebo-controlled trial evaluating efficacy and safety of namodenoson (CF102), an A3 adenosine receptor agonist (A3AR), as a second-line treatment in patients with Child-Pugh B (CPB) advanced hepatocellular carcinoma (HCC). *J Clin Oncol.* (2019) 37(15_suppl):2503. doi: 10.1200/JCO.2019.37.15_suppl.2503
191. Adel N. Current treatment landscape and emerging therapies for pancreatic cancer. *Am J Manag Care.* (2019) 25(1 Suppl):S3–S10.
192. McGuigan A, Kelly P, Turkington RC, Jones C, Coleman HG, McCain RS. Pancreatic cancer: a review of clinical diagnosis, epidemiology, treatment and outcomes. *World J Gastroenterol.* (2018) 24:4846–61. doi: 10.3748/wjg.v24.i43.4846
193. Rawla P, Sunkara T, Gaduputi V. Epidemiology of pancreatic cancer: global trends, etiology, and risk factors. *World J Oncol.* (2019) 10:10–27. doi: 10.14740/wjon1166
194. Brahmer JR, Tykodi SS, Chow LQ, Hwu WJ, Topalian SL, Hwu P, et al. Safety and activity of anti-PD-L1 antibody in patients with advanced cancer. *N Engl J Med.* (2012) 366:2455–65. doi: 10.1056/NEJMoa1200694
195. Royal RE, Levy C, Turner K, Mathur A, Hughes M, Kammula US, et al. Phase 2 trial of single agent Ipilimumab (anti-CTLA-4) for locally advanced or metastatic pancreatic adenocarcinoma. *J Immunother.* (2010) 33:828–33. doi: 10.1097/CJI.0b013e3181eec14c
196. O'Reilly EM, Oh DY, Dhani N, Renouf DJ, Lee MA, Sun W, et al. Durvalumab with or without tremelimumab for patients with metastatic pancreatic ductal adenocarcinoma: a phase 2 randomized clinical trial. *JAMA Oncol.* (2019) 5:1431–8. doi: 10.1001/jamaoncol.2019.1588
197. Nomi T, Sho M, Akahori T, Hamada K, Kubo A, Kanehiro H, et al. Clinical significance and therapeutic potential of the programmed death-1 ligand/programmed death-1 pathway in human pancreatic cancer. *Clin Cancer Res.* (2007) 13:2151–7. doi: 10.1158/1078-0432.CCR-06-2746
198. Yamaki S, Yanagimoto H, Tsuta K, Ryota H, Kon M. PD-L1 expression in pancreatic ductal adenocarcinoma is a poor prognostic factor in patients with high CD8(+) tumor-infiltrating lymphocytes: highly sensitive detection using phosphor-integrated dot staining. *Int J Clin Oncol.* (2017) 22:726–33. doi: 10.1007/s10147-017-1112-3
199. Zhuan-Sun Y, Huang F, Feng M, Zhao X, Chen W, Zhu Z, et al. Prognostic value of PD-L1 overexpression for pancreatic cancer: evidence from a meta-analysis. *Onco Targets Ther.* (2017) 10:5005–12. doi: 10.2147/OTT.S146383
200. Johnson BA 3rd, Yarchoan M, Lee V, Laheru DA, Jaffee EM. Strategies for increasing pancreatic tumor immunogenicity. *Clin Cancer Res.* (2017) 23:1656–69. doi: 10.1158/1078-0432.CCR-16-2318
201. Gunderson AJ, Kaneda MM, Tsujikawa T, Nguyen AV, Affara NI, Ruffell B, et al. Bruton tyrosine kinase-dependent immune cell cross-talk drives pancreas cancer. *Cancer Discov.* (2016) 6:270–85. doi: 10.1158/2159-8290.CD-15-0827
202. Masso-Valles D, Jauset T, Serrano E, Sodir NM, Pedersen K, Affara NI, et al. Ibrutinib exerts potent antifibrotic and antitumor activities in mouse models of pancreatic adenocarcinoma. *Cancer Res.* (2015) 75:1675–81. doi: 10.1158/0008-5472.CAN-14-2852
203. Thomas D, Radhakrishnan P. Tumor-stromal crosstalk in pancreatic cancer and tissue fibrosis. *Mol Cancer.* (2019) 18:14. doi: 10.1186/s12943-018-0927-5
204. Tempero MA, Coussens LM, Fong L, Manges R, Singh P, Cole YL, et al. A randomized, multicenter, double-blind, placebo-controlled study of the Bruton tyrosine kinase inhibitor, ibrutinib, versus placebo in combination with nab-paclitaxel and gemcitabine in the first-line treatment of patients with metastatic pancreatic adenocarcinoma (RESOLVE). *J Clin Oncol.* (2016) 34(4_suppl):tps483. doi: 10.1200/jco.2016.34.4_suppl.tps483
205. Jakel C, Bergmann F, Toth R, Assenov Y, van der Duin D, Strobel O, et al. Genome-wide genetic and epigenetic analyses of pancreatic acinar cell carcinomas reveal aberrations in genome stability. *Nat Commun.* (2017) 8:1323. doi: 10.1038/s41467-017-01118-x
206. Waters AM, Der CJ. KRAS: the critical driver, and therapeutic target for pancreatic cancer. *Cold Spring Harb Perspect Med.* (2018) 8. doi: 10.1101/cshperspect.a031435
207. Udyavar AR, DiRenzo D, Piovesan D, Ashok D, Anderson AE, Young SW, et al. Altered pan-Ras pathway and activating mutations in EGFR result in elevated CD73 in multiple cancers. In: *AACR abstract #2526*, Arcus Biosciences Poster. (2019). Available online at: https://www.arcusbio.com/static/media/Adenosine_PanRAS_EGFR-Relationship-Akshata-AACR-2019--1.7b11622c.pdf
208. Oliveira-Cunha M, Newman WG, Siriwardena AK. Epidermal growth factor receptor in pancreatic cancer. *Cancers.* (2011) 3:1513–26. doi: 10.3390/cancers3021513
209. Zhi X, Wang Y, Yu J, Yu J, Zhang L, Yin L, et al. Potential prognostic biomarker CD73 regulates epidermal growth factor receptor expression in human breast cancer. *IUBMB Life.* (2012) 64:911–20. doi: 10.1002/iub.1086
210. Hiraoka N, Onozato K, Kosuge T, Hirohashi S. Prevalence of FOXP3+ regulatory T cells increases during the progression of pancreatic ductal adenocarcinoma and its premalignant lesions. *Clin Cancer Res.* (2006) 12:5423–34. doi: 10.1158/1078-0432.CCR-06-0369
211. Schuler PJ, Saze Z, Hong CS, Muller L, Gillespie DG, Cheng D, et al. Human CD4+ CD39+ regulatory T cells produce adenosine upon co-expression of

surface CD73 or contact with CD73+ exosomes or CD73+ cells. *Clin Exp Immunol.* (2014) 177:531–43. doi: 10.1111/cei.12354
212. Gorzalczany Y, Merimsky O, Sagi-Eisenberg R. Mast cells are directly activated by cancer cell-derived extracellular vesicles by a CD73-, and adenosine-dependent mechanism. *Transl Oncol.* (2019) 12:1549–56. doi: 10.1016/j.tranon.2019.08.005
213. Gorzalczany Y, Akiva E, Klein O, Merimsky O, Sagi-Eisenberg R. Mast cells are directly activated by contact with cancer cells by a mechanism involving autocrine formation of adenosine and autocrine/paracrine signaling of the adenosine A3 receptor. *Cancer Lett.* (2017) 397:23–32. doi: 10.1016/j.canlet.2017.03.026
214. Barilla RM, Diskin B, Caso RC, Lee KB, Mohan N, Buttar C, et al. Specialized dendritic cells induce tumor-promoting IL-10(+)IL-17(+) FoxP3(neg) regulatory CD4(+) T cells in pancreatic carcinoma. *Nat Commun.* (2019) 10:1424. doi: 10.1038/s41467-019-09416-2
215. Yao JC, Eisner MP, Leary C, Dagohoy C, Phan A, Rashid A, et al. Population-based study of islet cell carcinoma. *Ann Surg Oncol.* (2007) 14:3492–500. doi: 10.1245/s10434-007-9566-6
216. Yao JC, Hassan M, Phan A, Dagohoy C, Leary C, Mares JE, et al. One hundred years after "carcinoid": epidemiology of and prognostic factors for neuroendocrine tumors in 35,825 cases in the United States. *J Clin Oncol.* (2008) 26:3063–72. doi: 10.1200/JCO.2007.15.4377
217. Ono K, Shiozawa E, Ohike N, Fujii T, Shibata H, Kitajima T, et al. Immunohistochemical CD73 expression status in gastrointestinal neuroendocrine neoplasms: a retrospective study of 136 patients. *Oncol Lett.* (2018) 15:2123–30. doi: 10.3892/ol.2017.7569
218. Filippini D, Agosto S, Delfino P, Simbolo M, Piro G, Rusev B, et al. Immunoevolution of mouse pancreatic organoid isografts from preinvasive to metastatic disease. *Sci Rep.* (2019) 9:12286. doi: 10.1038/s41598-019-48663-7
219. Yang D, Zhang Q, Ma Y, Che Z, Zhang W, Wu M, et al. Augmenting the therapeutic efficacy of adenosine against pancreatic cancer by switching the Akt/p21-dependent senescence to apoptosis. *EBioMedicine.* (2019) 47:114–27. doi: 10.1016/j.ebiom.2019.08.068
220. Kunzli BM, Bernlochner MI, Rath S, Kaser S, Csizmadia E, Enjyoji K, et al. Impact of CD39 and purinergic signalling on the growth and metastasis of colorectal cancer. *Purinergic Signal.* (2011) 7:231–41. doi: 10.1007/s11302-011-9228-9
221. Cronin KA, Lake AJ, Scott S, Sherman RL, Noone AM, Howlader N, et al. Annual report to the nation on the status of cancer, part I: national cancer statistics. *Cancer.* (2018) 124:2785–800. doi: 10.1002/cncr.31551
222. Arnold M, Sierra MS, Laversanne M, Soerjomataram I, Jemal A, Bray F. Global patterns and trends in colorectal cancer incidence and mortality. *Gut.* (2017) 66:683–91. doi: 10.1136/gutjnl-2015-310912
223. Johnson CM, Wei C, Ensor JE, Smolenski DJ, Amos CI, Levin B, et al. Meta-analyses of colorectal cancer risk factors. *Cancer Causes Control.* (2013) 24:1207–22. doi: 10.1007/s10552-013-0201-5
224. Dekker E, Tanis PJ, Vleugels JLA, Kasi PM, Wallace MB. Colorectal cancer. *Lancet.* (2019) 394:1467–80. doi: 10.1016/S0140-6736(19)32319-0
225. Crooke H, Kobayashi M, Mitchell B, Nwokeji E, Laurie M, Kamble S, et al. Estimating 1- and 5-year relative survival trends in colorectal cancer (CRC) in the United States: 2004 to 2014. *J Clin Oncol.* (2018) 36(4_suppl):587. doi: 10.1200/JCO.2018.36.4_suppl.587
226. Kalyan A, Kircher S, Shah H, Mulcahy M, Benson A. Updates on immunotherapy for colorectal cancer. *J Gastrointest Oncol.* (2018) 9:160–9. doi: 10.21037/jgo.2018.01.17
227. Camici M, Tozzi MG, Allegrini S, Del Corso A, Sanfilippo O, Daidone MG, et al. Purine salvage enzyme activities in normal and neoplastic human tissues. *Cancer Biochem Biophys.* (1990) 11:201–9.
228. Eroglu A, Canbolat O, Demirci S, Kocaoglu H, Eryavuz Y, Akgul H. Activities of adenosine deaminase and 5'-nucleotidase in cancerous and noncancerous human colorectal tissues. *Med Oncol.* (2000) 17:319–24. doi: 10.1007/BF02782198
229. Zhang B, Song B, Wang X, Chang XS, Pang T, Zhang X, et al. The expression and clinical significance of CD73 molecule in human rectal adenocarcinoma. *Tumour Biol.* (2015) 36:5459–66. doi: 10.1007/s13277-015-3212-x
230. Koivisto MK, Tervahartiala M, Kenessey I, Jalkanen S, Bostrom PJ, Salmi M. Cell-type-specific CD73 expression is an independent prognostic factor in bladder cancer. *Carcinogenesis.* (2019) 40:84–92. doi: 10.1093/carcin/bgy154
231. McGranahan N, Swanton C. Clonal heterogeneity, and tumor evolution: past, present, and the future. *Cell.* (2017) 168:613–28. doi: 10.1016/j.cell.2017.01.018
232. Blank A, Roberts DE II, Dawson H, Zlobec I, Lugli A. Tumor heterogeneity in primary colorectal cancer, and corresponding metastases. does the apple fall far from the tree? *Front Med.* (2018) 5:234. doi: 10.3389/fmed.2018.00234
233. Guinney J, Dienstmann R, Wang X, de Reynies A, Schlicker A, Soneson C, et al. The consensus molecular subtypes of colorectal cancer. *Nat Med.* (2015) 21:1350–6. doi: 10.1038/nm.3967
234. Cushman SM, Jiang C, Hatch AJ, Shterev I, Sibley AB, Niedzwiecki D, et al. Gene expression markers of efficacy and resistance to cetuximab treatment in metastatic colorectal cancer: results from CALGB 80203 (Alliance). *Clin Cancer Res.* (2015) 21:1078–86. doi: 10.1158/1078-0432.CCR-14-2313
235. Sveen A, Bruun J, Eide PW, Eilertsen IA, Ramirez L, Murumagi A, et al. Colorectal cancer consensus molecular subtypes translated to preclinical models uncover potentially targetable cancer cell dependencies. *Clin Cancer Res.* (2018) 24:794–806. doi: 10.1158/1078-0432.CCR-17-1234
236. Wu R, Chen Y, Li F, Li W, Zhou H, Yang Y, et al. Effects of CD73 on human colorectal cancer cell growth *in vivo* and *in vitro*. *Oncol Rep.* (2016) 35:1750–6. doi: 10.3892/or.2015.4512
237. Van Cutsem E, Nordlinger B, Cervantes A, Group EGW. Advanced colorectal cancer: ESMO clinical practice guidelines for treatment. *Ann Oncol.* (2010) 21(Suppl. 5):v93–7. doi: 10.1093/annonc/mdq222
238. Messaoudi N, Henault D, Stephen D, Cousineau I, St-Hilaire, PA, Vandenbroucke-Menu F, et al. Prognostic value of CD73 expression in resected colorectal cancer liver metastasis. *J Clin Oncol.* (2018) 36:3584. doi: 10.1200/JCO.2018.36.15_suppl.3584
239. Sun X, Wu Y, Gao W, Enjyoji K, Csizmadia E, Muller CE, et al. CD39/ENTPD1 expression by CD4+Foxp3+ regulatory T cells promotes hepatic metastatic tumor growth in mice. *Gastroenterology.* (2010) 139:1030–40. doi: 10.1053/j.gastro.2010.05.007
240. Jackson SW, Hoshi T, Wu Y, Sun X, Enjyoji K, Cszimadia E, et al. Disordered purinergic signaling inhibits pathological angiogenesis in cd39/Entpd1-null mice. *Am J Pathol.* (2007) 171:1395–404. doi: 10.2353/ajpath.2007.070190
241. Wu Z, Yang L, Shi L, Song H, Shi P, Yang T, et al. Prognostic impact of adenosine receptor 2 (A2aR), and programmed cell death ligand 1 (PD-L1) expression in colorectal cancer. *Biomed Res Int.* (2019) 2019:8014627. doi: 10.1155/2019/8014627
242. Yu M, Guo G, Huang L, Deng L, Chang CS, Achyut BR, et al. CD73 on cancer-associated fibroblasts enhanced by the A2B-mediated feedforward circuit enforces an immune checkpoint. *Nat Commun.* (2020) 11:515. doi: 10.1038/s41467-019-14060-x
243. Gessi S, Cattabriga E, Avitabile A, Gafa R, Lanza G, Cavazzini L, et al. Elevated expression of A3 adenosine receptors in human colorectal cancer is reflected in peripheral blood cells. *Clin Cancer Res.* (2004) 10:5895–901. doi: 10.1158/1078-0432.CCR-1134-03
244. Gessi S, Merighi S, Varani K, Cattabriga E, Benini A, Mirandola P, et al. Adenosine receptors in colon carcinoma tissues and colon tumoral cell lines: focus on the A(3) adenosine subtype. *J Cell Physiol.* (2007) 211:826–36. doi: 10.1002/jcp.20994
245. Ohana G, Bar-Yehuda S, Arich A, Madi L, Dreznick Z, Rath-Wolfson L, et al. Inhibition of primary colon carcinoma growth and liver metastasis by the A3 adenosine receptor agonist CF101. *Br J Cancer.* (2003) 89:1552–8. doi: 10.1038/sj.bjc.6601315
246. Fishman P, Bar-Yehuda S, Ohana G, Barer F, Ochaion A, Erlanger A, et al. An agonist to the A3 adenosine receptor inhibits colon carcinoma growth in mice via modulation of GSK-3 beta, and NF-kappa B. *Oncogene.* (2004) 23:2465–71. doi: 10.1038/sj.onc.1207355
247. Bar-Yehuda S, Madi L, Silberman D, Gery S, Shkapenuk M, Fishman P. CF101, an agonist to the A3 adenosine receptor, enhances the chemotherapeutic effect of 5-fluorouracil in a colon carcinoma murine model. *Neoplasia.* (2005) 7:85–90. doi: 10.1593/neo.04364
248. Merighi S, Benini A, Mirandola P, Gessi S, Varani K, Simioni C, et al. Caffeine inhibits adenosine-induced accumulation of hypoxia-inducible factor-1alpha, vascular endothelial growth factor, and interleukin-8 expression

in hypoxic human colon cancer cells. *Mol Pharmacol.* (2007) 72:395–406. doi: 10.1124/mol.106.032920
249. Imamura T, Kikuchi H, Herraiz MT, Park DY, Mizukami Y, Mino-Kenduson M, et al. HIF-1alpha, and HIF-2alpha have divergent roles in colon cancer. *Int J Cancer.* (2009) 124:763–71. doi: 10.1002/ijc.24032
250. Xue X, Ramakrishnan SK, Shah YM. Activation of HIF-1alpha does not increase intestinal tumorigenesis. *Am J Physiol Gastrointest Liver Physiol.* (2014) 307:G187–95. doi: 10.1152/ajpgi.00112.2014
251. Siu LL, Burris H, Le DT, Hollebecque A, Steeghs N, Delord, JP, et al. Abstract CT180: preliminary phase 1 profile of BMS-986179, an anti-CD73 antibody, in combination with nivolumab in patients with advanced solid tumors. *Cancer Res.* (2018) 78. doi: 10.1158/1538-7445.AM2018-CT180. Available online at: https://cancerres.aacrjournals.org/content/78/13_Supplement/CT180
252. Powderly JD, de Souza PL, Gutierrez R, Horvath L, Seitz L, Ashok D, et al. AB928, a novel dual adenosine receptor antagonist, combined with chemotherapy or AB122 (anti-PD-1) in patients (pts) with advanced tumors: Preliminary results from ongoing phase I studies. *J Clin Oncol.* (2019) doi: 10.1200/JCO.2019.37.15_suppl.2604
253. Garrido F, Cabrera T, Aptsiauri N. "Hard" and "soft" lesions underlying the HLA class I alterations in cancer cells: implications for immunotherapy. *Int J Cancer.* (2010) 127:249–56. doi: 10.1002/ijc.25270
254. Lampen MH, van Hall T. Strategies to counteract MHC-I defects in tumors. *Curr Opin Immunol.* (2011) 23:293–8. doi: 10.1016/j.coi.2010.12.005
255. Laheru D, Jaffee EM. Immunotherapy for pancreatic cancer - science driving clinical progress. *Nat Rev Cancer.* (2005) 5:459–67. doi: 10.1038/nrc1630
256. Rezvani K, de Lavallade H. Vaccination strategies in lymphomas and leukaemias: recent progress. *Drugs.* (2011) 71:1659–74. doi: 10.2165/11593270-000000000-00000
257. Blankenstein T, Coulie PG, Gilboa E, Jaffee EM. The determinants of tumour immunogenicity. *Nat Rev Cancer.* (2012) 12:307–13. doi: 10.1038/nrc3246
258. Pradeu T, Carosella ED. On the definition of a criterion of immunogenicity. *Proc Natl Acad Sci USA.* (2006) 103:17858–61. doi: 10.1073/pnas.0608683103
259. Gelfo V, Rodia MT, Pucci M, Dall'Ora M, Santi S, Solmi R, et al. A module of inflammatory cytokines defines resistance of colorectal cancer to EGFR inhibitors. *Oncotarget.* (2016) 7:72167–83. doi: 10.18632/oncotarget.12354
260. Cheng Y, Tian H. Current development status of MEK inhibitors. *Molecules.* (2017) 22:1551. doi: 10.3390/molecules22101551
261. Eng C, Kim TW, Bendell J, Argiles G, Tebbutt NC, Di Bartolomeo M, et al. Atezolizumab with or without cobimetinib versus regorafenib in previously treated metastatic colorectal cancer (IMblaze370): a multicentre, open-label, phase 3, randomised, controlled trial. *Lancet Oncol.* (2019) 20:849–61. doi: 10.1016/S1470-2045(19)30027-0
262. Canon J, Rex K, Saiki AY, Mohr C, Cooke K, Bagal D, et al. The clinical KRAS(G12C) inhibitor AMG 510 drives anti-tumour immunity. *Nature.* (2019) 575:217–23. doi: 10.1038/s41586-019-1694-1
263. Leone RD, Horton MR, Powell JD. Something in the air: hyperoxic conditioning of the tumor microenvironment for enhanced immunotherapy. *Cancer Cell.* (2015) 27:435–6. doi: 10.1016/j.ccell.2015.03.014
264. Zangl Q, Martignoni A, Jackson SH, Ohta A, Klaunberg B, Kaufmann I, et al. Postoperative hyperoxia (60%) worsens hepatic injury in mice. *Anesthesiology.* (2014) 121:1217–25. doi: 10.1097/ALN.0000000000000447

Conflict of Interest: The authors declare that the research was conducted in the absence of any commercial or financial relationships that could be construed as a potential conflict of interest.

frontiers in Immunology

ORIGINAL RESEARCH
published: 23 February 2021
doi: 10.3389/fimmu.2021.601611

Correlation Between Immune Lymphoid Cells and Plasmacytoid Dendritic Cells in Human Colon Cancer

*Jing Wu[1], Hang Cheng[1,2], Helei Wang[1,3], Guoxia Zang[1], Lingli Qi[1,4], Xinping Lv[1], Chunyan Liu[1,5], Shan Zhu[1], Mingyou Zhang[6], Jiuwei Cui[7], Hideki Ueno[8], Yong-Jun Liu[9], Jian Suo[3] and Jingtao Chen[1,10]**

[1] Institute of Translational Medicine, The First Hospital, Jilin University, Changchun, China, [2] Department of Pediatrics, The First Hospital, Jilin University, Changchun, China, [3] Department of Stomach Colorectal Anal Surgery, The First Hospital, Jilin University, Changchun, China, [4] Department of Pediatric Gastroenterology, The First Hospital, Jilin University, Changchun, China, [5] Department of Gynecology, The First Hospital, Jilin University, Changchun, China, [6] Department of Cardiovascular Center, The First Hospital, Jilin University, Changchun, China, [7] Cancer Center, The First Hospital, Jilin University, Changchun, China, [8] Department of Microbiology, Icahn School of Medicine at Mount Sinai, New York, NY, United States, [9] Department of Research and Development of Sanofi, Cambridge, MA, United States, [10] Key Laboratory of Organ Regeneration & Transplantation of the Ministry of Education, The First Hospital of Jilin University, Changchun, China

OPEN ACCESS

Edited by:
Erica Villa,
University of Modena and Reggio Emilia, Italy

Reviewed by:
Robert J. Canter,
University of California, Davis, United States
Guilan Shi,
University of South Florida, United States

***Correspondence:**
Jingtao Chen
jtchen@jlu.edu.cn

Specialty section:
This article was submitted to Cancer Immunity and Immunotherapy, a section of the journal Frontiers in Immunology

Received: 01 September 2020
Accepted: 11 January 2021
Published: 23 February 2021

Citation:
Wu J, Cheng H, Wang H, Zang G, Qi L, Lv X, Liu C, Zhu S, Zhang M, Cui J, Ueno H, Liu Y-J, Suo J and Chen J (2021) Correlation Between Immune Lymphoid Cells and Plasmacytoid Dendritic Cells in Human Colon Cancer. Front. Immunol. 12:601611. doi: 10.3389/fimmu.2021.601611

Background: Innate lymphoid cells (ILCs), so far studied mostly in mouse models, are important tissue-resident innate immune cells that play important roles in the colorectal cancer microenvironment and maintain mucosal tissue homeostasis. Plasmacytoid dendritic cells (pDCs) present complexity in various tumor types and are correlated with poor prognosis. pDCs can promote HIV-1–induced group 3 ILC (ILC3) depletion through the CD95 pathway. However, the role of ILC3s in human colon cancer and their correlation with other immune cells, especially pDCs, remain unclear.

Methods: We characterized ILCs and pDCs in the tumor microenvironment of 58 colon cancer patients by flow cytometry and selected three patients for RNA sequencing.

Results: ILC3s were negatively correlated, and pDCs were positively correlated, with cancer pathological stage. There was a negative correlation between the numbers of ILC3s and pDCs in tumor tissues. RNA sequencing confirmed the correlations between ILC3s and pDCs and highlighted the potential function of many ILC- and pDC-associated differentially expressed genes in the regulation of tumor immunity. pDCs can induce apoptosis of ILC3s through the CD95 pathway in the tumor-like microenvironment.

Conclusions: One of the interactions between ILC3s and pDCs is *via* the CD95 pathway, which may help explain the role of ILC3s in colon cancer.

Keywords: ILC, ILC3, pDC, colon cancer, RNA-Seq, apoptosis

INTRODUCTION

Colon cancer is the third most commonly diagnosed cancer worldwide (1–3); furthermore, its incidence has significantly increased recently (4) and is expected to further rise by 50% in the next five years (5). Epidemiological studies show that the causes of colon cancer are related to environmental, lifestyle, and genetic factors, and that age, intestinal polyps, and ulcerative colitis also represent high-risk factors (6, 7); however, the specific pathogenesis of colon cancer remains unclear.

Currently, treatment of primary colon cancer is mainly surgical; however, postoperatively there is still a risk of recurrence and metastases (8). Therefore, it is important to fully understand the causes of colon cancer to promote the discovery of novel and effective therapeutic targets; this reflects an urgent clinical need from both a theoretical and a practical point of view.

With the rapid rate of discoveries in the field of immunology, cancer immunotherapy has attracted increasing attention (9). The immune system plays an important role in the protection of the host against tumor onset (i.e., tumor immunosurveillance) (10). In addition to tumor cells, stromal and immune cells are also present in the tumor microenvironment, where tumor cells often either recruit or locally induce their proliferation or differentiation to release an array of cytokines that participate in the immune response (10–12). In colon cancer, T and B lymphocytes have been found in proximal colon tumor tissue (5), and natural killer (NK) cells, monocytes/macrophages, dendritic cells (DCs), mast cells, and neutrophils have been detected in the colon tumor microenvironment (12). Notably, the differential distribution of these cells in the tumor microenvironment reflects the diversity of tumor biology (13).

Innate lymphoid cells (ILCs) are a characterized subset of innate lymphocytes (14) that includes three groups: group 1 ILCs (ILC1s) consist of NK cells that express the transcription factor T-bet and secrete interferon (IFN)-γ; group 2 ILCs (ILC2s) express the transcription factor GATA-binding protein 3 and secrete interleukin (IL)-5 and IL-13; and group 3 ILCs (ILC3s) express the transcription factor RAR-related orphan receptor-γt and secrete IL-17 and IL-22 (15–17). ILCs lack an antigen-specific receptor; however, they can still be activated by danger signals from injured mucosal tissue and quickly produce an array of effective cytokines to repel pathogens and tumor cells, thereby sustaining mucosal integrity (18, 19). A previous study has suggested that ILCs may exert both pro- and antitumor functions depending on the phase of cancer and environmental context (20). Until now, most studies on ILCs have focused on mouse models, and very few studies on human colon cancer. Recently, Salimi et al. investigated 13 patients with gastrointestinal (including esophageal, gastric, colon, and rectal) tumors and found a significantly higher frequency of group 1 ILCs (p value: 0.001) in malignant gastrointestinal tumors than in benign tissues (21). Ikeda et al. collected 28 samples from colon cancer patients and reported that the number of NKp44$^+$ ILC3s from colorectal cancer tissue was decreased in T3/T4 tumors, with associated decreases in tertiary lymphoid structure induction (22). In this study, we expanded the number of research samples to further study the distribution characteristics of ILCs in colon cancer and their correlation with other immune cells. We investigated the role of ILCs in the colon tumor microenvironment to identify potential strategies for the induction of antitumor immune responses in colon cancer.

Abbreviations: DC, dendric cell; pDCs, plasmacytoid dendritic cells; ILCs, innate lymphoid cells; NK, natural killer; ILC1s, group 1 ILCs; ILC2s, group 2 ILCs; ILC3s, group 3 ILCs; IFN: interferon; IL, interleukin; TCR, T cell receptor; MNCs, mononuclear cells; NCR, natural cytotoxicity receptor; BDCA2, blood DC antigen 2; DEGs, differentially expressed genes; RNA-Seq, RNA sequencing; KEGG, Kyoto Encyclopedia of Genes and Genomes; FPKM, fragments per kilobase of transcript per million; mDC, myeloid DC; Breg, B regulatory; CCR6, C-C motif chemokine receptor 6.

MATERIALS AND METHODS

Patient Tissue Specimens

Fresh tumor specimens, including those from tumor-proximal and distal regions, were collected from 58 patients with colon cancer who did not receive radiotherapy or chemotherapy prior to surgery at the Department of Gastric Colorectal Anal Surgery, First Affiliated Hospital, Jilin University (Changchun, China). Patient clinicopathological characteristics were determined according to the National Comprehensive Cancer Network (NCCN) guidelines for colon cancer (Version 2.2018). Proximal tissue was defined as a 2-cm to 5-cm zone bordering the tumor margin. Distal tissue was located >5 cm from the tumor and was considered to be a normal tissue sample and used as a control. There were no restrictions on cancer subtype, age, or sex, and tumor types were identified by histological analysis.

Patients were divided based on TNM stage and tumor histological stage. The TNM staging system is based on the extent of the tumor (T), the extent of spread to the lymph nodes (N), and the presence of metastasis (M). Tumors were classified as stage I, II, III, or IV based on TNM stage and prognosis, where a higher number indicated a more advanced cancer and, likely, a worse outcome. Among them, stage III patients are the most common type. Additionally, the patients were classified as having either glandular or mucous carcinoma.

Tables 1 and **2** show the clinical characteristics of the patients included in this study. The relationship between these indicators and the frequency of ILCs and plasmacytoid dendritic cells (pDCs) in different patients were analyzed and have been shown in **Tables 1** and **2**.

Tissue Digestion for Single-Cell Suspension

Freshly resected colon tissues from patients with colon cancer and tonsil tissues from children with tonsillar hypertrophy were minced into small pieces in RPMI-1640 medium (Invitrogen, Carlsbad, CA, USA) supplemented with 1% fetal calf serum (Lonza, Basel, Switzerland) and were sequentially digested with collagenase D (1 mg/ml; Sigma-Aldrich, St. Louis, MO, USA) and DNase I (50 μg/ml; Sigma-Aldrich) at 37°C for 40 min and 30 min, respectively. The cell suspensions were

TABLE 1 | Correlations between tumor infiltrating ILC3s and clinicopathological factors of colon cancer.

Factors	N	ILC3s[#]	*P*-value
Age			
< 65	23	0.48 (0.38, 0.75)	0.29
≥ 65	35	0.62 (0.37, 0.98)	
Sex			
Male	32	0.50 (0.29, 0.79)	0.26
Female	26	0.64 (0.41, 0.80)	
Region			
Ascending/Transverse	40	0.62 (0.38, 0.92)	0.34
Descending/Sigmoid	18	0.60 (0.30, 0.74)	
T stage			
T2/T3	37	0.56 (0.40, 0.87)	0.54
T4	21	0.51 (0.33, 0.75)	
N stage			
N0/N1	26	0.51 (0.29, 0.79)	0.38
N3/N4	32	0.67 (0.43, 0.84)	
M stage			
M0	52	0.59 (0.38, 0.87)	0.20
M1	6	0.47 (0.20, 0.65)	
AJCC stage			0.04
I /II	24	0.70 (0.43, 1.27)	
III/IV	34	0.48 (0.31, 0.71)	

[#]*The percentage of ILC3s in tumor versus distal tissue.*

TABLE 2 | Correlations between tumor infiltrating pDCs and clinicopathological factors of colon cancer.

Factors	N	pDCs[#]	*P*-value
Age			
< 65	23	3.14 (1.83, 4.47)	0.08
≥ 65	35	4.49 (2.86, 8.44)	
Sex			
Male	32	4.13 (2.68, 7.87)	0.43
Female	26	3.70 (1.92, 5.44)	
Region			
Ascending/Transverse	40	4.13 (2.32, 5.95)	0.04
Descending/Sigmoid	18	3.15 (2.43, 10.99)	
T stage			
T2/T3	37	4.12 (2.30, 6.55)	0.90
T4	21	3.69 (2.41, 6.39)	
N stage			
N0/N1	26	2.27 (1.44, 4.13)	<0.001
N3/N4	32	4.83 (3.63, 8.07)	
M stage			
M0	52	3.68 (2.26, 5.33)	0.01
M1	6	10.44 (5.37, 14.37)	
AJCC stage			
I /II	24	2.21 (1.30, 3.79)	<0.001
III/IV	34	5.14 (3.69, 8.54)	

[#]*The percentage of pDCs in tumor versus distal tissue.*

then passed through 100-μm and 40-μm cell strainers (BD Biosciences, Franklin Lakes, NJ, USA) to remove debris. The cell suspensions were resuspended in RPMI 1640 medium (Invitrogen) supplemented with 10% fetal calf serum (FCS; Lonza) and 1% penicillin/streptomycin (Sigma-Aldrich) before isolation of mononuclear cells (MNCs) by centrifugation over a Ficoll–Hypaque density gradient centrifugation for 30 minutes at 24°C for further analysis.

Isolation of ILC3s and pDCs

For further purification, MNCs from freshly resected patient tissue specimens were subjected to Ficoll-Hypaque gradient centrifugation for 30 min at 24°C. Next, the MNC layer was transferred to a new tube, washed twice with phosphate-buffered saline (PBS), and suspended in PBS. ILCs were sorted using a BD FACSAria system (BD Bioscience) as Lin^--enriched MNCs as Lin cocktail$^-$ (CD3, CD19, CD20, and CD14), CD94$^-$ CD34$^-$ CD1a$^-$ TCRα/β$^-$ TCRγ/δ$^-$ CD45$^+$ CD127$^+$ CRTH2$^{+/-}$ CD117$^{+/-}$ cells using FITC anti-Lin (643510; BD Bioscience), CD94 (305504; Biolegend, San Diego, CA, USA), CD34 (343504; Biolegend), CD1a (300104; Biolegend), T cell receptor (TCR)α/β (306706; Biolegend), TCRγ/δ (331208; Biolegend), allophycocyanin (APC)-H7 anti-CD45 (56017; Biolegend), Percp-cy5.5 anti-CD127 (351322; Biolegend), phycoerythrin (PE)-Cy7 anti-CRTH2 (350118; Biolegend), and BV605 anti-CD117 (562687; Biolegend). pDCs were sorted as Lin$^-$ CD94$^-$ CD34$^-$ CD1a$^-$ TCRα/β$^-$ TCRγ/δ$^-$ CD45$^+$ BDCA2$^+$ cells using FITC anti-Lin, CD94, CD34, CD1a, TCRα/β, TCRγ/δ, APC-H7 anti-CD45, and APC anti-BDCA2 (17-9818-42; Biolegend). Purity was routinely >99%. Cell viability was determined by trypan blue staining and was >99% after isolation.

Flow Cytometric Analysis

ILCs and pDCs were identified as described. ILC3s were further divided into NKp44$^+$ ILC3s, and NKp44$^-$ ILC3s were identified as Lin$^-$ CD94$^-$ CD34$^-$ CD1a$^-$ TCRα/β$^-$ TCRγ/δ$^-$ CD45$^+$ CD127$^+$ CRTH2$^-$ CD117$^+$ NKp44$^{+/-}$ cells using AF647 anti-NKp44 (558564; BD Bioscience). Myeloid DCs (mDCs) were identified as Lin$^-$ CD45$^+$ CD11b$^+$ CD11c$^+$ cells using FITC anti-Lin, APC-H7 anti-CD45, PE-conjugated anti-CD11b (555388; BD Bioscience), and AF700 anti-CD11c (561352; BD Bioscience). Treg cells were identified as CD45$^+$ CD4$^+$ CD25$^+$ forkhead box (Fox) P3$^+$ cells utilizing APC-H7 anti-CD45, PE-Cy7 anti-CD4 (557852; BD Bioscience), FITC anti-CD25 (555431; BD Bioscience), and Percp-cy5.5 anti-FoxP3 (561493; BD Bioscience). B regulatory (Breg) cells were identified as CD45$^+$ CD19$^+$ CD24$^+$ CD38$^+$ cells using APC-H7 anti-CD45, APC anti-CD19 (555415; BD Bioscience), BV605 anti-CD24 (562788; BD Bioscience), and PerCP-Cy5.5 anti-CD38 (551400; BD Bioscience). T cells were identified as CD45$^+$ CD3$^+$ cells utilizing APC-H7 anti-CD45 and PerCP-Cy5.5 anti-CD3 (560835; BD Bioscience). B cells were identified as CD45$^+$ CD19$^+$ cells using APC-H7 anti-CD45 and APC anti-CD19. NK cells were identified as CD45$^+$ CD56$^+$ cells using APC-H7 anti-CD45 and AF700 anti-CD56 (557919; BD Bioscience). Monocytes were identified as CD45$^+$ CD14$^+$ cells utilizing APC-H7 anti-CD45 and FITC anti-CD14 (555397; BD Bioscience). pDCs from tissue and blood were stained with the following monoclonal antibodies: PE-conjugated anti-HLA-DR, and PE-Cy7 anti-CD86 (BD PharMingen, San Jose, CA, USA). Viability was assessed with an Aqua system (BD PharMingen).

For surface marker staining, MNCs were incubated with antibodies at 4°C for 30 minutes and then washed twice before flow cytometric analysis. For the staining of apoptotic marker active caspase-3, cells were stained with a surface marker first

and then permeabilised using a Cytofix/Cytoperm kit (BD Bioscience) and stained for intracellular protein caspase-3 with PE-conjugated anti-caspase 3 monoclonal antibodies (BD PharMingen). Fluorescence-associated cell sorting (FACS) plots depict the mean fluorescence intensity values of Ab staining after subtracting the mean fluorescence intensity of the respective isotype control (BD Bioscience).

Immunohistochemistry

Standard H&E staining was used for colon tissue localisation. Paraffin-embedded, 4-μm-thick tumor sections and tumor-proximal and distal tissue specimens from five patients with colon cancer were selected for immunohistochemistry analysis. Tissue sections were dewaxed and subjected to heat-induced epitope retrieval with preheated antigen-retrieval buffer (pH 9.0; Dako; Agilent Technologies, Santa Clara, CA, USA). Endogenous peroxidase activity was then blocked, and the sections were incubated overnight at 4°C with anti-human BDCA2 (10 μg/ml; clone 124B3.13; Dendritics, Lyon, France). After incubation with a horseradish peroxidase-conjugated secondary antibody (Invitrogen) and development with diaminobenzidine, sections were counterstained with hematoxylin. PBS was used in place of the primary antibody for the negative controls. Images of tissue slides were acquired with a light microscope (BX51N-34-FL-1-D; Olympus, Tokyo, Japan) and analyzed with CellSens Dimension software (Universal Imaging, Bedford Hills, NY, USA).

RNA-Seq and Analysis

We used freshly sorted ILC3s and pDCs from tumors, proximal and distal regions, and peripheral blood from three patients with stage III colon cancer for RNA-Seq analysis. A total of 200 sorted cells (ILCs or pDCs) were utilized. Cells were sorted into an Eppendorf tube containing 4 μl of lysis buffer (Beijing Genomics Institute, Shenzhen, China) and quickly transferred to liquid nitrogen. RNA-Seq analysis was performed by the Beijing Genomics Institute. The data discussed in this publication have been deposited in NCBI's Gene Expression Omnibus (23) and are accessible through GEO Series accession number GSE127934 (https://www.ncbi.nlm.nih.gov/geo/query/acc.cgi?acc=GSE127934).

To remove low-quality data, adapters were trimmed using Cutadapt 1 and low-quality bases were removed by ERNE2. To analyse differentially expressed genes, the quality-checked reads were processed using TopHat version 2.0.0 (Bowtie 2 version 2.2.0) as FASTQ files. Reads were mapped to the human reference genome GRCh37/hg19. Read abundance was evaluated and normalized using Cufflinks 3 for each gene, and Cuffdiff from the Cufflinks 2.2.0 package was used to calculate the differential expression levels and to evaluate the statistical significance of these changes in expression. The number of reads per sample is shown in **Tables S1** and **S2**. Only protein-coding genes were considered, and gene level expression values were determined as fragments per kilobase million mapped (FPKM). All genes with FPKM > 1 were designated as expressed and analyzed with an established p-value < 0.05. Pathway enrichment analysis based on the Kyoto Encyclopedia of Genes and Genomes (KEGG) was performed and significantly enriched terms based on low p-values.

Preparation of Colon Tumor-Derived Supernatant

Single-cell suspensions isolated from three patients with stage III colon cancer were incubated at a final concentration of 2.5×10^6 cells/ml in complete RPMI in a 6-well tissue culture plate. Tumor supernatant (TS) was collected after 24 hours, filtered at 0.2 μm, and frozen at -80 °C until use.

Co-Culture of ILC3s and pDCs

ILC3s and pDCs from normal tonsil tissue were prepared and cultured separately at 1×10^6 cells/ml in complete RPMI (RPMI 1640 containing 10% heat-inactivated fetal bovine serum, 100 U/ml penicillin, 100 mg/ml streptomycin sulfate, 100 U/ml IL-2, and 50 ng/ml IL-7, Cellgro) in the presence or absence of 25% TS, IFN-a (1,000 IU/ml, Millipore), and anti-IFNα (10 ug/ml, Millipore) for 72 hours. Cells and culture supernatant were then harvested for subsequent experiments. Flow cytometric analysis was used for the expression of apoptosis-related genes and the survival rate of ILC3s. ELISA was used to detect the secretion of IL-22 in co-culture supernatant. Giemsa staining was used to detect the morphology of ILC3s and pDCs.

ELISA

ELISA kits for hIFN-α and hIL-22 (R&D Systems, USA) were used according to the manufacturer's instructions. For hIFN-α, pDCs were cultured at 2.5×10^6 cells/ml with TS, TLR7 ligand IMQ (1.5 μM, Invivogen) or anti-IFNα (10 ug/ml, Millipore) in RPMI medium supplemented with 10% FCS, 1% Pen/Strep, nonessential amino acids, sodium pyruvate, and β-mercaptoethanol. Supernatants were collected after 2 days and analyzed with ELISA. For hIL-22, culture supernatant was collected from co-cultured ILC3s and pDCs. All ELISA results are expressed in pg/ml.

Giemsa Staining

For Giemsa staining, ILC3s and pDCs were seeded on glass coverslips and co-cultured in the presence of 25% TS for 72 hours. Coverslips were air-dried, fixed in methanol, and stained with modified Giemsa stain GS500 (Sigma Diagnostics, USA). Each slide specimen was observed under a light microscope (BX51N-34-FL-1-D, Olympus Corporation, Tokyo, Japan).

Statistics

Continuous variables were reported as median with interquartile range (IQR), compared using Student's t-test or Mann-Whitney u-test whenever appropriate. Categorical variables were assessed using the Chi-Square test. Correlation analysis was performed using the Spearman test. All statistical analyses were performed using GraphPad Prism 5 software (GraphPad Software, San Diego, CA, USA). $P < 0.05$ was considered statistically significant.

RESULTS

Number of ILC3s in Colon Cancer Tissue Specimens Is Negatively Correlated With Tumor Pathological Stage

In our study, following collection of tissue samples from 58 patients with colon cancer, flow cytometric analysis of MNCs

isolated from the tissue showed that nearly 1% of $CD45^+$ colon lymphocytes exhibited an ILC phenotype (Lin^-CD127^+) (**Figure 1A** and **Figure S1**). Further subtyping revealed that these ILCs comprised chemoattractant receptor-homologous molecules expressed on Th2 cells (CRTH2) $^+$ ILC2s, $CRTH2^-$ $CD117^+$ $NKp44^{+/-}$ ILC3s, and $CRTH2^-$ $CD117^-$ $NKp44^-$ ILC1s (**Figure 1A**). Additionally, we found that the percentage of total ILCs among the $CD45^+$ lymphocytes in the tumor tissue was lower than that in regions proximal and distal to the tumor (**Figure 1B**), with the ILC3 percentage lower than that in the proximal and distal regions (**Figure 1C**) and higher in the proximal region than in the distal region (**Figure 1C**). However, there was no difference in the percentage of ILC1s and ILC2s in the investigated tissue regions (**Figure 1C**). These findings are not consistent with the results of Salimi et al. (21), but consistent with the results of Ikeda et al., which may be due to differences in the investigated tissue samples. Additionally, variations in $NKp44^{+/-}$ ILC3 levels, especially those of $NKp44^+$ ILC3s, among the $CD45^+$ lymphocytes followed a similar pattern (**Figure 1D**). Because ILC3s can also be classified as $CCR6^{+/-}$, $NKp30^{+/-}$, and $NKp46^{+/-}$ (24), we investigated other subtypes and observed no significant differences in the percentages of the other ILC3 subtypes in the examined regions (**Figure S2A**).

A major prognostic factor for the survival of patients with colon cancer is the pathological tumor stage; therefore, we analyzed possible correlations between ILC3s or $NKp44^{+/-}$ ILC3s and the pathological cancer stage, and observed a negative correlation with ILC3s, especially $NKp44^+$ ILC3s, and stage (**Figures 1E, F**; **Table 1**). These data were consistent with previously reported results and showed that natural cytotoxicity receptor $(NCR)^+$ ILC3s are more prevalent in stage I/II non-small cell lung cancer than in more advanced-stage tumors, and that they contribute to the formation of protective tumor-associated tertiary lymphoid structures (24). However, in the present study, we found no correlation between $NKp44^-$ ILC3s and the pathological stage (**Figure 1F**).

Su et al. (25) reported the clinical significance of circulating immune cells at different colon tumor locations. In the present study, our results showed no correlation between ILC3 percentage and the different tumor regions (**Figure S2B** and **Table 1**). Glandular and mucous carcinomas are common forms of colon cancer. We found similar variations in ILC3 levels among $CD45^+$ lymphocytes in colon glandular cancer and mucous carcinoma with the percentage of tumor ILC3s lower than that of proximal and distal ILC3s and the percentage of proximal ILC3s higher than that of distal ILC3s (**Figure 1G**).

Decreased Numbers of ILC3s in Colon Cancer Tissues Are Correlated With Higher pDC Levels

pDCs have clinical importance in different tumor types (26) and play a critical role in the tumor microenvironment to promote cancer progression through stimulation of Th2 and regulatory immunity (27). Su et al. (28) showed that the percentage of ILC3s was negatively correlated with pDC levels in lymphoid organs of NRG humanized mice with a persistent HIV-1 infection. Because ILC3 depletion by HIV-1 infection is dependent upon pDCs and IFN-I activity, we hypothesised that the frequency of the two cell types is also correlated in colon cancer. To test this hypothesis, we detected the incidence of pDCs in colon cancer tissues. Flow cytometric analysis of MNCs isolated from colon cancer tissue specimens showed that nearly 0.5% of $CD45^+$ colon leukocytes exhibited a pDC phenotype (Lin^- $CD45^+$ blood DC antigen 2, $BDCA2^+$) (**Figure 2B** and **Figure S3**) with the percentage of pDCs higher than that in proximal and distal regions (**Figure 2C**); furthermore, the pDC percentage was higher in the proximal region than in the distal region (**Figure 2C**). Immunohistochemistry staining of BDCA2 revealed that pDCs were present in colon tumor tissue specimens in similar proportions to those obtained by flow cytometry (tumor > proximal > distal; **Figure 2A**).

Additionally, we found a positive correlation between the number of pDCs and pathological tumor stage (**Figure 2D** and **Table 2**). Interestingly, there was also a positive correlation between the percentage of pDCs and the examined tumor region (**Figure 2E** and **Table 2**). Moreover, the variations in pDC levels among $CD45^+$ cells in colon glandular cancer tissue and mucous carcinoma were similar, as the percentage of tumor pDCs was higher than that of pDCs in the proximal and distal regions, and the percentage of proximal pDCs was higher than that of distal pDCs (**Figure 2F**).

Next, we determined the correlation between ILC3 frequency and pDCs among tumor infiltrating $CD45^+$ cells and observed a negative correlation between the number of ILC3s and pDCs in colon cancer tissues (**Figure 2G**). We then detected the percentage of other immune cells in colon tissues (tumor, proximal, and distal) and found that the percentage of Treg cells among the $CD45^+$ cells was higher than that in the proximal and distal regions. However, there was no difference in the percentages of mDCs, $CD4^+$ T cells, $CD8^+$ T cells, Breg cells, B cells, NK cells, or monocytes among the $CD45^+$ cells in the investigated regions (**Figure S4**). Additionally, there was no correlation between the change in the number of ILC3s and that of other immune cells.

Correlation Between ILC3s and pDCs at the Level of Differentially Expressed Genes (DEGs)

To investigate gene expression in ILC3s, and to further assess the correlation between ILC3s and pDCs in colon cancer tissues, we performed RNA-Seq. The experimental group was tumor-derived (T) ILC3s or pDCs and the control group was distal (D) ILC3s or pDCs.

For the ILC3s, >60 million clean reads were obtained from each sample group with a Q20 score >98% and a mapping rate to the reference genome of each sample varying from 73.89% to 91.40% (**Table S1**), indicating that the data were reliable and could be used for further analysis. A total of 14,943 and 4213 genes were upregulated and downregulated, respectively, in tumor ILC3s relative to distant ILC3s (**Figure 3A**); among them, 7352 genes were related to cancer (**Figure 3B**). Kyoto

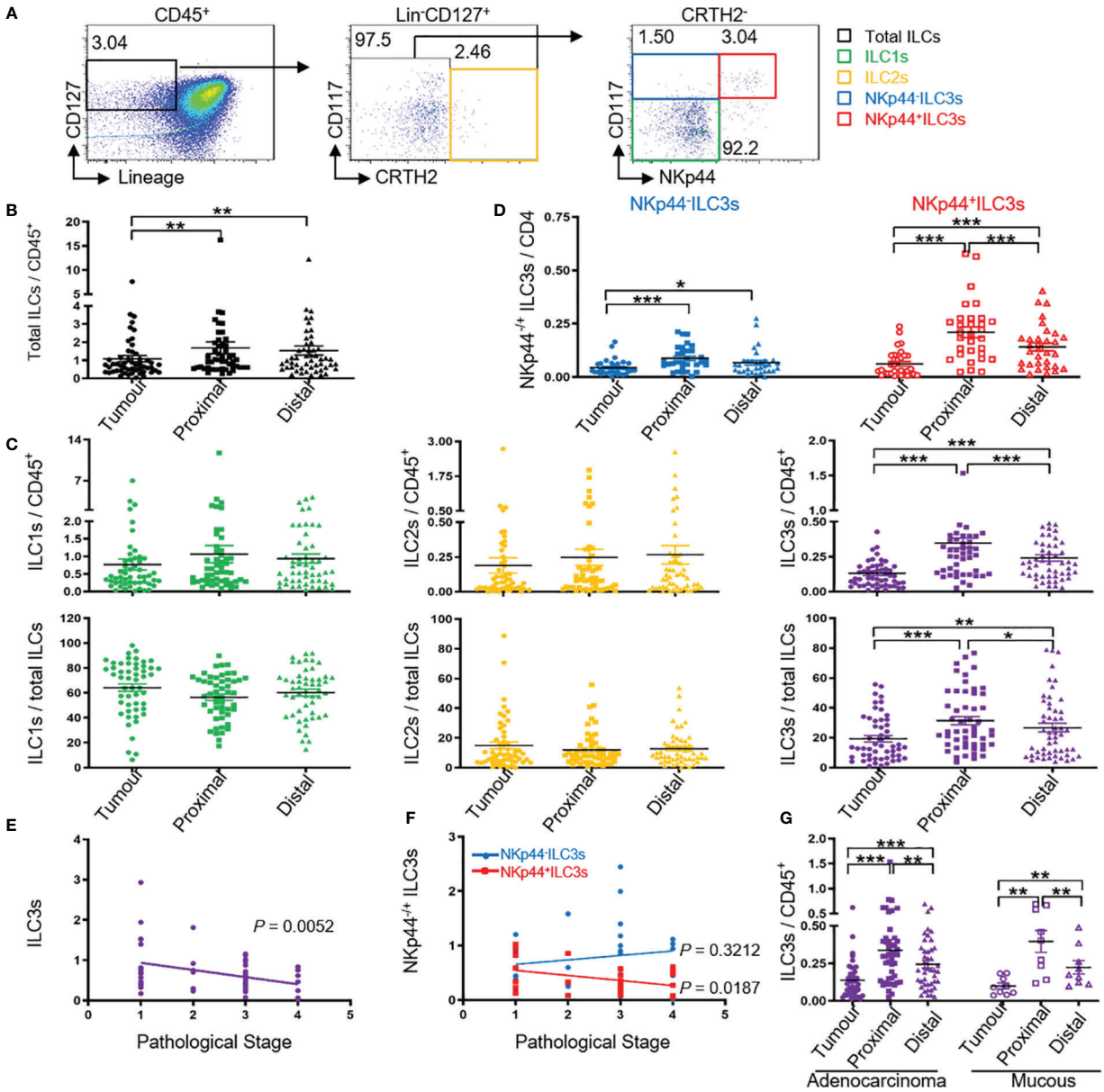

FIGURE 1 | Tumor ILC3s, especially NKp44$^+$ ILC3s are negatively correlated with pathological stage. Distribution of ILCs and ILC subtypes by FACS. MNCs from tumor, proximal, and distal regions of 58 patients with colon cancer were prepared. **(A)** The gating used to define ILC subtypes: MNCs were stained for Lin cocktail (CD3, CD14, CD19, and CD20), CD94, CD34, CD1a, TCRα/β, TCRγ/δ, CD45, CD127, CRTH2, and CD117. Total ILCs were identified as Lin$^-$ CD94$^-$ CD34$^-$ CD1a$^-$ TCRα/β$^-$ TCRγ/δ$^-$ CD45$^+$ CD127$^+$, ILC1s were identified as Lin$^-$ CD94$^-$ CD34$^-$ CD1a$^-$ TCRα/β$^-$ TCRγ/δ$^-$ CD45$^+$ CD127$^+$ CRTH2$^-$ CD117$^-$, ILC2s were identified as Lin$^-$ CD94$^-$ CD34$^-$ CD1a$^-$ TCRα/β$^-$ TCRγ/δ$^-$ CD45$^+$ CD127$^+$ CRTH2$^+$, and ILC3s were identified as Lin$^-$ CD94$^-$ CD34$^-$ CD1a$^-$ TCRα/β$^-$ TCRγ/δ$^-$ CD45$^+$ CD127$^+$ CRTH2$^-$ CD117$^+$. ILC3s were further divided into NKp44$^{+/-}$ ILC3s. **(B)** ILC levels among the CD45$^+$ cells in the indicated tissues. **(C)** Percentage of ILC1s, ILC2s, and ILC3s among CD45$^+$ cells and total ILCs in the indicated tissues. **(D)** Percentage of NKp44$^{+/-}$ ILC3s among CD45$^+$ cells in the indicated tissues. **(E, F)** Correlation between the percentage of ILC3s or NKp44$^{+/-}$ ILC3s in tumor (T) versus distal **(D)** tissue and the pathological stage of cancer. The distal tissue was considered normal tissue and was used for normalization to the background, here T/D. **(G)** Percentage of ILC3s among CD45$^+$ cells in colon glandular cancer and mucous carcinoma tissue. In **(B–D, G)**, each symbol represents the indicated tissue from one patient (circle, tumor; square, proximal region; triangle, distal region). In **(A, E, F)**, each dot represents one patient. A paired *t*-test and Spearman test were used for statistical comparison. *$P < 0.05$; **$P < 0.01$; ***$P < 0.001$.

Encyclopedia of Genes and Genomes (KEGG) pathway analysis confirmed a significant enrichment of genes involved in cancer-associated and RNA-degradation pathways (**Figure 3C**), with more upregulated than downregulated genes. These results show that the tumor environment altered the expression of many ILC3 genes.

After removing genes which could not be confidently mapped to existing entries in any public sequence database, we calculated

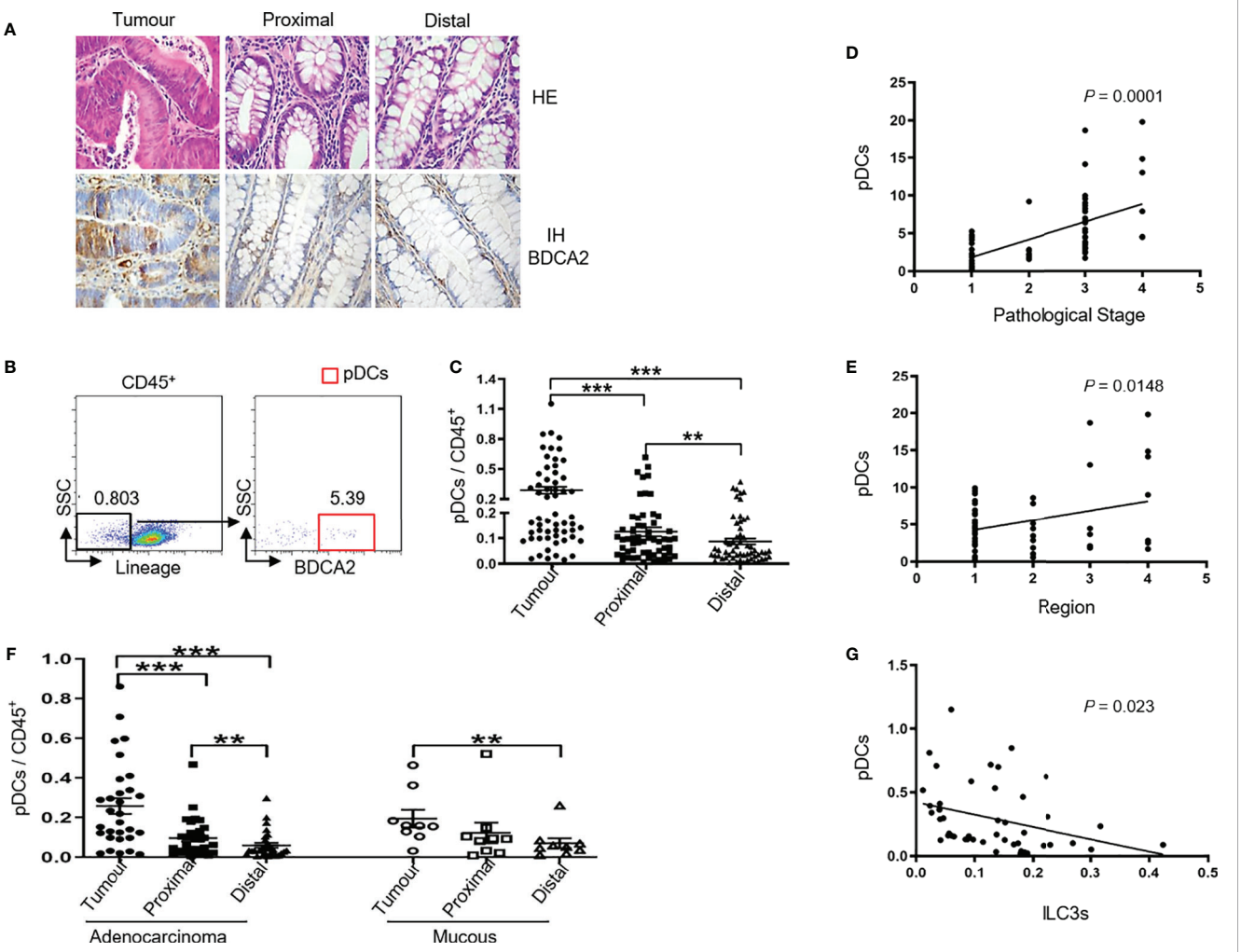

FIGURE 2 | Tumor ILC3s are negatively correlated with tumor pDC levels. MNCs from tumor, proximal, and distal regions of 58 patients with colon cancer were prepared. **(A)** Representative H&E and immunohistochemistry staining of BDCA2 in tumor, proximal, and distal tissues from patients are shown (magnification, 400×). **(B)** The gating used to define pDCs: MNCs were stained for Lin, CD94, CD34, CD1a, TCRα/β, TCRγ/δ, CD45, BDCA2, and pDCs were identified as Lin^- $CD94^-$ $CD34^-$ $CD1a^-$ $TCR\alpha/\beta^-$ $TCR\gamma/\delta^-$ $CD45^+$ $BDCA2^+$. **(C)** pDC levels among $CD45^+$ cells in the indicated tissues. **(D)** Correlation between the percentage of pDCs in tumor (T) versus distal **(D)** tissue specimens and the pathological stage of colon cancer. **(E)** Correlation between the percentage of pDCs in tumor (T) versus distal **(D)** tissue specimens and the region of the tumor in the colon: 1, 2, 3, and 4 represent ascending, transverse, descending, and sigmoid colon, respectively. **(F)** Percentage of pDCs among $CD45^+$ cells in colon glandular cancer and mucous carcinoma tissues. **(G)** Correlation between the number of ILC3s and pDCs among tumor infiltrating $CD45^+$ cells. In **(B**, **D**, **E**, **G)**, each dot represents one patient. In **(C**, **F)**, each symbol (circle, tumor; square, proximal region; triangle, distal region) represents the indicated tissue specimen from one patient. A paired *t*-test and Spearman test were used for statistical comparisons. $^*P < 0.05$; $^{**}P < 0.01$; $^{***}P < 0.001$.

the log value and fragments per kilobase of transcript per million (FPKM) reads value for each sample. We identified tumor-related genes with significant differences, including 29 upregulated genes and 2 downregulated genes identified from the comparison of tumor and distal regions in four patients (**Figure 3D**). The upregulated genes included those associated with tumor development (*PBX3*, *ARID3B*, *NID2*, *PRR11*, *COL23A1*, *TGIF2*, *SEMA4A*, *COL23A1*, and *SLC25A29*) and inhibition of tumor development (*LTBP4*, *KANK2*, *RTEL1*, *ANGPTL4*, and *SCIN*) (**Figure 3D**), whereas the downregulated genes included one associated with tumor development (*CSE1L*) (**Figure 3D**). These data suggest that ILC3s in tumor tissue might play dual roles during tumor development, in agreement with a previous report (20).

In addition, we analyzed the expression of inflammatory factors and chemokines on ILC3s. The analysis showed that 22 inflammatory genes and 13 chemokines were significantly expressed on ILC3s (**Figure 3D**). Of the inflammatory factors, 19 upregulated genes and three downregulated genes were identified from the comparison of tumor and distal regions in three patients (**Figure 3D**). Of the chemokines, eight upregulated genes and five downregulated genes were identified from the comparison of tumor and distal regions in four patients (**Figure 3D**).

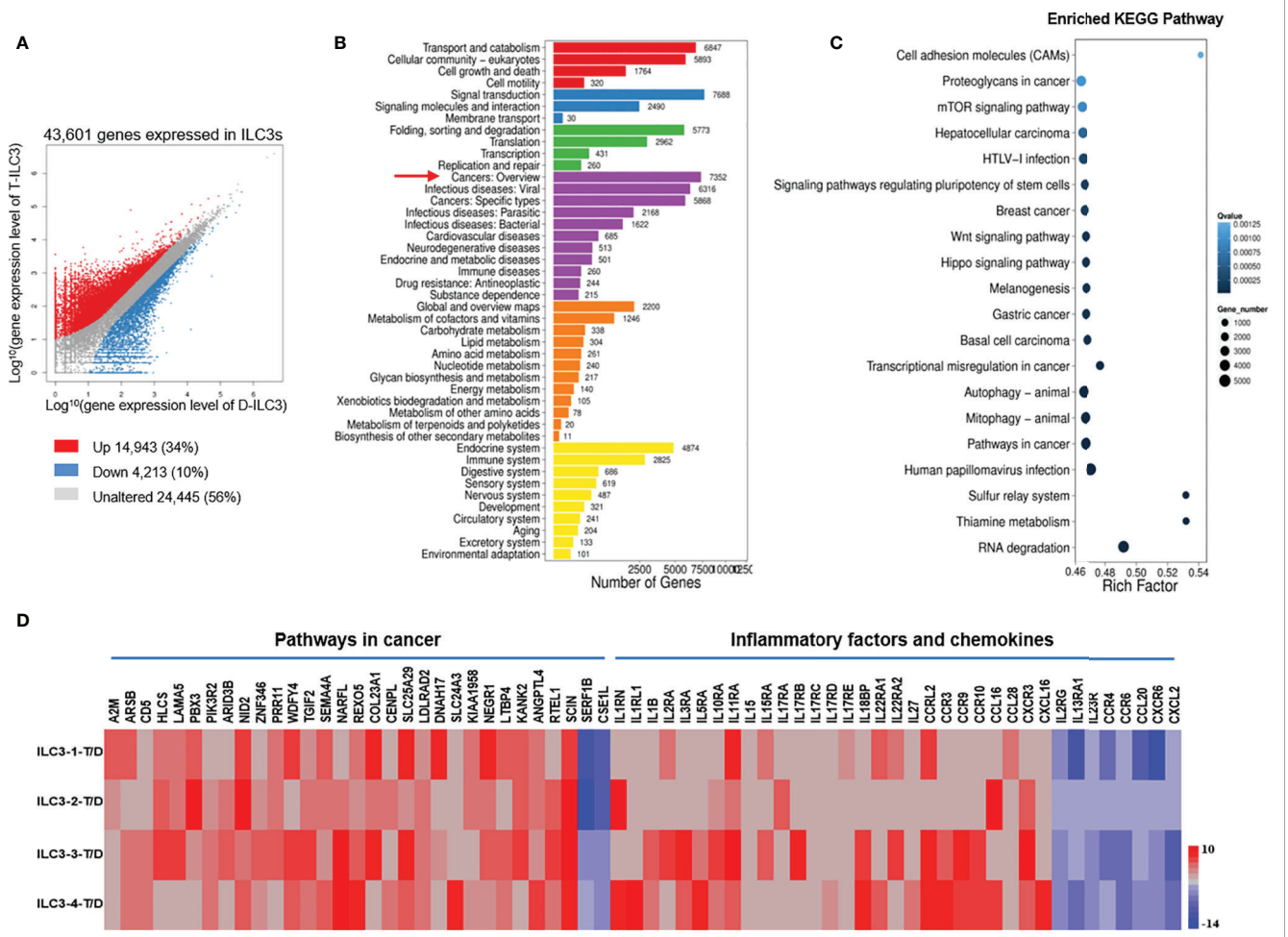

FIGURE 3 | DEGs in ILC3s are associated with both tumor development and inhibition. Analysis of gene expression in tumor and distal ILC3s and identification of significant pathways regulated by the DEGs. **(A)** Scatter plot of DEGs: X and Y axes represent log_{10}-transformed gene expression levels. Upregulated, downregulated, and unchanged genes are presented in red, blue, and gray, respectively. **(B)** Pathways regulated by the DEGs: The X-axis represents the number of DEGs, whereas the Y-axis represents the functional classification. **(C)** Pathway functional enrichment of DEGs: The X-axis represents the enrichment factor, and the Y-axis represents the pathway name. The color indicates the q-value (high: white; low: blue). A lower q-value signifies a more significant enrichment. Point size indicates the DEG number. Rich Factor refers to the value of the enrichment factor, which is the quotient of the foreground value (the number of DEGs) and the background value (total number of genes). The larger the value, the more significant the enrichment. **(D)** RNA-Seq analysis of DEGs in tumor versus distal ILC3s. Data from four separate tumor ILC3s (T, experimental group) versus data from four separate distal ILC3s (D, control group).

For the pDCs, we obtained >60 million clean reads with a Q20 score >97% and a mapping rate to the reference genome of each sample varying from 75.74% to 88.42% (**Table S2**). A total of 10,840 and 11,549 genes were upregulated and downregulated, respectively, in tumor pDCs as compared with distal pDCs (**Figure 4A**); among them, 6446 genes were related to cancer (**Figure 4B**). KEGG pathway analysis confirmed the enrichment of cancer-associated genes (**Figure 4C**), and as with the ILC3 results, the data show that the tumor environment altered the expression of multiple genes. We identified tumor-related genes with significant differences, including 14 upregulated and 10 downregulated genes from tumor versus distal pDCs in three patients (**Figure 4D**). We found that the upregulated genes were associated with tumor development (*ARHGAP4*, *HSPD1*, *HNRNPA2B1*, *UBAP2L*, *STAG1*, *TUBB*, *GPX2*, *CD44*, *PEBP4*, and *CD274*) (**Figure 4D**), and the downregulated genes were associated with tumor inhibition (*SNAP23*, *PTPRE*, *RPS13*, and *OGT*) (**Figure 4D**). These findings were consistent with previously reported results, showing that pDCs in the tumor microenvironment are associated with the development and maintenance of immunosuppression (27, 29–31).

In addition, we analyzed the expression of inflammatory factors and chemokines on pDCs. Nine inflammatory genes and one chemokine were significantly expressed on pDCs (**Figure 4D**). Of the inflammatory factors, seven upregulated genes and two downregulated genes were identified from the comparison of tumor and distal regions in three patients (**Figure 4D**). Of the chemokines, one downregulated gene was identified

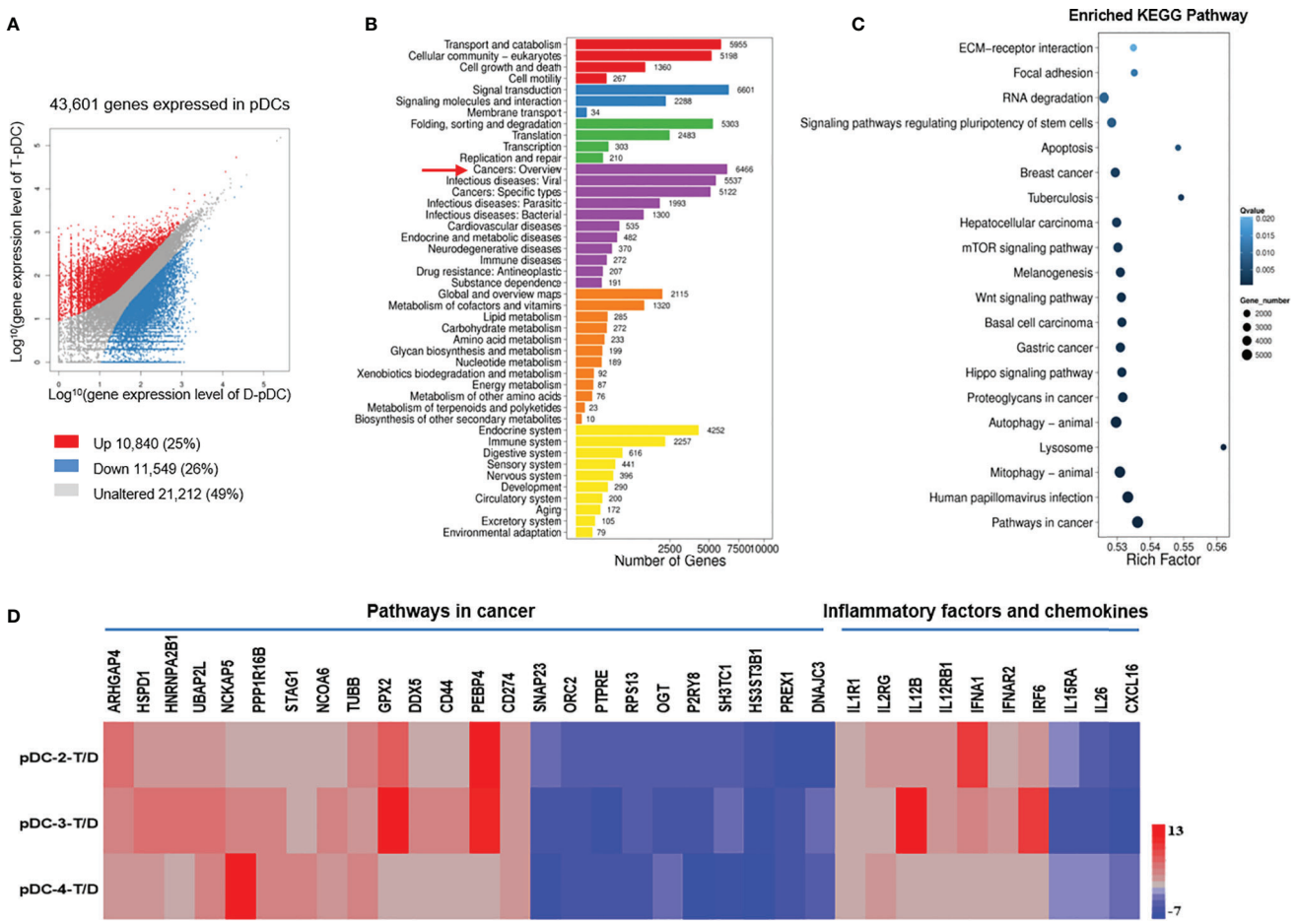

FIGURE 4 | DEGs in pDCs are associated with tumor development. Analysis of gene expression in tumor and distal pDCs and identification of significant pathways regulated by the DEGs. **(A)** Scatter plot of DEGs: X and Y axes represent $\log_{10}$-transformed gene expression levels. Upregulated, downregulated, and unchanged genes are presented in red, blue, and gray, respectively. **(B)** Pathways regulated by the DEGs: The X-axis represents the number of DEGs, whereas the Y-axis indicates the functional classification. **(C)** Pathway functional enrichment of DEGs: The X-axis represents the enrichment factor and the Y-axis signifies the pathway name. The color indicates the q-value (high: white; low: blue). A lower q-value represents a more significant enrichment. Point size indicates DEG number. Rich Factor refers to the value of the enrichment factor, which is the quotient of the foreground value (the number of DEGs) and the background value (total number of genes). The larger the value, the more significant the enrichment. **(D)** RNA-Seq analysis of DEGs in tumor versus distal pDCs. Data from three separate tumor pDCs (T, experimental group) versus data from three separate distal pDCs (D, control group). Many of the DEGs in pDCs were associated with tumor development and metastases.

from the comparison of tumor and distal regions in three patients (**Figure 4D**).

To assess correlations between ILC3s and pDCs in colon cancer tissues, we further analyzed the RNA-Seq data. Among the upregulated genes, 3,408 genes were co-expressed in ILC3s and pDCs (**Figure 5A**). Among the downregulated genes, 962 genes were co-expressed in ILC3s and pDCs (**Figure 5B**). Moreover, calculation of the Pearson correlation coefficient from RNA-Seq data from all tumor samples revealed an obvious correlation between ILC3s and pDCs in each tissue sample (**Figure 5C**). The analysis of DEGs in ILC3s (**Figure 3C**) versus pDCs (**Figure 4C**) revealed that most upregulated and downregulated ILC3 genes were associated with RNA degradation, metabolic, and apoptotic pathways, whereas most upregulated and downregulated pDC genes were associated with tumor development or inhibition (**Figure 5D**). In addition, some inflammatory factors and chemokines were highly expressed on ILCs or pDCs (**Figure 5D**), particularly ILC3s. These findings were consistent with our flow cytometry results, which showed a negative correlation between the numbers of ILC3s and pDCs in colon cancer tissues (**Figure 2G**).

pDCs Can Induce Apoptosis of ILC3s in a Tumor-Like Microenvironment

Our results showed a negative correlation between the numbers of ILC3s and pDCs in colon cancer tissues; the number was low for ILCs and high for pDCs (**Figure 2G**). The RNA-Seq results showed that ILC3s showed high expression of apoptosis-related genes such as *CD95*, *TNFRSF21*, *caspase 8*, and *caspase 3*, and pDCs showed high expression of IFN-a-related genes such as *IFNA1*, *IFNAR2*,

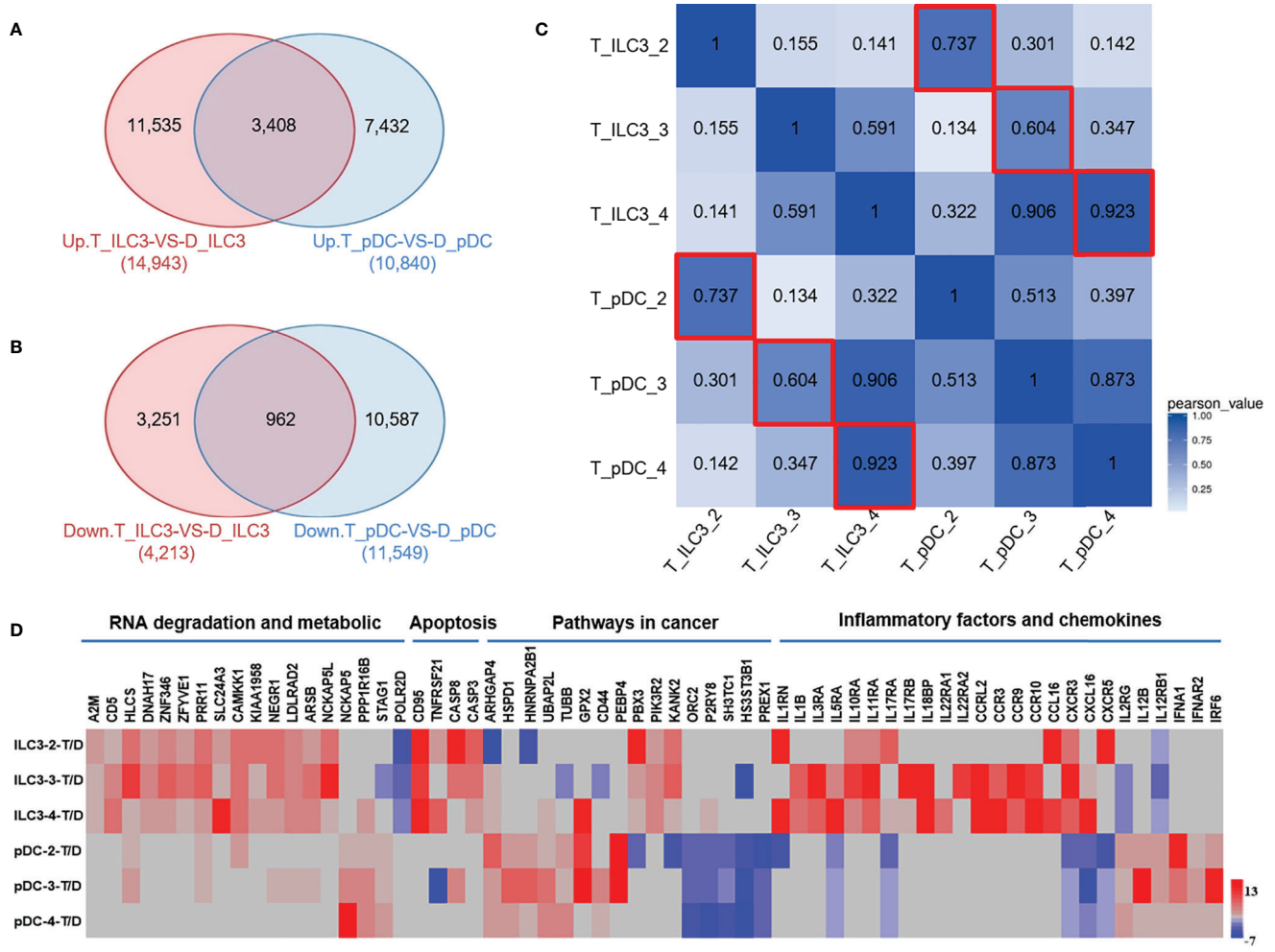

FIGURE 5 | Inverse correlation between ILC3s and pDCs in colon cancer tissues as assessed by RNA-Seq. **(A)** The Venn diagram represents the overlap between the number of upregulated genes in tumor ILC3s versus distal ILC3s (red, left) and tumor pDCs versus distal pDCs (blue, right). **(B)** The Venn diagram represents the overlap between the number of downregulated genes in tumor ILC3s versus distal ILC3s (red, left) and tumor pDCs versus distal pDCs (blue, right). **(C)** Heatmap of Pearson correlations between samples. Both the X and Y axes represent each sample. The colors indicate the degree of the Pearson correlation (high: blue; low: white). **(D)** RNA-Seq analysis of DEGs in tumor ILC3s versus pDCs. Data are from three separate comparisons of tumor ILC3s versus distal ILC3s and tumor pDCs versus distal pDCs.

and *IRF6* in tumors (**Figure 5D**). Su et al. (28) showed that ILC3 depletion by HIV-1 infection is dependent upon pDCs and IFN-I activity. Therefore, we tested whether the low number of ILC3s in the tumor microenvironment is related to pDCs.

First, we used flow cytometry to further verify the expression of apoptosis-related genes in ILC3s in the tumor tissues of colon cancer patients. The results showed that ILC3s overexpressed CD95 and caspase 3 in the tumor tissue compared with that in the distal tumor control group (**Figures 6A, B**). Secretion of cytokineIFN-a was detected in the TS (**Figures 6A, D**).

Previous studies have reported that IFN-a is mainly secreted by pDCs (32). As such, we wanted to detect whether pDCs in the tumor microenvironment secrete IFN-a. Owing to the limited number of pDCs in colon tissue and peripheral blood, we isolated pDCs from normal tonsil tissue for subsequent *in vitro* culture experiments. We added TS to the pDC culture system and used IMQ as a positive control to detect the secretion of cytokine IFN-a. TS was able to promote the secretion of IFN-a from pDCs compared with the TS itself (**Figures 6C, D**). After added anti-IFNα to the pDC culture system with TS, the release of IFN-a is significantly reduced (**Figures 6C, D**).

To test whether pDCs can affect the survival of ILC3s through IFN-a in the tumor microenvironment, we co-cultured pDCs and ILC3s from normal tonsil tissue in the presence or absence of TS, IFN-a, and anti-IFNα to detect the expression of apoptosis-related genes and the survival rate of ILC3s. After co-culturing ILC3s and pDCs with TS or IFN-a, the expression of apoptosis-related genes caspase 3 and CD95 on ILC3s was significantly upregulated (**Figures 6E, F**); the survival rate of ILC3s was significantly reduced (**Figures 6E, G**); and the main factor secreted by ILC3s

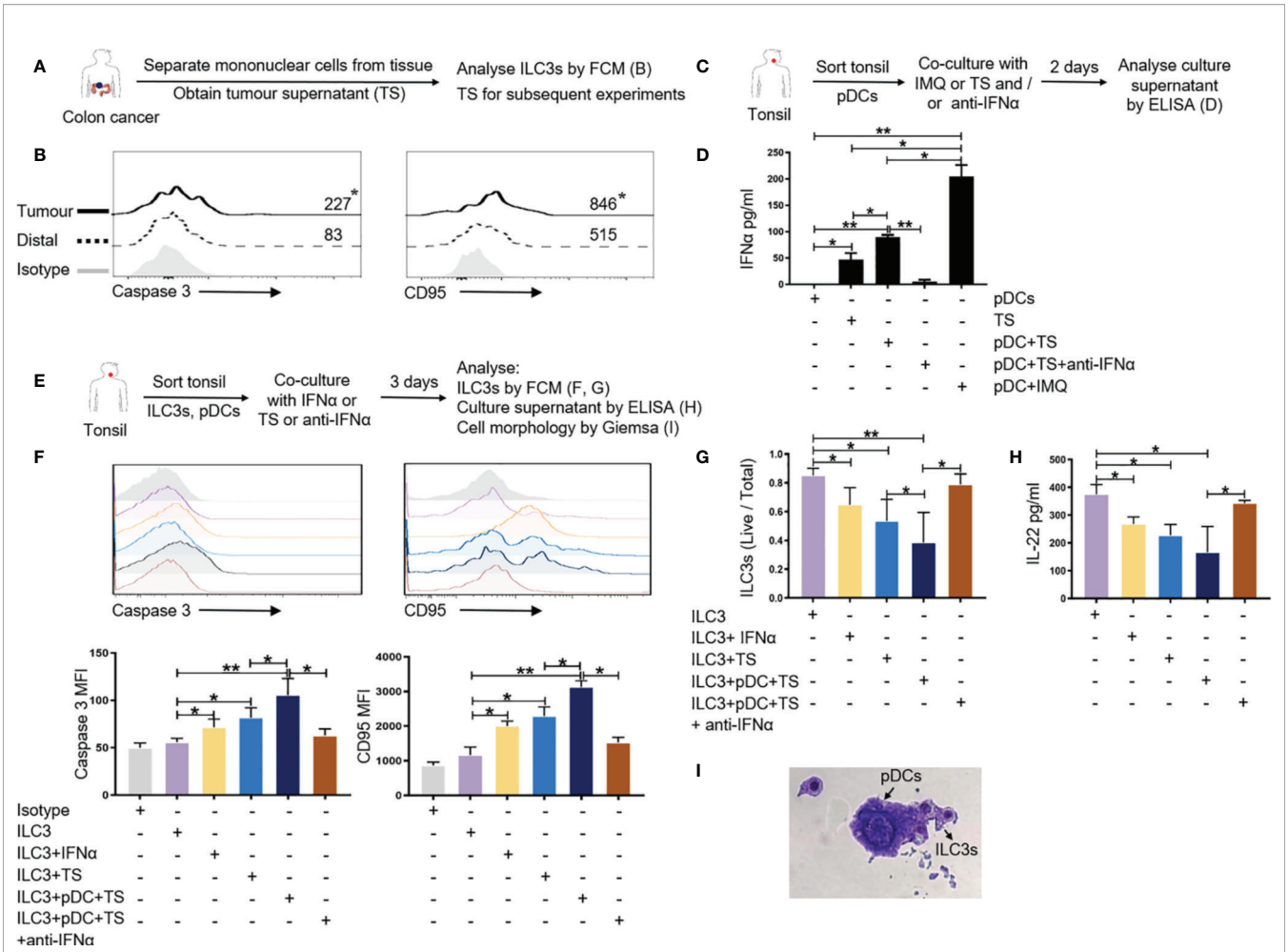

FIGURE 6 | pDCs can affect the survival of ILC3s in the tumor-like microenvironment. **(A, B)** MNCs from tumor and distal regions from three patients with colon cancer were prepared. Flow cytometric analysis was performed for the expression of apoptosis-related genes caspase 3 and CD95 on ILC3s in the tumor and distal tissue control groups. **(C, D)** pDCs from normal tonsil tissue were prepared. TS was added to the pDC culture system and the culture supernatant was collected to detect the secretion of cytokine IFN-a from pDCs by ELISA; IMQ was used as a positive control; anti-IFNα was used to neutralize IFN-a. TS is from tumors of three patients with colon cancer. **(E–I)** ILC3s and pDCs from normal tonsil tissue were prepared. TS, IFN-a, and anti-IFNα was added to the culture system of ILC3s and pDCs. Flow cytometric analysis of the expression of apoptosis-related genes **(F)** and the survival rate of ILC3s **(G)** are shown. ELISA was used to detect the secretion of IL-22 in co-culture supernatant **(H)**. Giemsa staining was used to detect the morphology of ILC3s and pDCs **(I)** (magnification, 50×). Each experiment was repeated three times. A paired *t*-test and Spearman test were used for statistical comparisons. $^{*}P < 0.05$; $^{**}P < 0.01$.

(IL-22) was also significantly downregulated (**Figures 6E, H**). After added anti-IFNα to neutralize IFN-a, the above effect is obviously weakened (**Figures 6E–H**). Giemsa staining results revealed that the ILC3 cell membrane was incomplete and there were scattered apoptotic bodies (**Figure 6I**), this result needs further verification. The above results indicate that pDCs can induce apoptosis of ILC3s through the CD95 pathway by releasing IFN-a in the tumor-like microenvironment.

DISCUSSION

ILCs are important tissue-resident innate immune cells; the numbers and relative percentages of the three subtypes (ILC1, ILC2, and ILC3) vary in different organs (33, 34). In response to acute environmental challenges and as tissue-resident cells, ILCs can renew and expand in both lymphoid and non-lymphoid organs (34). A change in the ILC population in human tissues is associated with the pathogenesis and progression of chronic infections and inflammatory diseases (18, 28, 35). Recently, Ikeda et al. reported that the number of NKp44^{+} ILC3s from colorectal cancer tissue is associated with tumor-associated tertiary lymphoid structures (22). Our group collected 58 samples from colon cancer patients to further study the distribution characteristics of ILCs in colon cancer and their correlation with other immune cells.

Flow cytometry showed that the numbers of ILC3s and NKp44^{+} ILC3s in colon tumor tissues were lower than those in distal regions and negatively correlated with the pathological stage of cancer; however, there was no correlation between the number of

ILC3s and patient age, sex, tumor location, tumor size, lymphatic metastases, or distant metastases. RNA-Seq showed that among the DEGs in tumor versus distal ILC3s, many were associated with tumor development or inhibition (**Figure 3**); however, most of the DEGs were involved in tumor suppression, especially *SCIN*, which was upregulated in tumor ILC3s. These data concur with previous studies suggesting that ILC3s in the tumor microenvironment might have dual functions depending on the cancer phase and environmental context (20, 36–38).

Human ILC3s are the most heterogeneous ILCs. In addition to conventional NK cells, the ILC3 population can also express NCRs and can be divided according to this expression into $NKp44^{+/-}$ ILC3s, $NKp30^{+/-}$ ILC3s, and $NKp46^{+/-}$ ILC3s (24). Additionally, ILC3s can be classified according to the C-C motif chemokine receptor (CCR) 6 expression into $CCR6^{+}$ and $CCR6^{-}$ ILC3s (18). In the present study, changes in the $NKp44^{+/-}$ ILC3 population in tumors and proximal and distal regions were similar to those in total ILC3s, especially the $NKp44^{+}$ ILC3 population; however, changes in the number of ILC1s and ILC2s among the analyzed locations were not significant. These results may be due to insufficient tissue sample size. In future investigations, we will expand the sample size and repeat this analysis.

pDCs are type-I IFN-producing cells that bridge the innate and adaptive immune systems (32) and are specialized in endosomal TLR7/9-mediated recognition of viral nucleic acids with their response involving massive secretion of type-I IFNs to promote virus removal (39). pDCs in the tumor microenvironment mainly exist in a non-activated state and are associated with the development and maintenance of an immunosuppressive environment (27, 29–31). Functional alterations of pDCs in the tumor microenvironment are associated with tumor immune-escape mechanisms (29, 40, 41). In the present study, the number of pDCs in flow cytometric analysis of colon tumor tissues was higher than that in distal regions and positively correlated with tumor location, pathological stage, lymphatic metastases, and especially distant metastases of colon cancer. However, we did not find any correlation between the number of pDCs and patient age, sex, or tumor size. Our RNA-Seq results showed that, among the genes upregulated in tumor pDCs (versus distal pDCs), many were associated with tumor development, whereas many of the downregulated genes were associated with tumor inhibition (**Figure 4**). These data suggest that pDCs might participate in tumor progression and immune escape.

Zhang et al. (28) reported that chronic HIV-1 infection induces ILC3 apoptosis *via* pDC activation, induction of type-I IFN expression, and CD95-mediated apoptosis. Additionally, Maazi et al. (42) showed that pDC activation alleviates airway hyperreactivity and inflammation by suppressing ILC2 function and survival. However, the relevance of ILCs and pDCs in the tumor microenvironment has not been reported. Our flow cytometric data showed a negative correlation between ILC3s and pathological stage and a positive correlation between pDCs and pathological stage. Additionally, we found a negative correlation between percentages of ILC3s and pDCs, with RNA-Seq analysis subsequently confirming this result. The analysis of ILC3 versus pDC DEGs showed that many tumor ILC3 DEGs were involved in RNA degradation, metabolic, and apoptotic pathways, whereas most tumor pDC DEGs were associated with tumor development or inhibition. Julieta et al. (43) reported mRNA degradation as an early apoptotic event in colon cancer, which is concordant with our findings.

In the *in vitro* experiments, after co-culturing ILC3s and pDCs with TS or IFN-a, the expression of apoptosis-related genes caspase 3 and CD95 on ILC3s was significantly upregulated; the survival rate of ILC3s was significantly reduced. In addition to molecules caspase 3 and CD95, other apoptosis-related genes on ILC3s may play important roles in the way pDCs affect ILC3s; this needs further verification. For pDCs, KEGG pathway analysis showed that many of the DEGs were associated with cancer. This supports the results reported by Zhang et al. (28) that pDCs might induce ILC3s apoptosis during chronic HIV-1 infection. Additionally, in the colon cancer environment, pDCs may induce ILC3 apoptosis and promote tumor progression, which would explain the difference in percentage of ILC3s and pDCs in tumor tissues (ILC3s, low; pDCs, high). Moreover, we found multiple upregulated and downregulated genes with similar patterns between ILC3s and pDCs. Pearson correlation analysis of all samples showed obvious correlations between ILC3s and pDCs in colon cancer tissue samples. In our future work, we will confirm these results using *in vivo* experiments.

Su et al. (25) reported that different levels of circulating immune cells are associated with tumor location, stage, differentiation status, and lymphatic metastases in patients with colon cancer. Additionally, they found that the epidemiology, pathogenesis, genetic and epigenetic alterations, molecular pathways, and prognoses differed in patients with left-sided and right-sided colon cancers. In the present study, we found that the percentage of pDCs in the tumor tissue was correlated with the region of the colon with the tumor and that the number of pDCs progressively decreased in the sigmoid, descending, transverse, and ascending colon. However, there was no correlation between the percentage of ILC3s and the region of the colon with the tumor or between the pathological stage and the tumor region (**Figures S2B, C**).

Interestingly, our results showed that the number of ILC3s in the tumor was lower than that in distal and proximal regions, but the number of ILC3s in the proximal region was higher than that in the distal region. Additionally, we found a negative correlation between ILC3s from proximal regions and the pathological stage of cancer (data not shown). RNA-Seq analysis revealed thousands of DEGs between proximal and distal ILC3s (data not shown), including oncogenes. In our future work, we plan to investigate the role of ILC3s in tumor and proximal regions in colon cancer.

CONCLUSIONS

In summary, our data reveal that ILC3s and pDCs represent important cellular components in colon cancer that may participate in tumor progression or inhibition. Specifically,

pDCs may induce immune tolerance and promote tumor metastasis in the tumor microenvironment. Furthermore, our findings suggest that ILC3s and pDCs may represent novel therapeutic targets for the modulation of the immune response against colon cancer. Moreover, the identification of ILC3s and pDCs in tumor specimens may represent a new immune score factor to aid in prognostic determination for patients undergoing surgery for colon cancer.

DATA AVAILABILITY STATEMENT

The datasets presented in this study can be found in online repositories. The names of the repository/repositories and accession number(s) can be found in the article/**Supplementary Material**.

ETHICS STATEMENT

The studies involving human participants were reviewed and approved by Ethical Committee of the First Affiliated Hospital, Jilin University (approval reference 2017-118). The patients/participants provided their written informed consent to participate in this study. Written informed consent was obtained from the individual(s) for the publication of any potentially identifiable images or data included in this article.

AUTHOR CONTRIBUTIONS

JTC and JW conceived the study. JW, HC, and GZ performed the experiments and analyzed the data. MZ, HW, JWC, and JS recruited and curated the patient samples and information for flow cytometric. XL and SZ contributed to the flow cytometric studies. JW, CL, and LQ generated and analyzed the RNA-Seq data. JS, Y-JL, and JTC conceived and designed the experiments and supervised the work, with participation from JWC and HU. All authors contributed to data analysis and reviewed and edited the manuscript. All authors contributed to the article and approved the submitted version.

FUNDING

This work was supported by the National Natural Science Foundation of China (Grant Nos. 81571534, 81870152, 81901591, and 81800021), the Key Scientific Project of Jilin Province (20140204024YY), the Scientific and Technological Developing Plan of Jilin Province (20160520141JH and 20180101097JC), the 62nd batch of the China Postdoctoral Science Foundation Fund (801171172842), the "13th Five-Year" Science and Technology Research of the Education Department of Jilin Province (YYKH20190043KJ), the Jilin Provincial Key Laboratory of Biotherapy (20170622011JC), the Program for JLU Science and Technology Innovative Research Team (2017TD-08), and the Fundamental Research Funds for the Central Universities.

ACKNOWLEDGMENTS

This manuscript has been released as a pre-print at Research Square (44).

SUPPLEMENTARY MATERIAL

The Supplementary Material for this article can be found online at: https://www.frontiersin.org/articles/10.3389/fimmu.2021.601611/full#supplementary-material

REFERENCES

1. Li SK, Martin A. Mismatch Repair and Colon Cancer: Mechanisms and Therapies Explored. *Trends Mol Med* (2016) 22(4):274–89. doi: 10.1016/j.molmed.2016.02.003
2. Kang M, Martin A. Microbiome and colorectal cancer: Unraveling host-microbiota interactions in colitis-associated colorectal cancer development. *Semin Immunol* (2017) 32:3–13. doi: 10.1016/j.smim.2017.04.003
3. Hjerkind KV, Qureshi SA, Moller B, Weiderpass E, Deapen D, Kumar B, et al. Ethnic differences in the incidence of cancer in Norway. *Int J Cancer* (2017) 140(8):1770–80. doi: 10.1002/ijc.30598
4. Arnold M, Sierra MS, Laversanne M, Soerjomataram I, Jemal A, Bray F. Global patterns and trends in colorectal cancer incidence and mortality. *Gut* (2017) 66(4):683–91. doi: 10.1136/gutjnl-2015-310912
5. Laskowski P, Klim B, Ostrowski K, Szkudlarek M, Litwiejko-Pietrynczak E, Kitlas K, et al. Local inflammatory response in colorectal cancer. *Polish J Pathol* (2016) 67(2):163–71. doi: 10.5114/pjp.2016.61453
6. Li QL, Ma XY, Yu LL, Xue F, Ma WL, Yao KY. [Age-specific detection rates of colorectal neoplasms by colonoscopic screening in high-incidence rural area]. *Zhonghua zhong liu za zhi Chin J Oncol* (2013) 35(2):154–7 doi: 10.3760/cma.j.issn.0253-3766.2013.02.018
7. Subramanian V, Chatu S, Echterdiek F, Banerjee A, Finlayson C, Pollok RCG. Patients with Endoscopically Visible Polypoid Adenomatous Lesions Within the Extent of Ulcerative Colitis Have an Increased Risk of Colorectal Cancer Despite Endoscopic Resection. *Dig Dis Sci* (2016) 61(10):3031–6. doi: 10.1007/s10620-016-4246-7
8. Bellik L, Gerlini G, Parenti A, Ledda F, Pimpinelli N, Neri B, et al. Role of conventional treatments on circulating and monocyte-derived dendritic cells in colorectal cancer. *Clin Immunol (Orlando Fla)* (2006) 121(1):74–80. doi: 10.1016/j.clim.2006.06.011
9. Menon S, Shin S, Dy G. Advances in Cancer Immunotherapy in Solid Tumors. *Cancers* (2016) 8(12):106-27. doi: 10.3390/cancers8120106
10. Di Franco S, Turdo A, Todaro M, Stassi G. Role of Type I and II Interferons in Colorectal Cancer and Melanoma. *Front Immunol* (2017) 8:878. doi: 10.3389/fimmu.2017.00878
11. Candido J, Hagemann T. Cancer-related inflammation. *J Clin Immunol* (2013) 33(Suppl 1):S79–84. doi: 10.1007/s10875-012-9847-0
12. Legitimo A, Consolini R, Failli A, Orsini G, Spisni R. Dendritic cell defects in the colorectal cancer. *Hum Vaccines Immunother* (2014) 10(11):3224–35. doi: 10.4161/hv.29857
13. Galon J, Fridman WH, Pages F. The adaptive immunologic microenvironment in colorectal cancer: a novel perspective. *Cancer Res* (2007) 67(5):1883–6. doi: 10.1158/0008-5472.CAN-06-4806
14. Salome B, Jandus C. Innate lymphoid cells in antitumor immunity. *J Leukoc Biol* (2018) 103(3):479–83 doi: 10.1189/JLB.5MR0617-266R
15. Simoni Y, Fehlings M, Kloverpris HN, McGovern N, Koo SL, Loh CY, et al. Human Innate Lymphoid Cell Subsets Possess Tissue-Type Based

Heterogeneity in Phenotype and Frequency. *Immunity* (2017) 46(1):148–61. doi: 10.1016/j.immuni.2016.11.005
16. Vivier E, Artis D, Colonna M, Diefenbach A, Di Santo JP, Eberl G, et al. Innate Lymphoid Cells: 10 Years On. *Cell* (2018) 174(5):1054–66. doi: 10.1016/j.cell.2018.07.017
17. Krabbendam L, Nagasawa M, Spits H, Bal SM. Isolation of Human Innate Lymphoid Cells. *Curr Protoc Immunol* (2018) 122(1):e55. doi: 10.1002/cpim.55
18. Cheng H, Jin C, Wu J, Zhu S, Liu YJ, Chen J. Guards at the gate: physiological and pathological roles of tissue-resident innate lymphoid cells in the lung. *Protein Cell* (2017) 8(12):878–95. doi: 10.1007/s13238-017-0379-5
19. Wang S, Xia P, Chen Y, Qu Y, Xiong Z, Ye B, et al. Regulatory Innate Lymphoid Cells Control Innate Intestinal Inflammation. *Cell* (2017) 171 (1):201–16.e18 doi: 10.1016/j.cell.2017.07.027
20. Carrega P, Campana S, Bonaccorsi I, Ferlazzo G. The Yin and Yang of Innate Lymphoid Cells in Cancer. *Immunol Lett* (2016) 179:29–35. doi: 10.1016/j.imlet.2016.06.003
21. Salimi M, Wang R, Yao X, Li X, Wang X, Hu Y, et al. Activated innate lymphoid cell populations accumulate in human tumour tissues. *BMC Cancer* (2018) 18(1):341. doi: 10.1186/s12885-018-4262-4
22. Ikeda A, Ogino T, Kayama H, Okuzaki D, Nishimura J, Fujino S, et al. Human NKp44+ group 3 innate lymphoid cells associate with tumor-associated tertiary lymphoid structures in colorectal cancer. *Cancer Immunol Res* (2020) 8(6):724–31. doi: 10.1158/2326-6066.CIR-19-0775.canimm.0775.2019
23. Edgar R, Domrachev M, Lash AE. Gene Expression Omnibus: NCBI gene expression and hybridization array data repository. *Nucleic Acids Res* (2002) 30(1):207–10. doi: 10.1093/nar/30.1.207
24. Carrega P, Loiacono F, Di Carlo E, Scaramuccia A, Mora M, Conte R, et al. NCR(+)ILC3 concentrate in human lung cancer and associate with intratumoral lymphoid structures. *Nat Commun* (2015) 6:8280. doi: 10.1038/ncomms9280
25. Di J, Zhuang M, Yang H, Jiang B, Wang Z, Su X. Clinical significance of circulating immune cells in left- and right-sided colon cancer. *PeerJ* (2017) 5: e4153. doi: 10.7717/peerj.4153
26. Li S, Wu J, Zhu S, Liu YJ, Chen J. Disease-Associated Plasmacytoid Dendritic Cells. *Front Immunol* (2017) 8:1268. doi: 10.3389/fimmu.2017.01268
27. Aspord C, Leccia MT, Charles J, Plumas J. Plasmacytoid dendritic cells support melanoma progression by promoting Th2 and regulatory immunity through OX40L and ICOSL. *Cancer Immunol Res* (2013) 1(6):402–15. doi: 10.1158/2326-6066.CIR-13-0114-T
28. Zhang Z, Cheng L, Zhao J, Li G, Zhang L, Chen W, et al. Plasmacytoid dendritic cells promote HIV-1-induced group 3 innate lymphoid cell depletion. *J Clin Invest* (2015) 125(9):3692–703. doi: 10.1172/JCI82124
29. Sisirak V, Faget J, Gobert M, Goutagny N, Vey N, Treilleux I, et al. Impaired IFN-alpha production by plasmacytoid dendritic cells favors regulatory T-cell expansion that may contribute to breast cancer progression. *Cancer Res* (2012) 72(20):5188–97. doi: 10.1158/0008-5472.CAN-11-3468
30. Dubrot J, Duraes FV, Potin L, Capotosti F, Brighouse D, Suter T, et al. Lymph node stromal cells acquire peptide-MHCII complexes from dendritic cells and induce antigen-specific CD4(+) T cell tolerance. *J Exp Med* (2014) 211 (6):1153–66. doi: 10.1084/jem.20132000
31. Wu J, Li S, Yang Y, Zhu S, Zhang M, Qiao Y, et al. TLR-activated plasmacytoid dendritic cells inhibit breast cancer cell growth in vitro and in vivo. *Oncotarget* (2017) 8(7):11708–18. doi: 10.18632/oncotarget.14315
32. Liu YJ. IPC: professional type 1 interferon-producing cells and plasmacytoid dendritic cell precursors. *Annu Rev Immunol* (2005) 23:275–306. doi: 10.1146/annurev.immunol.23.021704.115633
33. Riedel JH, Becker M, Kopp K, Duster M, Brix SR, Meyer-Schwesinger C, et al. IL-33-Mediated Expansion of Type 2 Innate Lymphoid Cells Protects from Progressive Glomerulosclerosis. *J Am Soc Nephrol: JASN* (2017) 28(7):2068–80. doi: 10.1681/ASN.2016080877
34. Gasteiger G, Fan X, Dikiy S, Lee SY, Rudensky AY. Tissue residency of innate lymphoid cells in lymphoid and nonlymphoid organs. *Science (New York NY)* (2015) 350(6263):981–5. doi: 10.1126/science.aac9593
35. Hazenberg MD, Spits H. Human innate lymphoid cells. *Blood* (2014) 124 (5):700–9. doi: 10.1182/blood-2013-11-427781
36. Guillerey C. Roles of cytotoxic and helper innate lymphoid cells in cancer. *Mamm Genome* (2018) 29(11–12):777–89. doi: 10.1007/s00335-018-9781-4
37. Fung KY, Nguyen PM, Putoczki T. The expanding role of innate lymphoid cells and their T-cell counterparts in gastrointestinal cancers. *Mol Immunol* (2017) 110:48–56. doi: 10.1016/j.molimm.2017.11.013
38. Wu J, Lv X, Zhu S, Li T, Cheng H, Chen J. Critical Roles of Balanced Innate Lymphoid Cell Subsets in Intestinal Homeostasis, Chronic Inflammation, and Cancer. *J Immunol Res* (2019) 2019:1325181. doi: 10.1155/2019/1325181
39. Arimura K, Takagi H, Uto T, Fukaya T, Nakamura T, Choijookhuu N, et al. Crucial role of plasmacytoid dendritic cells in the development of acute colitis through the regulation of intestinal inflammation. *Mucosal Immunol* (2017) 10(4):957–70. doi: 10.1038/mi.2016.96
40. Sawant A, Ponnazhagan S. Role of plasmacytoid dendritic cells in breast cancer bone dissemination. *Oncoimmunology* (2013) 2(2):e22983. doi: 10.4161/onci.22983
41. Mitchell D, Chintala S, Dey M. Plasmacytoid dendritic cell in immunity and cancer. *J Neuroimmunol* (2018) 322:63–73. doi: 10.1016/j.jneuroim.2018.06.012
42. Maazi H, Banie H, Aleman Muench GR, Patel N, Wang B, Sankaranarayanan I, et al. Activated plasmacytoid dendritic cells regulate type 2 innate lymphoid cell-mediated airway hyperreactivity. *J Allergy Clin Immunol* (2018) 141 (3):893–905.e6. doi: 10.1016/j.jaci.2017.04.043
43. Del Prete MJ, Robles MS, Guao A, Martinez AC, Izquierdo M, Garcia-Sanz JA. Degradation of cellular mRNA is a general early apoptosis-induced event. *FASEB J* (2002) 16(14):2003–5. doi: 10.1096/fj.02-0392fje
44. Jing Wu HC, Wang H, Zang G, Qi L, Lv X, Liu C, et al. Correlation between immune lymphoid cells and plasmacytoid dendritic cells in human colon cancer. *Research Square* (2020). doi: 10.21203/rs.3.rs-46781/v1

Conflict of Interests: The authors declare that the research was conducted in the absence of any commercial or financial relationships that could be construed as a potential conflict of interest.

frontiers in Oncology

ORIGINAL RESEARCH
published: 19 March 2021
doi: 10.3389/fonc.2021.636751

CD169 Expression on Lymph Node Macrophages Predicts in Patients With Gastric Cancer

Keiichiro Kumamoto[1,2], Takashi Tasaki[1,3], Koji Ohnishi[4], Michihiko Shibata[2], Shohei Shimajiri[1], Masaru Harada[2], Yoshihiro Komohara[4,5] and Toshiyuki Nakayama[1]*

[1] Department of Pathology, University of Environmental and Occupational Health, Fukuoka, Japan, [2] Third Department of Internal Medicine, University of Occupational and Environmental Health, Fukuoka, Japan, [3] Department of Pathology, Graduate School of Medical and Dental Sciences, Kagoshima University, Kagoshima, Japan, [4] Department of Cell Pathology, Graduate School of Medical Sciences, Kumamoto University, Kumamoto, Japan, [5] Center for Metabolic Regulation of Healthy Aging, Kumamoto University, Kumamoto, Japan

OPEN ACCESS

Edited by:
Erica Villa, University of Modena and Reggio Emilia, Italy

Reviewed by:
Yoshihiko Hirohashi, Sapporo Medical University, Japan
Hiroya Kobayashi, Asahikawa Medical University, Japan

***Correspondence:**
Yoshihiro Komohara
ycomo@kumamoto-u.ac.jp

Specialty section:
This article was submitted to Cancer Immunity and Immunotherapy, a section of the journal Frontiers in Oncology

Received: *02 December 2020*
Accepted: *01 March 2021*
Published: *19 March 2021*

Citation:
Kumamoto K, Tasaki T, Ohnishi K, Shibata M, Shimajiri S, Harada M, Komohara Y and Nakayama T (2021) CD169 Expression on Lymph Node Macrophages Predicts in Patients With Gastric Cancer. Front. Oncol. 11:636751. doi: 10.3389/fonc.2021.636751

The induction of an anti-cancer immune responses is potentially associated with the efficacy of anti-cancer therapy. Recent studies have indicated that sinus macrophages in regional lymph nodes are involved in anti-cancer immune responses in the cancer microenvironment. In the present study, we investigated the correlation between lymphocyte infiltration in cancer tissues and macrophage activation in regional lymph nodes. We retrospectively identified 294 patients with gastric cancer who underwent surgery from 2008 to 2012. Using immunohistochemistry, we evaluated CD169-expression on CD68-positive macrophages, and the density of CD8-postive lymphocytes in tumor microenvironment. We statistically examined the correlation between CD169 and CD8 expression, and performed Cox regression analysis of potential prognostic factors, including CD169 and CD8 expression, for cancer-specific survival (CSS) in patients with total and advanced gastric cancer. CD169 overexpression in lymph node sinus macrophages (LySMs) was positively correlated to the density of CD8-positive lymphocytes in primary cancer tissues ($R = 0.367$, $p < 0.001$). A high density of CD8-positive T lymphocytes in the primary site and a high level of CD169 expression in LySMs were independently associated with greater CSS in patients with total and advanced gastric cancer ($p < 0.05$ for all). The expression on CD169 in LySMs is a predictor of a favorable clinical course in patients with gastric cancer, and might be useful for evaluating anti-cancer immune responses.

Keywords: lymph node, macrophage, CD169, gastric cancer, lymphocyte

INTRODUCTION

Gastric cancer is one of the most common cancers, with about 865,000 patients with this disease dying worldwide each year (1). Various treatments including cancer immunotherapies have been used to treat gastric cancer, but the prognosis remains poor. Recently, immune checkpoint inhibitors have been approved to treat patients with gastric cancer. Tumor-infiltrating lymphocytes (TILs) are involved in anti-cancer immune responses with a high density of such cells in cancer tissues associated with a favorable prognosis in various cancers, including gastric cancer (2–5). A high density of TILs in cancer tissues is suggested to be associated with a better clinical effect of chemotherapy in patients with advanced gastric cancer (6). Thus, the induction of an anti-cancer immune responses is necessary to improve the efficacy of anti-cancer therapy.

Lymph nodes, as immune organs, play an important role in the induction of specific immune responses to cancer (7, 8). Various antigens from peripheral tissues flow into lymph nodes, where dendritic cells and macrophages act as antigen-presenting cells (9, 10). It is well-known that dendritic cells have strong antigen-presenting ability. In addition to dendritic cells, lymph node sinus macrophages (LySMs) have also been suggested to have antigen-presenting capacity in animal studies.

CD169, also called sialoadhesin, is the foremost member of the sialic acid-binding lectin (Siglec) superfamily (7). It binds sialylated glycoproteins including CD43 (sialophorin) and MUC1 and is involved in cell–cell adhesion as well as cell–pathogen interactions (11–14). CD169 expression is found in splenic marginal metallophilic macrophages and in certain tissue macrophages in bone marrow, colon, liver, and lung, as well as in LySMs (11, 15). CD169-positive macrophages express both M1- and M2-related genes, and are considered as a unique subset that differ from M1/M2-like macrophages (16, 17). CD169-positive LySMs were involved in antigen presentation and the induction of cytotoxic T lymphocytes, in addition to dendritic cells, in a mouse model (18, 19). The downregulation of CD169 in pre-metastatic regional lymph nodes was associated with lymph node metastasis in a rat model (20). In histopathological studies using human resected samples, a correlation between a high CD169 expression level in LySMs and a favorable clinical course has been reported in several cancers including colorectal cancer (21). A correlation between anti-cancer immune responses and a high level of CD169 expression has also been suggested in these tumors. These findings indicated that LySMs in regional lymph nodes are closely associated with anti-cancer immune responses since they engulf dead cells and debris from tumor tissues (22). However, the direct mechanisms underlying the role of CD169 in the induction of immune responses have not yet been clarified. Because CD169 expression is up-regulated by type I interferons, CD169 expression has been considered a surrogate marker of active immune responses in lymph nodes (23).

No studies have yet examined the role of LySMs in patients with gastric cancer. In the present study, we aimed to elucidate the association between CD169 LySMs and prognosis in gastric cancer, including its pathological stage and subgroups: histology, tumor-stroma ratio, distant metastasis, and LN metastasis. In order to determine the significance of CD169 expression in patients with gastric cancer, we used tissue specimens to investigate the correlation between CD169 expression on LySMs and $CD8^+$ T-cell infiltration in primary lesions. We also examined the relationship between CD169 expression and various clinicopathological factors.

MATERIALS AND METHODS

Samples

We conducted a retrospective analysis in accordance with the Declaration of Helsinki and with the approval of the Hospital of the University of Environmental and Occupational Health (UOEH), and Wakamatsu Hospital of UOEH (H30-172). The present study utilized paraffin-embedded specimens of primary lesions and regional lymph nodes (RLNs) resected from 294 patients with gastric cancer who had undergone surgery at the Hospital of the UOEH from 2008 to 2012 and Wakamatsu Hospital of the UOEH from 2011 to 2012. We excluded patients who died from non-primary cancer causes or patients who were no longer available for follow-up within a year after surgery. We also excluded cases in which the lymph nodes were difficult to evaluate and in which no lymph node resection had been performed.

Histology

Samples from 294 gastric cancer cases were stained with hematoxylin and eosin (HE) and evaluated histopathologically by two or three pathologists (KK, TT, and TN) who were blinded to clinical outcomes. As previously published, the tumor-stroma ratio (TSR) was calculated as the percentage of stroma relative to tumor area; tumors were subgrouped as having a high (>50%) or low TSR (24–26). We selected the most invasive tumor area (0.25 -0.50 mm^2 total area) for TSR evaluation, and excluded areas with necrosis or mucin deposition. TSR evaluation was also conducted by two or three pathologists (KK, TT, and TN) who were blinded to clinical outcomes.

Immunohistochemistry

Tumor tissues and RLNs were fixed in 10% neutral formalin and embedded in paraffin. Anti-CD169 (clone HSn 7D2; Santa Cruz Biotechnology, CA, USA), anti- CD68 (clone PG-M; Agilent Technologies, CA, USA), and anti-CD8 (clone C8/144B; Nichirei, Tokyo, Japan) antibodies were used as primary antibodies for immunohistochemistry (IHC). Antigen retrieval and IHC were performed as previously published (27). Lymph nodes without metastasis were used as controls for CD68 and CD169 expressions. For counting $CD169^+$ and $CD68^+$ cells in RLNs and $CD8^+$ cells in tumors, we used the HALO 2.3 system (Indica Labs, Albuquerque, NM, USA). We selected four random fields (0.25 mm^2 per field, total 1.00 mm^2) from the primary tumor to count $CD8^+$ T cells. To count $CD68^+$ and $CD169^+$ macrophages in RLNs, we delineated the RLN sinus with a line in two to four fields (0.10 to 0.25 mm^2 per field, total 0.50 mm^2) in serial sections. After counting cells and measuring these areas, we calculated the density of $CD8^+$ T cell infiltration into the tumor, and the ratio of $CD169^+$ cells in $CD68^+$ LySMs. For double-IHC, HistoGreen substrate (green color; AYS-

E109, Eurobio Scientific, Les Ulis, France) was used for peroxidase-based immunostaining.

Statistical Analysis

We carried out statistical analyses using SPSS 25 software (IBM, Chicago, IL, USA). Bivariate comparisons of clinicopathological features between patients with high (n = 135) and low (n = 159) ratios of $CD169^+$ to $CD68^+$ LySMs were performed using a χ^2-test. The relationship between two numerical factors was analyzed using Spearman's correlation analysis. The association of multiple prognostic factors with cancer-specific survival was assessed using univariate and multivariate Cox proportional hazard model analysis. Multivariate analysis included age, sex, histology, depth of invasion, LN metastasis, distant metastasis, lymphatic invasion, vascular invasion, tumor-stroma ratio, density of $CD8^+$ T cells, and the ratio of $CD169^+$ to $CD68^+$ LySMs. Survival curves were calculated using the Kaplan-Meier method, and the difference between survival curves was analyzed using the log-rank test. Differences were considered statistically significant at *P*-values of < 0.05.

RESULTS

CD169 Expression in LySMs Was Significantly Associated With the Density of Infiltrating $CD8^+$ T Cells in Primary Cancer Lesion

Immunohistochemistry for CD68 and CD169 was performed using RLN specimens, and that for CD8 was done using primary cancer specimens in 294 gastric cancer cases. The density of positive cells was evaluated by the HALO 2.3 system as described in the Materials and Methods section (**Figures 1A, B**). As shown in **Figure 1**, the density of CD8-positive cells ranged from 8.33 to 2399.26 cells/mm^2 (mean, 394.33 cells/mm^2; median, 286.81 cells/mm^2). The ratio of $CD169^+$ to $CD68^+$ cells ranged from 0.00% to 132.78% (mean, 62.14%; median, 71.38%; **Figure 1D**). Representative IHC images of samples of two patients are shown in **Figure 2**. Since it is well known that CD169 expression was restricted in $CD68^+$ LySMs in the lymph node, the expression on CD169 in LySMs was evaluated as the ratio of $CD169^+$ to $CD68^+$ cells (**Figure 2B**). The direct cell-cell interaction between $CD169^+$ LySM and $CD8^+$ TIL was detected in sinus area of lymph node (**Figure 2C**). Next, we tested the correlation between $CD8^+$ TILs in tumor tissues and CD169 expression in LySM. We found that the ratio of $CD169^+$ to $CD68^+$ cells was positively correlated to the density of $CD8^+$ TILs in both total and advanced gastric cancer (total; $R = 0.367$, $p < 0.001$; advanced; $R = 0.317$, $p < 0.001$; **Figures 2D, E**). These observations indicated a significant correlation between high CD169 expression in LySMs and high immune responses in the tumor microenvironment.

High CD169 Expression in LySMs and a High Density of Infiltrating $CD8^+$ T Cells in Primary Cancer Lesion Were Associated With a Favorable Clinical Course

Patients were divided into $CD169^{low}$ and $CD169^{high}$ groups, with the cut-off value set to 65% (**Figure 1**) and the relationship with clinicopathological features analyzed. The expression on CD169 in LySMs was not associated with age, sex, histological subtype, depth of invasion, lymphovascular invasions or metastasis (**Table 1**). Next, we tested the correlation between cancer-specific overall survival time (CSS)/relapse-free survival time (RFS), and CD169 expression. The $CD169^{high}$ group showed greater overall survival as compared to the $CD169^{low}$ group; the 5-year CSS was 85.25% in the $CD169^{high}$ group and 72.46% in the $CD169^{low}$ group ($p = 0.004$; **Figure 3A**). In addition, a high density of $CD8^+$ TILs was associated with a greater

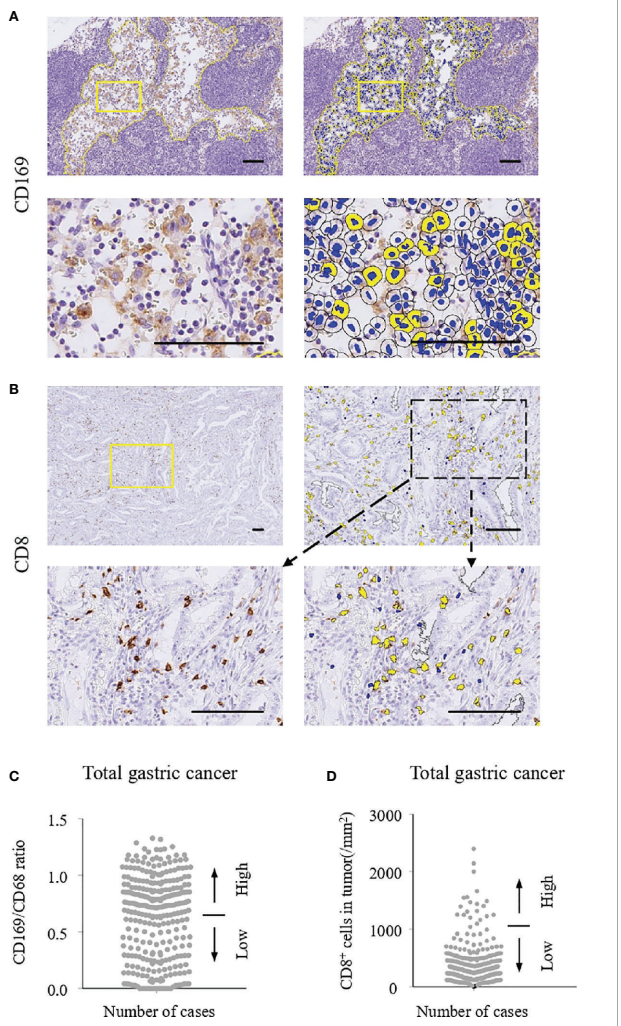

FIGURE 1 | Immunohistochemistry and cell counting system. The numbers of $CD169^+$ and $CD68^+$ cells in regional lymph nodes (RLNs) and $CD8^+$ cells in tumors were evaluated using HALO 2.3 as described in Materials and Methods. Scale bar = 100 μm. Representative immunohistochemistry (IHC) stains of CD169 **(A)** and CD8 **(B)** are shown. Positive cells in selected areas surrounded by yellow lines were counted automatically by HALO 2.3. **(C)** Number of CD169/CD68 ratio in lymph node sinus macrophages (LySMs). **(D)** Number of CD8 expressions in primary tumor. Patients were divided into two groups according to their CD169/CD68 ratio: < 0.65 was defined as low and ≥ 0.65 was defined as high. With regard to $CD8^+$ cells, the patients were divided into two groups according to cell density: < 287/mm^2 was defined as low and ≥ 287/mm^2 was defined as high.

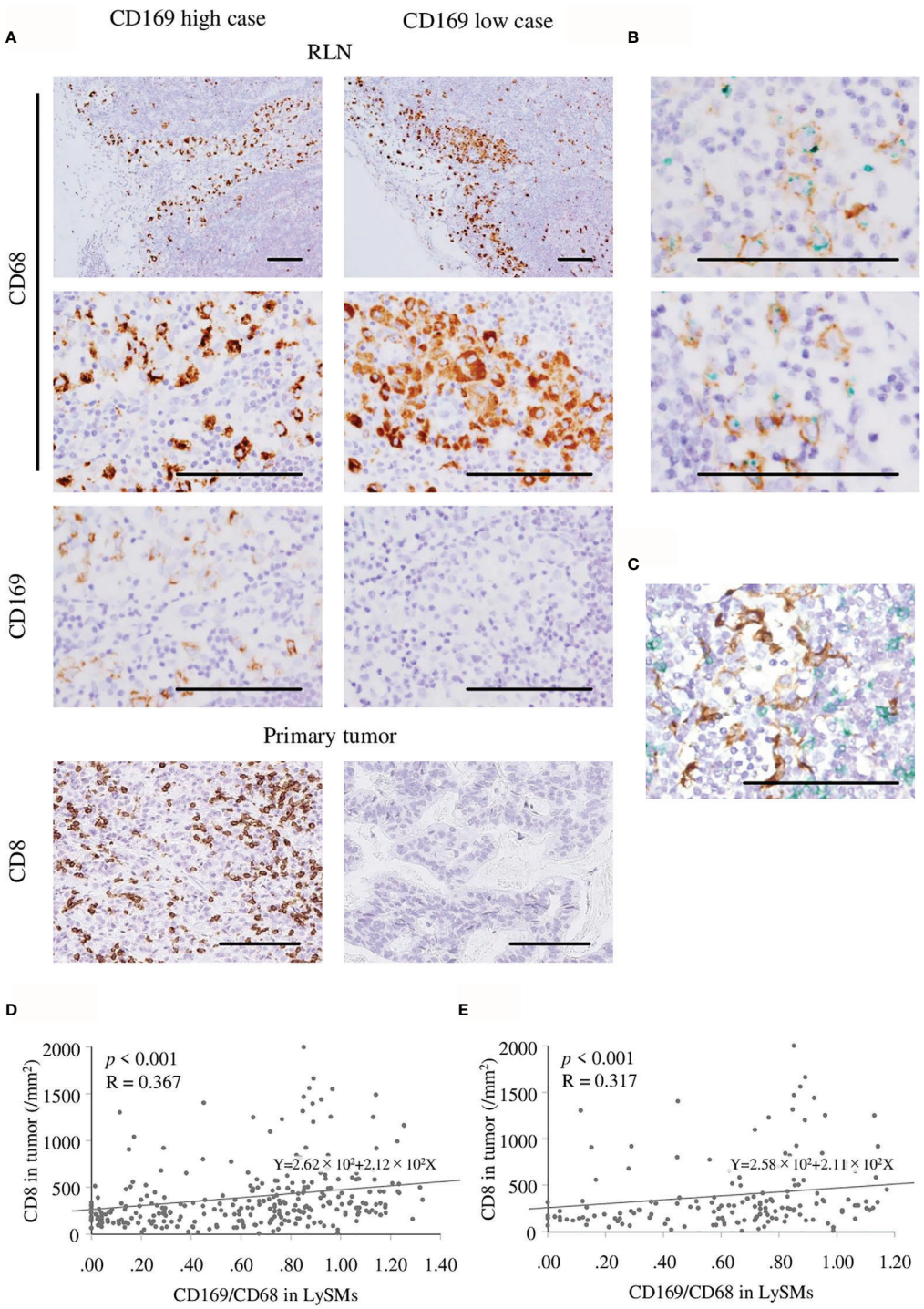

FIGURE 2 | Immunohistochemistry of CD169^{+} and CD68^{+} macrophage in regional lymph nodes (RLN), and CD8^{+} cells in primary tumor. Scale bar = 100 μm. **(A)** Representative figures of immunohistochemistry (IHC) images from CD169 high and low cases are shown. Lymph node sinus macrophages (LySMs) were positive for CD68 in both two patients, although, CD169 expression differed. High infiltration of CD8^{+} T cells in primary tumor tissues was seen in a CD169^{high} case and low infiltration of CD8^{+} T cells in primary tumor tissues was seen in a CD169^{low} case. **(B)** Double IHC of CD68(green) and CD169(brown) showed CD169 was expressed on CD68-positive macrophages. Correlation between the number of CD8^{+} T cells in primary tumor tissues and CD169/CD68 ratio in LySMs were tested by Spearman's correlation test. **(C)** Double IHC of CD8(green) and CD169(brown) showed the direct cell-cell interaction between LySM and T cells in sinus area. Scatter plots of total **(D)** and in advanced **(E)** gastric cancer cases were shown. RLN, regional lymph node.

CSS; the 5-year CSS was 93.60% in the $CD8^{high}$ group and 65.36% in the $CD8^{low}$ group ($p < 0.001$; **Figure 3C**). High CD169 expression and a high density of $CD8^+$ T cells were independent prognostic factors in a multivariate analysis respectively (**Table 2**; **Figure 3E**). A high density of $CD8^+$ TILs was also associated with a greater RFS; the 5-year RFS was 95.61% in the $CD8^{high}$ group and 68.03% in the $CD8^{low}$ group ($p < 0.001$; **Figure 3D**), However, the $CD169^{high}$ group did not show a greater RFS compared to the $CD169^{low}$ group; the 5-year RFS was 86.47% in $CD169^{high}$ and 77.71% in $CD169^{high}$ ($p = 0.112$, **Figure 3B**) groups, respectively. Additionally, in multivariate analysis, a high density of $CD8^+$ T cells was an independent prognostic factors, but high CD169 expression was not an independent prognostic factor (**Table 3**; **Figure 3F**).

A Significant Association Between CD169 Expression in LySMs and Clinical Course in Advanced Gastric Cancer Cases

We divided all cases into two groups: early and advanced gastric cancer cases. The $CD169^{high}$ group showed greater CSS and RFS as compared to the $CD169^{low}$ group. The 5-year CSS was 76.19% for the $CD169^{high}$ group, and 48.92% for the $CD169^{low}$ group ($p < 0.001$; **Figure 4A**). The 5-year RFS was 77.58% for the $CD169^{high}$ group and 53.16% for the $CD169^{low}$ group ($p = 0.004$; **Figure 4B**) in advanced gastric cancer. In addition, high CD169 expression was an independent prognostic factor in multivariate analysis (**Tables 2**, **3**, **Figures 4E, F**). However, in early gastric cancer, a significant difference between the ratio of macrophages and prognosis was not noted (**Figures 4C, D**). The 5-year CSS was 97.03% for the $CD169^{high}$ group and 98.48% for the $CD169^{low}$ group ($p = 0.354$; **Figure 4C**). The 5-year RFS was 98.48% for the $CD169^{high}$ group and 97.04% for the $CD169^{low}$ group ($p = 0.354$; **Figure 4D**).

TABLE 1 | Clinicopathological features and $CD169^+/CD68^+$ ratio in lymph node sinus macrophages (LySMs) from 294 patients with gastric cancer.

Clinicopathological feature	n	$CD169^+$cells/$CD68^+$cells in LySMs		
		<0.65	≥0.65	P
Age				
< 70 (y)	147	62	85	0.198
≥ 70 (y)	147	73	74	
Sex				
Female	109	49	60	0.799
Male	185	86	99	
Histology				
Intestinal type	142	64	78	0.778
Diffuse type	152	71	81	
Depth of invasion				
m, sm	135	66	69	0.346
mp, ss, se, si	159	69	90	
LN metastasis				
Negative	175	80	95	0.932
Positive	119	55	64	
Distant metastasis				
Negative	270	123	147	0.675
Positive	24	12	12	
Lymphatic invasion				
Negative	92	45	47	0.487
Positive	202	90	112	
Vascular invasion				
Negative	141	63	78	0.683
Positive	153	72	81	
Tumor-stroma ratio				
Low	202	96	106	0.413
High	92	39	53	
$CD8^+$cells/mm^2 in tumor				
< 287	147	90	57	<0.001
≥ 287	147	45	102	

LySMs, lymph node sinus macrophages; m, mucosa; sm, submucosa; mp, muscularis propria; ss, subserosa; se, serosa exposure; si, serosa invasion; LN, lymph node.

Significant Association Between CD169 Expression in LySMs and Clinical Course Was Not Dependent on Histological Subtype, Distant Metastasis, Etc.

Because we found a more significant association between CD169 expression in LySM and a clinical course in advanced gastric cancer, we performed a prognostic study of advanced gastric cancer cases only. The $CD169^{high}$ group showed better cancer specific survival in advanced gastric cancer with various subgroups, such as histology, and LN metastasis, in Kaplan-Meier analysis. The 5-year CSS was 76.49% for the $CD169^{high}$ group and 52.54% for the $CD169^{low}$ group for the intestinal type group ($p = 0.024$; **Figure 5A**), and 75.85% in the $CD169^{high}$ group and 45.60% in the $CD169^{low}$ group for the diffuse type group ($p < 0.001$; **Figure 5B**). The 5-year CSS was 67.48% for the $CD169^{high}$ group and 28.27% for the $CD169^{low}$ group for the LN metastasis-positive group ($p < 0.001$; **Figure 5D**); however, no significant difference was seen in cases without LN metastasis (**Figure 5C**). The 5-year CSS was 85.59% for the $CD169^{high}$ group and 59.35% for the $CD169^{low}$ group in a group without distant metastasis ($p < 0.001$; **Figure 5E**). Although a significant difference in cases with distant metastasis was not observed, the $CD169^{high}$ group tended to have a more favorable prognosis. The 5-year CSS was 11.11% for the $CD169^{high}$ group and 0% for the $CD169^{low}$ group ($p = 0.050$, **Figure 5F**). With regards to the RFS, a similar observation that high CD169 expression was associated with a more favorable clinical course tended to be seen. A significant correlation was seen in the diffuse type group but not in the intestinal type group (**Figures 6A, B**). A significant association between high CD169 expression and a more favorable clinical course was seen in a group, with or without LN metastasis, or with or without distant metastasis (**Figures 6C–F**).

Tumor-Stroma Ratio (TSR) Affected the Correlation Between CD169 Expression in LySMs and the Density of TILs

Because the TSR is a recognized prognostic factor for various solid tumors, we divided advanced gastric cancer into two groups: low and high TSR (**Figure 7A**) as described in the Materials and Methods section. Interestingly, the density of TILs was lower in the high compared with low TSR group (**Figure 7B**). A correlation between CD169 expression and CD8-positive T lymphocytes in the low TSR group was not noted ($p = 0.140$; **Figure 7C**), whereas CD169 expression was positively correlated with the density of CD8-positive T lymphocytes in the high TSR group ($R = 0.325$, $p = 0.014$; **Figure 7D**). The $CD169^{high}$ group showed greater CSS as

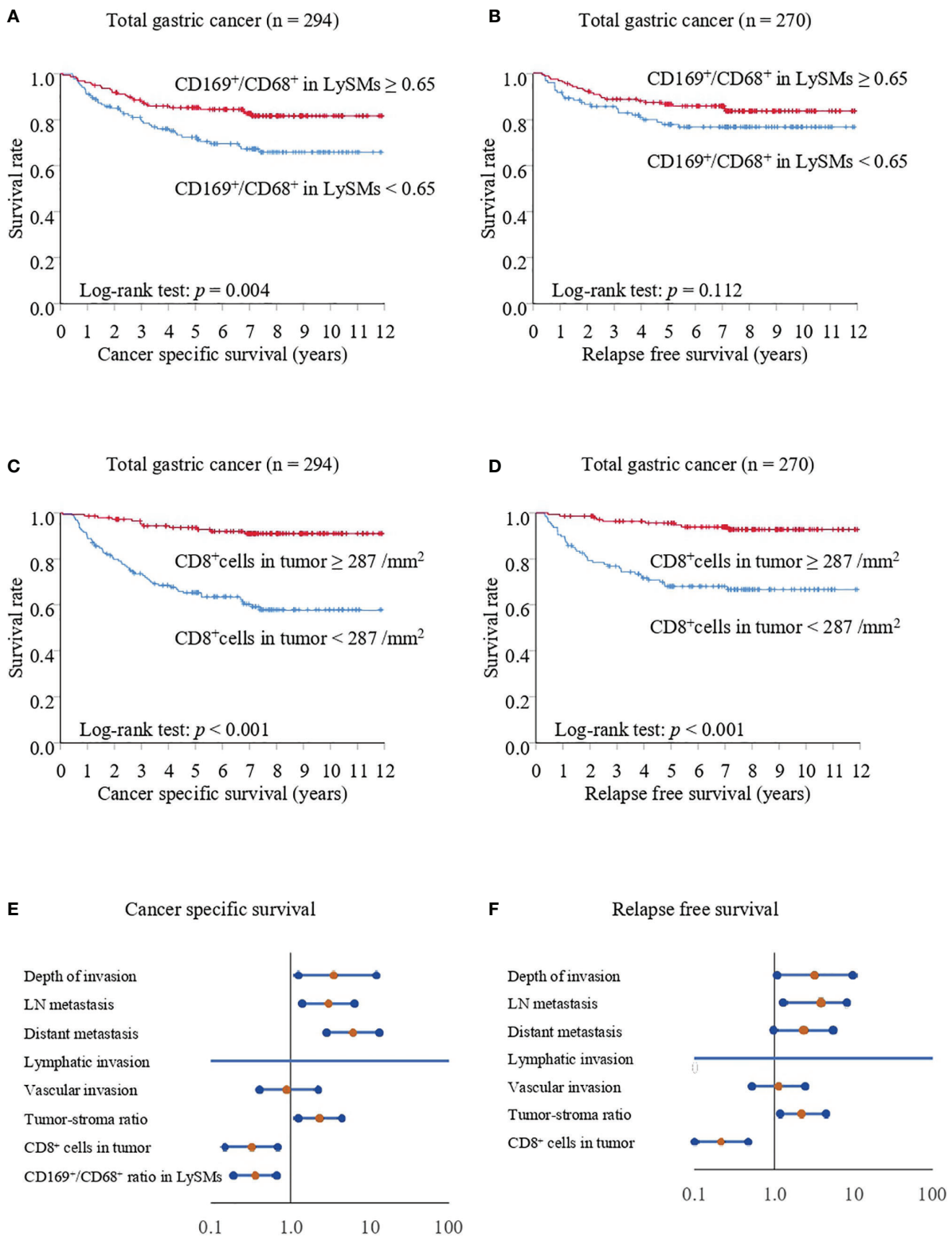

FIGURE 3 | Kaplan-Meier cancer-specific survival and relapse-free survival curves for total gastric cancer cases. The patients were divided into two groups according to their CD169/CD68 ratio: < 0.65 was defined as low and ≥ 0.65 was defined as high **(A, B)** or divided into two groups according to their density of $CD8^+$ cells: < 287/mm^2 was defined as low and ≥ 287/mm^2 was defined as high **(C, D)**. **(A, C)** Cancer-specific survival (CSS) curves for patients with total gastric cancer. **(B, D)** Relapse-free survival (RFS) curves for patients with total gastric cancer. **(E)** Forest plot analysis of CSS. **(F)** Forest plot analysis of RFS.

TABLE 2 | Univariate and multivariate Cox regression analysis of potential prognostic factors for cancer specific survival in patients with total gastric cancer (n = 294) and advanced gastric cancer (n = 159).

	Clinicopathological feature	n	Univariate analysis			Multivariate analysis		
			HR	(95%CI)	p	HR	(95%CI)	p
Total gastric cancer	Age							
	<70 (y)	147	1.00					
	≥70 (y)	147	1.02	(0.64 - 1.64)	0.930			
	Sex							
	Female	109	1.00					
	Male	185	1.70	(1.00 - 2.89)	0.050			
	Histology							
	Intestinal type	142	1.00					
	Diffuse type	152	1.20	(0.74 - 1.93)	0.467			
	Depth of invasion							
	m, sm	135	1.00					
	mp, ss, se, si	159	17.06	(6.21 - 46.90)	<0.001	3.60	(1.23 - 10.56)	0.019
	LN metastasis							
	Negative	175	1.00					
	Positive	119	10.96	(5.39 - 19.67)	<0.001	3.08	(1.54 - 6.16)	0.002
	Distant metastasis							
	Negative	270	1.00					
	Positive	24	22.95	(12.90 - 40.84)	<0.001	5.70	(3.02 - 10.76)	<0.001
	Lymphatic invasion							
	Negative	92	1.00					
	Positive	202	40.88	(5.14 - 325.30)	<0.001	4.87×10^{4}	$(0.00 - 5.65\times10^{102})$	0.925
	Vascular invasion							
	Negative	141	1.00					
	Positive	153	6.52	(3.33 - 12.77)	<0.001	1.01	(0.49 - 2.09)	0.984
	Tumor-stroma ratio							
	Low	202	1.00					
	High	92	6.88	(4.08 - 11.62)	<0.001	2.29	(1.30 - 4.02)	0.004
	$CD8^{+}$cells/mm^2 in tumor							
	<287	147	1.00					
	≥287	147	0.17	(0.09 - 0.32)	<0.001	0.37	(0.19 - 0.74)	0.005
	CD169/CD68 ratio in LySMs							
	<0.65	135	1.00					
	≥0.65	159	0.49	(0.30 - 0.80)	0.004	0.41	(0.25 - 0.69)	<0.001
Advanced gastric cancer	Age							
	<70 (y)	80	1.00					
	≥70 (y)	79	0.94	(0.58 - 1.54)	0.807			
	Sex							
	Female	54	1.00					
	Male	105	1.62	(0.93 - 2.83)	0.089			
	Histology							
	Intestinal type	77	1.00					
	Diffuse type	82	1.41	(0.86 - 2.32)	0.175			
	Depth of invasion							
	mp, ss	121	1.00					
	se, si	38	7.64	(4.56 - 12.81)	<0.001	2.86	(1.44 - 5.720)	0.003
	LN metastasis							
	Negative	57	1.00					
	Positive	102	4.21	(2.14 - 8.29)	<0.001	3.40	(1.64 - 7.08)	0.001
	Distant metastasis							
	Negative	135	1.00					
	Positive	24	12.61	(7.00 - 22.70)	<0.001	2.91	(1.32 - 6.43)	0.008
	Lymphatic invasion							
	Negative	4	1.00					
	Positive	155	21.10	$(0.04 - 1.15\times10^{4})$	0.343			
	Vascular invasion							
	Negative	32	1.00					
	Positive	127	1.78	(0.88 - 3.61)	0.108			
	Tumor-stroma ratio							
	Low	84	1.00					
	High	75	4.84	(0.12 - 0.42)	<0.001	2.54	(1.37 - 4.68)	0.003

(Continued)

TABLE 2 | Continued

	Clinicopathological feature	n	Univariate analysis			Multivariate analysis		
			HR	(95%CI)	p	HR	(95%CI)	p
	$CD8^+$cells/mm^2 in tumor							
	<287	92	1.00					
	≥287	67	0.22	(0.12 - 0.42)	<0.001	0.42	(0.20 - 0.84)	0.015
	CD169/CD68 ratio in LySMs							
	<0.65	69	1.00					
	≥0.65	90	0.36	(0.22 - 0.60)	<0.001	0.38	(0.22 - 0.66)	<0.001

HR. hazard ratio; CI, confidence interval; m, mucosa; sm, submucosa; mp, muscularis propria; ss, subserosa; se, serosa exposure; si, serosa invasion; LN, lymph node; LySMs, lymph node sinus macrophages.

TABLE 3 | Univariate and multivariate Cox regression analysis of potential prognostic factors for relapse free survival in patients with total gastric cancer (n = 270) and advanced cancer (n = 135).

	Clinicopathological feature	n	Univariate analysis			Multivariate analysis		
			HR	(95%CI)	p	HR	(95%CI)	p
Total gastric cancer	Age							
	<70 (y)	139	1.00					
	≥70 (y)	131	0.74	(0.42 - 1.32)	0.308			
	Sex							
	Female	101	1.00					
	Male	169	1.83	(0.97 - 3.46)	0.061			
	Histology							
	Intestinal type	134	1.00					
	Diffuse type	136	0.84	(0.48 - 1.48)	0.550			
	Depth of invasion							
	m, sm	135	1.00					
	mp, ss, se, si	135	13.33	(4.79 - 37.09)	<0.001	3.14	(1.07 - 9.23)	0.037
	LN metastasis							
	Negative	172	1.00					
	Positive	98	9.88	(4.79 - 20.38)	<0.001	3.85	(1.82 - 8.15)	<0.001
	Distant metastasis							
	Negative	262	1.00					
	Positive	8	13.90	(6.05 - 31.93)	<0.001	2.34	(0.99 - 5.57)	0.054
	Lymphatic invasion							
	Negative	92	1.00					
	Positive	178	42.94	(3.87 - 4.77×10^2)	0.002	2.66×10^4	(0.00 - 2.17×10^{90})	0.920
	Vascular invasion							
	Negative	138	1.00					
	Positive	132	6.19	(2.90 - 13.21)	<0.001	1.12	(0.53 - 2.69)	0.660
	Tumor-stroma ratio							
	Low	196	1.00					
	High	74	5.63	(3.14 - 10.07)	<0.001	2.22	(1.21 - 4.07)	0.010
	$CD8^+$cells/mm2 in tumor							
	<287	127	1.00					
	≥287	143	0.17	(0.08 - 0.17)	<0.001	0.21	(0.10 - 0.45)	<0.001
	$CD169^+/CD68^+$cells in RLNs							
	<0.65	119	1.00					
	≥0.65	151	0.64	(0.36 - 1.12)	0.115			
Advanced gastric cancer	Age							
	<70 (y)	72	1.00					
	≥70 (y)	63	0.65	(0.35 - 1.18)	0.156			
	Sex							
	Female	46	1.00					
	Male	89	1.82	(0.92 - 3.58)	0.086			
	Histology							
	Intestinal type	69	1.00					

(Continued)

TABLE 3 | Continued

Clinicopathological feature	n	Univariate analysis			Multivariate analysis		
		HR	(95%CI)	p	HR	(95%CI)	p
Diffuse type	66	1.00	(0.56 - 1.80)	0.991			
Depth of invasion							
mp, ss	116	1.00					
se, si	19	5.53	(2.93 - 10.42)	<0.001	3.64	(1.64 - 8.11)	0.002
LN metastasis							
Negative	54	1.00					
Positive	81	4.03	(1.87 - 8.67)	<0.001	4.97	(2.19 - 11.27)	<0.001
Distant metastasis							
Negative	127	1.00					
Positive	8	7.00	(3.03 - 16.18)	<0.001	1.46	(0.48 - 4.46)	0.507
Lymphatic invasion							
Negative	4	1.00					
Positive	131	21.24	(0.02 - 2.38×10^4)	0.394			
Vascular invasion							
Negative	29	1.00					
Positive	106	1.62	(0.72 - 3.63)	0.240			
Tumor-stroma ratio							
Low	78	1.00					
High	57	4.15	(2.20 - 7.82)	<0.001	2.03	(1.01 - 4.10)	0.048
$CD8^+$cells/mm in tumor							
<287	72	1.00					
≥287	63	0.21	(0.10 - 0.44)	<0.001	0.24	(0.10 - 0.53)	<0.001
$CD169^+/CD68^+$cells in RLNs							
<0.65	53	1.00					
≥0.65	82	0.43	(0.24 - 0.78)	0.005	0.37	(0.19 - 0.72)	0.003

HR. hazard ratio; CI, confidence interval; m, mucosa; sm, submucosa; mp, muscularis propria; ss, subserosa; se, serosa exposure; si, serosa invasion; LN, lymph node; LySMs, lymph node sinus macrophages.

compared to the $CD169^{low}$ group for both low and high TSR groups. The 5-year CSS was 90.00% in the $CD169^{high}$ group and 71.84% in the $CD169^{low}$ group for the low TSR group ($p = 0.031$; **Figure 7E**), and 58.33% for the $CD169^{high}$ group and 28.34% for the $CD169^{low}$ group for the high TSR group ($p = 0.001$; **Figure 7F**). Although, a significant difference in the low TSR group in RFS was not observed ($p = 0.887$; **Figure 6G**), the $CD169^{high}$ group showed a superior RFS in high TSR group ($p < 0.001$; **Figure 6H**).

DISCUSSION

In the present study, we found that a high CD169 expression level was associated with a more favorable overall survival. The observation that CD169 expression was positively associated with the density of CD8-positive cytotoxic T cells (TILs) indicated a significant association between CD169 expression in LySMs and anti-cancer immune responses. These findings are consistent with our previous research findings in colorectal cancer, melanoma, esophageal cancer, and bladder cancer (21, 28–30). Since CD169 overexpression has been suggested to be linked to interferon production (21), this might indicate an inflammatory reaction in lymph nodes.

Immune checkpoint blockade targeting programmed death 1 (PD-1)/programmed death ligand 1 (PD-L1) and cytotoxic T lymphocyte-associated protein 4 (CTLA-4) has become a promising approach for anti-cancer immunotherapy (31). The ATTRACTION-2 study was conducted in patients with gastric cancer who had become resistant to second- and third-line treatments. A significant difference in overall survival (OS) was observed between nivolumab and placebo groups (32). PD-1 ligands are expressed not only on cancer cells, but also on immune cells. Among immune cells, antigen-presenting cells, such as macrophages and dendritic cells, express high levels of PD-1 ligands (33, 34). Recently, it was reported that PD-L1 expression was significantly elevated in myeloid cells in the lymph nodes of cancer-bearing mice, and anti-PD-1 therapy induced T cell activation and proliferation in the lymph nodes (35). The study also demonstrated that resection of draining lymph nodes completely abrogated anti-tumor immune responses that were induced by PD-1/PD-L1 blockade therapy. These data indicated that PD-1/PD-L1 signals work as a negative regulator at regional lymph nodes, and that lymph nodes are pivotal sites for the induction of anti-tumor T cells.These findings suggest that CD169 positive macrophages may involve the mechanisms that are described in **Figure 8**.

Interestingly, the $CD169^{high}$ group had greater CSS than the $CD169^{low}$ group in the TSR high group. Because the stromal component of tumors has been proven to have a significant impact on tumor development (36), it has been recognized as a potential prognostic factor for various solid tumors (37). Cancer-associated fibroblasts (CAFs), which produce a desmoplastic stromal component, are thought to be important in considering

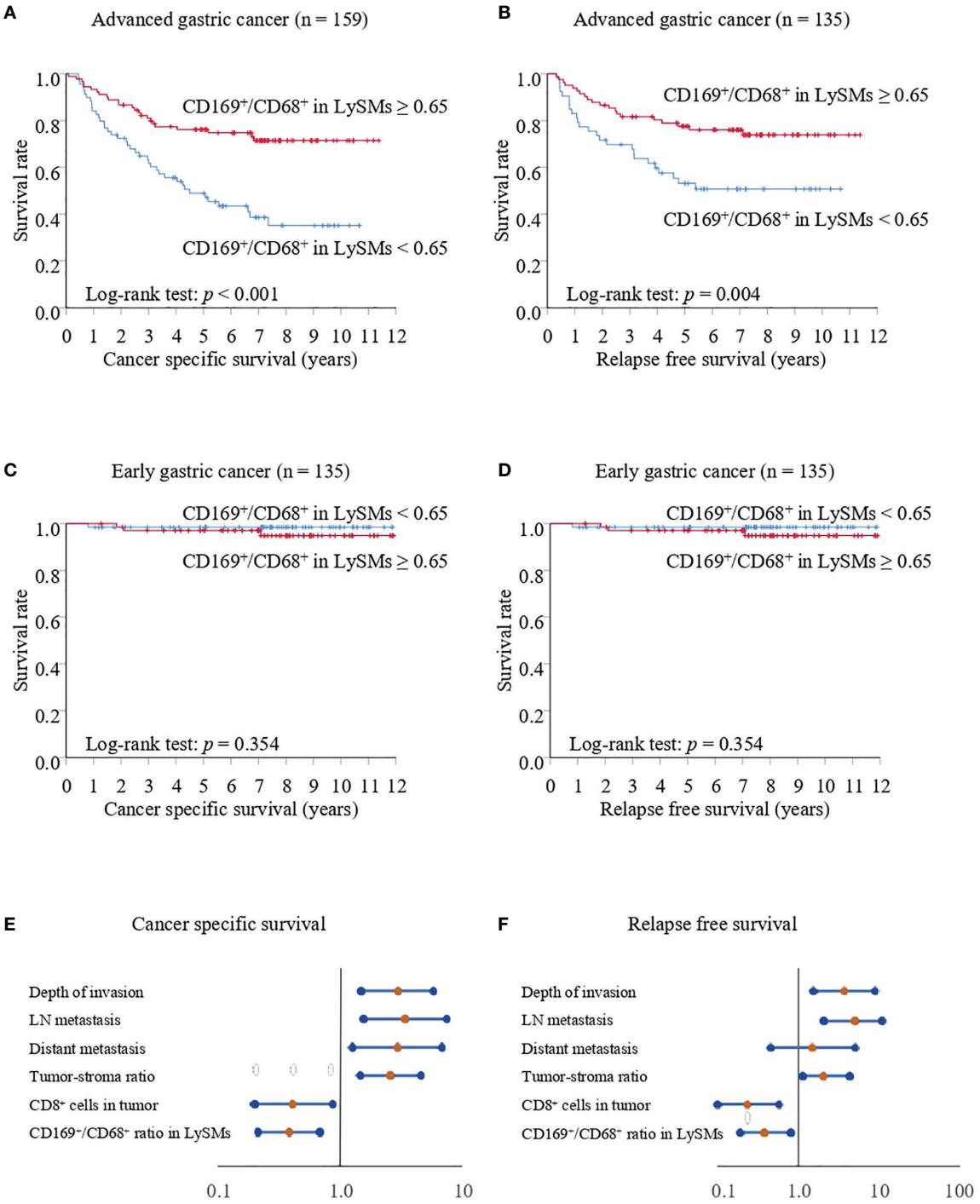

FIGURE 4 | Kaplan-Meier cancer-specific survival and relapse-free survival curves for patients with advanced or early gastric cancer. For all Kaplan-Meier curves, the patients were divided into two groups according to their CD169/CD68 ratio: < 0.65 was defined as low and ≥ 0.65 was defined as high. **(A)** Cancer-specific survival (CSS) curves for patients with advanced gastric cancer. **(B)** Relapse-free survival (RFS) curves for patients with advanced gastric cancer. **(C)** CSS curves for patients with early gastric cancer. **(D)** RFS curves for patients with early gastric cancer. **(E)** Forest plot analysis of CSS in advanced gastric cancer. **(F)** Forest plot analysis of RFS in advanced gastric cancer.

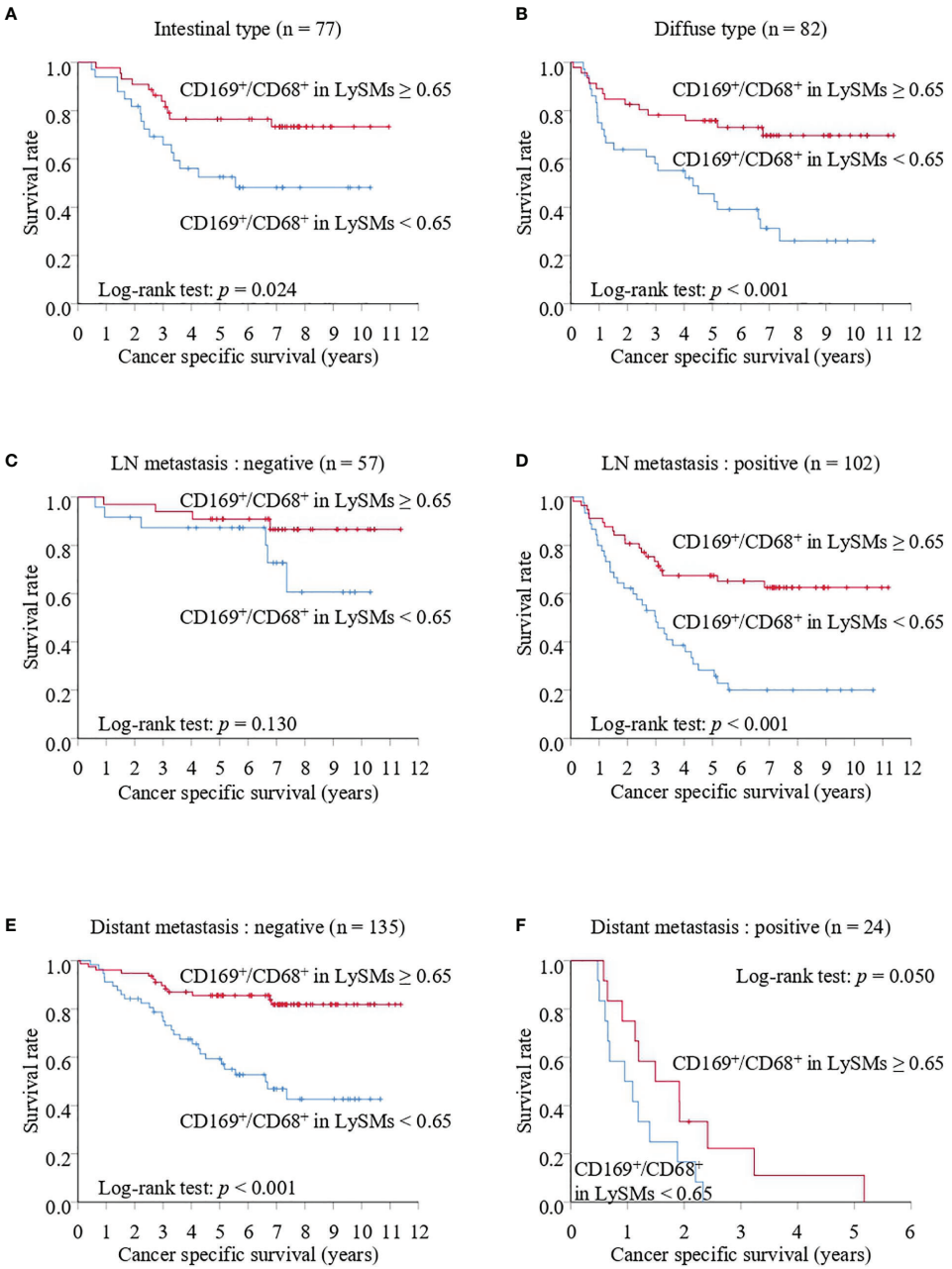

FIGURE 5 | Kaplan-Meier cancer-specific survival (CSS) curves of $CD169^+/CD68^+$ ratios in lymph node sinus macrophages (LySMs) of advanced gastric cancer patients with various tumor subtypes: intestinal type **(A)** or diffuse type **(B)**; lymph node (LN) metastasis negative **(C)** and positive **(D)**; distant metastasis negative **(E)** and positive **(F)**.

the TSR (38). It is possible that CD169-positive cells have some effect on CAFs. The $CD169^{high}$ group also had a significantly greater RFS in patients with gastric cancer in a high recurrence group, including diffuse type, LN metastasis, distant metastasis, and high TSR, suggesting a better prognosis because of reduced recurrence.

Regardless of CD169 expression in LySMs, significant high density of CD8-lymphocytes was counted in some cases. Some of these cases were suggesting medullary carcinoma or gastric carcinoma with lymphoid stroma. It is speculated that these cases could potentially contain EBV-positive or MSI-high gastric carcinoma, although these were not sufficiently investigated in this study.

In conclusion, CD169 overexpression in LySMs is a predictor of a more favorable clinical course in association with anti-cancer

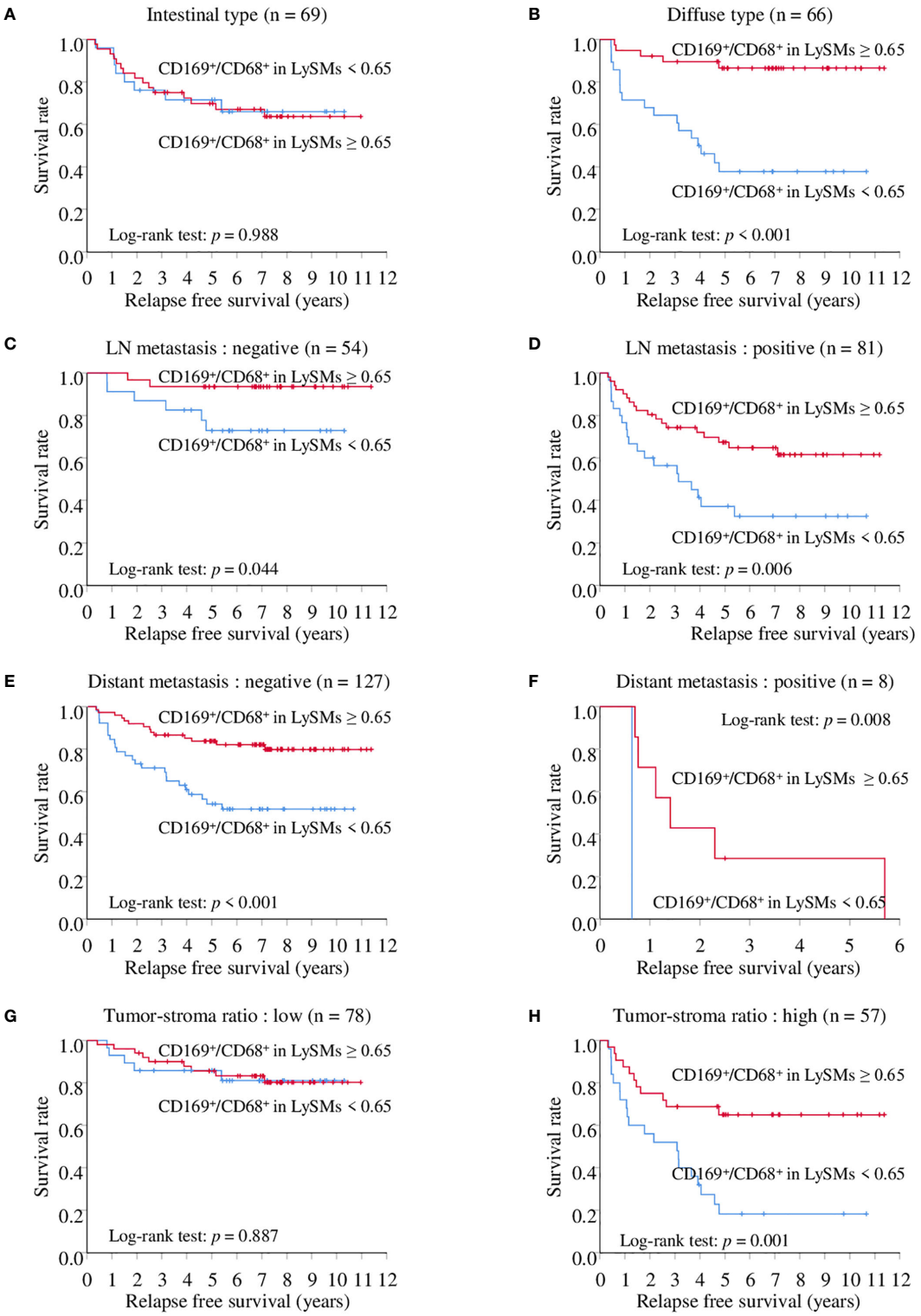

FIGURE 6 | Kaplan-Meier relapse free survival (RFS) curves of $CD169^+/CD68^+$ ratios in lymph node sinus macrophages (LySMs) of advanced gastric cancer patients with various tumor subtypes: intestinal type **(A)** and diffuse type **(B)**; lymph node (LN) metastasis negative **(C)** and positive **(D)**; distant metastasis negative **(E)** and positive **(F)**, tumor-stroma ratio; low **(G)** and high **(H)**.

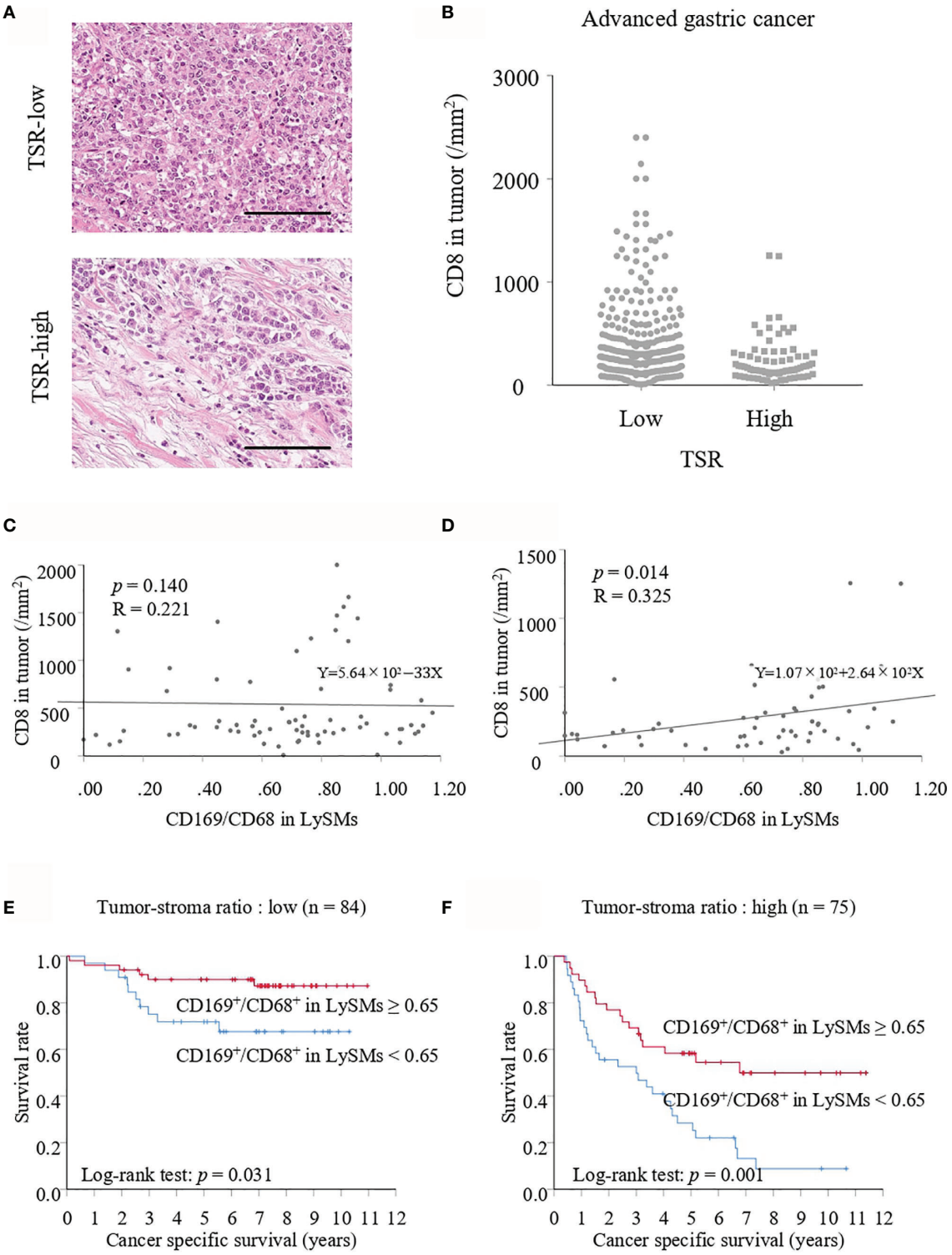

FIGURE 7 | **(A)** Hematoxylin and eosin staining of tumor-stroma ratio (TSR)- low and high. Scale bar = 100 μm. **(B)** Number of $CD8^+$ T cells in TSR-low or high advanced cancer tissues. Correlation between the number of $CD8^+$ T cells in TSR-low or high tumor tissues and the CD169/CD68 ratio in lymph node sinus macrophages (LySMs) were tested by Spearman's correlation test. Scatter plot in TSR-low advanced gastric cancer cases **(C)** and in TSR-high advanced gastric cancer cases **(D)** were shown. **(E)** Kaplan-Meier cancer-specific survival (CSS) curves in patients with TSR-low advanced gastric cancer. **(F)** Kaplan-Meier CSS curves in patients with TSR-high advanced gastric cancer.

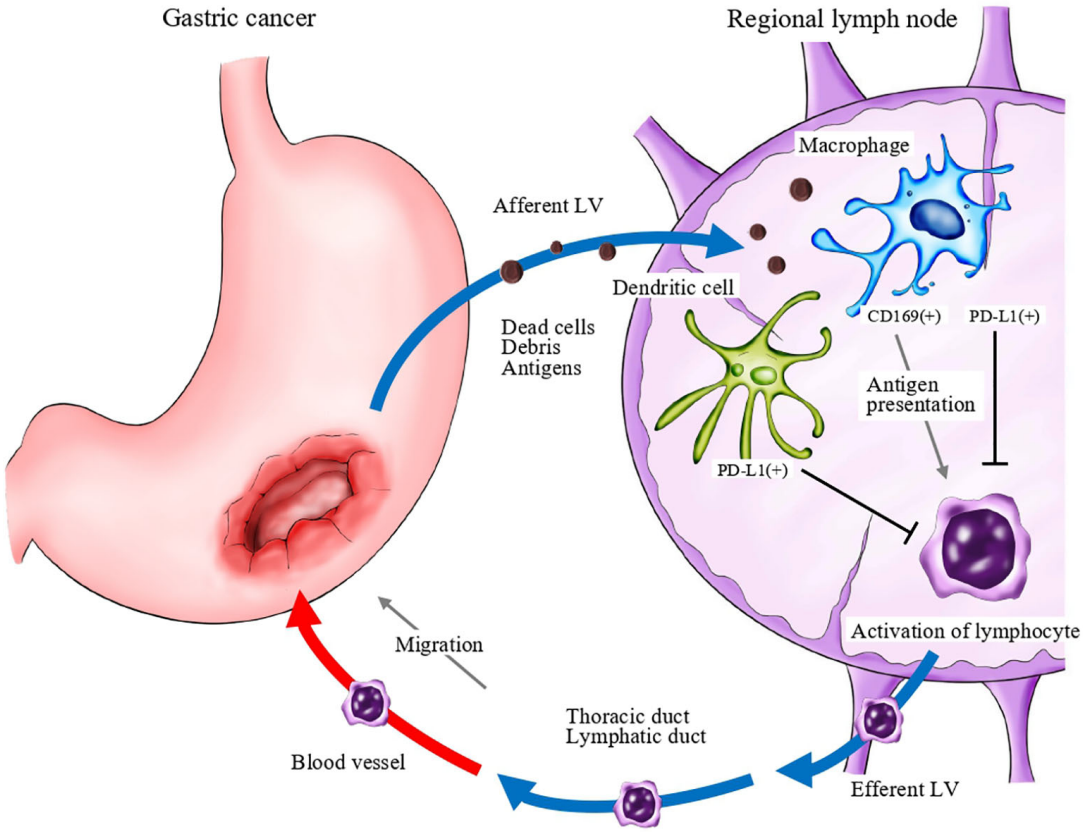

FIGURE 8 | A schema of the anti-cancer immune response associated with regional lymph nodes. Dead cells and debris, including tumor-specific antigens, drain into lymph node sinuses *via* lymphatic vessels (LV). Antigen-presenting cells, such as macrophages and dendritic cells, capture and engulf these antigens and activate antigen-reactive T lymphocytes. Programmed death ligand 1 (PD-L1; and potentially PD-L2) expressed on antigen-presenting cells may negatively regulate the activation of T lymphocytes.

immune responses. In addition, CD169 expression in LySMs as well as the density of TILs were identified as independent prognostic factors in the multivariate analysis. The evaluation of CD169 in RLNs might enable us to predict the anti-cancer immune responses in gastric cancer.

DATA AVAILABILITY STATEMENT

The original contributions presented in the study are included in the article/supplementary material. Further inquiries can be directed to the corresponding author.

ETHICS STATEMENT

The studies involving human participants were reviewed and approved by Ethics Committee of Medical Research, University of Occupational and Environmental Health, Japan. The patients/participants provided their written informed consent to participate in this study.

AUTHOR CONTRIBUTIONS

KK, KO and YK designed the study. KK and YK executed experimental work. KK, TT, KO, SS, YK and TN analyzed and interpreted data. KK, MS and YK performed the statistical analysis. KK drafted the manuscript. All authors contributed to the article and approved the submitted version.

FUNDING

This work was supported by grants from the Ministry of Education, Culture, Sports, Science and Technology of Japan (Nos. 18K06991) and Takeda Science Foundation.

ACKNOWLEDGMENTS

We thank Ms. Hana Nishimura and Ms. Rie Soeda for their technical assistance.

REFERENCES

1. Fitzmaurice C, Abate D, Abbasi N, Abbastabar H, Abd-Allah F, Abdel-Rahman O, et al. Global, regional, and national cancer incidence, mortality, years of life lost, years lived with disability, and disability-Adjusted life-years for 29 cancer groups, 1990 to 2017: A systematic analysis for the global burden of disease study. *JAMA Oncol* (2019) 5(12):1749–68. doi: 10.1001/jamaoncol.2019.2996
2. Lee HE, Chae SW, Lee YJ, Kim MA, Lee HS, Lee BL, et al. Prognostic implications of type and density of tumour-infiltrating lymphocytes in gastric cancer. *Br J Cancer* (2008) 99(10):1704–11. doi: 10.1038/sj.bjc.6604738
3. Kondratiev S, Sabo E, Yakirevich E, Lavie O, Resnick MB. Intratumoral CD8+ T lymphocytes as a prognostic factor of survival in endometrial carcinoma. *Clin Cancer Res* (2004) 10(13):4450–6. doi: 10.1158/1078-0432.CCR-0732-3
4. Sharma P, Shen Y, Wen S, Yamada S, Jungbluth AA, Gnjatic S, et al. CD8 tumor-infiltrating lymphocytes are predictive of survival in muscle-invasive urothelial carcinoma. *Proc Natl Acad Sci U.S.A.* (2007) 104(10):3967–72. doi: 10.1073/pnas.0611618104
5. Baker K, Lachapelle J, Zlobec I, Bismar TA, Terracciano L, Foulkes WD. Prognostic significance of CD8+ T lymphocytes in breast cancer depends upon both oestrogen receptor status and histological grade. *Histopathology* (2011) 58(7):1107–16. doi: 10.1111/j.1365-2559.2011.03846.x
6. Lu J, Xu Y, Wu Y, Huang XY, Xie JW, Bin WJ, et al. Tumor-infiltrating CD8+ T cells combined with tumor-associated CD68+ macrophages predict postoperative prognosis and adjuvant chemotherapy benefit in resected gastric cancer. *BMC Cancer* (2019) 19(1):1–10. doi: 10.1186/s12885-019-6089-z
7. Gray EE, Cyster JG. Lymph node macrophages. *J Innate Immun* (2012) 4:424–36. doi: 10.1159/000337007
8. Chen DS, Mellman I. Oncology meets immunology: The cancer-immunity cycle. *Immunity* (2013) 39(1):1–10. doi: 10.1016/j.immuni.2013.07.012
9. Steinman RM. Decisions about dendritic cells: Past, present, and future.s. *Annu Rev Immunol* (2012) 30:1–22. doi: 10.1146/annurev-immunol-100311-102839
10. Gasteiger G, Ataide M, Kastenmüller W. Lymph node - An organ for T-cell activation and pathogen defense. *Immunol Rev* (2016) 271(1):200–20. doi: 10.1111/imr.12399
11. Martinez-Pomares L, Gordon S. CD169 + macrophages at the crossroads of antigen presentation. *Trends Immunol* (2012) 33(2):66–70. doi: 10.1016/j.it.2011.11.001
12. Nath D, Hartnell A, Happerfield L, Miles DW, Burchell J, Taylor-Papadimitriou J, et al. Macrophage-tumour cell interactions: Identification of MUC1 on breast cancer cells as a potential counter-receptor for the macrophage-restricted receptor, sialoadhesin. *Immunology* (1999) 98 (2):213–9. doi: 10.1046/j.1365-2567.1999.00827.x
13. van den Berg TK, Nath D, Ziltener HJ, Vestweber D, Fukuda M, van Die I, et al. Cutting Edge: CD43 Functions as a T Cell Counterreceptor for the Macrophage Adhesion Receptor Sialoadhesin (Siglec-1). *J Immunol* (2001) 166(6):3637–40. doi: 10.4049/jimmunol.166.6.3637
14. Klaas M, Crocker PR. Sialoadhesin in recognition of self and non-self. *Semin Immunopathol* (2012) 34(3):353–64. doi: 10.1007/s00281-012-0310-3
15. Hartnell A, Steel J, Turley H, Jones M, Jackson DG, Crocker PR. Characterization of human sialoadhesin, a sialic acid binding receptor expressed by resident and inflammatory macrophage populations. *Blood* (2001) 97(1):288–96. doi: 10.1182/blood.v97.1.288
16. Liu Y, Xia Y, Qiu CH. Functions of cd169 positive macrophages in human diseases (Review). *BioMed Rep* (2021) 14(2):1–9. doi: 10.3892/br.2020.1402
17. Komohara Y, Harada M, Ohnishi K, Kumamoto K, Nakayama T. PD-L1 expression in regional lymph nodes and predictable roles in anti-cancer immune responses. *J Clin Exp Hematop* (2020) 60(3):113–6. doi: 10.3960/jslrt.20015
18. Asano K, Nabeyama A, Miyake Y, Qiu CH, Kurita A, Tomura M, et al. CD169-Positive Macrophages Dominate Antitumor Immunity by Crosspresenting Dead Cell-Associated Antigens. *Immunity* (2011) 34(1):85–95. doi: 10.1016/j.immuni.2010.12.011
19. Bernhard CA, Ried C, Kochanek S, Brocker T. CD169+ macrophages are sufficient for priming of CTLs with specificities left out by cross-priming dendritic cells. *Proc Natl Acad Sci U S A* (2015) 112(17):5461–6. doi: 10.1073/pnas.1423356112
20. Strömvall K, Sundkvist K, Ljungberg B, Halin Bergström S, Bergh A. Reduced number of CD169+ macrophages in pre-metastatic regional lymph nodes is associated with subsequent metastatic disease in an animal model and with poor outcome in prostate cancer patients. *Prostate* (2017) 77(15):1468–77. doi: 10.1002/pros.23407
21. Ohnishi K, Komohara Y, Saito Y, Miyamoto Y, Watanabe M, Baba H, et al. CD169-positive macrophages in regional lymph nodes are associated with a favorable prognosis in patients with colorectal carcinoma. *Cancer Sci* (2013) 104(9):1237–44. doi: 10.1111/cas.12212
22. Komohara Y, Ohnishi K, Takeya M. Possible functions of CD169-positive sinus macrophages in lymph nodes in anti-tumor immune responses. *Cancer Sci* (2017) 108(3):290–5. doi: 10.1111/cas.13137
23. Saito Y, Ohnishi K, Miyashita A, Nakahara S, Fujiwara Y, Horlad H, et al. Prognostic significance of CD169+ lymph node sinus macrophages in patients with malignant melanoma. *Cancer Immunol Res* (2015) 13(12):1356–63. doi: 10.1158/2326-6066.CIR-14-0180
24. Zhou ZH, Ji CD, Zhu J, Xiao HL, Bin ZH, YH C, et al. The prognostic value and pathobiological significance of Glasgow microenvironment score in gastric cancer. *J Cancer Res Clin Oncol* (2017) 143(5):883–94. doi: 10.1007/s00432-017-2346-1
25. Lee D, Ham IH, Son SY, Han SU, Kim YB, Hur H. Intratumor stromal proportion predicts aggressive phenotype of gastric signet ring cell carcinomas. *Gastric Cancer* (2017) 20(4):591–601. doi: 10.1007/s10120-016-0669-2
26. Kemi N, Eskuri M, Herva A, Leppänen J, Huhta H, Helminen O, et al. Tumour-stroma ratio and prognosis in gastric adenocarcinoma. *Br J Cancer* (2018) 119(4):435–9. doi: 10.1038/s41416-018-0202-y
27. Nakagawa T, Ohnishi K, Kosaki Y, Saito Y, Horlad H, Fujiwara Y, et al. Optimum immunohistochemical procedures for analysis of macrophages in human and mouse formalin fixed paraffin-embedded tissue samples. *J Clin Exp Hematop* (2017) 57(1):31–6. doi: 10.3960/jslrt.17017
28. Ohnishi K, Yamaguchi M, Erdenebaatar C, Saito F, Tashiro H, Katabuchi H, et al. Prognostic significance of CD169-positive lymph node sinus macrophages in patients with endometrial carcinoma. *Cancer Sci* (2016) 107(6):846–52. doi: 10.1111/cas.12929
29. Takeya H, Shiota T, Yagi T, Ohnishi K, Baba Y, Miyasato Y, et al. High CD169 expression in lymph node macrophages predicts a favorable clinical course in patients with esophageal cancer. *Pathol Int* (2018) 68(12):685–93. doi: 10.1111/pin.12736
30. Asano T, Ohnishi K, Shiota T, Motoshima T, Sugiyama Y, Yatsuda J, et al. CD169-positive sinus macrophages in the lymph nodes determine bladder cancer prognosis. *Cancer Sci* (2018) 109(5):1723–30. doi: 10.1111/cas.13565
31. Zou W, Wolchok JD, Chen L. PD-L1 (B7-H1) and PD-1 pathway blockade for cancer therapy. *Sci Transl Med* (2016) 8(328):1–34. doi: 10.1126/scitranslmed.aad7118
32. Kang YK, Boku N, Satoh T, Ryu MH, Chao Y, Kato K, et al. Nivolumab in patients with advanced gastric or gastro-oesophageal junction cancer refractory to, or intolerant of, at least two previous chemotherapy regimens (ONO-4538-12, ATTRACTION-2): a randomised, double-blind, placebo-controlled, phase 3 trial. *Lancet* (2017) 390(10111):2461–71. doi: 10.1016/S0140-6736(17)31827-5
33. Yamazaki T, Akiba H, Iwai H, Matsuda H, Aoki M, Tanno Y, et al. Expression of Programmed Death 1 Ligands by Murine T Cells and APC. *J Immunol* (2002) 169(10):5538–45. doi: 10.4049/jimmunol.169.10.5538
34. Ishida M, Iwai Y, Tanaka Y, Okazaki T, Freeman GJ, Minato N, et al. Differential expression of PD-L1 and PD-L2, ligands for an inhibitory receptor PD-1, in the cells of lymphohematopoietic tissues. *Immunol Lett* (2002) 84(1):57–62. doi: 10.1016/s0165-2478(02)00142-6
35. Curiel TJ, We S, Dong H, Alvarez X. Blockade of B7-H1 improves myeloid dendritic cell–mediated antitumor immunity. *Nat Med* (2003) 9(5):562–7. doi: 10.1038/nm863
36. Quail D, Joyce J. Microenvironmental regulation of tumor progression and metastasis DF. *Nat Med* (2013) 19(11):1423–37. doi: 10.1038/nm.3394
37. Wu J, Liang C, Chen M, Su W. Association between tumor-stroma ratio and prognosis in solid tumor patients: A systematic review and meta-analysis. *Oncotarget* (2016) 7(42):68954–65. doi: 10.18632/oncotarget.12135

38. Marsh T, Pietras K, McAllister SS. Fibroblasts as architects of cancer pathogenesis. *Biochim Biophys Acta* (2013) 1832(7):1070–8. doi: 10.1016/j.bbadis.2012.10.013

Conflict of Interest: The authors declare that the research was conducted in the absence of any commercial or financial relationships that could be construed as a potential conflict of interest.

frontiers in Oncology

ORIGINAL RESEARCH
published: 12 April 2021
doi: 10.3389/fonc.2021.646979

The Efficacy and Safety of Apatinib Plus Camrelizumab in Patients With Previously Treated Advanced Biliary Tract Cancer: A Prospective Clinical Study

Dongxu Wang[1†], Xu Yang[1†], Junyu Long[1†], Jianzhen Lin[1], Jinzhu Mao[1], Fucun Xie[1], Yunchao Wang[1], Yanyu Wang[1], Ziyu Xun[1], Yi Bai[1], Xiaobo Yang[1], Mei Guan[2], Jie Pan[3], Samuel Seery[4,5], Xinting Sang[1] and Haitao Zhao[1]*

[1] Department of Liver Surgery, State Key Laboratory of Complex Severe and Rare Disease, Peking Union Medical College Hospital, Chinese Academy of Medical Sciences and Peking Union Medical College, Beijing, China, [2] Department of Medical Oncology, Peking Union Medical College Hospital, Chinese Academy of Medical Sciences and Peking Union Medical College, Beijing, China, [3] Department of Radiology, Peking Union Medical College, Chinese Academy of Medical Sciences and Peking Union Medical College, Beijing, China, [4] Department of Humanities and Social Sciences, Peking Union Medical College, Chinese Academy of Medical Sciences and Peking Union Medical College, Beijing, China, [5] Faculty of Health and Medicine, Division of Health Research, Lancaster University, Lancaster, United Kingdom

Background: PD-1/L1 inhibitor-based immunotherapy is currently under investigation in biliary tract cancer (BTC). Apatinib combined with camrelizumab has achieved promising results in various tumor types. The aim of this study was to assess the safety and efficacy of apatinib plus camrelizumab for advanced biliary tract cancer patients who have received previously treatments.

Methods: This prospective, non-randomized, open-label trial was conducted at Peking Union Medical College Hospital (PUMCH). All included patients received apatinib orally at 250 mg per a day and camrelizumab intravenously at 200 mg every three weeks until disease progression or intolerable toxicity occurred. Efficacy was evaluated based on the Response Evaluation Criteria in Solid Tumors RECIST Version 1.1 (RECIST 1.1). Adverse events (AEs) were assessed by the National Cancer Institute Common Terminology Criteria for Adverse Events (CTCAE version 4.0).

Results: A total of 22 patients were consecutively enrolled from 1st December, 2018 until 1st August, 2020. Among 21 patients for whom we could conduct efficacy evaluations, no patients achieved a complete response (CR), 4 patients (19%) achieved partial response (PR), and 11 patients had stable disease with a disease control rate of 71.4%. The median overall survival was 13.1 months (95% CI, 8.1-18.2), and the median progression-free survival was 4.4 months (95% CI, 2.4-6.3). All patients experienced treatment related AEs, and grade 3 or 4 AEs occurred in 14 (63.6%) of 22 patients. No treatment related deaths were observed.

OPEN ACCESS

Edited by:
Maria L. Martinez Chantar, CIC bioGUNE, Spain

Reviewed by:
Matias Antonio Avila, University of Navarra, Spain
Naminatsu Takahara, The University of Tokyo Hospital, Japan

***Correspondence:**
Haitao Zhao
ZhaoHT@pumch.cn

†These authors have contributed equally to this work

Specialty section:
This article was submitted to Cancer Immunity and Immunotherapy, a section of the journal Frontiers in Oncology

Received: *28 December 2020*
Accepted: *18 March 2021*
Published: *12 April 2021*

Citation:
Wang D, Yang X, Long J, Lin J, Mao J, Xie F, Wang Y, Wang Y, Xun Z, Bai Y, Yang X, Guan M, Pan J, Seery S, Sang X and Zhao H (2021) The Efficacy and Safety of Apatinib Plus Camrelizumab in Patients With Previously Treated Advanced Biliary Tract Cancer: A Prospective Clinical Study. Front. Oncol. 11:646979. doi: 10.3389/fonc.2021.646979

Conclusions: This is the first report focusing on the efficacy and safety of camrelizumab plus apatinib in pretreated biliary tract cancer patients. The finding suggests this regimen has favorable therapeutic effects with relatively manageable toxicity. Further trials with a control arm are required to investigate.

Clinical Trial Registration: identifier NCT04642664.

Keywords: apatinib, camrelizumab (SHR-1210), advanced biliary tract cancer, combination therapy, PD-1/L1 blockade, target therapy, immunotherapy, cholangiocarcinoma

INTRODUCTION

Biliary tract cancers (BTCs) are a heterogeneous group of cancers derived from the epithelial cells lining the biliary tree, which generally divided into intrahepatic and extrahepatic cholangiocarcinomas (ICC, ECC) and gallbladder cancers (GBC) (1). Even though BTC are traditionally regarded as rare malignant neoplasms, it is the second most common primary liver tumor and accounts for approximately 10%-15% of all hepatobiliary malignancies (2). Consistent with other gastrointestinal neoplasms, radical surgery with negative resection margins is the only potentially curative therapy. However, approximately 60-70% patients are diagnosed at late disease stages and are ineligible for surgical resection (3). Moreover, the treatment regimens for advanced BTC patients are extremely scarce with limited efficacy. Only a few chemotherapies including gemcitabine plus cisplatin or another platinum derivative have been approved as first-line interventions, with only modest efficacy, and there are no consensus standard regimens for second-line and later therapy (4, 5). Given these factors, effective treatments are needed to fill in gaps in current BTC treatment approaches and prolong the survival of patients (6).

Programmed cell death protein 1 or ligand 1 (PD-1/L1) blockades are relatively novel therapeutics which have been tested for a variety of tumors and have found to have robust, durable antitumor activity. However, the efficacy of PD-1/L1 inhibitor monotherapy in gastrointestinal malignancies is not ideal owing to the complex tumor microenvironment, for example the presence of abundant fibrotic stroma that surrounds and infiltrates the tumor structures can hinder the antitumor functions of T cells (7). For BTCs, the objective response rate (ORR) of PD-1 blockade monotherapy is approximately 4%-18%, although accumulating findings demonstrate patients with cholangiocarcinoma with specific pathological and genomic characteristics might benefit from immunotherapy (8, 9). As such, immunotherapeutic research in this field has tended to focus on seeking combinations which destroy stroma while promoting tumor antigens presentation and enabling immune recognition (7). With the substantial progress in research regarding the tumorigenesis and genetic landscape of BTCs, targeted drugs including multiple small-molecule tyrosine kinase inhibitors are also being actively explored. Current evidence indicates that 53% intrahepatic cholangiocarcinoma harbor vascular endothelial growth factor (VEGF) overexpression which is related to poorer prognosis (10). Preclinical models appear to suggest that agents targeting VEGF, FEGF, EGFR and other signaling pathways can convert the tumor microenvironment and reprogram the immune responses to suppress tumorigenesis (11).

Apatinib, a multitarget tyrosine kinase inhibitor (TKI) that selectively inhibits VEGFR-2, has proven beneficial for various solid tumors including gastric cancer and hepatocellular carcinoma (12). A small sample study of patients with unresectable intrahepatic cholangiocarcinoma revealed that apatinib has manageable toxicities with a median progression-free survival (PFS) of 4.5 months and overall survival (OS) of 6.5 months (13). Meanwhile, another study include patients with primary liver cancer showed that apatinib achieved 16% ORR (14). Camrelizumab (SHR-1210), a PD-1 inhibitor, has been shown to block the binding of PD-1 to PD-L1 and consequently inhibit the immune escape of tumour cells. Therefore, considering the potential synergistic efficacy of targeted therapy combined with immune checkpoint inhibitor, apatinib plus camrelizumab might be a potentially effective combination for various tumors (15). For patients with advanced HCC, apatinib combined with camrelizumab achieved a 34.3% objective response as the first-line and 22.5% as the second-line therapy (16). Similar results were also observed in osteosarcoma, gastric cancer, advanced triple-negative breast cancer and a variety of other tumors (17–19). Nevertheless, thus far, no studies have reported results regarding this regimen in patients with BTC. As such, we conducted this prospective clinical trial to evaluate the efficacy and safety of apatinib in previously treated patients with advanced BTC in hopes of providing an alternative treatment regimen.

Abbreviations: HCC, hepatocellular carcinoma; AE, adverse event; PFS, progression free survival; HR, hazard ratio; CI, confidence interval; BCLC, Barcelona Clinic Liver Cancer; AFP, alpha-fetoprotein; HBV, hepatitis B virus; OS, overall survival; ORR, objective response rate; TTP, time-to-progression; RCT, randomized controlled trials; DCR, disease control rate; RDI, relative dose intensity; TACE, transarterial chemoembolization; HCV, hepatitis C virus; RECIST 1.1, Response Evaluation Criteria in Solid Tumours version 1.1; CR, complete response; PR, partial response; SD, stable disease; PD, progressive disease; CTCAE, common terminology criteria for adverse events; HBsAg, hepatitis B virus surface antigen; ECOG-PS, Eastern Cooperative Oncology Group performance status; ALBI, albumin-bilirubin; K-M, Kaplan-Meier; OR, odds ratios; EHS, extrahepatic spread; PVT, portal vein thrombus; MVI, macrovascular invasion; TKI, tyrosine kinase inhibitors; FGFR, fibroblast growth factor receptor; FGF, fibroblast growth factor; VEGF, vascular endothelial growth factor.

METHODS

Study Design and Participants

This was a prospective, single institution, open-label, nonrandomized trial designed to evaluate the efficacy and safety of apatinib in combination with camrelizumab for advanced BTC patients. The study protocol adhered to the principles of the Declaration of Helsinki and was approved by the Institutional Review Board and Ethics Committee of Peking Union Medical College Hospital (PUMCH-JS-2160). The clinical trial is registered at ClinicalTrials.gov (NCT04642664).

All patients were required to provided written informed consent before participating. Patients were enrolled from 1st December, 2018 until 1st August, 2020. The primary inclusion criteria were patients older than 18 years with either histologically or cytologically confirmed BTC diagnosis, including ICC, ECC and GBC. The patients had at least one measurable tumor lesion at baseline per the Response Evaluation Criteria in Solid Tumors, version 1.1 (RECIST v1.1) and had received at least a previous systemic anti-tumor therapy. Patients had Child Pugh A or B liver function status (score ≤7) and presented with an Eastern Cooperative Oncology Group performance status (ECOG PS) value of 0-2.

The exclusion criteria mainly included intolerance to apatinib or PD-1 blockade, life expectancy of ≤3 months and inadequate organ function including Child-Pugh liver function class C, active or prior autoimmune disease, concurrent use of immunosuppressive medicaments and other contraindicators associated with apatinib or camrelizumab. Patients with severe esophageal varices or those who presented with positive fecal occult blood were also excluded. The detailed study criteria are available in the Supplement.

Assessment of Efficacy and Treatment Related Adverse Events (AEs)

Patients received apatinib orally at 250 mg per day, irrespective of body mass. During treatment, apatinib could be reduced to a half dose or administered once every other day considering the grade of treatment-related AEs. Camrelizumab was administered intravenously at a dosage of 200mg over 30 minutes every 3 weeks. The interruption period of camrelizumab was no longer than six weeks. All patients continued combination treatment until disease progression, unacceptable toxicity or discontinuation for any reasons.

Tumor were assessed using enhanced computed tomography, magnetic resonance imaging (MRI) or other available imaging technologies at baseline and every 4-8 weeks until disease progression or treatment discontinuation. The therapeutic efficacy assessment included the ORR, disease control rate (DCR), PFS, OS and clinical benefit rate (CBR) according to RECIST 1.1. The CBR was defined as the proportion of patients who achieved a radiologically confirmed objective response (CR or PR) or those who encountered stable disease longer than 6 months. Patients who had progressive disease could continue treatment, if the investigator determined patients would benefit from continuing. When patients discontinued treatment, follow-up was conducted every month to assess survival.

During the observation period, tolerability and toxicity were collected in detail and assessed according to the National Cancer Institute Common Terminology Criteria for Adverse Events version 4.0 (CTCAE 4.0). Patients who received at least one dose of camrelizumab plus apatinib were included in the safety assessment set, and AEs were collected until 30 days after the last dose. According to the study protocol, when grade 3 or more severe AEs occurred, dose reduction was implemented or a temporary interruption commenced until symptoms subsided to pharmaceutically manageable grades 1 or 2. Patients with grade 3 or more severe AEs were followed up to 90 days after the lase dose or until the new anticancer treatment.

Multivariate Analysis of Characteristics and Therapeutic Response Predictions

Baseline characteristics including age, sex, hepatitis B virus (HBV) infection status, ECOG performance score, histopathological grade, site of metastases and number of previous treatments were analyzed using multivariate method to explore the potential factors affecting PFS or OS. Patients who were evaluated as having stable disease were further divided into two groups: those with a reduction in tumor size and those with an increase in tumor size. Carbohydrate antigen 19-9 (CA19-9) values were recorded before and after treatment within first evaluation period to develop response predictions for tumor size changes. On the basis of the previous studies, patients who are Lewis-antigen-negative (7% of the general population) have undetectable CA 19–9 levels. If patient's CA199 level was within the normal range before and after treatment, we excluded these patients from the further analysis.

In addition, we assessed PD-L1 expression in this BTC population. Tumor tissue samples for analyzing PD-L1 expression were collected from patients. Preserved tumor specimens were formalin-fixed, paraffin-embedded (FFPE) and then cut into 4-5 μm thick sections for further staining. The primary antibody used was anti-PD-L1 (IHC 22C3 pharmDx, Dako North America, Agilent Technologies). Specimens in which PD-L1 was expressed in 1% or more tumor cells and 1% or more tumor-associated immune cells were defined as positive for PD-L1 expression.

Statistical Analysis

Baseline data were calculated and presented as the means with corresponding standard deviations or as simple numbers and percentages. Categorical variables in the different subgroups were compared using the Fisher's exact test. The Kaplan-Meier method was applied to generate PFS and OS curves, and the log-rank test was used to compare curves from different PD-L1 expression subgroups. Two tailed P values of less than 0.05 were considered to be indicative of statistical significance. Sensitivity was calculated as the number of correctly classified divided by total true decreased individuals, and specificity was calculated as the number of true negatives divided by all non-decreased individuals. Univariate and multivariate analysis of baseline characteristics for overall survival and progression-free survival were conducted by Cox proportional hazards regression. All statistical analyses were performed using IBM SPSS 22.0 and R software (version 3.6.5).

RESULTS

Patients Characteristics

From December 01, 2018 to August 01, 2020, the study totally evaluated 28 patients and six patients were excluded according to the inclusion criteria; at last, 22 patients were consecutively enrolled for drug administration, one patient was excluded from the study due to the lack of necessary evaluations (**Figure 1**). The median patient age was 58 years (range, 39-72) and 11 patients (52%) were male. Most patients (16 [76.2%]) had an Eastern Cooperative Oncology Group performance status of 1 and 7 patients (33.3%) presented with HBV infection. Fifteen patients (71%) had intrahepatic cholangiocarcinoma, 4 patients (19%) had extrahepatic cholangiocarcinoma, and 2 (9%) patients had gallbladder cancer. Regarding the histopathological grade of cholangiocarcinoma, 4 patients (19%) had undetermined grade, eight patients (38.1%) had poorly differentiated tumors, seven patients (33.3%) had moderately differentiated tumors, and two patients (9.5%) had well differentiated tumors. Of the 21 patients, 20 patients (95.2%) presented with metastatic disease, and 12 patients (57.2%) experienced recurrence after radical resection. Regarding the site of metastases, most patients (17, 80.9%) had intrahepatic or lymph nodes metastases, and the lung metastases occurred in 8 patients (38.1%). Twenty patients (95.2%) underwent systemic chemotherapy, and 10 patients (47.6%) received at least two kinds of treatment regimens. In addition, CA19-9 levels exceeding 150 ng/ml were observed in twelve patients (57.1%) (**Table 1**).

Assessment of Efficacy and AEs During the Entire Treatment Period

Among the 21 patients who had evaluation data with imaging examination, ten patients (47%) exhibited a reduction in tumor size as the best response during the treatment period, while 11 patients (52%) exhibited an increase in tumor size, of which two patients experienced new lesions (**Figure 2**). According to the RECIST 1.1, no CR was observed, 4 patients (19%) achieved a partial response (PR) with an ORR of 19%, and 11 patients had stable disease with a DCR of 71.4% (**Table 2**). An objective response was observed in 3 of 15 patients (25%) with intrahepatic cholangiocarcinoma, and a PR was observed in one patient with gallbladder cancer. As of the data cut-off date of August 01, 2020, the median duration of follow-up was 13.4 months (IQR 11.9-14.8), the median duration of treatment was 4.9 (IQR, 3.8-5.9) months, and 4 (19%) of 21 patients were still receiving treatment (**Table 3**). In the entire cohort, the median OS was 13.1 months (95% CI, 8.1-18.2), and the median PFS was 4.4 months (95% CI, 2.4-6.3) (**Figure 1**).

The observed treatment-related AEs are summarized in **Table 4**. All patients experienced at least one kind of adverse event, and grade 3 or 4 AEs occurred in 14 (63.6%) of 22 patients. The most common treatment-related AEs of any grade were asthenia (15, 68.2%), decreased appetite (10, 45.5%) and hypertension (7, 31.8%). The most common grade 3 or 4 AEs were hypertension (3, 13.6%), blood bilirubin increase (3, 13.6%) and platelet count decrease (3, 13.6%). Eighteen patients (81.8%) experienced treatment interruption or modification and three patients (13.6%)

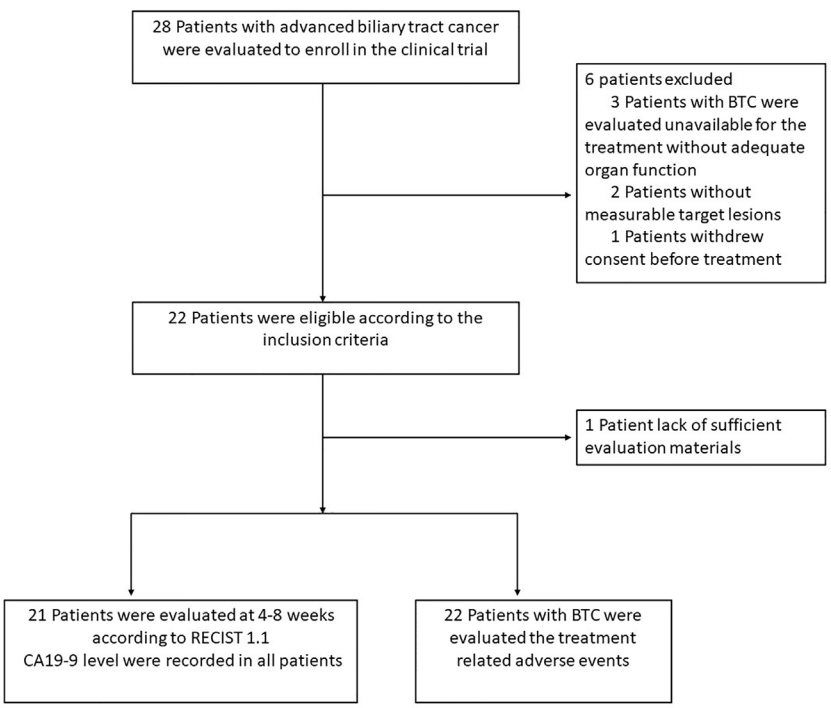

FIGURE 1 | Flow diagram of study population.

TABLE 1 | Patient baseline demographics and disease characteristics.

	ALL (n=21)
Age (median, range)	60 (39-72)
Sex (female: male)	10:11
BMI (mean (SD))	23 (3.5)
Hepatitis (HBV) infection n, (%)	7 (33.3)
ECOG performance n, (%)	
0	2 (9.5)
1	16 (76.2)
2	3 (14.3)
Tumor subtype n, (%)	
ICC	15 (71.4)
ECC	4 (19.0)
GBC	2 (9.5)
Histopathologyical grade	
Well differentiated (low grade)	2 (9.5)
Moderately differentiated (intermediate grade)	7 (33.3)
Poorly differentiated (high grade)	8 (38.1)
Unable to determine	4 (19.0)
Extent of disease n, (%)	
Metastatic	20 (95.2)
Recurrent	12 (57.2)
Site of Metastases n, (%)	
Intrahepatic	17 (80.9)
Lymph nodes	17 (80.9)
Lung	8 (38.1)
Others	5 (23.8)
Number of previous treatment regimens n, (%)	
1	11 (52.4)
≥2	10 (47.6)
Previous treatment regimens n, (%)	
Systemic chemotherapy	20 (95.2)
Targeted therapy	6 (28.6)
Regional radiotherapy or ablation	5 (23.8)
Transarterial chemoembolization	5 (23.8)
CA19-9> 150 n, (%)	12 (57.1)
Size of target lesion (mean (SD)	7.3 (3.5)

BMI, body mass index; ECOG, Eastern Cooperative Oncology Group; HBV, hepatitis type B virus; CA19-9, carbohydrate antigen 19-9; ICC, intrahepatic cholangiocarcinoma; ECC, extrahepatic cholangiocarcinoma; GBC, gallbladder cancer.

discontinued combination therapy due to treatment related AEs. No deaths related to treatment were observed.

Subgroup Analyses and Therapeutic Response Predictions

Among 21 available tumor samples, 4 patients (19%) were positive for PD-L1 staining in tumor cells or immune cells (**Figure 3**). Of the four PD-L1-positive patients, three patients experienced tumor reduction, but only one patient had experienced PR. Median PFS and OS were not significantly different (p=0.58, p=0.83) between the patients with PD-L1 expression ≥1% and those with PD-L1 expression <1% (**Figure 4**). Although the limited sample in current study, considering the heterogeneity of biliary tract cancer, we analyzed the efficacy and safety of different tumor subtypes. The results showed that there was no significant difference among intrahepatic cholangiocarcinoma, extrahepatic cholangiocarcinoma and gallbladder carcinoma regarding the ORR ($\chi 2 = 2.666$, p=0.264), grade 3-4 AEs ($\chi 2 = 0.649$, p=0.723) and PFS (p=0.958), OS (p=0.725) (**Supplement Table 1**). The Cox-regression analysis results regarding the relationship between baseline characters and PFS or OS were summarized in the forest plot (**Figure 5**) and **Supplement Table 2**. The CA19-9 serum value decreased in 10 patients (47.6%) after treatment (**Supplement Table 3**). The decrease in CA19-9 value was able to predict the tumor size reduction with a sensitivity and specificity of 63.6% and 66.7%, respectively.

DISCUSSION

Currently, the exploration of immune monotherapy faces many challenges in terms of various gastrointestinal malignancies. The efficacy of PD-1/L1 inhibitor monotherapy in BTC remains significantly uncertainty (ORR range 3%-22%) (20). Combining PD1/L1 inhibitor with other available anticancer therapies can improve the efficacy of immunotherapies has reached a general consensus (7). In the Makoto et al. study, only one of 30 patients who received nivolumab monotherapy achieved an objective response, with a median OS of 5.2 months and a median PFS of 1.4 months. However, in the combined therapy cohort (nivolumab and cisplatin plus gemcitabine), 11 of 30 patients achieved an objective response, the median OS and PFS were 15.4 months and 4.2 months, respectively (21). In this study, apatinib in combination with camrelizumab also showed a potent efficacy in terms of the ORR, PFS and OS and had manageable toxicity. This is the first report of this regimen in advanced BTC, and these results were superior to the previously reported efficacy of apatinib alone in BTC (13, 14).

Although camrelizumab combined with apatinib has achieved promising results in the treatment of various tumors, including hepatocellular carcinoma, osteosarcoma and triple-negative breast cancer, this regimen has not been reported in cholangiocarcinoma (16, 17, 19). Currently, most trials combining multitarget TKIs with PD-1 blockade for BTC are in the recruitment phase, and few studies have reported detailed results. A study evaluating lenvatinib plus pembrolizumab as a non-first-line treatment in 32 patients with advanced BTC demonstrated that the ORR could reach 25% with a PFS of 4.9 months (95% CI: 4.7-5.2) and OS of 11.0 months (95% CI: 9.6-12.3) (22). In this study, almost all the patients (95.2%) were previously treated with at least one kind of systemic chemotherapy, and 47.6% of patients had received two or more anticancer treatments, which demonstrated that the population of this study was not similar to that of other previous studies regarding immunotherapy for BTC. In spite of this, 19% patients in this study achieved a partial response with a favorable survival. 42.8% patients who were confirmed progressive disease continued other immunotherapy or targeted drugs, which might explain this prolonged OS.

Higher PD-L1 expression is related to the favorable efficacy of immunotherapy have been reported by several studies (7, 8). In BTCs, Kabir Mody et al. analyzed the PD-L1 expression of 652 tumors by immunohistochemistry (IHC) and found that 8.6% of specimens [GBC, 12.3% (25/203); ICC, 7.3% (27/372); and ECC, 5.2% (4/77)] had PD-L1-positive tumor cells. In addition, recently published results from a BTC patient cohort receiving

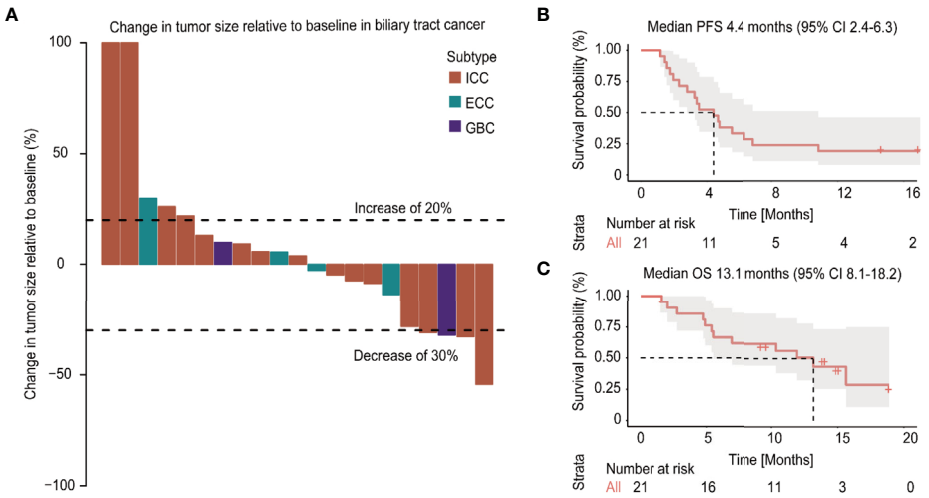

FIGURE 2 | Changes in tumor burden from baseline of the response-evaluable patients and survival plot **(A)**. Kaplan-Meier curves of the progression-free survival (PFS) **(B)** and overall survival (OS) **(C)** of patients with biliary tract cancer (BTC) treated with apatinib plus camrelizumab.

TABLE 2 | Clinical efficacy in BTC patients treated with apatinib plus camrelizumab.

Investigator review according to RECIST 1.1	All (n=21)
Objective response rate (%, 95% CI)	19.0% (7-40)
Complete response (n, %)	0
Partial response (n, %)	4 (19%)
Stable disease (n, %)	11 (52.3%)
Progressive disease (n, %)	6 (28.5%)
Disease control rate (%, 95% CI)	71.4% (50-86.1)
Clinical benefit rate (%, 95% CI)	33.3% (17.1-54.6)
Progression-free survival (months, 95% CI)	4.4 (2.4-6.3)
Overall survival (months, 95% CI)	13.1 (8.1-18.2)
Decreased CA19-9 predicts tumor reduction	
Se (%, 95% CI)	63.6% (35.3-84.8)
Sp (%, 95% CI)	66.7% (35.4-87.9)

BTC, biliary tract cancer; RECIST 1.1, response evaluation criteria in solid tumors, version 1.1; CA19-9, carbohydrate antigen 19-9; Se, sensitivity; Sp, specificity.

TABLE 3 | Clinical characters of BTC patients treated with Apatinib plus Camrelizumab.

	All (n=21)
median Follow-up time (months, 95% CI)	13.4 (11.9-14.8)
median Treatment time (months, 95% CI)	4.9 (3.8-5.9)
Patients still receive the treatment	4/21
Patients of PD-L1 positive	4/21
Continue Treatment after Progression Disease	9/21
Continue Targeted	9/21
Continue PD-1/L1 inhibitor	7/21

BTC, biliary tract cancer.

TABLE 4 | Treatment-related AEs in all patients with biliary tract cancer.

	All treated patients (n=22)	
	Any grade n, (%)	Grade 3/4 n, (%)
Asthenia	15 (68.2)	1 (4.5)
Decreased appetite	10 (45.5)	
Hypertension	7 (31.8)	3 (13.6)
Increased alanine aminotransferase	7 (31.8)	2 (9.1)
Rash	7 (31.8)	2 (9.1)
Abdominal pain	7 (31.8)	
Increased blood bilirubin	6 (27.3)	3 (13.6)
Pain	6 (27.3)	1 (4.5)
Hypoalbuminemia	6 (27.3)	
RCCEP	6 (27.3)	
Increased aspartate aminotransferase	5 (22.7)	2 (9.1)
Abdominal distention	9 (40.9)	
Nausea	5 (22.7)	
Decreased platelet count	4 (18.2)	3 (13.6)
Hypothyroidism	4 (18.2)	
Vomiting	3 (13.6)	1 (4.5)
Proteinuria	3 (13.6)	
Fever	3 (13.6)	
Palmar–plantar erythrodysesthesia	3 (13.6)	
syndrome	3 (13.6)	
Digestive tract hemorrhage	2 (9.1)	2 (9.1)
Decreased leukopenia	2 (9.1)	
Diarrhea	2 (9.1)	
Decreased neutropenia	1 (4.5)	
Decreased hemoglobin	1 (4.5)	

immunotherapy reported a positive rate of PD-L1 expression of between 9% and 11.6% (23, 24). In our present study, PD-L1 expression was found in four patients (19%), and there was no significant difference between the PD-L1-positive and PD-L1-negative patients, which is consistent with the results for advanced biliary cancer in the Keynote 158 study (25). After careful analysis of the treatment regimens of the PD-L1 positive patients and their clinical characteristics, we found that the ECOG PS of these two patients differed and that they had both received multiline treatment, which potentially affected the efficacy of immunotherapy. The limited sample size of this

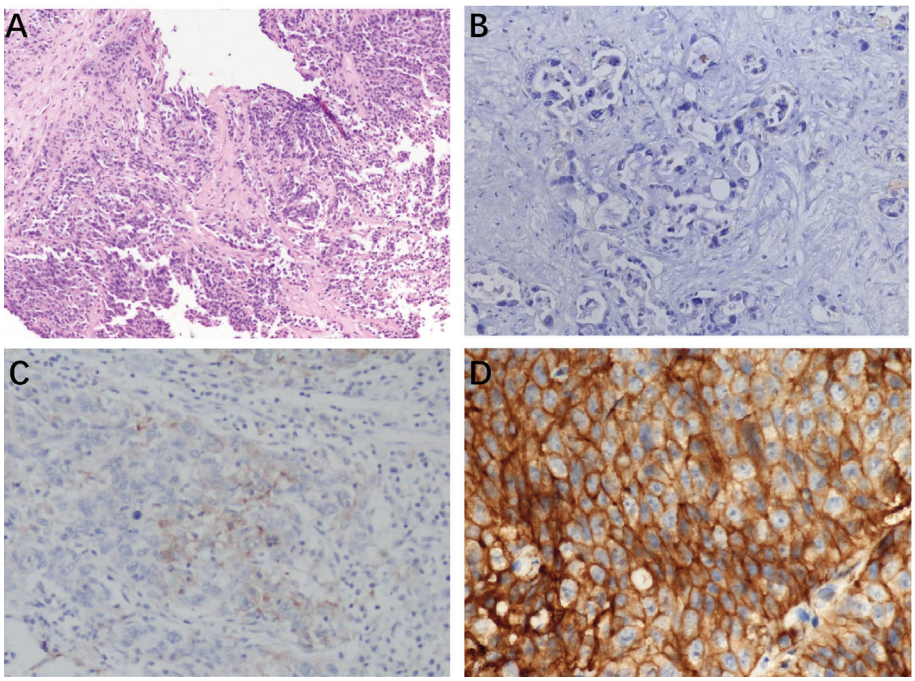

FIGURE 3 | Typical photomicrographs of PD-L1 immunohistochemistry in patents' archived pretreatment formalin-fixed and paraffin-5 embedded tumor tissue: **(A)** HE staining, 100×; **(B)**PD-L1 negative, 200×; **(C)** PDL1-stained tumor cell (3%) 100×; **(D)** positive PD-L1 expression (50%) 400×.

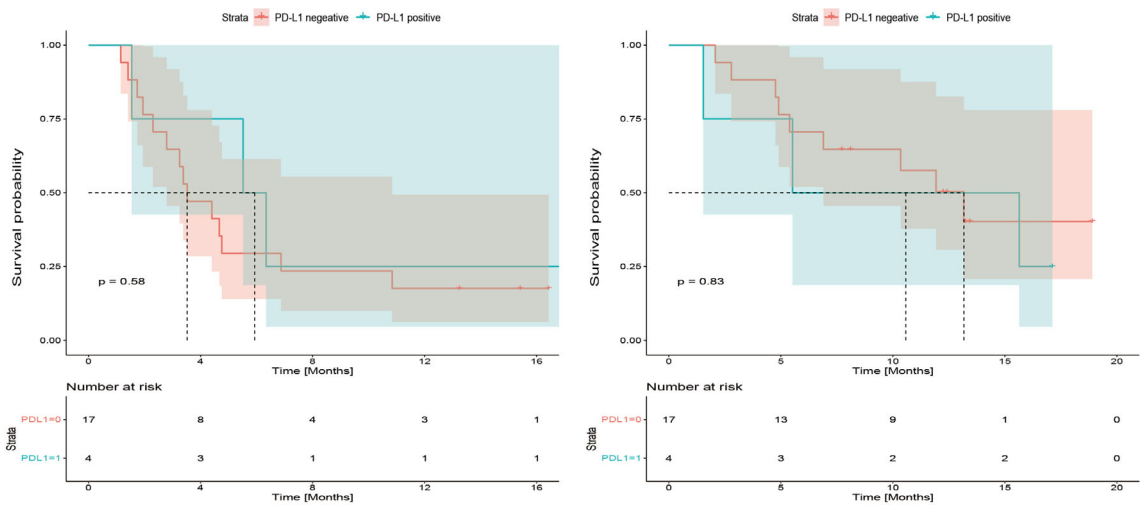

FIGURE 4 | Kaplan-Meier plot for progression-free survival (PFS) and overall survival (OS) based on programmed cell death 1 ligand-1 (PD-L1) immunohistochemical expression.

study may also explain the lack of significance regarding efficacy in PD-L1 positive patients. In the Kim et al. study, nivolumab treatment in a single group of patients with refractory BTCs resulted in a 22% ORR with a median PFS of 4.0 months. Although the PD-L1 expression rate of tumor cells was 43% higher than that in previous studies, which potentially means that PD-L1 expression in BTC remains a good prognostic biomarker for immunotherapy, a more comprehensive

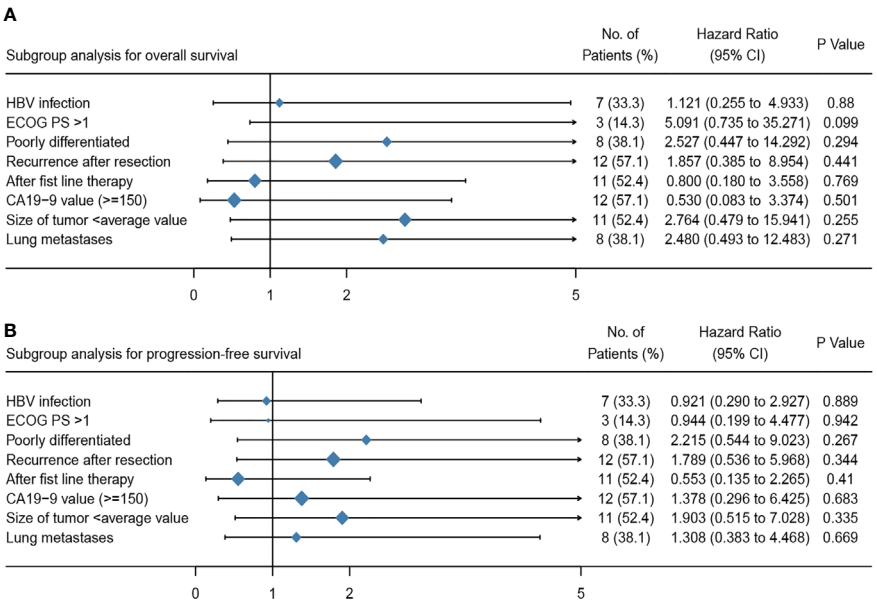

FIGURE 5 | Multivariate analyses of the overall survival **(A)** and progression free survival **(B)** for patients treated with apatinib plus camrelizumab. ECOG PS, Eastern Cooperative Oncology Group performance status; CA19-9, carbohydrate antigen 19-9.

evaluation of efficacy is required for future clinical trials (26). As reported in BTC patients undergoing chemotherapy, pretreatment CA19-9 levels and the decrease in CA19-9 after treatment are of prognostic relevance. In our study, CA19-9 may be another predictive biomarker for potentially judging the response to the current treatment. But it's important to note that patients who are Lewis-antigen-negative (7% of the general population) have undetectable CA 19–9 levels (27, 28). In addition, although apatinib has various tumor targets, the strong inhibitory effect mainly focus on VEGFR-2. Monitoring the expression of VEGFR-2 will also contribute to the prediction and evaluation of therapeutic efficacy.

The safety profile and tolerance of apatinib combined with camrelizumab in this study were similar to those in previous studies exploring apatinib, camrelizumab or combination regimens in gastroenteric neoplasms (14). Based on previous studies regarding the AEs of apatinib, this study excluded patients who had potential risk of gastrointestinal bleeding (29). Although every patient had experienced at least one kind of treatment related adverse event, most of these AEs were grade 1-2 and were well tolerated. Moreover, there were no treatment related deaths, and 63.6% of patients reporting treatment related grade 3-4 AEs had well control after stopping drug delivery. As reported in a study regarding nivolumab monotherapy for BTC (26), among the 3-4 grade AEs in this study, hepatic toxic effects were prominent and included an increase in ALT, AST and serum bilirubin levels and a decrease in platelet counts. These results demonstrate that immunotherapy alone or in combination with targeted drugs probably leads to a decrease in liver function because certain types of treatment related AEs may be affected by disease sites (30). The targets of apatinib are VEGFR-2, PDGFRβ, SRC, c-KIT and RET, and its IC 50 is lower than that of other VEGF inhibitors, which suggest that it has more AEs than some other targeted drugs applying to liver cancer. However, this study administered the lowest dose of apatinib, 250mg, and the regimens of administration were flexible, allowing patients to take the medicine every other day, take half of the 250 mg dose or take the drug for five days and stop for two days if the patients experienced 3-4 grade AEs. This flexible regimen can effectively prevent the further escalation of AEs when apatinib is readministered. In addition, the rate of reactive cutaneous capillary endothelial proliferation (27.3%) was reduced in this study compared with that reported in previous camrelizumab monotherapy studies (67%) (31).

BTC is a group of relatively rare heterogeneous cancers. In various clinical studies, the number of patients with cholangiocarcinoma is still one of the main factors that prevent a better interpretation of the results and a more scientific design of the trial. Similar to other previous studies, the main limitation of this study was its small sample size, which may lead the bias of the multivariate analysis and subgroup analysis of tumor types. Moreover, the study was a single center-initiated clinical trial that lacked a control cohort. Up to now, most studies on immunotherapy for cholangiocarcinoma are in an exploratory stage, and no phase III clinical data have been published. In general, this study was a tentative first step to explore the safety and efficacy of apatinib combined with camrelizumab in heavily pretreated BTC patients, and offers detailed clinical trial experience that can be applied to subsequent investigations.

DATA AVAILABILITY STATEMENT

The original contributions presented in the study are included in the article/**Supplementary Material**. Further inquiries can be directed to the corresponding author.

ETHICS STATEMENT

The studies involving human participants were reviewed and approved by Institutional Review Board and Ethics Committee of Peking Union Medical College Hospital (PUMCH-JS-2160). The patients/participants provided their written informed consent to participate in this study. Written informed consent was obtained from the individual(s) for the publication of any potentially identifiable images or data included in this article.

AUTHOR CONTRIBUTIONS

DW, XY, JYL, and JZL collected the data and wrote the manuscript. JM, FX, YCW, YYW, ZX, and YB helped to collect literature and participated in discussions. XBY, MG, JP, XS, and HZ designed and verified the study. SS and HZ examined the language of this study. All authors contributed to the article and approved the submitted version.

FUNDING

This work was supported by the International Science and Technology Cooperation Projects (2016YFE0107100), the Capital Special Research Project for Health Development (2014-2-4012), the Beijing Natural Science Foundation (L172055 and 7192158), the National Ten-thousand Talent Program, the Fundamental Research Funds for the Central Universities (3332018032), the CAMS Innovation Fund for Medical Science (CIFMS) (2017-I2M-4-003 and 2018-I2M-3-001) and the Innovation Fund for Graduate Students of Peking Union Medical College.

SUPPLEMENTARY MATERIAL

The Supplementary Material for this article can be found online at: https://www.frontiersin.org/articles/10.3389/fonc.2021.646979/full#supplementary-material

REFERENCES

1. Razumilava N, Gores GJ. Cholangiocarcinoma. *Lancet* (2014) 383:2168–79. doi: 10.1016/S0140-6736(13)61903-0
2. Asrani SK, Devarbhavi H, Eaton J, Kamath PS. Burden of liver diseases in the world. *J Hepatol* (2019) 70:151–71. doi: 10.1016/j.jhep.2018.09.014
3. Bridgewater J, Galle PR, Khan SA, Llovet JM, Park JW, Patel T, et al. Guidelines for the diagnosis and management of intrahepatic cholangiocarcinoma. *J Hepatol* (2014) 60:1268–89. doi: 10.1016/j.jhep.2014.01.021
4. Valle J, Wasan H, Palmer DH, Cunningham D, Anthoney A, Maraveyas A, et al. Cisplatin plus gemcitabine versus gemcitabine for biliary tract cancer. *N Engl J Med* (2010) 362:1273–81. doi: 10.1056/NEJMoa0908721
5. Tella SH, Kommalapati A, Borad MJ, Mahipal A. Second-line therapies in advanced biliary tract cancers. *Lancet Oncol* (2020) 21:e29–41. doi: 10.1016/S1470-2045(19)30733-8
6. Rizvi S, Khan SA, Hallemeier CL, Kelley RK, Gores GJ. Cholangiocarcinoma - evolving concepts and therapeutic strategies. *Nat Rev Clin Oncol* (2018) 15:95–111. doi: 10.1038/nrclinonc.2017.157
7. Wang D, Lin J, Yang X, Long J, Bai Y, Yang X, et al. Combination regimens with PD-1/PD-L1 immune checkpoint inhibitors for gastrointestinal malignancies. *J Hematol Oncol* (2019) 12:42. doi: 10.1186/s13045-019-0730-9
8. Blair AB, Murphy A. Immunotherapy as a treatment for biliary tract cancers: A review of approaches with an eye to the future. *Curr Probl Cancer* (2018) 42:49–58. doi: 10.1016/j.currproblcancer.2017.10.004
9. Job S, Rapoud D, Dos Santos A, Gonzalez P, Desterke C, Pascal G, et al. Identification of Four Immune Subtypes Characterized by Distinct Composition and Functions of Tumor Microenvironment in Intrahepatic Cholangiocarcinoma. *Hepatology* (2020) 72:965–81. doi: 10.1002/hep.31092
10. Sia D, Tovar V, Moeini A, Llovet JM. Intrahepatic cholangiocarcinoma: pathogenesis and rationale for molecular therapies. *Oncogene* (2013) 32:4861–70. doi: 10.1038/onc.2012.617
11. Fabris L, Sato K, Alpini G, Strazzabosco M. The Tumor Microenvironment in Cholangiocarcinoma Progression. *Hepatology* (2020) 73 Suppl 1(Suppl 1):75–85. doi: 10.1002/hep.31410
12. Scott LJ. Apatinib: A Review in Advanced Gastric Cancer and Other Advanced Cancers. *Drugs* (2018) 78:747–58. doi: 10.1007/s40265-018-0903-9
13. Hu Y, Lin H, Hao M, Zhou Y, Chen Q, Chen Z. Efficacy and Safety of Apatinib in Treatment of Unresectable Intrahepatic Cholangiocarcinoma: An Observational Study. *Cancer Manag Res* (2020) 12:5345–51. doi: 10.2147/CMAR.S254955
14. Zhen L, Jiali C, Yong F, Han X, Hongming P, Weidong H. The Efficacy and Safety of Apatinib Treatment for Patients with Unresectable or Relapsed Liver Cancer: a retrospective study. *J Cancer* (2018) 9:2773–7. doi: 10.7150/jca.26376
15. Athauda A, Fong C, Lau DK, Javle M, Abou-Alfa GK, Morizane C, et al. Broadening the therapeutic horizon of advanced biliary tract cancer through molecular characterisation. *Cancer Treat Rev* (2020) 86:101998. doi: 10.1016/j.ctrv.2020.101998
16. Xu J, Shen J, Gu S, Zhang Y, Wu L, Wu J, et al. Camrelizumab in combination with apatinib in patients with advanced hepatocellular carcinoma (RESCUE): a non-randomized, open-label, phase 2 trial. *Clin Cancer Res* (2021) 27 (4):1003–11. doi: 10.1158/1078-0432.CCR-20-2571
17. Liu J, Liu Q, Li Y, Li Q, Su F, Yao H, et al. Efficacy and safety of camrelizumab combined with apatinib in advanced triple-negative breast cancer: an open-label phase II trial. *J Immunother Cancer* (2020) 8(1):e000696. doi: 10.1136/jitc-2020-000696
18. Liang L, Wen Y, Hu R, Wang L, Xia Y, Hu C, et al. Safety and efficacy of PD-1 blockade-activated multiple antigen-specific cellular therapy alone or in combination with apatinib in patients with advanced solid tumors: a pooled analysis of two prospective trials. *Cancer Immunol Immunother* (2019) 68:1467–77. doi: 10.1007/s00262-019-02375-z
19. Xie L, Xu J, Sun X, Guo W, Gu J, Liu K, et al. Apatinib plus camrelizumab (anti-PD1 therapy, SHR-1210) for advanced osteosarcoma (APFAO) progressing after chemotherapy: a single-arm, open-label, phase 2 trial. *J Immunother Cancer* (2020) 8(1). doi: 10.1136/jitc-2020-000798
20. Franses JW, Hong TS, Zhu AX. Nivolumab with gemcitabine plus cisplatin for biliary cancers: as easy as ABC? *Lancet Gastroenterol Hepatol* (2019) 4:575–7. doi: 10.1016/S2468-1253(19)30148-7
21. Ueno M, Ikeda M, Morizane C, Kobayashi S, Ohno I, Kondo S, et al. Nivolumab alone or in combination with cisplatin plus gemcitabine in Japanese patients with unresectable or recurrent biliary tract cancer: a non-randomised, multicentre, open-label, phase 1 study. *Lancet Gastroenterol Hepatol* (2019) 4:611–21. doi: 10.1016/S2468-1253(19)30086-X

22. Lin J, Yang X, Long J, Zhao S, Mao J, Wang D, et al. Pembrolizumab combined with lenvatinib as non-first-line therapy in patients with refractory biliary tract carcinoma. *Hepatobiliary Surg Nutr* (2020) 9(4):414–24. doi: 10.21037/hbsn-20-338
23. Fontugne J, Augustin J, Pujals A, Compagnon P, Rousseau B, Luciani A, et al. PD-L1 expression in perihilar and intrahepatic cholangiocarcinoma. *Oncotarget* (2017) 8:24644–51. doi: 10.18632/oncotarget.15602
24. Walter D, Herrmann E, Schnitzbauer AA, Zeuzem S, Hansmann ML, Peveling-Oberhag J, et al. PD-L1 expression in extrahepatic cholangiocarcinoma. *Histopathology* (2017) 71:383–92. doi: 10.1111/his.13238
25. Piha-Paul SA, Oh DY, Ueno M, Malka D, Chung HC, Nagrial A, et al. Efficacy and safety of pembrolizumab for the treatment of advanced biliary cancer: Results from the KEYNOTE-158 and KEYNOTE-028 studies. *Int J Cancer* (2020) 147:2190–8. doi: 10.1002/ijc.33013
26. Kim RD, Chung V, Alese OB, El-Rayes BF, Li D, Al-Toubah TE, et al. A Phase 2 Multi-institutional Study of Nivolumab for Patients With Advanced Refractory Biliary Tract Cancer. *JAMA Oncol* (2020) 6:1–8. doi: 10.1001/jamaoncol.2020.0930
27. Yamashita S, Passot G, Aloia T, Chun Y, Javle M, Lee J, et al. Prognostic value of carbohydrate antigen 19-9 in patients undergoing resection of biliary tract cancer. *J Br Surg* (2017) 104:267–77. doi: 10.1002/bjs.10415
28. Nehls O, Gregor M, Klump B. Serum and bile markers for cholangiocarcinoma. *Semin Liver Dis* (2004) 24:139–54. doi: 10.1055/s-2004-828891
29. Shao F, Zhang H, Yang X, Luo X, Liu J. Adverse events and management of apatinib in patients with advanced or metastatic cancers: A review. *Neoplasma* (2020) 67:715–23. doi: 10.4149/neo_2020_190801N701
30. El-Khoueiry AB, Sangro B, Yau T, Crocenzi TS, Kudo M, Hsu C, et al. Nivolumab in patients with advanced hepatocellular carcinoma (CheckMate 040): an open-label, non-comparative, phase 1/2 dose escalation and expansion trial. *Lancet* (2017) 389:2492–502. doi: 10.1016/S0140-6736(17)31046-2
31. Qin S, Ren Z, Meng Z, Chen Z, Chai X, Xiong J, et al. Camrelizumab in patients with previously treated advanced hepatocellular carcinoma: a multicentre, open-label, parallel-group, randomised, phase 2 trial. *Lancet Oncol* (2020) 21:571–80. doi: 10.1016/S1470-2045(20)30011-5

Conflict of Interest: The authors declare that the research was conducted in the absence of any commercial or financial relationships that could be construed as a potential conflict of interest.

frontiers in Oncology

REVIEW
published: 13 April 2021
doi: 10.3389/fonc.2021.644454

Exploring the Modulatory Effects of Gut Microbiota in Anti-Cancer Therapy

Wenyu Li[1,2], *Xiaorong Deng*[1*] and *Tingtao Chen*[1,3*]

[1] Department of Gastrointestinal Surgery, The Second Affiliated Hospital of Nanchang University, Nanchang, China, [2] Queen Mary School, Nanchang University, Nanchang, China, [3] National Engineering Research Center for Bioengineering Drugs and the Technologies, Institute of Translational Medicine, The First Affiliated Hospital, Nanchang University, Nanchang, China

In the recent decade, gut microbiota has received growing interest due to its role in human health and disease. On the one hand, by utilizing the signaling pathways of the host and interacting with the immune system, the gut microbiota is able to maintain the homeostasis in human body. This important role is mainly modulated by the composition of microbiota, as a normal microbiota composition is responsible for maintaining the homeostasis of human body, while an altered microbiota profile could contribute to several pathogenic conditions and may further lead to oncogenesis and tumor progression. Moreover, recent insights have especially focused on the important role of gut microbiota in current anticancer therapies, including chemotherapy, radiotherapy, immunotherapy and surgery. Research findings have indicated a bidirectional interplay between gut microbiota and these therapeutic methods, in which the implementation of different therapeutic methods could lead to different alterations in gut microbiota, and the presence of gut microbiota could in turn contribute to different therapeutic responses. As a result, manipulating the gut microbiota to reduce the therapy-induced toxicity may provide an adjuvant therapy to achieve a better therapeutic outcome. Given the complex role of gut microbiota in cancer treatment, this review summarizes the interactions between gut microbiota and anticancer therapies, and demonstrates the current strategies for reshaping gut microbiota community, aiming to provide possibilities for finding an alternative approach to lower the damage and improve the efficacy of cancer therapy.

Keywords: gut microbiota, neoplasms, cancer therapy, probiotics, fecal microbiota transplantation, diet therapy

OPEN ACCESS

Edited by:
Maria L. Martinez Chantar, CIC bioGUNE, Spain

Reviewed by:
Chuan Wang, Sichuan University, China
Degang Song, Janssen Pharmaceuticals, Inc., United States

***Correspondence:**
Tingtao Chen
chentingtao1984@163.com
Xiaorong Deng
dengxr77@163.com

Specialty section:
This article was submitted to Cancer Immunity and Immunotherapy, a section of the journal Frontiers in Oncology

Received: *21 December 2020*
Accepted: *18 March 2021*
Published: *13 April 2021*

Citation:
Li W, Deng X and Chen T (2021) Exploring the Modulatory Effects of Gut Microbiota in Anti-Cancer Therapy. Front. Oncol. 11:644454. doi: 10.3389/fonc.2021.644454

INTRODUCTION

Cancer is one of the leading causes of death worldwide. It arises as a result of accumulated genetic disorders that leads to dysregulations in cell cycle, having the potential to undergo unlimited times of division and imposing a strong negative impact on the normal physiological functions of the host (1). As the mutations accumulate, the life quality of the patient is largely impaired, and most importantly the life span is reduced (2).

Finding a cure for cancer to prolong the lifespan has long been the greatest challenge during the development of medical research. Over the years, researchers have worked out a variety of

therapeutic methods against cancer, including chemotherapy, radiotherapy, immunotherapy, surgery and so on. Although these methods are able to inhibit the progression or even eliminate some types of cancer cells, there are still limitations due to acquired resistance as well as undesirable side effects caused by the low selectivity of anti-cancer agents between normal cells and cancer cells (3). For example, previous research findings suggest that collateral damage in the abdominopelvic region caused by radiotherapy can lead to bowel injury (4), and 80% of cancer patient suffer from chemotherapy-induced gastrointestinal toxicity (CIGT), with symptoms of diarrhea and abdominal pain (5). As these adverse effects seriously interfere with the anticancer therapy, finding an adjuvant method to ultimately overcome these complications becomes urgent for the clinical research.

The human microbiota consists of microoganisms (bacteria, archaea, fungi and viruses) present in the epithelial barriers of the host (6), with the most abundant being the commensal bacteria that coexist with human cells in the gastrointestinal tract (7). With the development of high-throughput sequencing technology, the composition of gut microbiota can be clearly identified. It mainly consists of 5 bacteria in healthy individuals: *Firmicutes*, *Bacteriodes*, *Actinobacteria*, *Proteobacteria* and *Fusobacteria* (8). This microbiota profile stays relatively unchanged throughout life once established (9), forming a unique "signature" in each individual with important functions associated with both innate and adaptive immune systems (9). In recent years, the gut microbiota has increasingly come under focus due to its impact on many human diseases, including diabetes, obesity, psychiatric disorders and gastrointestinal diseases (10). They regulate the balance between health and disease by maintaining local homeostasis to systematically regulating metabolism, hematopoiesis, inflammation, immunity and preventing pathogen infection (9), and the host can in turn "communicate" with the microbiota with the aid of several host molecules such as host microRNA (miRNA), hormones, cytokines, metabolites and metabolic signaling pathways (11). Additionally, recent insights importantly highlighted the impact of gut microbiota on responses across several cancer therapies (12), suggesting that regulating gut microbiota may improve the effectiveness of many cancer treatments, with a reduced cytotoxic activity.

This article reviews how the gut microbiota, as an adjuvant therapy, affect the efficacy of four anti-cancer therapies including chemotherapy, radiotherapy, immunotherapy and surgery, at the same time reduce the adverse effects. These manipulations may be conducive to the promotion of personalized medicine and effective anti-cancer treatment.

THE IMPACT OF GUT MICROBIOTA ON ONCOGENESIS AND TUMOR PROGRESSION

There are many factors contributing to the oncogenesis of cancer, and the study of these oncogenic pathways have clearly given us insight into the nature of this devastating disease. In 2000, Hanahan and Weinberg presented six hallmarks of cancer, and updated in 2011 with two emerging hallmarks (13). By acquiring these properties, normal cells can undergo tumorigenic transformation and, in the end, become cancer cells. The hallmarks are: i) self-signaling for proliferation, ii) evading anti-growth signals, iii) invasion and metastasis, iv) immortality, v) angiogenesis, vi) resisting apoptosis, vii) deregulating energy metabolites, viii) evading immune system. The main mechanism by which normal cells gaining these cancer hallmarks are accumulated mutations in the genome, including somatic structural variants (SVs) and copy number alterations (CNAs), that interfere with the normal regulatory controls (14). In recent years, increasing researches have revealed the relation between microbiota (especially the gut microbiota) and carcinogenesis, suggesting that the gut microbiota can be involved as an environmental factor and contribute to genetic alterations as well.

The indirect bacterial mechanism of oncogenesis is represented in the process of chronic inflammations induced by bacterial infection. In this case, the microbiota chronically generates several inflammation mediators such as Tumor Necrosis Factor-α (TNF- α) and Interleukin-1 (IL-1), which further lead to the induction of transcription factor nuclear factor-κB (NF-κB) and contribute to carcinogenesis (15). In addition, the bacteria-induced oncogenesis could also be direct through the effect of microbial metabolites or toxins. Previous studies have shown that several strains of gut microbiota are responsible for the tumorigenesis of different cancer types, such as gastric cancer, colorectal cancer (CRC) and hepatocellular carcinoma (15, 16). Their carcinogenic processes are all linked to the production of microbial metabolites. the carcinogenic process of gastric cancer, CagA proteins produced by H. pylori are transferred into gastric epithelial cells and interact with pro-oncogenic phosphatase SHP2 and the polarity-regulating kinase PAR1/MARK, driving the host signaling pathways that favors carcinogenesis (17). *Bacteroides fragilis* is a strong risk factor of CRC, which could act as an opportunistic pathogen (15). In antigen-presenting cell (APC) mutant mice model which are predisposed to intestinal cancer formation, the enterotoxigenic *B. fragilis* (ETBF), one of the two subtype of *B. fragilis*, can induce colitis and inflammatory bowel disease (IBD) through the pathway of β-catenin/Wnt/NF-κB signaling, and further lead to the oncogenesis of CRC (15). On the other hand, *B. fragilis* toxin (Bft) can up-regulate spermine oxidase (SMO) in colon epithelial cells, causing reactive oxygen species (ROS) production and indirect DNA damage (18, 19). Other microbial metabolites associated with carcinogenesis include *Pasteurella multocida* toxin, cytolethal distending Toxin (CDT) (15) and inositol phosphate phosphatase D (IpgD) (16). These could all contribute to the cell transformation, in which the normal cell responses are altered, and further elevate the risk for developing cancer.

Given the association between the gut microbiota and carcer development, it should be considered that a healthy gut microbiota profile is both sufficient and necessary for maintaining a healthy microenvironment. Therefore, by

targeting dysbiosis, the efficacy of some anti-cancer therapies may be improved, with a better prognosis and reduced side effects.

THE INTERPLAY BETWEEN GUT MICROBIOTA AND CANCER THERAPY

Microbiota and Chemotherapy

Chemotherapy is one of the most potent approach to treat cancer systematically at present. As the chemotherapy drugs can be delivered through blood circulating system, it can act on hematopoietic malignancies or tumor with metastasis (20), targeting DNA, topoisomerase or tubulin to prevent the growth and proliferation of cancer cells (21). However, due to the lack of specific targets of chemotherapy drugs, there are still unavoidable complications caused by cytotoxic effect. In further studies, the mechanisms of chemotherapy toxicity revealed a bidirectional interaction between gut microbiota and cytotoxic drugs.

The Influence of Chemotherapy on the Gut Microbiota: Composition and Translocation

The chemotherapy-induced change in microbiota composition has been widely studied in a considerable number of pre-clinical models, demonstrating a decreased total number and diversity. Although different chemotherapy drugs may exert different influences (22, 23), the overall impact was concluded as a reduced *Lactobacillus* and *Bifidobacterium*, together with an increased *Escherichia coli* (E. coli) and *Staphylococcus*, consisting with the result of clinical studies (5). This disruption in microbiota composition is associated with an activated inflammatory pathway and an impaired barrier function, which makes the host more vulnerable to pathogens (5, 22).

In addition to changes of microbiota composition, chemotherapy can also induce microbiota translocations, which is often due to the injured epithelium of the gut (24). During this process, the gram-positive bacteria strains, such as *Lactobacillus johnsonii*, *Lactobacillus murinus* and *Enterococcus hirae*, are transferred by the circulation system to peripheral lymphoid organs such as mesenteric lymph nodes and spleen (25). There, the microbiota facilitates the stimulation of memory T helper 1 (Th1) and the conversion of naïve $CD4^+$ T cells to T helper 17 (Th17) that secrete IL-17, together with an increased production of other secreting molecules such as interferon gamma (IFN-γ) which further contribute to the healing of mucosa and anticancer responses (25).

The Direct Influence of Microbiota on Chemotherapy: Drug Pharmacokinetics and ROS Production

As the influence between gut microbiota and chemotherapy is bidirectional, the microbiota can in turn affect the efficacy of chemotherapy (**Figure 1**). One of the mechanisms is that, orally administrated drugs and some injected drugs depend on gut microbiota to be converted into active form to exert the anticancer function (6, 26). For example, CPT-11 (Irinotecan) is a prodrug administrated intravenously in CRC treatment, and is converted into its active form SN-38 by carboxylesterase (26). The active drug works as topoisome-1 inhibitor, which induces single and double strand breaks of the DNA by blocking DNA ligation, leading to tumor cell death (26). Then the drug is detoxified by uridine diphosphate-glucuronosyl transferase (UDP-transferase) (26). However, experiment showed that the amount of SN-38 was elevated from 2% of administered dose to 12% in feces (27), because the intestinal microbiota-produced β-glucuronidases are able to convert the detoxicated SN-38-glucurone back to its active form SN-38 by deconjugation, and the increased concentration of SN-38 in the colon could cause diarrhea and intestinal injury (28). The result verified the role of microbiota in drug pharmacokinetics, providing a potential target for reducing side effects.

On the other hand, gut microbiota can facilitate the production of drug metabolite which inhibits a critical enzyme used for the detoxification of another drug, leading to enhanced side effects. Many studies have focused on the toxicity of 5-fluorouracil (5-FU) induced by microbiota, for example if Sorivudine and 5-FU are taken together by rats, Sorivudine would be metabolized to bromovinyluracil, and further inhibit the enzyme dihydropyrimidine dehydrogenase responsible for the detoxification of 5-FU (26). As 5-FU is an inhibitor of thymidylate synthase critical in DNA replication, the increased duration and concentration of 5-FU in the body will cause serious systemic effects including diarrhea and even reduction in leukocytes and platelets (29–31). Interestingly, this conversion only happened *in vivo*, especially in the intestinal contents, and it was then confirmed by experiment that gut microbiota species was responsible for the production of bromovinyluracil (32), indicating the key role of gut microbiota in the chemotherapy-induced toxicity.

Moreover, in contrast to increasing chemotherapy-induced toxicity, the gut microbiota could also facilitate the anticancer activity of chemotherapy drugs. This is achieved through inducing the expression of enzymes which are responsible for ROS production. Oxaliplatin, a commonly used chemotherapeutic agents, can generate ROS in tumor cells to induce cell apoptosis by damaging DNA (33). According to experiment results, the anticancer effect will be reduced in germ free mice or if the mice are treated with antibiotic cocktail (ABX), as the impaired microbiota function could lead to reduced expression levels of Nox1 and Cybb genes coding for NADPH oxidase 2 (Nox2) (34). This altered gene expression would contribute to compromised therapeutic effect, as Nox2 can transfer electrons to generate superoxide (O_2^-) and further lead to H_2O_2 production by an enzyme called compartment-specific superoxide dismutase (SOD), having the ability to induce DNA damage in tumor cells and permit cell apoptosis (33). Furthermore, there is also a second pathway by which gut microbiota could facilitate the myeloid cell-produced ROS through Toll-like receptor (TLR) agonist releasing and the downstream expression of myeloid differentiation primary response gene 88 (MyD88) (34). This pathway further activates

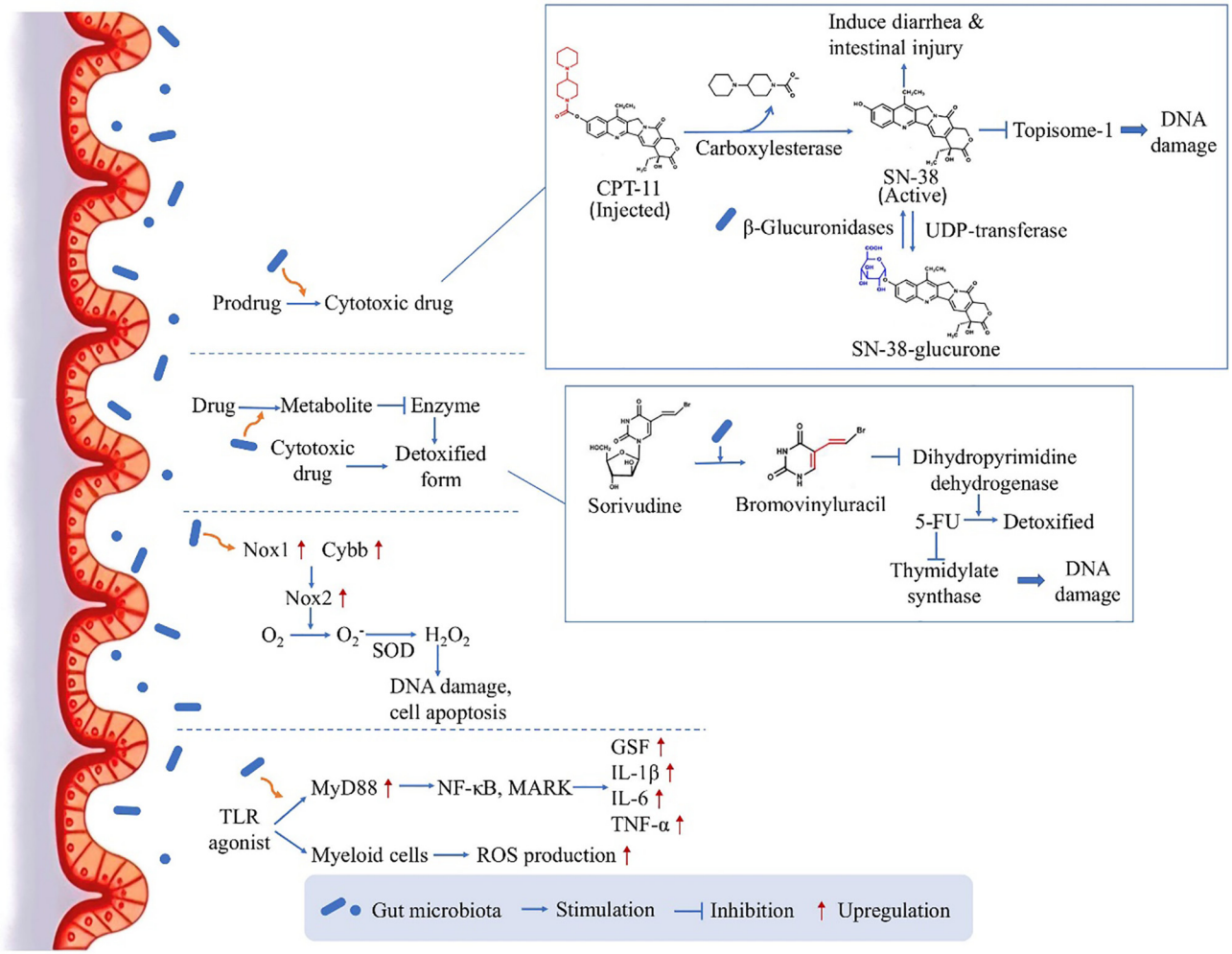

FIGURE 1 | The direct influence of microbiota on chemotherapy: drug pharmacokinetics and ROS production. By several mechanism pathways, the gut microbiota can directly act on the drug conversion and gene transcription, leading to an either enhanced therapeutic effect or enhanced side effect.

NF-κB õand MAPKs and induces the expression of several genes coding for inflammatory cytokines, including granulocyte colony-stimulating factor, Interleukin-1β (IL-1β), Interleukin-6 (IL-6) and TNF-α (35). This study substantiated the ROS-generating pathway used by microbiota to modulate tumor microenvironment and further affect the outcome of chemotherapy, highlighting a mechanism for obtaining optimal anticancer responses.

The Indirect Influence of Microbiota on Chemotherapy: The Immune System

As the microbiota and chemotherapy drugs can both act on the immune system, they could use it as a medium to interact with each other. When the component of gut microbiota is changed by the chemotherapy as a side effect of the treatment, the alteration can further influence the function of innate immune system by reducing APCs (36) and produce inflammatory cytokines (37), which lead to the progression of Chemotherapy-induced gastrointestinal toxicity (CIGT) (5). Furthermore, certain phyla of microbiota could play an indispensable role in anticancer chemotherapy by regulating the immune response. One of the chemotherapeutic agents, Cyclophosphamide (CTX), is able to exert systemically anticancer effect through inducing naïve $CD4^+$ T cells to Th1 and Th17 fate (25). This process is microbiota-dependent: the entry of symbiotic bacteria (such as *Lactobacillus johnsonii* and *Enterococcus hirae*) into mesenteric lymph nodes promotes the induction of Th17 and Th1 memory responses in the spleen in the presence of bone marrow-derived dendritic cells, performing tumor antigen cross-presentation with the help of TLR and its adaptor MyD88 (25). It is critical for achieving successful therapeutic outcome of CTX (25). Similarly, another experiment demonstrates that the colonization of *Barnesiella intestinihominis* in the colon is able to modulate tumor

microenvironment, promoting Interferon-γ (IFN-γ) production and reducing Treg cells (38). In this research, the immunogenic microbiota is referred to as "oncomicrobiotics", cooperating with CTX against many types of cancers by unknown mechanisms (38).

Gut Microbiota Induces Chemoresistance

Resistance and heterogeneous responses to chemotherapeutic drugs are a major challenge in cancer treatment (39). Currently, researchers have identified several different intrinsic cellular mechanisms involved in chemotherapeutic resistance, and the microbiota-induced drug resistance has gradually received attention in recent years.

Based upon the fact that in recurrent CRC patients the microbiota *Fusobacterium nucleatum* (Fn) is especially enriched (40), it is found that this microbiota phyla is able to induce chemoresistance in a FadA-dependent manner: the oncogenic and inflammatory pathway are stimulated by the binding of FadA and E-cadherin and the downstream β-catenin signaling, which further elevated the expression of transcription factors and genes including oncogenes and Wnt, resulting in increased inflammation and tumor cell growth (41). This study pointed to the potential role of Fn in chemoresistance, indicating that the colonization of specific phyla of microbiota could be a general characteristic of cancer patients.

In addition to utilizing the signaling pathways of the host, the gut microbiota could also induce chemoresistance by inactivating the chemotherapy drug. For example, *Gammaproteobacteria* is a microbiota species especially abundant in the duodenum, and could convert the chemotherapy drug gemcitabine (a chemotherapy drug used to treat cancers of pancreatic, lung, breast or bladder) to its inactive metabolite by expressing a long isoform of the enzyme cytidine deaminase (CDD_L), contributing to the drug resistance.

Altogether, these research findings underline the importance of gut microbiota in the development of chemoresistance, which may provide an alternative target to deal with this obstacle.

Microbiota and Immunotherapy

Immunotherapy is a promising therapeutic method for cancer treatment, acting on cancer types which develop resistance to conventional anti-cancer therapies (6). It targets cancer cells with the aid of host immune system, and has already proved to be effective in many clinical trials (42). The first attempt of cancer immunotherapy dates back to 1890s when Coley developed the first cancer vaccine, and the approval of the first immune checkpoint inhibitor in 2011 represents a new era of anti-cancer treatment (43). The recent decades witnessed a surge in exploring various methods for anti-cancer immunotherapy. Some of the promising immunotherapy methods include adoptive T cell transfer (i.e., transferring cytotoxic T cells which are tumor-specific to patients), CpG-oligodeoxynucleotide (i.e., a TLR9 agonist, containing unmethylated CG dinucleotide and has immune stimulation similar to bacterial DNA, which triggers the body's defense mechanism and causes obvious and diversified immune response through a series of signal cascade transduction), immune checkpoint inhibitors (i.e., antibodies that target immune checkpoints to prevent tumor cells from escaping antitumor immunity, which has proved to be effective in advanced and metastatic cancer) (6). The US Food and Drug Administration has approved three immune checkpoint inhibitors: cytotoxic T lymphocyte-associated antigen-4 monoclonal antibody (CTLA-4), programmed cell death protein-1 (PD-1), and programmed cell death-ligand 1 (PD-L1) (44). Though they act *via* different mechanisms, the rationale is the same: to block the protective signaling pathway of Tregs hijacked by tumor cells, and reactivate the suppressed immune effectors. This can further restore the immune responses against cancerous cells when T cells are exhausted by the chronic activation of tumor antigen, achieving a better therapeutic outcome (45). As the gut process a great number of innate and adaptive immune cells, the interactions between immune cells and the commensal gut microbes could contribute to a robust immune response which protect the body from pathogens (46).

Gut Microbiota Influences the Immune System and Immunotherapy

In general, the impact of gut microbiota on the immune system can be involved in all anticancer therapies. The effects can be local, which is restricted to the gut mucosa, or can be systemic, which is due to primed dendritic cell that travel through circulation system (47). The local tolerance is mediated by the induction of Tregs *via* several signaling pathways, including interleukin 10 (IL-10), polysaccharide A and TLR (47). Short chain fatty acids (SCFAs) produced by microbiota are also able to affect local immunity *via* IgA, contributing to an enhanced immunity (48). In contrast to the local effect, the distant effects of gut microbiota on immunity requires another mechanism named "cancer-immunity cycle" model, which depends on the tumor antigen-activated T cells for recognizing and killing tumor cells (49).

There are also associations between specific strains of gut microbiota and the development of immune cells. *Segmented filamentous* bacterium (SFB) can induce $CD4^+$ T helper cell fate as well as an increased resistance against *Citrobacter rodentium* (50), and *Clostridium* strain contributes to the differentiation of $CD4^+$ T regulatory cells (51). Similarly, dendritic cells can also be regulated by gut microbiota, through the process of cytokine secretion, antigen presentation and T cell activation (52).

In addition to the impact on host's original immune responses, it is also suggested that the composition of intestinal microbiota may influence the response of several immunotherapies such as immune checkpoint inhibitors (52, 53). Previous studies have indicated that the anti-CTLA activity is related to *Bacteroides*, while the effect of anti-PD-L1 is *Bifidobacterium*-dependent (54). The anti-CTLA therapy could not exert its function in germ-free mice or mice treated with antibiotics, but this situation could be improved by orally feeding the mice with *Bacteroides thetaiotaomicron*, *Bacterooides fragilis* or *Burkholderia cepacia* to induce dendritic cell and IL-12-dependent Th1 cell responses. One of the mechanisms that contribute to restoration of anti-CTLA activity is that *Bf* could utilize the TLR2/TLR4 signaling pathways to activate immunoprotection. The distribution of *Bf* on the intestinal

mucosa is also responsible for the microbiota-dependent immunomodulatory effects of CTLA-4 antibody (53). In 2019, 11 strains of bacteria isolated in the gut of human were shown to possess the ability to facilitate immune checkpoint inhibitors by inducing IFN-γ^+ $CD8^+$ T cells, which strains include *Parabacteroides* spp., *Alistipes senegalensis*, five *Bacteroides* spp., *Eubacterium limosum*, *Ruminococcaceae bacterium cv2*, *Phascolarctobacterium faecium* and *Fusobacterium ulcerans* (55). Collectively, these research findings suggest that the immunostimulatory function of immunotherapy is strongly microbiota dependent.

The Immunotherapy Affects Gut Microbiota

From another point of view, the immunotherapy can in turn alter the composition of gut microbiota. The anti-CTLA-4 treatment is able to induce decrease in *Bacteroidales* and *Burkholderiales* and increase in *Clostridiales*, whereas the amount of *Bacteroides fragilis* is relatively unchanged (6). Similarly, in a study using anti-PD-1 to treat patients with melanoma, the abundant of different strains of gut microbiota was altered after the therapy, with an increase in *Clostridiales/Ruminococcaceae* in responders and an increase in *Bacteroidales* in non-responders (56). Other immunotherapy methods like allogeneic stem cell transplant (allo-HSCT) can also alter the abundance of *Enterococcus*, *Streptococcus* and *Proteobacteria* (57). As a result, the altered composition of gut microbiota caused by the exposure to immunotherapy can induce a negative impact on the effectiveness of further treatment, including colitis, thyroid dysfunction and even autoimmune disease in which the enteric bacteria become the target of host antibodies (53).

Microbiota and Surgery

For solid cancers, especially in the situations which the tumor is in the early stage or with no metastasis, performing surgery to remove the neoplasm lesion can be an effective treatment (58). In these cases, the potential influence of intestinal microbiota on surgical outcomes is possibly due to the direct interaction between intestinal microbiota and the site of resection. This association has been demonstrated mostly in CRC. Although the therapy for CRC is usually multidisciplinary, the major surgical treatment for non-metastatic or locally advanced rectal cancer is total mesorectal excision (TME) (59). The research findings have shown that after surgery, the amount of some obligate anaerobes which are responsible for gastrointestinal homeostasis such as *Clostridium coccoides*, *C. leptum*, *B. fragilis*, *Bifidobacterium*, *Atopobium* and *Prevotella* are reduced, together with an increase in pathogens including the *Facultative anaerobes*, *Enterobacteriaceae*, *Enterococcus*, *Staphylococcus* and *Pseudomonas* (60). In turn, this disturbed gut microbiota community could affect the outcome of the therapy, responsible for an increased recurrence rate and a decreased disease-free survival (60).

In addition to dysbiosis, anastomotic leak (AL) is also a most common life-threatening complication after CRC. Despite improvements in perioperative medical care, the AL rate has remained between 1% and 19% over the past few decades (61, 62) while little is known about the microbial characteristics and mechanisms associated with AL. Then in 2013, Stern et al. first demonstrated that harmful intestinal factors (such as bacteria) may invade the intestinal tissue when the epithelial barrier is impaired, which may delay the healing of the anastomosis and lead to AL (63). This suggests that anastomotic healing after colorectal surgery is greatly depend on the restoration of epithelial barrier integrity. Recently, van Praagh et al. employed 16S MiSeq sequencing on colorectal anastomosis tissue samples and reported that AL development was associated with a low microbial diversity, which was characterized by a high abundance of the dominant Lachnospiraceae and Bacteroidaceae families and a low abundance of *Prevotella oralis* (64). Collectively, these experimental phenomena shed light on the importance of gut microbiota manipulation during post-operative care, suggesting that it is the part that should not be ignored.

Microbiota and Radiotherapy

Radiotherapy is a commonly used anticancer therapy using ionizing irritation to generate reactive chemical species such as ROS or reactive nitrogen (RNS). It directly induces DNA damage, including single-strand breaks and double-strand breaks, through energy transfer (6, 65–67). Radiotherapy is also commonly associated with immunogenic process, as it can induce immunogenic cell death (ICD) which evokes subsequent immune responses by antigen presenting cells and cytotoxic T cells. The close association of radiotherapy and immunotherapy allows radiotherapy to not only deal with local lesions, but also have a systemic effect for treating distant malignancies *via* migrating DC and cytotoxic T cells, known as abscopal effect. Therefore, radiotherapy and immunotherapy are often combined to achieve a better efficacy (67).

The side effects induced by total body irritation (TBI) mainly result from the fact that radiotherapy could affect tumor cells and surrounding normal cells alike. Inflammation is a common consequence of radiation irritation not only due to weakened immune system, but also caused by altered gut microbiota. The reduced integrity of gut epithelium leads to microbiota translocation to mesenteric lymph nodes, together with an increased lipopolysaccharide (LPS) derived by microbiota (68). Similarly, the radiotherapy used for treating head and neck cancer such as nasopharyngeal carcinoma can lead to oral mucositis, compromising the anticancer therapy (69). On the other hand, several studies have also proved that radiation irritation is able to induce reduction in microbiota diversity (70–72). In a pilot study of three pediatric cancer patients with pelvic rhabdomyosarcoma, the radiotherapy and antibiotic treatment caused a decreased abundant of *Firmicutes* and increased *Proteobacteria* (73).Compared to the healthy controls and the patients who didn't undergo microbiota change after radiotherapy, the patients with dysbiosis are prone to develop pathologic conditions like diarrhea (72), inflammatory bowel disease (IBD) and type 2 diabetes (T2D) (70). Moreover, the gut microbiota could also affect the therapeutic effects of radiotherapy. A preclinical study revealed the presence of gut microbiota is responsible for increased radio-sensitivity of the

intestinal endothelium, showing that the production of angiopoietin type 4 in germ free mice model could lead to reduced endothelial cell apoptosis and lymphocyte infiltration (74, 75). Further explorations are promising for discovering the mechanisms and potential therapeutic modulation of gut microbiota on the therapeutic effects of ionizing radiation.

MANIPULATING GUT MICROBIOTA TO ACHIEVE BETTER THERAPEUTIC EFFICACY

There are lines of evidence implicating that different patients respond differently to anticancer therapy. The reasons are concluded as different host genes, different tumor mutations, different environmental factors, and to some extent the different gut microbiota composition (52). Therefore, the manipulation of gut microbiota could be an effective method to improve the efficacy of conventional anticancer therapy.

Probiotics

According to the research findings discussed in previous sections, those mechanism pathways could be considered in combination therapy for cancer treatment. On the one hand, reducing the amount of genus that could impair the efficacy of anticancer therapy, for example providing antibiotics to target the strains that could induce resistance, is a goal of microbiota-targeted combination therapy. On the other hand, as dysbiosis is one of the side effects brought by anticancer therapy, targeting the abnormal microbiota profile by providing patients with beneficial bacterial strains can also effectively reestablish the microbiota community, and further restore the abilities of microbiota involved in drug-microbiota interaction (76, 77).

Given these notions, the use of probiotics has become a significant research field. Probiotics refer to the live bacterial species introduced into human body, exerting their beneficial effects by reestablishing the normal microbiota community (78). Much attention has been paid to the effect of probiotics on tumor-treatment-related toxicity (79) and its potential in improving the efficiency of cancer treatment (80). According to research findings, the preoperative administration of probiotics, prebiotics and synbiotics (the combination of probiotics and prebiotics) effectively attenuates the post-operational infection, with a reduced inflammation, morbidity and hospital stay (81, 82). This is achieved by modulating the composition of microbiota and improve the intestinal barrier (82). Additionally, the use of probiotic nutrition strategies has also been proved to be effective against radiotherapy-induced side effects through enhancing immune response, including the administration of probiotic Bifico against chemoradiotherapy-induced oral mucositis (69) and the use of "designer probiotics" in CRC and breast cancer (47). Notably, there is emerging evidence suggesting that the administration of specific bacteria strains, such as *Lactobacillus* spp. and *Bifidobacteriales*, is associated with better anticancer efficacy. A recent clinical trial showed that providing probiotics containing *Lactobacillus* and *Bifidobacteria* to post-operative CRC patients for six mouths effectively reduced the expression of many pro-inflammatory cytokines, including TNF-α, IL-6, IL-10 and IL-12, but the level of IFN-γ is relatively unchanged (83). In mice with adverse intestinal microbiota, oral probiotics containing *Bifidobacterium* could restore the anti-tumor effect of PD-L1 blockade, mainly by promoting the maturation of dendritic cells so as to improve the activity of tumor-specific $CD8^+$ T cells (52). Similarly, the decreased Firmicutes/Baxteroides ratio also leads to a decreased tumorigenic outcome (84).

Looking into the mechanisms, it is found that *Bifidobacteria* could act on the host immune system through the IFN-γ pathway (52). By treating the mice with probiotic Bifidobacteria, the number of major histocompatibility complex-II (MHC-II) dendritic cells within the tumor were elevated due to the secreted costimulatory molecules (85), together with the tumor specific T cells, both in periphery and in tumor. On the other hand, *Bifidobacterium* spp. can activate the transcription of up to 760 genes in tumor-infiltrating dendritic cells which are related to antitumor responses, such as Cd70 and Icam1 gene for $CD8^+$ T cell activation, Relb for dendritic cell maturation, and Rab27a for antigen processing and cross presentation (52).

In addition to the direct interaction of bacteria and immune system, the probiotics can also exert its function by secreting several probiotic-derived molecules. The effector molecules that have been shown to be associated with anticancer property are competence and sporulation factor (CSF), inorganic polyphosphates, ferrichrome, and some other peptides such as P75 and P40 (86). These secreting molecules can act through different mechanisms and pathways. CSF is a type of quorum-sensing pentapeptide, and is able to induce the upregulation of heat shock proteins (Hsps). This further activates epithelial cell survival pathway of protein kinase B/Akt and p38 MAP kinase by organic cation transporter 2 (OCTN2). The inorganic polyphosphate can also induce Hsps expression and act on the integrin β_1-p38 MAPK pathway, and the peptides P75 and P40 is associated with the activation of Akt cell survival pathway. The molecule ferrichrome, derived from probiotic *Lactobacillus casei*, can selectively act on colon cancer cells to induce the cleaving of Caspase-3 and PARP and activate the apoptosis pathway through DDIT3-JNK signaling-mediated ER stress response pathway, with a therapeutic effect even better than cisplatin and 5-FU (86).

Fecal Microbiota Transplantation (FMT)

The concept of fecal microbiota transplantation (FMT) was initially established for treating *Clostridium difficile* infection (CDI). In 1958, Eiseman and colleagues first described this therapeutic method for presumed severe CDI in a case series, which is to transplant functional microbiota from healthy individuals into the gastrointestinal tract of patients to rebuild the normally functioning intestinal microbiota (87, 88). It was not until 2012 that FMT was first linked to cancer treatment by Neemann et al., and in this case by performing FMT, a patient with acute lymphocytic leukemia (ALL) successfully recovered from severe CDI induced by the immunocompromised condition after allogeneic hematopoietic stem cell transplant (89). Later, this therapy was put into practice in the treatment of many other hematological malignancies, in which immunocompromised

condition and dysbiosis often occurred as a post-transplantation complication, leading to *C. difficile* overgrowth and symptoms like diarrhea, abdominal pain and hematochezia (90, 91). Clinical trials of the use of FMT in the treatment of cancer patients are still in their early stages, but has proved its effect on many types of complications during anticancer treatment, including CDI that are resistant to traditional therapies (92), graft-versus-host disease after allogeneic stem cell transplantation (93), inflammatory bowel disease (94) and active ulcerative colitis (95). However, in some cases post-FMT complications such as bacteremia may occur (91), and the mechanism is still unclear. Further studies are required to identify the risk factors for FMT and improve the safety.

Dietary Factors

Short Chain Fatty Acids (SCFA)

Dietary factors have been considered to play a vital role in human health and disease for centuries. Over the last decade, there have been increasing interests in the research on the interplay between diet and the gut microbiota, and it is now widely accepted that gut microbiota can be shaped by dietary factors, leading to enriched beneficial microbiota strains and the production of SCFA. Generally, SCFA has an anti-inflammatory and anti-tumorigenic effect, but there are also exceptions in which specific SCFA could induce different outcomes. For example, being the focus of many studies, the butyrate, one of the SCFA, has a tumor suppressing effect (96), while acetate is a metabolite that has shown to be potentially oncogenic.

Being one of the dietary factors, dietary fibers have shown to effectively prevent CRC with an anti-inflammatory property due to its effect of maintaining the amount of microbiota that produce butyrate (47, 97). Another dietary factor is resistant starch, also a contributing factor of decreased risk of CRC and colitis. It can be converted to SCFA by fermentation in the large intestine, and can lead to reduction in gene expression associated with immune responses and inflammatory conditions including cyclooxygenase 2 (COX-2), NF-κB, IL-1β and TNF-α, having an anti-tumorigenic effect by either activating the expression of G-protein coupled receptor 43 (GPR43) which induces anti-inflammatory property, or inhibiting histone deacetylase (97). In addition, it can inhibit the cell proliferation by inhibiting the translocation of β-catenin from the membrane into the nucleus, preventing the downstream expression of growth factors related to cell growth (97). These findings have strong implications in searching an alternative approach to shape gut microbiota with dietary factors, which can be easily controlled by patients even in everyday life.

Vitamin D

Previous studies have demonstrated that vitamin D has an important immunomodulatory function. Several immune cells (such as T cells, B cells, neutrophils and APCs) express vitamin D receptor, allowing vitamin D to regulate the balance between pro-inflammatory and anti-inflammatory state (98). It can also mediate the antimicrobial peptide (CAMP) expression downstream of TLR activation, leading to phagosome formation and antimicrobial activity against pathogens (98).

In addition, vitamin D has shown to be effective against complications caused by radiotherapy *via* restoring the population of gut microbiota and reducing the number of opportunistic pathogens (99). In induced colitis, the vitamin D deficient mice have the characteristics of a reduced antimicrobial activity of angiogenin-4 protein (Ang4) (100).The relationships among vitamin D, gut microbiota and radiation-induced resistance were described as a "love-hate triangle", indicating that these three factors could interact with each other during the process of the anticancer therapy (99). However, further studies are still needed for the understanding of the molecular mechanisms.

CONCLUSIONS AND FUTURE DIRECTIONS

As cancer is the leading cause of death worldwide, finding a cure for this devastating disease has long been a challenge for the research field. The current anticancer therapies mentioned above have proved to be effective in providing curative or palliative managements against cancer, but there are still several side effects during this process, leading to reduced efficacy and prognosis. Reports on the role of microbiota in cancer, combined with preclinical and clinical research, have led to the revelation of this topic as a potentially dominant mediator in response to cancer treatment. With the rapid development of the understanding of human gastrointestinal microbiota, there exists a close symbiotic relationship between the gastrointestinal microbiota and the host. In the context of many diseases of the digestive system, the disturbance of the composition of the gastrointestinal microbiota can be observed. Whether gastrointestinal microbiota imbalance is the cause or outcome of the disease, it may exacerbate the disease progression and influence the associated treatment strategies. In addition, it is demonstrated that the cancer treatment response can be enhanced by modulating the intestinal microbiome such as providing beneficial bacteria strains as probiotics or preforming FMT, and future therapy could utilize these methods to achieve a precise regulation of the microbiota composition, such as the specific amount of a particular microbiota genus. However, it is not clear which intestinal microbiome composition is best suited to promote the anti-tumor immune response, which needs to be carefully tested through clinical trials. It is also necessary to find out other important factors to modulate the intestinal microbiome, such as adjustment of preparation before the use of antibiotics. Only by fully understanding these mechanisms can we better optimize the regulation of the intestinal microbiota, and improve the potential for immune surveillance and cancer treatment.

AUTHOR CONTRIBUTIONS

TC conceived the idea for the review and designed its framework. WL and XD conducted the research and wrote the manuscript. All authors edited the manuscript. All authors contributed to the article and approved the submitted version.

FUNDING

This study was supported by the National Natural Science Foundation of China (Grant no. 82060638, 81960103), Academic and technical leaders of major disciplines in Jiangxi Province (Grant no. 20194BCJ22032), and Double thousand plan of Jiangxi Province (high end Talents Project of scientific and technological innovation).

REFERENCES

1. Inaki K, Liu ET. Structural mutations in cancer: mechanistic and functional insights. *Trends Genet* (2012) 28(11):550–9. doi: 10.1016/j.tig.2012.07.002
2. Samuel SR, Maiya AG, Fernandes DJ, Guddattu V, Saxena PUP, Kurian JR, et al. Effectiveness of exercise-based rehabilitation on functional capacity and quality of life in head and neck cancer patients receiving chemo-radiotherapy. *Support Care Cancer* (2019) 27(10):3913–20. doi: 10.1007/s00520-019-04750-z
3. Chen T, Zhao X, Ren Y, Wang Y, Tang X, Tian P, et al. Triptolide modulates tumour-colonisation and anti-tumour effect of attenuated Salmonella encoding DNase I. *Appl Microbiol Biotechnol* (2019) 103(2):929–39. doi: 10.1007/s00253-018-9481-8
4. Kumagai T, Rahman F, Smith AM. The Microbiome and Radiation Induced-Bowel Injury: Evidence for Potential Mechanistic Role in Disease Pathogenesis. *Nutrients* (2018) 10(10):1045. doi: 10.3390/nu10101405
5. Secombe KR, Coller JK, Gibson RJ, Wardill HR, Bowen JM. The bidirectional interaction of the gut microbiome and the innate immune system: Implications for chemotherapy-induced gastrointestinal toxicity. *Int J Cancer* (2019) 144 (10):2365–76. doi: 10.1002/ijc.31836
6. Roy S, Trinchieri G. Microbiota: a key orchestrator of cancer therapy. *Nat Rev Cancer* (2017) 17(5):271–85. doi: 10.1038/nrc.2017.13
7. Gori S, Inno A, Belluomini L, Bocus P, Bisoffi Z, Russo A, et al. Gut microbiota and cancer: How gut microbiota modulates activity, efficacy and toxicity of antitumoral therapy. *Crit Rev Oncol Hematol* (2019) 143:139–47. doi: 10.1016/j.critrevonc.2019.09.003
8. AlHilli MM, Bae-Jump V. Diet and gut microbiome interactions in gynecologic cancer. *Gynecol Oncol* (2020) 159(2):299–308. doi: 10.1016/j.ygyno.2020.08.027
9. Rodriguez JM, Murphy K, Stanton C, Ross RP, Kober OI, Juge N, et al. The composition of the gut microbiota throughout life, with an emphasis on early life. *Microb Ecol Health Dis* (2015) 26:26050. doi: 10.3402/mehd.v26.26050
10. Aarnoutse R, Ziemons J, Penders J, Rensen SS, de Vos-Geelen J, Smidt ML. The Clinical Link between Human Intestinal Microbiota and Systemic Cancer Therapy. *Int J Mol Sci* (019) 20(17):4145. doi: 10.3390/ijms20174145
11. White JR, Dauros-Singorenko P, Hong J, Vanholsbeeck F, Phillips A, Swift S. The role of host molecules in communication with the resident and pathogenic microbiota: A review. *Med Microecology* (2021) 4:100005. doi: 10.1016/j.medmic.2020.100005
12. Kroemer G, Zitvogel L. Cancer immunotherapy in 2017: The breakthrough of the microbiota. *Nat Rev Immunol* (2018) 18(2):87–8. doi: 10.1038/nri.2018.4
13. Hanahan D, Weinberg RA. Hallmarks of cancer: the next generation. *Cell* (2011) 144(5):646–74. doi: 10.1016/j.cell.2011.02.013
14. Ewing A, Semple C. Breaking point: the genesis and impact of structural variation in tumours. *F1000Research* (2018) 7:1814. doi: 10.12688/f1000research.16079.1
15. Dejea C, Wick E, Sears CL. Bacterial oncogenesis in the colon. *Future Microbiol* (2013) 8(4):445–60. doi: 10.2217/fmb.13.17
16. Tsvetikova SA, Koshel EI. Microbiota and cancer: host cellular mechanisms activated by gut microbial metabolites. *Int J Med Microbiol* (2020) 310 (4):151425. doi: 10.1016/j.ijmm.2020.151425
17. Hatakeyama M. Structure and function of Helicobacter pylori CagA, the first-identified bacterial protein involved in human cancer. Proceedings of the Japan Academy Series B. *Phys Biol Sci* (2017) 93(4):196–219. doi: 10.2183/pjab.93.013
18. Goodwin AC, Destefano Shields CE, Wu S, Huso DL, Wu X, Murray-Stewart TR, et al. Polyamine catabolism contributes to enterotoxigenic Bacteroides fragilis-induced colon tumorigenesis. *Proc Natl Acad Sci USA* (2011) 108 (37):15354–9. doi: 10.1073/pnas.1010203108
19. Raza MH, Gul K, Arshad A, Riaz N, Waheed U, Rauf A, et al. Microbiota in cancer development and treatment. *J Cancer Res Clin Oncol* (2019) 145(1):49–63. doi: 10.1007/s00432-018-2816-0
20. Blagosklonny MV. How Avastin potentiates chemotherapeutic drugs: action and reaction in antiangiogenic therapy. *Cancer Biol Ther* (2005) 4(12):1307–10. doi: 10.4161/cbt.4.12.2315
21. Winkler GC, Barle EL, Galati G, Kluwe WM. Functional differentiation of cytotoxic cancer drugs and targeted cancer therapeutics. *Regul Toxicol Pharmacol* (2014) 70(1):46–53. doi: 10.1016/j.yrtph.2014.06.012
22. Lin XB, Dieleman LA, Ketabi A, Bibova I, Sawyer MB, Xue H, et al. Irinotecan (CPT-11) chemotherapy alters intestinal microbiota in tumour bearing rats. *PloS One* (2012) 7(7):e39764. doi: 10.1371/journal.pone.0039764
23. Imaoka A, Setoyama H, Takagi A, Matsumoto S, Umesaki Y. Improvement of human faecal flora-associated mouse model for evaluation of the functional foods. *J Appl Microbiol* (2004) 96(4):656–63. doi: 10.1111/j.1365-2672.2004.02189.x
24. Hekmatshoar Y, Rahbar Saadat Y, Hosseiniyan Khatibi SM, Ozkan T, Zununi Vahed F, Nariman-Saleh-Fam Z, et al. The impact of tumor and gut microbiotas on cancer therapy: Beneficial or detrimental? *Life Sci* (2019) 233:116680. doi: 10.1016/j.lfs.2019.116680
25. Viaud S, Saccheri F, Mignot G, Yamazaki T, Daillère R, Hannani D, et al. The intestinal microbiota modulates the anticancer immune effects of cyclophosphamide. *Science (New York NY)* (2013) 342(6161):971–6. doi: 10.1126/science.1240537
26. Klaassen CD, Cui JY. Review: Mechanisms of How the Intestinal Microbiota Alters the Effects of Drugs and Bile Acids. *Drug Metab Dispos* (2015) 43 (10):1505–21. doi: 10.1124/dmd.115.065698
27. Kaneda N, Yokokura T. Nonlinear pharmacokinetics of CPT-11 in rats. *Cancer Res* (1990) 50(6):1721–5. doi: 10.1016/S1872-2075(08)60042-4
28. Takasuna K, Hagiwara T, Hirohashi M, Kato M, Nomura M, Nagai E, et al. Involvement of beta-glucuronidase in intestinal microflora in the intestinal toxicity of the antitumor camptothecin derivative irinotecan hydrochloride (CPT-11) in rats. *Cancer Res* (1996) 56(16):3752–7. doi: 10.1002/(SICI)1097-0142(19960815)78:4<912::AID-CNCR31>3.0.CO;2-W
29. Desgranges C, Razaka G, De Clercq E, Herdewijn P, Balzarini J, Drouillet F, et al. Effect of (E)-5-(2-bromovinyl)uracil on the catabolism and antitumor activity of 5-fluorouracil in rats and leukemic mice. *Cancer Res* (1986) 46 (3):1094–101. doi: 10.1016/0304-3835(86)90058-3
30. Nishiyama T, Ogura K, Okuda H, Suda K, Kato A, Watabe T. Mechanism-based inactivation of human dihydropyrimidine dehydrogenase by (E)-5-(2-bromovinyl)uracil in the presence of NADPH. *Mol Pharmacol* (2000) 57 (5):899–905.
31. Okuda H, Nishiyama T, Ogura K, Nagayama S, Ikeda K, Yamaguchi S, et al. Lethal drug interactions of sorivudine, a new antiviral drug, with oral 5-fluorouracil prodrugs. *Drug Metab Dispos* (1997) 25(2):270–3. doi: 10.1016/S1359-6446(96)10051-9
32. Nakayama H, Kinouchi T, Kataoka K, Akimoto S, Matsuda Y, Ohnishi Y. Intestinal anaerobic bacteria hydrolyse sorivudine, producing the high blood concentration of 5-(E)-(2-bromovinyl)uracil that increases the level and toxicity of 5-fluorouracil. *Pharmacogenetics* (1997) 7(1):35–43. doi: 10.1097/00008571-199702000-00005
33. Schieber M, Chandel NS. ROS function in redox signaling and oxidative stress. *Curr Biol* (2014) 24(10):R453–62. doi: 10.1016/j.cub.2014.03.034
34. Iida N, Dzutsev A, Stewart CA, Smith L, Bouladoux N, Weingarten RA, et al. Commensal bacteria control cancer response to therapy by modulating the tumor microenvironment. *Science (New York NY)* (2013) 342(6161):967–70. doi: 10.1126/science.1240527
35. Chang CW, Lee HC, Li LH, Chiang Chiau JS, Wang TE, Chuang WH, et al. Fecal Microbiota Transplantation Prevents Intestinal Injury, Upregulation of Toll-Like Receptors, and 5-Fluorouracil/Oxaliplatin-Induced Toxicity in Colorectal Cancer. *Int J Mol Sci* (2020) 21(2):386. doi: 10.3390/ijms21020386
36. Xu C, Ruan B, Jiang Y, Xue T, Wang Z, Lu H, et al. Antibiotics-induced gut microbiota dysbiosis promotes tumor initiation via affecting APC-Th1

development in mice. *Biochem Biophys Res Commun* (2017) 488(2):418–24. doi: 10.1016/j.bbrc.2017.05.071
37. Schirmer M, Smeekens SP, Vlamakis H, Jaeger M, Oosting M, Franzosa EA, et al. Linking the Human Gut Microbiome to Inflammatory Cytokine Production Capacity. *Cell* (2016) 167(4):1125–36.e8. doi: 10.1016/j.cell.2016.10.020
38. Daillère R, Vétizou M, Waldschmitt N, Yamazaki T, Isnard C, Poirier-Colame V, et al. Enterococcus hirae and Barnesiella intestinihominis Facilitate Cyclophosphamide-Induced Therapeutic Immunomodulatory Effects. *Immunity* (2016) 45(4):931–43. doi: 10.1016/j.immuni.2016.09.009
39. Wang Y, Li Y, Shang D, Efferth T. Interactions between artemisinin derivatives and P-glycoprotein. *Phytomedicine* (2019) 60:152998. doi: 10.1016/j.phymed.2019.152998
40. Kostic AD, Gevers D, Pedamallu CS, Michaud M, Duke F, Earl AM, et al. Genomic analysis identifies association of Fusobacterium with colorectal carcinoma. *Genome Res* (2012) 22(2):292–8. doi: 10.1101/gr.126573.111
41. Rubinstein MR, Wang X, Liu W, Hao Y, Cai G, Han YW. Fusobacterium nucleatum promotes colorectal carcinogenesis by modulating E-cadherin/β-catenin signaling via its FadA adhesin. *Cell Host Microbe* (2013) 14(2):195–206. doi: 10.1016/j.chom.2013.07.012
42. Couzin-Frankel J. Breakthrough of the year 2013. Cancer immunotherapy. *Science (New York NY)* (2013) 342(6165):1432–3. doi: 10.1126/science.342.6165.1432
43. Billan S, Kaidar-Person O, Gil Z. Treatment after progression in the era of immunotherapy. *Lancet Oncol* (2020) 21(10):e463–e76. doi: 10.1016/S1470-2045(20)30328-4
44. Hahn AW, Gill DM, Pal SK, Agarwal N. The future of immune checkpoint cancer therapy after PD-1 and CTLA-4. *Immunotherapy* (2017) 9(8):681–92. doi: 10.2217/imt-2017-0024
45. Peggs KS, Quezada SA, Korman AJ, Allison JP. Principles and use of anti-CTLA4 antibody in human cancer immunotherapy. *Curr Opin Immunol* (2006) 18(2):206–13. doi: 10.1016/j.coi.2006.01.011
46. Cohen I, Ruff WE, Longbrake EE. Influence of immunomodulatory drugs on the gut microbiota. *Trans Res J Lab Clin Med* (2021) S1931-5244(21):00023–2. doi: 10.1016/j.trsl.2021.01.009
47. Gopalakrishnan V, Helmink BA, Spencer CN, Reuben A, Wargo JA. The Influence of the Gut Microbiome on Cancer, Immunity, and Cancer Immunotherapy. *Cancer Cell* (2018) 33(4):570–80. doi: 10.1016/j.ccell.2018.03.015
48. Pabst O. New concepts in the generation and functions of IgA. *Nat Rev Immunol* (2012) 12(12):821–32. doi: 10.1038/nri3322
49. Chen DS, Mellman I. Oncology meets immunology: the cancer-immunity cycle. *Immunity* (2013) 39(1):1–10. doi: 10.1016/j.immuni.2013.07.012
50. Ivanov II, Atarashi K, Manel N, Brodie EL, Shima T, Karaoz U, et al. Induction of intestinal Th17 cells by segmented filamentous bacteria. *Cell* (2009) 139 (3):485–98. doi: 10.1016/j.cell.2009.09.033
51. Atarashi K, Tanoue T, Shima T, Imaoka A, Kuwahara T, Momose Y, et al. Induction of colonic regulatory T cells by indigenous Clostridium species. *Science (New York NY)* (2011) 331(6015):337–41. doi: 10.1126/science.1198469
52. Sivan A, Corrales L, Hubert N, Williams JB, Aquino-Michaels K, Earley ZM, et al. Commensal Bifidobacterium promotes antitumor immunity and facilitates anti-PD-L1 efficacy. *Science (New York NY)* (2015) 350 (6264):1084–9. doi: 10.1126/science.aac4255
53. Vetizou M, Pitt JM, Daillere R, Lepage P, Waldschmitt N, Flament C, et al. Anticancer immunotherapy by CTLA-4 blockade relies on the gut microbiota. *Science (New York NY)* (2015) 350(6264):1079–84. doi: 10.1126/science.aad1329
54. Huang J, Jiang Z, Wang Y, Fan X, Cai J, Yao X, et al. Modulation of gut microbiota to overcome resistance to immune checkpoint blockade in cancer immunotherapy. *Curr Opin Pharmacol* (2020) 54:1–10. doi: 10.1016/j.coph.2020.06.004
55. Tanoue T, Morita S, Plichta DR, Skelly AN, Suda W, Sugiura Y, et al. A defined commensal consortium elicits CD8 T cells and anti-cancer immunity. *Nature* (2019) 565(7741):600–5. doi: 10.1038/s41586-019-0878-z
56. Gopalakrishnan V, Spencer CN, Nezi L, Reuben A, Andrews MC, Karpinets TV, et al. Gut microbiome modulates response to anti-PD-1 immunotherapy in melanoma patients. *Science (New York NY)* (2018) 359(6371):97–103. doi: 10.1126/science.aan4236
57. Holler E, Butzhammer P, Schmid K, Hundsrucker C, Koestler J, Peter K, et al. Metagenomic analysis of the stool microbiome in patients receiving allogeneic stem cell transplantation: loss of diversity is associated with use of systemic antibiotics and more pronounced in gastrointestinal graft-versus-host disease. *Biol Blood marrow Transplant* (2014) 20(5):640–5. doi: 10.1016/j.bbmt.2014.01.030
58. Gao Y, Shang Q, Li W, Guo W, Stojadinovic A, Mannion C, et al. Antibiotics for cancer treatment: A double-edged sword. *J Cancer* (2020) 11(17):5135–49. doi: 10.7150/jca.47470
59. Mari GM, Achilli P, Maggioni D, Crippa J, Costanzi ATM, Scotti MA, et al. Creation of a rectal cancer registry in Italy by the Advanced International Mini-Invasive Surgery (AIMS) academy clinical research network. *F1000Research* (2019) 8:1736. doi: 10.12688/f1000research.20702.1
60. Gaines S, Shao C, Hyman N, Alverdy JC. Gut microbiome influences on anastomotic leak and recurrence rates following colorectal cancer surgery. *Br J Surg* (2018) 105(2):e131–e41. doi: 10.1002/bjs.10760
61. Alves A, Panis Y, Trancart D, Regimbeau JM, Pocard M, Valleur P. Factors associated with clinically significant anastomotic leakage after large bowel resection: multivariate analysis of 707 patients. *World J Surg* (2002) 26 (4):499–502. doi: 10.1007/s00268-001-0256-4
62. Borowski DW, Bradburn DM, Mills SJ, Bharathan B, Wilson RG, Ratcliffe AA, et al. Volume-outcome analysis of colorectal cancer-related outcomes. *Br J Surg* (2010) 97(9):1416–30. doi: 10.1002/bjs.7111
63. Stern JR, Olivas AD, Valuckaite V, Zaborina O, Alverdy JC, An G. Agent-based model of epithelial host-pathogen interactions in anastomotic leak. *J Surg Res* (2013) 184(2):730–8. doi: 10.1016/j.jss.2012.12.009
64. van Praagh JB, de Goffau MC, Bakker IS, van Goor H, Harmsen HJM, Olinga P, et al. Mucus Microbiome of Anastomotic Tissue During Surgery Has Predictive Value for Colorectal Anastomotic Leakage. *Ann Surg* (2019) 269 (5):911–6. doi: 10.1097/SLA.0000000000002651
65. Baskar R, Dai J, Wenlong N, Yeo R, Yeoh KW. Biological response of cancer cells to radiation treatment. *Front Mol Biosci* (2014) 1:24. doi: 10.3389/fmolb.2014.00024
66. Shuryak I. Review of microbial resistance to chronic ionizing radiation exposure under environmental conditions. *J Environ Radioact* (2019) 196:50–63. doi: 10.1016/j.jenvrad.2018.10.012
67. Derer A, Deloch L, Rubner Y, Fietkau R, Frey B, Gaipl US. Radio-Immunotherapy-Induced Immunogenic Cancer Cells as Basis for Induction of Systemic Anti-Tumor Immune Responses - Pre-Clinical Evidence and Ongoing Clinical Applications. *Front Immunol* (2015) 6:505. doi: 10.3389/fimmu.2015.00505
68. Nelson MH, Diven MA, Huff LW, Paulos CM. Harnessing the Microbiome to Enhance Cancer Immunotherapy. *J Immunol Res* (2015) 2015:368736. doi: 10.1155/2015/368736
69. Jiang C, Wang H, Xia C, Dong Q, Chen E, Qiu Y, et al. A randomized, double-blind, placebo-controlled trial of probiotics to reduce the severity of oral mucositis induced by chemoradiotherapy for patients with nasopharyngeal carcinoma. *Cancer* (2019) 125(7):1081–90. doi: 10.1002/cncr.31907
70. Nam YD, Kim HJ, Seo JG, Kang SW, Bae JW. Impact of pelvic radiotherapy on gut microbiota of gynecological cancer patients revealed by massive pyrosequencing. *PloS One* (2013) 8(12):e82659. doi: 10.1371/journal.pone.0082659
71. Manichanh C, Varela E, Martinez C, Antolin M, Llopis M, Doré J, et al. The gut microbiota predispose to the pathophysiology of acute postradiotherapy diarrhea. *Am J Gastroenterol* (2008) 103(7):1754–61. doi: 10.1111/j.1572-0241.2008.01868.x
72. Wang A, Ling Z, Yang Z, Kiela PR, Wang T, Wang C, et al. Gut microbial dysbiosis may predict diarrhea and fatigue in patients undergoing pelvic cancer radiotherapy: a pilot study. *PloS One* (2015) 10(5):e0126312. doi: 10.1371/journal.pone.0126312
73. Sahly N, Moustafa A, Zaghloul M, Salem TZ. Effect of radiotherapy on the gut microbiome in pediatric cancer patients: a pilot study. *PeerJ* (2019) 7:e7683. doi: 10.7717/peerj.7683
74. Crawford PA, Gordon JI. Microbial regulation of intestinal radiosensitivity. *Proc Natl Acad Sci USA* (2005) 102(37):13254–9. doi: 10.1073/pnas.0504830102

75. Tonneau M, Elkrief A, Pasquier D, Paz Del Socorro T, Chamaillard M, Bahig H, et al. The role of the gut microbiome on radiation therapy efficacy and gastrointestinal complications: A systematic review. *Radiother Oncol* (2020) 156:1–9. doi: 10.1016/j.radonc.2020.10.033
76. Bhatt AP, Pellock SJ, Biernat KA, Walton WG, Wallace BD, Creekmore BC, et al. Targeted inhibition of gut bacterial β-glucuronidase activity enhances anticancer drug efficacy. *Proc Natl Acad Sci USA* (2020) 117(13):7374–81. doi: 10.1073/pnas.1918095117
77. Zhou Z, Chen X, Sheng H, Shen X, Sun X, Yan Y, et al. Engineering probiotics as living diagnostics and therapeutics for improving human health. *Microb Cell Fact* (2020) 19(1):56. doi: 10.1186/s12934-020-01318-z
78. Gareau MG, Sherman PM, Walker WA. Probiotics and the gut microbiota in intestinal health and disease. *Nat Rev Gastroenterol Hepatol* (2010) 7(9):503–14. doi: 10.1038/nrgastro.2010.117
79. Hendler R, Zhang Y. Probiotics in the Treatment of Colorectal Cancer. *Medicines (Basel Switzerland)* (2018) 5(31):101. doi: 10.3390/medicines5030101
80. Górska A, Przystupski D, Niemczura MJ, Kulbacka J. Probiotic Bacteria: A Promising Tool in Cancer Prevention and Therapy. *Curr Microbiol* (2019) 76 (8):939–49. doi: 10.1007/s00284-019-01679-8
81. Kinross JM, Markar S, Karthikesalingam A, Chow A, Penney N, Silk D, et al. A meta-analysis of probiotic and synbiotic use in elective surgery: does nutrition modulation of the gut microbiome improve clinical outcome? *JPEN J Parenter Enteral Nutr* (2013) 37(2):243–53. doi: 10.1177/0148607112452306
82. Polakowski CB, Kato M, Preti VB, Schieferdecker MEM, Ligocki Campos AC. Impact of the preoperative use of synbiotics in colorectal cancer patients: A prospective, randomized, double-blind, placebo-controlled study. *Nutrition (Burbank Los Angeles County Calif)* (2019) 58:40–6. doi: 10.1016/j.nut.2018.06.004
83. Zaharuddin L, Mokhtar NM, Muhammad Nawawi KN, Raja Ali RA. A randomized double-blind placebo-controlled trial of probiotics in post-surgical colorectal cancer. *BMC Gastroenterol* (2019) 19(1):131. doi: 10.1186/s12876-019-1047-4
84. Zhu Q, Jin Z, Wu W, Gao R, Guo B, Gao Z, et al. Analysis of the intestinal lumen microbiota in an animal model of colorectal cancer. *PloS One* (2014) 9 (6):e90849. doi: 10.1371/journal.pone.0090849
85. López P, Gueimonde M, Margolles A, Suárez A. Distinct Bifidobacterium strains drive different immune responses in vitro. *Int J Food Microbiol* (2010) 138(1-2):157–65. doi: 10.1016/j.ijfoodmicro.2009.12.023
86. Konishi H, Fujiya M, Tanaka H, Ueno N, Moriichi K, Sasajima J, et al. Probiotic-derived ferrichrome inhibits colon cancer progression via JNK-mediated apoptosis. *Nat Commun* (2016) 7:12365. doi: 10.1038/ncomms12365
87. Eiseman B, Silen W, Bascom GS, Kauvar AJ. Fecal enema as an adjunct in the treatment of pseudomembranous enterocolitis. *Surgery* (1958) 44(5):854–9.
88. Grigoryan Z, Shen MJ, Twardus SW, Beuttler MM, Chen LA, Bateman-House A. Fecal microbiota transplantation: Uses, questions, and ethics. *Med Microecology* (2020) 6:100027. doi: 10.1016/j.medmic.2020.100027
89. Neemann K, Eichele DD, Smith PW, Bociek R, Akhtari M, Freifeld A. Fecal microbiota transplantation for fulminant Clostridium difficile infection in an allogeneic stem cell transplant patient. *Transplant Infect Dis* (2012) 14(6): E161–5. doi: 10.1111/tid.12017
90. de Castro CGJr, Ganc AJ, Ganc RL, Petrolli MS, Hamerschlack N. Fecal microbiota transplant after hematopoietic SCT: report of a successful case. *Bone marrow Transplant* (2015) 50(1):145. doi: 10.1038/bmt.2014.212
91. Lee MSL, Ramakrishna B, Moss AC, Gold HS, Branch-Elliman W. Successful treatment of fulminant Clostridioides difficile infection with emergent fecal microbiota transplantation in a patient with acute myeloid leukemia and prolonged, severe neutropenia. *Transplant Infect Dis* (2020) 22(1):e13216. doi: 10.1111/tid.13216
92. Borody TJ, Warren EF, Leis SM, Surace R, Ashman O, Siarakas S. Bacteriotherapy using fecal flora: toying with human motions. *J Clin Gastroenterol* (2004) 38(6):475–83. doi: 10.1097/01.mcg.0000128988.13808.dc
93. Kakihana K, Fujioka Y, Suda W, Najima Y, Kuwata G, Sasajima S, et al. Fecal microbiota transplantation for patients with steroid-resistant acute graft-versus-host disease of the gut. *Blood* (2016) 128(16):2083–8. doi: 10.1182/blood-2016-05-717652
94. Ding X, Yang X, Wang H. Methodology, efficacy and safety of fecal microbiota transplantation in treating inflammatory bowel disease. *Med Microecology* (2020) 6:100028. doi: 10.1016/j.medmic.2020.100028
95. Moayyedi P, Surette MG, Kim PT, Libertucci J, Wolfe M, Onischi C, et al. Fecal Microbiota Transplantation Induces Remission in Patients With Active Ulcerative Colitis in a Randomized Controlled Trial. *Gastroenterology* (2015) 149(1):102–9.e6. doi: 10.1053/j.gastro.2015.04.001
96. Zitvogel L, Daillère R, Roberti MP, Routy B, Kroemer G. Anticancer effects of the microbiome and its products. *Nat Rev Microbiol* (2017) 15(8):465–78. doi: 10.1038/nrmicro.2017.44
97. Hu Y, Le Leu RK, Christophersen CT, Somashekar R, Conlon MA, Meng XQ, et al. Manipulation of the gut microbiota using resistant starch is associated with protection against colitis-associated colorectal cancer in rats. *Carcinogenesis* (2016) 37(4):366–75. doi: 10.1093/carcin/bgw019
98. Malaguarnera L. Vitamin D and microbiota: Two sides of the same coin in the immunomodulatory aspects. *Int Immunopharmacol* (2020) 79:106112. doi: 10.1016/j.intimp.2019.106112
99. Huang R, Xiang J, Zhou P. Vitamin D, gut microbiota, and radiation-related resistance: a love-hate triangle. *J Exp Clin Cancer Res* (2019) 38(1):493. doi: 10.1186/s13046-019-1499-y
100. Assa A, Vong L, Pinnell LJ, Rautava J, Avitzur N, Johnson-Henry KC, et al. Vitamin D deficiency predisposes to adherent-invasive Escherichia coli-induced barrier dysfunction and experimental colonic injury. *Inflamm Bowel Dis* (2015) 21(2):297–306. doi: 10.1097/MIB.0000000000000282

Conflict of Interest: The authors declare that the research was conducted in the absence of any commercial or financial relationships that could be construed as a potential conflict of interest.

frontiers in Immunology

ORIGINAL RESEARCH
published: 05 October 2021
doi: 10.3389/fimmu.2021.687874

Suppression of Transmembrane Tumor Necrosis Factor Alpha Processing by a Specific Antibody Protects Against Colitis-Associated Cancer

Hongping Ba[1], Rui Jiang[1], Meng Zhang[1], Bingjiao Yin[1], Jing Wang[1], Zhuoya Li[1], Baihua Li[1] and Xiaoxi Zhou[2]**

[1] Department of Immunology, Tongji Medical College, Huazhong University of Science and Technology, Wuhan, China,
[2] Department of Hematology, Tongji Hospital, Huazhong University of Science and Technology, Wuhan, China

OPEN ACCESS

Edited by:
Catherine Sautes-Fridman,
INSERM U1138 Centre de Recherche des Cordeliers (CRC), France

Reviewed by:
Virginia Tirino,
Università della Campania Luigi Vanvitelli, Italy
Tiziana Schioppa,
University of Brescia, Italy

***Correspondence:**
Xiaoxi Zhou
cello316@163.com
Baihua Li
libaihua1986@126.com

Specialty section:
This article was submitted to Cancer Immunity and Immunotherapy, a section of the journal Frontiers in Immunology

Received: 30 March 2021
Accepted: 16 September 2021
Published: 05 October 2021

Citation:
Ba H, Jiang R, Zhang M, Yin B, Wang J, Li Z, Li B and Zhou X (2021) Suppression of Transmembrane Tumor Necrosis Factor Alpha Processing by a Specific Antibody Protects Against Colitis-Associated Cancer. Front. Immunol. 12:687874. doi: 10.3389/fimmu.2021.687874

Soluble tumor necrosis factor-α (sTNF-α) plays an important role in colitis-associated cancer (CAC); however, little is known about transmembrane TNF-α (tmTNF-α). Here, we observed an increase in sTNF-α mainly in colitis tissues from an azoxymethane/dextran sodium sulfate (DSS)-induced CAC mouse model whereas tmTNF-α levels were chiefly increased on epithelial cells at the tumor stage. The ratio of intracolonic tmTNF-α/sTNF-α was negatively correlated with the levels of pro-inflammatory mediators (IL-1β, IL-6, and NO) and M1 macrophages but positively correlated with the infiltration of myeloid-derived suppressor cells, regulatory T cells, and the level of the anti-inflammatory cytokine IL-10, suggesting an anti-inflammatory effect of tmTNF-α. This effect of tmTNF-α was confirmed again by the induction of resistance to LPS in colonic epithelial cell lines NCM460 and HCoEpiC through the addition of exogenous tmTNF-α or transfection of the tmTNF-α leading sequence that lacks the extracellular segment but retains the intracellular domain of tmTNF-α. A tmTNF-α antibody was used to block tmTNF-α shedding after the first or second round of inflammation induction by DSS drinking to shift the time window of tmTNF-α expression ahead to the inflammation stage. Antibody treatment significantly alleviated inflammation and suppressed subsequent adenoma formation, accompanied by increased apoptosis. An antitumor effect was also observed when the antibody was administered at the malignant phase of CAC. Our results reveal tmTNF-α as a novel molecular marker for malignant transformation in CAC and provide a new insight into blocking the pathological process by targeting tmTNF-α processing.

Keywords: transmembrane tumor necrosis factor-α, soluble tumor necrosis factor-α, colitis-associated cancer, antibody-based therapy, cytokines, macrophages, regulatory T cells, myeloid-derived suppressor cells

INTRODUCTION

Up to 20% of all human cancers result from chronic inflammation and persistent infection. Patients who suffer from inflammatory bowel disease (IBD) have a high risk of developing colitis-associated colorectal cancer (CAC) and have a high mortality from the disease (1, 2). Chronic inflammation contributes to the development of low- and high-grade dysplasia that further converts colitis into colorectal cancer (CRC). Proinflammatory cytokines and tumor-infiltrating myeloid and immune cells play critical roles in the initiation, promotion, and progression to malignant transformation (3–8).

Tumor necrosis factor-α (TNF-α) exists in two bioactive forms: 26-kDa transmembrane TNF-α (tmTNF-α) and 17-kDa soluble TNF-α (sTNF-α). tmTNF-α on the cell surface is cleaved by a metalloproteinase, TNF-α-converting enzyme (TACE), to release sTNF-α. Both forms of TNF-α are bioactive and display distinct functions. sTNF-α, a proinflammatory factor, plays a pivotal role in the pathogenesis of IBD. The expression of TNF-α is elevated in biopsies and peripheral blood cells (PBC) obtained from patients with ulcerative colitis (UC) and Crohn's disease (CD) (9, 10). Serum levels of sTNF-α are markedly increased by 1.7-fold in patients with active UC (11), which contributes to the mucosal damage and chronic inflammation responsible for the signs and symptoms of active UC. The release of sTNF-α also increases in the mouse colon following azoxymethane/dextran sodium sulfate (AOM/DSS) treatment, and ablation of TNF receptor (TNFR) 1 results in reduced mucosal damage, macrophage and neutrophil recruitment, and tumor formation in mouse colon, suggesting a tumor-promoting role of TNF-α in CAC (12). In addition, TNF-α also promotes CRC metastasis. The efficacy of blocking TNF-α signaling by anti-TNF-α agents has been reported in the treatment of IBD (13, 14). TNF-α antagonists not only inhibit CAC induction in mice by limiting TNF-induced infiltration of neutrophils and macrophages (12) but also reduce the risk of both dysplasia and CAC when combined with other anti-inflammatory medications in the clinic (15).

The role of tmTNF-α in IBD has been clarified in studies on the mechanisms of anti-TNF-α agents. Although the affinity of anti-TNF-α agents for tmTNF-α is lower than that for sTNF-α, the binding and neutralization of tmTNF-α by these agents is presumed to be crucial for their different clinical efficacies, as the neutralization of sTNF-α alone or transferring T cells expressing a non-cleavable tmTNF-α mutant that does not produce sTNF-α did not protect the mice from intestinal inflammation (16, 17). However, a deficiency in both IL-10 and TNF-α exacerbates enterocolitis in mice, indicating some protective effects of TNF-α on this condition (18). Selective inhibition of sTNF-α by XPro1595-DN-TNF significantly prevents chemical-induced carcinogenesis (19), indicating a possible protective effect of tmTNF-α. In addition, tmTNF-α functions not only as a ligand that binds TNFRs to induce forward signaling but also as a receptor to transduce outside-to-inside signals, namely, reverse signaling. The mechanisms underlying the benefit of anti-TNF agents in patients with IBD are not limited to the neutralization of both forms of TNF-α, as these agents activate reverse signaling from tmTNF-α. Binding of infliximab to tmTNF-α not only induces apoptosis but also downregulates proinflammatory mediators and upregulates the anti-inflammatory cytokines IL-10 and TGF-β (20–23), indicating that tmTNF-α-mediated reverse signaling promotes the resolution of inflammation. However, little is known about tmTNF-α expression and its function during the development of CAC. Here, we found that sTNF-α levels increased in the inflammation phase, while tmTNF-α expression was enhanced in colon tissues during malignant transformation in AOM/DSS-induced CAC mice. The administration of a tmTNF-α antibody to shift the time window of tmTNF-α expression ahead to the inflammation phase significantly suppressed inflammation and limited subsequent tumor formation.

MATERIALS AND METHODS

Mouse Model

All animal experiments were approved by the Animal Care and Use Committee of Huazhong University of Science and Technology. Male C57BL/6 mice, 4 to 6 weeks old, were purchased from Beijing HFK Bioscience Company (Beijing, China) and housed under specific pathogen-free conditions with free access to food and water. Mice were intraperitoneally injected with 10 mg/kg AOM (Sigma-Aldrich, St. Louis, MO, USA) on day -7, followed by three 5 day cycles of administration of 2.5% DSS (MP Biomedicals, Santa Ana, CA) in the drinking water with a 14 day intercycle interval starting 1 week after the AOM injection (day 0). Mice were sacrificed 13 days after the end of the last cycle. Mice were weighed every three days. Colon tissues were dissected from the mice, flushed and cleaned with PBS, and cut open longitudinally to examine tumor nodules. The tumor diameter was measured with Vernier calipers.

Disease Activity Index (DAI)

Body weight, stool consistency, and occult or gross blood were analyzed every three days. The disease activity index score was assessed in a blind manner as follows (24): (1) Body weight loss: 0: none; 1: 1–5%; 2: 6–10%; 3: 11–20%; 4: > 20%; (2) Stool consistency: 0: normal; 2: loose stool; 3 and 4: diarrhea (adhering to the anus); and (3) Hematochezia: 0: negative; 2: positive hemoccult; and 4: gross bleeding.

The hemoccult test was performed using a solution composed of 1% o-tolidine in 80 ml of glacial acetic acid, 20 ml of absolute ethanol, and 3% hydrogen peroxide (25).

Cell Culture, Transfection, and Stimulation

Two human colonic cell lines - NCM460, a gift from Prof. Junbo Hu (Department of Gastrointestinal Surgery Center, Tongji Hospital, Tongji Medical College, Huazhong University of Science and Technology, Wuhan, China) and HCoEpiC (Otwo Biotech, Shenzhen, China) were cultured at 37°C in a 5% CO_2 atmosphere with DMEM medium (Life Technologies, USA) supplemented with 10% heat-inactivated, pyrogen-free fetal calf serum (FCS, Sijiqing, Hangzhou, China), 1 mM sodium

pyruvate, 2 mM L-glutamine, 100 U/ml penicillin, and 100 mg/ml streptomycin.

The full-length human TNF-α cDNA and its leader sequence (LS) mutant were generated by PCR from the pCDNA 3.0 plasmid containing TNF-α or TNF-LS (26) and cloned into the pHAGE-CMV-MCS-PGK puro vector at the Bam HI and Xho I sites. The primers were synthesized by TSINGKE Biological Technology (Beijing, China), and their sequences are listed in **Supplementary Table 1**. The two constructs were verified by DNA sequencing (TSINGKE Biological Technology, Beijing, China). Recombinant lentiviruses were produced by transient four-plasmid cotransfection into 293T cells and purified by ultracentrifugation (27). NCM460 cells were transfected with the lentivirus in antibiotic-free growth medium containing 2 μg/ml polybrene (Sigma-Aldrich, St. Louis, MO, USA) and incubated overnight. Cells were selected with 2 μg/ml puromycin for 2 weeks and subcloned using the limiting dilution method. The expression of TNF-α and TNF-LS on the cell surface was monitored for positive clone selection. HCoEpiC cells were transiently transfected with pCDNA 3.0 plasmid containing TNF-α or TNF-LS using polyethylenimine Max, Linear, MW 40,000 (Polysciences Inc., Illinois, USA) for 48 h.

For the detection of tmTNF-α–mediated forward signaling, 293T cells stably transfected with human tmTNF-α were fixed with 4% paraformaldehyde for 30 min at room temperature (RT) and used as the source of exogenous tmTNF-α (28). 100 ng/ml sTNF-α (Peprotech, Rocky Hill, NJ) or tmTNF-α-overexpressing 293T cells as effector cells were cocultured with NCM460 or HCoEpiC cells as target cells at an effector/target (E/T) ratio of 10:1 in the presence of 10 ng/ml LPS (from *Escherichia* coli 026:B6, no. L2654, Sigma-Aldrich, St. Louis, MO, USA) for different times.

Preparation of the Single-Cell Suspension and Flow Cytometry

Cell suspensions from mouse spleen were prepared as previously described (29). Cell suspensions were prepared from mesenteric lymph nodes (MLNs) by mechanically disrupting MLNs, and colonic epithelial cell suspensions were prepared by digesting colon tissues with 1 mM EDTA and 1 mm dithiothreitol (30). Single-cell suspensions were obtained by filtering the aforementioned cell suspensions through a 75 μm 200 mesh filter (24).

Splenic or MLN cells were stained with the following fluorescent dye-conjugated antibodies (eBioscience, San Diego, CA, USA) for 30 min at 4°C: APC-F4/80 (Cat# 17-4801), PE-CD11b (Cat# 12-0122), FITC-Gr1 (Cat# 11-6041), FITC-CD4 (Cat# 11-0041), APC-IL-17 (Cat# 17-7177), APC-CD25 (Cat# 17-0251) and PE-Foxp3 (Cat# 12-4771). For the analysis of tmTNF-α expression, NCM460 cells, HCoEpiC cells or colonic epithelial cells were stained with a monoclonal antibody against tmTNF-α (31) for 30 min at 4°C, followed by a FITC-conjugated secondary antibody (FeiYi, Wuhan, China, Cat# ZF-0312). The stained cells were analyzed using an LSRII flow cytometer (Becton Dickinson, San Jose, CA, USA).

Culture of Colonic Tissue for the Detection of Both Forms of TNF-α

Fifty milligrams of tissue from the distal portion of the colon were washed with 1x PBS and then cut into segments of ≈ 1 cm^2. Colonic tissue samples were cultured in RPMI 1640 containing 5% fetal bovine serum in a 24-well culture plate for 24 h (24). Supernatants were collected for the detection of sTNF-α; and membrane proteins were extracted according to the manufacturer's protocol (Biovision, Milpitas, CA, USA) for the detection of tmTNF-α. Concentrations of both forms of TNF-α in colonic tissue or serum sTNF-α were detected using a TNF-α ELISA kit (eBioscience, San Diego, CA, USA). The ratio of tmTNF-α and sTNF-α in colonic tissue was calculated.

Detection of Cytokines and Nitric Oxide (NO)

For the preparation of tissue homogenates, distal colons (2 cm in length; 1 cm away from the anus) were cut and flushed with 1x PBS to remove gut contents and homogenized in RIPA buffer (Beyotime Biotechnology, Shanghai, China), followed by centrifugation at 12000 rpm for 20 min.

The concentrations of IL-1β, IL-6, IL-10, and TGF-β in colonic homogenates or in supernatants of cultured cells were detected using ELISAs (eBioscience, San Diego, CA, USA) according to the manufacturer's instructions. NO was quantified using a spectrophotometric assay based on the Griess reaction with a commercial NO assay kit (Beyotime Biotechnology, Shanghai, China).

Western Blot Analysis

Total protein was extracted by lysing cells in lysis buffer (20 mM HEPES, pH 7.4, 20 mM NaCl, 10% glycerol, and 1% Triton X-100). Colonic membrane proteins were prepared using a Membrane Protein Extraction Kit (Biovision, Milpitas, CA, USA) and soluble proteins were isolated from colon homogenates using methanol and chloroform (28). All protein samples were subjected to 12% SDS-polyacrylamide gel electrophoresis and transferred to PVDF membranes (Millipore, Merck KGaA, Darmstadt, Germany). Immunoblotting was performed with the following primary antibodies: anti-tmTNF-α (home-made) (31), anti-TNF-α (Cat# 3707s), anti-PARP (Cat# 9532s), anti-cleaved caspase 3 (Asp175) (Cat# 9661s) from Cell Signaling Technology (Danvers, MA, USA), anti-IκB-α (Santa Cruz, CA, USA, Cat# sc-1643), anti-p65 (Cat# A19653), anti-p-p65 (Cat# AP0475), anti-caspase 3 (Cat# A17900), anti-Na^+/K^+ ATPase (Cat# A12405), and anti-β-actin (Cat# AC026) from Abclonal (Wuhan, China). HRP-conjugated secondary antibodies (Cell Signaling Technology, Danvers, MA, USA, Cat# 7074) were subsequently applied to the membrane. Bands were visualized using an enhanced chemiluminescence system (ECL; TIANGEN, Beijing, China).

Real-Time PCR

Total RNA was extracted from NCM460 cells using TRIzol reagent (Invitrogen, USA). The cDNA templates were reverse transcribed from 1 μg of RNA with a HiFiScript cDNA Synthesis Kit (Yeasen, Shanghai, China) according to the manufacturer's

instructions. Relative mRNA levels of *IL-6* and *iNOS* were determined using real-time PCR with UltraSYBR Mixture (Yeasen, Shanghai, China). PCR was performed using the following conditions: 95°C for 10 min, followed by 40 cycles of 95°C for 15 s and 60°C for 1 min. The results were analyzed using the $2^{-\triangle\triangle Ct}$ method and normalized to the corresponding levels of GAPDH. The primers were synthesized by Sangon Biotech (Shanghai, China) and are listed in **Supplementary Table 1**.

Histopathology and Immunohistochemistry

Colonic tissue sections (4 μm) were deparaffinized, rehydrated, and stained with hematoxylin and eosin (H&E). Colonic tissue sections (4 μm) were dewaxed with xylene and rehydrated in graded ethanol solutions. Antigen retrieval was performed on the sections using Antigen Unmasking Solution (Boster Biological Technology, Wuhan, China). Immunohistochemical staining was performed using the avidin–biotin complex method with anti-mouse TNF-α (Boster Biological Technology, Wuhan, China, Cat# BA0131), anti-mouse F4/80 (eBioscience, San Diego, CA, USA, Cat# 14-4801), anti-mouse CD16/32 and anti-mouse IL-17 (BD Biosciences, San Jose, CA, USA, Cat# 553141 and Cat# 559501), anti-mouse CD206 (AbD Serotec, Kidlington, UK, Cat# MCA2235GA), anti-mouse Foxp3 (Cat# 12653s), and anti-mouse Gr1 monoclonal antibodies (Cat# 31469s) from Cell Signaling Technology (Danvers, MA, USA), followed by HRP-conjugated universal anti-mouse IgG/anti-rabbit IgG antibody (Boster Biological Technology, Wuhan, China, Cat# SA1052/Cat# SA1055). Signals were visualized using an ImmPACT DAB peroxidase substrate (Boster Biological Technology, Wuhan, China), followed by counterstaining with hematoxylin (Sigma Aldrich, St. Louis, MO). Images were viewed and captured with an Olympus BH-2 light microscope (Olympus, Tokyo, Japan) attached to a computerized imaging system. The positive cells in five randomly selected fields were counted at 200× or 400× magnification with Image-Pro Plus Version 6.0 software (Media Cybernetics, Bethesda, MD, USA).

Apoptosis Detection

In situ TUNEL staining was performed using an *In Situ* Cell Death Detection Kit (Roche Diagnostics, Basel, Switzerland) according to the manufacturer's instructions. In brief, sections of colonic tissue were deparaffinized, repaired with proteinase K at 37°C for 25 min, and permeabilized at RT for 20 min. Sections were incubated with TdT and fluorescent dye-labeled dUTP for 1 h at 37°C, followed by DAPI staining at RT for 10 min. Apoptotic cells were observed using a laser scanning confocal microscope (Nikon D-Eclipse CI, Tokyo, Japan).

Statistical Analysis

Student's t-test and one-way or two-way analysis of variance followed by Tukey's *post hoc* test were used to compare data from two or multiple groups with GraphPad Prism 6.0 software (San Diego, CA, USA). *P* values less than 0.05 were considered statistically significant.

RESULTS

sTNF-α Levels Increase in the Inflammatory Phase, While tmTNF-α Levels Are Elevated in the Tumor Phase of the Mouse AOM/DSS-Induced CAC Model

Mice were intraperitoneally injected with AOM (10 mg/kg) on day -7, followed by three cycles of drinking 2.5% DSS-containing water for 5 days with an interval of 14 days (**Figure 1A**) to determine the dynamical changes in the levels of both forms of TNF-α during the transformation from colitis to tumors. After the first round of drinking DSS-containing water (day 8), the mice developed acute colitis, showing diarrhea, weight loss (**Figure 1B**), fecal occult blood (**Figure 1C**) and even rectal bleeding, an increased DAI score (**Figure 1D**), and an obvious hyperemic, shortened colon filled with bloody stools (**Figure 1E**). The histopathological changes included the infiltration of a large number of inflammatory cells into the lamina propria of the colon and significant damage to the intestinal epithelial barrier (**Figure 1F**). These symptoms and pathological changes were markedly alleviated after a two-week interval (day 19), and the body weight and intestinal structure were close to normal. After the second round of DSS administration (day 25), repeated inflammation was induced, inflammatory cells infiltrated the submucosal layer, and the intestinal glands significantly proliferated (day 38). After the third round of DSS administration (day 44), adenomas were observed with dysplastic cells, and later (day 70) tumors developed (**Figure 1F**).

In this animal model, serum sTNF-α levels increased gradually and peaked on day 19, followed by a relative decrease, but slightly raised again at the tumor stage (**Figure 2A**). We cultured colon tissue for 24 h to measure the levels of sTNF-α released in the supernatant and tmTNF-α in the membrane proteins using an ELISA in order to accurately evaluate and compare the changes between the levels of both forms of TNF-α in the colon tissue. sTNF-α levels increased significantly in mice with DSS-induced inflammation but then declined during 2-week intervals, and were enhanced again to a certain degree at the tumor stage (**Figure 2B**). In contrast, tmTNF-α levels remained unchanged and began to increase in the second round of inflammation and peaked at the tumor stage (**Figure 2C**). The ratio of tmTNF-α to sTNF-α was approximately 0.85 in the normal group but decreased significantly during the first and second rounds of DSS consumption (**Figure 2D**), indicating that sTNF-α predominated in the inflammation phases. In contrast, this ratio was significantly increased at the uncontrolled inflammation stage and the tumor stage, suggesting that increased tmTNF-α expression was associated with malignant transformation. Western blot analysis showed similar results: intracolonic sTNF-α levels increased dominantly in the inflammation phase, but tmTNF-α levels in the membrane protein fraction were significantly elevated in the tumor phase (**Figure 2E**). Immunohistochemical staining using a tmTNF-α-specific antibody that is not cross reactive to sTNF-α (28) revealed that tmTNF-α was expressed on infiltrated leukocytes on day 38 but expressed on glandular epithelial cells or tumor cells in addition

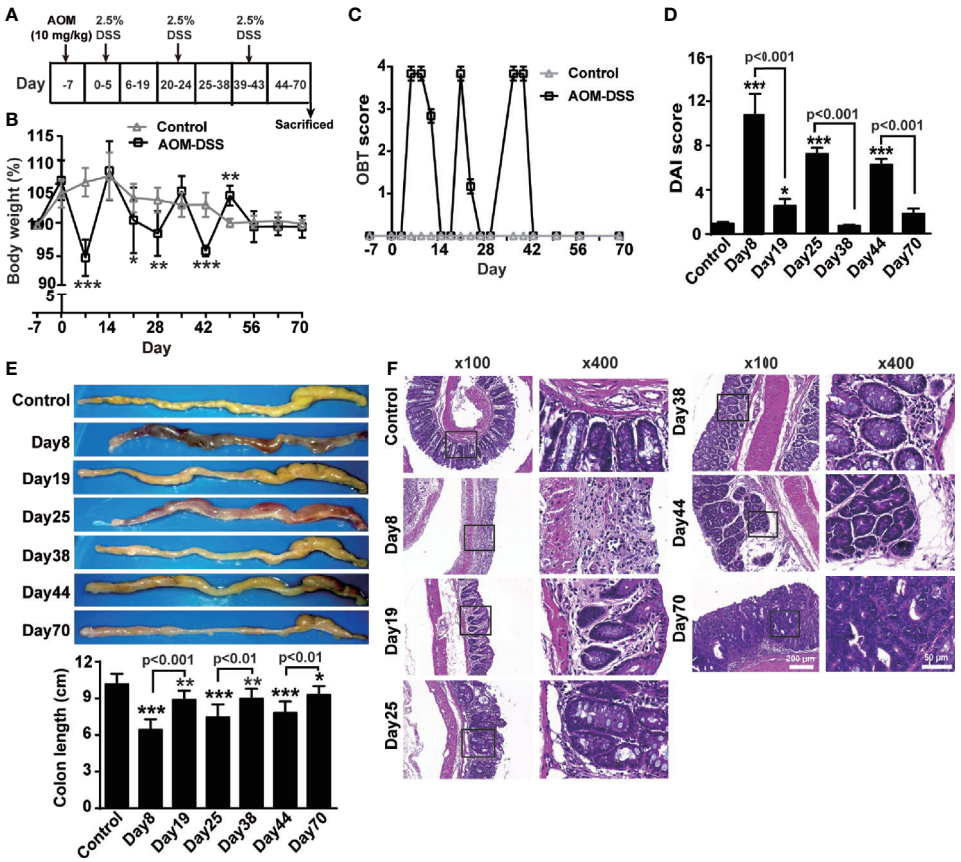

FIGURE 1 | AOM/DSS induced CAC. **(A)** Schematic treatment of mice with AOM and DSS. Mice were intraperitoneally administered with AOM (10 mg/Kg) at day -7, followed by three cycles of drinking 2.5% DSS-containing water for 5 days with interval of 14 days (n = 6, each group). Time course for body weight **(B)**, score of occult blood test (OBT) **(C)** and disease activity index (DAI) **(D)**. **(E)** Representative images and quantitative data of colon length. **(F)** Colons tissue sections were stained with hematoxylin and eosin. Representative histopathological images (×100, ×400). All quantitative data are expressed as means ± SEM. *P < 0.05, **P < 0.01, ***P < 0.001 versus control.

to infiltrated leukocytes in the tumor stage (**Figure 2F**). We further isolated diseased colonic epithelial cells and found that tmTNF-α expression did not significantly increase in colonic epithelial cells until malignant transformation and peaked in the tumor stage (**Figure 2G**).

The tmTNF-α/sTNF-α Ratio Is Associated With the Accumulation of MDSCs and Treg Cells in a Mouse AOM/DSS-Induced CAC Model But Negatively Correlates With Macrophages

Next, we measured changes in immune cells, such as macrophages and Th17 cells, and immunosuppressive cells, including $CD4^+CD25^+$ regulatory T cells (Tregs) and myeloid-derived suppressor cells (MDSCs), using flow cytometry and immunohistochemistry to determine potential relationships between both forms of TNF-α and these cells in the mouse AOM/DSS-induced CAC model. The number of $F4/80^+$ macrophages increased during inflammation and peaked on day 19 and day 44, but returned to baseline levels in the spleen and mesenteric lymph nodes at the tumor stage (**Supplementary Figures S1A, B**). However, in the colonic tissue, infiltrated $F4/80^+$ macrophages were detected at approximately all time-points, except the first interval in which the infiltration significantly decreased (**Figure 3A**). Moreover, the number of $CD16/32^+$ M1 macrophages significantly increased when mice drank DSS-containing water but decreased during the intervals (**Figure 3B**), while the number of $CD206^+$ M2 type macrophages began to increase on day 25 and peaked at the tumor stage (**Figure 3C**). The number of $CD4^+CD17A^+$Th17 cells with proinflammatory and tumor-promoting effects increased slightly and peaked on day 19 in the spleen, but did not increase until day 70 in the mesenteric lymph nodes (**Supplementary Figures S1C, D**), while the number of Th17 cells in the colonic tissue was significantly enhanced on day 25 and peaked on day 70 (**Supplementary Figure S1E**). Importantly, the ratio of intracolonic tmTNF-α/sTNF-α negatively correlated with the infiltrated $F4/80^+$ macrophages and M1 macrophages in the colon (**Figure 3D**), but not with M2 macrophages or Th17 cells (**Figure 3D** and **Supplementary Figure S1F**).

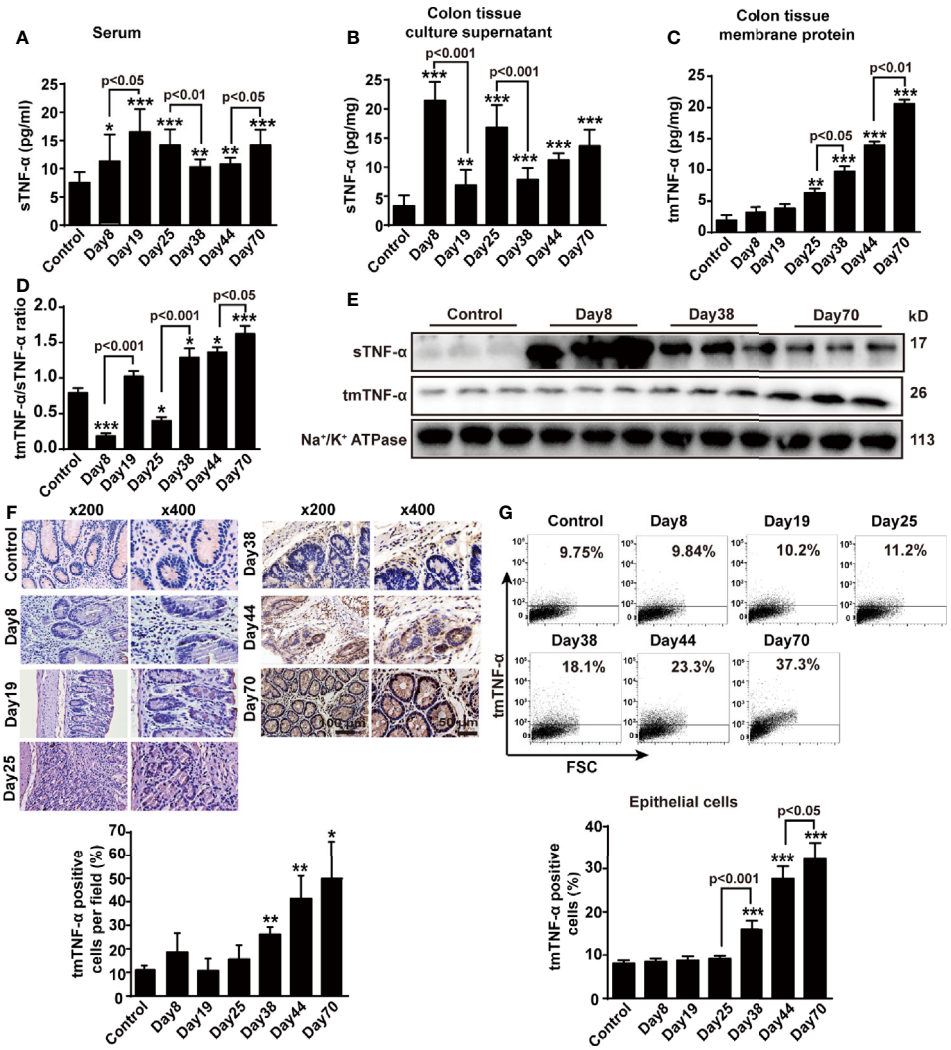

FIGURE 2 | sTNF-α levels are increased at the inflammation stage, but tmTNF-α expression is enhanced at the tumor stage. Mice were treated with AOM and DSS as described in **Figure 1A** (n = 6, each group). **(A)** Serum concentrations of sTNF-α detected by ELISA. Levels of sTNF-α released in supernatants **(B)** and tmTNF-α expression in the membrane protein **(C)** of 24-h-cultured colonic tissues detected by ELISA and their ratios **(D)**. **(E)** Western blot analysis of sTNF-α in colonic homogenates and tmTNF-α in colonic membrane protein. **(F)** Representative immunohistochemical staining for intracolonic expression of tmTNF-α (x200, ×400) and their quantitative data. **(G)** Representative cytogram for tmTNF-α expression on colonic epithelial cells isolated from AOM/DSS-treated mice analyzed by flow cytometry and their quantitative data. All quantitative data are expressed as means ± SEM, *P < 0.05, **P < 0.01, ***P < 0.001 versus control.

The number of $CD11b^+Gr1^+$MDSCs, a heterogeneous population of immature myeloid cells with a remarkable ability to suppress T cell responses that are characterized by co-expression of CD11b and GR1 in mice (32–34), peaked on day 19 in the spleen and on day 25 in mesenteric lymph nodes and then decreased significantly with disease progression (**Supplementary Figures S1G, H**). In contrast, the number of MDSCs in the colonic tissue was augmented on days 8 and 25 in animals with DSS-induced inflammation, further increased with the disease development, and reached a peak at the tumor stage (**Figure 3E**). The number of another type of immunosuppressive cell, $CD4^+CD25^+Foxp3^+$Treg cells, increased in the spleen at all time points, except at the tumor stage (**Supplementary Figure S1I**), but the number of Treg cells increased during DSS drinking and returned to baseline levels in mesenteric lymph nodes during intervals between DSS consumption (**Supplementary Figure S1J**). However, a certain number of Treg cells was present in the lamina propria of colonic tissue of normal mice but did not increase during the inflammation stage until malignant transformation (**Figure 3F**). Interestingly, the ratio of intracolonic tmTNF-α/sTNF-α positively correlated with the infiltration of both MDSCs and Treg cells in the colonic tissues (**Figures 3G, H**). Based on these data, tmTNF-α expression in the colon was closely associated with intracolonic infiltration of MDSCs and Treg cells.

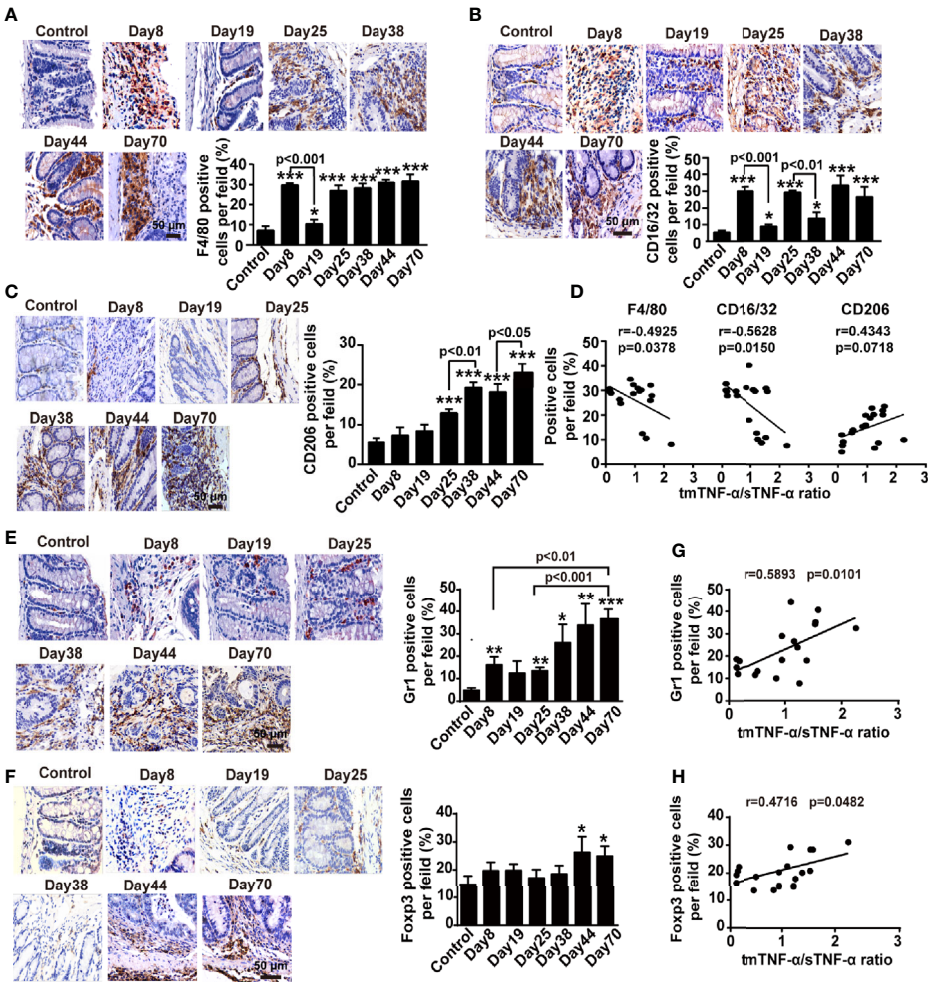

FIGURE 3 | The tmTNF-α/sTNF-α ratio negatively correlates with the accumulation of macrophages but positively associates with the infiltration of MDSCs and Treg cells in the colonic tissue of CAC. Mice were treated with AOM and DSS as described in **Figure 1A** (n = 6-8, each group). Representative immunohistochemistry images of F4/80$^+$ macrophages **(A),** CD16/32$^+$ M1 type **(B)** or CD206$^+$ M2 type macrophages **(C),** Gr1$^+$ MDSCs **(E)** and Foxp3$^+$ Treg cells **(F)** infiltrated in colonic tissues (×400) and their quantitative data. The correlation of the tmTNF-α/sTNF-α ratio with percentages of F4/80$^+$ macrophages, CD16/32$^+$ M1 type or CD206$^+$ M2 type macrophages **(D)**, MDSCs **(G)** and Treg cells **(H)** (n = 18). All quantitative data are expressed as means ± SEM. *P < 0.05, **P < 0.01, ***P < 0.001 versus control.

The tmTNF-α/sTNF-α Ratio Is Negatively Correlated With Proinflammatory Mediators but Positively Correlated With the Anti-inflammatory Cytokine IL-10

We detected cytokines and NO in colonic tissue homogenates from the AOM/DSS mouse model to analyze the correlations between both forms of tmTNF-α and pro- and anti-inflammatory factors. The concentrations of IL-1β and IL-6 were increased while animals drank DSS-containing water and were reduced in the intervals between DSS consumption (**Figures 4A, B**); the release of NO peaked on day 8 (**Figure 4C**). In contrast, IL-10 and TGF-β levels increased when animals were drinking DSS-containing water compared to the control, but were further enhanced in the intervals between DSS consumption, with the exception of TGF-β at the tumor stage (**Figures 4D, E**). Interestingly, the ratio of tmTNF-α/sTNF-α was negatively correlated with the levels of proinflammatory mediators, including IL-1β, IL-6, and NO (**Figures 4F, G**), but was positively correlated with the level of the anti-inflammatory cytokine IL-10 (**Figure 4H**) in colonic tissues from mice with AOM/DSS-induced CAC. However, this ratio was not associated with the secretion of TGF-β (**Figure 4H**). Our data suggested an association of tmTNF-α with inflammation resolution during disease progression.

Increasing tmTNF-α Expression by Treatment With an Antibody in the Inflammation Stage Suppresses Inflammation and Tumor Formation

Our results indicate an association of tmTNF-α with the inhibition of inflammation; however, tmTNF-α expression

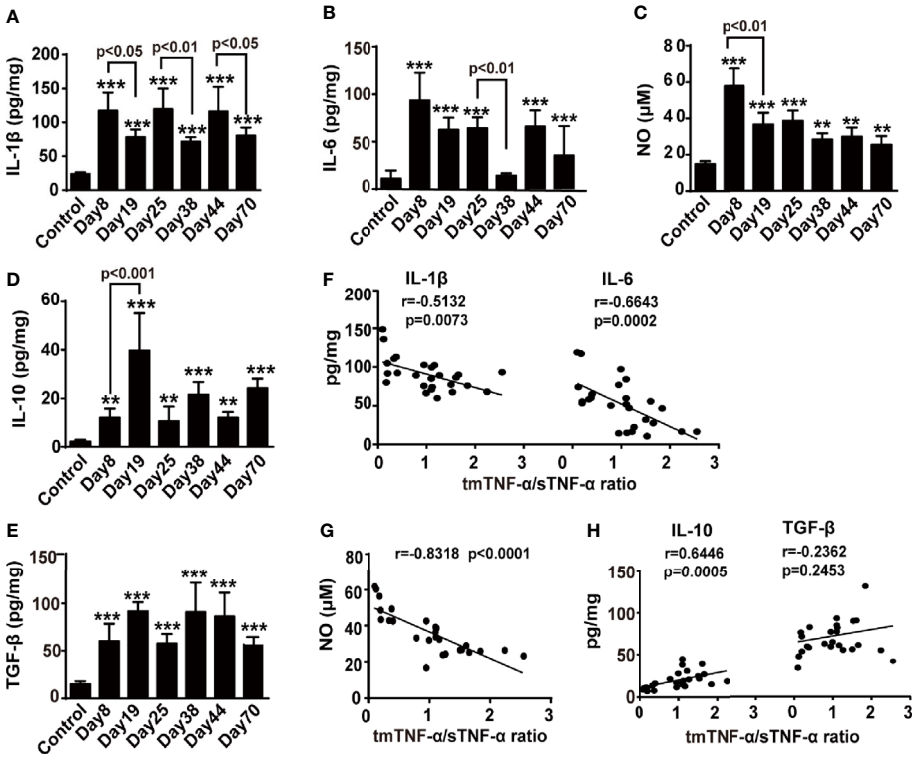

FIGURE 4 | The tmTNF-α/sTNF-α ratio negatively correlates with proinflammatory mediators but positively correlates with IL-10. Mice were treated with AOM and DSS as described in **Figure 1A** (n = 5-8, each group). Concentrations of IL-1β **(A)**, IL-6 **(B)**, IL-10 **(D)**, and TGF-β **(E)** in colonic tissue homogenates detected at indicated time points by ELISA. The levels of NO **(C)** in colonic tissue homogenates measured by Griess method. The correlation of tmTNF-α/sTNF-α ratio with concentrations of IL-1β and IL6 **(F)**, or NO **(G)**, or IL-10 and TGF-β **(H)** [n = 26, except IL-10 (n = 25)]. All values represent the mean ± SEM. **P < 0.01, ***P < 0.001 versus control.

began to increase in the later stage of colitis. If the tmTNF-α expression time window can be shifted beforehand to the early stage of inflammation, disease progression may be interrupted. Previously, we developed a monoclonal antibody specific to human tmTNF-α and a polyclonal antibody specific to murine tmTNF-α. Both antibodies inhibit tmTNF-α shedding by competing with TACE that is responsible for tmTNF-α processing (28), increasing tmTNF-α expression and decreasing sTNF-α release. To test our hypothesis, mice were intraperitoneally injected with 600 μg of the murine tmTNF-α polyclonal antibody twice a week beginning on the day after the first cycle of drinking DSS water (**Figure 5A**). The effects of the antibody were detected at the inflammation stage on day 38 and at the tumor stage on day 70. Indeed, the antibody decreased sTNF-α levels in serum and cultured colonic tissue supernatant (**Figures 5B, C**), while the antibody increased tmTNF-α expression in colonic tissues (**Figure 5D**) with an elevated ratio of intracolonic tmTNF-α/sTNF-α (**Figure 5E**) observed on day 38 and on day 70. In addition, immunohistochemical staining revealed that the antibody increased tmTNF-α expression in both infiltrated cells and glandular epithelial cells on day 38 and day 70 (**Supplementary Figure S2A**). Importantly, antibody treatment remarkably suppressed the formation of inflammation-associated tumors, as the number and size of tumors were significantly reduced (**Figures 5F, G**). TUNEL staining showed that the antibody induced apoptosis mainly in tumor cells (**Figure 5H**), and the western blot analysis of diseased colonic tissue revealed that the antibody induced caspase 3 activation and cleavage of its substrate PARP (**Figure 5I**).

Next, we observed whether the antibody suppressed inflammation in the inflammation stage on day 38 and the tumor stage on day 70. Although a significant improvement in weight loss or DAI score was not observed (**Supplementary Figures S2B, C**), treatment with the tmTNF-α antibody significantly inhibited the production of proinflammatory mediators, including IL-1β, IL-6, and NO, but prompted the release of the anti-inflammatory cytokine IL-10 in colonic tissue homogenates at both the inflammation and tumor stages (**Figures 6A–D**). Interestingly, the antibody induced apoptosis mainly in infiltrated cells on day 38 (**Figures 6E, F**), which might contribute to inhibiting inflammation. Furthermore, the tmTNF-α antibody markedly reduced the intracolonic infiltration of F4/80$^+$ macrophages and M1 type macrophages (**Figures 6G, H**), rather than M2 type macrophages (**Figure 6I**) at inflammation and tumor stages. However, the antibody promoted the infiltration of immunosuppressive Treg cells and MDSCs at the inflammation

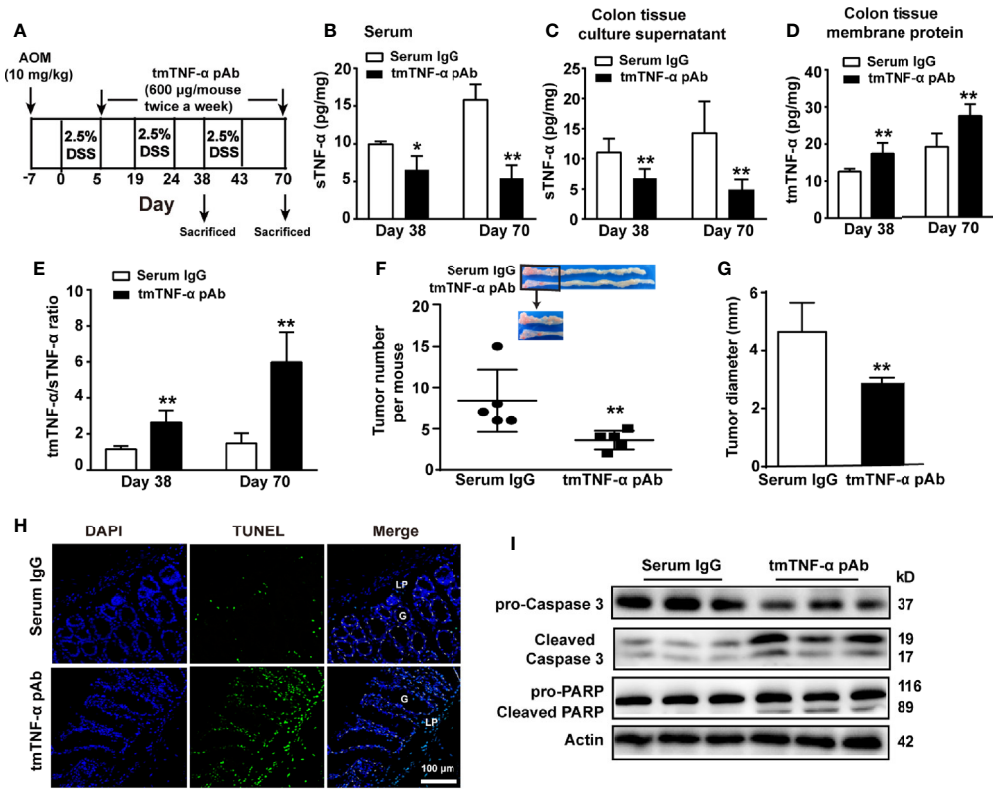

FIGURE 5 | tmTNF-α antibody treatment in the first inflammation stage suppresses tmTNF-α shedding and tumor growth. **(A)** Schematic treatment of mice with tmTNF-α polyclonal antibody (pAb) in AOM/DSS-induced CAC. Mice were intraperitoneally injected with 600 μg of tmTNF-α pAb twice a week, and the treatment was from day 5 to day 70. Normal rabbit serum IgG served as a control. (n = 5, each group) **(B)** Serum concentrations of sTNF-α detected by ELISA. Levels of sTNF-α released in supernatants **(C)** and tmTNF-α expression in the membrane protein **(D)** of 24-h-cultured colonic tissues detected by ELISA and their ratios **(E)** on day 38 and day 70. **(F, G)** Tumor number and size. **(H, I)** Representative images of apoptosis in diseased colons detected by TUNEL (×200), and western blot analysis for cleavage of caspase 3 and PARP on day 70. G: glands; LP: lamina propria. All quantitative data represent the mean ± SEM. *P < 0.05, **P < 0.01 versus serum IgG.

stage but reduced their accumulation at the tumor stage (**Figures 6J, K**). The data indicate that the tmTNF-α antibody not only suppressed inflammation at the inflammation stage but also inhibited tumor-associated inflammation.

In addition, we treated mice with tmTNF-α antibody twice a week starting at the end of the second cycle of drinking DSS water (**Supplementary Figure S3A**), and found that the tmTNF-α antibody inhibited tmTNF-α shedding, decreased sTNF-α levels in the serum and cultured colonic tissue supernatant (**Supplementary Figures S3B, C**), increased the expression of the transmembrane molecule in the diseased colonic tissue (**Supplementary Figures S3D, F**), and increased the ratio of intracolonic tmTNF-α/sTNF-α (**Supplementary Figure S3E**). The tmTNF-α antibody also remarkably reduced the number and size of tumors and increased apoptosis in both tumor cells and infiltrated leukocytes (**Supplementary Figures S3G–I**) through the activation of caspase 3 and cleavage of PARP (**Supplementary Figure S3J**). Similarly, the tmTNF-α antibody suppressed the production of proinflammatory mediators (**Supplementary Figures S4A–C**), promoted the release of IL-10 (**Supplementary Figure S4D**), and inhibited the infiltration of macrophages, Treg cells, and MDSCs at the tumor stage (**Supplementary Figures S4E–G**). Thus, suppressing tmTNF-α processing at the inflammation stage might attenuate inflammation and limit subsequent tumor formation.

Treatment With the tmTNF-α Antibody at the Tumor Stage Suppresses Tumor Growth

To observe the effect of the antibody on CRC, we treated mice with the tmTNF-α antibody twice a week starting at the end of the third cycle of drinking DSS-containing water (**Figure 7A**). Administration of the tmTNF-α antibody decreased sTNF-α release (**Figures 7B, C**) and increased tmTNF-α expression (**Figures 7D, F**) with a raised ratio of tmTNF-α/sTNF-α in colonic tissue (**Figure 7E**). The antibody remarkably reduced the number and size of tumors (**Figures 7G, H**) by promoting apoptosis (**Figures 7I, J**). Moreover, the tmTNF-α antibody significantly inhibited the production of IL-1β, IL-6, and NO and increased IL-10 release in colonic tissue homogenates (**Figures 7K–N**). The antibody also significantly reduced the intracolonic infiltration of macrophages, Tregs, and MDSCs

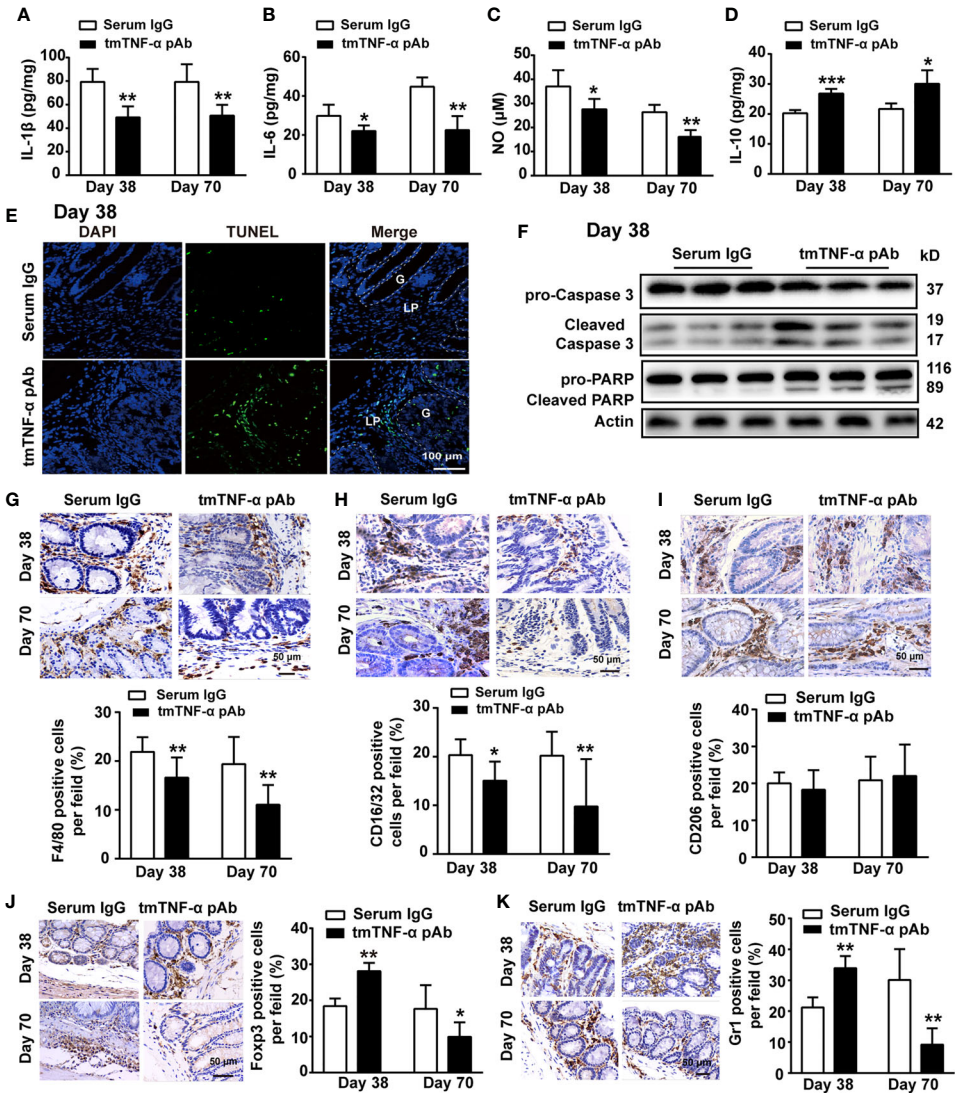

FIGURE 6 | tmTNF-α antibody treatment in the first inflammation stage inhibits inflammation. tmTNF-α pAb was administered in the inflammation stage as described in **Figure 5A** (n = 5, each group). Concentrations of IL-1β **(A)**, IL-6 **(B),** and IL-10 **(D)** in colonic tissue homogenates detected by ELISA. The levels of NO **(C)** in colonic tissue homogenates measured by Griess method. **(E, F)** Representative images of apoptosis in diseased colons detected by TUNEL (×200), and the western blot analysis for cleavage of caspase 3 and PARP on day 38. G: glands; LP: lamina propria. **(G–K)** Representative immunohistochemistry images of F4/80$^+$ Macrophages, CD16/32$^+$ type 1 or CD206$^+$ type 2 macrophages, Foxp3$^+$ Tregs and Gr1$^+$ MDSCs in colonic tissues (×400) and their quantitative data. All quantitative data represent the mean ± SEM. *P < 0.05, **P < 0.01, ***P < 0.001 versus serum IgG.

(**Figures 7O–Q**). The data indicate an antitumor effect of the antibody through the induction of apoptosis and inhibition of inflammation.

tmTNF-α, Rather Than sTNF-α, Actively Suppresses LPS-Induced Production of Inflammatory Mediators

To further explore the mechanism by which the tmTNF-α antibody exerted anti-inflammatory effects and therefore inhibited inflammation-associated cancer, a human colon mucosal epithelial cell line NCM460 was stimulated with LPS (10 ng/ml) to induce tmTNF-α expression. LPS-induced tmTNF-α expression at 6 h was significantly enhanced by treatment with the human tmTNF-α monoclonal antibody (mAb, **Figure 8A**). Consistent with the results obtained from the mouse model, the antibody effectively suppressed LPS-induced mRNA expression of proinflammatory factors, including *IL-6* and *iNOS* (**Supplementary Figure S5A**), and the release of IL-6 and NO (**Figure 8B**). In addition, LPS-induced IκBα degradation and phosphorylation of NF-κB p65 were effectively blocked by the antibody (**Figure 8C**). In line with the *in vitro* results, treatment of AOM/DSS mice with the tmTNF-α antibody significantly inhibited IκBα degradation and phosphorylation of NF-κB p65 on day 8 and day 38

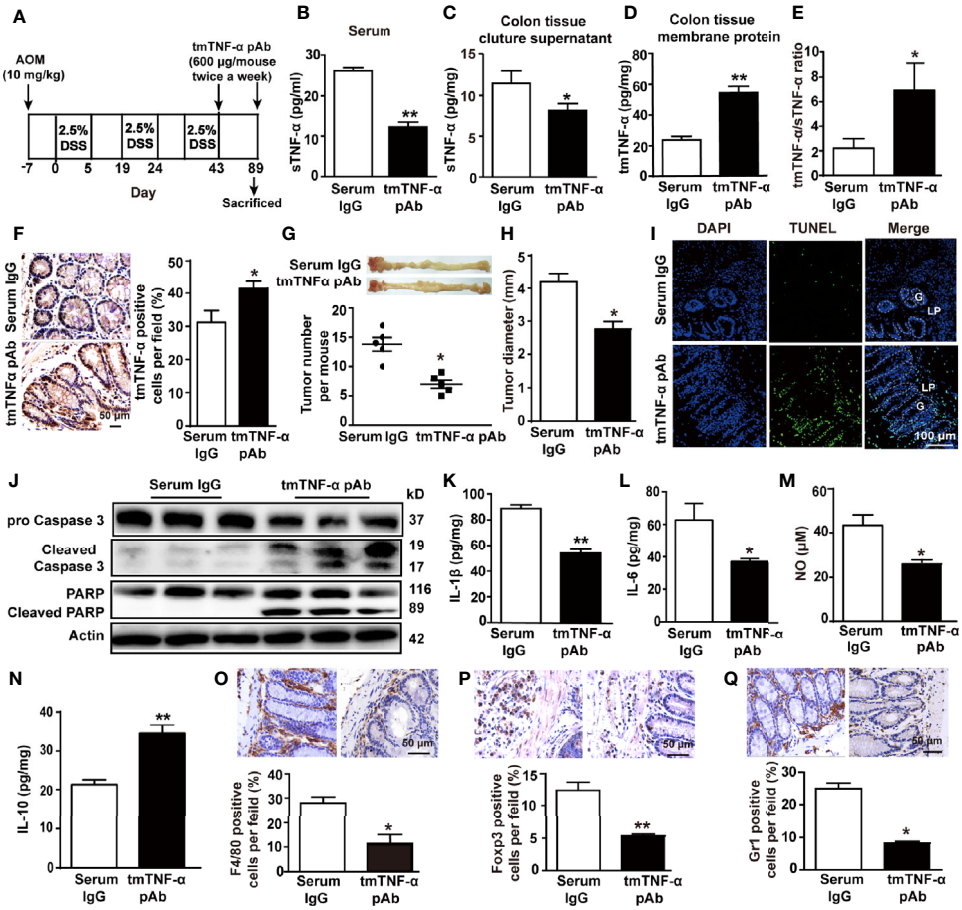

FIGURE 7 | tmTNF-α antibody treatment in the tumor stage inhibits inflammation and tumor growth. **(A)** Schematic treatment of mice with tmTNF-α pAb in AOM/DSS-induced CAC. Mice were intraperitoneally injected with 600 μg of tmTNF-α pAb twice a week, and the treatment was from day 43 to day 89. Normal rabbit serum IgG served as a control (n = 5, each group). **(B)** Serum concentrations of sTNF-α detected by ELISA. Levels of sTNF-α released in supernatants **(C)** and tmTNF-α expression in the membrane protein **(D)** of 24-h-cultured colonic tissues detected by ELISA and their ratios **(E).** Representative immunohistochemical staining of tmTNF-α positive cells in colons (×400) and their quantitative data **(F)**. **(G, H)** tumor number and size. **(I, J)** Representative images of apoptosis in colonic tissues detected by TUNEL (×200), and western blot analysis for cleavage of caspase 3 and PARP. G: glands; LP: lamina propria. Concentrations of IL-1β **(K)**, IL-6 **(L)** and IL-10 **(N)** in colonic tissue homogenates detected by ELISA. The levels of NO **(M)** in colonic tissue homogenates measured by Griess method. **(O–Q)** Representative immunohistochemistry images of F4/80$^+$ Macrophages, Foxp3$^+$ Tregs and Gr1$^+$ MDSCs in colonic tissues (×400) and their quantitative data. All quantitative data represent the mean ± SEM. *P < 0.05, **P < 0.01 versus serum IgG.

(**Figures 8D, E**), indicating that the anti-inflammatory effects of the tmTNF-α antibody were mediated by suppressing the NF-κB pathway.

The suppressive effect of the tmTNF-α antibody on the LPS response might be due to increased tmTNF-α expression and reduced sTNF-α release. We stably transfected 293T cells with tmTNF-α (**Supplementary Figure S5B**) and fixed these cells as effector cells to determine whether tmTNF-α was responsible for this anti-inflammatory effect of the antibody. tmTNF-α-overexpressing cells or sTNF-α were added to NCM460 cells to compare the effect of the two forms of exogenous TNF-α on the LPS response (**Figure 8F**). As expected, LPS-induced expression of *IL-6* mRNA and *iNOS* mRNA (**Supplementary Figure S5C**) and release of IL-6 and NO (**Figure 8G**) were suppressed by tmTNF-α but increased by sTNF-α. Additionally, LPS-induced activation of NF-κB was also suppressed by tmTNF-α but promoted by sTNF-α (**Figure 8H**).

Since tmTNF-α functions as a receptor and transmits outside-to-inside (reverse) signals to tmTNF-α-bearing cells, we transferred the full-length gene encoding TNF-α or its leading sequence (LS) mutant into NCM460 cells. The transfectants overexpressed tmTNF-α and TNF-LS on the cell surface (**Supplementary Figure S5D**). TNF-α-overexpressing cells secreted high levels of sTNF-α; however, TNF-LS-overexpressing cells did not secrete sTNF-α (**Supplementary Figure S5E**) because of the lack of an extracellular sTNF-α segment. Therefore, TNF-LS cannot bind to the TNF-α receptor (excluding forward signaling) but retains the intracellular segment of tmTNF-α for reverse signaling (**Figure 8I**). Interestingly, LPS-induced IL-6 and NO production and

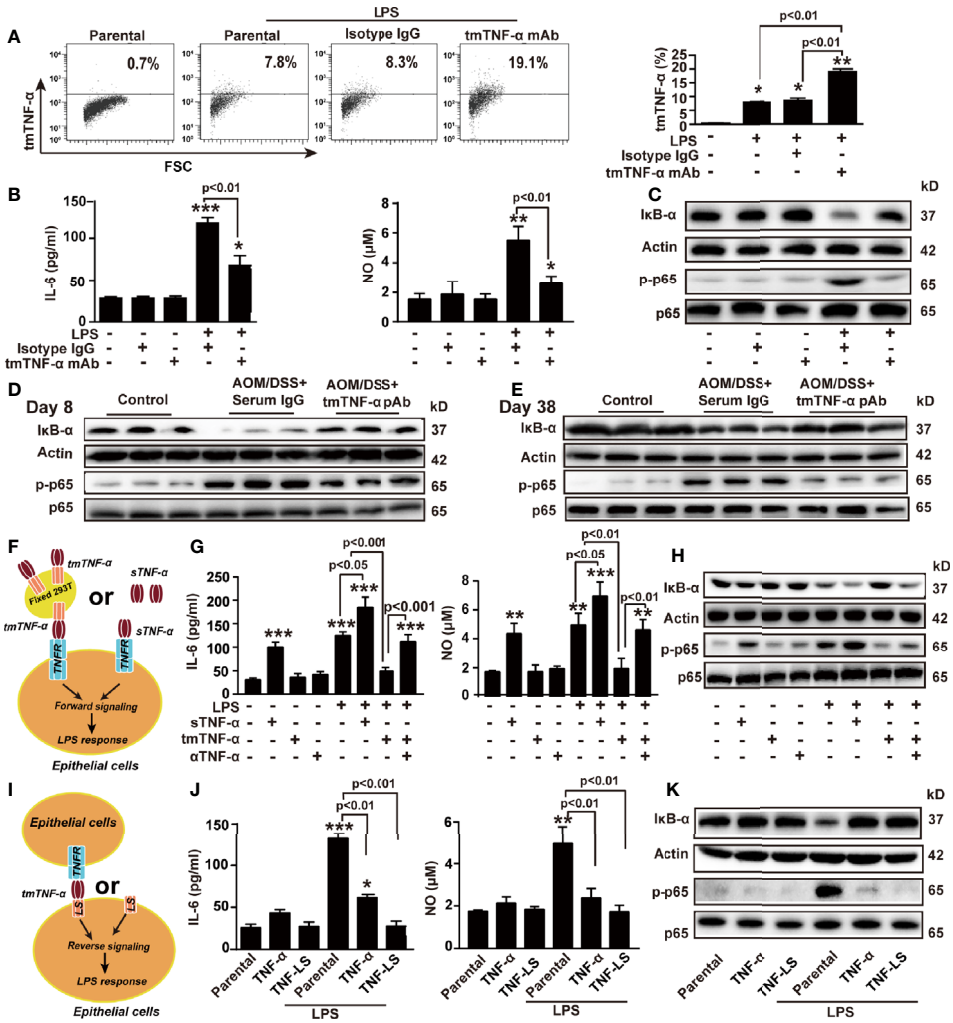

FIGURE 8 | tmTNF-α actively suppresses LPS-induced production of inflammatory mediators *via* dual signaling. NCM460 cells were stimulated with 10 ng/ml LPS combined with 2 μg/ml of tmTNF-α mAb for 6 h. Isotype IgG served as a control. **(A)** tmTNF-α expression on the cell surface assessed by flow cytometry and quantitative data. **(B)** Concentrations of IL-6 and NO in culture supernatants at 10 h after stimulation. **(C)** Representative western blot of three independent experiments for IκBα degradation and p65 phosphorylation at 1 h after stimulation. **(D, E)** Mice were intraperitoneally injected with 600 μg tmTNF-α pAb twice a week starting on day 5 followed by AOM/DSS treatment. Normal rabbit serum IgG served as a control. Western blot analysis of the NF-κB pathway on day 8 and day 38. **(F–H)** NCM460 cells were cocultured with 100 ng/ml sTNF-α or tmTNF-α stably expressed on the cell surface of fixed 293T cells at a ratio of 1:10 in the presence of 10 ng/ml LPS **(F)**. Concentrations of IL-6 and NO in culture supernatants at 10 h after stimulation **(G)**, and representative western blot of three independent experiments for the NF-κB pathway at 1 h after stimulation **(H)**. **(I–K)** TNF-α and TNF-LS stably transfected NCM460 cells **(I)** and their parental cells were stimulated with 10 ng/ml LPS for 10 h **(J)** Levels of IL-6 and NO. **(K)** Representative western blot of three independent experiments for the NF-κB pathway at 1 h after LPS stimulation. All quantitative data represent as means ± SEM of four independent experiments. *P < 0.05, **P < 0.01, ***P < 0.001 versus control for **(A, B, G)**, versus parental for **(J)**.

activation of NF-κB were significantly inhibited by the transfection of TNF-α but completely blocked by the transfection of the TNF-LS mutant (**Supplementary Figure S5F** and **Figures 8J, K**). Although TNF-α transfectants secreted a large amount of sTNF-α, tmTNF-α overexpression still blocked the LPS response of colonic epithelial cells. The inhibitory effect of TNF-LS indicates an active anti-inflammatory role of tmTNF-α-mediated reverse signaling. Similar phenomena were observed in another human colon mucosal epithelial cell line, HCoEpiC (**Supplementary Figures S6A-H**).

DISCUSSION

Here, we described dynamic changes in the ectodomain shedding of tmTNF-α during AOM/DSS-induced CAC, namely, the processing of tmTNF-α was markedly increased during the inflammation phase but decreased during malignant transformation (**Figures 9A, B**). The ratio of intracolonic tmTNF-α/sTNF-α was associated with increased anti-inflammatory responses and decreased release of pro-inflammatory mediators, indicating an anti-inflammatory effect

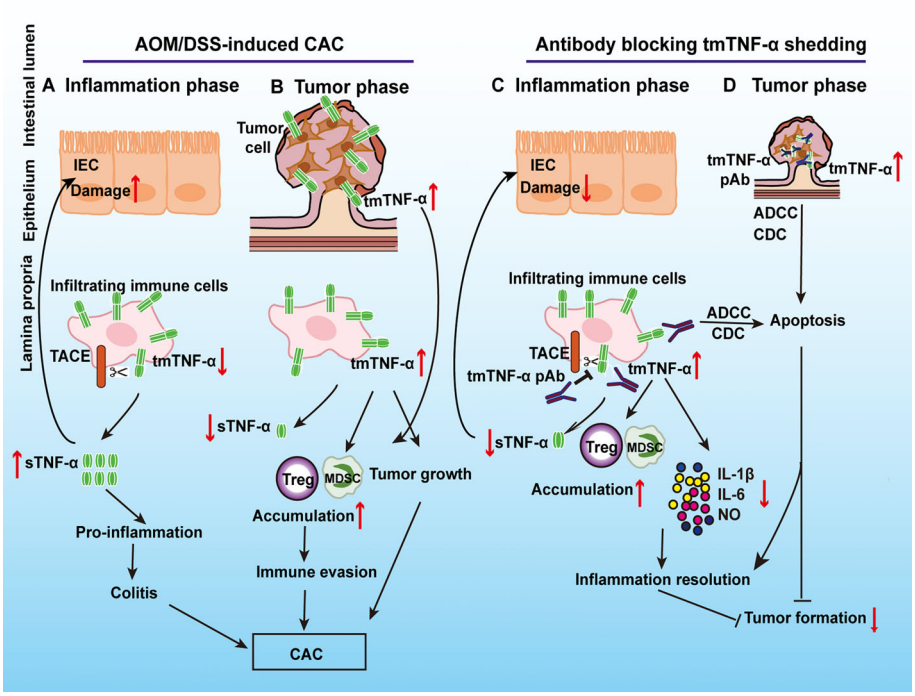

FIGURE 9 | Schematic summary of the protective effect of tmTNF-α on CAC by a specific antibody that prevents tmTNF-α shedding. In AOM/DSS-induced CAC, tmTNF-α is rapidly processed into sTNF-α that is mainly released by inflammatory cells in the inflammation phase to promote colitis **(A)**, while tmTNF-α expression is increased on epithelial cells in addition to infiltrated leukocytes in malignant transformation to facilitate CAC development. Increased tmTNF-α expression promotes the accumulation of MDSCs and Treg cells, which leads to immune evasion **(B)**. Using a specific antibody to prevent tmTNF-α shedding and increase tmTNF-α expression in the inflammation phase inhibits the production of inflammatory mediators (IL-1β, IL-6, and NO) and the infiltration of M1 macrophages, induces apoptosis of inflammatory cells, and promotes intracolonic accumulation of MDSCs and Treg cells **(C)**. As a result, inflammation resolution is facilitated and subsequent tumor formation is suppressed. In addition, the antibody induces apoptosis of tmTNF-α-positive tumor cells by ADCC and CDC **(D)**.

of tmTNF-α. The administration of a tmTNF-α antibody that prevents the ectodomain shedding of tmTNF-α at the inflammation stage significantly suppressed inflammation and subsequent tumor formation (**Figures 9C, D**).

Although TNF-α expression is increased at the mRNA and protein levels in IBD and AOM/DSS-induced CAC (12), the changes in TNF-α at the posttranslational level in this pathological process remain unclear. Our results originally revealed that sTNF-α levels were increased in the inflammation phase, while tmTNF-α levels were enhanced during malignant transformation and peaked in the tumor phase. These findings suggest that tmTNF-α was rapidly processed into sTNF-α that promoted colitis, since sTNF-α, a pro-inflammatory cytokine, promotes colonic inflammation by inducing the expression of IL-1β and IL-6 in colonic epithelial cells through activating the NF-κB pathway (35). In contrast, the ectodomain shedding of tmTNF-α was decreased during malignant transformation, as evidenced by the elevated tmTNF-α expression levels and reduced sTNF-α release in the colonic tissue. Consequently, the ratio of tmTNF-α/sTNF-α was significantly increased. Interestingly, the ratio of tmTNF-α/sTNF-α was positively correlated with the production of the anti-inflammatory cytokine IL-10 and intracolonic infiltration of immunosuppressive MDSCs and Treg cells but negatively correlated with the release of inflammatory mediators, including IL-1β, IL-6, and NO, and M1 macrophage accumulation, suggesting an anti-inflammatory effect of tmTNF-α. As shown in our previous study and studies from other researchers, tmTNF-α functions in the resolution of inflammation by suppressing LPS/TLR4 signaling and the production of IL-1β and IL-6 in macrophages (28, 36). Furthermore, in addition to the different expression windows of both forms of TNF-α during CAC development, the cell types expressing these proteins were not quite the same. sTNF-α has been reported to be mainly released from infiltrated myeloid cells (12), and our results revealed that tmTNF-α was expressed at high levels on enterocytes, including intestinal adenomatous cells, in addition to infiltrated immune cells. Notably, tmTNF-α expression by colonic epithelial cells did not increase until the precancerous stage, indicating that it might be a biomarker for the malignant transformation of CAC. Based on our findings and those from other researchers, tmTNF-α expressed by tumor cells not only promotes proliferation, transformation, chemoresistance, and metastasis (31, 37, 38) but also facilitates immune evasion by promoting the suppressive activities of MDSCs and accumulation of Treg cells (39, 40). tmTNF-α expression in intestinal epithelial cells likely facilitates

malignant transformation and tumor formation. Therefore, tmTNF-α functions as a double-edged sword, an anti-inflammatory molecule and a tumor promoter, in CAC.

Although tmTNF-α exerts an anti-inflammatory effect, its expression was too low because of high-level processing of tmTNF-α in the inflammation phase. We assumed that if the time window of tmTNF-α expression was shifted ahead to the inflammation stage, malignant transformation might be suppressed. We used a specific antibody that prevents tmTNF-α ectodomain shedding to treat mice in the inflammation phase and successfully increased tmTNF-α expression and decreased sTNF-α release, along with a raised tmTNF-α/sTNF-α ratio. As expected, the antibody significantly reduced the infiltration of M1 macrophages and the production of IL-1β, IL-6, and NO but promoted IL-10 release and the accumulation of Treg cells and MDSCs in the diseased colonic tissue during the inflammation phase. Importantly, the subsequent tumor formation was effectively inhibited, as the number and size of the tumors were significantly decreased. The benefit of the antibody was attributed to increased tmTNF-α expression that suppressed the release of inflammatory mediators. This was supported by the following evidence: 1) The antibody increased tmTNF-α expression and exerted anti-inflammatory effects by inhibition of the NF-κB pathway *in vivo* and *in vitro*; 2) Direct addition of exogenous tmTNF-α or sTNF-α to the culture of colonic epithelial cell lines NCM460 and HCoEpiC led to the opposite effects on the response to LPS *via* TNFR. In contrast to the proinflammatory effect of sTNF-α, tmTNF-α actively suppressed LPS-induced activation of the NF-κB pathway and production of IL-6 and NO, indicating tmTNF-α-induced LPS resistance through its forward signaling; and 3) Transfection of TNF-α or TNF-LS (lack of sTNF-α and TNFR binding but retention of the intracellular fragment of tmTNF-α to transduce reverse signaling) into NCM460 and HCoEpiC suppressed LPS-induced activation of the NF−κB pathway and production of IL-6 and NO, indicating tmTNF-α-induced LPS resistance through its reverse signaling. Second, the anti-inflammatory effect of the tmTNF-α antibody was activation of immunosuppressive cells by increased tmTNF-α expression. This was supported by our original evidence that the antibody significantly promoted intracolonic infiltration of MDSCs and Tregs at the inflammation stage. We have previously found that MDSCs exert a cardioprotective effect in heart failure (41) and tmTNF-α promotes suppressive activities of MDSCs (39). Furthermore, tmTNF-α is a primary ligand for TNFR2 (42) and the interaction of tmTNF-α with TNFR2 results in activation of Tregs and induction of their expansion (40). Thus, the resolution of inflammation through tmTNF-α was the main mechanism by which the antibody suppressed tumor formation in the mouse AOM/DSS-induced CAC model.

Another important mechanism of the tmTNF-α antibody was the induction of apoptosis. Our results revealed that the antibody induced apoptosis not only in infiltrated cells but also in tumor cells; the former led to inflammation resolution and the latter resulted in inhibition of tumor formation and growth. The tmTNF-α density on leukocytes is associated with the primary response to infliximab, including apoptosis of peripheral blood mononuclear cells in IBD. Additionally, infliximab induces apoptosis of monocytes from patients with active Crohn's disease in a caspase-dependent manner (20). Namely, anti-TNF-α agents, such as infliximab, can bind to tmTNF-α and induce apoptosis of tmTNF-α-bearing cells *via* reverse signaling (43). Although our antibody is unable to directly activate tmTNF-α-mediated reverse signaling as its recognized epitope does not exist in TNFR binding site, it was possible that sTNFR or membrane TNFR, as a ligand, bound to tmTNF-α (as a receptor) that was upregulated by the antibody, which activated tmTNF-α-mediated reverse signaling, and thus induced apoptosis. Moreover, our previous study documented that the tmTNF-α antibody is cytotoxic to tmTNF-α-expressing breast cancer cells *via* antibody-dependent cell-mediated cytotoxicity (ADCC) and complement-dependent cytotoxicity (CDC) (31). In this study, antibody treatment during the tumor stage also effectively suppressed the growth of tmTNF-α-expressing adenoma by inducing apoptosis and inhibiting tumor-associated inflammation.

In summary, in a mouse AOM/DSS-induced CAC model, sTNF-α was mainly released in the inflammation phase to promote colitis, while tmTNF-α was expressed by adenoma cells to facilitate tumor development. We have not yet clearly determined whether this phenomenon also exists in patients with CAC, although a report has shown that tmTNF-α is expressed in colorectal cancer (37). Since tmTNF-α functions as a double-edged sword in AOM/DSS-induced CAC, changing its expression window to the inflammation stage may benefit the patients by promoting inflammation resolution *via* tmTNF-α-mediated signaling. The tmTNF-α antibody that targets tmTNF-α processing, unlike selective inhibitors of sTNF-α, anti-TNF antibodies, or soluble TNFR, not only reduced sTNF-α levels but also increased tmTNF-α expression and thus effectively prevented AOM/DSS-induced CAC through the inhibition of inflammation and induction of apoptosis, which provides a new insight into the blockade of this pathological process.

DATA AVAILABILITY STATEMENT

The original contributions presented in the study are included in the article/**Supplementary Material**. Further inquiries can be directed to the corresponding authors.

ETHICS STATEMENT

The animal study was reviewed and approved by the Ethics Committee of Tongji Medical College of HUST.

AUTHOR CONTRIBUTIONS

HB, BL, RJ, MZ, and XZ planned and performed the experiments. HB and BL analyzed the data. ZL, BY, and JW

initiated the project and designed the study. XZ and ZL drafted and wrote the manuscript. All authors contributed to the article and approved the submitted version.

FUNDING

This study was supported by the National Natural Science Foundation of China (Major research program 91029709 and General program 31671470 to ZL) and by China Postdoctoral Science Foundation (2018M642852 to HB).

ACKNOWLEDGMENTS

We appreciate the assistance of Dr. Yaqi Duan (Department of Pathology, Tongji Hospital, Tongji Medical College, Huazhong University of Science and Technology) in pathological analysis.

SUPPLEMENTARY MATERIAL

The Supplementary Material for this article can be found online at: https://www.frontiersin.org/articles/10.3389/fimmu.2021.687874/full#supplementary-material

REFERENCES

1. Feagins LA, Souza RF, Spechler SJ. Carcinogenesis in IBD: Potential Targets for the Prevention of Colorectal Cancer. *Nat Rev Gastroenterol Hepatol* (2009) 6(5):297–305. doi: 10.1038/nrgastro.2009.44
2. Lakatos PL, Lakatos L. Risk for Colorectal Cancer in Ulcerative Colitis: Changes, Causes and Management Strategies. *World J Gastroenterol* (2008) 14(25):3937–47. doi: 10.3748/wjg.14.3937
3. Banat GA, Tretyn A, Pullamsetti SS, Wilhelm J, Weigert A, Olesch C, et al. Immune and Inflammatory Cell Composition of Human Lung Cancer Stroma. *PloS One* (2015) 10(9):e0139073. doi: 10.1371/journal.pone.0139073
4. Elinav E, Nowarski R, Thaiss CA, Hu B, Jin C, Flavell RA. Inflammation-Induced Cancer: Crosstalk Between Tumours, Immune Cells and Microorganisms. *Nat Rev Cancer* (2013) 13(11):759–71. doi: 10.1038/nrc3611
5. Liu H, Zhang Z, Tabuchi T, Wang S, Wang J. The Role of Pro-Inflammatory Cytokines and Immune Cells in Colorectal Carcinoma Progression. *Oncol Lett* (2013) 5(4):1177–82. doi: 10.3892/ol.2013.1176
6. Man YG, Stojadinovic A, Mason J, Avital I, Bilchik A, Bruecher B, et al. Tumor-Infiltrating Immune Cells Promoting Tumor Invasion and Metastasis: Existing Theories. *J Cancer* (2013) 4(1):84–95. doi: 10.7150/jca.5482
7. Nakagawa H, Sido JM, Reyes EE, Kiers V, Cantor H, Kim HJ. Instability of Helios-Deficient Tregs Is Associated With Conversion to a T-Effector Phenotype and Enhanced Antitumor Immunity. *Proc Natl Acad Sci USA* (2016) 113(22):6248–53. doi: 10.1073/pnas.1604765113
8. Yoshimura A. Signal Transduction of Inflammatory Cytokines and Tumor Development. *Cancer Sci* (2006) 97(6):439–47. doi: 10.1111/j.1349-7006.2006.00197.x
9. Mazlam MZ, Hodgson HJ. Peripheral Blood Monocyte Cytokine Production and Acute Phase Response in Inflammatory Bowel Disease. *Gut* (1992) 33 (6):773–8. doi: 10.1136/gut.33.6.773
10. Noguchi M, Hiwatashi N, Liu Z, Toyota T. Secretion Imbalance Between Tumour Necrosis Factor and Its Inhibitor in Inflammatory Bowel Disease. *Gut* (1998) 43(2):203–9. doi: 10.1136/gut.43.2.203
11. Komatsu M, Kobayashi D, Saito K, Furuya D, Yagihashi A, Araake H, et al. Tumor Necrosis Factor-Alpha in Serum of Patients With Inflammatory Bowel Disease as Measured by a Highly Sensitive Immuno-PCR. *Clin Chem* (2001) 47(7):1297–301. doi: 10.1093/clinchem/47.7.1297
12. Popivanova BK, Kitamura K, Wu Y, Kondo T, Kagaya T, Kaneko S, et al. Blocking TNF-Alpha in Mice Reduces Colorectal Carcinogenesis Associated With Chronic Colitis. *J Clin Invest* (2008) 118(2):560–70. doi: 10.1172/JCI32453
13. Nielsen OH, Ainsworth MA. Tumor Necrosis Factor Inhibitors for Inflammatory Bowel Disease. *N Engl J Med* (2013) 369(8):754–62. doi: 10.1056/NEJMct1209614
14. Rutgeerts P, Van Assche G, Vermeire S. Optimizing Anti-TNF Treatment in Inflammatory Bowel Disease. *Gastroenterology* (2004) 126(6):1593–610. doi: 10.1053/j.gastro.2004.02.070
15. Nowacki TM, Bruckner M, Eveslage M, Tepasse P, Pott F, Thoennissen NH, et al. The Risk of Colorectal Cancer in Patients With Ulcerative Colitis. *Dig Dis Sci* (2015) 60(2):492–501. doi: 10.1007/s10620-014-3373-2
16. Corazza N, Brunner T, Buri C, Rihs S, Imboden MA, Seibold I, et al. Transmembrane Tumor Necrosis Factor Is a Potent Inducer of Colitis Even in the Absence of Its Secreted Form. *Gastroenterology* (2004) 127(3):816–25. doi: 10.1053/j.gastro.2004.06.036
17. Perrier C, de Hertogh G, Cremer J, Vermeire S, Rutgeerts P, Van Assche G, et al. Neutralization of Membrane TNF, But Not Soluble TNF, Is Crucial for the Treatment of Experimental Colitis. *Inflammation Bowel Dis* (2013) 19 (2):246–53. doi: 10.1002/ibd.23023
18. Hale LP, Greer PK. A Novel Murine Model of Inflammatory Bowel Disease and Inflammation-Associated Colon Cancer With Ulcerative Colitis-Like Features. *PloS One* (2012) 7(7):e41797. doi: 10.1371/journal.pone.0041797
19. Sobo-Vujanovic A, Vujanovic L, DeLeo AB, Concha-Benavente F, Ferris RL, Lin Y, et al. Inhibition of Soluble Tumor Necrosis Factor Prevents Chemically Induced Carcinogenesis in Mice. *Cancer Immunol Res* (2016) 4(5):441–51. doi: 10.1158/2326-6066.CIR-15-0104
20. Lugering A, Schmidt M, Lugering N, Pauels HG, Domschke W, Kucharzik T. Infliximab Induces Apoptosis in Monocytes From Patients With Chronic Active Crohn's Disease by Using a Caspase-Dependent Pathway. *Gastroenterology* (2001) 121(5):1145–57. doi: 10.1053/gast.2001.28702
21. Mitoma H, Horiuchi T, Hatta N, Tsukamoto H, Harashima S, Kikuchi Y, et al. Infliximab Induces Potent Anti-Inflammatory Responses by Outside-to-Inside Signals Through Transmembrane TNF-Alpha. *Gastroenterology* (2005) 128(2):376–92. doi: 10.1053/j.gastro.2004.11.060
22. Van den Brande JM, Braat H, van den Brink GR, Versteeg HH, Bauer CA, Hoedemaeker I, et al. Infliximab But Not Etanercept Induces Apoptosis in Lamina Propria T-Lymphocytes From Patients With Crohn's Disease. *Gastroenterology* (2003) 124(7):1774–85. doi: 10.1016/s0016-5085(03)00382-2
23. Van den Brande JM, Koehler TC, Zelinkova Z, Bennink RJ, te Velde AA, ten Cate FJ, et al. Prediction of Antitumour Necrosis Factor Clinical Efficacy by Real-Time Visualisation of Apoptosis in Patients With Crohn's Disease. *Gut* (2007) 56(4):509–17. doi: 10.1136/gut.2006.105379
24. Siegmund B, Lehr HA, Fantuzzi G, Dinarello CA. IL-1 Beta-Converting Enzyme (Caspase-1) in Intestinal Inflammation. *Proc Natl Acad Sci USA* (2001) 98(23):13249–54. doi: 10.1073/pnas.231473998
25. Sun L, Yuan M. Application Evaluation of O-Toluidine Method and Monoclonal Antibody Method for Detecting Fecal Occult Blood. *Lab Med Clin* (2011) 8(20):2526–7. doi: 10.3969/j.issn.1672-9455.2011.20.054
26. Yan D, Qin N, Zhang H, Liu T, Yu M, Jiang X, et al. Expression of TNF-Alpha Leader Sequence Renders MCF-7 Tumor Cells Resistant to the Cytotoxicity of Soluble TNF-Alpha. *Breast Cancer Res Treat* (2009) 116(1):91–102. doi: 10.1007/s10549-008-0111-5
27. Amendola M, Venneri MA, Biffi A, Vigna E, Naldini L. Coordinate Dual-Gene Transgenesis by Lentiviral Vectors Carrying Synthetic Bidirectional Promoters. *Nat Biotechnol* (2005) 23(1):108–16. doi: 10.1038/nbt1049
28. Li C, Gu H, Yu M, Yang P, Zhang M, Ba H, et al. Inhibition of Transmembrane TNF-Alpha Shedding by a Specific Antibody Protects Against Septic Shock. *Cell Death Dis* (2019) 10(8):586. doi: 10.1038/s41419-019-1808-6
29. Ba H, Li B, Li X, Li C, Feng A, Zhu Y, et al. Transmembrane Tumor Necrosis Factor-Alpha Promotes the Recruitment of MDSCs to Tumor Tissue by Upregulating CXCR4 Expression *via* TNFR2. *Int Immunopharmacol* (2017) 44:143–52. doi: 10.1016/j.intimp.2016.12.028
30. O'Keeffe J, Lynch S, Whelan A, Jackson J, Kennedy NP, Weir DG, et al. Flow Cytometric Measurement of Intracellular Migration Inhibition Factor and

Tumour Necrosis Factor Alpha in the Mucosa of Patients With Coeliac Disease. *Clin Exp Immunol* (2001) 125(3):376–82. doi: 10.1046/j.1365-2249.2001.01594.x
31. Yu M, Zhou X, Niu L, Lin G, Huang J, Zhou W, et al. Targeting Transmembrane TNF-Alpha Suppresses Breast Cancer Growth. *Cancer Res* (2013) 73(13):4061–74. doi: 10.1158/0008-5472.CAN-12-3946
32. Gabrilovich DI, Nagaraj S. Myeloid-Derived Suppressor Cells as Regulators of the Immune System. *Nat Rev Immunol* (2009) 9(3):162–74. doi: 10.1038/nri2506
33. Kusmartsev S, Nefedova Y, Yoder D, Gabrilovich DI. Antigen-Specific Inhibition of CD8+ T Cell Response by Immature Myeloid Cells in Cancer Is Mediated by Reactive Oxygen Species. *J Immunol* (2004) 172(2):989–99. doi: 10.4049/jimmunol.172.2.989
34. Ostrand-Rosenberg S, Sinha P. Myeloid-Derived Suppressor Cells: Linking Inflammation and Cancer. *J Immunol* (2009) 182(8):4499–506. doi: 10.4049/jimmunol.0802740
35. Onizawa M, Nagaishi T, Kanai T, Nagano K, Oshima S, Nemoto Y, et al. Signaling Pathway *via* TNF-Alpha/NF-KappaB in Intestinal Epithelial Cells May Be Directly Involved in Colitis-Associated Carcinogenesis. *Am J Physiol Gastrointestinal Liver Physiol* (2009) 296(4):G850–9. doi: 10.1152/ajpgi.00071.2008
36. Meusch U, Rossol M, Baerwald C, Hauschildt S, Wagner U. Outside-To-Inside Signaling Through Transmembrane Tumor Necrosis Factor Reverses Pathologic Interleukin-1beta Production and Deficient Apoptosis of Rheumatoid Arthritis Monocytes. *Arthritis Rheum* (2009) 60(9):2612–21. doi: 10.1002/art.24778
37. Li X, Wang S, Ren H, Ma J, Sun X, Li N, et al. Molecular Correlates and Prognostic Value of tmTNF-Alpha Expression in Colorectal Cancer of 5-Fluorouracil-Based Adjuvant Therapy. *Cancer Biol Ther* (2016) 17(6):684–92. doi: 10.1080/15384047.2016.1187551
38. Zhang Z, Lin G, Yan Y, Li X, Hu Y, Wang J, et al. Transmembrane TNF-Alpha Promotes Chemoresistance in Breast Cancer Cells. *Oncogene* (2018) 37(25):3456–70. doi: 10.1038/s41388-018-0221-4
39. Hu X, Li B, Li X, Zhao X, Wan L, Lin G, et al. Transmembrane TNF-Alpha Promotes Suppressive Activities of Myeloid-Derived Suppressor Cells *via* TNFR2. *J Immunol* (2014) 192(3):1320–31. doi: 10.4049/jimmunol.1203195
40. Zou H, Li R, Hu H, Hu Y, Chen X. Modulation of Regulatory T Cell Activity by TNF Receptor Type II-Targeting Pharmacological Agents. *Front Immunol* (2018) 9:594. doi: 10.3389/fimmu.2018.00594
41. Zhou L, Miao K, Yin B, Li H, Fan J, Zhu Y, et al. Cardioprotective Role of Myeloid-Derived Suppressor Cells in Heart Failure. *Circulation* (2018) 138(2):181–97. doi: 10.1161/CIRCULATIONAHA.117.030811
42. Grell M, Douni E, Wajant H, Lohden M, Clauss M, Maxeiner B, et al. The Transmembrane Form of Tumor Necrosis Factor Is the Prime Activating Ligand of the 80 kDa Tumor Necrosis Factor Receptor. *Cell* (1995) 83(5):793–802. doi: 10.1016/0092-8674(95)90192-2
43. Lugering A, Lebiedz P, Koch S, Kucharzik T. Apoptosis as a Therapeutic Tool in IBD? *Ann NY Acad Sci* (2006) 1072:62–77. doi: 10.1196/annals.1326.013

Conflict of Interest: The authors declare that the research was conducted in the absence of any commercial or financial relationships that could be construed as a potential conflict of interest.

Publisher's Note: All claims expressed in this article are solely those of the authors and do not necessarily represent those of their affiliated organizations, or those of the publisher, the editors and the reviewers. Any product that may be evaluated in this article, or claim that may be made by its manufacturer, is not guaranteed or endorsed by the publisher.

Advantages of publishing in Frontiers

OPEN ACCESS
Articles are free to read for greatest visibility and readership

FAST PUBLICATION
Around 90 days from submission to decision

HIGH QUALITY PEER-REVIEW
Rigorous, collaborative, and constructive peer-review

TRANSPARENT PEER-REVIEW
Editors and reviewers acknowledged by name on published articles

Frontiers
Avenue du Tribunal-Fédéral 34
1005 Lausanne | Switzerland

Visit us: www.frontiersin.org
Contact us: frontiersin.org/about/contact

REPRODUCIBILITY OF RESEARCH
Support open data and methods to enhance research reproducibility

DIGITAL PUBLISHING
Articles designed for optimal readership across devices

FOLLOW US
@frontiersin

IMPACT METRICS
Advanced article metrics track visibility across digital media

EXTENSIVE PROMOTION
Marketing and promotion of impactful research

LOOP RESEARCH NETWORK
Our network increases your article's readership